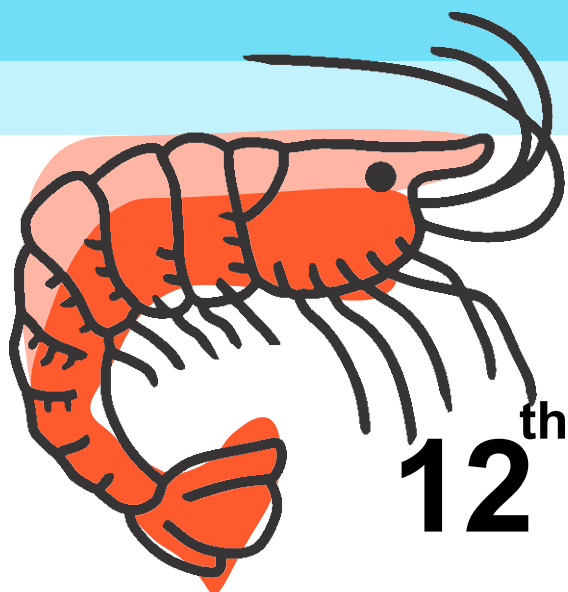


ISBN 978-85-63191-03-8 (v.14)



Sociedad Iberoamericana de Quitina



6th Iberoamerican Chitin
Symposium

&

12th International Conference on
Chitin and Chitosan

ADVANCES IN CHITIN SCIENCE VOLUME XIV

PROCEEDINGS

VI SIAQ / XII ICC
São Carlos / Brazil
2014

EDITED BY

Sergio Paulo Campana Filho
Marisa Masumi Beppu
Anderson Fiamingo



S I A Q

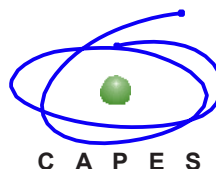
Sociedad Iberoamericana de Quitina

**VI Iberoamerican Chitin Symposium
&
XII International Conference on
Chitin and Chitosan
São Carlos, Brazil
2014**

**ADVANCES IN CHITIN SCIENCE
VOLUME XIV**

**EDITED BY
Sergio Paulo Campana Filho
Marisa Masumi Beppu
Anderson Fiamingo**

Sponsors



6th Iberoamerican Chitin Symposium
&
12th International Conference on Chitin and Chitosan
September 2nd to 5th, 2012
Fortaleza, Brazil

Iberoamerican Chitin Society Board

Sergio Paulo Campana Filho (President)

Gustavo Cabrera (Vice-President)

Paola Ximena Anaya (Secretary)

Cristiana Yoshida (Treasurer)

Jaime Lizardi

Ficha catalográfica elaborada pela Seção de Tratamento da Informação do Serviço de Biblioteca e Informação do IQSC/USP

S13 Sociedade Iberoamericana de Quitina
Advances in chitin science [recurso eletrônico] /
organizadores Sergio Paulo Campana Filho, Marisa Masumi
Beppu, Anderson Fiamingo. — São Carlos : IQSC, 2014.
Modo de acesso: World Wide Web
Texto (livro eletrônico)
ISBN 978-85-63191-03-8 (v.14)

1. Química. 2. Quitina. I. Campana Filho, Sergio
Paulo. II. Beppu, Marisa Masumi. III. Fiamingo,
Anderson. IV. Título.

CDD 547.84

Conference Chairs

Marisa M. Beppu

Sérgio P. Campana-Filho

Haroldo C. B. de Paula

Local Committee

Marisa M. Beppu (UNICAMP)

Sérgio P. Campana-Filho (USP)

Haroldo C. B. de Paula (UFC)

Regina de Paula (UFC)

Sueli Rodrigues (UFC)

Rodrigo Vieira (UFC)

Cristiana Yoshida (UNIFESP)

International Advisory Board

Marisa Beppu (Brazil)

Sergio Paulo Campana-Filho (Brazil)

Rong-Huei Chen (Taiwan)

Chong-Su Cho (South Korea)

Veronique Coma (France)

Carlos Peniche Covas (Cuba)

Laurent David (France)

Nguyen Anh Dzung (Vietnam)

Francisco M. Goycoolea (Germany)

Saburo Minami (Japan)

Bruno Moerschbacher (Germany)

Hong Kyoon No (South Korea)

Gregory F. Payne (USA)

Martin G. Peter (Germany)

Sevda Senel (Turkey)

Valery Varlamov (Russia)

Kjell Varum (Norway)

Yumin Du (China)

PREFACE

“Advances in Chitin Science vol. XIV” records some of the most important contributions presented during the joint event 6th Iberoamerican Chitin Symposium & 12th Internacional Conference on Chitin and Chitosan (VI SIAQ & XII ICCC), which took place in Fortaleza/Brazil in September 2012.

It is noteworthy to add that for the first time the Iberoamerican Chitin Society co-organized its own scientific event, mostly dedicated to the iberoamerican community, together with the international conference on chitin and chitosan, making the joint event an unique opportunity to bring together the international community of researchers, industrials and students working on basic science and technological applications of chitin and chitosan.

Indeed, the number of participants of the VI SIAQ & XII ICCC was the highest (over 140 participants registered) ever attained in scientific events organized by the Iberoamerican Chitin Society and its international character was evidenced by the nationality of these participants which represented twenty eight (28) countries.

During the VI SIAQ & XII ICCC, fifty two (52) oral contributions were presented, including seven (7) plenary and seven (7) invited lectures, and one hundred fifty eight (158) posters.

The authors were invited to submit extended versions of their contributions for reviewing and publication in the “Advances in Chitin Science vol. XIV” and fifty one (51) papers integrate this book which groups the contributions according to the following themes: i) Sources, Production and Technological Processes; ii) Enzymology, Biochemistry, Biological and Ecological Aspects; iii) Chemical and Physicochemical Properties; iv) Chemical Modifications and Advanced Materials; v) Nanotechnology; vi) Applications in Life Science; vii) Applications in Material Science and viii) Intellectual Properties.

The organizers of the VI SIAQ & XII ICCC and the editors of the “Advances in Chitin Science vol. XIV” are greatly thankful to all those who contributed to make it possible and special thanks are directed to the Brazilian agencies, CAPES and FAPESP, for financial support and to the Brazilian academic institutions, namely the Universidade de São Paulo, Universidade Federal do Ceará, Universidade Federal de São Paulo and Universidade Estadual de Campinas.

Sergio Paulo Campana-Filho

Universidade de São Paulo

Brazil

E-mail: scampana@iqsc.usp.br

Content

Sources, Production and Technological Processes

**CALCIUM LACTATE PRODUCTION DURING
DEMINERALIZATION OF CRAB (*Callinectes bellicosus*) SHELLS
WITH LACTIC ACID** **2**

N. Ayala-Mendivil, W. Argüelles-Monal, E. Carvajal-Millán, Y. López-Franco, M. Plascencia-Jatomea, J. Lizardi-Mendoza

**EFFECT OF SUPERCRITICAL WATER TREATMENT ON
ENZYMATIC SACCHARIFICATION OF CHITIN** **8**

M. Osada, C. Miura, Y.S. Nakagawa, M. Kaihara, M. Nikaido, K. Totani

**CHEMICAL COMPOSITION AND QUALITY OF CHITIN FROM
WHITE SHRIMP AND BLACK TIGER SHRIMP** **14**

T.T. Khong, H.D.T. Ngo, N.D. Ngo, T.S. Trang, K.M. Vårum

**NARROW POLYDISPERSITY OF CHITOSAN BY SUPERCRITICAL
CARBON DIOXIDE WITH ACETIC ACID AQUEOUS SOLUTION** **21**

M.-L. Tsai, W.-K. Lee

**MORPHOLOGICAL CHARACTERIZATION OF CHITIN
EXTRACTION** **27**

A.S.R.R.M. Cavalcanti, M.V.L. Fook, G.T. Furtado, H.M. Lisboa

**CHARACTERIZATION OF CHITOSAN BASED FILM WITH *ALOE
VERA* GEL INCORPORATION** **33**

A. Valbuena, A. Garcia, M. Colina, J. Molina, J. Caldera, O. Leon, R. Cambar

Enzymology, Biochemistry, Biological and Ecological Aspects

**CHITIN AND CHITOSAN MODIFYING ENZYMES: VERSATILE
NOVEL TOOLS FOR THE ANALYSIS OF STRUCTURE-FUNCTION
RELATIONSHIPS OF PARTIALLY ACETYLATED CHITOSANS** **40**

N.E. Gueddari, S. Kolkenbrock, A. Schaaf, N. Chilukoti, F. Brunel, C. Gorzelanny, S. Fehser, S. Chachra, F. Bernard, M. Nampally, T. Kalagara, P. Ihmor, B.M. Moerschbacher

**SUBMERGED AND SOLID SUPPORT PRODUCTION AND
MOLECULAR IDENTIFICATION OF CHITIN DEACETYLASES
FROM PHYTOPATHOGENIC FUNGI** **48**

F. Muñiz-Paredes, C.P. Larralde-Corona, F.J. Fernandez, J.D. Sepúlveda, K. Shirai

ENZYMATIC HYDROLYSIS OF CHITOSAN TO OBTAIN OLIGOMERS USING A CELLULASE ENZYMATIC COMPLEX AND ITS SCALING AT PILOT PLANT LEVEL	55
H. Ortega-Ortiz ¹ , B. Gutiérrez-Rodríguez, G. Cadenas-Pliego	
CRUDE ENZYME OF <i>Colletotrichum gloeosporioides</i> WITH CHITIN DEACETYLASE ACTIVITY ON CHITINOUS SUBSTRATES	61
N. Pacheco, S. Trombotto, L. David, C.P. Larralde-Corona, K. Shirai	
ENZYMATIC HYDROLYSIS OF CHITIN BY CHITINASES FROM <i>Lecanicillium lecanii</i>	67
G. Villa-Lerma, H. González-Márquez, M. Gimeno, A. López, K. Shirai	
SYNTHESIS OF GALACTOOLIGOSACCHARIDES FROM LACTOSE BY β-GALACTOSIDASE IMMOBILIZED ON GLUTARALDEHYDE-TREATED CHITOSAN	73
A.E.C. Fai, T.C.M. Stamford, T.L.M. Stamford, H.Y. Kawaguti, I. Thomazelli, G.M. Pastore	
IMMOBILIZATION OF MARINE FUNGUS <i>Penicillium citrinum</i> CBMAI 1186 ON CHITOSAN FOR REDUCTION OF KETONES	79
L.C. Rocha, S.P. Campana Filho, A.L.M. Porto, A.H. Jeller	
SELECTIVE ISOLATION OF TRYPSIN INHIBITOR FROM SOYBEAN WHEY BY CHITOSAN/TRIPOLYPHOSPHATE/GENIPIN CO-CROSSLINKED BEADS	92
M.-L. Tsai ¹ , R.H. Chen, C.-H. Hsu, Y.-L. Chang	
SYNTHESIS OF CHITOSAN DERIVATIVES WITH ANTIFUNGAL AND ANTIBACTERIAL PROPERTIES	98
A. Valbuena-Inciarte, C. Valbuena, M. Colina, N. Diaz	

Chemical and Physicochemical Properties

USE OF HIGHLY DEACETYLATED CHITOSAN FOR THE REMOVAL Cr (VI) FROM AQUEOUS SOLUTIONS BY ADSORPTION: THERMODYNAMIC PARAMETERS	105
T. R. S. Cadaval, A. S. Camara, G. L. Dotto, L. A. A. Pinto	
PHYSICO-CHEMICAL STUDIES ON THE CARBOXYMETHYLATION OF CHITOSAN	111
D. S. Silva, S. P. Campana Filho	

Chemical Modifications and Advanced Materials

- PREPARATION, CHARACTERIZATION AND RELEASING STUDIES OF A CAPTOPRIL CHITOSAN SALT** 119
M.B. Luppi, R.C. da Silva, E.T.G. Cavalheiro
- INFLUENCE OF STARCH OXIDATION IN DRUG DELIVERY BEHAVIOR OF CHITOSAN/ CORN STARCH FILMS** 126
M.B. Simões, M.M. Horn, V.C.A. Martins, A.M.G. Plepis
- SURFACE MODIFIED CHITOSAN FILM FOR TRANSDERMAL DRUG DELIVERY** 132
A. Tourrette, S. Chamary, D. Geyter, R. Morent, P. Kirilov, S. Cazalbou

Nanotechnology

- PREPARATION OF OPTICALLY TRANSPARENT CHITIN NANOFIBER/POLYSILSESQUOXANE COMPOSITES** 139
S. Ifuku¹, A. Ikuta, M. Morimoto, H. Saimoto
- “SMART” CO-CROSSLINKED CHITOSAN-BASED NANOPARTICLES FOR NANOBIO TECHNOLOGY** 145
C. Vila-Sanjurjo, C. Remuñán-López, L. David, C. Rochas, F.M. Goycoolea

Applications in Life Science

- ANTIFUNGAL POTENTIAL OF MICRO AND NANOPARTICLES OF CHITOSAN CROSSLINKED WITH SODIUM TRIPOLYPHOSPHATE** 157
O. Cota-Arriola, M.O. Cortez-Rocha, J. Lizardi-Mendoza, J.M. Ezquerrabauer, M. Robles-Sánchez, M. Plascencia-Jatomea
- BARRIER PROPERTIES OF CHITOSAN FILM INCORPORATED WITH ESSENTIAL OIL** 163
H. S. Debone, C. M. P. Yoshida, C. F. Da Silva
- EQUILIBRIUM AND KINETIC STUDIES ON THE ADSORPTION OF RED 2 BY CHITOSAN-CELLULOSE BEADS** 169
E. Alva-Navarrete, B. García-Gaitán, J. L. García-Rivas, R. E. Zavala-Arce, J. G. Luna-Bárceñas, M. C. Díaz-Nava, C. R. Muro-Urista

RUBUS FRUTICOSUS SUSPENSION-CULTURED CELLS ELICITED WITH CHITOOLIGOSACCHARIDES PRODUCED FROM POLYMERIC CHITOSAN USING CHITOSANOLYTIC ENZYMES FROM SOLID STATE FERMENTATION	175
T. L. Honorato, S. Rodrigues, N. E. El Gueddari, B. M. Moerschbacher, T.T. Franco	
CHARACTERIZATION OF A NEW H₂S CHITOSAN INTELLIGENT SENSOR AND STUDY OF THE INFLUENCE OF MOISTURE CONTENT	181
E.T. Kato-Junior, E. Guibal, C.M.P. Yoshida, T.T. Franco	
PREPARATION AND CHARACTERIZATION OF A CHITOSAN/PECTIN POLYELECTROLYTE COMPLEX	190
V. Maciell, C. Yoshida, T. Franco	
EFFECT OF CHITIN NANOFIBRILS ON ULCERATIVE COLITIS MOUSE MODEL AND ITS MECHANISM	196
S. Minami, K. Azuma, T. Osaki, S. Ifuku, H. Saimoto, T. Tsuka, T. Imagawa, Y. Okamoto	
SYNTHESIS, CHARACTERIZATION AND STUDY OF AMPHIPHILIC QUARTENARY DERIVATIVES OF CHITOSAN: IN VITRO STUDY AGAINST <i>Aspergillus flavus</i>	205
M. Takaki, R.O. Pedro, R.H.F.V. de Souza, A.M. Dias, J.S. Gabriel, M.J. Tiera, V.A.O. Tiera	
CHITOSAN BASED SUTURE – FOCUSING ON THE REAL ADVANTAGES OF AN OUTSTANDING BIOMATERIAL	211
R. Montenegro, J.R.G. Godeiro	
CHITOSAN IN BIOMEDICINE. FROM GELS TO NANOPARTICLES	217
L. Becherán, M. Bocourt, J. Pérez, C. Peniche	
THE BIODEGRADABILITY OF CHITOSAN FILM-COATED KRAFT PAPER SHEETS	225
A.B.Reis, C.M.P. Yoshida, I.S. Melo, T.T. Franco	
SYNTHESIS AND CHARACTERIZATION OF ANTIMICROBIAL CHITOSAN COCITRIC FILMS	232
I. Corona, M. Gimeno, A. Tecante, J. Sepúlveda, K. Shirai	
STRESS-RESPONSE OF <i>Aspergillus niger</i> EXPOSED TO CHITOSAN: COMPARISON OF THE GROWTH KINETICS MODELS IN SOLID AND LIQUID MEDIA	238
J.M. Velez-Haro, E.C. Rosas-Burgos, M.O. Cortez-Rocha, F.J. Almendariz-Tapia, M. Plascencia-Jatomea	
KINETIC AND ISOTHERMS STUDIES OF Cu⁺² SORPTION USING CHITOSAN-CELLULOSE CRYOGEL	244
R. Garcia-Gonzalez, R.E. Zavala-Arce, P. Avila-Perez, R.M. Gomez-Espinosa, B. Garcia-Gaitan, F. Cortes	

MELON PRODUCTION (<i>Cucumis melo L.</i>) AS AFFECTED BY SOIL APPLICATIONS OF CHITOSAN OLIGOMERS UNDER VARYING LEVELS OF IRRIGATION	250
C.A. Pérez-Cabrera, H. Ortega-Ortiz, E. Treviño-López, M.C. Fuente, A. Benavides-Mendoza, E. Cruz-Lázaro	
PREPARATION AND CHARACTERIZATION OF POROUS CHITOSAN AND CARBOXYMETHYLCHITOSAN MEMBRANES FOR PREVENTING POSTSURGICAL PERICARDIAL ADHESIONS	256
A. Fiamingo, J.B. Lopes, S.P. Campana-Filho	
INFLUENCE OF COPPER SPECIES ON CHITOSAN MEMBRANES FOR CHROMIUM ADSORPTION – AN XPS STUDY	262
M.M. Beppu, F.C. Godoi, R.B. Rabelo, E. Rodriguez-Castellon, E. Guibal	
ANTIBACTERIAL ACTIVITY OF FUNGAL CHITOSAN	268
W.S. Paiva, F.E. Souza Neto, G.G. Reboucas, F.H.A. Praxedes Júnior, A.C.L. Batista	
EVALUATION OF CHITOSAN BASED FILMS IN PRESERVATION OF MEXICAN FRESH CHEESE “QUESO RANCHERO”	274
M. Lopez-Chavez, A.Tecante, A. Lopez-Luna, K. Shirai	
BIODIESEL PRODUCTION FROM SUNFLOWER OIL REFINED USING CHITOSAN SPHERES WITH CALCIUM AS HETEROGENEOUS CATALYST	281
L.M. Correia, N.S. Campelo, R.S. Vieira	
INFLUENCE OF THE ADDITION OF POTATO STARCH TO CHITOSAN MATRICES USED FOR CONTROLLED RELEASE	288
M.V. Debandi, M.E. Daraio, N.J. Francois	
CONTROLLED RELEASE OF FERTILIZERS: INFLUENCE OF XANTHAN AND HIDROXYPROPYLMETHYLCELLULOSE ADDITION TO CHITOSAN MATRICES	294
M.A. Melaj, E. Andisco, N.J. Francois, M.E. Daraio	
EFFECT OF USING FREEZE-THAWING CYCLES ON THE PROPERTIES OF CHITOSAN FILMS	300
S. Allo, M. Daraio, N. Francois	

Applications in Material Science

PERFORMANCE EVALUATION OF MECHANICAL CHITOSAN/HYDROXYAPATITE BIOCOMPOSITES	307
R.C.A. Leal, I.V.S.R. Nascimento, I.P. Rabello, V.P. Ferreira, M.V.L. Fook, H.M. Lisboa	

CHITOSAN-POLY (LACTIC ACID) COMPOSITE FILMS: MECHANICAL, THERMAL, AND ANTIFUNGAL PROPERTIES	314
A.P. Martinez-Camacho, M.M. Castillo-Ortega, J.M. Ezquerra-Brauer, P. Herrera-Franco, M.O. Cortez-Rocha, M. Plascencia-Jatomea	
EFFECT OF INTRINSIC FACTORS OF CHITOSAN ON PROPERTIES OF CHITOSAN/2-GLYCEROPHOSPHATE THERMOSENSITIVE HYDROGEL CONTAINING SILVER NANOPARTICLES	320
M.-L. Tsai, H.-W. Chang, Y.-S. Lin, Y.-D. Tsai	
ANTIFUNGAL PROPERTIES OF NEUTRALIZED AND NON- NEUTRALIZED CHITOSAN/POLYLACTIC ACID COMPOSITE FILMS	326
M.A. Méndez-Encinas, A.P. Martínez-Camacho, E.C. Rosas-Burgos, A.Z. Graciano- Verdugo, M.S. Yépiz-Gómez, M. Plascencia-Jatomea	
3D STRUCTURED CHITOSAN SCAFFOLDS FOR TISSUE ENGINEERING	332
G.Y.H. Sampaio, A.C.B.M. Fook, T.B. Fidéles, H.M.L. Oliveira, A.S. R.R.M. Cavalcanti, M.V.L. Fook	

Intellectual Properties

EACH COIN HAS TWO SIDES: SCIENTIFIC AND COMMERCIAL ASPECTS OF CHITIN / CHITOSAN	339
M.G. Peter	

Sources, Production and Technological Processes

CALCIUM LACTATE PRODUCTION DURING DEMINERALIZATION OF CRAB (*Callinectes bellicosus*) SHELLS WITH LACTIC ACID

N. Ayala-Mendivil¹, W. Argüelles-Monal², E. Carvajal-Millán¹, Y. López-Franco¹,
M. Plascencia-Jatomea³, J. Lizardi-Mendoza^{1*}

¹ Biopolímeros CTAOA. Centro de Investigación en Alimentación y Desarrollo AC, Carretera a la Victoria km 0.6, Apartado Postal 1735, Hermosillo, Sonora, México 83000.

² Centro de Investigación en Alimentación y Desarrollo AC, Unidad Guaymas. Carretera al Varadero Nacional km 6.6, Apartado Postal 284, Guaymas, Sonora, México 85400.

³ Departamento de Investigación y Posgrado en Alimentos, Universidad de Sonora, Blvd. Rosales y Luis Encinas s/n. Hermosillo, Sonora, México 83000.

*E-mail address: jalim@ciad.mx

ABSTRACT

Processing of crab generates considerable quantities of solid waste. This rejects has been used as source of protein, pigments and chitin; however its main constituent, the mineral salts, are not usually recovered. Using organic acids for demineralization the recovery of the resulting salts is feasible. In this work lactic acid was used to demineralize the crab shells in order to produce calcium lactate. Demineralization conditions were optimized using response surface methodology considering reaction time, lactic acid concentration and solid to liquid ratio as main factors. At the end of the treatment calcium lactate was recovered from the reaction liquid. Conventional demineralization method was also performed as reference. At optimal conditions a 99.3% of demineralization of crab shell was reached. Also it was possible to recover calcium lactate, identified by FTIR, from the demineralization reaction effluent. The chitin obtained using the proposed lactic acid treatment for demineralization had a purity of 90.9% as some protein and lipids were retained, compared to 98.9% chitin purity obtained by a conventional chemical isolation procedure. No substantial difference were found on the acetylation degree of the obtained chitins but the molecular weight of the lactic acid treated chitin was lower.

Keywords

Chitin, Calcium lactate, Crab shells, Demineralization.

INTRODUCTION

Food processing of crustaceans species generates considerable quantities of solid waste. For crab the fraction regarded as waste is estimated in approximately 50 % (wet weight) of the processed biomass. Such rejects has been used as source of chitin and other valuable by-products. In this way, considerable biomass is used as raw material of a profitable activity that could contribute to avoid contamination problems or to facilitate the observance of regional environmental regulations.

Chitin isolation processes are usually used as starting point to recover other valuable compounds present in crab shells. Methodological modifications are often proposed to maximize the recovery of proteins or carotenoid pigments. However, the calcium salts, that are among the main constituents of the crab shell, are not usually recovered. Most conventional processes of chitin isolation use strong acids for the demineralization step.

The use of such type of acids, i.e. hydrochloric acid, results in the production of highly soluble salts (i.e calcium chloride) that are difficult to recover from the reaction effluent. The use of organic acids for crab shells demineralization makes the recovery of the resulting calcium compounds feasible.

Organic acids, as acetic or lactic acid, have been proposed for the demineralization of crustacean shells, commonly with acceptable results. Several biotechnological methods for chitin isolation are based on the action of organic acids either added or produced *in situ*, as in lactic fermentations [1]. Demineralization of crab shells with lactic acid produces calcium lactate. Similarly, this calcium salt is produced commercially treating calcium compounds with lactic acid. The uses of calcium lactate are diverse and are particularly interesting those in food technology and biomedical applications.

It is considered that lactic acid production could be incorporated to the chitin isolation process from crab shells without compromising the quality of the obtained polysaccharide. Thus the process of demineralization of crab shells treated with lactic acid was optimized using response surface methodology (RSM). Also the recovery of calcium lactate and the quality of the isolated chitin was evaluated.

MATERIALS and METHODS

Ground dry Crab (*Callinectes bellicosus*) shell waste was kindly provided by the Biopigmentos S.A. company at Cd. Obregon, Sonora, México. The shell waste, which consisted mainly on particles of 1 mm or less, was washed thoroughly with running water and dried again at 60 °C before use it. For all the experiments bi-distillate water and chemical compounds of analytical reagent grade from recognized commercial brands were used.

The crab shell waste was demineralized using lactic acid. Demineralization conditions were optimized using response surface methodology (RSM). A rotatable central composite design was applied considering three independent variables as main factors: lactic acid concentration, reaction time and solid to liquid ratio. The test values ranging between 8-12 %, 1-3 hours and 1:20-1:30 (g:mL), respectively. The response variable was the percentage of demineralization (DM) defined as (equation 1):

$$DM (\%) = 100 \times (A_i \cdot W_i - A_f \cdot W_f) / (A_i \cdot W_i) \quad (1)$$

Where A_i and A_f are the inorganic content (measured as ash; g/g) before and after demineralization, respectively; similarly, W_i and W_f are the weight of the samples previously and after the treatment with lactic acid (adapted from [2]).

At the end of the demineralization treatment calcium lactate was recovered from the reaction liquid as follows. The reaction liquid was filtered through a No 4 Whatman paper filter to remove all suspended debris. Afterward, the liquid was concentrated by heating at 90 °C until reach an approximate calcium lactate concentration of 100 mg/mL. The concentrated liquid was left to cool down at room temperature and then stored at 4 °C up to 72 hours to promote the crystallization of the calcium lactate. The obtained calcium lactate crystallites were decanted and washed thoroughly with 50 % ethanol. Finally it was dried at 100 °C for 24 h. in a convection oven.

Chitin was isolated from the crab shell waste using the optimal conditions determined for demineralization with lactic acid treatment and the chemical deproteinization treatment described by Beaney and collaborators (2005) [3]. Simultaneously the complete chemical procedure of such authors was followed to produce chitin from the crab shell waste to compare the products. In summary, two chitin lots were obtained from the same raw material, one using the optimized lactic acid treatment (Cn-L) and the other using hydrochloric acid for demineralization (Cn-C); both were deproteinized with sodium hydroxide treatment at the same conditions.

The products, calcium lactate and both chitins, were chemically identified by infrared spectroscopy analysis (Nicolet Protege 460 ESP, FTIR spectrometer). They proximate compositions were also determined. Total ash content was determined gravimetrically after incinerate a known weight sample at 800 °C for 4 h in a furnace. Humidity, lipids and total nitrogen content were determined by standard methods (AOAC 991.01, 7.060 and 992.15; respectively). Protein content in the chitin samples was estimated using the stoichiometric nitrogen relationship proposed by Diaz-Rojas and collaborators (2006) [4]. The degree of acetylation (DA) of the chitins was calculated from the FTIR spectra [5] and their viscosity average molecular mass (M_v) was determined using capillary viscometry data and the constants K= 0.10 and α= 0.68 for the Mark-Houwink-Sakurada equation [6].

RESULTS and DISCUSSION

Following the setup of the RSM the obtained experimental data were analyzed by linear multiple regression (Minitab software v. 15). Equation 2 represent the best fit model obtained.

$$Y = -0.238 + 0.088 \cdot X_1 + 0.15 \cdot X_2 + 0.036 \cdot X_3 - 0.001 \cdot X_1^2 - 0.01 \cdot X_2^2 - 0.0003 \cdot X_3^2 - 0.009 \cdot X_1 \cdot X_2 - 0.001 \cdot X_1 \cdot X_3 - 0.00009 \cdot X_2 \cdot X_3 \quad (2)$$

Where: Y is the predicted response variable, DM (%); and X₁-X₃ are the coded values for the independent variables, acid lactic concentration (%), reaction time (h) and ratio solid to liquid (g:mL), respectively. The correlation coefficient (R² = 0.9421) for the Equation 2 suggest that 94 % of the total variation is attributed to the effect of independent variables and only about 6 % of such variation cannot be explained by the model.

The optimal levels of the three independent variables for maximum demineralization were: Lactic acid concentration of 7.17 %, 3.5 h of reaction time and 1:33 of solid to liquid ratio. According to the model, these conditions predicted a value of 99.9 % of DM. On trial tests it was possible to obtain an average of 99.4% of DM on dry crab shell waste using these optimal conditions. This DM value is higher than others reported for crustacean shells demineralization procedures with added lactic acid [7–9].

Calcium lactate was recovered from the demineralization reaction liquid obtaining yields over 75 % (w/w) respect to the estimated mineral content of the crab shell waste. It was positively identified by FTIR spectral analysis (Figure 2). Characteristics bands related with calcium lactate were observed: at 1126 and 1090 cm⁻¹ (CO), at 1589 and 1429 cm⁻¹ CO₂ and at 863 cm⁻¹ (C-CO₂) [10]. Furthermore, no substantial differences were found when the product spectrum (Figure 2-B) was compared with a reagent grade calcium lactate (CAS 5743-47-5, Sigma-Aldrich) spectrum (Figure 2-A). The produced calcium lactate contained 18.8% of calcium compared with the 18.3 % of formula value. This could indicate some presence of other calcium salts.

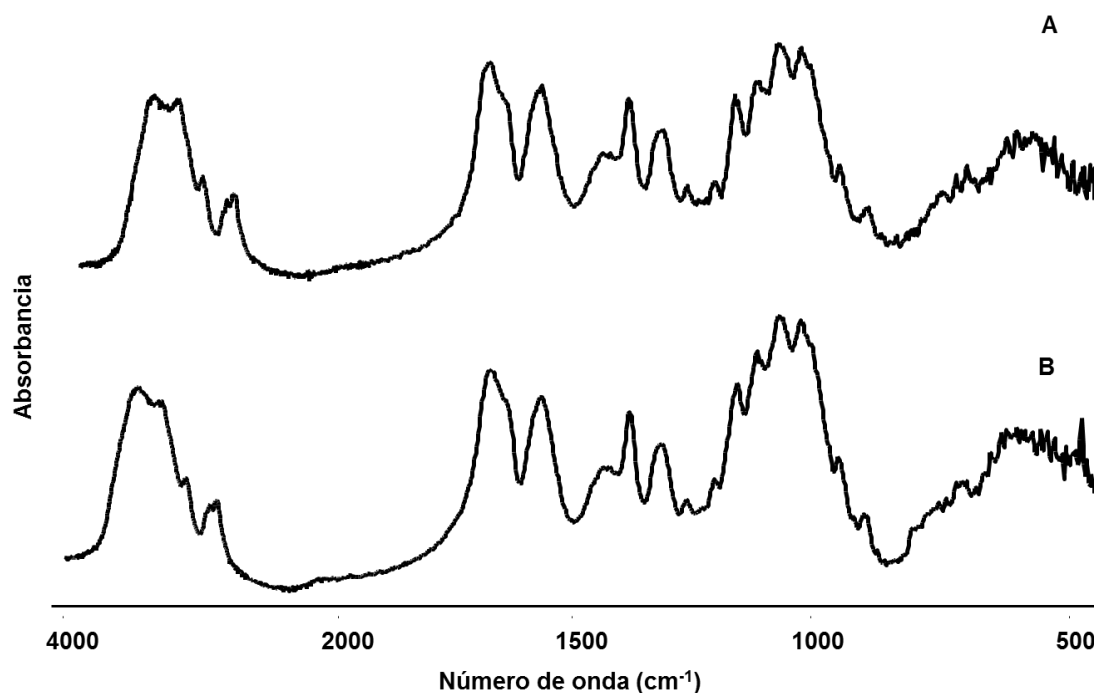


Figure 2. FTIR spectra of reagent grade calcium lactate (A) and the compound recovered from the reaction liquid of crab shells waste demineralization (B).

The composition and main physicochemical characteristics of the obtained chitins are included in Table 1. It could be observed that the chitin obtained by conventional chemical process (Cn-C) has a less impurities. Conversely, some protein and lipids fractions are retained in the lactic acid treated chitin (Cn-L). However, both chitins have similar content of inorganic matter (ash), this indicates that the proposed lactic acid treatment is as effective as the conventional process to demineralize crab shell waste. The overall results are comparable to those obtained by the biotechnological process reported by Beaney and col. (2005) [3]. Apparently the chitins isolated by milder procedures tend to retain organic impurities to some extent. This could be result of relatively lower protein hydrolyzing proficiency or compounds re-adsorption facilitated by the physicochemical conditions of such procedures.

Table 1. Composition and main characteristics of the isolated chitins.

Sample	Protein ^a (% wt.)	Chitin ^a (% wt.)	Ash (% wt.)	Lipids (% wt.)	DA (%)	Mv (g·mol ⁻¹)
Cn-L	1.1	90.9	0.85 ± 0.13	5.4 ± 0.1	~ 100	5.5 × 10 ⁴
Cn-C	~ 0.0	98.9	0.82 ± 0.06	2.4 ± 0.1	~ 100	6.2 × 10 ⁵

^a Estimated from total nitrogen and proximate analysis data (as in [4])

The degree of acetylation of both obtained chitins were high, accordingly to the FTIR spectra analysis practically all the sugar units of the polysaccharides were acetylated. Conversely, the molecular weight of Cn-L was lower than the Mv of the Cn-C. The higher hydrolysis suffered by Cn-L could be related to the longer reaction time used to demineralize the crab shell waste with lactic acid. It has been reported that demineralization procedures with reaction times over 3 h can cause partial depolymerization of chitin, even when diluted acidic conditions are used [11].

Summarizing, the optimal conditions to demineralize crab shell waste with lactic acid treatment were determined by response surface methodology. The DM reached at the proposed conditions was higher than the obtained by other reported procedures using added lactic acid for crustacean shells demineralization. Furthermore, it was comparable to the DM achieved by a conventional chemical process. On the other hand, it was possible to recover most of the calcium lactate produced during the demineralization of crab shell waste. The quality of the chitin isolated using the optimized lactic acid treatment (Cn-L) was lower compared to chitin obtained by usual chemical method. This was consequence of the presence of residual protein and lipids in the Cn-L and also because of its lower molecular weight. These results could help to incorporate the calcium lactate production in a scheme of profitable complete utilization of crustacean shells waste. However, further effort is required to improve the quality of the obtained chitin.

ACKNOWLEDGEMENTS

The authors wish to recognize the financial support of the FOMIX-Sonora Project No. 80891. We are grateful to Karla Martinez Robinson, Rene Valenzuela Miranda and Alma Campa Mada for the help conducting part of the experimental work of this study. NAM acknowledges the postgraduate grant from CONACYT.

REFERENCES

- [1] Bautista J, Jover M, Gutierrez JF, Corpas R, Cremades O, Fontiveros E, Iglesias F, Vega J (2001) Preparation of crayfish chitin by in situ lactic acid production. *Process Biochem.* 37, 229–234.
- [2] Ghorbel-Bellaaj O, Hmidet N, Jellouli K, Younes I, Maalej L, Hachicha R, Nasri M (2011) Shrimp waste fermentation with *Pseudomonas aeruginosa* A2: Optimization of chitin extraction conditions through Plackett-Burman and response surface methodology approaches. *Int J Biol Macromol.* 48, 596–602.
- [3] Beaney P, Lizardi-Mendoza J, Healy M (2005) Comparison of chitins produced by chemical and bioprocessing methods. *J Chem Technol Biotechnol.* 80, 145–150.
- [4] Diaz-Rojas EI, Arguelles-Monal WM, Higuera-Ciapara I, Hernandez J, Lizardi-Mendoza J, Goycoolea FM (2006) Determination of chitin and protein contents during the isolation of chitin from shrimp waste. *Macromol Biosci.* 6, 340–347.
- [5] Brugnerotto J, Lizardi J, Goycoolea FM, Arguelles-Monal W, Desbrieres J, Rinaudo M (2001) An infrared investigation in relation with chitin and chitosan characterization. *Polymer* 42, 3569–3580.
- [6] Einbu A, Naess SN, Elgsaeter A, Varum KM (2004) Solution properties of chitin in alkali. *Biomacromol.* 5, 2048–2054.
- [7] Mahmoud NS, Ghaly AE, Arab F (2007) Unconventional Approach for Demineralization of Deproteinized Crustacean Shells for Chitin Production. *Am J Biochem Biotechnol.* 3, 1–9.
- [8] Jung WJ, Jo GH, Kuk JH, Kim KY, Park RD (2005) Demineralization of crab shells by chemical and biological treatments. *Biotechnol Bioprocess Eng.* 10, 67–72.
- [9] Das S, Ganesh EA (2010) Extraction of Chitin from Trash Crabs (*Podophthalmus vigil*) by an Eccentric Method. *Curr Res J Biol Sci.* 2, 72.

- [10] Cassanas G, Morssli M, Fabrègue E, Bardet L (1991) Vibrational spectra of lactic acid and lactates. *J Raman Spectrosc.* 22, 409–413.
- [11] Percot A, Viton C, Domard A (2003) Optimization of chitin extraction from shrimp shells. *Biomacromol.* 4, 12–8.

EFFECT OF SUPERCRITICAL WATER TREATMENT ON ENZYMATIC SACCHARIFICATION OF CHITIN

Mitsumasa OSADA*, Chika MIURA, Yuko S. NAKAGAWA, Mikio KAIHARA, Mitsuru NIKAIDO, and Kazuhide TOTANI

Department of Chemical Engineering, Ichinoseki National College of Technology, Ichinoseki, Iwate, 021-8511, Japan.

**E-mail address: osada@ichinoseki.ac.jp*

ABSTRACT

We examined the effect of supercritical water treatment on enzymatic saccharification from chitin to *N,N'*-diacetylchitobiose ((GlcNAc)₂). The enzymatic saccharification ratio after hydrothermal treatment was up to 37%, whereas that of untreated chitin was only 5%. XRD analysis revealed that the *d*-spacing and the crystallite size increased by supercritical water treatment, which indicates the swelling of chitin occurs in high-temperature and high-pressure water. The swelling of the chitin crystal structure improved enzymatic saccharification, allowing the enzymes to easily access and exert the catalytic action.

Keywords

Chitin, Enzymatic saccharification, Hydrothermal treatment, *N*-acetyl glucosamine

INTRODUCTION

Water near its critical point ($T_c = 374.3^\circ\text{C}$, $P_c = 22.1\text{ MPa}$) possesses properties very different from those of ambient liquid water. The dielectric constant is much lower, and the number and persistence of hydrogen bonds are both diminished. As a result, high-temperature water behaves like many organic solvents in that organic compounds enjoy complete miscibility with supercritical water. The ion product, or dissociation constant (K_w) for water as it approaches the critical point, is about 3 orders of magnitude higher than it is for ambient liquid water. Accordingly, in addition to supercritical water being an excellent solvent for organic compounds, it can also boast a higher H^+ and OH^- ion concentration than liquid water under certain conditions [1].

N,N'-diacetylchitobiose ((GlcNAc)₂) is a disaccharide of *N*-acetylglucosamine (GlcNAc). GlcNAc produced from crustacean chitin (α -chitin) possesses versatile functional properties as skin moisturizers, joint-pain relievers, and antitumoral and antimicrobial agents. (GlcNAc)₂ has potentially milder or other physiological activities compared to GlcNAc and is expected to be a source for oligosaccharides production. Although the market is rapidly expanding, the production of (GlcNAc)₂ and GlcNAc from crab shells takes a large number of processes and strong acid because of the hard crystallinity and insolubility of α -chitin. In light of the difficulties associated with traditional (GlcNAc)₂ and GlcNAc production processes, environmentally compatible and reproducible enzymatic saccharification alternatives are desired. If chitin could be completely degraded by enzymes, it would not be necessary to use deleterious substances or to produce excessive amounts of waste water, allowing the establishment of an environmentally conscious process. However, α -chitin is not soluble in water under

ambient conditions and their crystallinity is potentially too high to be degraded enzymatically. To solve these problems, pretreatment of α -chitin is widely considered to be important.

The aim of this study is the production of $(\text{GlcNAc})_2$ from chitin by a combination of and supercritical water pretreatment and enzymatic saccharification. There are some reports that sub- and supercritical water treatment on its own is not sufficient to obtain $(\text{GlcNAc})_2$ and GlcNAc from chitin because, under these conditions, they decompose at the same time as the chitin is hydrolyzed [2]. In this study, we used pretreatment of chitin in supercritical water for enzymatic saccharification and investigated conditions that promote enzymatic degradation without including decomposition of $(\text{GlcNAc})_2$ and GlcNAc.

MATERIALS and METHODS

A. Materials and enzymes

Crab chitin (Yaizu suisankagaku industry) was used for material. The shape of chitin is flake and its size is about 3 mm. For the enzymatic saccharification, crude enzyme from *Streptomyces griseus* (Eikon CHL from Rakuto kasei industrial) was used as chitinase. For saccharification each substrate, we used 90 U of enzyme. The enzyme produces $(\text{GlcNAc})_2$ as a major product from chitin. In this work, we mainly obtained $(\text{GlcNAc})_2$, which could be hydrolyzed to GlcNAc by other enzymes [1,3].

B. Supercritical water treatment

Supercritical water treatment for chitin was conducted in a SUS 316 tube reactor of 6 cm³ in volume. After chitin flakes and water (2/30 w/w) were loaded in the reactor, the reactor was submerged into a molten-salt bath (KNO_3 – NaNO_3) kept at 400. Figure 1 shows the internal temperature profile of the reactor at 400°C setting. In this paper, the reaction starting point was set at the moment when the reactor was submerged into the molten-salt bath; therefore, the reaction time includes the initial heating period. After a given reaction time, the reactor was taken out from the molten-salt bath and rapidly quenched in a water bath to cool down to room temperature. After cooling, the products were collected from the reactor and divided into the water-soluble and solid fractions (chitin) with a membrane filter (pore size: 0.20 μm , Millipore). After supercritical treatment, chitin was dried at 90°C for 24 h.

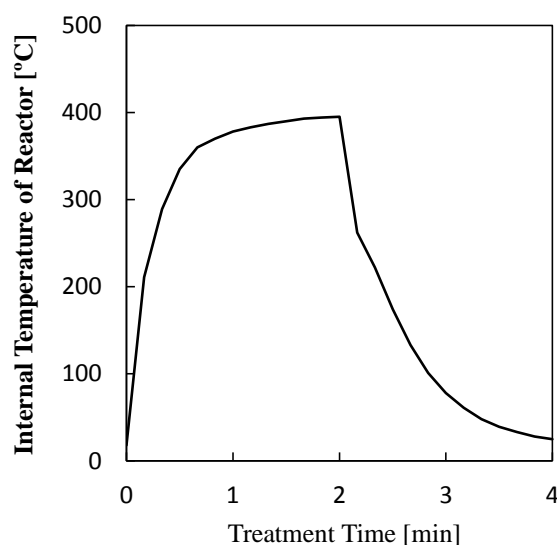


Figure1. Internal temperature profile of the reactor

C. Enzymatic saccharification of chitin

The enzymatic saccharification of chitin was conducted as follows. 20 mg of chitin (1% of final concentration) was mixed with 1.8 mL of 10 mmol/L phosphate buffer (pH 6.0) and 0.2 mL of 10 mg/mL enzyme diluted with 10 mmol/L phosphate buffer (0.1% of final concentration, about 100 U). The reaction mixture was shaken at 1400 rpm at 40 °C, and 0.4 mL of the mixture was harvested at the appropriate time. The harvested reaction solution was filtered (pore size 0.45 μm, ADVANTEC) after boiling for 10 min, and centrifuged.

D. High-performance liquid chromatography (HPLC)

The harvested reaction solution was filtered (pore size 0.45 μm, ADVANTEC) after boiling for 10 min, and centrifuged. The HPLC system consisted of a Model 300S ELSD detector (SoftA), and L-2000 system (Hitachi). Sugars were separated on a Shodex SUGAR KS-802 column (ϕ 0.8 × 30 cm) using ultrapure water (Millipore) as the mobile phase, at a flow rate of 0.6 mL/min at 60 °C. Yield was calculated from the area of the peak of the enzymatic reaction mixture and two standards of (GlcNAc)₂ and GlcNAc. The product yield was divided by the chitin concentration and reported as a percent.

E. Characterization of the chitin by X-ray diffraction (XRD)

Equatorial diffraction profiles were obtained with Cu-K α from a powder X-ray generator (Japan Electronic Organization Co. Ltd., JDX-3530) operating at 30 kV and 30 mA. The crystallinity index was calculated from normalized diffractograms according to Equation below. The intensities of the peaks at [110] lattice (I_{110} , at $2\theta = 20$ corresponding to the maximum intensity of chitin) and I_{am} at $2\theta = 16$ (amorphous diffraction) were used to calculate the crystallinity index [4].

$$\text{Crystallinity index (\%)} = (I_{110} - I_{am}) / I_{110} \times 100 \quad (1)$$

The d -spacing of the peaks at [110] lattice was calculated using the Bragg's equation

$$2d \sin\theta = \lambda \quad (2)$$

where d is the spacing between the planes in the lattice; θ is the Bragg angle; and λ is the X-ray wavelength.

The crystallite size of chitin at [110] lattice was calculated using the Scherrer equation

$$L = 0.9\lambda / (H \cos\theta) \quad (3)$$

where L is the crystallite size perpendicular to the plane; and H is the full-width at half-maximum in radians.

RESULTS and DISCUSSION

A. Effect of supercritical water treatment on enzymatic saccharification

Figure 2 shows the yield of (GlcNAc)₂ by enzymatic saccharification of untreated and supercritical water treated chitin at 400°C for 1 min. Some experiments were repeated two to three times to quantify run-to-run variability. The averages of these trials are included in the Figure 2 along with the standard deviations. For untreated chitin, the yield of (GlcNAc)₂ at 72 h was only 5%. The yield of (GlcNAc)₂ of supercritical water treated chitin reached 37%. From Figure 2, the enzymatic saccharification would be completed at a reaction time of 48 h. In addition, the yield of GlcNAc at 72h was only 1.7%, therefore, we will discuss on (GlcNAc)₂. We also analyzed the aqueous solution recovered after supercritical water treatment; however, (GlcNAc)₂ and GlcNAc were not detected.

Figure 3 shows the effect of supercritical water treatment time on the yield of (GlcNAc)₂ by enzymatic saccharification at a reaction time of 48 h. At 400°C, the yield of (GlcNAc)₂ increased with treatment time and reached 37% at 1 min. Then the yield of (GlcNAc)₂ decreased with treatment time and it became about 2% at 2 min.

In absence of water condition at 400°C and 1 min, namely thermal treatment, the chitin flaks changed to a black solid like char. The yield of (GlcNAc)₂ by enzymatic saccharification of the black solid was 0%, indicating that it was not saccharificated by enzyme. Therefore, we could confirm the necessity of water for pretreatment of chitin.

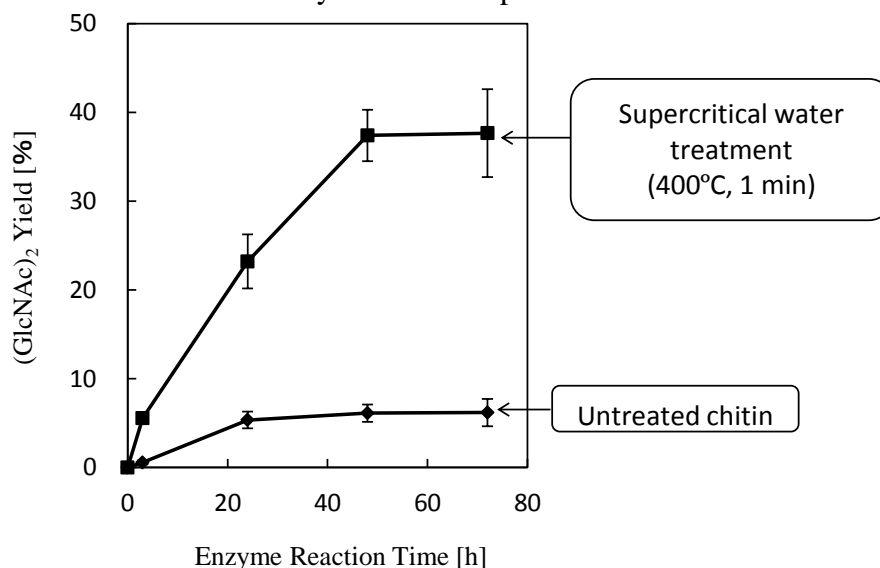


Figure 2. Reaction time profile of enzymatic saccharification of untreated chitin and supercritical water treated chitin at 400°C for 1 min

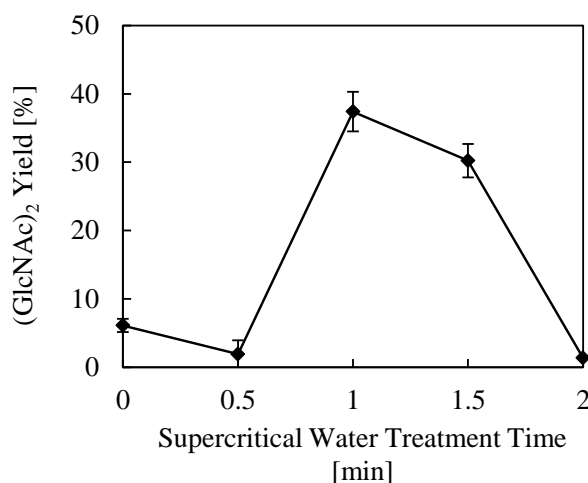


Figure 3. Effect of supercritical water treatment time at 400°C on enzymatic saccharification of chitin at an enzyme reaction time of 48 h

B. Properties of supercritical water treated chitin

The size of untreated chitin flakes is about 3 mm and it does not change so much until 1.5 min of supercritical water treatment at 400°C. However, the chitin flakes crumbled after 2 min of supercritical water treatment at 400°C and it became powder.

The results shown in Figure 4 and 5 are obtained by XRD analysis. Figure 4 shows the effect of supercritical water treatment temperature and time on the crystallinity index of chitin flakes. The crystallinity index slightly decreased until 1.5 min and then drastically decreased at 2 min.

Figure 5 shows the effect of the supercritical water treatment on the d -spacing and crystallite of chitin flakes. The d -spacing increased until 1.5 min, indicating that the lattice spacing became wider. Then the d -spacing slightly decreased at 2 min. On the other hand, the crystallite size increased with treatment time, indicating that the crystal grows by supercritical water treatment. Then the crystallite size slightly decreased at 2 min.

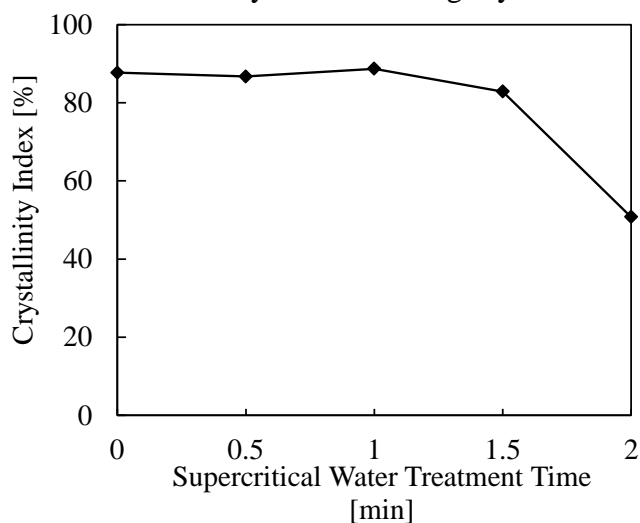


Figure 4. Effect of supercritical water treatment time at 400°C on crystallinity index of chitin

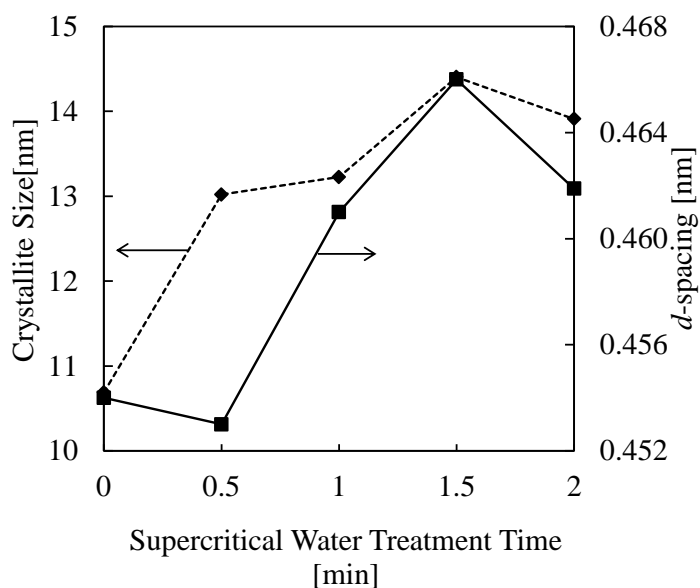


Figure 5. Effect of supercritical water treatment at 400°C on crystallite size and d -spacing of chitin

C. Effect of supercritical water treatment

In the literature, it is reported that the conversion of microcrystalline cellulose in supercritical condition as following steps (1) swelling, (2) dissolution, and (3) hydrolysis [5]. In this work, we used the batch type reactor and the treatment time reported includes heat-up time as shown in Figure 1. From Figure 3, the chitin is stable and does not change until 0.5 min at 400°C because the yield of $(\text{GlcNAc})_2$ was almost the same as untreated chitin. At from 1.0 to 1.5 min, the swelling of the chitin would mainly occur, which is consistent with the shape of the chitin flakes was kept. The swelling chitin in high-temperature high-pressure water was rapidly cooled down. Therefore, the crystallinity

index was kept; however, the *d*-spacing slightly increased by the swelling. The increase of *d*-spacing causes an increase of the crystallite size. After 2 min, the dissolution and the hydrolysis of the chitin occurred, which was indicated by that the crystallinity index, *d*-spacing, the crystallite size decreased suddenly as shown in Figure 4 and 5, and the shape of the chitin flakes was crumbled. We analyzed the solution recovered after 2 min of supercritical water treatment; however, (GlcNAc)₂ and GlcNAc were not detected, indicating that these compounds immediately decomposed during supercritical water treatment as reported in the literature [2]. The results show that it is important to control the optimum pretreatment condition for leading the swelling of the chitin during supercritical water treatment not dissolution and hydrolysis.

From our group's previous research, the crystallinity index was one of the important factors to promote the enzymatic saccharification of chitin [3]. In the previous research, we reported that the crystallinity index of chitin decreased by mechanochemical grinding with a ball mill and the enzymatic saccharification ratio increased with the decrease of the crystallinity index. However, supercritical water treated chitin of crystallinity index was not changed so much until 1.5 min (at 400 °C) as shown in Figure 4. On the other hand, the yield of (GlcNAc)₂ increased as shown in Figure 3. It is reported that the chitin pretreated by phosphoric acid or hydrochloric acid solution at ambient temperature showed high enzymatic saccharification ratio, whereas the crystallinity index of these chitins was not changed [6]. These results indicate that the decrease of the crystallinity index is not necessarily for the promotion of the enzymatic saccharification of chitin.

The reason of enhancement of enzymatic saccharification after supercritical water treatment will be discussed. The *d*-spacing of the chitin after supercritical water treatment became greater than untreated, indicating that hydrogen bonds between hydroxyl groups of chitin chains became weak. The increase of the *d*-spacing causes the increase of the crystallite size. The swelling of chitin during supercritical water treatment causes the increase of *d*-spacing and crystallite size. Therefore, the number of the hydroxyl groups which does not form hydrogen bonds increase. The free hydroxyl groups after supercritical water treatment would lead to more hydrophilic chitin than untreated one. The hydrophilic chitin would improve enzymatic saccharification, allowing the enzymes to easily access and exert the catalytic action.

REFERENCES

- [1] Osada, M., Miura, C., Nakagawa, Y. S., Kaihara, M., Nikaido, M., and Totani, K. (2012). Effect of sub- and supercritical water pretreatment on enzymatic degradation of chitin. *Carbohydrate Polymers*, 88, 308-312.
- [2] Sakanishi, K., Ikeyama, N., Sakaki, T., Shibata, M., and Miki, T. (1999). Comparison of the hydrothermal decomposition reactivities of the chitin and cellulose. *Industrial & Engineering Chemistry Research*, 38, 2177-2181.
- [3] Nakagawa, Y., Oyama, Y., Kon, N., Nikaido, M., Tanno, K., Kogawa, J., Inomata, S., Masui, A., Yamamura, A., Kawasuchi, M., Matahira, Y., and Totani, K. (2011). Development of innovative technologies to decrease the environmental burdens associated with using chitin as a biomass resource: Mechanochemical grinding and enzymatic degradation. *Carbohydrate Polymers*, 83, 1843-1849.
- [4] Lavall, R. L., Assis, O. B. G., and Campana-Filho, S. P. (2007). β -Chitin from the pens of *Loligo* sp.: Extraction and characterization. *Bioresource Technology*, 98, 24-65-2472.
- [5] Sasaki, M., Adschiri, T., Arai, K. (2004). Kinetics of Cellulose Conversion at 25 MPa in Sub- and Supercritical Water. *AIChE Journal*, 50, 192-202.
- [6] Ilankovan, P., Hein, S., Ng, C. H., Trung, T. S., & Stevens, W. F. (2006). Production of *N*-acetyl chitobiose from various chitin substrates using commercial enzyme. *Carbohydrate Polymers* 63, 245-250.

CHEMICAL COMPOSITION AND QUALITY OF CHITIN FROM WHITE SHRIMP AND BLACK TIGER SHRIMP

T.T. Khong^{1,2*}, H.D.T. Ngo², N.D. Ngo², T.S. Trang², K.M. Vårum¹

¹ Norwegian Biopolymer Laboratory (NOBIPOL), Department of Biotechnology, Norwegian University of Science and Technology (NTNU), 7491 Trondheim, Norway.

² Nha Trang University, Nha Trang, Vietnam
E-mail address: thang.khong@biotech.ntnu.no

ABSTRACT

The chemical composition of head and shell of white shrimp (WS) (*Penaeus vannamei*) and black tiger shrimp (BT) (*Penaeus monodon*) was analyzed. The results showed that the chemical composition of head and shell from the two shrimp species was very similar. However, there were large differences between head and shell. The protein content of head was 44.39 ± 0.50 and 48.56 ± 1.33 of the dry weight in WS and BT, respectively, which was ca. 50% higher than in the shell. The chitin content of shell was 27.37 ± 1.82 and 29.29 ± 1.78 of the dry weight in WS and BT, respectively, which was more than 2.5 times higher than in the head. The amino acid contents of the proteins were similar for both species, and for head and shell, and with a profile that was suitable as a source for fish feed. The differences in chemical composition of head and shell had consequences for optimal extraction conditions in order to isolate a pure and high molecular weight chitin. Demineralization and deproteinization conditions were optimized for head and shell, and chitin with relatively low ash (< 0.3%) and protein (<0.8%), relatively high molecular weight (1100-1300 kDa) and a high degree of acetylation (98%) were isolated.

Keywords chitin, shrimp by-product, chemical composition, demineralization, deproteinization

INTRODUCTION

Vietnam is a major producer of aquacultured shrimps in Asia, with annual production of 450 000 metric tons of the two major species white shrimp (WS) (*Penaeus vannamei*) and black tiger shrimp (BT) (*Penaeus monodon*) in 2010 [1]. In the shrimp processing lines, head and shell are manually peeled in two different operation units, meaning that they can be easily separated. The main components of shrimp by-product (head and shell) are minerals, proteins and chitin, a linear homopolymer of $\beta(1-4)$ -linked 2-acetamido-2-deoxy-D-glucose which could be deacetylated to different extents [2]. Today the main application of Vietnamese shrimp waste material, which constitutes about 30% of the total shrimp weight, is for chitin production. However, crustacean waste contains, in addition to chitin, proteins that have not so far been exploited.

Chemical isolation of chitin from crustacean shell involves demineralization and deproteinization. The acid treatment in the demineralization step is the main cause of the degradation of chitin, while the alkali treatment in the chemical deproteinization step is the main cause of chitin de-N-acetylation [3-5]. Thus, chitin extraction must be optimized to minimize the degradation of chitin, while at the same time bringing down the levels of other compounds.

In this study, we have characterized head and shell from the two major species of Vietnamese aquacultured shrimps, and determined the conditions for extraction of chitin of high-quality, which was characterized.

MATERIALS and METHODS

Materials

Shrimp by-products (separated head and shell) of BT were collected from factories in Camau province, while WS samples were from factories in Nha Trang city.

Dry weight, ash, chitin, protein and heavy metals content

The dry weight was determined after drying for 24 h at 105⁰C. The ash content was determined after heating to 550⁰C for 20 h. The chitin content was determined gravimetrically as previously described [5]. The protein content of raw material was determined by Biuret method. The heavy metals were analyzed using AOAC methods.

Amino acid composition

Samples were pulverized, and to 0.500 g (head) or 1.000 g (shell) of the sample 1 mL of 6M HCl was added and incubated at 105⁰C for 22 h. The hydrolysate was neutralized to pH of 6.5-7.5, filtered, adjusted to 10 mL with distilled water. This solution was, after appropriate dilution, subjected to amino acid composition analysis using the method of Lindroth and Mopper [6] as modified by Flynn [7]. Glycine and arginine co-eluted and appeared in the chromatogram as a single peak. Tryptophan was not detected because of destruction during the acid hydrolysis [8].

Chitin extraction

Demineralization was carried out in 0.25 M HCl solutions (shell) and 0.75 M HCl (head). Fresh frozen shell or head (150 g) were thawed at room temperature and extracted with HCl at ambient temperature for different time with a solid-to-solvent ratio of 1:3 (head) or 1:4 (shell). Following demineralization, the decalcified shell or head were washed using running tap water. Then dilute NaOH solutions, i.e. 2% for the shell and 3% for the head, were used for the deproteinization at 75⁰C with a solid-to-solvent ratio of 1:5. After decantation, the residues were washed using running tap water and finally dried. In the case a second demineralization step was needed (as judged from the ash content), the precipitate was isolated by decantation, and extraction with HCl solution was repeated using the same procedure as with the first demineralization. In order to determine conditions for obtaining chitin with less than 1% protein, the demineralized shell or head (from the optimized demineralization process, see above) were extracted with alkali (deproteinized) using the alkali extraction conditions as described above but for varying time intervals. The isolated chitin samples were analyzed for their protein contents.

Chitin characterization

The protein content of chitin was determined by Micro-Biuret method [9]. The intrinsic viscosity of chitin was determined based on the method described by Einbu [10]. The degree of acetylation (DA) was determined by proton NMR-spectroscopy [2].

Statistical analysis

The statistically differences between means ($p < 0.05$) were tested using one way analysis of variance (one way ANOVA) with the Pairwise Multiple Comparison Procedures (Tukey Test). Statistical analyses were performed using SigmaPlot for Windows version 11.0.

RESULTS and DISCUSSIONS

Chemical composition of raw materials

Table 1 shows the content of the three main constituents of WS and BT head and shell, i.e. ash, protein, and chitin. The ash content of head and shell varied from 25.61 % to 32.18 % of dry weight, and the ash content of shell of BT (32.18%) was significantly higher than the other samples (25.61 to 27.09%). However, BT head and shell have higher ash content when compared to those of WS, which is conceivable as the shell structure of BT is more rigid and thicker [11]. Ngoan [12] determined the relative proportions of head/shell of common shrimp species in Vietnam, and showed that the head constituted from 72.5% to 78.4% of by-product, and the shell with tail from 21.6 to 27.5%. In their study, the ash content of BT by-product was 21.9%, which is lower than our data. However, our data of ash content for BT were in the same range of those reported by Narayan [13] and Charoenvuttitham [14].

Table 1. Chemical compositions of shell and head of WS and BT as percentage of dry weight.

Composition	White shrimp (WS)		Black tiger shrimp (BT)	
	Shell (WS-S)	Head (WS-H)	Shell (BT-S)	Head (BT-H)
Ash	26.66 ± 1.81 ^a	25.61 ± 1.03 ^a	32.18 ± 1.13 ^b	27.09 ± 1.58 ^a
Protein	33.11 ± 1.56 ^a	44.39 ± 0.50 ^b	34.92 ± 0.59 ^a	48.56 ± 1.33 ^c
Chitin	27.37 ± 1.82 ^a	11.40 ± 1.83 ^b	29.29 ± 1.78 ^a	12.14 ± 0.94 ^b

* Values are given as means ± standard deviation (n = 3 – 6)

** Different superscript in the same row indicate significant differences (p < 0.05)

Protein is an important constituent of shrimp by-product. There is a large difference in the protein content of head and shell of both shrimp species, where head contain ca. 50% more in protein than shell. This is the first time that separate values of protein from Vietnamese shrimp shell and head are reported.

The chitin content in the shell of both shrimp species was more than two times higher than in the head. The chitin content of shell and head of WS were 27.37 and 11.40%, respectively, while those of BT were 29.29 (shell) and 12.14% (head).

Table 2. Amino acid composition of different parts of WS and BT (g/100 g amino acid)

Amino acid	White shrimp			Black tiger shrimp		
	Shell	Head	Flesh	Shell	Head	Flesh
Asp/Asn	10.5	10.8	9.9	10.2	10.1	9.8
Glu/Gln	12.9 ^a	14.3 ^b	15.1 ^c	12.3 ^d	13.4 ^e	14.4 ^b
His	2.1	2.0	1.9	2.2	2.5	1.7
Ser	5.3	4.1	4.1	6.2	4.2	4.0
Gly/Arg	24.2 ^a	20.6 ^b	25.6 ^a	27.8 ^c	23.3 ^d	28.6 ^c
Thr	4.9	4.6	4.1	5.0	4.6	4.0
Ala	9.7 ^a	7.9 ^b	6.9	9.6 ^a	7.5 ^c	6.1
Tyr	4.0 ^a	3.9 ^a	2.7 ^b	3.2 ^c	3.6 ^c	2.7 ^b
Met	1.7 ^a	2.4 ^b	2.5	1.5 ^c	2.3 ^b	2.5
Val	4.6	4.6	3.2	4.1	4.5	3.2
Phe	5.4	4.9	3.8	5.2	5.0	3.7
Ile	3.1	3.8	3.1	2.5	3.7	3.0
Leu	5.7 ^a	8.5 ^b	7.1	4.8 ^c	6.7 ^a	7.2
Lys	5.9 ^a	7.7 ^b	10.0 ^c	5.4 ^a	8.4 ^d	9.2 ^e

* Values are the means of three determinations.

** Different superscript in the same row indicate significant differences (p < 0.05)

Amino acid composition

In Table 2 was shown the 14 amino acids of flesh, shell and head of the two shrimp species, showing remarkably similar in the amino acid compositions in flesh, shell and head, and also in the two shrimp species. During acid hydrolysis of the proteins, asparagine and glutamine are converted to aspartic acid and glutamic acid, respectively. Glycine/arginine, glutamic acid/glutamine, aspartic acid/asparagine, and alanine are the dominant amino acid and accounted for more than 50% of the total amino acid content. Our data on amino acid content are in good agreement with those reported by Ngoan [12], Narayan [13] for BT. We also calculated the chemical score of amino acid from shrimp waste with reference protein required for common carp, as previously reported by Narayan [13], showing that chemical scores for all essential amino acid, except methionine, were

higher than those in the reference protein. Thus, the amino acid compositions of shrimp by-products meet the requirements of feed for fish.

Heavy metals

The content of selected heavy metals of the shell and head of both shrimp species are given in Table 3. Generally, the contents were low, and contents of As, Cd, Hg, and Se were lower than the limit of detection. The heavy metals in the head of both shrimp species were higher than that in the shell. Stanley and Wilt (quoted by Heu [15]) stated the heavy metal safety values to be 1.5-3.5 ppm for cadmium, 42-173 ppm for copper, 2.0 ppm for lead, 1000-2000 ppm for zinc, and 0.2 ppm for mercury. Thus, the by-product of BT and WS are safe to be used for feed production with respect to heavy metals.

Chitin extraction and characterization

Demineralization. The acid treatment solubilizes the inorganic carbonates (mainly CaCO_3) in the by-product. This process is often done by mineral acid such as hydrochloric acid, and it is highly efficient. The concentration of HCl ranges from 0.25 to 2 M, and is performed from 4 to 100^oC for 1-48 h [5, 16].

The demineralization step is crucial to preserve the chain length of the chitin molecules [5]. Therefore, to minimize the degradation of chitin during demineralization, low concentration of HCl and low temperature are beneficial. Percot et al. [16] presented examples of demineralization using 0.25 M HCl at ambient temperature within 15 minutes with materials that were carefully prepared (e.g. cryo-milling to obtain small particle size). Rodde et al. [5] used cold 0.25 M HCl for demineralization of northern shrimp with short extraction time (5 and 30 minutes). However, no data on the ash content of the chitin were given. In both these reports [5, 16], high molecular weight chitin were isolated.

Table 3. Heavy metals of the head and shell of WS and BT (mg/kg)

	White shrimp		Black tiger shrimp	
	Shell (WS-S)	Head (WS-H)	Shell (BT-S)	Head (BT-H)
As	nd, LOD = 0.01	0.16	nd, LOD = 0.01	0.16
Cd	nd, LOD = 0.005	0.0062	0.0063	0.031
Pb	0.034	0.033	0.042	0.04
Cu	18.12	20.71	20.8	35.66
Zn	11.08	17.48	12.72	23.07
Hg	nd, LOD = 0.01	nd, LOD = 0.01	nd, LOD = 0.01	nd, LOD = 0.01
Fe	15.67	24.6	28.13	40.92
Se	nd, LOD = 0.01	nd, LOD = 0.01	nd, LOD = 0.01	nd, LOD = 0.01

* nd: not detected, LOD: Limit of detection

Based on the previously reported studies and preliminary experiments with the Vietnamese raw material, we chose 0.25 M (shell) and 0.75 M HCl (head) at ambient temperature, and the demineralization of shrimp shell or head was followed as a function of time. In Figure 1 is shown the ash content of the isolated chitin from shell of the two species. For WS shell, it is clearly seen that the demineralization process was quite effective so that the ash content of the chitin was below 3% after 3h, then slowly decreasing to about 1.5% after 24h. For BT shell, the demineralization process was much slower compared to WS shell (Figure 1, right). The ash content of the chitin was only reduced to 7% and 5% after 7h and 24h acid treatment, respectively. This is most probably due to difference in the thickness of the shell, as black tiger shrimp is a larger species than white shrimp. However, differences in the organization of the biomaterial such as chitin-protein interactions (covalent and non-covalent) are also possible.

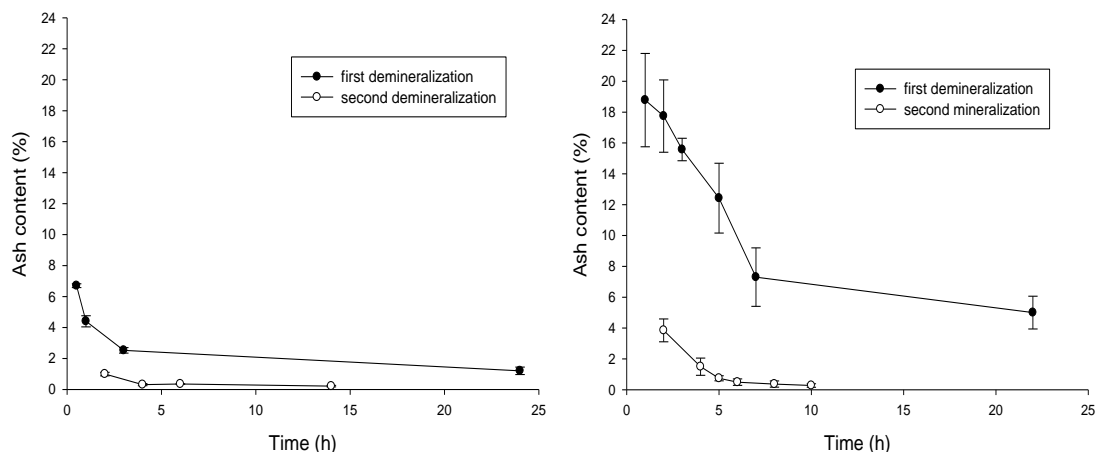


Figure 1. Effect of time of acid treatment on ash content of chitin from WS (left) and BT shell (right)

The relatively high ash content of the chitin after the first acid treatment (1.5% and 5% after 24h for WS shell and BT shell, respectively) motivated to a second demineralization step (Figure 1). This second acid treatment reduced the ash content to less than 0.3% after 4 and 10h for WS and BT, respectively. The acid treatment time in this study was longer than previously reported [16] which is most probably due to the smaller particle size (<80 μm). The demineralization condition for WS shell which is required to obtain chitin with a low ash content is less severe than for BT shell, which can be attributed to the thicker and more rigid shell structure of black tiger species.

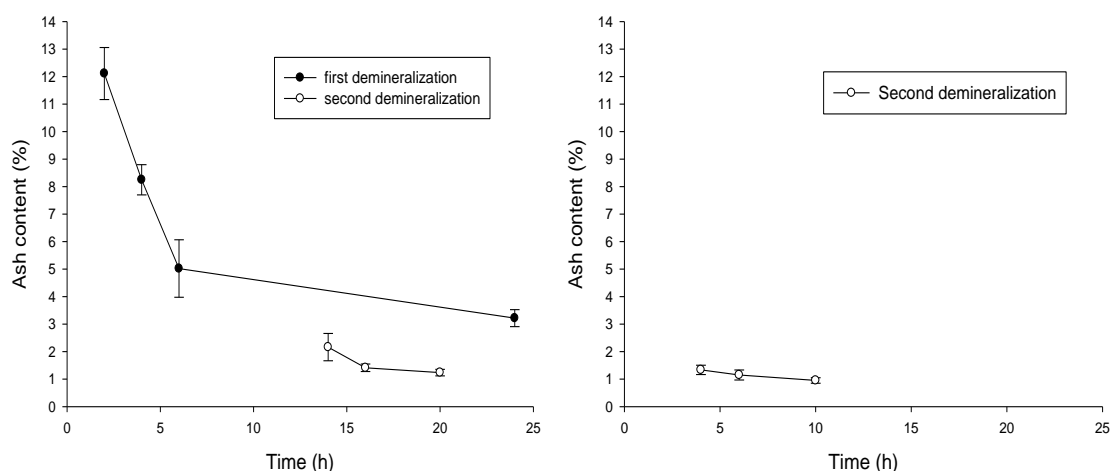


Figure 2. Effect of time of acid treatment on ash content of chitin from WS (left) and BT head (right)

Next, we determined the demineralization conditions with shrimp head as raw material. It was difficult to reduce the ash content of the isolated chitin below 1% when using 0.75 M HCl in two successive treatments. As shown in Figure 2 (left), the chitin from WS head still had an ash content of over 3% after 24h treatment. During the second demineralization, the ash content of the chitin from WS head after 20h still was at about 1% (Figure 2, left). The same trend was observed for BT head, the chitin ash content was only reduced to about 1% after 10h in the second demineralization step (Figure 2, right).

Table 4 shows the intrinsic viscosities and viscosity-average molecular weights of the isolated chitins. The WS shell chitin exhibited the highest intrinsic viscosities, 1479, 1406, and 1291 mL/g after treatment of 4, 6, and 15h in the second demineralization step, respectively. The BT shell chitin had similar intrinsic viscosities, from 1292 to 1321 mL/g.

These values are somewhat higher as compared to the chitins isolated from northern shrimp of 1150-1250 mL/g [5]. Both chitin from WS head and BT head exhibited slightly lower intrinsic viscosities than those from the shell of 1160 and 1219 mL/g, respectively. The reason for this is probably the higher concentration of the acid and longer exposure time.

Deproteinization. The deproteinization was carried out using 2% NaOH for shell and 3% NaOH for head at 75^oC for increasing time intervals. Table 4 shows the protein content and degree of acetylation (DA) of the isolated chitins. For shrimp shell, the results show that the alkali treatment for 10h was sufficient to reduce the protein level to less than 1%. For shrimp head, longer treatment time with NaOH was necessary to reduce the protein content of the chitin to below 1%, as expected from a raw material containing higher protein content.

Table 4. Characterization of the isolated chitins

Chitin from	1st demineralization (h)	2nd demineralization (h)	Viscosity (mL/g)	Viscosity-average MW (kDa)*	Deproteinization time (h)	Protein (%)	DA
WS-S	3	4	1479 ± 20	1356			
	3	6	1406 ± 67	1259			
	3	15	1291	1110	8	1.11 ± 0.06	
					12	0.83 ± 0.02	0.982
				15	0.71 ± 0.03	0.988	
BT-S	7	4	1292 ± 12	1112			
	7	6	1321 ± 31	1149			
	7	8	1307 ± 41	1131	8	1.17 ± 0.05	
					10	0.52 ± 0.13	0.981
				12	0.38 ± 0.03	0.971	
WS-H	8	16	1160 ± 11	949	9	1.23 ± 0.17	
					15	0.87 ± 0.17	0.962
BT-H	15	6	1219	1021	8	1.12 ± 0.09	0.973
					12	1.16 ± 0.18	0.968

* calculated using the Mark-Houwink-Sakurada (MHS) equation with K=0.10, a=0.68 [10]

During the alkali treatment in the deproteinization process, deacetylation will occur, and the rate of this deacetylation reaction will increase strongly with increasing alkali concentration and temperature [4]. As shown in the table 4, the degrees of acetylation of the isolated chitins were high, 96 - 99%. The highly acetylated chitins isolated from Vietnamese raw materials using the conditions described herein are very well suited as raw material for production of N-acetyl glucosamine in high yield [2].

CONCLUSIONS

There are large differences in protein and chitin content between the head and the shell with ca. 50% higher protein content in the head, and chitin contents in the shell are more than two times higher than in the head. Therefore, the head is suitable as raw material for protein, while the shell is more suitable for chitin production. The amino acid compositions of the proteins make them very well suited as fish feed. Their relatively low content of heavy metals also contributes to a safe application as feed ingredients. The difference in chemical composition of head and shell has consequences for their extraction conditions to obtain chitins of reasonable molecular weight and purity.

ACKNOWLEDGEMENTS

This research was financially supported by the SRV 2701 Project, Improving the teaching and researching capacity of Nha Trang University, funded by the Norwegian Royal Government. Ann-Sissel Teialeret Ulset and Tom Hallvard Jakobsen (NTNU) are acknowledged for performing the amino acid analysis.

REFERENCES

- [1] Industry, M.o.T.a. **Statistics on cultured shrimp production in Vietnam by provinces.** 2012 [cited 2012 September 14]; Available from: <http://ttm.vecita.gov.vn/dstk.aspx?NewID=181E&CateID=95>.
- [2] Einbu, A. and K.M. Varum (2008). **Characterization of chitin and its hydrolysis to GlcNAc and GlcN.** *Biomacromolecules.* **9**(7): p. 1870-1875.
- [3] Einbu, A. and K.M. Varum (2007). **Depolymerization and de-N-acetylation of chitin oligomers in hydrochloric acid.** *Biomacromolecules.* **8**(1): p. 309-314.
- [4] Khong, T.T., F.L. Aachmann, and K.M. Varum (2012). **Kinetics of de-N-acetylation of the chitin disaccharide in aqueous sodium hydroxide solution.** *Carbohydrate Research.* **352**: p. 82-87.
- [5] Rodde, R.H., A. Einbu, and K.M. Varum (2008). **A seasonal study of the chemical composition and chitin quality of shrimp shells obtained from northern shrimp (*Pandalus borealis*).** *Carbohydrate Polymers.* **71**(3): p. 388-393.
- [6] Lindroth, P. and K. Mopper (1979). **High-Performance Liquid-Chromatographic Determination of Subpicomole Amounts of Amino-Acids by Precolumn Fluorescence Derivatization with Ortho-Phthaldialdehyde.** *Analytical Chemistry.* **51**(11): p. 1667-1674.
- [7] Flynn, K.J. (1988). **Some Practical Aspects of Measurements of Dissolved Free Amino Acids in Natural Waters and Within Microalgae by the Use of HPLC.** *Chemistry and Ecology.* **3**(4): p. 269-293.
- [8] Bueno-Solano, C., J. Lopez-Cervantes, O.N. Campas-Baypoli, et al. (2009). **Chemical and biological characteristics of protein hydrolysates from fermented shrimp by-products.** *Food Chemistry.* **112**(3): p. 671-675.
- [9] Van Toan, N., C.H. Ng, K.N. Aye, et al. (2006). **Production of high-quality chitin and chitosan from preconditioned shrimp shells.** *Journal of Chemical Technology and Biotechnology.* **81**(7): p. 1113-1118.
- [10] Einbu, A., S.N. Naess, A. Elgsaeter, et al. (2004). **Solution properties of chitin in alkali.** *Biomacromolecules.* **5**(5): p. 2048-2054.
- [11] Chen, P.Y., A.Y.M. Lin, J. McKittrick, et al. (2008). **Structure and mechanical properties of crab exoskeletons.** *Acta Biomaterialia.* **4**(3): p. 587-596.
- [12] Ngoan, L.D., J.E. Lindberg, B. Ogle, et al. (2000). **Anatomical proportions and chemical and amino acid composition of common shrimp species in Central Vietnam.** *Asian-Australasian Journal of Animal Sciences.* **13**(10): p. 1422-1428.
- [13] Narayan, B., S.P. Velappan, S.P. Zituji, et al. (2010). **Yield and chemical composition of fractions from fermented shrimp biowaste.** *Waste Management & Research.* **28**(1): p. 64-70.
- [14] Charoenvuttitham, P., J. Shi, and G.S. Mittal (2006). **Chitin extraction from black tiger shrimp (*Penaeus monodon*) waste using organic acids.** *Separation Science and Technology.* **41**(6): p. 1135-1153.
- [15] Heu, M.S., J.S. Kim, and F. Shahidi (2003). **Components and nutritional quality of shrimp processing by-products.** *Food Chemistry.* **82**(2): p. 235-242.
- [16] Percot, A., C. Viton, and A. Domard (2003). **Optimization of chitin extraction from shrimp shells.** *Biomacromolecules.* **4**(1): p. 12-8.

NARROW POLYDISPERSITY OF CHITOSAN BY SUPERCRITICAL CARBON DIOXIDE WITH ACETIC ACID AQUEOUS SOLUTION

Min-Lang Tsai*, Wang-Kun Lee

Department of Food Science, National Taiwan Ocean University, 2 Pei-Ning Road, Keelung 20224, Taiwan, ROC.

*E-mail address: tml@mail.ntou.edu.tw

ABSTRACT

The aim of this study is to fractionate lower molecular weight and polydispersity chitosan via supercritical carbon dioxide with 1% acetic acid solution as a cosolvent. The chitosan, with a degree of deacetylation of 62.5%, molecular weight of 508 kDa and polydispersity of 6.35, was fractionated with supercritical carbon dioxide + 1% acetic acid solution at 35, 45, 50°C and 20, 30, 40 MPa for 2 h. The yield, degree of deacetylation, molecular weight and polydispersity of the fractionated chitosan were then determined. Since hardly any chitosan could be extracted with supercritical carbon dioxide, a 1% acetic acid solution was added as a cosolvent to achieve chitosan extraction of 1.9-3.1%. This method could extract a lower molecular weight (336-483 kDa) and polydispersity (1.93-2.49) chitosan fraction, and also increased the degree of deacetylation (72.0-77.1%). Thereby, a new preliminary method for fractionating chitosan by supercritical carbon dioxide + 1% acetic acid solution was established.

Keywords

Chitosan, Supercritical carbon dioxide, Degree of deacetylation, Molecular weight, Polydispersity, Cosolvent

INTRODUCTION

Chitosan is a high molecular weight polysaccharide composed of glucosamine and *N*-acetyl-glucosamine. The physicochemical properties of chitosan depend on intrinsic factors such as the degree of deacetylation (DD), the distribution of the acetyl group, molecular weight (MW), polydispersity, etc [1,2]. The DD, MW and polydispersity of chitosan affect the rheological properties, chain flexibility, mechanical properties and pore size of membranes and microcapsules, water-holding capacity of cosmetics, immunoadjuvant, antimicrobial activity, enzyme-binding ability, metal binding, etc [2,3].

Supercritical carbon dioxide (SC-CO₂) is an environmentally friendly solvent and has been widely applied in many fields. SC-CO₂ is non-polar and unsuitable for the separation of carbohydrates; however, using a polar organic cosolvent can considerably increase the solubility of carbohydrates in SC-CO₂ [4]. The solubility of chitosan in SC-CO₂ is nearly zero [5]. Therefore, in order to improve the solubility of chitosan in SC-CO₂, the addition of a cosolvent is necessary. Reverchon and Antonacci [5] reported that chitosan in 1% acetic acid aqueous solution had been successfully micronized using an SC-CO₂ atomization system. Some process parameters such as the precipitation temperature and chitosan concentration had been explored to evaluate their influence on the morphology and the size of precipitated particles. The diameters of 99% particles were 0.1-1.5 μm when precipitated from solutions with chitosan concentrations ranging between 1 and 10 mg/ml.

In general, methods such as gel permeation chromatography, size exclusion chromatography and membrane separation are used for molecular weight fraction of polysaccharides. However, these methods have shortcomings; these include: working with

a small amount, low concentration, a large amount of waste, the tendency of the membrane to become easily plugged, etc. Fractioning with solubility of polysaccharides may be a better method due to the relative ease of operation and mass production.

In this paper, SC-CO₂ was used concurrently with the cosolvent to control the treatment temperature and pressure when fractioning chitosan. Then, the DD, MW and the polydispersity of the fractionated chitosan were determined. An attempt was made to establish a new fraction method to fractionate chitosan by SC-CO₂ with a 1% acetic acid solution cosolvent.

MATERIALS and METHODS

Preparation of chitosan

β -Chitin was prepared from squid pens (*Illex argentinus*). The squid pens were ground to a 40–60 mesh size. Each 100 g batch of powder was immersed overnight in 500 ml of 1 M of hydrochloric acid solution. The sample was washed to neutrality and drained. Then, the sample was soaked overnight in 500 ml of 2 M of sodium hydroxide at an ambient temperature, washed and drained. Subsequently, the sample was reacted in 500 ml of 2 M of sodium hydroxide solution at 100°C for 4 h, washed to neutrality and dried.

β -Chitin was added to a 50% (w/w) sodium hydroxide solution at a ratio of 1 (g solid):10 (ml solution). The deacetylation reaction took place at 100°C for 1 h. Then the chitosan was collected and washed to neutrality and freeze-dried [6].

Measurement DD of chitosan

The DDs of the chitosans were determined with infrared spectrometry [7]. Chitosan powder was sieved through a 200 mesh and then mixed with KBr (1:100), dried at 60°C for 3 days to prevent interference of the -OH group in FTIR measurements, and pressed into a pellet. The absorbance of amide 1 (1655 cm⁻¹) and the hydroxyl band (3450 cm⁻¹) were measured using a Bio-Rad FTS-155 infrared spectrophotometer (Hercules, CA, USA). The band of the hydroxyl group at 3450 cm⁻¹ was used as an internal standard to correct for disc thickness and for differences in chitosan concentration when making the KBr disc. The percentage of the amine group's acetylation in a sample was given by $(A_{1655}/A_{3450}) \times 115$. Here, A_{1655} and A_{3450} were the absorbances at 1655 cm⁻¹ and 3450 cm⁻¹, respectively. Every sample measurement was repeated three times.

Measurement MW and polydispersity of chitosan

The MWs and PDs of chitosans were determined with the size exclusion high-performance liquid chromatography (SE-HPLC) [8]. A column (7.8 mm x 30 cm) packed with TSK gel G4000 PW_{XL} and G5000 PW_{XL} (Tosoh Co. Ltd, Japan) was used. The mobile phase consisted of 0.2 M of acetic acid/0.1 M sodium acetate and 0.008 M of sodium azide. A sample concentration of 0.1 % (w/v) was loaded and eluted with a flow rate of 0.6 ml/min by a pump (Shimadzu LC-10T AP, Kyoto, Japan). The elute peak was detected by a RI detector (Shodex RI-71, Tokyo, Japan). The data were analyzed by Chem-Lab software (SISC 3.0, Scientific Information Service, Taipei, Taiwan). Pullulan standards with different MWs were used as markers. The MWs and polydispersities of the samples were calculated from the pullulan calibration curve with Chem-Lab software

Supercritical carbon dioxide fraction

The fractional procedure was performed in a batch manner. At the beginning, 1 g of chitosan was loaded into the extraction vessel of supercritical fluid extractor (Figure 1) (Supercritical Fluid Technologies, Inc., SFT-100, Newark, Delaware, USA). The 30 ml

pure water or 1% acetic acid solution as cosolvent was added into the extraction vessel, respectively. Then chitosan was treated with SC-CO₂ (Ching Feng Heng Inc., Taipei, Taiwan) which operative temperature and pressure were controlled to 35, 45, 50°C and 20, 30, 40 MPa, respectively. The flow rate of SC-CO₂ was 8 ml/min. The treatment time was 2 h, starting from the time the experimental conditions reached the setting temperature and pressure, respectively. After depressurization, the chitosan dissolved fraction was collected in a collection vessel. Then the sample was freeze-dried and the DD and MW were determined.

Calculation of extraction ratio

The extraction ratio of treated chitosan from the extraction vessel to the collection vessel was calculated as follows:

$$\text{Extraction ratio (\%)} = [(B - A)/C] \times 100\%$$

A: the weight of the collection vessel

B: the weight of the collection vessel and the freeze-dried chitosan

C: the weight of the loaded chitosan

Statistical analysis

Analysis of variance was used to determine any significant difference ($p < 0.05$). Duncan's new Multiple Range Test was used to further test their differences by the SAS system for windows Version 8.1 (SAS Institute Inc., Cary, Ca., USA, 1988).

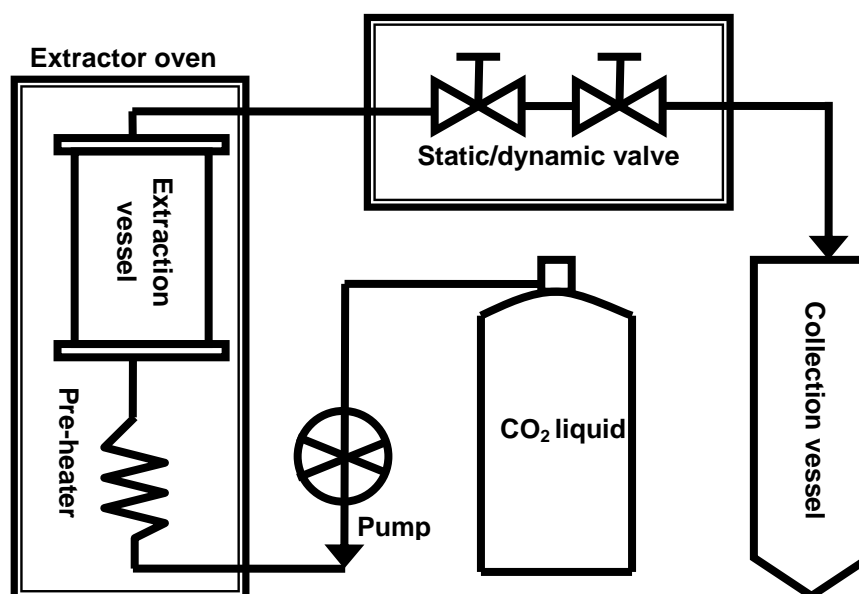


Figure 1. Flow diagram of the extraction process. The volumes of the extraction and collection vessels are 100 and 30 mL, respectively

RESULTS and DISCUSSION

Chitosan was treated with SC-CO₂ at 40 MPa, 45°C for 2 h and the substance was scarcely fractionated and collated in the collection vessel (Figure 2A). The solubility of chitosan in SC-CO₂ was close to zero [5]. However, 1% acetic acid solution as a cosolvent was added into this system and treated under the same conditions. About 10 ml of chitosan solution was fractionated into the collection vessel (Figure 2B). It is clear that chitosan can be dissolved in SC-CO₂ + 1% acetic acid solution. Subsequently, the chitosan solution was freeze-dried and became a sponge-like form (Figure 2C). The difference in appearance between the freeze-dried fractionated chitosan and the untreated chitosan was insignificant.

The 62.5% DD chitosan was treated with SC-CO₂ + 1% acetic acid solution at 20, 30 and 40 MPa, 35, 45 and 50°C for 2 h; then the samples were collected and freeze-dried. The extraction ratio of treated chitosan from the extraction vessel to the collection vessel was calculated (Table 1). The result shows that the extraction ratios were 1.9-3.1% at various operation conditions. These data were insignificantly different. However, the result shows that the highest extraction ratio was 3.1% at 20 MPa-45°C, 20 MPa-50°C and 40 MPa-35°C, respectively.

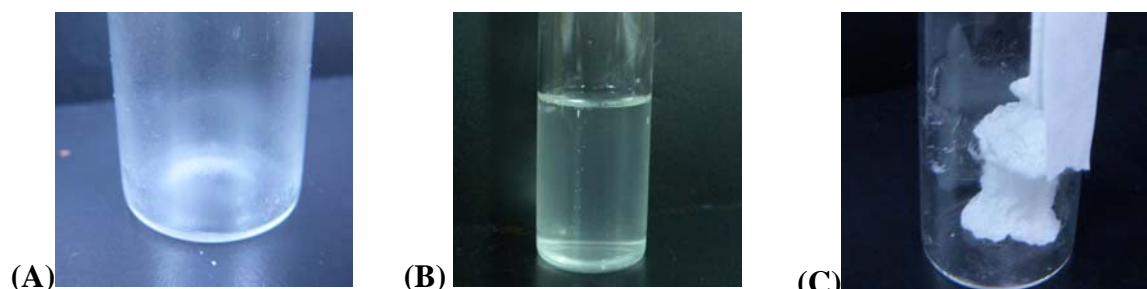


Figure 2. Photos of chitosan in collection vessel that was treated with SC-CO₂ at 40 MPa, 45°C for 2 h. (A) without cosolvent; (B) with 1% acetic acid solution; (C) with 1% acetic acid solution followed by freeze-dried.

Table 1. Effect of temperature (T) and pressure (P) of SC-CO₂ processing with 1% acetic acid cosolvent on the yield, degree of deacetylation (DD), molecular weight (MW) and polydispersity (PD) of fractionated chitosan.

P (MPa)	T (°C)	Yield (%)	DD (%)	MW (kDa)	PD
---	---	---	62.5±3.3a	508±18a	6.35±0.64a
20	35	2.9±0.8a	73.4±2.4bc	443±59abc	2.37±0.31b
	45	3.1±1.0a	72.8±2.1bc	363±56bc	2.13±0.54b
	50	3.1±1.5a	74.7±1.8bc	399±95abc	2.02±0.19b
30	35	2.8±0.7a	77.1±2.2c	414±68abc	2.24±0.34b
	45	2.9±0.7a	72.0±3.3b	412±63abc	2.49±0.82b
	50	2.9±1.5a	75.9±2.6bc	415±89abc	2.16±0.06b
40	35	3.1±0.3a	75.0±3.0bc	336±9c	2.04±0.55b
	45	2.6±0.6a	76.1±2.1bc	483±29ab	2.32±0.85b
	50	1.9±1.1a	74.7±3.0bc	435±125abc	1.93±0.32b

* Untreated chitosan. Values are mean±S.D (n=3). a-c Different letters in the same column indicate significant differences ($p < 0.05$) between samples.

Controlling the operation conditions (pressure and temperature) and the density of SC-CO₂ could affect the extraction ratio of the solute. However, the effect of these factors on the extraction ratio of chitosan in SC-CO₂ + 1% acetic acid solution was insignificantly different. This may be due to the soluble behavior of chitosan in this system being predominated by the cosolvent, leading to pressure, temperature and density insignificantly affecting the extraction ratio.

Table 1 also shows the DD of chitosan, both untreated and treated with SC-CO₂ + 1% acetic acid solution. The result reveals that the DD of untreated chitosan was 62.5±3.3%; however, the DDs of all fractionated chitosans were significantly higher than untreated chitosan. The DDs of fractionated chitosans were between 72.0±3.3% to 77.1±2.2%. The highest DD of chitosan was treated at 30 MPa and 35°C.

The solubility of the solvent system (SC-CO₂ + 1% acetic acid solution) was not very good for 62.5% DD chitosan. The higher DD chitosan fraction was more easily solved and extracted under supercritical processing. As a result, fractionated chitosans had higher DD than untreated chitosan did. Additionally, the fact that modulating the supercritical conditions, including pressure, temperature and density, insignificantly affects the DD of

chitosan; this may be due to the extraction ratio being too low and the soluble behavior being predominated by 1% acetic acid solution.

Figure 3 shows the elution patterns of size-exclusion high-performance liquid chromatography of chitosans that were untreated and treated with supercritical CO₂ + 1% acetic acid solution at 30 MPa and 35°C. It indicated that the MW and polydispersity of fractionated chitosan were smaller than those of untreated chitosan.

The MWs and polydispersities of fractionated chitosan by SC-CO₂ + 1% acetic acid solution at various conditions are also listed in Table 1. The result shows that the MW and polydispersity of untreated chitosan were 508±18 kDa and 6.35±0.64, respectively. The MWs and polydispersities of all fractionated chitosans by SC-CO₂ + 1% acetic acid solution were smaller than those of untreated chitosan. The values of MWs and polydispersities were 336-483 kDa and 1.93-2.49, respectively. In general, low MW polymer fraction is more easily dissolved in the dissolution process. The solvent of SC-CO₂ + 1% acetic acid solution for chitosan was not very good, and the soluble chitosan fraction was lower MW fraction consequentially. MWs and polydispersities of fractionated chitosans were smaller than those of untreated chitosan.

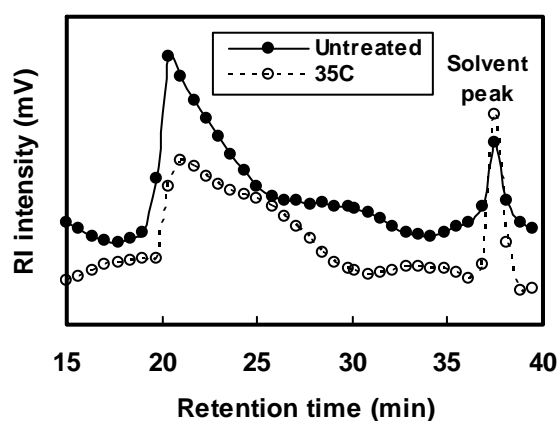


Figure 3. Elution patterns of HP-SEC of chitosan treated with SC-CO₂ + 0.1% acetic acid solution at 30 MPa and 35°C for 2 h.

CONCLUSIONS

Chitosan was scarcely fractionated with supercritical carbon dioxide (SC-CO₂) at 35, 45, 50°C and 20, 30, 40 MPa for 2 h. However, adding a cosolvent such as 1% acetic acid solution could lead to the extraction of 1.9-3.1% chitosan. The MWs and polydispersities of fractionated chitosans were decreased from 508 kDa to 336-483 kDa and 6.35 to 1.93-2.49, respectively. However, the DDs of fractionated chitosans were increased from 62.5% to 72.0-77.1%. This SC-CO₂ method with 1% acetic acid solution cosolvent could fractionate lower MW and polydispersity chitosan fraction but cause DD to increase. The change of DD, MW and polydispersity of fractionated chitosan due to higher DD and lower MW chitosan fraction was more easily dissolved and fractionated. The effects of temperature and pressure of SC-CO₂ on the extraction ratio of chitosan were insignificant. The result fell short of our expectations. This may be due to the low extraction ratio and the soluble behavior of chitosan in this system being predominated by the cosolvent (1% acetic acid solution).

ACKNOWLEDGEMENTS

The authors wish to express their appreciation for the financial support from National Science Council, ROC (NSC 100-2313-B-019-004-MY3).

REFERENCES

- [1] Chen, R. H., Huang, J. R., Tsai, M. L., Tseng, L. Z., Hsu, C. H. (2011). Differences in degradation kinetics for sonolysis, microfluidization and shearing treatments of chitosan. *Polym. Int.*, 60, 897-902.
- [2] Moura, C. M. d., Moura, J. M. d., Soares, N. M., Pinto, L. A. d. A. (2011). Evaluation of molar weight and deacetylation degree of chitosan during chitin deacetylation reaction: Used to produce biofilm. *Chem. Eng. Process.*, 50, 351-355.
- [3] Tsaih, M. L., Chen, R. H. (2003). The effect of reaction time and temperature during heterogenous alkali deacetylation on degree of deacetylation and molecular weight of resulted chitosan. *J. Appl. Polym. Sci.*, 88, 2917-2923.
- [4] Montañés, F., Fornari, T., Stateva, R. P., Olano, A., Ibáñez, E. (2009). Solubility of carbohydrates in supercritical carbon dioxide with (ethanol + water) cosolvent. *J. Supercrit. Fluid*, 49, 16-22.
- [5] Reverchon, E., Antonacci, A. (2006). Chitosan microparticles production by supercritical fluid processing. *Ind. Eng. Chem. Res.*, 45, 5722-5728.
- [6] Tsai, M. L., Chang, H. W., Yu, H. C., Lin, Y. S., Tsai, Y. D. (2011). Effect of chitosan characteristics and solution conditions on gelation temperatures of chitosan/2-glycerophosphate/nanosilver hydrogels. *Carbohydr. Polym.*, 84, 1337-1343.
- [7] Baxter, A., Dillon, M., Taylor, K. D. A., Roberts, G. A. F. (1992). Improved method for i.r. determination of the degree of N-acetylation of chitosan. *Int. J. Biol. Macromol.*, 14, 166-169.
- [8] Tsai, M. L., Bai, S. W., Chen, R. H. (2008). Cavitation effects versus stretch effects resulted in different size and polydispersity of ionotropic gelation chitosan-sodium tripolyphosphate nanoparticle. *Carbohydr. Polym.*, 71, 448-457.

MORPHOLOGICAL CHARACTERIZATION OF CHITIN EXTRACTION

**Anna Sylvia R. R. Cavalcanti¹, Marcus Vinicius L. Fook¹,
Gloria T. Furtado¹, Hugo M. Lisboa¹**

¹*CertBio, Unidade Acadêmica de Engenharia De Materiais, Universidade Federal Campina Grande, Campina Grande, PB, Brasil
(e-mail: cavalcantiannas@gmail.com)*

ABSTRACT

In the present study, scanning electron microscopy (SEM) was used to monitor the extraction of chitin from shrimp shell. The aim of the work is to study the morphology and the macromolecular arrangement of each component on the shell. Using a SEM device that allows non-destructive characterization of the samples, tests were made to shrimp shell from the specie *Litopenaeus vannamei* Boone as received, after demineralization and after deproteinization. It is further considered that morphological study of shrimp shell can provide important data for production of biocompatible composites using biomineralization techniques that mimic the macromolecular organization of the shell.

Keywords: Chitin extraction, Morphology, Biomineralization

INTRODUCTION

With the development of nanometric structures in biomaterials for medical application, technique like biomerization has received some interest. Furthermore, it was verified that skeletal structures like human bone and crustacean sea shell have similar features requiring a more profound study of crustacean shells to serve as model for new composites for biomedical applications. [1]

Several species of crustacean, like shrimps, with the purpose of protection from the environment and predators, develop an exoskeleton [2]. There is several different names used for the different layers composing this exoskeleton. In this work is considered that crustacean shells are composed of 3 principal layers: Epicuticle, Exocuticle and Endocuticle. From a chemical point of view, this exoskeleton is composed by inorganic and organic materials, in a proportion of respectively 60:40. [3]

Shrimp shells can then be considered as a natural composite [4] because it associates an organic matrix composed by the chitin-protein complex with carbonate calcium, where it grows and nucleates as calcite. In terms of structure it is well known that the macromolecular arrangement in twisted plywoods facilitates the deposition and growth of the calcite crystals [5].

Presently several studies concerning crustacean shells morphology and composition focus the organized layered structure in twisted plywood as described by Bouligand 1972. [6,7]. Other papers studied this natural composite of a mechanical point of view, trying to identify the reasons for their performance. [8,9] However, to our knowledge, none of these studies relate the steps of extraction of chitin with the

morphology of the shells, or shell from shrimps of the species *Litopenaeus vannamei* Boone which is considered an important product in the economy of Brazil.

The objective of this study is try to understand the layout of the various components in the peel shrimp, identifying areas of higher accumulation of each of them, thus helping to understand some phenomena associated with the extraction process. The shell structuring can also help the developing of nanostructures that enable the biomimicking processes.

MATERIALS and METHODS

Extraction: The shrimp shell specie used was *Litopenaeus Vannamei Boone* obtained from a fish farm at Brazilian Northeast. The shell was received frozen and after thawing was dried. The extraction procedures were used in the entire shell and only in the abdomen. Aqueous solutions of HCl and NaOH 1.0M were employed for 24 hours for demineralization and deproteinization, respectively.

Scanning Electron Microscopy / Energy Dispersive X-ray: Microscopic assays were performed in dried shells, after demineralization and after deproteinization. Images were taken using a scanning electron microscope bench model TM-1000, Hitachi, with magnifications from 180x to 10000x, 15 kV, without metal plating.

RESULTS and DISCUSSION

Raw Shell

The present study was carried out by SEM visualization of shrimp shell samples at 3 distinct stages. The components comprising the shell have been successively removed and observations were made at the end of each extraction. We tried to use an extraction method that could guarantee the complete removal of the elements that compose the shell, since once we used the whole shell (no grinding) the reaction kinetics decreases making the diffusional issues more relevant.

To simplify the analysis of the results we selected only the shell of the shrimp corresponding to the body, and observations were made on the upper surface side surface. In the observations made on the upper part of the shell, it was not possible to identify the different layers constituting shell, but when observed lateral surface layers became evident. In Figure 1a, it is possible to easily identify the epicuticle (a), the exocuticle (b) and endocuticle (c). Using image analysis software, the size of each of these layers was measured, these values lying summarized in Table 1. It is found that in each layer comes a repetitive structure forming thin layers which will overlap each other. These layers originate cells secreting the components that go outwards, pushing the older successive layers to the outside. These layers have smaller as the main component chitin-protein complex, as well as calcite deposited on the nanofibrils formed by said complex. Epicuticle exhibits a higher density as compared to the other layers, possibly due to the accumulation of a higher amount of calcium in this zone.

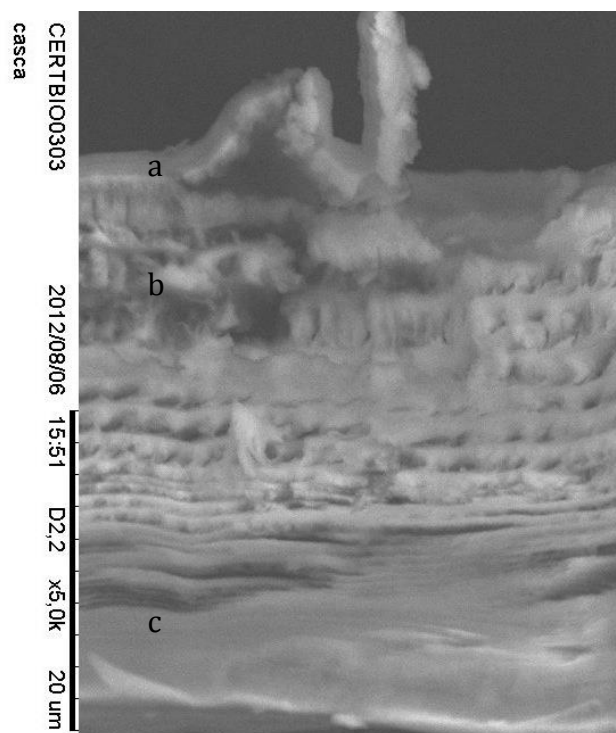


Figure 1. SEM image of a lateral cross section of the crude shell

Demineralized Shell

In Figure 2, shows the lateral section of the demineralized shell. Comparing with Figure 1 it can be seen that some areas change their color, particularly in the area of Endocuticle. It is believed that the removal of calcium salts present in that area gave further evidence to the chitin-protein structure. In this image it is possible to check the increase in size of each sublayer as they approach the Epicuticle, which in turn disappeared, confirming that this layer is mainly composed of calcium carbonate crystals. The values for the dimensions mentioned, are shown in Table 1. The increasing in the size of this small layers comprising the chitin-protein complex may be related to the ability of the calcium chelate amino acids, thus playing the role of a cross-linker and on its removal, the macromolecules complex gain freedom. This is further verified by the swelling upon contact with aqueous solutions. This question also supports the selection of demineralization as the first process of extraction of chitin. Regarding the EDX analysis, the calcium disappeared in all layers, confirming that the demineralization procedure was effective to remove it. At this moment the presence of nitrogen, which was not detected in the crude shell, possibly due to the higher concentration of elements such as calcium and carbon masking the presence of Nitrogen, was detected.

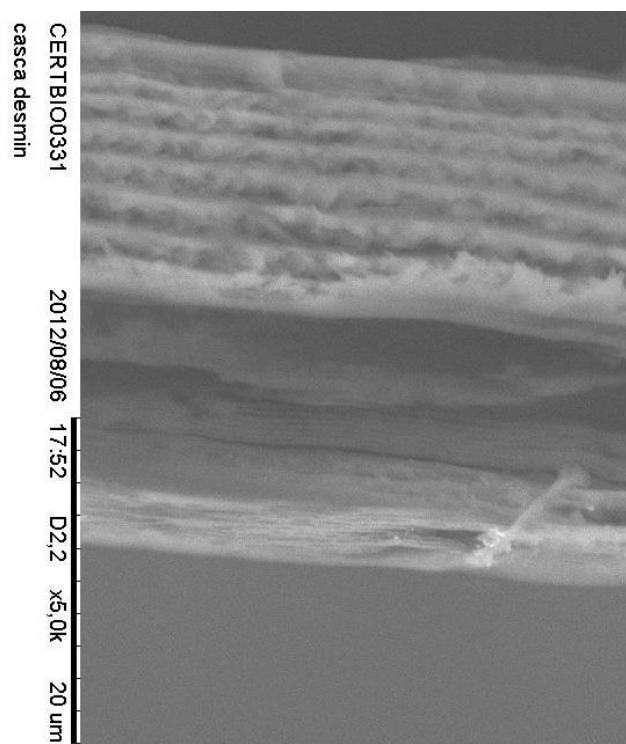


Figure 2. SEM image of a lateral cross section of the demineralized shell

Table 1. Summary of the measurement of different layers

Layers	As received (um)	Demineralized (um)	Chitin (um)
Epicuticle	1,47 ± 0,1	-	
Exocuticle	10,93 ± 1,2	19,07 ± 0,17	20
Endocuticle	25,57 ± 1,8	12,6 ± 0,84	
Total	37,97	31,65	20

Deproteinized Shell

At this moment, the obtained shell can be regarded as chitin, because theoretically this is the only remaining phase. The appearance of the shell is virtually transparent, with denser areas especially in the joints. The piece of chitinous shell tends to bend over himself when in contact with distilled water, possibly revealing the hydrophobicity characteristic of chitin. Regarding the analysis by SEM, Figure 3 presents another cross-section. In this image is no longer possible to differentiate with great clarity the constituent layers, and has become a kind of chitinous skeleton which should serve as a support for the integration of other components. The structure also shows the organization of sublayers, and as they approach the epicuticle zone (outside) become increasingly smaller. Note that the extraction processes were not sufficient to disrupt this chitin structure, thus this fact may explain the difficulty of alpha-chitin deacetylation, and diffusional issues related to the interior of the polymer chains. In

terms of dimensions this is the smallest structure, assuming that the protein is of great importance for structural while regulating the mechanisms of calcification.

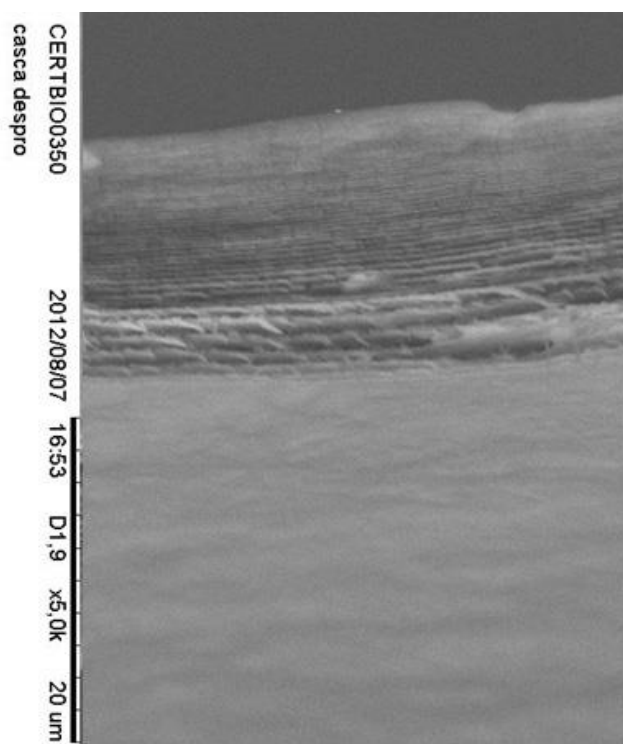


Figure 3. SEM image of a lateral cross section of the chitinous shell

Table 2. Elemental Analysis by EDX of the different shell layers

		C	N	O	Ca
As received	Epicuticle	49,6	ND	29,9	19,1
	Exocuticle	55,6	ND	34,1	10,3
	Endocuticle	60,9	ND	35,9	2,8
Demineralized	Epicuticle	NF	NF	NF	NF
	Exocuticle	53,0	13,2	33,8	ND
	Endocuticle	53,2	11,3	35,5	ND
Chitin	Epicuticle	NF	NF	NF	NF
	Exocuticle	66,2	7,8	26,1	ND
	Endocuticle	68,6	12,3	19,3	ND
ND- Not Detected		NF-Not Found			

CONCLUSION

This work followed the extraction of the elements that comprise the shell of the shrimp specie *Litopenaeus Vannamei Boone*. During the test it was possible to identify the differences resulting from the extraction, confirming that chitin has a determining effect on the structure of the shell. The presence of repetitive multilayer composite chitin-protein-calcium should be responsible for the mechanical characteristics of the shell and can serve as an inspiration for the development of new biomaterials.

ACKNOWLEDGEMENTS

Anna Sylvia Cavalcanti acknowledges financial support provided by **CAPES** fellowship

REFERENCES

1. Marie-Madeleine Giraud-Guille *, Emmanuel Belamie, Gervaise Mosser Organic and mineral networks in carapaces, bones and biomimetic materials, *C. R. Palevol* 3 (2004) 503–513
2. P.Y. Chen, A.Y.M. Lin, Y.S.Lin, Y. Seki, A.G. Stokes, J. Peyras, E.A. Olevsky, M.A. Meyers, J. McKittrick. Structure and mechanical properties of selected biological materials *Journal of the Mechanical Behavior of Biomedical Materials* 1 (2008) 208 – 226
3. Waraporn Promwikorn, Piyakorn Boonyoung, Pornpimol Kirirat Histological characterization of cuticular depositions throughout the molting cycle of the black tiger shrimp (*Penaeus monodon*) *Songklanakarinn J. Sci. Technol.*, 2005, 27(3) : 499-509
4. Julian F.V. Vincent Arthropod cuticle: a natural composite shell system, *Composites: Part A* 33 (2002) 1311–1315
5. Manoli F, Koutsopoulos S, Dalas E. Crystallization of calcite on chitin. *J Cryst Growth* 1997;182:116.
6. Bouhgand. Y. (1972) Twisted fibrous arrangements in biological materials and cholesteric mesophase. *Tissue & Cell*. 4, 189-217.
7. Marie-Madeleine Giraud-Guille, Fine Structure on Chitin-Protein System in the crab cuticle, *Tissue and Cell* 1984, 16 (1) 75-92
8. Po-Yu Chen *, Albert Yu-Min Lin, Joanna McKittrick, Marc AndreÅL Meyers Structure and mechanical properties of crab exoskeletons *Acta Biomaterialia* 4 (2008) 587–596
9. D. Raabe *, C. Sachs, P. Romano The crustacean exoskeleton as an example of a structurally and mechanically graded biological nanocomposite material *Acta Materialia* 53 (2005) 4281–4292

CHARACTERIZATION OF CHITOSAN BASED FILM WITH *ALOE VERA* GEL INCORPORATION

A. VALBUENA^{1,2}, A.GARCIA¹; M. COLINA^{✉1,2}; J. MOLINA²; JOSE CALDERA¹; O.LEON³; R. CAMBAR¹.

(1) *Laboratorio de Química Ambiental. Universidad del Zulia Facultad Experimental de Ciencias. Maracaibo 4011. Venezuela.*

(2) *Empresa Mixta Innovación Ambiental Quitosano CA. (INNOVAQUITO CA) Av. 4 San Francisco Sector El Bajo detrás de la Bomba Beta Petrol. Maracaibo. Venezuela.*

(3) *Laboratorio de Polímeros. Universidad del Zulia. Facultad de Ingeniería. Maracaibo 4011. Venezuela.*

✉ *Corresponding author: colinamarinela@gmail.com*

ABSTRACT

In this research, the effect of *Aloe Vera* gel incorporation at different proportions on chitosan-based films in their mechanical properties was investigated. For the preparation of the films, the hydrogel of chitosan was elaborated by adding 5 g of chitosan to 200 mL of water in a blender for 10 min until the hydrogel was formed. Different mixtures of chitosan- *Aloe Vera* gel were elaborated 90- 10; 80-20; 50-50; 100 % chitosan and 100% *Aloe Vera*. After filtration, the hydrogels were introduced to plastic molds for drying during for 24 h in the dark to avoid chitosan and *Aloe Vera* degradation. The mechanical properties are affected by the gel incorporation and the type of drying. The thickness of films decreased from 0 (plain chitosan film) to 50 % (the film containing 50% *Aloe vera* gel). The films elaborated with 100% of *aloe vera* were not tested because they did not present a good consistence for the analysis. FTIR bands were used to characterized the films. To investigate the morphology, scanning electron microscopy in environmental mode (ESEM) was used. The better mixture films were obtained 90-10; 80-20 percentage chitosan- *Aloe Vera* respectively.

INTRODUCTION

Chitin and its deacetylated derivative chitosan have received much recent attention in various fields. The reason is the unique chemical and physicochemical and biological properties of both and the unlimited source for their production. Chitosan was used as a film-forming polymer and *Aloe vera* gel was added as an additive at different proportions to the chitosan solution. Commercial *Aloe Vera* 1X was used to obtain the films. Chitosan has been reported as an excellent film-forming substance, wherein positively charged groups occurring in chitosan can come in interaction with groups possessing opposite charges and yield three-dimensional networks. However, the properties of the obtained chitosan films are mainly proportional to several variants including chitin source, chitosan characteristics (i.e., molecular weight and deacetylation degree), type and amount of solvents, plasticizers, copolymers, dispersants, compatibilizers, among others and the method used for film preparation. The objective of this research was to investigate the effect of *Aloe vera* gel incorporation at different proportions on chitosan-based films in their mechanical properties [1], [2].

EXPERIMENTAL PART

1. Materials

Chitosan ($M_v = 540$ kDa, degree of deacetylation 85%) was obtained from Innovaquito (Innovación Ambiental Quitosano CA, El Bajo, Estado Zulia, Venezuela). *Aloe Vera* gel 1X was obtained from *Aloe Vera* Company from Maracaibo, Venezuela.

2. Film's elaboration procedure

The hydrogel of chitosan was elaborated by adding 5 g of chitosan to 200 mL of water in a blender for 10 min until the hydrogel was formed. Different mixtures of chitosan- *Aloe Vera* gel were elaborated 90-10; 80-20; 50-50; 100 % chitosan. (CHAV3, CHAV2, CHAV1, CHAV0, respectively), The film 100 % *Aloe Vera* couldn't be elaborated. After filtration, the hydrogels were introduced to plastic molds for drying during for 24 h in the dark to avoid degradation and dried using lyophilization a -51°C a 4000X10-03 Mbar during for 7 h.

3. Characterization

The spectra of chitosan films were obtained using an I.R instrument (SHIMADZU-8400, Japan) with a frequency range from 4000 to 400 cm^{-1} . All mechanical properties of the films were determined by a texture analyzer using a modified ASTM D00882-00 (ASTM, 2000b). The films were cut into $1\text{ cm} \times 6\text{ cm}$ strips for testing. The measurements were performed using a cross-head speed of 50 mm min^{-1} with an exposed area of $1\text{ cm} \times 4\text{ cm}$ for each film strip. Four strips were prepared from each film. The tensile stress was plotted against the elongation in order to give a stress-strain curve, and the ultimate tensile strength (TS, in MPa), elongation at break (%E) as well as elastic modulus (EM, in MPa) of films were reported. The films thickness (mm) was measured, using a hand-held digital micrometer (Mitutoyo, Japan), at five different positions in each specimen to the nearest 0.001 mm.

RESULTS AND DISCUSSION

The films are formed for the re-arrangement of the molecules during the drying of the gel or chitosan solution. In this investigation was observed that the films cannot be exposed to high temperatures due to the fact that they fracture, this is due to break of the bonds of hydrogen that keep the molecules close to the polymer, neither they can be exposed to the solar light. The films only can part with molds of plastic or teflon, on having used glass molds remain adhered completely being very difficult its detachment. This owes to that the surface of the glass contains silicates with charges (-), in the completions of Si-O (-) which have very strong interactions with the ammine protonated groups (+) of the chitosan. On the other hand, the plastic polymers have functional olefinic groups C=C which do not have affinity with the chitosan. Chemical coatings have been brought of chitosan on glass. The chitosan also is absorbent, whereas the plastic ones are hydrophobic. Therefore that to do

the above mentioned coverings carry out chemical modifications of the chitosan to improve its adsorption to plastic and this way they can be sprayed on them .

In the Figure 1 is shown the chitosan film FTIR spectra a) commercial (Biopiel), and b) experimental without sulphite, in both the appearance of a band observes to 1560 cm^{-1} corresponding to the flexion N-H of the primary amine formed by means of the deacetylation. These films possess the same appearance, they are transparent, stick fast easily in the skin, and take the improving of the skin as a usefulness for a burn cure. There is a displacement of bands from the experimental films without sulphite, for the addition of acetic acid, with respect to the commercial films. The bands at 1530 cm^{-1} is observed which correspond to the group ammonium NH_3^+ formed by means of the acidification.

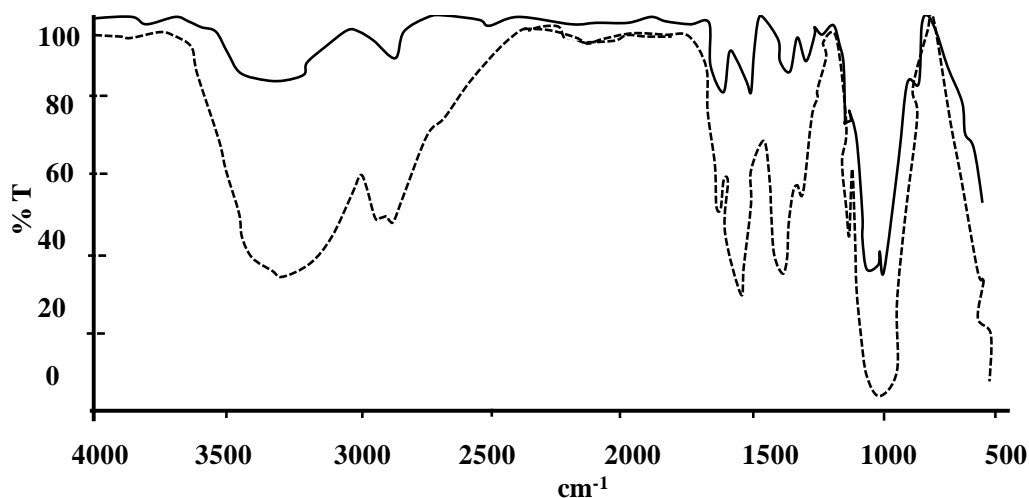


Figure 1. FTIR spectra of chitosan film a) commercial chitosan (---) (Biopiel) (DD 80 %) y b) experimental(—) (without sulphite, DD 82 %).

In Figure 2 is shown a 100% chitosan film. In the FTIR analysis, the bands were observed, NH tension at 1528 cm^{-1} from amine group and 1628 cm^{-1} of the acetamide group, these are signals typical of chitosan,. In addition, in the Figure is shown the spectra of chitosan film with *Aloe Vera* gel, showing a thickened band system (C-O-C).

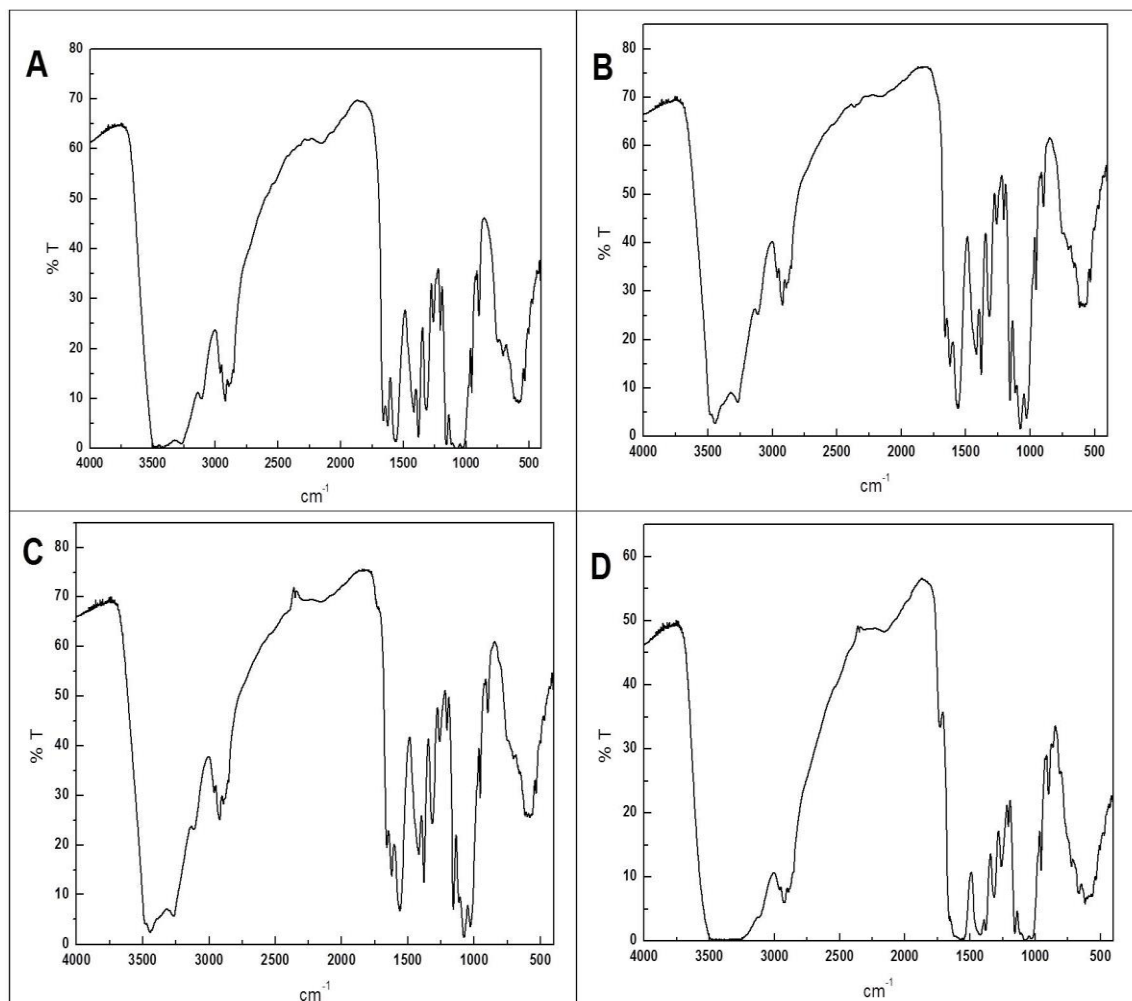


Figure 2. FT-IR spectra of films (A) CHAV0 (100 % chitosan), (B) CHAV1, (C) CHAV2, (D) CHAV3.

The results of film's mechanical analysis are summarized in Table 1. All mechanical properties, tensile strength (TS, in MPa) indicating the maximum tensile stress that the film can sustain, elongation at break (E, in %) as the maximum change in the length of a test film before being broken, and elastic modulus (EM, in MPa) which is a measure of the stiffness of the film, as a function of *Aloe vera* gel incorporation, showed the same behaviour pattern. These mechanical characteristics started to increase slightly as a result of increasing the *Aloe Vera* gel ratio, from plain chitosan films to the highest values in blend films containing 20% *Aloe Vera* gel, however this increase did not obtain any significant difference, except for elongation at break. This increase was followed by a significant reduction in all mechanical properties by introducing higher quantities of *Aloe vera* gel, as the lowest values obtained by blend films containing 50% *Aloe vera* gel, which can be related to the high moisture content, since the moisture has been reported as an effective plasticizer. Clearly, the blend films containing 20% *Aloe vera* gel showed the highest values for mechanical characteristics, with suitable toughness and flexibility (Table 1).

Table 1. Thickness and mechanical properties of plain chitosan and chitosan–*Aloe Vera* gel blend films

Film's Code	Ratio	Thickness (mm)		E^a (%)		TS^b (MPa)		EM^c (MPa)	
		DRT ^d	DL ^e						
CHAV0	100% chitosan/ <i>Aloe vera</i> gel 0%	0.1589	0.2305	66.80	70.56	8.56	9.56	8.23	9.26
CHAV1	90% chitosan/ <i>Aloe vera</i> gel 10%	0.1757	0.2003	69.35	80.37	9.45	9.67	7.88	8.35
CHAV2	80% chitosan/ <i>Aloe vera</i> gel 20%	0.2013	0.2207	80.23	92.46	9.35	9.85	6.94	7.06
CHAV3	50% chitosan/ <i>Aloe vera</i> gel 50%	0.1807	0.2269	60.24	65.23	7.12	8.25	7.23	8.45

^a Elongation at break, ^b Tensile strength, ^c Elastic modulus, ^d Dried at Room Temperature and ^e Dried by Lyophilization.

The above corresponds to the mechanical properties of the films dried at room temperature: In the case of the films dried by lyophilization the elongation properties are magnified because this drying system promotes the formation of sheets with higher molecular arrangement, this is can be seen in Tables 1. In Table 2, the differences of flexibility of the films are shown, for 100 % of chitosan films, completely transparence is seen but for not for the lyophilized films, however they presented more flexibility as is shown in the picture for 50% of *aloe vera*-chitosan.

Table 2. The consistence of the films depending on the mix chitosan – *Aloe Vera* and the dryness type.

Treatment	DRT	DL
100% chitosan/ <i>Aloe vera</i> gel 0%		
80% chitosan/ <i>Aloe vera</i> gel 20%		
50% chitosan/ <i>Aloe vera</i> gel 50%		

The use of the two components chitosan- *Aloe vera* for the film making should increase the properties for burn cure as both of them have been reporter as good for that medical treatment.

CONCLUSIONS

The results of this study suggested that the incorporation of *Aloe Vera* gel into film-forming chitosan solution can have a considerable influence on the properties of the obtained chitosan–*Aloe Vera* gel blend films. Additional to that, the drying process for obtaining the films has influence on the mechanical properties of the films.

REFERENCES

- [1]Chávez, A; Colina, M.; Valbuena, A. and López, A. (2012) Obtención y caracterización de películas de quitosano elaborado a partir de los desechos de la industria cangrejera. *Revista Iberoamericana de Polímeros*, 13, 3, 77-88.
- [2] Wani, M. Y., Hasan, N. & Malik, M. A. (2010). Chitosan and *Aloe vera*: two gifts of nature. *Journal of Dispersion Science and Technology*, 31(6), 799–811.

**Enzymology, Biochemistry, Biological
and Ecological Aspects**

CHITIN AND CHITOSAN MODIFYING ENZYMES: VERSATILE NOVEL TOOLS FOR THE ANALYSIS OF STRUCTURE-FUNCTION RELATIONSHIPS OF PARTIALLY ACETYLATED CHITOSANS

Nour Eddine El Gueddari, Stephan Kolkenbrock, Andreas Schaaf, Neeraja Chilukoti, Fabrice Brunel, Christian Gorzelanny, Sabine Fehser, Sonia Chachra, Frank Bernard, Malathi Nampally, Thejaswi Kalagara, Philipp Ihmor, Bruno M. Moerschbacher*

*Institute for Biology and Biotechnology of Plants – IBBP,
Westphalian Wilhelm’s-University Münster – WWU, Schlossplatz 8, 48143 Münster, Germany.*

**E-mail address: moersch@uni-muenster.de*

ABSTRACT

The past decade has seen remarkable progress in understanding structure-function relationships of partially acetylated chitosans. In particular, the roles of the degree of polymerisation (DP) and degree of acetylation (DA) of chitosans in defining their physico-chemical properties and their biological activities have been investigated. In contrast, the role of the pattern of acetylation (PA) has not yet been studied, mostly due to a lack of analytical methods to determine PA, and to the non-availability of chitosans with non-random PA. We here describe how chitin and chitosan modifying enzymes, such as chitin deacetylases and chitosan hydrolases, can be used for analysis and synthesis of chitosans. Chitin deacetylases can convert chitin oligomers or highly acetylated chitosan polymers with random PA into chitosan oligomers or less acetylated chitosan polymers with defined, non-random PAs. Sequence specific chitosan hydrolases can be used in enzymatic / mass-spectrometric fingerprinting assays to determine the PA of chitosan polymers, while the PA of chitosan oligomers even in complex mixtures can be determined using quantitative mass spectrometric sequencing. Thus, bio-engineering of designer chitosans with known structures and defined functions becomes feasible, as a prerequisite for the development of reliable chitosan-based products, e.g. for plant disease protection or scar-free wound healing.

Keywords

chitin deacetylase, chitinase, chitosanase, patterns of acetylation, enzymatic mass-spectrometric fingerprinting, chitosan affinity protein

THE ALL-IMPORTANT “S”: FROM CHITOSAN TO CHITOSANS

Chitosans – a family of partially de-N-acetylated derivatives of one of the world’s most abundant renewable resources, chitin – are among the most versatile and most promising functional biopolymers. However, the commercial exploitation of chitosans still lags behind initial expectations, and this is mostly due to poor reproducibility of many of their alleged biological activities. We have argued that this is at least in part brought about by a lack of detailed understanding of structure/function relationships of partially acetylated chitosans at the molecular or nano-level [1]. We have therefore, in collaborations with European and international partners and in a series of European research projects, set out to

analyse structure-function relationships of chitosans concerning their physico-chemical properties and their biological activities, as a basis to studying their molecular and cellular modes of action and, eventually, the knowledge-based development of commercially viable applications, e.g. as plant strengtheners or plant protectants, as trans-mucosal, sustained release nanoparticle carriers of drugs, genes, or vaccines, or to support scar-free wound healing, to name a few.

The notion that the biological activities of partially acetylated chitosans crucially depend on the physico-chemical properties of the chitosan used was supported by two landmark papers, by Kauss et al. [2] and Vander et al. [3], studying the effect of different, well defined chitosans on plants. While Kauss et al. concluded that the resistance eliciting activities of chitosans in vinca cells were most likely the result of electrostatic interactions of polycationic chitosan polymers with the negatively charged surface of phospholipid containing membranes, Vander et al. postulated the presence of chitin and/or chitosan specific receptors on the wheat cell surface. We believe today that both modes of action are likely to occur in parallel and to act in concert and synergistically (Fig. 1). This concept puts microbial chitin synthases and chitin deacetylases as well as host derived chitosanolytic enzymes in the focus of our current research.

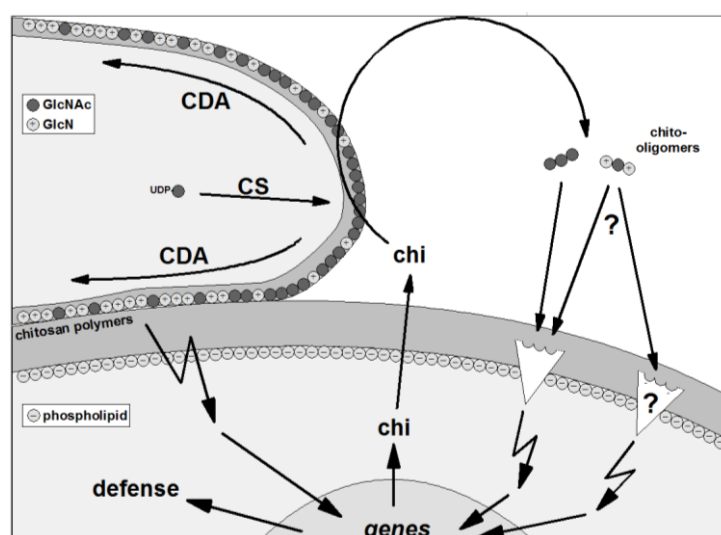


Figure 1. Possible modes of action of chitosans as elicitors of plant defense reactions.
(CS, chitin synthase; CDA, chitin deacetylase; chi, chitinase)

Chitosans are linear copolymers of N-acetylglucosamine and glucosamine units and, thus, they differ in their degrees of polymerisation (DP), degrees of acetylation (DA), and patterns of acetylation (PA). In the CARAPAX project (www.uni-muenster.de/biologie.ibbp/carapax), we had generated and characterised series of chitosans differing in only one parameter, DP or DA, while keeping all other parameters constant [4]. This allowed us to show that both the physico-chemical properties and the antimicrobial activities of partially acetylated chitosans as well as their resistance eliciting activities in plants depended strongly on their DA and, above a threshold DP and to a lesser extent, on their DP [5]. One first and highly significant result of the CARAPAX project was Domard's famous "general law of behavior" of partially acetylated chitosans in aqueous solution defining three different DA ranges – the polyelectrolyte range at low DAs from 0 to ca. 25%, the transition range at intermediate DAs from ca. 25 to ca. 50%, and the hydrophobic range at high DAs from ca. 50 to ca. 70%, beyond which chitosans become insoluble in aqueous solution [6].

LOW DA / MEDIUM DP IS BEST FOR ANTIMICROBIAL ACTIVITIES

The antimicrobial activity against gram-positive and gram-negative bacteria as well as against ascomycete, basidiomycete, zygomycete and oomycete fungi was highest for chitosans with very low DA – i.e. in the polyelectrolyte range – and intermediate DP of ca. 50 to 200. As we also observed that the antimicrobial activity decreased with increasing pH, we concluded that the positive charge of the chitosans was mostly responsible for their antimicrobial activities [5]. We also found that invariably, microorganisms with a high tolerance to chitosans were characterised by strong chitosanolytic activities [7]. These results have since been confirmed in many studies [8], proving that the choice of chitosan crucially determines its effect e.g. when used as an antimicrobial agent, an observation that has prompted us to talk of “chitosans” rather than of “chitosan”, and to regard chitosans as a family of related biopolymers with distinct properties and functionalities.

MEDIUM DA / HIGH DP IS BEST FOR PLANT STRENGTHENING ACTIVITIES

Similarly, we found that the plant strengthening activities of chitosans crucially depend on their DA and, again to a lesser extent, on their DP. Here, the picture was less uniform. Different plant species reacted best to different chitosans, and even different aspects of resistance in the same plant species were best induced by different chitosans. Still, the emerging overall picture showed that chitosans with high DP of around 1000 and intermediate DA – i.e. in the transition range – were typically best suited to elicit complex resistance responses [5]. We have speculated that this is due to the presence of chitinases in plant tissues which will degrade partially acetylated chitosans to yield oligomers with rather low DP and rather high DA concomitant with chitosan polymers of higher DP and lower DA (otherwise, if they had a higher DA, they would be further degraded to yield oligomers). As depicted in Fig. 1, these two products of plant chitinases acting on chitosans present in fungal cell walls inside their host tissues may have different modes of action. The rather cationic polymers might interact electrostatically with the plant plasma-membrane, triggering the synthesis of precursor metabolites, while the rather chitin-like oligomers might be perceived via receptors triggering the conversion of the precursor metabolites into defense molecules such as lignin or antimicrobial phytoalexins. While chitosans with intermediate DA might give rise to both types of synergistically acting molecules, those of low DA or high DA might yield only one of them, explaining their reduced activity in eliciting complex defense reactions. This hypothesis is currently being investigated in our lab using state-of-the-art molecular genetic methods, such as DNA arrays to study gene expression patterns triggered by different types of chitosans, or gene knock-out studies to identify the receptors and signal transduction chains involved.

At the end of the CARAPAX project, we had reduced the 40 kg/ha required of raw chitosan to achieve reliable plant disease protection to a mere 160 g/ha. However, as the efficacy of our knowledge-based chitosans was only around 50% – meaning that disease incurred losses could be cut by half – this was not considered good enough for the development of a successful product for the European agro-market. However, our long-term chitosan producer (Mahtani Chitosan in Gujarat, India) built on our results and further improved the efficacy, eventually launching three products containing different, specifically optimised chitins or chitosans for soil amendment, seed dressing, and foliar spray, acting at only 40 g/ha. Two of them are currently approved in India, one in France, and we are now optimizing them for other climates and markets around the world.

HUMAN CHITOTRIOSIDASE IS A CHITOSANOLYTIC ENZYME

In the subsequent NANOBIO SACCHARIDES project and its international satellite project NBS-TTC (www.nanobiosaccharides.org), we extended the proof-of-principle studies of the CARAPAX project to investigate structure-function relationships of partially acetylated chitosans in the formation of hydrogels and nanoparticles and in the biological activities towards human cells. Here, the picture became even more complex and difficult, suggesting to us an even more important role of chitosanolytic enzymes present in target tissues. We argued that in addition to DP and DA, the biological functionalities of chitosans will be strongly influenced by their PA if a sequence-specific chitosan hydrolase is present [9]. In such cases, both the turnover rate of the potentially bioactive polymer and the rates, qualities, and quantities of the resulting and potentially biologically active oligomeric products will be strongly influenced by the PA of the initial polymer applied. And the bioactivities of the resulting chitosan oligomers which are likely to exert their biological activities through interaction with target molecules such as receptors, can be expected to depend crucially on the spatial distribution of the hydrophobic acetyl groups and the hydrophilic, at slightly acidic pH values even positively charged free amino groups as these different patches will be crucial for binding.

At the time, lysozyme was considered to be the most relevant chitinolytic enzyme in humans, and its inability to cleave chitosans with less than very high DA had led to the general assumption that human tissues do not contain a chitosanolytic enzyme [10]. However, we found that one of the other two known human chitinases, namely chitotriosidase, is a processively acting endochitinase of the glycosyl hydrolase family GH18 with the ability for non-productive binding, quite similar to well known bacterial chitinases [11]. While chitotriosidase has a preference for cleaving the linkage between two acetylated units, the specificity is absolute only at the -1 subsite, but less pronounced at the +1 subsite, so that even chitosans with rather low DA are slowly hydrolysed. We were also able to show that the products obtained from a chitotriosidase digestion of chitosans were biologically active in human macrophages, triggering increased chitotriosidase activities and thus initiating a positive feedback cycle. Clearly, then, the pattern of acetylation of a partially acetylated chitosan will matter for its biological activity in human tissues where chitotriosidase is present.

However, while the importance of DP and DA for different biological activities of chitosans is broadly accepted now and investigated intensively in many groups around the world, little is known about the influence of PA. In fact, the potential role of PA is not yet even considered by most of the chitosan researchers. This lack of knowledge and appreciation is due firstly to the fact that today's chemical methods of chitosan production, whether by hetero- or homogeneous de-N-acetylation of chitin or by re-N-acetylation of polyglucosamine, invariably lead to random PAs, so that chitosans with non-random PAs are not at all available for testing [12]. Secondly, there is a notable lack of suitable analytical methods to determine different PAs, especially in the case of polymeric chitosans. We have, therefore, begun to develop tools for the generation and analysis of chitosans with non-random PA. All of these methods are using chitin and chitosan modifying enzymes (CCME), typically heterologously expressed, and sometimes engineered recombinant proteins. We hypothesise that CCME such as chitin deacetylases or sequence-specific chitosan hydrolases can be used to generate chitosan polymers and oligomers with non-random PA, and also to analyse the PA using computer assisted, enzymatic / mass spectrometric fingerprinting techniques.

TOWARDS CHITOSANS WITH NON-RANDOM PA

In a number of bilateral collaboration projects with partners mainly in India as well as in our current European research project, PolyModE (www.polymode.eu), we have established knowledge-based and un-biased, e.g. metagenomic, discovery approaches for CCME, and we have developed screening methods for their identification. We have cloned and heterologously expressed genes coding for a variety of CCME in a number of pro- and eukaryotic expression systems, and we have begun to optimise them using genetic engineering. We are using these CCME for the production of chitosan polymers and oligomers which are then analysed in detail concerning their DP, DA, and PA.

While the DP of chitosan polymers can be analysed rather accurately using viscosimetry or, better, HP-SEC coupled to RI and MALLS detectors, and the DA can be analysed more or less accurately using potentiometry or, better, NMR, the analysis of the PA has received less attention so far. Diad analysis by ^{13}C -NMR remains the gold standard for PA determination for chitosan polymers [13]. MS can easily yield information on DP and DA of chitosan oligomers even in complex mixtures, and sequencing is possible using MSⁿ techniques when the mixtures are not too complex [14]. We are now developing fingerprinting techniques for sensitive and accurate PA analysis of chitosans. These entail the use of chitosan hydrolases with defined and known subsite specificities followed by quantitative MSⁿ of the oligomers produced, and computer assisted analysis of the results using our proprietary “chitinator” program [15].

Using a number of recombinant bacterial and fungal chitin deacetylases for the further enzymatic deacetylation of chemically produced chitosans of high DA, we were able to produce chitosan polymers of low DA which appear to have non-random PAs. A first evidence of non-random PA was given by the observation that enzymatic deacetylation of chitosan polymers is typically not complete, so that e.g. a chitosan with an initial DA of 56% yielded a chitosan with a DA of 35% which even after prolonged incubation, addition of fresh enzyme, and removal of free acetate, did not decrease further. However, a chitosan with an initial DA of 36% is readily deacetylated by the same chitin deacetylase to yield a chitosan with a DA of 10%. We concluded that the enzymatically produced chitosan of DA 35% must differ from the chemically produced chitosan of 36%. As the DP and polydispersity index I_p of all chitosans used was very similar, we assume that they differ in PA, the chemically produced ones having a random PA while the enzymatically produced ones having a non-random PA. This hypothesis was further strengthened by a fingerprinting analysis in which we digested both chitosans with chitinases and chitosanases of known cleavage specificities. These yielded significantly different products upon mass spectrometric analysis, the most pronounced one being the presence of higher amounts of the fully deacetylated dimer in the chitosanase digest of the enzymatically produced chitosan. This is in agreement with the assumption that the chitin deacetylase has a processive mode of action, thus creating a block of deacetylated residues when gliding along the chitosan chain (Fig. 2). This block is then an ideal substrate for the chitosanase cleaving only between two deacetylated residues and yielding glucosamine dimers in the process. We are currently extending these investigations using different chitin deacetylases and different fingerprinting enzymes.

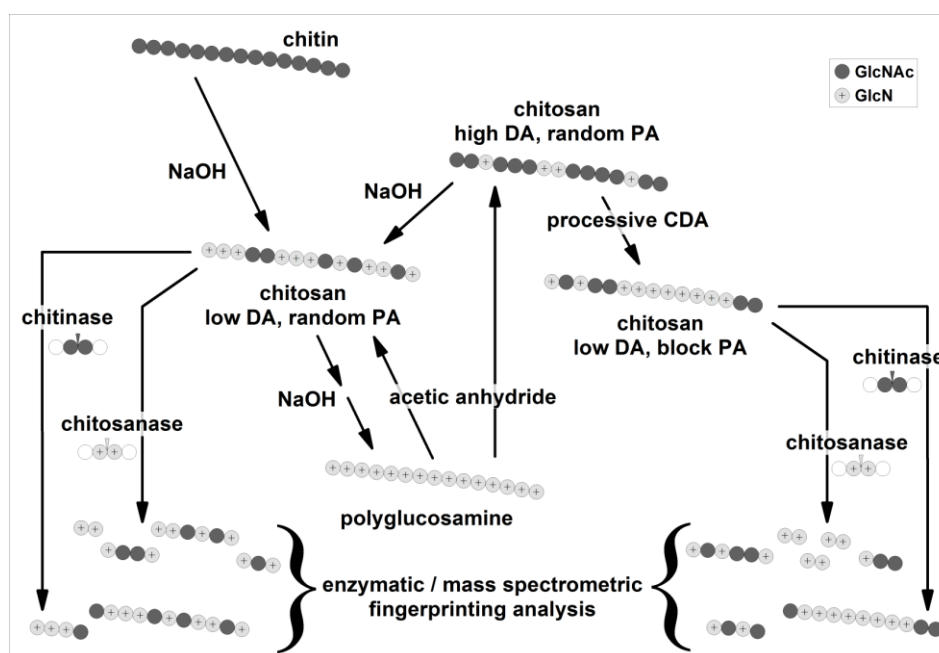


Figure 2. Chemical versus enzymatic generation of chitosans and enzymatic / mass spectrometric fingerprinting for PA analysis.

Concurrently, we have optimised the mass spectrometric analysis of the oligomeric products to allow quantitative sequencing, by the re-N-acetylation of partially deacetylated chitosan oligomers using deuterated acetic anhydride to give fully acetylated chitin oligomers where three additional mass units on the acetyl group mark the positions of formerly deacetylated residues. Exact quantitation is then possible relative to a series of doubly isotopically labeled chitin oligomers, allowing the sequencing of partially acetylated chitosan oligomers even in a mixture of several isobars (oligomers with identical DP and DA and, thus, identical molar mass, but different PAs) and the determination of the relative abundance of each isobar in the mixture. This method has allowed us to further extend the capabilities of our “chitinator” program with which we can now determine the subsite specificities of an unknown chitosan hydrolase.

TOWARDS ENGINEERING FULLY DEFINED DESIGNER CHITOSANS

In another European research project, the ERA-IB project ChitoBioEngineering (www.chitobioengineering.eu), we are currently using the chitin deacetylases in a biotechnological approach to produce useful amounts of partially acetylated chitosan oligomers with fully defined architecture – i.e. known DP, DA, and PA. This can be done either in vitro by enzymatic deacetylation of fully acetylated chitin oligomers or in vivo when the gene coding for the chitin deacetylase is combined with a suitable chitin synthase gene in a host strain such as *E. coli* [16]. The first such fully defined chitosan oligomers are now available on a small scale and are being tested in a number of different bioassays involving plant and human cells and tissues.

Finally, we have converted a chitosanase into a fluorescing chitosan affinity protein (CAP) by inactivating it using site directed mutagenesis and fusing it to a fluorescent protein such as GFP [16]. This CAP now allows us the in situ detection of chitosan, e.g. in the hyphae of pathogenic fungi or on the surface of human cells treated with chitosans. We are now developing CAP into a whole family of versatile tools for the analysis and localisation of chitosans.

Thus, CCME-based tools can be used for the generation and for the structural and functional analysis of partially acetylated chitosan polymers and oligomers, yielding an increasing portfolio of third-generation bioengineered chitosans with defined DP, DA, and PA. These tools which we continue to improve promise to further reveal molecular, nano-scale details of structure-function relationships of chitosans, in particular concerning the hitherto possibly grossly underestimated role of PA, to allow the knowledge-based development of reliable applications, e.g. in biotechnology, biomedicine, agriculture, or food sciences.

ACKNOWLEDGEMENTS

We gratefully acknowledge financial support from the European Union through the CARAPAX, NanoBioSaccharides and NBS-TTC, and PolyModE projects, from German Federal Ministry for Research and Education BMBF through the ERA-IB project Chito-BioEngineering and the Indo-German Public Private Partnership “2+2” project CuChi-BCA, from the German Research Council DFG through the Indo-German International Research Training Group IRTG on Molecular and Cellular Glyco-Sciences MCGS, from German Academic Exchange Service DAAD through exchange programs and doctoral fellowships. Also, we thank our partners in these projects, above all Dominique Gillet, Alain Domard, Kjell Vårum, Stefan Schillberg, Vassilis Bouriotis, Maria Alonso, Francisco Goycoolea, Stefan Schneider, Thierry Delair, Willem Stevens, Appa Rao Podile, Telma Franco, Amie van der Westhuizen, T.S. Suryanarayanan, Suseelendra Desai, Martin Peter, Wim Soetaert, Toni Planas, Michael Mormann, Heinrich Luftmann, and Naoto Shibuya for support, ideas, discussions, and more.

REFERENCES

- 1 El Gueddari, N. E., Moerschbacher, B. M. (2004) A bioactivity matrix for chitosans as elicitors of disease resistance reactions in wheat. *Adv. Chitin Sci.*, 7, 56-59.
- 2 Kauss, H., Jeblick, W., Domard, A. (1989) The degrees of polymerization and N-acetylation of chitosan determine its ability to elicit callose formation in suspension cells and protoplasts of *Catharanthus roseus*. *Planta*, 178, 385-392.
- 3 Vander, P., Vårum, K. M., Domard, A., El Gueddari, N. E., Moerschbacher, B. M. (1998) Comparison of the ability of partially N-acetylated chitosans and chitooligosaccharides to elicit resistance reactions in wheat leaves. *Plant Physiol.*, 118, 1353-1359.
- 4 Domard, A. (2011) A perspective on 30 years research on chitin and chitosan. *Carbohydrate Polymers*, 84, 696-703.
- 5 Moerschbacher, B. M. (2005) Bio-activity matrices of chitosans in plant protection. In: S. S. Gnanamanickam, R. Balasubramanian, N. Anand, eds., *Emerging Trends in Plant-Microbe Interactions*. University of Madras, Chennai, pp. 186-190.
- 6 Lamarque, G., Lucas, J. M., Viton, C., Domard, A. (2005) Physicochemical behavior of homogeneous series of acetylated chitosans in aqueous solution: role of various structural parameters. *Biomacromolecules*, 6, 131-142.
- 7 Oliveira, E. N. Junior, El Gueddari, N. E., Moerschbacher, B. M., Peter, M. G., Franco, T. T. (2008) Growth of phytopathogenic fungi in the presence of partially acetylated chitooligosaccharides. *Mycopathologia*, 166, 163-174.

- 8 Kong, M., Chen, X. G., Xing, K., Park, H. J. (2010) Antimicrobial properties of chitosan and mode of action: A state of the art review. *Int. J. Food Microbiol.*, 144, 51-63.
- 9 Kohlhoff, M., El Gueddari, N. E., Gorzelanny, C., Haebel, S., Alonso, M. J., Franco T. T., Moerschbacher, B. M. (2009) Bio-engineering of chitosans with non-random patterns of acetylation - a novel sequence-specific chitosan hydrolase generating oligomers with block-PA. *Adv. Chitin Sci.*, 11, 463-468.
- 10 Nordtveit, R. J., Vårum, K. M., Smidsrød, O. (1996) Degradation of partially N-acetylated chitosans with hen egg white and human lysozyme. *Carbohydr. Polym.*, 29, 163-167.
- 11 Gorzelanny, C., Pöppelmann, B., Pappelbaum, K., Moerschbacher, B. M., Schneider, S. W. (2010) Human macrophage activation triggered by chitotriosidase-mediated chitin and chitosan degradation. *Biomaterials*, 31, 8556-8563.
- 12 Weinhold, M. X., Sauvageau, J. C. M., Kumirska, J., Thöming, J. (2009) Studies on acetylation patterns of different chitosan preparations. *Carbohydr. Polym.*, 78, 678-684.
- 13 Vårum, K. M., Anthonsen, M. W., Grasdalen, H., Smidsrød, D. (1991) ¹³C-NMR studies of the acetylation sequences in partially N-deacetylated chitins (chitosans). *Carbohydr. Res.*, 217, 19-27.
- 14 Haebel, S., Bahrke, S., Peter, M. G. (2007) Quantitative sequencing of complex mixtures of heterochitooligosaccharides by vMALDI-linear ion trap mass spectrometry. *Anal. Chem.*, 79, 5557-5566.
- 15 Moerschbacher, B. M., Bernard, F., El Gueddari, N. E. (2011) Enzymatic / mass spectrometric fingerprinting of partially acetylated chitosans. *Adv. Chitin Sci.*, 13, 185-191.
- 16 Samain, E., Drouillard, S., Heyraud, A., Driguez, H., Geremia, R. A. (1997) Gram-scale synthesis of recombinant chitooligosaccharides in *Escherichia coli*. *Carbohydr. Res.*, 302, 35-42.
- 17 Nampally M., Moerschbacher, B. M., Kolkenbrock, S. (2012) A novel genetically engineered chitosan affinity GFP-fusion protein to specifically detect chitosan in vitro and in situ. *Appl. Environm. Microbiol.*, 78, 3114-3119.

SUBMERGED AND SOLID SUPPORT PRODUCTION AND MOLECULAR IDENTIFICATION OF CHITIN DEACETYLASES FROM PHYTOPATHOGENIC FUNGI

F. Muñiz-Paredes¹, C. P. Larralde-Corona², F. J. Fernandez¹, J. D. Sepúlveda¹, K. Shirai^{1*}

¹Universidad Autónoma Metropolitana-Iztapalapa, Departamento de Biotecnología, Mexico.

²Instituto Politécnico Nacional - Centro de Biotecnología Genómica, Mexico.

*E-mail address: smk@xanum.uam.mx

ABSTRACT

Production of chitin deacetylases (CDAs) from *Colletotrichum gloeosporioides*, *Colletotrichum acutatum* and *Fusarium solani* was conducted in submerged (SmC) and solid-state culture (SSC), the later using polyurethane foam as an inert support. Growth kinetics and enzymatic activity determination were carried out using glutamic acid and glucose media in both SmC and SSC. *C. gloeosporioides* displayed CDA activity in both cultures, but enzyme activity was higher in SmC than that in SSC. CDA activity for *C. acutatum* and *F. solani* only was detected when cultured in SSC, but it was lower than that produced with *C. gloeosporioides*. Scanning electron microscopy (SEM) was performed in order to observe the infective structures, *C. gloeosporioides* and *F. solani* showed appresoria only when cultured in SSC, while *C. acutatum* showed appresoria in both cultures. In addition, the molecular identification of CDA genes of *C. acutatum* and *C. gloeosporioides* was conducted by sequencing of PCR products and analyzed by BLAST, resulting on 84% and 75% CDA maximal identities to genes of *Colletotrichum lindemuthianum* and *Magnaporthe grisea*, respectively.

Keywords Chitin deacetylases, submerged culture, solid state culture, phytopathogenic fungi.

INTRODUCTION

CDAs play an important role in the development of cell wall in plant-pathogen interactions. CDA is responsible for hydrolysis of the *N*-acetamide bonds in chitin toward chitosan [1]. The callus formation, lignification and synthesis of coumarin derivatives and defense proteins including chitinases are mechanisms of plant defense against parasitic fungi. Chitin oligomers (from tetramers to hexamers) and fungal chitin induce these plant defense mechanisms; however, the deacetylated forms do not activate plant defense mechanisms. It has been suggested that CDA could act on chitin oligomers involved in cell wall synthesis thus reducing the activity of plant chitinases and decreasing their defensive activity [2].

The deacetylation of chitin by these enzymes also facilitates the penetration process of the fungal hyphae in plant tissues, because it reduces the levels of acetylation of fungal chitin, decreasing the activity of plant endochitinases [3].

Despite of reports on the purification of CDA from fungi *Mucor rouxii* [4], *Absidia coerulea* [5] and *Colletotrichum lindemuthianum* [1] hitherto, there is no information on the production from *Colletotrichum gloeosporioides*, *Colletotrichum acutatum* and *Fusarium solani*. Therefore, the aim of this work was to determine CDA production of these phytopathogenic fungi in SmC and SSC cultures. On the other hand, we were looking at the molecular identification of CDA genes produced by these fungi.

MATERIALS and METHODS

Microorganisms. The strains *Aspergillus niger*, *Colletotrichum gloeosporioides*, *Colletotrichum acutatum* and *Fusarium solani* were cultivated in slants on potato dextrose agar. Spore suspensions were obtained by mechanical stirring with a sterile solution of 0.1% (v/v) Tween 80.

Media. Basal composition for SmC and SSC (weight/L water): 15 g of glucose, 6.6 g of glutamic acid, 1 g of K₂HPO₄, 0.5 g of MgSO₄·7H₂O, 1.8 mg of ZnSO₄·7H₂O, 1 mg of FeSO₄·7H₂O, 0.3 mg of MnSO₄·H₂O, 0.4 mg of CuSO₄·5H₂O, 1 mg of thiamine and 1 mg of nicotinic acid [1].

SmCs were carried out in 50 ml medium. Then medium was inoculated with 1×10^6 spores/ml and incubated at 28°C. Samples were taken in duplicates at 24, 48, 72 and 96 h. Cultures were filtered and biomasses were determined as dry weight. The filtrates from cultures were used as crude enzymes.

SSC was carried out in glass columns packed with 0.3 g of polyurethane foam (PUF) with size *ca.* 0.125 cm^3 . PUF was impregnated with the medium previously inoculated (1.8×10^8 spores/g PUF) in a ratio of 4.5 ml of medium per 0.3 g of PUF. The columns were incubated at 28°C. Samples were taken in duplicates at 24, 48, 72 and 96 h. SSC solid support was collected from each column and compressed to 1,000 psi and the resulting medium collected, and then the support was washed with 4.5 ml of distilled water and compressed again. Crude enzyme was obtained by mixing the two liquid fractions and then filtered through a $0.45 \mu\text{m}$ pore size sterile filter. Biomass was determined as dry weight of the PUF after culture.

CDA assay. CDA activity was determined in the crude enzyme following the method of Kauss and Bausch [6] using ethyleneglycol chitin as substrate and *D*-glucosamine-HCl ($0.035 \mu\text{mol/ml}$) as standard. One unit of CDA was defined as *the amount of enzyme required to release 1 μmol of acetate per minute at standard condition.*

Results were expressed as mg of biomass and yields of CDA based on initial dry weight substrate (U/g IDS), considering glucose, glutamic acid and minerals as substrates.

SEM analysis was carried out in scanning electron microscope (JEOL JSM-5900 LV, Tokyo, Japan) with samples withdrawn at the highest CDA activities. PUF of SSC and pellets of *SmC* were fixed in glutaraldehyde (5% v/v), treated with OsO_4 (1% w/v) and dehydrated with methanol; then covered with gold prior to SEM analyses.

Gene identification. Molecular identification was done by PCR using primers designed from consensus regions found on *C. lindemuthianum* [7] and *Magnaporthe grisae* [8] and reported CDA genes in the Genbank database using the BioEdit Sequence Alignment Editor 5.0.6. Forward primer (F-Deg) was degenerated in 3 nucleotides (5'-GACGACGWTCCTTCACTWCAC-3') and Reverse primer (R-CDA) was identical to the consensus region (5'-CCGAGGCACTCGCCGACGGTGACGGC-3'). Genomic DNA from *C. acutatum* and *C. gloeosporioides* was obtained by phenol-chloroform extraction [9]. PCR amplification was performed in 25 μL of PCR reaction mix containing 2.5 μL of reaction buffer, 1 unit of Taq polymerase, 6 mM MgCl_2 , 5 μM of each primer, 2.5 mM dNTPs, 50 ng of template gDNA and 0.25 mg of BSA. Amplification was carried out with an initial denaturation of 5 min at 95 °C, followed by 35 cycles of 30 s at 94 °C, 1.5 min at 58-65 °C and 1 min at 72 °C with a final extension of 7 min at 72 °C. Amplicons (5 μl) were confirmed by electrophoresis on 1.5% agarose gel in TBE buffer (108g TrisHCl, 55g boric acid, 40 ml of EDTA 0.5mM, pH 8.0 on 1 liter of distilled water). Total PCR products (20 μl) were separated by agarose gel (1.8%) electrophoresis. Bands were excised and purified according to the Wizard® SV Gel and PCR Clean-Up System. Purified bands were reamplified to corroborate the quality of the products. Finally, bands were directly sequenced in a automatic sequencer (ABI 377 DNA-sequencer, Applied Biosystems, USA) by the BigDye terminator cycle sequencing-ready reaction kit according to the instructions of manufacturer (Applied Biosystems, USA) and analyzed with BLAST, BLASTX and TBLASTX.

RESULTS and DISCUSSION

The biomass production was lower in *SmC* than in SSC, which might be explained by the duration of lag phases and thus fungi did not reach the stationary phase in *SmC* (Figure 1a). This is in agreement to previous reports [10], in which fungi are well adapted to grow in moist substrates as in SSC as in their natural conditions, hence fungal growth is favored and culture time might be shorter. Herein most of tested fungi reached the stationary phase at 48 h and only *A. niger* grew faster (Figure 1).

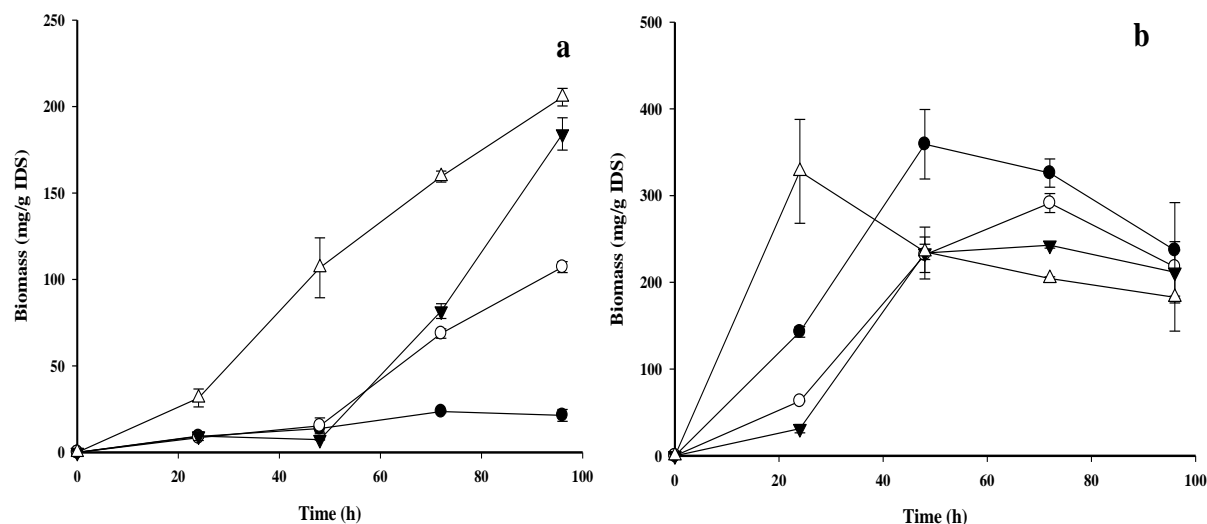


Figure 1 Kinetics of biomass production of the phytopathogenic fungi in: (a) SmC and (b) SSC. Symbols ● *C. gloeosporioides*, ○ *C. acutatum*, ▼ *F. solani*, △ *A. niger*.

Kinetics of CDA activity displayed the highest for *C. gloeosporioides* in SmC, whereas *C. acutatum* and *F. solani* only presented CDA activities in SSC. CDA production with *C. acutatum* and *C. gloeosporioides* in SSC were not significantly different ($\alpha \leq 0.05$) (Figure 2). *A. niger* did not show CDA activity in any culture, regardless previous reports on its purification [11] and its identification of several CDA genes [12] in *Aspergillus fumigatus*.

This atypical behavior of higher enzyme production in SmC than that in SSC has been also observed in the production of exopectinases of *A. niger* cultured with pectin as carbon source [13]. SSC only was advantageous when sucrose was added as carbon source owing to catabolic repression of this saccharide over exopectinases. Another report on production of laccases by *Pleurotus ostreatus* [14], in which higher activity in SmC than SSC was claimed and attributed to lower protease activity in SmC than that in SSC, thereby the stability of laccases was better preserved in SmC. De-Santiago [15] did not find significant differences in the production of CDA of *C. gloeosporioides* between SmC and SSC (with perlite as inert support). CDA production by *C. lindemuthianum* was previously reported [16], to reach 460 U/g IDS using wheat bran supplemented with chitosan, while 392 U/g IDS was obtained with shrimp shell chitin waste. This higher activity was attributed to the organic support that serves as nutritional source, as well as chitosan and chitin, which stimulate CDA production [15, 17, 18].

SEM

CDA production has been reported to start with appresoria formation in *Uromyces viciae-fabae* [19] and *Colletotrichum lagenarium* [20]. Therefore, SEM was carried out in order to observe whether these infective structures were developed in both cultures within the maximum CDA production for each phytopathogenic fungi. Spores were observed with a typical length (10µm) and morphology of *C. gloeosporioides* [21], appresoria were also noticed but only in SSC, and these were developed over the PUF surface (Figure 3). SEM from samples of SmC and SSC of *C. acutatum* at 24 h showed spores with similar length and morphology to *C. gloeosporioides* (Figure 4) and appresoria were observed in both cultures, according to previous reports potassium and calcium ions, simple sugars and pH and temperature gradients can also stimulate appresoria formation [22]. In addition, SEM from samples of SmC and SSC of *F. solani* at 24 h (Figure 5) showed typical spores of the genus *Fusarium*. Appresoria were present in low number only in SSC, whereas growing mycelia was observed in SmC with the absence of infective structures or spores. This indicates that CDA production in *F. solani* is dependent on appresoria formation, thereby the lack of CDA activity in SmC.

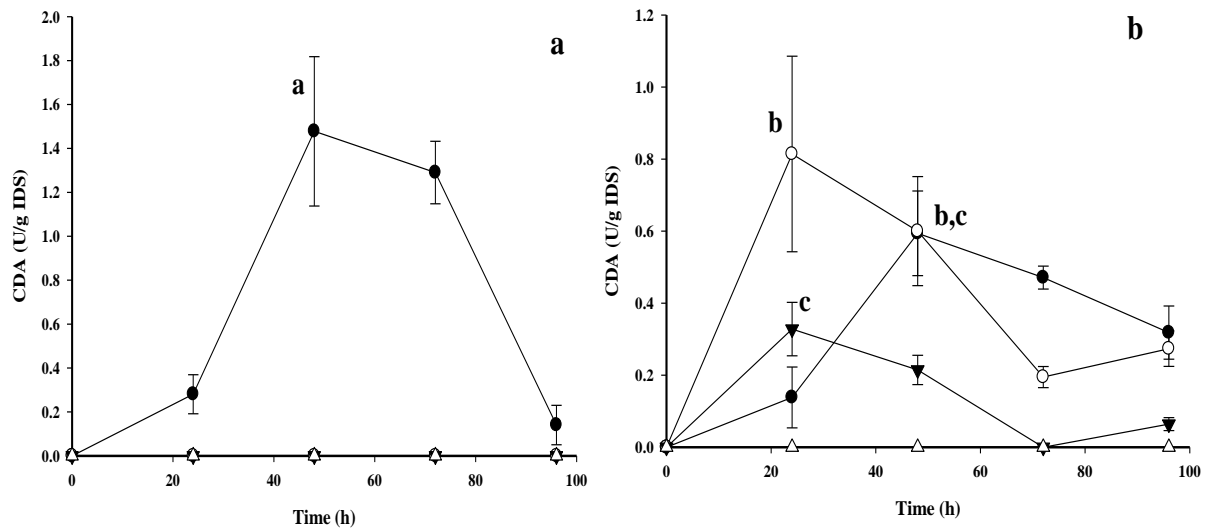


Figure 2 Kinetics of CDA production of the phytopathogenic fungi in: (a) SmC and (b) SSC. Symbols ● *C. gloeosporioides*, ○ *C. acutatum*, ▼ *F. solani*, △ *A. niger*. Means with the same letter are not significantly different ($\alpha \leq 0.05$).

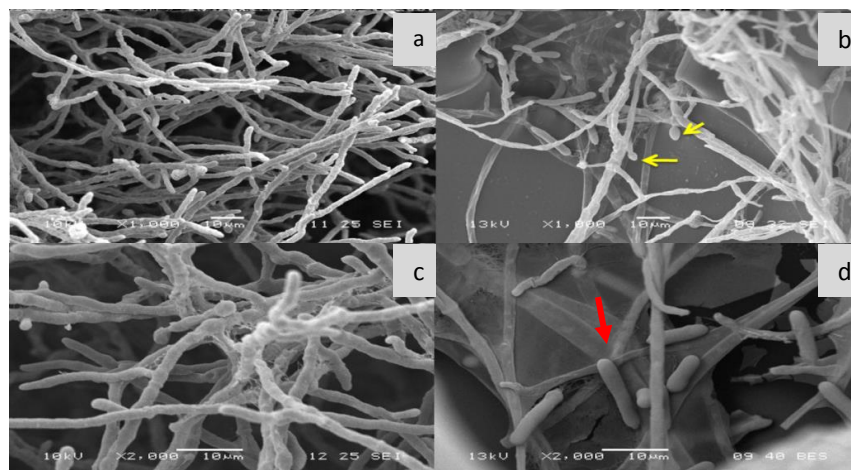


Figure 3 SEM of *C. gloeosporioides* in SmC (a and c) and SSC (b and d) at 48 h. Appresoria are indicated by yellow arrows and spores by red arrows.

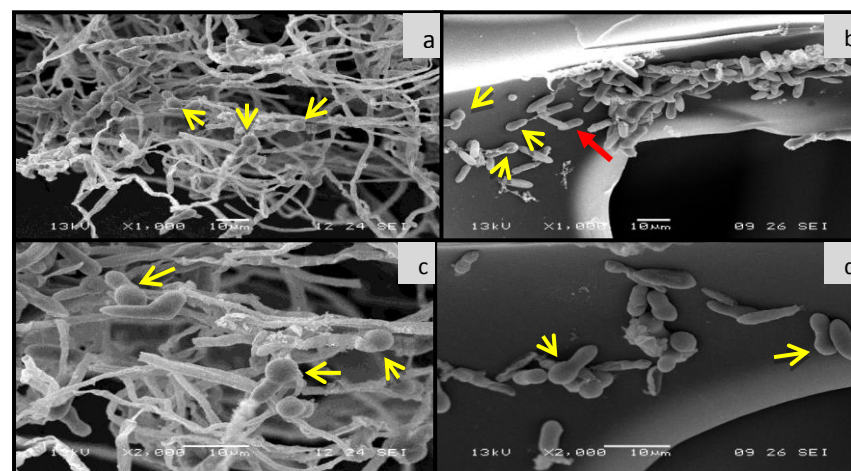


Figure 4 SEM of *C. acutatum* in SmC (a and c) and SSC (b and d) at 24 h. Appresoria are indicated by yellow arrows and spores by red arrows.

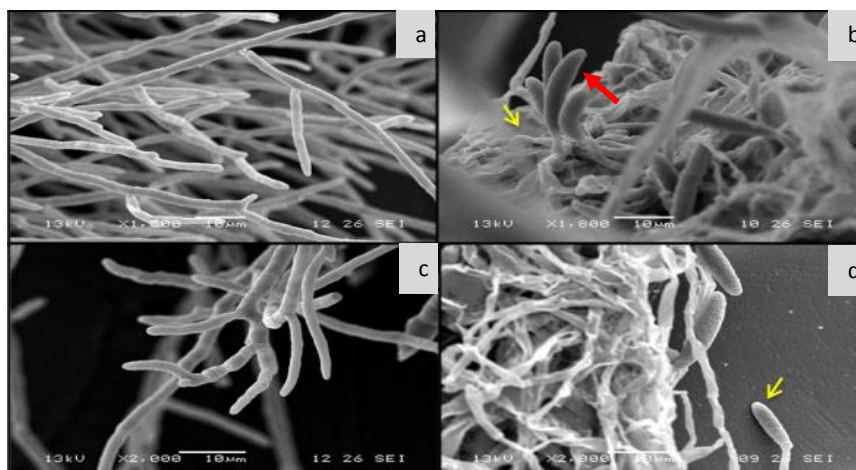


Figure 5 SEM of *F. solani* in SmC (a and c) and SSC (b and d) at 24 h. Appressoria are indicated by yellow arrows and spores by red arrows.

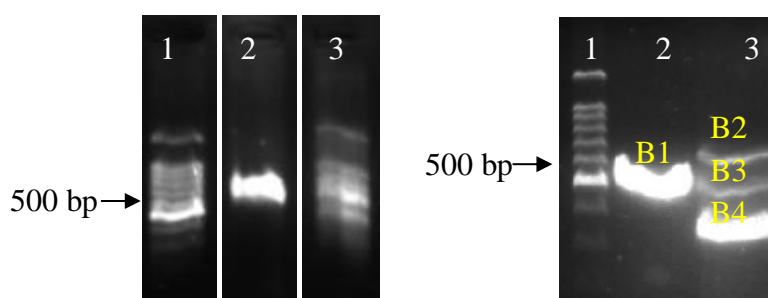


Figure 6 (a) PCR amplification of *C. acutatum* and *C. gloeosporioides*: 1) 100 pb MWM, 2) *C. acutatum* F-Deg/R-CDA and 3) *C. gloeosporioides* F-Deg/R-CDA. (b) Electrophoresis of PCR products of *C. acutatum* and *C. gloeosporioides* in a 1.8% agarose gel: 1) 100 pb MWM, 2) *C. acutatum* F-Deg/R-CDA (B1) and 3) *C. gloeosporioides* F-Deg/R-CDA (B2, B3 and B4)

The obtained sequences are the following:

Band B1 of *C. acutatum* using primer F-Deg: CGACCGTCGCCGCAACAACGTCAAGG
CCACCTTCTTCGTC AACGGCAACA ACTGGGGCAACATCGAGACGGCACCCGGCCC
GGACAACATCCGCCGCATGAAGGCCGAGGGTCACCTCATCGGCTCTCACACCTACT
CTCACCCGGATCTGAGCACCCTCTCCTCGGCGGACCGCATCTCTCAGATGACCCAG
CTCGAGGACGCGACCCGCCGTATCGCCGGCTTCGCGCCCAAGTACATGCGCGCGCC
GTTCTCTCCTGCGACGCCGCTTGCCCTGAGCGATATGGCCAGCCTGGGCTACCACG
TCATCGACACCAGCCTCGATACAAAGGATTACGAGAACGACACCCCCGAGACCAC
GCACATCTCGGCTGAGAAGTTCAACAACGAGCTTAGCGCCGACGCCGCGAGCAAC
AGCTACATTGTCCTCTCCACGATGTCCACCAGCAGACTGTCTGTTTCTCTGGTGCAG
AAGATGATCGACAACCTCAAGTCCAAGGGCTACCGCGCCGTCACCGTCCGGCGAGT
GCCTCGG

Band B2 of *C. gloeosporioides* using primer F-Deg: GCGACGCCTATCCTCCACGTCA
GCTGTGCACATCGATCATCGCTGGAGACACATTAGTAGGACATGATCAACGGC
TCCGTCAGCACCCCTGCAGGAAGTACCCCAAACCTGCCCGTAATCTGGCCGAGATC
TGACTACATCAGCACATGATTGCCGAGGGTACCAGGTCGCCAGCCACACGTGGT
TCACGAGAACCTCGACTCCTTGACACTGTCCAGCGCCAGAACCAGATGGTGTACA
ACGAGATCGCCTTACCAGACATCTTGGGCTTCTACCCTACTTACATGCGTCTCCTT
ACTCCATCTGCGGATCCGAGTGCCAGGGACAGATGGCCGATCTTGGTTACCACATC
ACCTACTTTGATCTCGACACTCAGGGTTACCTGCACACCGACCCTAGCCAGATCGG
CGTCAGCGTCAACCTGTGGGGACCAAGCCATGCTGGCCAGGTCTCCTTGGCACGGG
CTCCTACTTGCACATCGAGGCACGACATTCACCAGCAGATTGCCAGGTTCTTACT
CCTCACATTCTGGACCTCCGTCGTTGCCAACGGCTGGAGGGCCGTCACCGTCCGGCG
AGTGCGCTCAG

Analysis of sequences provided similarity to other CDA genes and proteins (Table 1). *C. acutatum* band B1 showed more similarity to CDA genes and proteins from *C. lindemuthianum*, while *C. gloeosporioides* band B2 showed similarity to CDA genes and proteins of other *Colletotrichum* genus and fungi.

CONCLUSION

The type of culture, SSC or SmC, influenced the production of CDAs and the highest activity was found in SmC with *C. gloeosporioides*. Nonetheless, SSC is still challenging because the production of CDA occurred only in SSC for some fungi.

Table 1 Analysis of the obtained sequences from *C. acutatum* and *C. gloeosporioides* with BLAST, BLASTX and TBLASTX tools (NCBI).

Fungi	Band	Description	E value	Max. identity	Genebank ID	Reference	Analysis tool
<i>C. acutatum</i>	B1	<i>C. lindemuthianum</i> CDA gene sequence	10^{-40}	84%	AY633657.1	[7]	BLAST
		Chain A, structure of CDA from <i>C. lindemuthianum</i>	3×10^{-99}	79%	2IW0_A	[23]	BLASTX
		<i>C. lindemuthianum</i> CDA gene sequence	3×10^{-92}	NA	AY633657.1	[7]	TBLASTX
<i>C. gloeosporioides</i>	B2	<i>M. grisea</i> CDA complete gene	10^{-31}	75%	AB535713.1	[8]	BLAST
		Chitin binding protein from <i>Colletotrichum higginsianum</i>	10^{-61}	73%	CCF45230.1	NA	BLASTX
		<i>Myceliophthora thermophila</i> carbohydrate esterase family 4 protein mRNA	6×10^{-41}	NA	XM_003662913.1	[24]	TBLASTX

NA Not available.

ACKNOWLEDGEMENTS

The authors acknowledge the financial support from CONACYT Government of Mexico (Project No.105628) and for scholarship (FM).

REFERENCES

1. Tsigos I. And Bouriotis V. (1995). J Biol Chem. 270: 26286-26291.
2. El Gueddari N., Rauchhaus U., Moerschbacher B., Deising H. (2002). New Phytol 156:103-112.
3. Tsigos I., Martinou A., Kafetzopoulos D., Bouriotis V. (2000). Trends Biotechnol 18: 305-311.
4. Araki Y., Ito E. (1975). Eur J Biochem. 55, 71-78.
5. Gao X., Katsumoto T., Onodera K. (1995). J Biochem 117, 257-263.
6. Kauss H. and Bauch B. (1988). Method Enzymol. 161, 518-523.
7. Shrestha B., Blondeau K., Stevens W., Hegarat F. (2004). Protein Expres Purif. 38, 196-204.
8. Murata S., Ohno Y., Nakajima Y., Kamakura T. (2009). Unpublished. Accession in NCBI: AB535713.1
9. Brown T. (1993). Essential molecular biology: A practical approach. IRL Press at Oxford University Press. Volume I.
10. Hölker U., Lenz J. (2005). Curr Opin Microbiol. 8,301–306.
11. Alfonso C., Nuero O., Santamaría F., Reyes F. (1995). Curr Microbiol. 30, 49-54.
12. Nierman W., Pain A., Anderson M., Wortman J., Kim H., Arroyo J., Berriman M., Abe K., Archer D., Bermejo C., Bennett J., Bowyer P., Chen D., Collins M., Coulson R., Davies R., Dyer P., Farman M., Fedorova N., Fedorova N., Feldblyum T., Fischer R., Fosker N., Fraser A., Garcia J., Garcia M., Goble A., Goldman G., Gomi K., Griffith-Jones S., Gwilliam R., Haas B., Haas H., Harris D., Horiuchi H., Huang J., Humphray S., Jimenez J., Keller N., Khouri H., Kitamoto K., Kobayashi T., Konzack S., Kulkarni R., Kumagai T., Lafon A., Latge J., Li W., Lord A., Lu C., Majoros W., May G., Miller B., Mohamoud Y., Molina M., Monod M., Mouyna I., Mulligan S., Murphy L., O'Neil S., Paulsen I., Peñalva M., Perteau M., Price C., Pritchard B., Quail M., Rabinowitsch E., Rawlins N., Rajandream M., Reichard U., Renauld H., Robson G., Rodriguez de Cordoba S., Rodriguez-Peña J., Ronning C., Rutter S., Salzberg S., Sanchez M., Sanchez-Ferrero J., Saunders D., Seeger K., Squares R., Squares S., Takeuchi M., Tekaiia F., Turner G., Vazquez de Aldana C., Weidman J., White O., Woodward J., Yu J., Fraser C., Galagan J, Asai K., Machida M., Hall N., Barrell B., Denning D. (2005). Nature. 438, 1151-1156.

13. Díaz-Godínez G., Soriano-Santos J., Augur C., Viniestra-González G. (2001). *J Ind Microbiol Biot.* 26, 271-275.
14. Téllez-Téllez M., Fernández F. J., Montiel-González A., Sánchez C., Díaz-Godínez G. (2008). *Appl Microbiol Biot.* 81, 675-679.
15. De Santiago C. (2011). Estudio del efecto de inductores sobre la actividad quitina desacetilasa de hongos fitopatógenos. Master degree Thesis. UAM.
16. Suresh P., Sachindra N., Bhaskar N. (2011). *J Food Sci Tech.* 48, 349-356.
17. El Ghaouth A., Arul J., Grenier J., Asselin A. (1992). *Exp Mycol.* 16, 173-177.
18. Murad A., Noronha E., Miller R., Costa F., Pereira C., Mehta A., Caldas R., Franco O. (2008). *Microbiology.* 154, 3766-3774.
19. Deising H. and Seigrist J. (1995). *FEMS Microbiol Lett.* 127, 207-212.
20. Siegrist J. and Kauss H. (1990). *Physiol Mol Plant P.* 36, 267-275.
21. Zulfikar M., Brlansky R., Timmer L. (1996). *Mycologia.* 88:121-128.
22. Hoch H., and Staples R. (1991). New York: Plenum. 25-46.
23. Blair D. Hekmat O., Schuttelkopf A., Shrestha B., Toyuyasu K., Withers S., Van Aalten D. (2006). *Biochemistry.* 45, 9416-9426.
24. Berka R., Grigoriev I., Otiillar R., Salamov A., Grimwood J., Reid I., Ishmael N., John T., Darmond C., Moisan M., Henrissat B., Coutinho P., Lombard V., Natvig D., Lindquist E., Schmutz J., Lucas S., Harris P., Powlowski J., Bellemare A., Taylor D., Butler G., de Vries R., Allijn I., van den Brink J., Ushinsky S., Storms R., Powell A., Paulsen I., Elbourne L., Baker S., Magnuson J., Laboissiere S., Cluterbuck A., Martinez D., Wogulis M., de Leon A., Rey M., Tsang A. (2011). *Nat Biotechnol.* 29, 922-927.

ENZYMATIC HYDROLYSIS OF CHITOSAN TO OBTAIN OLIGOMERS USING A CELLULASE ENZYMATIC COMPLEX AND ITS SCALING AT PILOT PLANT LEVEL

H. Ortega-Ortiz^{1*}, B. Gutiérrez-Rodríguez², G. Cadenas-Pliego¹

¹Centro de Investigación en Química Aplicada, Blvd. E. Reyna #140, Saltillo, México. CP. 25294. Tel. +52 844 438 98 30.

²UAdeC, Depto. de Biotecnología, Blvd V. Carranza e Ing. J. Cárdenas V., Saltillo, México. CP 25208.

*Email: hortensia.ortega@ciqa.edu.mx

ABSTRACT

Chitin is a polysaccharide formed from units of N-acetyl-D-glucose-2-amine; they are linked together through links β -1,4 in the same way as the glucose units do in cellulose. Chitin is the second most abundant natural polymer after cellulose and the chitosan its deacetylated derivative. The production of oligosaccharides from enzymatic hydrolysis of chitosan has many advantages compared to other hydrolysis methods reported before, like well defined molecular weight, narrower molecular weight distributions and purer products. In this paper, we report the scaling at pilot plant level of chitosan oligomers synthesis, using a cellulase enzymatic complex from *Trichoderma viride*, from the reaction conditions set up at laboratory level in an earlier work of the group. The results showed that the scaling process is feasible and also inexpensive. Furthermore, the molecular weights of the reaction products can be easily controlled by the concentration of enzymatic complex.

Keywords

Chitosan oligomers, enzymatic complex, enzymatic hydrolysis.

INTRODUCTION

Chitin is a lineal polysaccharide composed by linkages of (β -1-4)-2-acetylamino-2-deoxy- β -D glucopyranoside. It is obtained from exoskeletons of crustaceans and in the last years has significantly increased its production, due to the multiple applications of this polymer and its derivatives in medicine, nutrition, cosmetic industry and agriculture [1]. Chitin is also the second most abundant polymer in nature after cellulose, it is relatively easy to obtain and is a renewable resource.

Chitosan is the main derivative of chitin and is obtained by its partial or complete deacetylation, which increases the ability of the polymer to become soluble in water. Among the advantages of chitosan are its usage in agriculture, its solubility in water or weak diluted alkalines, and unlike chitin, its growth inhibitory activity for a large amount of phytopathogen fungi [2,3], the induction of defensive responses and protection against pathogens in plants [4, 5, 6] and the increase in the yield of several crops [7].

The degree of acetylation [GA] and degree of polymerization [GP] of chitosans are key in the anti-fungal activity against phytopathogens and in the induction of defensive responses

in the plant. Several authors have demonstrated the increase of induction of several defensive responses like peroxidase activity (PAL) and increase of when acetylation values of chitosans are increased, achieving maximum values of such activities with GA above 20% in chitosan [4, 8]. However, the growth inhibitory activity of phytopathogen fungi increases as the degree of acetylation increases in the polymer [2]. On the other hand, GP of chitosan has an outstanding effect in its biological activity, related to the growth inhibitory activity of pathogens [2], to the induction of defensive responses [4] and protection against pathogens [5, 6].

For the above mentioned, chitosan degradation, either chemical or enzymatic, releases portions which, depending on the parameters indicated (GP and GA) and on the pathogen or plant variety used, cause a wide range of responses. Actually, these responses are under major researches in this field [4, 5, 8]. And because enzymatic degradation is more specific, it makes easier to control the preparation of bioactive oligomers and it has been demonstrated the ability of chitosan to be hydrolyzed by a large number of enzymes, among the most important are the cellulases [9 - 13].

Taking this in consideration, the aim of this work was to assess the potential to use a cellulase enzymatic complex for degradation of chitosan and to use its low molecular weight oligomers at laboratory level and scale it at pilot plant level (100 liters)

MATERIALS and METHODS

Raw material. Chitosan from Marine Chemicals with a molecular weight of 200,000 (defined in a mixture of 0.3M of acetic acid solvents/ 0.2M of sodium acetate at 30°C), calculating with equation from Mark-Houwink where $\eta = KMv^\alpha$, $k = 7.6 \times 10^{-2}$ and $\alpha = 0.76$. Celobiridin, commercial compound from the company Bio Rad obtained from fungus *Trichoderma viride*. Such compound is comprised of a mixture of different cellulose enzymes, mainly endoglucanases, celobiohydrolases and other kinds of hydrolytic enzymes.

Chitosans characterization. The degree of deacetylation was defined by FTIR, preparing samples of KBr in an IR Nicolet 550 [14] spectrophotometer. Also, infrared spectra were obtained from each of chitosan oligomers, as well as their degree of deacetylation. On the other hand, the thermal behavior of chitosan and chitosan oligomers was studied. This was performed using differential scanning calorimeters (DSC) brand TA instruments model DSC 2920 Modulated DSC, with a heating rate of: 10°C/min and in a thermogravimetric analyzer (TGA) brand TA instruments model TGA Q/500 at a rate of 10°C/min under nitrogen atmosphere at 50 mL/min up to 600°C and from 600 to 750°C in oxygen ATM.

Enzymatic hydrolysis of chitosan at laboratory level. Enzymatic hydrolysis was made in glass Bath type reactors of 50mL with a control temperature level; mounted on a mechanical stirring device.

Experimental Procedure. The enzymatic hydrolysis was studied using a 50 mL glass reactor where chitosan solution in 0.05M acetates buffer was put and then stirring was applied during 5 minutes to keep the temperature constant, and then 0.5 mL of enzyme solution were added, being the total volume of reactor mixture of 10 mL and stirring during 6 hours, taking 1 mL aliquots to determine the reducing sugars content formed at the following hydrolysis times: 0.5, 1, 3 and 6 hours [15]. The enzymatic reaction was paused in each aliquot by the addition of Somogyi-Nelson reagent [16]. For each variable (pH, temperature, substrate concentration and enzyme concentration) five different values were used and they were

assessed three times. Each point of the plot is the mean of two independent hydrolysis experiments. The percentage of hydrolysis was calculated according to the amount of glucose produced at the end of the process [17].

Scaling at Pilot Plant Level. According to the results, different reaction conditions were selected to obtain the oligomers based on molecular weight in a 100 liters reactor at CIQA's pilot plant. The reaction conditions to obtain the three oligomers were the same, varying only the enzyme concentration. Chitosan oligomer 1: temperature of 40°C, pH of 4.5, substrate concentration of 1% and 20 mg/mL of enzymatic complex; for chitosan oligomer 2 the concentration of enzymatic complex was 40 mg/mL, and finally for the chitosan oligomer 3 the concentration of enzymatic complex was 80 mg/mL.

RESULTS and DISCUSSION

The optimum values for the variables of chitosan hydrolysis based on the formation of reducing sugars like reaction products were obtained after preliminary kinetic study: temperature of 50°C, pH of 4.0, substrate concentration of 0.5% and enzymatic complex concentration of 0.15 mg/mL.

The results were statistically processed by bifactorial analysis, using product and concentration as sources of variation, followed by Duncan's multiple range tests for the means at 1% of significance [17].

Similarly to other studies reporting use of inexpensive commercial enzymes like pectinases, cellulases, hemicellulases, among others, to degrade chitosans [18-20], which was effectively performed when highly specific enzymes are used, meaning an outstanding improvement for producing hydrolyzed chitosan under inexpensive and feasible way.

Study of chitosan hydrolysis with enzymatic complex. Table 1 shows the hydrolysis values of chitosan, detecting formation of oligomers by means of Somogy-Nelson's reducing sugars (RS); 6 hours after starting reaction a maximum conversion of 7% of substrate was achieved using 1mg/mL of complex concentration.

Table 1. Kinetics of chitosan hydrolysis at different concentrations of enzymatic complex.

[E] mg/mL	Time (h)	[RS] mg/mL
0.50	1	0.0052
0.50	3	0.0115
0.50	6	0.0205
0.67	1	0.0102
0.67	3	0.0203
0.67	6	0.0425
1.00	1	0.0204
1.00	3	0.0406
1.00	6	0.0736

[E].-enzymatic complex concentration. pH 4.0 and T=50°C.

When comparing initial reaction rates (Figure 1) it can be clearly detected the linearity of enzymatic process (0.0052, 0.0102 and 0.0204 mg/mL). This is an important result because

despite working with commercial extract composed of large variety of enzymes, the kinetic behavior is similar to pure enzyme. Taking into account the obtained results, the use of Celobiridin enzymatic complex to produce chitosan oligomers offers many advantages in terms of low molecular weight and highly homogeneous material according to the tests.

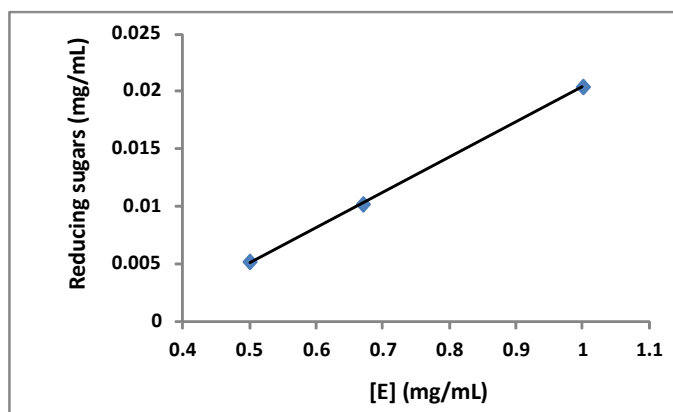


Figure 1. Initial rates of chitosan enzymatic hydrolysis.

On the other hand, the thermal behavior of commercially available chitosan and oligomers by DSC and TGA (Figure 2) showed that the commercial chitosan has the highest thermal transition corresponding to the lost of water around 120-122°C. For oligomers the thermal transitions were observed at lower temperatures (115°C).

In the TGA comparing a commercial chitosan with the oligomer which the last presents four different components, where the first two could be some volatile components and retained water, and the last two can be structures more stable corresponding to crosslink cycles, or glucosidic cycles, and the last one could correspond to some inorganic component left in the material, coming from the washing solution.

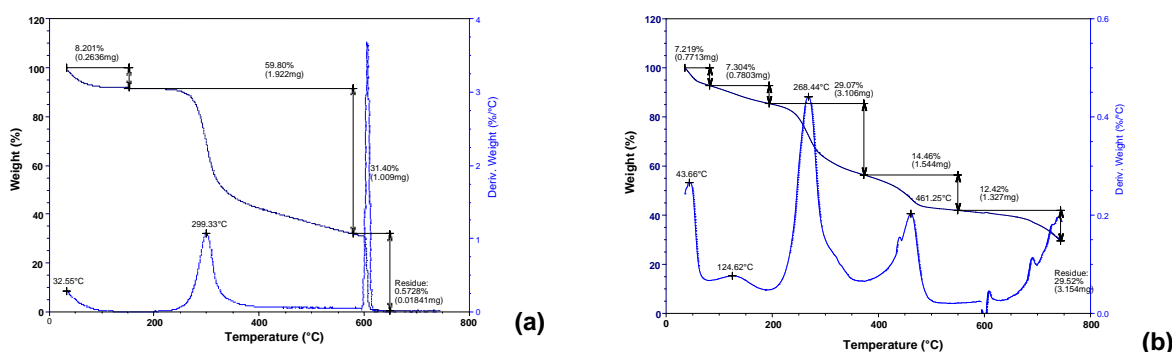


Figure 2. TGA of commercially available chitosan (a) and chitosan oligomer (b).

The graph that represents the molecular weights obtained at reaction conditions selected by laboratory kinetic studies is shown on Figure 3. Each oligomer was obtained from a batch process modifying only the concentration of enzymatic complex. According to these results it is concluded the feasibility to obtain chitosan oligomers of different molecular weights varying only some of the reaction variables, like enzyme concentration.

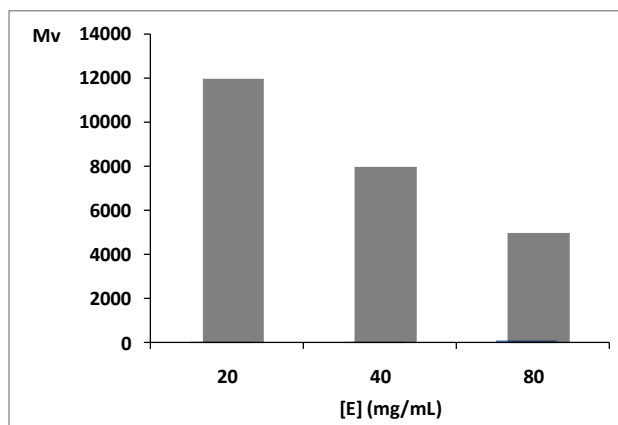


Figure 3. Molecular weights of chitosan oligomers obtained by enzymatic hydrolysis of commercially available chitosan with molecular weight $M_v=200,000$. Reaction conditions: $T=40^\circ\text{C}$, $\text{pH}=4.5$ and $[\text{Cs}]=1\%$.

In the infrared spectra it was possible to assess the deacetylation degree; being for the commercially available chitosan of 86% and 100% for the three oligomers obtained at pilot plant level using the formula reported by Brugnerotto, *et al.* [14].

CONCLUSIONS

Hydrolysis of high molecular weight chitosan was possible using commercially available enzymatic hydrolysis and the basis of a methodology to obtain chitosan oligomers at laboratory and pilot plant level was set.

Besides chitosan hydrolysis, enzymatic treatment allowed complete deacetylation of oligomers in one single step.

Thermogravimetric analysis shows that molecular weight has a significant impact on chitosan thermal properties.

ACKNOWLEDGMENTS

The authors wish to thank to CONACyT for the support given through project CB80425.

REFERENCES

[1] Leffler, M. (1997). Chitin Breakdown: The Bacterial Way, *Maryland Marine Notes*, 15(2), March-April.

- [2] El Gaouth, A.; Arul, J. (1992). Asselin, A. y Benhamou, N. Antifungal activity of chitosan on post-harvest pathogens: induction of morphological and cytological alterations in *Rhizopusstolonifer*. *Mycol. Res.*, 9, 769-779.
- [3] Laflamme, P.; Benhamou, N.; Bussi eres, A.; Dessureault, P. (1999). Differential effect of chitosan on root fungal pathogens in forest nurseries. *Can. J. Bot.*, 77, 1460-1468.
- [4] Kauss, H.; Jeblick, W.; Domard, A.; Siegrist, J. (1997). Partial acetylation of chitosan and a conditioning period are essential for elicitation of H₂O₂ in surface-abraded tissues from various plants. *Advances in Chitin Sciences*, 2, 94-101.
- [5] Struszczyk, H.; Schanzenbach, D.; Peter, M.; Pospieszny, H. (1999). Biodegradation of chitosan. In: Chitin and Chitosan. Polish and Russian monograph. pp. 59-75. Polish Chitin Society, Serie 1.
- [6] Pospieszny, H. (1999). Potential use of chitosan in plant protection. In: Chitin and Chitosan. Polish and Russian monograph. pp. 115-130. Polish Chitin Society, Serie 1.
- [7] Freepons, D. (1990). Plant growth regulators derived from chitin. US Patent 4964894.
- [8] Vander, P.; Varum, K. M.; Domard, A.; El Gueddari, N. E. and Moerschbacher, B. M. (1998). Comparison of the ability of partially N-acetylated chitosans and chitooligosaccharides to elicit resistance reactions in wheat leaves. *Plant Physiol.*, 118, 1353-1359.
- [9] Pantaleone, D.; Yalpani, M. and Scollar, M. (1992). Unusual susceptibility of chitosan to enzymatic hydrolysis. *Carbohydr. Res.*, 237, 325-332.
- [10] Aiba, S. (1994). Preparation of N-acetyl-oligosaccharides by hydrolysis of chitosan and chitinase followed by N-acetylation. *Carbohydr. Res.*, 265, 323-328.
- [11] Jeon, Y. and Kim, S. (2000). Production of chitooligosaccharides using an ultrafiltration membrane reactor and their antibacterial activity. *Carbohydr. Polymers*, 41, 133-141.
- [12] Shin-Yaa, Y.; Lee, M. Y.; Hinode, H. and Kajuchi, T. (2001). Effects of N-acetylation degree on N-acetylated chitosan hydrolysis with commercially available and modified pectinases. *Bioch. Engin. Journal*, 7, 85-88.
- [13] Aiba, S. and Muraki, E. (1998). Preparation of higher N-acetylchitooligosaccharides in high yields. Proceedings of the Third Asia-Pacific Chitin and Chitosan Symposium. Feelung, Taiwan, pp. 89-96.
- [14] Brugnerotto, J.; Desbrieres, J.; Roberts, G.; Rinaudo, M. (2001). An infrared investigation in relation with Chitin and chitosan characterization, *Polymer*, 4, 291-297.
- [15] Vazquez-Chaires Y., Ortega-Ortiz H. y Guti errez-Rodr guez B. (2007). "Hidr lisis enzimtica de quitosano mediante un complejo enzimtico Celuloltico", XII Congreso Nacional de Biotecnologa y Bioingeniera, Acapulco, Mxico.
- [16] Nelson, N. (1944). A photometric adaptation of the Shomogy method for the determination of glucose. *J. Biol. Chem.*, 153, 375-380.
- [17] Guti errez-Rodr guez, B.; Ortega-Ortiz, H.; Barrera,-Aguilar, E. (2009). "Optimizaci n de los Parmetros Cinticos de la Hidr lisis Enzimtica de Quitosano Mediante un Complejo Enzimtico Celuloltico", XIII Congreso Nacional de Biotecnologa y Bioingeniera, Morelia, Mxico.
- [18] Pantaleone, D., M. Yalpani, and M. Scollar. 1992. Unusual susceptibility of chitosan to enzymatic hydrolysis. *Carbohydr. Res.*, 237, 325-332.
- [19] Yalpani, M., & Pantaleone, D. (1994). An examination of the unusual susceptibilities of aminoglycans to enzymatic hydrolysis. *Carbohydrate Research*, 256, 159-175.
- [20] Terbojevich, M., Cosani, A. & Muzzarelli, R.A.A. (1996). Molecular parameter of chitosans depolymerized with the aid of papain. *Carbohydr. Polym.*, 29 (81), 63-68.

CRUDE ENZYME OF *Colletotrichum gloeosporioides* WITH CHITIN DEACETYLASE ACTIVITY ON CHITINOUS SUBSTRATES

Neith Pacheco,^{1,2} Stéphane Trombotto,³ Laurent David,³ Claudia Patricia Larralde-Corona,⁴ Keiko Shirai.^{1*}

¹Universidad Autónoma Metropolitana, Biotechnology Department, Laboratory of Biopolymers. Av. San Rafael Atlixco No. 186. Col. Vicentina, C.P. 09340. México City. Tel. (525)5804-49-21 Fax. (525) 5804-47-12. ²Present address: Centro de Investigación y Asistencia Tecnológica del Estado de Jalisco A.C. Unidad Sureste. ³Laboratoire des Matériaux Polymères et des Biomatériaux Université Lyon 1, France. ⁴Centro de Biotecnología Genómica, Instituto Politécnico Nacional.

*E-mail address: smk@xanum.uam.mx

ABSTRACT

Chitin deacetylases have been detected in the culture media of submerged fermentation of the phytopathogenic fungus *Colletotrichum gloeosporioides*. Maximal specific activity of 0.018 U/mg of protein was obtained after 96h of cultivation at pH 6 and 28°C. Two bands of proteins with molecular weights of 170 kDa and 35 kDa displayed chitin deacetylase activity determined by electrophoresis under semi native conditions. Extracellular crude enzymatic extract and reacylated commercial chitosan (52% acetylated) were used to estimate the kinetic parameters of acetate production as undirected deacetylation measurement. The highest acetate production rate of 0.26 1/h was attained with 75mg/ml of substrate. Acetylation degree, molecular weight and crystallinity index of chitinous substrates were evaluated following enzymatic deacetylation. This work provides novel information from a producer of chitin deacetylase and its activity towards biological production of chitosan.

Keywords

Chitin Deacetylases, *Colletotrichum gloeosporioides*, chitinous substrates, chitosan

INTRODUCTION

Chitin is a β -(1 \rightarrow 4)-linked polysaccharide composed mostly of N-acetyl-D-glucosamine (GlcNAc) residues. Chitosan, its n-deacetylated derivative, is a copolymer of D-glucosamine (GlcN) and GlcNAc residues [1]. The high alkali concentrations at high temperatures used in the chemical production of chitosan makes this process environmentally unsafe and not easily controlled [1,2,3]. On the other hand Chitin Deacetylases (CDAs) are glycoproteins with molecular masses ranging from 24 to 150 kDa with optimum temperature for enzyme activity of 50°C while optimum pH varies from 4.5 to 8.5 [4,2]. The use of CDAs is prompted as a useful tool to produce biotechnologically chitosan with unique properties suitable for specific applications [1,2,3] and an alternative to the chemical method. CDAs have been reported in several fungi as well as in some marine bacteria and insect species [5,6,7,8]. CDAs have shown an important role in chitosan biosynthesis in the cell wall of some fungi and in fungal growth in Zygomycetes. They are also involved in oligosaccharide deacetylation during autolysis and are suggested to have a biological role in plant-pathogen interactions [5,9]. Despite of all CDAs reported are active on chitin oligomers, it is still challenging to achieve a high degree of enzymatic deacetylation in chitin substrates mainly due to the insoluble and crystalline nature of this biopolymer. The aim of this work was to evaluated CDAs production from submerged

fermentation of the plant pathogenic fungus *C. gloeosporioides* and its application in chitinous substrates deacetylation.

MATERIALS and METHODS

Materials: *C. gloeosporioides* was isolated from sections of damaged plant tissues (fruits, calyxes and leaves) of *Citrus limon* var Eureka (Italian lemon) and identified as it is reported elsewhere [10]. Ethylene glycol chitosan from Sigma (USA) and commercial chitosan (Kitomer) were reacylated to activity determinations [11,8]. α -Chitin was obtained biologically and chemically [8]. β -chitin was also chemically purified [8].

Microorganism Cultivation and Submerged fermentation conditions: *C. gloeosporioides* was cultivated on potato dextrose agar (PDA) and a inoculum size of 1×10^6 spores/ml was obtained. Spore suspension was inoculated to a 3L instrumented bioreactor (Applikon B.V. Holland) containing a medium reported previously [6] during 6 days at 28°C and pH 6. Samples were taken every 24h, after centrifugation at 12 700 g and 4°C during 25 min pellets were recovered using deionized water, then filtered through filter paper (Whatman 40) and dried overnight at 100°C. Dry weight of mycelia was then determined. Supernatants obtained from the fungal culture were concentrated by salting out (40 and 80% wt/v of $(\text{NH}_4)_2\text{SO}_4$). The enzymatic assay and protein determinations were carried out in concentrated and non concentrated samples. Protein content was determined by Bradford method (1976) using serum albumin as standard.

Determination of Enzyme activity and detection of activity by SDS-PAGE: CDA activity was determined by a spectrophotometric method [11] and acetate production determined by gas chromatography [8]. In both cases one unit of activity was defined as the amount of enzyme necessary to release 1 μmol of acetate from ethylene glycol-chitin per minute. Acetate production rates were estimated by the Gompertz model using the non-linear regression program (STATISTICA StatSoft, Inc) as reported previously [8].

Culture filtrates and concentrated crude enzyme were subjected to sodium dodecyl sulfate polyacrylamide gel electrophoresis SDS-PAGE (mini Protean II Bio-Rad, Hercules, CA, USA) under semi native conditions, to detect activity according the methodology described elsewhere [13]. After CDA detection, the bands obtained were analyzed with the ImageJ software using a known molecular weight standard proteins (Bio-Rad), to determine molecular weight M_W of the enzymes under such conditions. SDS-PAGE was also conducted under denaturing conditions (mini Protean II Bio-Rad) [14]. A broad range of M_W protein standards (Bio-Rad) was used as a reference.

Chitin modifications and characterization: Chemically deacetylated chitins (CHC), Microwave deacetylated chitins (MiWe-BIOCH), Chitin sponge (BIOCH-Spg), precipitated chitins (Precipitated BIOCH-Spg), Hydrolyzed chitin (H-BIOCH) were produced by the method described else where [8]. Products were further characterized to determine solubility, molecular weight (M_W), acetylation degree (DA), Crystalline Index (I_{CR}) as reported previously [8,12], and evaluated as substrates for CDAs.

The data were subjected to analyses of variance and multiple comparison of means by Tukey Kramer test in order to determine significant differences of CDA activities among the chitinous substrates ($p < 0.05$) using the statistical program NCSS (NCSS, PASS and GESS, 2001).

RESULTS and DISCUSSION

Chitin deacetylases production and detection activity after SDS-page electrophoresis

The maximum CDA production of the fungus *C. gloeosporioides* in submerged culture was 0.018 (U/mg of protein) after 96h of cultivation. CDA secreted into the culture medium has been related with mycelia growth in *Absidia glauca* and *M. Anisopliae*, and associated to the end of fungal growth autolysis *C. lindemuthiaunum* [17,18]. Herein the maximum value of specific activity obtained from the culture filtrate was higher than that

reported in the literature for *C. lindemuthianum* (0.002 U/mg of protein) after 72h [6] and similar to that reported after 432h (0.019 U/mg of protein) [18]. After precipitation with 40% followed by 80% of ammonium sulfate a recovering of 68% of enzyme and concentration of 5-fold of CDAs activity was achieved. Crude enzyme and its concentrated extract were subjected to SDS-PAGE denaturing conditions. The protein profile of the produced extracellular enzymes is shown in Figure 1. M_w of proteins present in the crude enzyme after 96h of the *C. gloeosporioides* culture was estimated by SDS-PAGE under semi native conditions, after UV illumination two bands were observed corresponding to the molecular weights of 170 kDa and 35 kDa that displayed CDA activity, as revealed by the zymogram shown in Figure 2d. The molecular mass for most of chitin deacetylases reported in the literature is in the range of 25 – 80 kDa, although a 150kDa molecular mass was found in *C. lindemuthianum* DSM 63144 [17].

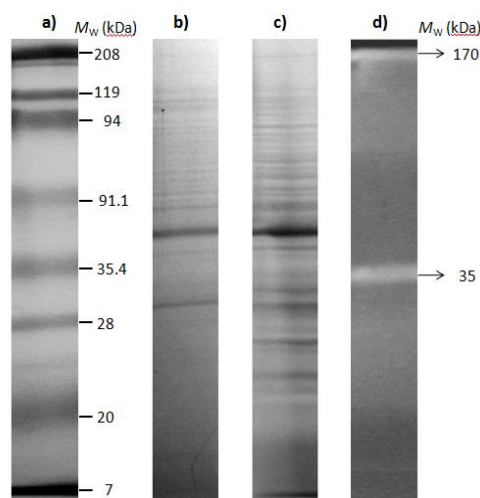


Figure 1. SDS-PAGE of: (a) Molecular weight standards, stained with coomassie blue; extracellular proteins from (b) crude enzyme (c) concentrated crude enzyme of *C. gloeosporioides* stained with coomassie blue; (d) Zymogram under seminative conditions with ethylene glycol chitin stained with Calcofluor white of concentrated crude enzyme.

CDA activity with different reacylated chitosan concentrations

A constant concentration of crude enzymatic extract with activity of 0.15 U/ml and a reaction time of 12h were used to evaluate the kinetics of different substrate concentrations, using reacylated chitosan as substrate. Acetate was rapidly produced during the first 2h of reaction for all substrate concentrations tested, and the steady state was reached after 3h. Acetate production values obtained during the deacetylation of each substrate concentration were adjusted to the Gompertz model ($R^2 < 0.98$). The higher acetate production of 12.59 $\mu\text{mol/mL}$ and 12.9 $\mu\text{mol/mL}$ were obtained using 5mg/mL and 7.5mg/mL of substrate, respectively, without significant differences ($p < 0.05$), as shown in Figure 2. The highest k obtained were 0.026 h^{-1} and 0.025 h^{-1} , corresponding to the substrate concentrations of 10 mg/mL and 12.5 mg/mL, respectively (Fig. 2). A higher substrate concentration could increase the rate of acetate production due to increased amount of *N*-acetyl groups; nevertheless a poor acetate production using higher concentrations can be explained due to less accessibility of the acetyl groups caused by a poor solubilization of the reacylated chitosan in the media.

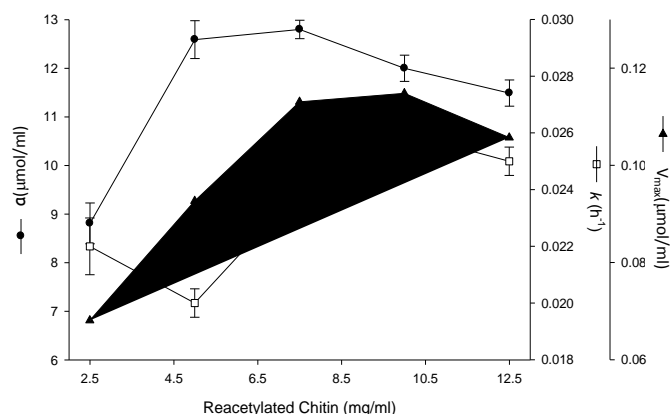


Figure 2. Kinetic parameters of acetate production estimated by Gompertz model obtained during chitin deacetylation after 180min of reaction.

Characterization of initial chitinous substrates and after CDA activity

Solubility, Crystalline index (I_{CR}), Molecular weight (M_W) and degree of acetylation (DA) of chitinous samples before enzyme evaluation are shown in table 1. X-ray diffraction profiles for BIOCH, CHC, MiWe-BIOCH, BIOCH-Spg and precipitated BIOCH-Spg displayed the five crystalline reflections corresponding to the α -chitin indexed as 020, 110, 120, 101 and 130 [12], are shown in Fig. 3. For the sponge samples a reflection located at $2\theta = 30$ was observed, that might correspond to the calcium carbonate use to the sponge preparation. β -chitin X-ray diffraction profile was similar to the profile reported previously [13] and D-BIOCH displayed only 3 reflections identified in β -chitin profile. Hydrolyzed chitin and reacylated chitosan did not show crystal reflections, indicative of an amorphous structure (Figure 3).

Table 1. Solubility and Crystalline index (I_{CR}) of initial samples; Molecular weight (M_W) and degree of acetylation (DA) of chitinous samples before and after enzyme evaluation.

Samples	Initial				Final	
	Solubility (%)	I_{CR}	M_W (1×10^3 g/mol)	DA(%)	M_W (1×10^3 g/mol)	DA(%)
Reacylated chitosan	69 ± 1.8	0	458 ± 32	52 ± 1	328 ± 56.2	37 ± 2
BIOCH ^a	0	86.4	1200 ± 73	95.5 ± 1	1198 ± 92.6	95.3 ± 1
CHC ^b	0	78.5	851 ± 96	94.5 ± 2	839 ± 82.3	94.41 ± 2
β -chitin	2 ± 0.4	84	831 ± 25	89.2 ± 1	799 ± 22.0	83.7 ± 1
D-BIOCH ^c	25 ± 1.1	72.7	783 ± 24	72.8 ± 1	713 ± 23.6	60.8 ± 1
MiWe-BIOCH ^d	1.6 ± 0.8	82.7	413 ± 12	91 ± 2	371 ± 5.8	88.38 ± 1
BIOCH-Spg ^e	10.4 ± 0.7	79.2	334 ± 26	92.4 ± 1	329 ± 8.3	86.29 ± 2
Precipitated BIOCH-Spg ^f	2.6 ± 1.3	74.7	267 ± 7	89.4 ± 2	275 ± 2.3	81.55 ± 1.6
H-BIOCH ^g	19.8 ± 1.6	59.4	102 ± 9	79.9 ± 2.9	86 ± 7.4	55.3 ± 3

^aBiological chitin, ^bChemical chitin, ^cBiologicalchitin chemically deacetylated, ^dMicrowave biological chitin, ^eBiological chitin sponge, ^fPrecipitated from biological chitin sponge, ^gHydrolyzedbiological chitin.

The reaction conditions obtained previously for CDA activity were applied in different chitinous substrates, the results showed that deacetylation was not possible in insoluble chitinous substrates, biological (BIOCH) and chemical (CHC) extracted chitin (table 1). This is in agreement with previous works [19, 20] for CDAs from *Absidia coerulea* and *Mucor rouxii*, respectively. The high I_{CR} in BIOCH made difficult the enzyme penetration which also agrees with reported elsewhere [1,3]. Although CHC presented a lower I_{CR} , no deacetylation was observed. On the other hand, β -chitin showed deacetylation of 5.5% after enzymatic process, even in the presence of a high crystalline ratio. This could be interpreted as a partial deacetylation restricted in the amorphous phase. The 3 samples of non modified chitin did not present significant differences ($p < 0.05$) on the evolution of M_W during the enzyme addition. For D-BIOCH, deacetylation of 12% was achieved. This

is in good agreement with higher solubility, lower I_{CR} and M_W values that could favor enzyme penetration due to the increment on the amorphous content. The initial DA also improved solubilization thus favoring the deacetylation. MiWe-BIOCH exhibited a lower M_W in comparison with BIOCH, but I_{CR} and solubility values were similar. After enzyme addition, only a slight deacetylation of not more than 3% was achieved. This result suggests that crystalline content and solubility have a higher impact in enzymatic deacetylation than M_W . BIOCH-Spg and precipitated BIOCH-Spg presented deacetylation of only 6% that may also be attributed to the crystalline structure, as values were higher than in D-BIOCH, thus reducing enzyme penetration keeping in mind that at low solubility might affect as well the deacetylation [3]. Crude enzyme of CDAs was able to induce up to 25% of deacetylation in hydrolyzed BIOCH: in this case a reduction around of 31% in I_{CR} , which could be a key factor to improve deacetylation [3] (Table 1).

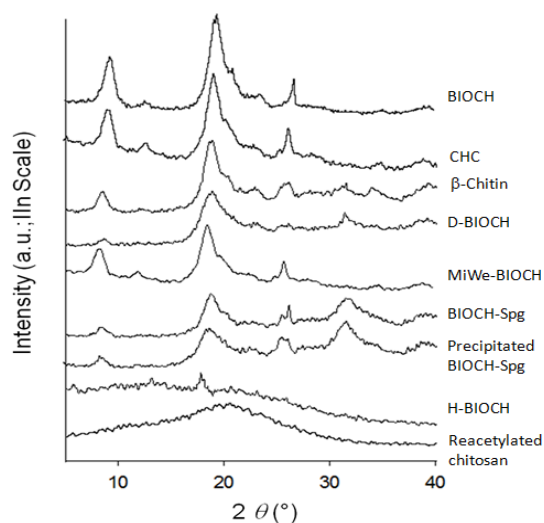


Figure 3. X-ray diffraction patterns of BIOCH, CH-C, β -chitin, D-BIOCH, MiWe-BIOCH, BIOCH-Spg, precipitated BIOCH-Spg, H-BIOCH and reacetylated chitosan.

CONCLUSION

The phytopathogenic fungus *Colletotrichum gloeosporioides* produced extracellular chitin deacetylases in a maximum of 0.018 U/mg of protein after 96h of cultivation at pH 6 and 28°C. Two bands of proteins with molecular weights of 170 kDa and 35 kDa displayed CDA activity as determined by electrophoresis under semi native conditions. Parameters of acetate production as undirected deacetylation measured with substrate concentration of 75mg/ml at its maximum reaction time (180min) were obtained using reacetylated chitosan with DA of 52%. I_{CR} and relative solubility proved to be key factors on enzymatic deacetylation of CDAs from *C. gloeosporioides*. A deacetylation of 25% on hydrolyzed chitins obtained by biological methods (HBIOCH) was attained with a high increase of solubility and a decrease of crystallinity index, and around 20% decrease on M_W . Thus, a controlled hydrolysis of initial chitin could be of great interest to produce chitosan by full or partial biological processes.

ACKNOWLEDGEMENTS

We gratefully thank CONACyT (project No. 105628) for research funding and for postdoctoral grant (NP). We thank Ruben Vera for assistance during the diffraction experiments (University Claude Bernard Lyon 1 Diffractometry Center).

REFERENCES

[1] Tsigos, I., Martinou, A., Kafetzopoulos, D., and Bouriotis, V. 2000. Chitin deacetylases: new versatile tools in biotechnology, *Tibtech*. 18: 305-312.

- [2] Aye, K. N., Karuppuswamy, R., Ahamed, T. and Stevens, W. F. 2006. Peripheral enzymatic deacetylation of chitin and reprecipitated chitin particles. *Bioresource Technol.* 97: 577-582.
- [3] Beaney, P. D., Gan, Q., Magee, T. R. A., Healy, M., Lizardi-Mendoza, J. 2007. Modification of chitin properties for enzymatic deacetylation. *J Chem. TechnolBiotechnol.* 82:165-173.
- [4] Young-Ju, K., Zhao, Y., Oh K-T., Nguyen, V-N. and Park, R-D. 2008. Enzymatic deacetylation of chitin by extracellular chitin deacetylases from a newly screened *Mortierella* sp. DY-52. *J. Microbiol. Biotechnol.* 18(4): 759-766.
- [5] Araki, Y. and Ito, E. 1975. A pathway of chitosan formation in *Mucorrouxii*. *Eur. J. Biochem.* 55, 71-78.
- [6] Tsigos, I and Bouriotis, V. 1995. Purification and characterization of chitin deacetylase from *Colletotrichumlindemuthianum*. *J BiolChem.* 270(44):26286-26291.
- [7] Win, N.N. and Stevens, W.F. 2001. Shrimp chitin as substrate for fungal chitin deacetylase. *Appl. Microbiol. Biotechnol.* 57: 334-341.
- [8] Pacheco, N. PhD Thesis 2009.
- [9] Siegrist, J., Kauss, H. 1990. Chitin deacetylase in cucumber leaves infected by *Colletotrichum lagenarium*. *Journal Physiological and Molecular Plant Pathology* 36 (4): 267-275.
- [10] Rosas-Hernández I., De Santiago C., Larralde-Corona CP., Arguijo de la Cruz E., Shirai K. and Narváez-Zapata JA. Occurrence and pathogenic evaluation of *Colletotrichum gloeosporoides* within an endophytic fungal community associated to *Citrus limon* var *Eureka*
- [11] Kauss, H. and Bauch, B. 1988. Chitin deacetylase from *Colletotrichumlindemuthianum*. *MethodsEnzymol.* 161:518-523.
- [12] Pacheco, N., Garnica-González, M., Gimeno, M., Bárzana, E., Trombotto, S., David, L., Shirai. 2011. Structural characterization of chitin and chitosan obtained by biological and chemical methods. *Biomacromolecules.* 12:3285-3290.
- [13] Trudel, J. and Asselin, A. 1990. Detection of chitin deacetylase activity after polyacrylamide gel electrophoresis. *Anal Biochem.* 189:249-253.
- [14] Laemmli UK. Cleavage of structural proteins during the assembly of the head of bacteriophage T4. *Nature* 1970;227:680-5.
- [15] Lamarque, G., Viton, C.M. and Domard, A. 2005. New Route of Deacetylation of α - and β -Chitins by Means of Freeze-Pump Out-Thaw Cycles. *Biomacromolecules.* 6: 1380-1388.
- [16] Focher, B.; Beltrame, P. L.; Naggi, A.; Torri, G. *Carbohydr.* 1990. Alkaline N-deacetylation of chitin enhanced by flash treatments. *Reactionkinetics and structuremodifications. Polym.,* 12, 405.
- [17] Zhao, Y., Park, R., Muzzarelli, R. 2010. Review: chitin deacetylases: Properties and Applications. *Mar. Drugs.* 8:24-46
- [18] Tokuyasu, K., --ohnishi-Kameyama, M., Hayashi, K. 1996. Purification and characterization of extracellular chitin deacetylase from *Colletotrichumlindemuthianum*. *Biosci. Biotech. Biochem.* 60(10):1598-1603.
- [19] Stevens W. F., Win, N.N., Ng, C. H., Pichayangkura, C., Chandkrachang, S. 1997. Towards technical biocatalyticdeacetylation of chitin. In :Domard A. Roberts GAF, Varum KM](eds). *Advances in chitinscience.,* 2:360-365.
- [20] Martinou, A., Kafetzopoulos, D. and Bouriotis, V. 1995. Chitin deacetylation by enzymatic means: monitoring of deacetylation processes. *Carbohydr Res.* 273(2): 235-242.

ENZYMATIC HYDROLYSIS OF CHITIN BY CHITINASES FROM *Lecanicillium lecanii*

Guadalupe Villa-Lerma,¹ Humberto González-Márquez,¹ Miquel Gimeno,² Alberto López,¹ Keiko Shirai*¹

¹ Universidad Autónoma Metropolitana, Departamento de Biotecnología, Laboratorio de Biopolímeros. San Rafael Atlixco 186. Mexico City C.P. 09340

² Universidad Nacional Autónoma de México, Facultad de Química, Ciudad Universitaria, Mexico City.

*E-mail address: smk@xanum.uam.mx

ABSTRACT

Production of chitinases and proteases from the fungus *Lecanicillium lecanii* were evaluated upon the effect of culture medium, the type of chitin and pH. The best conditions were found using Czapeck medium supplemented with 10 g/L of colloidal chitin and varying the pH from 5 to 8. The maximum enzyme production under these conditions was attained at 96 h and at pH 6 with activities of 0.029, 2.26 and 1.1 U/mL for *N*-acetylhexosaminidases (Nases), endochitinases (Endo) and proteases (Prot), respectively. Additionally, partial purification of the enzyme extract was conducted in order to separate proteases by salting out, followed by preparative size exclusion chromatography (SEC). After this purification, no proteolytic activity was detected on the fractions with the highest chitinolytic activity. These fractions were employed in the hydrolysis of raw and colloidal chitin, as well as, sonicated and steam exploded chitins. Results from hydrolases were compared and discussed herein.

Keywords: Chitin, *Lecanicillium lecanii*, Chitinases, steam explosion.

INTRODUCTION

Chitin, the linear polysaccharide composed of β -1-4-*N*-acetyl-D-glucosamine and *D*-glucosamine units, is one of the most abundant biopolymers and it is commercially extracted mainly from the exoskeletons of crustaceans. The hydrolysis of chitin between C1 and C4 of two consecutive monomer units of *N*-acetylglucosamine or *D*-glucosamine is catalyzed by chitinases. These enzymes are widely distributed in plants, animals and microorganisms [1]. In bacteria and fungi, chitinases are related to nutrition, morphogenesis, parasitism and pathogenesis. Chitinase activity of entomopathogenic fungi occurs during the invasion of the insect cuticle, which is regulated by chitin degradation products and pH [2,3]. Chitinolytic enzymes from *Serratia marscescens*, *Streptomyces griseus* and the fungi *Trichoderma harzianum* have wide range of potential applications in molecular biology, agriculture (biocontrol) and oligomers and NAG production [1]. On the other hand, the fungus *Lecanicillium lecanii* is an excellent biocontrol agent against insects. The antagonism process of these fungi is mediated by a massive invasion of external layers of the cuticle followed by penetration to the internal tissues. Therein, the actions of chitinases, proteases and lipases as well as mechanical pressure are key factors for the degradation of the cuticle of the insect [2]. We have previously reported the production of chitinases from *L. lecanii* in submerged and solid-substrate cultures [3-5], however, despite of the high production of chitinases in solid substrate cultures (SSC)s [4,5] there is a constraint in pH and temperature control in such systems. Alternatively, in submerged cultures (SmC)s pH and media composition might be evaluated as crucial factors toward production of chitinolytic enzymes of *L. lecanii*. In addition, removal of proteases to attain pure mixtures of chitinases is advantageous for their effective application in oligosaccharide production. Herein, we report the production of chitinolytic enzymes from *L. lecanii* by SmC, their partial purification and action on the hydrolyses of three chitin substrates, raw chitin, colloidal chitin, sonicated chitin and steam explosion-treated chitin.

MATERIALS and METHODS

Microorganism. *L. lecanii* ATCC 26854 was cultured on potato dextrose agar at 25 °C for 7 days and stored at 4°C. Spore suspension was prepared by mechanical agitation of with sporulated cultures with sterile solution of 1% (wt/v) of Tween 80 up to a concentration of 10⁷ spores/mL.

SmC. Cultures were carried out in a 3L reactor (Applikon BV, Holland) at 100 rpm, 1 vvm, at 25 °C for 144 h, using two culture media: Czapeck medium (QMC) and mineral medium (QMM). Two colloidal chitin concentrations were evaluated (g/L): 10 (QMC10, QMM10) and 30 (QMC30, QMM 30). Carbon source was tested using colloidal chitin and raw chitin (10.68% ash and 6.29% protein); the culture pH was kept at 6 by addition of HCl or NaOH (0.1N) and another maintaining pH 5 for 72 h and subsequently increasing one pH unit every 24 h up to 8 days.

Determination of enzymatic activities. Samples were centrifuged at 12,700 g and 4 °C for 25 min, the supernatants were considered crude enzyme and analyzed for Nhase activity using p-Nitrophenyl-β-N-acetylglucosamine [6]. Endo was determined using colloidal chitin [7]. Prot was determined by the method of Kunitz [8]. Protein concentration was determined by Bradford [9].

Precipitation with (NH₄)₂SO₄. Crude enzyme was precipitated by adding ammonium sulfate. The precipitated fraction was solubilized in 0.05M Tris-HCl buffer, 0.15 M NaCl at pH 7.8 and determined enzyme activities and protein.

SEC. Fractions from the ammonium sulfate precipitation were injected on a Sephacryl S-100 High Resolution 26/60 column (GE Healthcare, USA). Elution was carried out using an isocratic flow of 1.3 mL/min of solution buffer 0.05M Tris-HCl-0.15 M NaCl at pH 7.8.

SDS polyacrylamide gel electrophoresis (SDS-PAGE). Denaturing SDS-PAGE conditions were employed following the method of Laemmli [10]. Gels were stained by silver staining (Bio-Rad, USA, using wide range molecular mass markers (Bio-Rad). For zymograms the standard method of Laemmli was also used. Gels contained 0.01% (w / v) of 4-methylumbelliferyl-NNN-acetyl-β-D-glucosamine for Endo activity and 4-methylumbelliferyl-N-acetyl-β-D-glucosamine (Sigma Chemical) for Nhase.

Pretreatment of chitin for enzymatic hydrolysis. Chitin samples were pulverized and sieved to a particle size of 177 μm and then treated with the following procedures: i) suspended in citrate phosphate buffer (50 mM pH 6) and sonicated for 20 min [11]; ii) mixed with water using concentrations of 0.1, 0.2, 0.4, 2 g/mL and steam exploded within reaction times of 1, 3, 5 and 8 min at a temperature of 180°C [12].

Crystallinity Index (I_{CR}) and apparent crystal size (D_{ap}) of chitin treated with steam explosion. X-Ray diffraction measurements were carried out in a diffractometer (Bruker D8 Advance) with an incident radiation CuKα and wavelength of λ = 1.5418 Å in the range of 2θ = 4.5 – 50 °C with steps of 0.02°. I_{CR} of the samples was determined according to the method reported by Focher et al. [13].

Conditions for enzymatic hydrolysis. Sonicated and steam exploded samples were suspended in citrate phosphate buffer (50 mM; pH 6) at concentration of 2.5 mg/mL. Enzyme activity of 0.1 U/mL was used in a constant stirring (200 rpm) at 40 °C [14]. Finally, the reaction medium was centrifuged for 10 min at 399 g, supernatant was filtered through a 0.45 μm and the amount of reducing sugars was determined by the method of Miller [14].

RESULTS and DISCUSSION

Production of chitinases. QMC10 medium gave the highest Nhase (0.012 U/mL) and Endo (5.57 U/mL) productions and the lowest Prot (0.42 U/mL) (Table 1). This might be attributed to the high amount of carbon and nitrogen present in that medium, as reported by Giuliano et al. [15]. High levels of ammonia and glucose results in very low chitinolytic activity, thus affecting the inductive effect of chitin, thereby when both nutrients (nitrogen and carbon) are limited, activity is greatly increased [15]. Sun and Liu [16] reported carbon an interesting work on the requirements of entomopathogenic fungi, including *L. lecanii*, finding that the growth and sporulation were enhanced with monosaccharides and disaccharides such as sucrose, cellobiose, mannose and fructose as carbon sources, while the polysaccharides did not promote biomass production.

Chitin type. QMC10 medium was selected for further experiments owing to high Nhase and Endo but low Prot activities. The effect of chitin type (colloidal and raw) is shown in Table 2, where raw chitin involved the lowest Endo and Nhase activities. Raw is a less digestible substrate than the colloidal chitin because during the preparation of the latter concentrated HCl is employed, which might induce depolymerization. Contrarily to the results found in this work, Fenice and co-workers [17] evaluated raw and colloidal chitin as carbon sources for cultivation of *V. lecanii* and pointed to highest chitinolytic activities using raw chitin although the maximum activity was delayed up to 120 h. They also found that raw chitin sustained higher fungal growth, which led to an increased amount of protein in the crude enzyme thereby lower specific activity than that with colloidal chitin.

Table 1. Effect of media formulation and chitin amount in the enzyme production

Culture media	Nhase (U/mL)	Endo (U/mL)	Prot (U/mL)
QMM10	0.0006 ± 2.709E-05 d	2.6666 ± 0.1222 b	0.5611 ± 0.0673 a
QMM30	0.0027 ± 5.639E-05 c	2.32 ± 0.0002 c	0.4888 ± 0.0419 b
QMC10	0.0123 ± 0.0009 a	5.5733 ± 0.1222 a	0.4183 ± 0.0293 b
QMC30	0.0076 ± 0.0004 b	1.2267 ± 0.1665 d	0.4666 ± 0.0166 b

Data are the mean of three independent observations and their standard deviation. Different letters in the same column are significantly different ($p < 0.05$)

Table 2. Effect of type of chitin in volumetric activity of chitinases and proteases

Culture media	Nhase (U/mL)	Endo (U/mL)	Prot (U/mL)
QMC10 raw	0.0007 ± 1.628E-05 b	1.8133 ± 0.1222 b	0.1222 ± 0.0254 b
QMC10 colloidal	0.0109 ± 0.0008 a	5.5733 ± 0.1222 a	0.2488 ± 0.0092 a

Results showed are the mean of three independent observations and their standard deviation. Different letters in the same column are significantly different ($p < 0.05$)

Effect of pH. pH 6 displayed the highest activity, however increasing the pH from 7 to 8 both resolved in dramatic increase of Endo and Nhase activities, which might be attributed to the increase in proteolytic activity at 120 h. Prot might hydrolyze chitinases, therefore partial purification of the extracts was carried out to avoid that. Our results agree to those obtained by Ramirez-Coutiño [18] where at pH 6, Nhase and Endo were significantly higher than at pH 5. Figure 1 shows enzymatic activity upon pH variation, where maximum chitinolytic activities are attained at 96 h, reaching 0.029 U/mL and 2.26 U/mL for Nhases and Endo, respectively. On the other hand, during cultivation at constant pH Nhases and Endo were 0.012 and 5.57 U/mL, respectively. It is worth mentioning that although Endo volumetric activities are higher in QMC10 media with constant pH (5.57 U/mL), in terms of the specific activities those where 47.32 U/mg protein with varying pH of culture but 3.32 U/mg protein at constant pH, thus QCM10 media with pH variations was selected as the best condition for our purposes.

Fenice et al [19] reported with *L. muscarium* a pattern of at least 5 chitinolytic enzymes (including Endo and Exochitinases), which is typical behavior in mycoparasitic fungi such as those belonging to the genus *Trichoderma* [20]. Therein, maximum activity was found between 132 and 144 h to ca. 0.009 U/mL and 5.5 U/mL for Nhase and Endo, respectively. St. Leger et al. [21] reported that pH is one of the factors that most influence the production of chitinases, establishing that the pH at which the greatest amount of chitinolytic enzymes or any other type of

enzymes are produced is that at which enzyme exhibits its highest activity. The authors also pointed that this effect is due to the tendency of the microorganism to auto-regulate its environment.

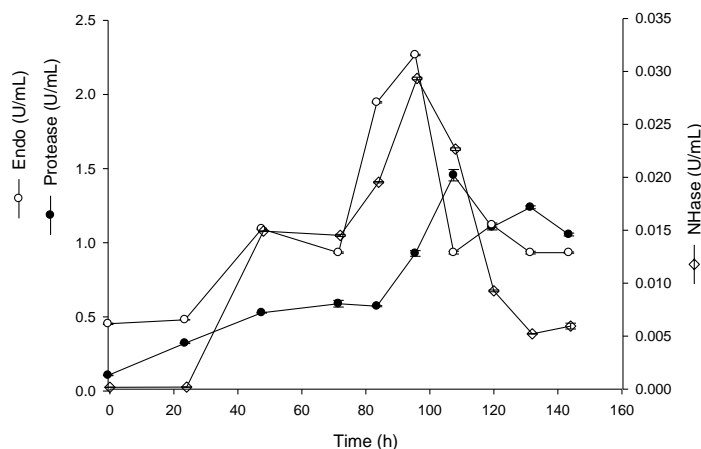


Figure 1. Kinetics of chitinolytic enzyme production with QMC10 medium and variation of pH

Partial purification of chitinases. The percentage of saturation that showed high activity was ranged between 60% (85.2 U/mg protein) and 80% (91.3 U/mg protein). Therefore, precipitate from 60% was chosen in further purification. After preparative SEC, the activity was 4,875 U/mg protein with a purification factor of 53.42 and a percentage of recovery of 12% (Table 3). Regarding the Endo purification, a specific activity of 13.84 U/mg of protein was attained with a purification factor of 3.21 and 24.32% recovery. SEC fractions signals for Nhase and Endo appeared between 19 to 23 min, with a peak in fractions 21 min and 22 min of 0195 U/mL and 0.72 U/ mL for Nhase and Endo, respectively. The SEC fractions were used for enzymatic hydrolysis of chitins. It is noteworthy that after SEC, there was no detection of proteolytic activity, whereas the crude enzyme subjected to ammonium sulfate precipitation gave a remaining protease activity of 3.42 U/ml.

Table 3. Summary Nhase and Endo purification process

Purification step	Protein (mg)	Activity (U)		Specific Activity (U/mg)		Recovery (%)		Purification fold	
		Endo	Nhase	Endo	Nhase	Endo	Nhase	Endo	Nhase
Crude enzyme (CE)	280 ± 0.12	74	40.6	0.264	0.14	100	100	1	1
Precipitate with 60% (NH ₄) ₂ SO ₄	64 ± 0.05	42.6	28.8	0.665	0.45	57.6	70.9	2.51	3.1
SEC (Fractions 19-23)	1.3 ± 0.002	18	4.875	13.84	3.75	24.32	12.00	3.21	53.42

SDS-PAGE and zymograms. Low intensity bands of protein were observed in the crude extract owing to the low concentration unlike the bands present in the precipitate with ammonium sulfate. After SEC, few bands were found, 75, 50 and 37 kDa (Figure 2a). Zymograms with the fractions with higher Endo activity (Figure 2b) and Nhase activities (Figure 2c) were performed, thus confirming the presence of both activities.

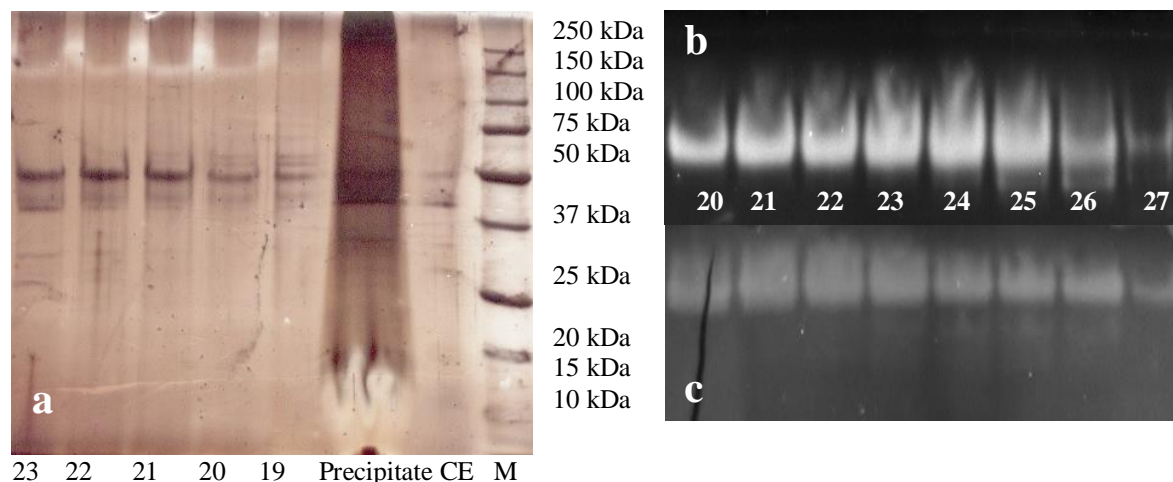


Figure 2. SDS-PAGE of fractions obtained from SEC (a). Zymograms of chitinolytic activity: Nhase (b); Endo (c).

Crystallinity analysis of chitin treated with steam explosion. I_{CR} (Figure 3a) was stable in treatments with high concentration (2 and 0.4), however when the water content increased in the samples resulted in significant decrease. Indeed, treatment with concentration of 0.1 mg/mL gave an I_{CR} decrease to *ca.* 19% compared to untreated chitin (88.13%). The D_{ap} (Figure 3b) analyses showed similar behavior observing its lowest value in the 0.1g/mL treatment for 8 min. Grethlein et al. [22] suggested that the effectiveness of steam explosion in facilitating enzymatic hydrolysis of wood is based on the increase of the total surface area by increasing pore volumes which leads to a larger contact surface for the enzymes. Additionally, the decrease in crystallinity might be a crucial factor, however, as can be corroborated herein in Figure 3a, the I_{CR} was unchanged, which is consistent with Focher et al. [13], whom mentioned that crystallinity of chitin is unaffected by steam explosion.

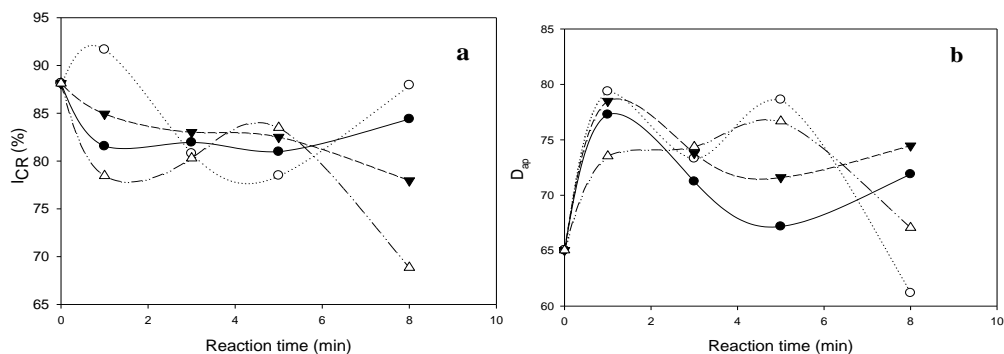


Figure 3. Effect of steam explosion in I_{CR} (a) and D_{ap} (b). Concentration (g/mL): 2 (●); 0.4 (○); 0.2 (▼); 0.1 (△).

Hydrolysis of sonicated and steam explosion treated chitin. The determination of reducing sugars was possible for all substrates and kinetics were performed up to 144 h (Figure 4). Maximum production (0.56 mmol/L) of chitin oligosaccharides was observed in sonicated chitin at 72 h. But greater production up to 1.7 mmol/L was attained using chitin treated with steam explosion at 144 h. It is noteworthy that, as shown in the Figure 4, presence of reducing sugars is detected since the beginning for the sonicated sample unlike steam explosion-treatment.

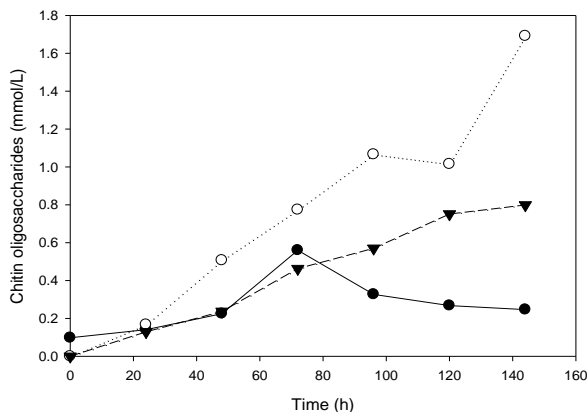


Figure 4. Kinetics of enzymatic hydrolysis with different substrates: sonication treatment (●); steam explosion treatment 0.1 g/mL and 8 min (○) and explosion treatment 0.4 g/mL for 5 min.

CONCLUSIONS

QMC10 supplemented with colloidal chitin and varying pH presented the highest production for chitinases, a reduction in production time was observed from 144 to 96 h under these conditions. SEC achieved the removal of proteases from the enzymatic extract remaining chitinolytic activities. Steam explosion as a pretreatment of chitin accomplished the decrease of the crystallinity of chitin without depolymerization, the treatments with the lowest ratio of chitin to water displayed the highest reduction in I_{CR} and D_{ap} . Steam explosion pre-treatment also enhanced the hydrolysis of chitin by partially purified chitinases.

ACKNOWLEDGEMENTS

The authors thank CONACYT Mexico (Project No.105628) for funding and scholarship (GVL).

REFERENCES

- Shirai K (2006) In: Guevara-González RG and Torres-Pacheco I (Ed) Fungal chitinases, in *Advances in Agricultural and Food Biotechnology Kerala (India)*.
- Askary H, Benhamou N, Brodeur J. (1999). *J Invert Pathol.* 74: 1-13.
- Rocha-Pino, Z., Viguera, G., Shirai, K., 2011. *Bioproc. Biosyst. Eng.* 34, 681-686.
- Matsumoto, Y., Saucedo, G., Revah, S., Shirai, K., (2004). *Process Biochem.* 39(6), 665-671.
- Marín-Cervantes M, Matsumoto Y, Ramírez-Coutiño L, Rocha-Pino Z, Vinięra G, Shirai K. (2008). *Process Biochem.* 43: 24-32.
- Coudron, T. A., Kroha, M. J., and Ignoffo, C. M. (1984). *Comp. Biochem. Physiol.* 79B, 339-348
- Tronsmo A., Hjeljord L., Klemsdal S. S., Varum K. M., Nordtveit H. R., & Harman G. E. (1996). *Chitin Enzymol.* 2:235-244.
- Kunitz M. (1947) *J. Gen Phys.*, 30: 291-310.
- Bradford, M.M. (1976). *Anal. Biochem.*, 72, 248-254
- Laemmli, U. K. (1970). *Nature* 227, 680-685.
- Barreto-Cardoso M., Signini R., Campana-Filho P., (2001). *Polym. Bull.* 47: 183-190.
- Jiebing L., Gunnar H., Göran G. (2007). *Bioresour. Technol.* 98, 3061-3068.
- Focher B., Beltrame P.L., Naggi A., Torri G. (1990). *Carbohydr. Polym.* 12: 405-418.
- Miller GL. (1959). *Anal. Chem.*, 31: 426-428.
- Giuliano B. y Harman G. (2001). *Appl. Environ. Microbiol.* 67(12): 5643-5647.
- Sun M., Liu X. (2006). *Mycopathologia* 161: 295-305
- Fenice M., Selbmann L., Di Giambattista R., Petruccioli M. (1996). *Chitin Enzymol* 2: 285-292
- Ramirez-Coutiño L, Espinosa-Marquez J, Peter M. G, Shirai K. (2010). *Bioresour. Technol.* 101: 9236-9240.
- Fenice M., Gooday G. (2006). *Ann. Microbiol.* 56:1-6
- Viterbo A, Montero M, Ramot O, Friesem D, Monte E, Llobell A. (2002). *Curr Genet.* 42:114-22.
- St. Leger R.J., Joshi L., Roberts D. (1998). 64: 709-713.
- Grethlein H. E., (1991). *Bioresour. Technol.* 36:77-82.

SYNTHESIS OF GALACTOOLIGOSACCHARIDES FROM LACTOSE BY β -GALACTOSIDASE IMMOBILIZED ON GLUTARALDEHYDE-TREATED CHITOSAN

Ana Elizabeth Cavalcante Fai¹*#; Thayza Christina Montenegro Stamford²; Tânia Lúcia Montenegro Stamford³; Haroldo Yukio Kawaguti¹; Isabela Thomazelli¹; Gláucia Maria Pastore¹

¹ Department of Food Science, Faculty of Food Engineering, University of Campinas, Campinas/SP, Brazil;

² Department of Tropical Medicine, Federal University of Pernambuco, Recife/PE, Brazil;

³ Department of Nutrition, Federal University of Pernambuco, Recife/PE, Brazil.

*E-mail address: bethfai@yahoo.com.br

Present address: Department of Food Technology, Nutrition School, Federal University of Rio de Janeiro State - UNIRIO, Rio de Janeiro/RJ, Brazil.

ABSTRACT

Aspergillus oryzae β -galactosidase was covalently immobilized on glutaraldehyde-treated chitosan powder. A fixed-bed reactor with lactose recycle was employed for galactooligosaccharides (GOS) synthesis and lactose hydrolysis by immobilized enzyme. The optimum pH for soluble and immobilized β -galactosidase were 4.6 and 5.0, respectively. The optimum temperature for the free enzyme was 40°C, yet this value was 10°C higher when characterizing the immobilized enzyme. Immobilized β -galactosidase had a good operational stability when used 10 times repeatedly and GOS synthesis had a maximum productivity of 14.42g/L.h from 400 g/L (w/v) lactose solution after two hours of reaction. Lactose was 44 % hydrolyzed in 12 hours.

Keywords: β -galactosidase; prebiotic; transgalactosylation; chitosan; covalent binding.

INTRODUCTION

Galactooligosaccharides (GOS), containing 3–10 molecules of galactose and glucose, selectively stimulating the beneficial colonic microflora, impart physiological benefits to the consumer and are among the most promising prebiotics [1;2]. GOS can be produced from lactose by enzymatic transgalactosylation using β -galactosidase (E.C.3.2.1.23) of great technological interest from various yeast [3], fungi [1;4;5] and bacteria [2].

Biocatalytic process economics can be enhanced by enzyme reuse and the improvement in enzyme stability afforded by immobilization [6]. Of the many carriers that have been studied for enzyme and cell immobilization considerable attention has been paid to chitosan, due to its appropriate characteristics: high affinity to proteins, availability of reactive functional groups, mechanical stability and ease of preparation in different geometrical configurations [7].

In the present study, *Aspergillus oryzae* β -galactosidase was covalently attached, via glutaraldehyde, to powder chitosan to produce GOS and hydrolyze lactose.

MATERIALS AND METHODS

Material

Aspergillus oryzae β -galactosidase (EC 3.2.1.23) and o-nitrophenyl- β -D-galactopyranoside (ONPG) was obtained from Sigma®. Commercial chitosan was purchased from Polymar, Brazil, with a deacetylation degree and apparent density of 91.1% and 0.64 g/mL, respectively, according to the manufacturer's protocol.

Preparation of immobilized enzyme

Chitosan in powder form was activated with glutaraldehyde 2.5% (v/v) in buffer acetate 0.2 M, pH 7.4 at 20 °C, 120 rpm, 30 min. The support was exhaustively washed with deionized water. β -galactosidase (5 mg) was then mixed with glutaraldehyde-activated chitosan (1.0 g suspended in 8 mL of 0.2 M acetate buffer, pH 5.0) and incubated overnight at 20 °C under constant shaking. The preparation was repeatedly washed with buffer until no protein and enzyme activity were detected. The chitosan-bound enzyme was suspended in 5 mL of the same buffer and used as an immobilized preparation for further studies. This methodology was adapted from Oliveira & Vieira [8].

Enzyme analysis

Activity of free and immobilized β -galactosidase was estimated by Food Chemical Codex method [9], using ONPG as substrate. An extinction coefficient for ONP of 4.3mM was calculated and used. Protein was determined by Bradford method using bovine serum albumin (BSA) as protein standard. Optimum temperature and pH were determined by changing individually the conditions of the β -galactosidase activity assay: pH from 4 to 9 and temperature from 30 to 70°C. K_m and V_{max} were determined using the Lineweaver–Burk plot method [10].

GOS synthesis

For the bath production, enzyme preparations were incubated with 40% lactose (w/v) solution in 0.2 M acetate buffer, pH 5.0 for 12 hours with intermittent stirring. Fixed-bed reactor studies were carried out in a jacketed glass column with 40% lactose recycle, using a MasterFlex® L/S peristaltic pump. The immobilized β -galactosidase (6.6 U/mg of support), obtained as previously described, was transferred to a jacketed column (2×8 cm). Temperature of the column was maintained at 45 °C using an ultrathermostate Quimis® Q-14 M2 bath. Sample aliquots (1 mL) were collected at various times from 2 to 24 hours and kept in boiling water bath for 10 min. Oligosaccharides formed were analyzed as described in 2.9.

Estimation of oligosaccharides

The identification and quantification of sugars was carried out by ion exchange chromatography with pulsed amperometric detection (HPLC-PAD). A DIONEX (USA) chromatograph, supplied with a Carbopac PA1 (4x250 mm) column, a PA1 (4x50 mm) guard column, with a GP50 gradient pump, ED40 electrochemical detector and PEAKNET software were used for the analyses. Sugars were eluted with 20 mM sodium hydroxide, at a flow rate of 1.0 mL/min at room temperature. Before injection, the samples were diluted with water and filtered through 0.22 μ m filters [3].

RESULTS AND DISCUSSION

In this study immobilized β -galactosidase retained 55% of its original activity. It was observed (Table 1) that optimum temperature for immobilized β -galactosidase was 10 °C higher when compared to the free enzyme.

Table 1: Characterization of free and immobilized *Aspergillus oryzae* β -galactosidase.

Parameters	Free enzyme	Immobilized enzyme
Enzymatic activity (U/mg)	12.03 \pm 0.22	6.6 \pm 0.57
pH optima	4.6 \pm 0.00	5.0 \pm 0.00
Temperature optima (°C)	40 \pm 0.00	50 \pm 0.00
Km (mM)	2.34 \pm 0.21	3 \pm 0.60
Vmax (μmol ONP/min.mg)	43.47 \pm 1.45	34.48 \pm 2.14

Optimal pH was slightly affected by immobilization procedure and was shifted up 0.4 unit to a more alkaline value. The Michaelis–Menten constant Km was found to be increased approximately 1.3-folds after immobilization. These variations are attributed to several factors such as protein conformational changes induced by the support, steric hindrances and diffusional effects [11]. In this study, catalytic efficiency (Vmax/Km) of β -galactosidase was decreased about 1.62-fold upon immobilization.

Chitosan covalent binding enzyme was reused for 10 cycles without significant loss in the enzymatic activity (retained at least 85% of its activity) and after 40 days of storage, suspended in 0.1 M acetate buffer, pH 4.5 at 3.5°C, retained 80% of its residual enzymatic activity.

As seen from Figure 1, a higher rate of GOS formation was obtained at 50 °C compared with others temperatures, which was consistent with our expectation since this was the optima temperature observed in enzymatic activity assays performed with ONPG. However, the packed bed reactor was used at 45 °C to increase thermal stability for a longer period of time.

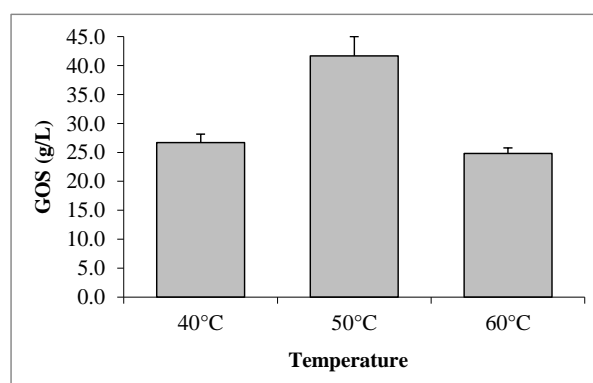


Figure 1: Effect of temperature on GOS production by immobilized enzyme in batch process from 40% (w/w) lactose, pH 5.0, 12 hours.

Time course of GOS production and lactose hydrolysis in fixed-bed reactor with lactose recycle were monitored and are shown in Figure 2 and 3, respectively.

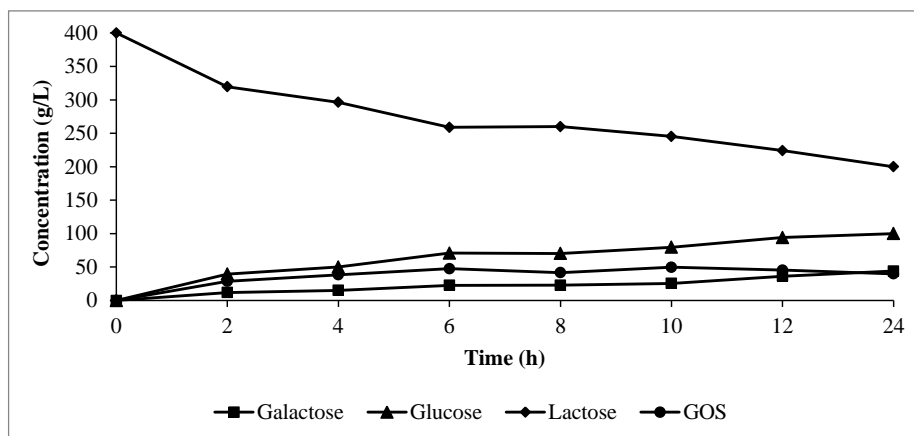


Figure 2: Reaction kinetics of GOS synthesis and lactose hydrolysis catalyzed by immobilized enzyme in the fixed-bed reactor in the first cycle, from 40% (w/w) lactose, pH 5.0, 45°C. Coefficient of variation (CV) % = range of 0.28 to 5.09.

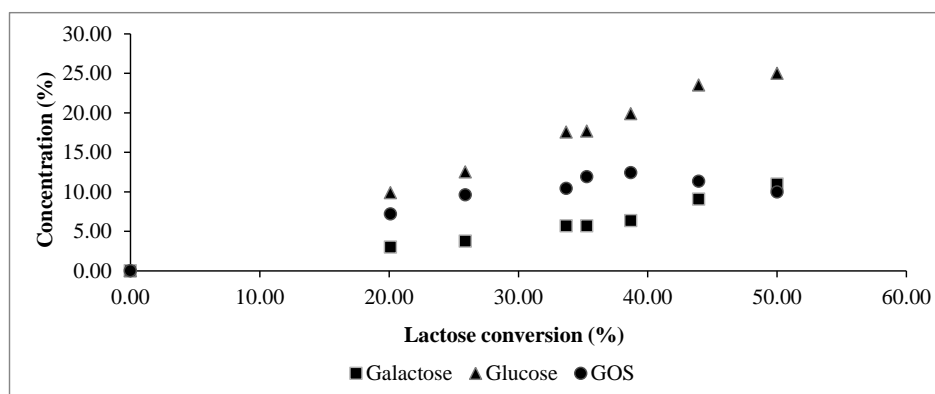


Figure 3: Lactose conversion, and other sugars concentration, catalyzed by immobilized enzyme in the fixed-bed reactor in the first cycle, from 40% (w/w) lactose, pH 5.0, 45°C. CV% = range of 0.28 to 4.89.

In the present study a maximum GOS production of 49.72 g/L, after 10 hours of reaction was achieved. Maximum productivity was 14.42 g/L.h after 2 hours of reaction (Figure 4). Glucose concentration was much higher than galactose which indicates involvement of galactose in GOS formation.

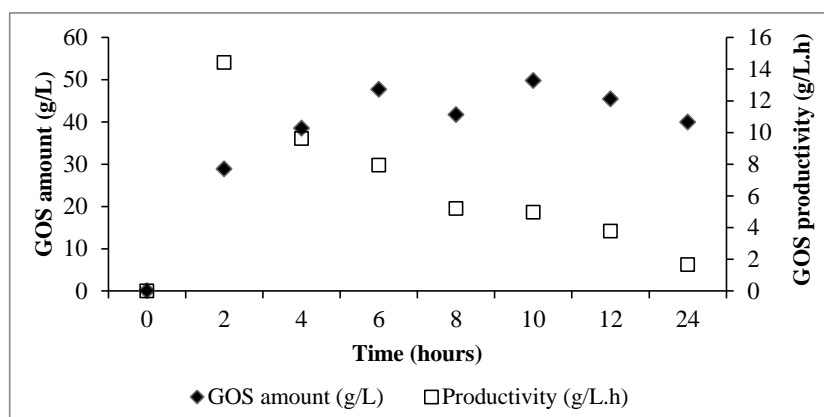


Figure 4: Kinetics of GOS synthesized and productivity catalyzed by immobilized enzyme in the fixed-bed reactor in the first cycle, from 40% (w/w) lactose, pH 5.0, 45°C. CV% = range of 0.48 to 4.50.

Gaur *et al.* [10] studied *A. oryzae* β -galactosidase covalently coupled to chitosan and aggregated by glutaraldehyde and reported a 17.3 and 4.6% oligosaccharide yield respectively, within 2 h in a 20% (w/v) lactose solution. This corresponds to a productivity of 17 and 4.6 g/L.h for the chitosan immobilized enzyme preparation and cross-linked aggregates, respectively.

In another study, Pectinex Ultra SP-L, a commercial enzyme preparation obtained from *Aspergillus aculeatus*, containing β -galactosidase activity, was immobilized onto Eupergit C and produced from 30 % (w/v) lactose by 24 h reaction 38.4 and 47.40 g/L of GOS for free and immobilized enzyme, respectively, corresponding to a productivity of 1.6 and 1.97 g/L/h [12].

β -Galactosidase from *Aspergillus oryzae*, immobilized on glutaraldehyde-treated chitosan beads, produced GOS in a plug reactor and maximum yields were 18, 21, 26% from a lactose solution of 100, 200 and 300 g/L, respectively [13].

As can be seen in Figure 3, GOS production kinetics is closely related to lactose conversion. As also shown, GOS production increased until a maximum was reached at 10 hours, at 44% lactose conversion and indicate that extending incubation time does not necessarily increase GOS amount. These results suggest that GOS formation precedes lactose hydrolysis as the dominant reaction before this point. Similar patterns were reported by other investigators [13; 14].

It is generally observed that the hydrolysis and transgalactosylation reactions occurred simultaneously. What dominates the product profile of the reaction is largely dependent on lactose concentration [15]. So the process of GOS formation may be concluded as a balance between hydrolysis and transgalactosylation [5]. This phenomenon was observed in the study as described above.

It is noteworthy that all types and sizes of GOS including transgalactosylated disaccharides are considered nondigestible oligosaccharides due to similar physiological characteristics, although some differences and strain specificities have also been reported [15].

CONCLUSIONS

Since the immobilization efficiency was satisfactory and immobilized enzyme retains its activity without decrease for 30 days, the covalent coupling *A. oryzae* β -galactosidase to chitosan could be used for the production of GOS and to hydrolyze lactose.

ACKNOWLEDGMENTS

The authors are grateful to Coordenação de Aperfeiçoamento de Pessoal de Nível Superior (Capes) and Universidade Estadual de Campinas (Unicamp) for financial support.

REFERENCES

- [1] LI, Z.; XIAO, M.; LU, L.; *et al.* (2008). Production of non-monosaccharide and high-purity galactooligosaccharides by immobilized enzyme catalysis and fermentation with immobilized yeast cells. *Process Biochemistry*, v. 43, p. 896-899.
- [2] GOSLING, A.; ALFTRÉN, J.; STEVENS, G.W.; *et al.* (2009). Facile pretreatment of *Bacillus circulans* β -Galactosidase increases the yield of galactosyl oligosaccharides in

milk and lactose reaction systems. *Journal of Agricultural and Food Chemistry*, v.59, n.7, p. 3366-3372.

[3] MANERA, A.P.; KUHN, G.; POLLONI, A.; *et al.* (2011). Effect of compressed fluids treatment on the activity, stability and enzymatic reaction performance of β -galactosidase. *Food Chemistry*, v.125, p. 1235-1240.

[4] HUERTA, L.M.; VERA, C.; GUERRERO, C.; *et al.* (2011). Synthesis of galactooligosaccharides at very high lactose concentrations with immobilized β -galactosidase from *Aspergillus oryzae*. *Process Biochemistry*, v. 46, p. 245–252.

[5] ZHENG, P.; YU, H.; SUN, Z.; *et al.* (2006). Production of galacto-oligosaccharides by immobilized recombinant β -galactosidase from *Aspergillus candidus*. *Biotechnology Journal*, v. 1, p. 1464-1470.

[6] BRADY, D.; JORDAAN, J. (2009). Advances in enzyme immobilization. *Biotechnology Letters*, v.31, n.11, p. 1639-1650.

[7] KRAJEWSKA, B. (2004). Application of chitin- and chitosan-based materials for enzyme immobilizations: a review. *Enzyme and Microbial Technology*, 35, 123-139.

[8] OLIVEIRA, I.R.W.Z.; VIEIRA, I.C. (2006). Construção e aplicação de biossensores usando diferentes procedimentos de imobilização da peroxidase de vegetal em matriz de quitosana. *Química Nova*, v.29, n.5, p.1932-939.

[9] FOOD CHEMICAL CODEX. (1981). *General Tests and Apparatus*, p. 491-492, National Academy Press, Washington, USA.

[10] GAUR, R.; PANT, H.; JAIN, R.; *et al.* (2006). Galacto-oligosaccharide synthesis by immobilized *Aspergillus oryzae* β -galactosidase. *Food Chemistry*, v.97, p.426-430.

[11] GURDAS, S.; GULEC, H.A.; MUTLU, M. (2010). Immobilization of *Aspergillus oryzae* β -galactosidase onto duolite A568 resin via simple adsorption mechanism. *Food and Bioprocess Technology*, DOI: 10.1007/s11947-010-0384-7.

[12] ASLAN, Y.; TANRISEVEN, A. (2007). Immobilization of Pectinex Ultra SP-L to produce galactooligosaccharides. *Journal of Molecular Catalysis B: Enzymatic*, v. 45, p. 73-77.

[13] SHEU, D.C.; LI, S.Y.; DUAN, K.J.; *et al.* (1998). Production of galactooligosaccharides by β -galactosidase immobilized on glutaraldehyde-treated chitosan beads. *Biotechnology Techniques*, v.12,n. 4, p. 273-276.

[14] NERI, D.F.M.; BALCÃO, V.M.; DOURADO, F.O.Q.; *et al.* (2009). Galactooligosaccharides production by β galactosidase immobilized onto magnetic polysiloxane-polyaniline particles. *Reactive & Functional Polymers*, v.69, p.264-251.

[15] ALBAYRAK, N.; YANG, S.T. (2002). Production of galactooligosaccharides from lactose by *Aspergillus oryzae* β -galactosidase immobilized on cotton cloth. *Biotechnology and Bioengineering*, v.77, n.1, p.8-19.

IMMOBILIZATION OF MARINE FUNGUS *Penicillium citrinum* CBMAI 1186 ON CHITOSAN FOR REDUCTION OF KETONES

Lenilson Coutinho Rocha¹, Sergio Paulo Campana Filho¹, André Luiz Meleiro Porto¹,
Alex Haroldo Jeller^{1,2*}

¹*Instituto de Química de São Carlos, Universidade de São Paulo, Av. Trabalhador São-carlense, 400, 13560-970, São Carlos, SP, Brazil*

^b*Coordenação de Química, Universidade Estadual de Mato Grosso do Sul, Rod. Itahum Km 12, s/n 79804-970, Dourados, MS, Brazil*

e-mail: alexjell@uems.br

Abstract

The objective of this study was to immobilize the marine fungus *Penicillium citrinum* CBMAI 1186 on chitosan and then use the immobilized mycelium to perform the reduction of ketones. The immobilized fungus catalyzed the reduction of 1-(4-methoxyphenyl)ethanone **1** to the (*S*)-1-(4-methoxyphenyl)ethanol **3b** with high selectivity (>99% *ee*) and 95% yield of isolated product. In contrast, ketone **1** was reduced to alcohol **3a** with only moderate selectivity (69% *ee*) and poor conversion (40%) by the free mycelia of *P. citrinum* CBMAI 1186. The free mycelia produced mainly the *R*-alcohol **3a**, the antipode of that produced by the immobilized cells. In addition, whole cells of *P. citrinum* immobilized on chitosan catalyzed the reduction of 2-chloro-1-phenylethanone **2** to the 2-chloro-1-phenylethanol **4a,b** but in this case without selectivity. Scanning electron micrographs showed that whole living hyphae of the fungus *P. citrinum* CBMAI 1186 were effectively immobilized on the chitosan.

Keywords: Bioreduction, *Penicillium citrinum*, Whole cells, Biocatalysis

1. Introduction

Biocatalysis consists of reactions of organic compounds catalyzed either by isolated enzymes or by whole cells of various origins, such as microorganisms or plants. Biocatalysts are used in industry for the production of pharmaceuticals, agrochemicals, fine chemicals, fragrances, nutritional compounds, and for bioremediation processes [1]. The main advantages of using enzymes in biocatalytic transformations are their chemo-, regio-, and stereospecificity as well as the mild reaction conditions that are used [2].

During biotransformation, several factors affect the stability and activity of the biocatalyst. Thus, a more efficient and stable biocatalyst the immobilization of whole microbial cells or isolated enzymes can provide many benefits for the biocatalytic process [3]. Immobilization techniques can involve adsorption, ionic or covalent bonding of the biocatalyst to an insoluble support, as well as entrapment of the biocatalyst in polymeric gels or encapsulation. The main advantage of using immobilized enzymes or whole cells as biocatalysts is the possibility of reusing them, since they can easily be recovered, making the process economically viable. Various immobilizing techniques and support materials have been studied, giving rise to a variety of immobilized preparations, with a wide range of efficiency, stability and activity. The properties of the support are important and must be considered: mechanical strength, chemical and physical stability, hydrophobic/hydrophilic character, enzyme loading capacity and cost, among others [1, 4,5].

In the literature, several classes of substances are transformed by immobilized enzymes and cells; for example racemic ibuprofen is resolved by a native enantioselective lipase from *Aspergillus niger*, both free and immobilized on five types of support (Accurel EP-100, Amberlite MB-1, Celite, Montmorillonite K10 and Silica gel) and polycyclic aromatic hydrocarbons are degraded by whole cells of the fungus *Mucor* sp. immobilized on maize cob [6,7].

New methods of immobilization and biodegradable supports need to be developed for biotransformation reactions, especially for classes of substances that are important for commercial synthesis, for example, the chiral alcohols. Thus, in this study whole cells of the marine fungus *Penicillium citrinum* CBMAI 1186 immobilized on chitosan were used to reduce the prochiral ketones **1-2**. Our research group recently published parts of this study and here we present more details of these reactions [8].

2. Experimental

2.1. General methods

The substrates 1-(4-methoxyphenyl)ethanone **1** and 2-chloro-1-phenylethanone **2** were purchased from Sigma-Aldrich. Sodium borohydride, sodium hydroxide and ethanol were purchased from Vetec or Synth. All manipulations involving the fungus *P. citrinum* CBMAI 1186 were carried out under sterile conditions in a Veco laminar flow cabinet. Technal TE-421 or Superohm G-25 orbital shakers were employed in the biocatalysed conversion experiments. The products of the reduction reactions were purified by column chromatography (CC) over silica gel (230-400 mesh). The column was eluted with mixtures of *n*-hexane and ethyl acetate (Hex:EtOAc - 9:1 and 8:2) and fractions were monitored by thin layer chromatography (TLC), using pre-coated silica gel 60 F254 layers (aluminum-backed: Sorbent). The alcohols were analyzed in a Shimadzu GC 2010 gas chromatograph equipped with an AOC 20i auto injector, flame ionization detector (FID) and a Varian chiral column CP-Chiralsil-DEX (β -cyclodextrin) (25 m x 0.25 mm x 0.39 μ m). For the GC analyses, the following conditions were employed: initial oven temperature 120 °C (2 min) raised to 165 °C (8 min) at a rate of 2 °C/min; total run time 32.5 min; injector temperature 200 °C; detector temperature 200 °C; injector split ratio 1:20; nitrogen carrier gas at a pressure of 69.2 kPa. The enantiomeric excesses (*ee*) of 1-(4-methoxyphenyl)ethanol **3a,b** and 2-chloro-1-phenylethanol **4a,b** were determined by GC-FID analysis. The retention times of the alcohols *S*-**3b**, *R*-**3a**, *S*-**4b** and *R*-**4a** were 15.2 min, 15.8 min, 16.5 min, and 17.0 min, respectively. For the gas chromatography-mass spectrometry analysis, a Shimadzu GC 2010 plus gas chromatograph with a 30 m x 0.25 mm x 0.25 DB5 fused silica column (J&W Scientific), coupled to a mass-selective detector (Shimadzu MS 2010 plus) in electron ionization (EI, 70 eV) mode was used.

2.2. Absolute configuration

The optical rotation of the purified products 1-(4-methoxyphenyl)ethanol **3** and 2-chloro-1-phenylethanol **4** were measured in a Perkin-Elmer (Waltham, MA, USA) 241 polarimeter with a 1 dm light path cuvette, at the sodium D-line. The absolute configurations of the alcohols **3a,b** and **4a,b** were determined by comparing the measurements of their specific rotations with those reported in the literature [9,10].

(*S*)-(-)-1-(4-methoxyphenyl)ethanol **3b** $[\alpha]_D^{25} = -45.13$ (*c* 0.5, CHCl₃; >99% *ee*); lit. [9] $[\alpha]_D^{25} = -23.2$ (*c* 1.0, CHCl₃; 91% *ee*); (*S*)-(+)-2-chloro-1-phenylethanol **4b** $[\alpha]_D^{25} = +17.08$ (*c* 3.2 CHCl₃; 50% *ee*); lit. [10] $[\alpha]_D^{25} = +54.9$ (*c* 1.0 CHCl₃).

2.3. Chemical synthesis of 1-(4-methoxyphenyl)ethanol **3a,b** and 2-chloro-1-phenylethanol **4a,b**

The racemic mixtures of 1-(4-methoxyphenyl)ethanol **3a,b** and 2-chloro-1-phenylethanol **4a,b** were synthesized by reduction of 1-(4-methoxyphenyl)ethanone **1** (100.0 mg, 0.70 mmol) and 2-chloro-1-phenylethanone **2** (100.0 mg, 0.65 mmol) with sodium borohydride (30.0 mg, 0.77 mmol) in 25 mL methanol [11]. The spectroscopic data (^1H and ^{13}C NMR, MS and IR) of alcohols **3a,b** and **4a,b** were in agreement with those reported in the literature [8,12].

2.4. Marine fungus

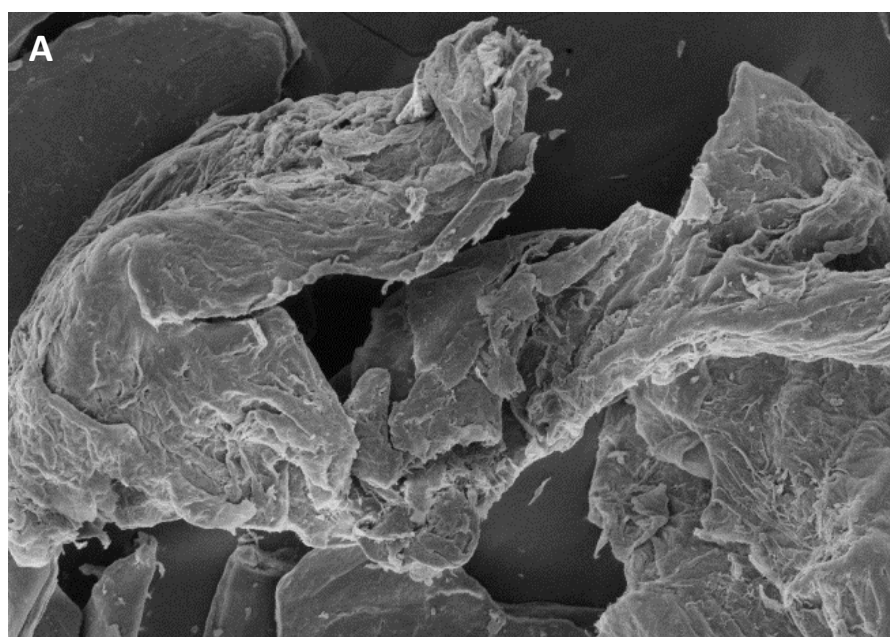
The marine fungus *P. citrinum* CBMAI 1186 was isolated from the marine alga *Caulerpa* sp., which was collected by Prof. R.G.S. Berlinck in the town of São Sebastião, on the coast of São Paulo State, Brazil. The fungus used in this work was identified by both conventional and molecular methods at the Chemical, Biological and Agricultural Multidisciplinary Research Center (CPQBA) at the State University of Campinas (UNICAMP), SP, Brazil [8,13,14].

2.5. Biocatalytic reduction of ketones **1** and **2** by free mycelium of marine fungus

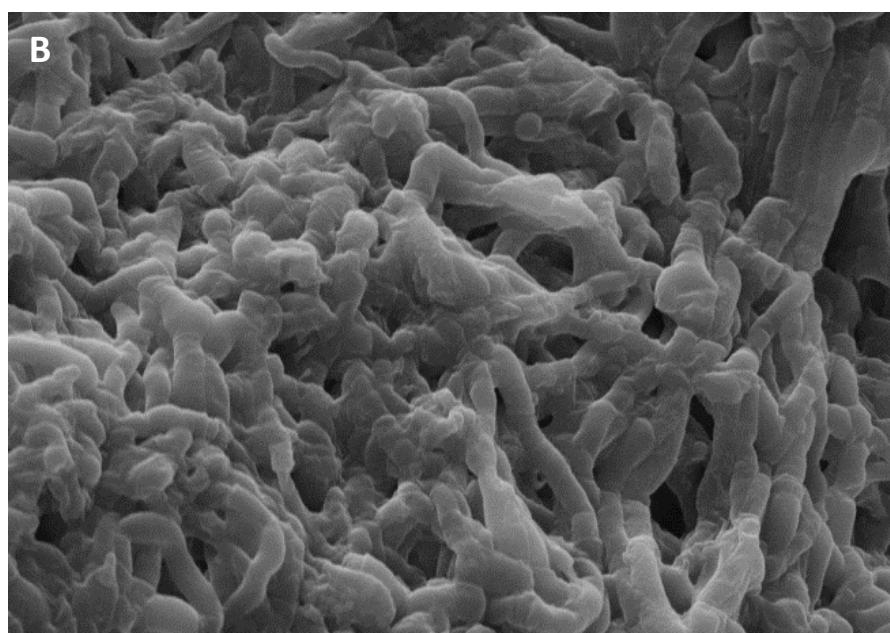
The cultured medium used to grow the marine fungus was artificial seawater [12]. Small slices of solid medium (0.5 × 0.5 cm) bearing mycelia of *P. citrinum* CBMAI 1186 were cut from the stock solid culture and used to inoculate 1 L of liquid culture medium contained in an Erlenmeyer flask (2 L). The mycelia were incubated at 32 °C for 9 days in a rotary shaker (120 rpm). After which the mycelia were harvested by Buchner filtration and suspended in a buffer solution contained in Erlenmeyer flasks (250 mL). The biocatalytic reductions were carried out with 5.0 g (wet weight) of mycelium and 0.50 mmol of ketone **1** or **2**, previously dissolved in 300 μL dimethyl sulfoxide and mixed into 100 mL phosphate buffer solution ($\text{Na}_2\text{HPO}_4/\text{KH}_2\text{PO}_4$, pH = 7, 0.1 M). The mixtures were incubated for 9 days, in an orbital shaker at 32 °C and 120 rpm. After this time, the samples were extracted with 2.0 mL ethyl acetate by mixing on a vortex and centrifuging at 6000 rpm for 6.0 min in a HERMLE Z-200 A, and analyzed by GC-FID and GC-MS. The products were purified by column chromatography over silica gel to yield the alcohols **3a,b** or **4a,b** (Scheme 1). All the reactions were performed in duplicate.

2.6. Immobilization of whole living hyphae of *P. citrinum* CBMAI 1186 on chitosan

The whole living hyphae of *P. citrinum* CBMAI 1186 were grown as described in Section 2.5. The mycelia were harvested by filtration and 5.0 g were suspended in 100 mL of phosphate buffer solution ($\text{Na}_2\text{HPO}_4/\text{KH}_2\text{PO}_4$, pH = 7, 0.1 M) in a 250 mL Erlenmeyer flask. The support matrix of commercial chitosan (3.0 g) was added to each Erlenmeyer flask. The mixtures were incubated for 24 h in an orbital shaker maintained at 32 °C and 120 rpm. After filtration, the immobilized mycelia were immediately used in the biocatalytic reduction reactions. The free and immobilized on hyphae were analyzed by scanning electron microscopy (SEM) (Figures 1-2), as described in the following section.



IQSC EHT=20.00 kV WD= 25 mm Mag= 250 X Detector= SE1
20µm H Photo No.=16 8-Jul-2010



IQSC EHT=20.00 kV WD= 25 mm Mag= 5.00 K X Detector= SE1
1µm H Photo No.=23 8-Jul-2010

Figure 1. Scanning microscopy micrographs of (A) chitosan support, (B) free mycelium of *P. citrinum* CBMAI

1186

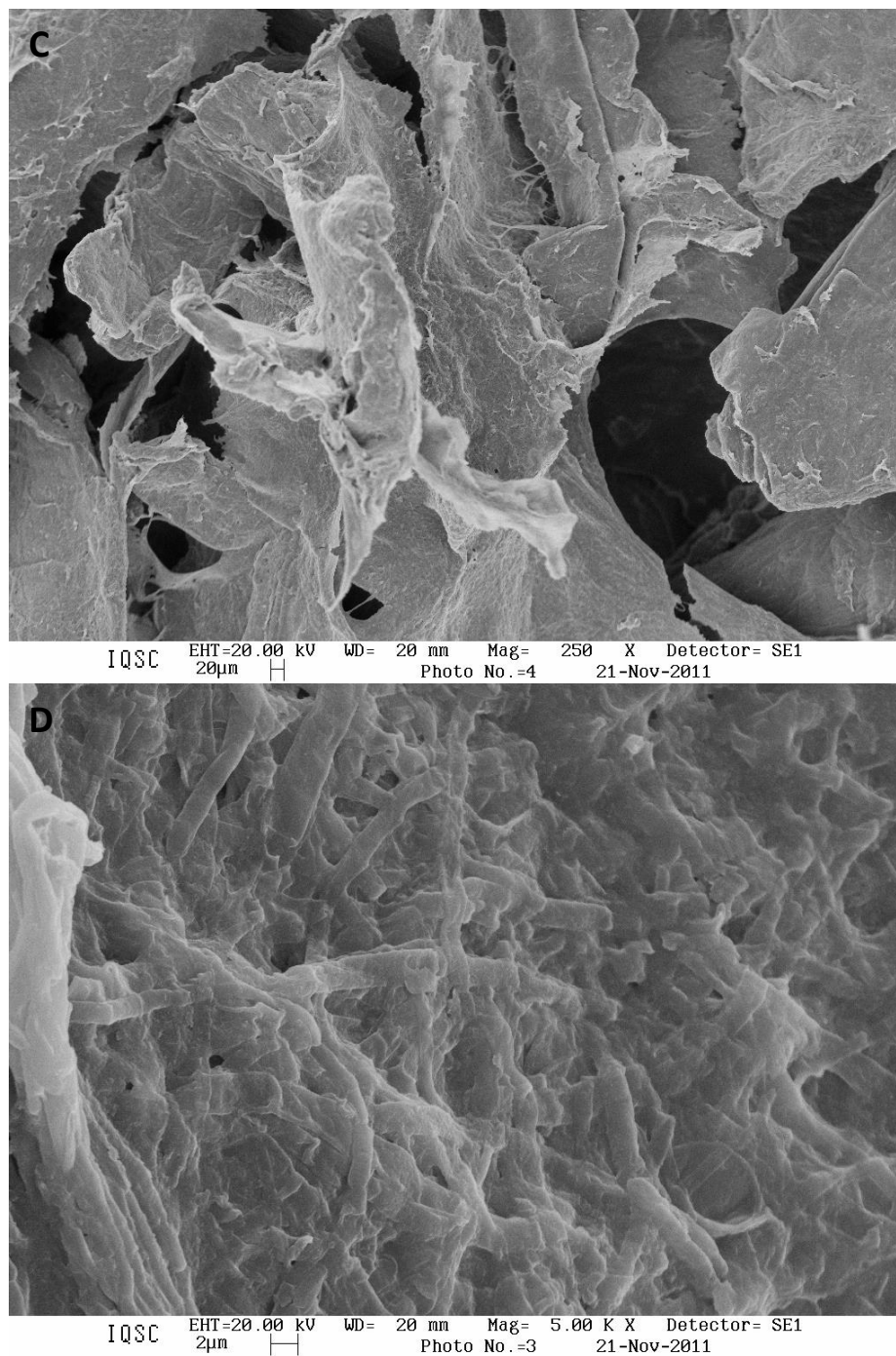


Figure 2. Scanning electron micrographs of (C-D) Whole hyphae of *P. citrinum* immobilized on chitosan

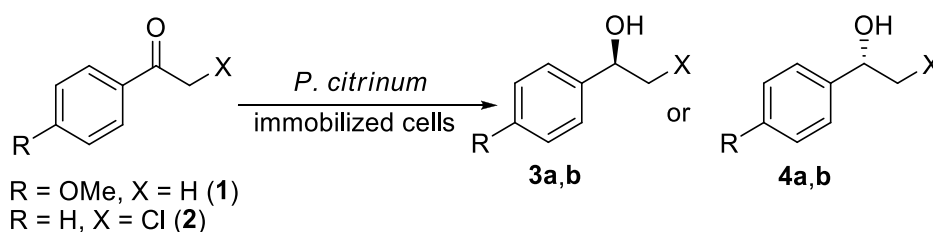
2.7. Scanning electron microscopy

For SEM analysis, the surfaces of immobilized mycelia of *P. citrinum* CBMAI 1186 were washed with water to remove the non-adhering support matrix. The whole mycelium from a

culture flasks was dehydrated in a graded series of 10 mL water-ethanol solutions (10%, 25%, 40%, 50%, 70%, 80%, 90% and 100%), in a 50 mL Erlenmeyer flasks, for 15 min at each step. Samples were air dried at room temperature, and coated with 8-10 nm of gold by argon ion sputtering in a Baltec MED 020 model sputter. Images were taken at magnifications of x 200 to 5000 a scanning electron microscope (Leica-Zeiss LEO 440) operating at an accelerating voltage of 20 kV with a Secondary Electron Detector positioned 13-25 away from the sample (Figures 1 and 2).

2.8. Reduction of ketones **1** and **2** by immobilized mycelia of *P. citrinum*

Biocatalytic reduction reactions were carried out with fungal mycelia immobilized on 7.0 g (wet weight) of chitosan. Ketones **1** and **2**, 0.5 mmol previously dissolved in 300 μ L of dimethyl sulphoxide, were added to 100 mL of phosphate buffer solution ($\text{Na}_2\text{HPO}_4/\text{KH}_2\text{PO}_4$, pH 7, 0.1 M). The mixtures containing the substrates and the immobilized mycelia were incubated for 9 days on an orbital shaker at 32 $^\circ\text{C}$ and 120 rpm. The cultures were extracted with ethyl acetate (1.0 mL) by vortexing and centrifuging (6000 rpm for 6.0 min in a HERMLE Z-200 A centrifuge) and analyzed by GC-FID and GC-MS. The products were purified by CC over silica gel, to yield the alcohols **3a,b** and **4a,b** (Scheme 1).



Scheme 1. Reduction of ketones **1-2** by immobilized cells of *P. citrinum* CBMAI 1186

3. Results and discussion

It is very common to use cell of yeast or bacteria in reduction reactions of organic compounds. However, the employment of immobilized cells of filamentous fungi for biocatalytic reactions is quite rare in the literature.

Our research group has used free whole mycelia of marine fungi to promote reactions such as the reduction of prochiral ketones [12,15], hydrolysis of epoxides [16] and biotransformation of nitriles [17]. More recently, our group used whole marine fungi immobilized on chitosan, silica xerogel and silica gel to promote biocatalytic reactions [8].

Following to the excellent results obtained in the biocatalytic reduction of ketones by free mycelium of marine fungi, in this study we investigated the immobilization of living mycelia of the marine fungus *P. citrinum* CBMAI 1186 on chitosan. Chitosan is the deacetylated form of chitin, the second most abundant polymer in nature after cellulose. It is a low cost, renewable and biodegradable natural product that is safe and easy to handle [5].

Figures 1 and 2 show SEM micrographs of chitosan, free hyphae of *P. citrinum* CBMAI 1186 and mycelia of *P. citrinum* CBMAI 1186 immobilized on the chitosan matrix, respectively. The whole living mycelium of *P. citrinum* CBMAI 1186 was successfully immobilized on chitosan, can be seen in the SEM micrographs. The support matrix chitosan was closely intertwined with the hyphae (Figures 2C,D). As can be seen in the micrographs, the mycelia were strongly bond to the support, yielding a uniform material. The chitosan support matrix appears to create an appropriate environment for the preservation of the living fungus. The biomaterial formed by the immobilization of the mycelia on the chitosan was used directly in the biocatalytic reduction of 1-(4-methoxyphenyl)ethanone **1** and 2-chloro-1-phenylethanone **2**. Control reactions were performed with free fungal mycelia, without the support matrix.

The whole cells free mycelia of *P. citrinum* CBMAI 1186 catalyzed the stereospecific reduction of 1-(4-methoxyphenyl)ethanone **1** and, after 9 days, the (*R*)-1-(4-methoxyphenyl)ethanol **3a** was obtained in moderate enantiomeric excess (69% *ee*) and low conversion (c 40%). The *R*-alcohol **3a** was isolated at a yield of 35% after purification by column chromatography over silica gel. When whole cells hyphae of *P. citrinum* CBMAI 1186 immobilized on chitosan were used, the performance of the bioreduction of **1** to alcohol **3** was improved dramatically. Thus, the enantiopure alcohol *S*-**3b** (>99% *ee*, c 100%) was obtained by biocatalytic reduction on immobilized chitosan. Interestingly, not only was the conversion greatly enhanced by this type of organic support matrix. In addition, the immobilization led to a total inversion of the configuration produced by free mycelium, yielding the *S*-alcohol **3b** (>99% *ee*) instead of the *R*-alcohol **3a** (Figure 3).

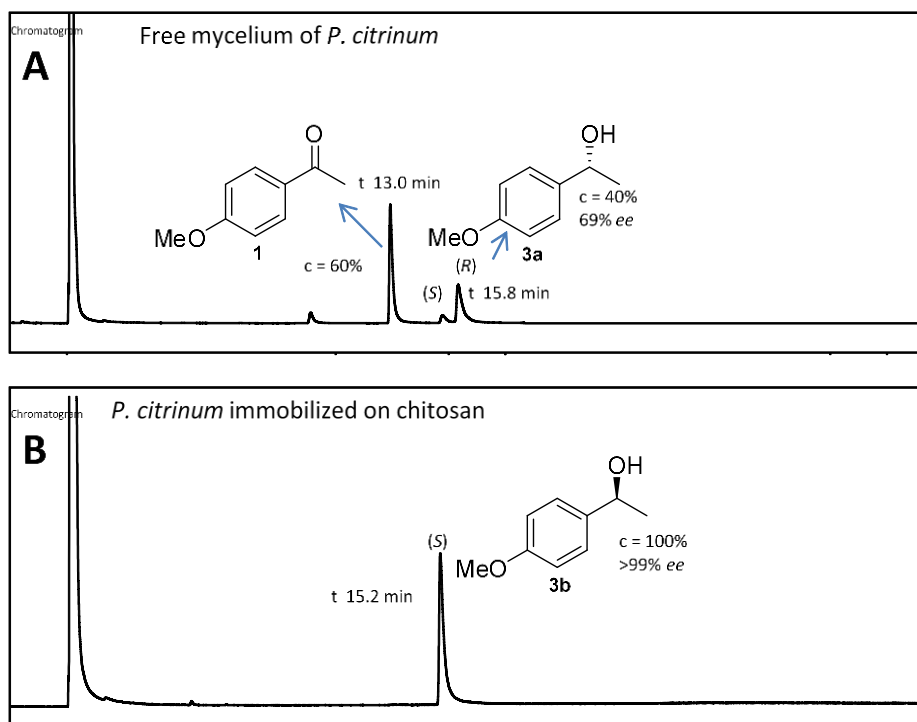


Figure 3. Chromatograms obtained by GC-FID of reaction extract for reduction of ketone **1** by *P. citrinum* CBMAI 1186. (A) Whole free mycelium. (B) Whole hyphae immobilized on chitosan.

From these results, we conclude that the whole marine fungus *P. citrinum* CBMAI 1186 immobilized on chitosan maintained the stability and activity of the enzymes and their cofactors responsible for the bioreduction of ketone **1**, proving the effectiveness of the support. The inversion of the configuration of the alcohol *R*-**3a** (not immobilized) to *S*-**3b** (immobilized hyphae) showed a strong interaction between the fungus and the support. Free and immobilized whole living hyphae of *P. citrinum* CBMAI 1186 were efficient at yielding both enantiomers by the action of a single microorganism, showing a further potential advantage of the immobilization of microbial cells: the synthesis of both enantiomers of a compound with only one biocatalyst. Such entanglement of hypha and chitosan is probably related to the surface charges on the surface of the matrix. The interactions between the organic matrix and mycelium probably enhanced the affinity for ketone **1** and preserved the activity of the enzyme that catalyzed the reduction of ketone **1** to enantiomerically pure *S*-alcohol-**3b**.

The free (not immobilized) live mycelia of *P. citrinum* CBMAI 1186 also catalyzed the reduction of 2-chloro-1-phenylethanone **2** and, after 9 days, the (*R*)-2-chloro-1-phenylethanol **4a** was produced with modest selectivity (31% *ee*) and conversion (*c* 70%). On the other hand, whole *P. citrinum* CBMAI 1186 hyphae immobilized on chitosan catalyzed the reduction of ketone **2** to alcohol **4a,b** in excellent yield (98% after purification by CC), but without selectivity (Figure 4).

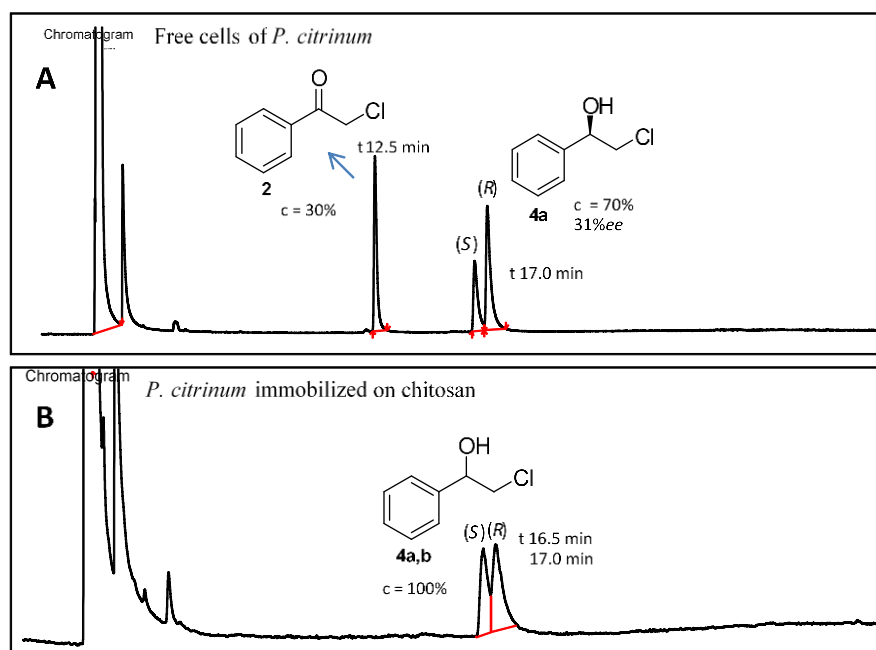


Figure 4. Chromatograms obtained by GC-FID of reaction extract for reduction of ketone **2** by *P. citrinum* CBMAI 1186. (A) Whole free mycelium. (B) Whole hyphae immobilized on chitosan.

In these studies, we have observed that chitosan shows clear advantages when used as a matrix for the immobilization of the filamentous fungus *P. citrinum* CBMAI 1186. Probably, the reactive hydroxyl and amino groups on the repeating units of the polymer chains interact with the wall of the fungus and promote strong interaction between matrix and mycelium. In addition, as chitosan is an organic polymer support matrix, it probably facilitates the interaction of the substrate with the immobilized hypha aiding the reactions to go to completion. It was therefore concluded that chitosan was an excellent support matrix for the immobilization of filamentous fungus, such as *P. citrinum*, with a beneficial influence on enzyme activity.

In the literature, chitosan has been immobilized onto a PNIPAAm gel/PP nonwoven composite surface by means of the crosslinking agent, glutaraldehyde. Preliminary results showed that chitosan hydrogels displayed antibacterial ability to *Escherichia coli* and *Staphylococcus aureus* [18].

As functional materials, chitin and chitosan offer a unique set of characteristics: biocompatibility, biodegradability to harmless products, nontoxicity, physiological inertness, antibacterial properties, heavy metal ion chelation, gel-forming properties, hydrophilicity and a remarkable affinity for proteins. Owing to these characteristics, chitin- and chitosan-based materials, as yet underutilized, are predicted to be widely exploited in the near future, especially

in environmentally benign applications in systems working in biological environments. Among these are fungus and enzyme immobilization supports [19].

Conclusion

In this study, we reported the immobilization of whole mycelia of marine fungus *P. citrinum* CBMAI 1186 for the biocatalytic reduction of ketones. The whole cells of *P. citrinum* free and immobilized on chitosan catalyzed reduction reactions of ketones **1** and **2** with high conversion. SEM micrographs showed a strong interaction between chitosan and the mycelium of *P. citrinum*. Chitosan proved to be an excellent matrix for the immobilization of the filamentous fungus *P. citrinum*.

Acknowledgements

The authors wish to thank Prof. R.G.S. Berlinck (Instituto de Química de São Carlos-USP) for providing the marine fungal strains and Prof. Timothy John Brockson (Universidade Federal de São Carlos-UFSCar) for optical rotation measurements in a Perkin-Elmer 241 polarimeter (Waltham, MA, USA). The English language was reviewed by Timothy Roberts, MSc., a native English speaker. We also acknowledge the Conselho Nacional de Desenvolvimento Científico e Tecnológico (CNPq) and Fundação de Amparo à Pesquisa do Estado de São Paulo (FAPESP) for financial support. We also thank the Coordenação de Aperfeiçoamento de Pessoal de Nível Superior (CAPES) for the scholarship grant to LCR.

References

- [1] Norouzian, D; Akbarzadeh, A; Inanlou, DN, *et al* (2003). Biotransformation of alcohols to aldehydes by immobilized cells of *Saccharomyces cerevisiae* PTCC5080. *Enzyme Microb. Technol.*, 33, 150-153.
- [2] Bornscheuer, UT (2003). Immobilizing enzymes: how to create more suitable biocatalysts. *Angew.*, 42, 3336-3337.
- [3] Halling, P (1994). Thermodynamic prediction for biocatalysis in non-conventional media; theory, test and recommendation for experimental design and analysis. *Enzyme Microb. Technol.*, 16, 176-205.
- [4] Contesini, FJ; Lopesa, DB; Macedo, GA; *et al* (2010). *Aspergillus* sp. lipase: Potential biocatalyst for industrial use. *J. Mol. Catal. B: Enzymatic*, 67, 163-171.

- [5] Mendes, AA; Oliveira, PC; Castro, HF; Giordano, RLC (2011). Application of chitosan as support for immobilization of enzymes of industrial interest. *Quím. Nova*, 34, 831-840.
- [6] Silva, VCF; Contesini, FJ; Carvalho, PO (2009). Enantioselective behavior of lipases from *Aspergillus niger* immobilized in different supports. *J. Ind. Microbiol. Biotechnol.*, 36, 949-954.
- [7] Su, D; Li, P; Wang, X; Stagnitti, F.; Xiong, X (2006). Biodegradation of benzo[a]pyrene in soil by immobilized fungus. *J. Environ. Sci.*, 18, 1204-1209.
- [8] Rocha, LC; Souza, AD; Rodrigues Filho, UP; *et al* (2012). Immobilization of marine fungi on silica gel, silica xerogel and chitosan for biocatalytic reduction of ketones. *J. Mol. Catal. B: Enzymatic*, 84, 160-165.
- [9] Yadav, JS; Reddy, BVS; Sreelakshmi, C; Rao, AB (2009). Enantioselective of prochiral ketones employing sprouted *Pisum sativa* as biocatalyst. *Synthesis*, 11, 1881-1885.
- [10] Xu, GC; Yu, HL; Zhang, XY; Xu JH (2012). Access to Optically Active Aryl Halohydrins Using a Substrate-Tolerant Carbonyl Reductase Discovered from *Kluyveromyces thermotolerans*. *Catalysis*, 2566-2571.
- [11] Pavia, DL; Lampman, GM; Kriz, GS; Engel, RG (1999). Introduction to organic laboratory techniques, 3rd ed., Sanders College Publishing, Orlando.
- [12] Rocha, LC; Ferreira, HV; Pimenta, EF; *et al* (2009). Bioreduction of α -chloroacetophenone by whole cells of marine fungi. *Biotechnol. Lett.*, 31, 1559-156.
- [13] De Vita-Marques, AM; Lira, SP; Berlinck, RGS; *et al* (2008). A multi-screening approach for marine-derived fungal metabolites and the isolation of cyclodepsipeptides from *Beauveria felina*. *Quim. Nova*, 31, 1099-1103.

- [14] Santos, RCB; Durrant, LR; Silva, M; *et al* (2010). Production of laccase, manganese peroxidase and lignin peroxidase by brazilian marine-derived fungi. *Enzyme Microb. Technol.*, 46, 32-37.
- [15] Mouad, AM; Martins, MP, Deboni, HM; *et al* (2011). Bioreduction of acetophenone derivatives by red marine algae *Bostrychia radicans* and *B. tenella*, and marine bacteria associated. *Helv. Chim. Acta*, 94, 1506-1514.
- [16] Martins, MP; Mouad, AM; Boschini, L; *et al* (2011). Marine fungi *Aspergillus sydowii* and *Trichoderma* sp. catalyze the hydrolysis of benzyl glycidyl ether. *Mar. Biotechnol.*, 13, 314-320.
- [17] Oliveira, JR; Mizuno, CM; Selegim, MHR; *et al* (2013). Biotransformation of phenylacetonitrile to 2-hydroxyphenylacetic acid by marine fungi. *Mar. Biotechnol.*, 15, 97-103.
- [18] Chen, TKS; Yuan-An, K.; Lee, CH, *et al* (2005). Immobilization of chitosan gel with cross-linking reagent on PNIPAAm gel/PP nonwoven composites surface. *Mat. Science and Engineering C*, 25, 472-478.
- [19] Krajewska, B. Application of chitin- and chitosan-based materials for enzyme immobilizations: a review (2004). *Enzyme and Microbial Technology*, 35, 126-139.

SELECTIVE ISOLATION OF TRYPSIN INHIBITOR FROM SOYBEAN WHEY BY CHITOSAN/TRIPOLYPHOSPHATE/GENIPIN CO-CROSSLINKED BEADS

Min-Lang Tsai^{1*}, Rong Huei Chen^{1,2*}, Chu-Hsi Hsu^{1,3}, Yu-Lung Chang¹

¹ Department of Food Science, National Taiwan Ocean University, 2 Pei-Ning Road, Keelung 20224, Taiwan, ROC

² Sea Party Technology LTD, No. 65, Sec. 3, Nanjing E. Rd. Taipei, Taiwan, ROC

³ Department of Food and Beverage Management, Yuanpei University, 306, Yuanpei Street, Hsinchu 30015, Taiwan, ROC

*E-mail address: chenrhntou@gmail.com (R.H. Chen) tml@mail.ntou.edu.tw (M.L. Tsai)

ABSTRACT

In this study, tripolyphosphate/genipin co-crosslinked chitosan beads were prepared in pH 5, 7 and 9 solutions (CB5, CB7 and CB9) and applied for selective adsorption of trypsin inhibitor from soybean whey solution at 15°C. Chitosan was prepared from squid pen. The degree of deacetylation and molecular weight of chitosan were 80% and 400 kDa, respectively. The co-crosslinking degrees of CB5, CB7 and CB9 were 74.6%, 65.3% and 59.2%, respectively. The major proteins of soybean whey were trypsin inhibitor and lectin. The best adsorption ratio of trypsin inhibitor and lectin of CBs occurred in pH 4.4 and 5.4 solution, respectively. The adsorption ratios of trypsin inhibitor were decreased with co-crosslinking degrees of CBs increasing. At 15°C, the best adsorption ratios of CB5, CB7 and CB9 adsorbed trypsin inhibitor from pH 4.4 soybean whey solutions being 70.4%, 85.2% and 94.2%, respectively. However, the adsorption ratios of CB5, CB7 and CB9 for lectin were very low at same adsorbed condition, it were 5.7%, 6.0% and 11.6%, respectively. The selective isolation for trypsin inhibitor from pH 4.4 soybean whey solution could be processed by CBs due to good selectivities.

Keywords

Chitosan/tripolyphosphate/genipin co-crosslinked bead; Selective isolation; Soybean whey; Trypsin inhibitor; Lectin

INTRODUCTION

Chitosan is a high molecular weight polysaccharide and is composed by glucosamine and N-acetyl-glucosamine. It is a widely distributed biopolymer since it is readily available via cationic polyelectrolyte in acid solution and because it is non-toxic, biocompatible and biodegradable. Chitosan is often considered to be an adsorbent due to its amino and hydroxyl groups as well as adsorption of protein, dye, metal, etc [1]. Advantages of chitosan-based material used as sorbent include the fact that it is an extremely cost-effective environmentally friendly natural polymer with outstanding metal and dye-binding capacities, high efficiency and selectivity in detoxifying both very dilute or concentrated solutions, exhibiting excellent diffusion properties and resulting in high-quality treated effluent; it is a versatile sorbent and easily regenerated if required [2].

The chitosan bead crosslinks with crosslinking agent could improve these drawbacks and increase the use of recycling. Tripolyphosphate (TPP) is a non-toxic polyanion which can interact with chitosan via electrostatic forces to form ionic crosslinked networks [3]. Genipin is a natural crosslinking agent. It is an aglucone of geniposide extracted from *Gardenia jasminoides* and obtained from geniposide via enzymatic hydrolysis. Genipin is considered an ideal biomedical material due to its being 10,000 times less toxic than glutaraldehyde [4-5]. Mi et al. [3] have explored the mechanism of the co-crosslinked reaction of chitosan and TPP/genipin.

Soybean whey is a by-product from the preparation of soybean products such as tofu, soy protein isolate, etc. It was deemed a waste product, and disposal constitutes an environmental and industrial problem. Soybean whey is composed of trypsin inhibitor, lectin, lipoxygenase, urease, β -amylase, phytic acid, etc [6]. The value of soybean will increase if the above compounds are recovered and used.

Several procedures have been proposed for separation of individual proteins from a mixture including salting-out, selective precipitation, chromatographic techniques, and membrane filtration. These processes have not been widely applied for large-scale purification because of their complexity, high cost, low overall yield, poor selectivity, and unacceptable product degradation associated with the extremes of heat, pH, or salt used during the process [7].

The concept of selective adsorption is to control some conditions and to make the adsorbent adsorbing only one ingredient from a mixture. Then, the adsorbent is collected and put into another solution. The desorptions are carried out under controlling conditions.

The aims of this study were explored the selective isolation of trypsin inhibitor from soybean whey solution by chitosan/TPP/genipin co-crosslinked bead (CB).

MATERIALS and METHODS

Preparation of chitosan

β -Chitin was prepared from squid pens (*Illex argentinus*). The squid pens were grounded to a 40–60 mesh size. Each 100 g batch of powder was immersed overnight in 500 ml of 1 M of hydrochloric acid solution. The sample was washed to neutrality and drained. Then, the sample was soaked overnight in 500 ml of 2 M of sodium hydroxide at an ambient temperature, washed and drained. Subsequently, the sample was reacted in 500 ml of 2 M of sodium hydroxide solution at 100°C for 4 h, washed to neutrality and dried.

β -Chitin was added to a 50% (w/w) sodium hydroxide solution at a ratio of 1 (g solid):10 (ml solution). The deacetylation reaction took place at 100°C for 3 h. Then the chitosan was collected and washed to neutrality and freeze-dried [8].

Measurement DD and MW of chitosan

The DD and MW of the chitosan were determined with infrared spectrometry [9] and size exclusion high-performance liquid chromatography [10], respectively. The DD and MW of the chitosan are 80% and 400 kDa, respectively.

Preparation of TPP/genipin co-crosslinked chitosan beads

The chitosan solution (1%) was dripped into 0.01 M TPP/0.01 M genipin solution with pH 7 and stored for 24 h to processed co-crosslinking. After crosslinking, the solidified beads were stirred for two days in ultrapure water (Millipore) to remove residual TPP and genipin, and was then stored at 4°C (Mi et al., 2003).

Adsorption ratio and desorption ratio

The CB was dipped in blank solutions at pH 2-6 for 4 h. The beads were then taken out and drained. The initial concentrations (C0) of trypsin inhibitor, lectin and phytic acid in soybean whey solutions were determined beforehand. The 0.1 g CB was added into 30 ml of pH 2-6 soybean whey solution, respectively. The solution was stirred at 100 rpm for 24 h at 5, 15, 25°C, respectively. Then, CB was taken out, the concentrations (C1) of phytic acid, trypsin inhibitor and lectin, of adsorbed soybean whey solution were determined with the Wade reagent method and HPLC, respectively [11]. At 25°C, the desorption of trypsin inhibitor, lectin and phytic acid from adsorbed CB is carried out in solutions at pH 7, 8 and 9, stirred at 100 rpm for 24 h. Then, the concentrations (C2) of

trypsin inhibitor, lectin and phytic acid were determined. The calculation equation for adsorption ratio and desorption ratio were as follows:

$$\text{Adsorption ratio (\%)} = [(C_0 - C_1)/C_0] \times 100$$

$$\text{Desorption ratio (\%)} = [C_2/(C_0 - C_1)] \times 100$$

$$\text{Recovery ratio (\%)} = C_2/C_0 \times 100$$

Preparation of soybean whey

The preparation method of soybean whey was expatiated by Sorgentini and Wagner [6].

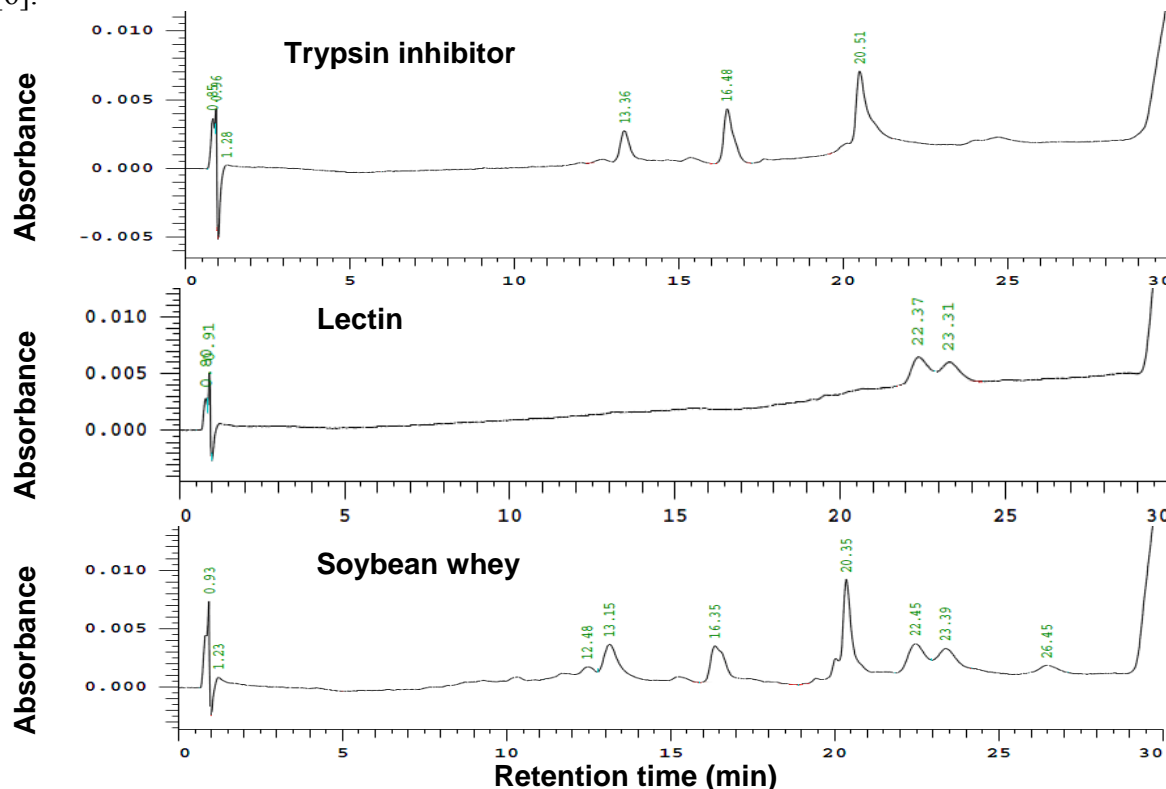


Figure 1. The elution patterns of reverse-phase high performance liquid chromatography of trypsin inhibitor, lectin and soybean whey.

Determination of trypsin inhibitor and lectin

The HPLC system equipped with L-2130 Pump and L-7455 Detector (Hitachi, Tokyo, Japan). A POROS R2/H perfusion column (100 mm x 2.1 mm I.D., Perseptive Biosystems, Framingham, MA, USA) was used for the separation of proteins. Mobile phase A consisted of ultrapure water and 0.05% (v/v) TFA. Mobile phase B was ACN with 0.05% (v/v) TFA. These separations were performed at a flow-rate of 0.5 ml/min (mobile phase A + B) using a solvent gradient from 5% to 16% B in 8 min, 16% to 20% B from 8 to 12.5 min, 20% to 24% B from 12.5 to 13.5 min, 24% to 40% B form 13.5 to 17.5 min, 40% to 45% B form 17.5 to 22.5 min, 45% to 50% B from 22.5 to 26.5 min, and 50% to 95% B form 26.5 to 27 min. The injected volume was 20 μ l, the operation temperature was 60°C and UV detection was performed at 254 nm. The standard curves were established via plot of peak area versus concentration of trypsin inhibitor and lectin, respectively [11].

RESULTS and DISCUSSION

Figure 1 shows the elution patterns of reverse-phase high performance liquid chromatography of trypsin inhibitor, lectin and soybean whey. The results indicate that the retention times of peaks of soybean whey at 13.15, 16.35 and 20.35 min were nearly the

same as the peaks of trypsin inhibitor; the peaks at 22.45 and 23.39 min were almost same as the peaks of lectin, since the major proteins of soybean whey were trypsin inhibitor and lectin. The result was similar to that of Sorgentini and Wanger [6].

Table 1. The adsorption ratio of 0.1 g chitosan/TPP/genipin bead for phytic acid, trypsin inhibitor and lectin adsorbed from soybean whey solution (pH 2) at 25°C.

Adsorption time (h)	Phytic acid ($\mu\text{g/ml}$)	Trypsin inhibitor ($\mu\text{g/ml}$)	Lectin ($\mu\text{g/ml}$)
0	178.48 \pm 0.64 ^a	1835 \pm 17 ^a	196 \pm 19 ^a
24	124.53 \pm 8.33 ^b	1766 \pm 122 ^a	193 \pm 11 ^a
Adsorption ratio(%)	30.23	3.76	1.53

Value are mean \pm S.D (n=3). ^{a,b} Different letters in the same column indicate significant difference ($p < 0.05$) between samples.

At 25°C, the adsorption of phytic acid, trypsin inhibitor and lectin from soybean whey solution by CB was carried out for 24 h (Table 1). The results show that the initial concentration and adsorbed concentration of phytic acid were 178.45 and 124.53 $\mu\text{g/ml}$, respectively. The initial concentration and adsorbed concentration of trypsin inhibitor and lectin changed insignificantly; they were 1835 to 1766 $\mu\text{g/ml}$ and 196 to 193 $\mu\text{g/ml}$, respectively. This indicates that CB could effectively adsorb phytic acid; the adsorption ratio was 30.23%. However, the adsorption ratios of trypsin inhibitor and lectin were very low: the values were 3.76% and 1.53%, respectively. The results indicate that CB had an acceptable adsorption ratio of phytic acid in pH 2 soybean whey solution at 25°C. But trypsin inhibitor and lectin were almost not adsorbed by this bead. In short, the selective adsorption of phytic acid can be executed by the CB in pH 2 soybean whey solution at 25°C.

At 25°C, the desorption of phytic acid from adsorbed phytic acid CB was carried out in pH 7, 8 and 9 solutions for 24 h. The desorption ratio of phytic acid from the CB desorbed in pH 7, 8 and 9 solution were 74.07%, 80.25% and 93.98%, respectively. This indicates that the desorption ratio of phytic acid increased with the increased solution pH value. In higher pH solution, the electrostatic force between the amino group of chitosan and phytic acid was weaker due to lower protonation of chitosan. This led to phytic acid being more easily desorbed from chitosan, and with a higher desorption ratio.

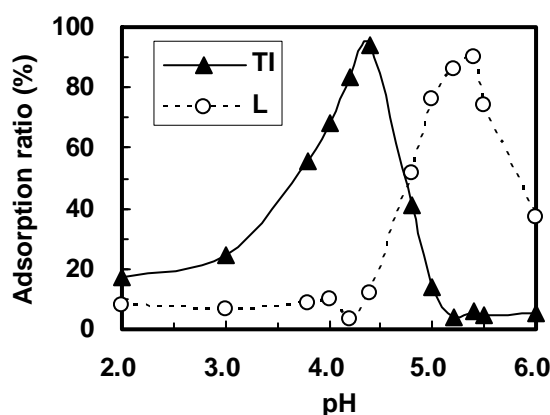


Figure 2. Effect of pH on the adsorption ratios (%) of CB9 adsorbed trypsin inhibitor (TI) and lectin (L) from soybean whey at 15°C for 24 h..

Figure 2 shows that the adsorption of trypsin inhibitor and lectin from soybean whey solution (pH 2.0-5.6) by CB was carried out for 24 h at 15°C. The results show that the highest adsorption ratio of trypsin inhibitor and lectin were 94.2% at pH 4.4 and 90.2% at pH 5.4, respectively. However, adsorption ratio of lectin and trypsin inhibitor were 11.6% at pH 4.4 and 6.0% at pH 5.4, respectively. The results indicate that selective adsorption of

trypsin inhibitor and lectin can be executed by CB in pH 4.4 and 5.4 soybean whey solution at 25°C.

The adsorption ratios of trypsin inhibitor were decreased with co-crosslinking degrees of CBs increasing (Figure 3). It indicated that free amino group of chitosan was served an important role in adsorption of protein. The results indicate that the maximum adsorption ratios of trypsin inhibitor and lectin were at pH 4.4 and pH 5.5, respectively. The specific pH values are near pI of trypsin inhibitor and lectin. The pIs of trypsin inhibitor and lectin are pH 4.5 and pH 5.6, respectively. This phenomenon may be due to amphoteric property of CB. Amino group of chitosan is positive charge, phosphate of TPP is negative charge. When solution pH is larger of smaller pI of protein, which is not favorable for adsorption of bead due to electrostatic repulsion between the protein and bead. Therefore, the proteins were adsorbed by CB thanks to both electrostatic interaction and hydrogen bonding. The hydrogen bonding may be as dominator in this adsorption system.

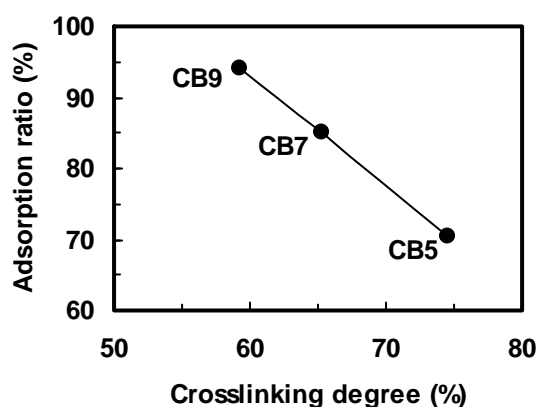


Figure 3. Effect of crosslinking degree on adsorption ratios (%) of chitosan/TPP/genipin beads adsorbed trypsin inhibitor from pH 4.4 soybean whey solution at 15°C.

Table 2. The adsorption ratios (%) and selectivities (Sel) of chitosan/TPP/genipin beads (CB5, CB7 and CB9) adsorbed trypsin inhibitor and lectin from pH 4.4 soybean whey solutions at 15°C.

	CB5	CB7	CB9
Trypsin inhibitor	70.4±2.5 ^a	85.2±1.0	94.2±0.3
Lectin	5.7±1.7	6.0±2.1	11.6±1.7
Sel ^b	12.4	14.2	8.1

^a Value of adsorption ratio represents mean±S.D. (n=3).

^b Sel was the ratio of adsorption ratio of trypsin inhibitor to lectin at pH 4.4.

At 15°C, the best adsorption ratios of CB5, CB7 and CB9 adsorbed trypsin inhibitor from pH 4.4 soybean whey solutions being 70.4%, 85.2% and 94.2%, respectively (Table 2). However, the adsorption ratios of CB5, CB7 and CB9 for lectin were very low at same adsorbed condition, it were 5.7%, 6.0% and 11.6%, respectively. In conclusion, the selective isolation for trypsin inhibitor from pH 4.4 soybean whey solution could be processed by chitosan/TPP/genipin beads due to good selectivities.

The maximum trypsin inhibitor and lectin of adsorbed CBs were desorbed in pH 9 solution for 24 h at 25°C, respectively. The results show the desorption ratio of trypsin inhibitor and lectin from CB were 80.9% and 81.0%, respectively. In short, selective isolation of trypsin inhibitor and lectin from soybean whey can be carried out by CB and recovery ratios were 74% and 72%, respectively.

CONCLUSIONS

At 25°C, under pH 2 soybean whey solution, CB7 could selectively adsorb phytic acid; the adsorption ratio was 30.23%, however, the adsorption ratios of trypsin inhibitor

and lectin were very low, only 3.76% and 1.53% respectively. The desorption ratio of phytic acid from the CB7 desorbed in pH 7, 8 and 9 solution were 74.07%, 80.25% and 93.98%, respectively.

At 15°C, under pH 4.4 soybean whey solution, CB9 could selectively adsorb trypsin inhibitor due to the adsorption ratio was 94.2%, however, the adsorption ratios of lectin were only 11.6%. Under pH 5.4 solution, CB9 could selectively adsorb lectin due to the adsorption ratio was 90.2%, however, the adsorption ratios of trypsin inhibitor were only 6.0%. The specific pH values are near pI of trypsin inhibitor and lectin. Therefore, both electrostatic interaction and hydrogen bonding are considered the interaction force between proteins and CB9. The hydrogen bonding may be as dominator in this adsorption system. The desorption ratio of trypsin inhibitor and lectin from CB9 were 80.9% and 81.0%, respectively. In short, selective isolation of trypsin inhibitor and lectin from soybean whey can be carried out by CB9 and recovery ratios were 76% and 73%, respectively.

ACKNOWLEDGEMENTS

The authors wish to express their appreciation for the financial support from National Science Council, ROC (NSC 97-2313-B-019-007-MY3; NSC 100-2313-B-019-004-MY3).

REFERENCES

- [1] Muzzarelli, R. A. A. (2011). Potential of chitin/chitosan-bearing materials for uranium recovery: an interdisciplinary review. *Carbohydr. Polym.*, 84, 54-63.
- [2] Crini, G. (2005). Recent developments in polysaccharide-based materials used as adsorbents in wastewater treatment. *Prog. Polym. Sci.*, 30, 38-70.
- [3] Mi, F. L., Sung, H. W., Shyu, S. S., Su, C. C., Peng, C. K. (2003). Synthesis and characterization of biodegradable TPP/genipin co-crosslinked chitosan gel beads. *Polymer*, 24, 6521-6530.
- [4] Muzzarelli, R. A. A. (2009). Genipin-chitosan hydrogels as biomedical and pharmaceutical aids. *Carbohydr. Polym.*, 77, 1-9.
- [5] Sung, H. W., Huang, R. N., Huang, L. L. H., Tsai, C. C. (1999). In vitro evaluation of cytotoxicity of a naturally occurring cross-linking reagent for biological tissue fixation. *J. Biomat. Sci.-Polym. E.*, 10, 63-78.
- [6] Sorgentini, D. A., Wanger, J. R. (1999). Comparative study of structural characteristics and thermal behavior of whey and isolate soybean proteins. *J. Food Biochem.*, 23, 489-507.
- [7] Casal, E., Montilla, A., Moreno, F. J., Olano, A., Corzo, N. (2006). Use of chitosan for selective removal of β -lactoglobulin from whey. *J. Dairy Sci.*, 89(5), 1384-1389.
- [8] Tsai, M. L., Chang, H. W., Yu, H. C., Lin, Y. S., Tsai, Y. D. (2011). Effect of chitosan characteristics and solution conditions on gelation temperatures of chitosan/2-glycerophosphate/nanosilver hydrogels. *Carbohydr. Polym.*, 84, 1337-1343.
- [9] Baxter, A., Dillon, M., Taylor, K. D. A., Roberts, G. A. F. (1992). Improved method for i.r. determination of the degree of N-acetylation of chitosan. *Int. J. Biol. Macromol.*, 14, 166-169.
- [10] Tsai, M. L., Bai, S. W., Chen, R. H. (2008). Cavitation effects versus stretch effects resulted in different size and polydispersity of ionotropic gelation chitosan-sodium tripolyphosphate nanoparticle. *Carbohydr. Polym.*, 71, 448-457.
- [11] Yang, C. Y., Hsu, C. H., Tsai, M. L. (2011). Effect of crosslinked condition on characteristics of chitosan/tripolyphosphate/genipin beads and their application in the selective adsorption of phytic acid from soybean whey. *Carbohydr. Polym.*, 86, 659-665.

SYNTHESIS OF CHITOSAN DERIVATIVES WITH ANTIFUNGAL AND ANTIBACTERIAL PROPERTIES

A.Valbuena-Inciarte¹, C. Valbuena¹, M. Colina^{✉1,2} y N. Diaz³

¹Laboratorio de Química Ambiental . Departamento de Química, Facultad Experimental de Ciencias. Universidad del Zulia. Maracaibo 4001, Venezuela.

²Empresa Mixta Innovación Ambiental Quitosano CA. (INNOVAQUITO CA) Av. 4 San Francisco Sector El Bajo No 29-25.

³Instituto de Estudios Avanzados IDEA Hoyo de la Puerta. Sartenejas. Edo. Miranda Venezuela.

✉corresponding author:E-mail address: colinamarinela@gmail.com

ABSTRACT

In this work, chitosan with 9 different degrees of deacetylation were obtained (73 - 97) %. The samples were characterized by FTIR, being observed the stretching OH about 3450 cm⁻¹, the flexion of the group CH₂ at 1420 cm⁻¹, the stretching C - O at 1030 cm⁻¹, the stretching C - O at 1070 cm⁻¹, the signal of the stretching of the glucosidic bonds C - O at 897 cm⁻¹ and the stretching C - O asymmetric (bridge C-O-C) at 1160 cm⁻¹. The index of crystallinity by XRD showed an increase with the degree of deacetylation, after an oxidative degradation of the chitosan samples (Q1, Q3, Q6 and Q9) with H₂O₂ activated with HCL. Analysis for FTIR and DRX of the degraded fractions were performance deciding for the not aqueous fractions supported by the typical spectral signals of chitosan with high degrees of deacetylation and high crystallinity ratio. The aqueous fractions showed the deformation of the plane for the group N=CHCOO- and low crystallinity. Antimicrobial test was established 5 mg/L as MIC for the *E.coli's* growth, and 70 mg/L for the *N. Crassa* growth, disabling more than 80 % of the bacterial and fungus population.

Keywords

Chitosan, Deacetylation, Degradation, MIC, *Escherichia Coli*, *Neurospora Crassa*.

INTRODUCTION

A great number of anti-fungal and bactericidal agents available on the market present characteristics not compatible with the environment, it is for this reason that diverse groups of researchers are developing alternative strategies for the bactericidal and antifungal obtaining from biomass such as chitin and chitosan[1] Chitin is the most abundant second polysaccharide in the nature after the cellulose. It is a type of renewable natural resource, which presents a specific number of properties, since biocompatibility, biodegradability and not toxic activity towards certain applications, for what it constitutes a raw material for obtaining a great number of anti fungal and bactericidal agents[2] They are found in the crustaceans, in the skeleton of some insects and in the cellular walls of many fungi and algae. The chitosan and its derivatives are produced from the hydrolysis of the chitin in alkaline way; it is composed of two subunits D-glucosamine and N-acetyl-D-glucosamine, which are connected by the (1-4) glycoside bond [3]. Currently, several authors [4-5] have established that the activity of the chitosan depends to some biological entities of their molecular size distribution, degree of deacetylation, chemical modification, substitution degree, pH, length and position of the substituents on the units repeating glucosamine and

the target organism. These variations may result in two different mechanisms of interaction of chitosan with the specific microorganism, the first is adsorption of chitosan in the cell walls forming a coating of chitosan membrane rupture and leak through this wall, the second is chitosan penetration into the walls leading to the inhibition of various enzymes, the significance of this work is that the modification of chitosan of different degrees of deacetylation through degradation oxidative, can generate better performing products fungicide and bactericide.[1]

MATERIALS AND METHODS

1. Sample collection and preparation of chitosan with different degrees of deacetylation

Crab shells were supplied from PROMARCA. The wastes were reacted for deproteinization with 10% (w/w) NaOH solution for 1 h at 65 °C with constant stirring at a solid/solvent ratio of 1:10 (w/v), they were washed with water for three times. Then they were demineralized with 1 N HCl for 30 min at 25 °C with a solid/solvent ratio of 1:15 (w/v). Crab shells were then decolorized with ethanol for 10 min and dried for 2 h at 25 °C, followed by bleaching with 0.315% (v/v) sodium hypochlorite (NaOCl) solution (containing 5.25% available chloride) for 5 min with a solid/solvent ratio of 1: 10 (w/v), based on dry shell. Samples were washed with tap water and dried at 25 °C for 24 h. Removal of acetyl groups from chitin was achieved by refluxing for different conditions (Table 1) with a solid/solvent ratio of 1:15(w/v). The resulting chitosan was washed to neutrality with tap water, rinsed with hot distilled water (90 °C), filtered and dried at 60 °C for 24 h in an oven.

2. Degradation of chitosan

2 g of chitosan (Q1, Q3, Q4, Q6 and Q9) was completely dissolved in 100 ml 0.5% hydrochloric acid solution, then 5 ml H₂O₂ aqueous solution (the concentration was 0.68 M) was added. The solution was stirred and reacted at the desired temperature of 50 °C for different times 30, 90, 150, 240 min, respectively. After the reaction, the solution was filtrated. The collected solid was washed with distilled water until reaching pH 7, and then dried in a vacuum. The obtained product was the water-insoluble chitosan denominated during for this work (FNA, Not aqueous fraction). The filtrate was adjusted to pH 7.0 with NaOH solution and a precipitate was obtained by adding ethanol, this was collected after drying the precipitate in vacuum, and named (FA, fraction aqueous). The resulting products were lyophilized in the follows conditions a -51°C a 4000X10-03 Mbar during for 7 h.

3. Characterization

The degree of deacetylation (DD) was assessed by FT-IR spectroscopy, this was used to characterize chemical functional groups of chitosan and degraded chitosan. FT-IR spectra (Shimadzu 8400) were collected using a KBr and ATR method. Elemental analysis to determine the degree of deacetylation measurement was carried out LECO/Truspec CHN. The crystal structure were recorded at room temperature by X-ray diffraction using a Bruker / D8 Focus with a Cu K α ($\lambda=1.54 \text{ \AA}$), 0.05 ° pass with a range from 5° to 40° and the cristallinity index was determined throught the equation $CI_{110} = [(I_{110} - I_{am}) / I_{110}] \times 100$ where I_{020} , I_{110} and I_{am} are peak intensities in the reflections (020), (110) and amorphous diffraction $2\theta = 12.6^\circ$, respectively.

The viscosity of chitosan solutions in CH₃COOH/CH₃COONa buffer (0.5:0.2M) was measured by using a Anton Parr Viscometer (SVM 3000) a constant temperature bath at 20.0±0.1 °C. The increment in the solution viscosity, η , with respect to that of the pure

solvent, η_0 , the relative viscosity, is the ratio $\eta_r = \eta/\eta_0$. The specific viscosity of solution of concentration c is $\eta_{sp} = (\eta - \eta_0)/\eta_0 = \eta_r - 1$ (1). A classical procedure for its determination consists of the determination of viscosities of various solutions with different concentrations, followed by extrapolation of η_{sp}/c to zero concentration. In a range of moderate concentrations, the dependence is linear and can be written as the Huggins equation: $\eta_{sp}/c = [\eta] + k_H[\eta]2c$ (3) where k_H is the (dimensionless) Huggins constant. Thus, $[\eta]$ can be obtained as the intercept in a linear least-squares fit. The molecular weight was calculated based on the Mark–Houwink–Sakurada (MHS) equation as follows: $[\eta] = KMv^\alpha$ (4), where $[\eta]$ is the intrinsic viscosity, K and α are viscometric parameters depending on the solvent. Chitosan was dissolved in 0.5M $\text{CH}_3\text{COOH}/0.2\text{MCH}_3\text{COONa}$. [3]

4. Antimicrobial test

Antibacterial activities of chitin, chitosan (Q3 – Q9) and degraded chitosan [(30, 90, 150, 240 min Q9), (30, 90, 150, 240 min Q4), (30, 90, 150, 240 min Q6)] were examined as the inhibitory effects against the growth of our Gram-negative bacteria: *Escherichia Coli* (*E. Coli*) CVCM2070, the inhibitory effect was estimated periodically by measuring turbidity of the cultured medium at 600 nm using a TECAN spectrophotometer. The minimum inhibitory concentration (MIC) was defined as the lowest concentration of chitosan or degraded chitosan required to completely inhibit bacterial growth after incubation at 37 °C for 72 h. For determination of the minimum inhibitory concentration for the samples (MIC) 1% (w/w) in 1% (w/w) acid) of each substances were added to grown medium LB Both for final chitosan concentrations of (2 – 600 ppm). For Fungicidal activities of *Neurospora Crassa* (*N. Crassa*), the inhibitory effect was estimated periodically by measuring consumption of glucose in TECAN spectrophotometer for a method enzymatic, the minimum inhibitory concentration (MIC) after incubation at 25 °C for 72 h in a MPPY grown medium.

RESULTS AND DISCUSSION

1. Preparation and characterization of chitosan with different degrees of deacetylation

The deacetylation of chitin (Q0) used for preparation of chitosans with different DD (Q1-Q9), the molecular weights decreased obviously as the deacetylation time increased and a long reaction time was required in heterogeneous deacetylation of chitin (Table 1).

Table 1. Reaction conditions, degree of deacetylation and viscosimetric molecular mass.

Sample	Reaction Time, h	[NaOH], % m/v	DD ^A , %	DD ^B , %	Mv, (KDa)
Q0	---	---	32,86	30,03	---
Q1	6 + 4 (10)	30	70,18	73,01	520,12
Q2	4 + 4 + 4 + 4 (16)	30	72,41	75,51	450,15
Q3	4 + 4 + 4 (12)	30	74,06	78,03	620,14
Q4	6 + 4 (10)	50	81,20	82,52	513,62
Q5	6 + 6 + 6 (18)	50	87,01	86,02	253,52
Q6	6 + 3 + 3 (12)	50	85,38	88,05	490,36
Q7	6 + 4 + 4 (14)	50	88,23	89,22	420,95
Q8	4 + 4 + 4 + 4 (16)	50	92,08	90,03	598,60
Q9	4 + 4 + 4 + 3 (15)	50	95,76	97,01	272,35

FTIR determination $DA^A = (((A_{1655}/A_{3450}) \times 100) / 1,33)$ y $DA^B = (((A_{1320}/A_{3450}) - 0,03146) / 0,0026)$. CHN determination $DD^B = [1 - (C/N - 5,145) / 1,716] \times 100$

In spectrum of the Q9 (Figure 1), strong characteristic band at 1590cm^{-1} is assigned to the N-H bending vibration of the primary amine. The bands at 1650cm^{-1} (amide I band), 1544cm^{-1} (amide II band), and 1454cm^{-1} (CH_3 in-plane bending) are greatly weakened in this spectrum of highly deacetylated chitosan.[1]

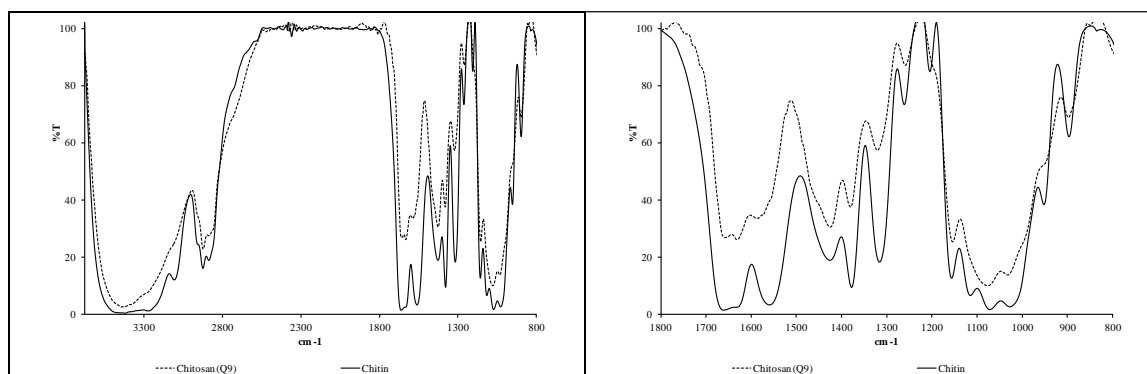


Figure 1. Infrared spectra Chitin and Chitosan (Q9) (A) infrared spectrum between 800 to 3900 cm^{-1} (B) Expansion of C-O-C area.

So far, the following six polymorphs have been proposed for chitosan: “tendon chitosan”, “annealed”, “1-2”, “L-2”, “form-I” and “form-II”. The single molecular chain in these polymorphs has always been observed to be extended 2-fold helical structure.[5].

The strongest reflection appears at $2\theta=11.4^\circ$, which is assigned to (100) reflection. The strongest reflection appears at $2\theta = 20.1^\circ$, which corresponds to the (100) reflection shown in Figure 2 (A) [2]. In Figure 2 (B) shows the reduction in crystallinity due to the increase in free amine groups in the polymer chain leads to increased intramolecular and intermolecular electrostatic forces, since the hydrogen bridge formation, decreasing this structural rigidity makes it less crystalline chitosan obtained as they have a high degree of deacetylation

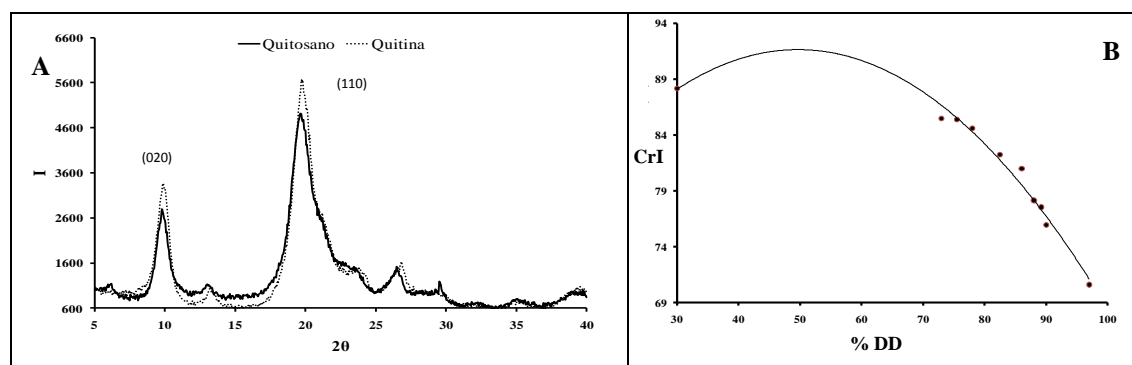


Figure 2. (A) XRD of Chitin and Chitosan. (B) Crystallinity Index Vs Degree of deacetylation.

2. Degradation and characterization of degradation products of chitosan with differents degree of deacetylation

The FT-IR spectra of chitosan (Q9 = 97 %), water soluble (FA) and water-insoluble chitosan (FNA), both obtained from chitosan Q9 = 97 %, are shown in Figure 3 (A and B), respectively. These data shows that the structures of the main chain of chitosan and FA are the same. In comparison with the FT-IR spectrum of chitosan, the FA shows a new peak at 1623cm^{-1} , which is assigned to the absorbance of C=O. It might be the new side group FA. In the FT-IR spectrum of water-soluble chitosan (Figure 3A), the peak at 777.5cm^{-1} is assigned to the out-of-plane deformation of the N=CHCOO- group, which is a

consequence of the N=C double bond. This suggests that Maillard reaction between –CHO of 2, 5-anhydro-D-mannose end group and –NH₂ of chitosan was occurred.

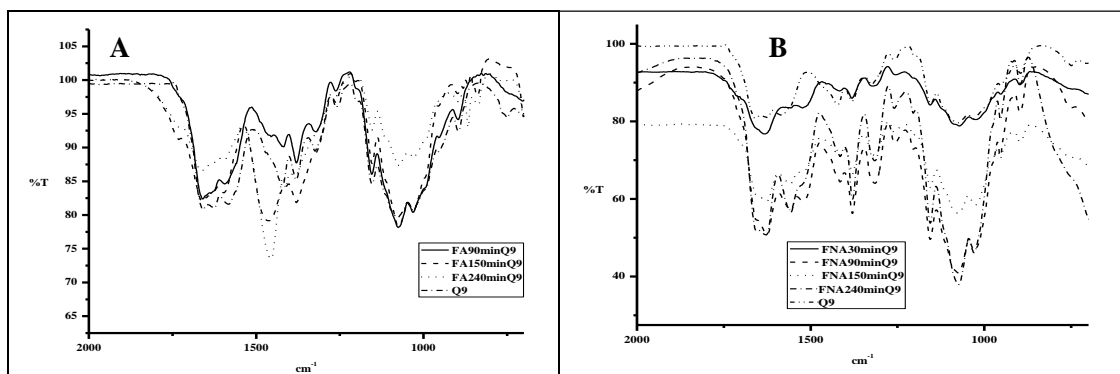


Figure 3.(A)FTIR spectra of the water soluble fractions Q9.(B)FTIR spectra of the fractions water-insoluble Q9.

FA and FNA was product of chitosan (Q9= 97%) depolymerized with H₂O₂ solution. As shown in Figure 4 (A and B), the intensity peak of FA were significantly lower than those of chitosan at $2\theta = 10.38^\circ$, $2\theta = 19.84^\circ$ and $2\theta = 22.46^\circ$, whose crystallinity degree is 20.06% decreased from 26.1% of the initial chitosan. This can be observed in the Figure 4 (A) where the chitosan with high deacetylation degree is easily depolymerized which is the normal mechanism of the chitosan depolymerization by H₂O₂. In acidic reaction system, more amino groups became protonated group, which improves the solubility of chitosan and helps to increase the pH of solution. This suggest that there are more free amine groups in the polysaccharide chains, the more easily NH₂ react with H₂O₂ to break down the chitosan chain. That indicated that the amine groups on C-2 of chitosan facilitated a site-specific for fragmentation of the glycosidic linkages while the N-acetyl group slowed the rearrangement of radicals during b-cleavage. During the depolymerization, the change in peaks was caused by that the amorphous part of chitosan which was referentially degraded and the crystal part was temporally maintained.

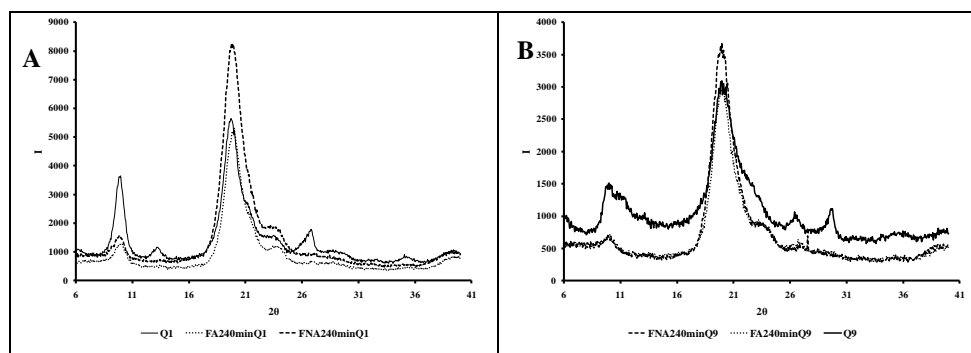


Figure 4. XRD degraded Chitosan samples (A) Q1, (B), Q9.

3. Antimicrobial activity

The efficient antibacterial and fungicide concentration of acetic acid was investigated in detail in Figure 5 (A and B) which shows the antimicrobial activity of the acetic acid with different concentrations for *E. coli* and *N. Crassa* at concentration ranges from 1 to 3 %. When the concentration of acetic acid was 1 %, the activity was a little lower than the control set. However, when the concentration was higher than 2 %, almost all the *E. coli* was killed. The minimal inhibitory concentrations (MIC) of degraded chitosan: 240

minQ9, 240 minQ4 and 240 minQ6 were lower compared to chitosan Q9, Q4 and Q6. In Figure 5 (C and D), differences in activity were exhibited between the type and/or molecular weight of the material against bacterial and fungus species.[1]

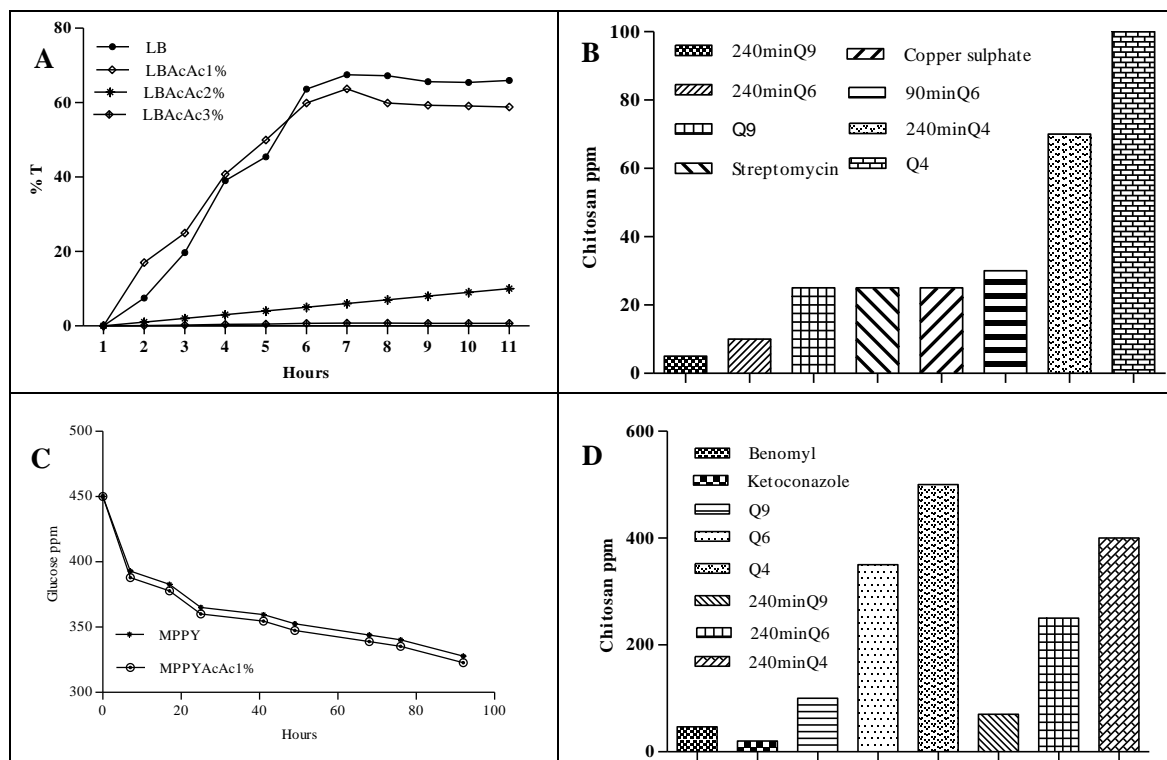


Figure 5. (A) and (C) Determination of minimal acetic acid concentration in Kinetic of *E. coli* and *N. Crassa* respectively. (B) and (D) Minimal Inhibitory Concentrations (MIC) of Chitosans and degraded chitosans against *E. Col.* and *N. Crassa* respectively.

CONCLUSIONS

The crystallinity index is inversely affected by the degree of deacetylation. In the depolymerization of chitosan by hydrogen peroxide, the breakage of 1,4-b-D-glucoside bonds in polysaccharide chain decreases the chitosan molecular weight. Degraded chitosan would have advantages as new antimicrobial agents due to their higher activity and since they are also more readily soluble in water than the native polysaccharides.

REFERENCES

- [1] Rabea, E.; Badawy, M. (2009). In vitro assessment of N-(benzyl)chitosan derivatives against some plant pathogenic bacteria and fungi. *Eur. Polym. J.*, 45, 237–245.
- [2] Zhong, Z.; Chen, R. (2007). Synthesis and antifungal properties of sulfanilamide derivatives of chitosan. *Carbohydr. Res.*, 342, 2390–2395.
- [3] Park, T.; Jeong, J.; Kim, S. (2006). Current status of polymeric gene delivery systems. *Adv. Drug. Deliv. Rev.*, 58, 467-486.
- [4] Pinottia, A.; Garcia, A. (2007). Study on microstructure and physical properties of composite films based on chitosan and methylcellulose. *Food Hydrocolloid.*, 21, 66–72.
- [5] Chavez, A., Colina, M., Valbuena, A. and López, A. (2012). Obtención y caracterización de películas de quitosano elaborado a partir de los desechos de la industria cangrejera. *Revista Iberoamericana de Polímeros*, 13, 2 -13.

Chemical and Physicochemical Properties

USE OF HIGHLY DEACETYLATED CHITOSAN FOR THE REMOVAL Cr (VI) FROM AQUEOUS SOLUTIONS BY ADSORPTION: THERMODYNAMIC PARAMETERS

T. R. S. Cadaval; A. S. Camara; G. L. Dotto; L. A. A. Pinto*

Unit Operation Laboratory, School of Chemistry and Food, Federal University of Rio Grande – FURG, Rio Grande, RS, Brazil.

*dqmpinto@furg.br

Abstract

In this work, highly deacetylated chitosan (HDC) was obtained from shrimp wastes (*Penaeus brasiliensis*) and used to remove chromium VI (Cr (VI)) from aqueous solutions by adsorption. The adsorption study was carried out by equilibrium isotherms and thermodynamic analysis. The equilibrium data were fitted with three models and also the thermodynamic parameters were estimated. The Sips model was the more appropriate to fit the experimental equilibrium data, being the maximum adsorption capacity of 97.4 mg g⁻¹, obtained at 298K. Negative values of ΔH^0 , ΔS^0 and ΔG showed that the adsorption was exothermic, spontaneous and favorable.

Keywords: Deacetylation degree; Cr (VI) adsorption; Isotherms; Chitosan.

INTRODUCTION

Heavy metals occur in natural waters due to the discharge of contaminated effluents from various industries [1]. Effluents containing Cr (VI) are very difficult to treat, since it is highly soluble [2]. The conventional methods for water purification are unfavorable economically and/or technically complex [3]. In this manner, adsorption is an alternative to removal Cr (VI) from aqueous solutions due its easy operation and application, high efficiency, and cost-effectiveness. Commercially, activated carbon is the most common adsorbent to remove heavy metals, however, alternative adsorbents have been studied [4].

Chitosan is a good scavenger for metal ions due its versatility, high efficiency, high selectivity, fast kinetics, availability and cost effectiveness [5,6]. In this context, studies demonstrated the chitosan applicability to removal metals [5-7]. However, these studies used this biopolymer in the commercial form or modified by many chemical means. An alternative to improve the chitosan performance as adsorbent, is obtain this biopolymer with high deacetylation degree, changing its production process [8].

In this work, highly deacetylated chitosan (HDC) was used to remove Cr (VI) from aqueous solutions by adsorption. HDC was obtained from shrimp wastes and characterized. Batch experiments were carried out at different temperatures to obtain the equilibrium isotherms. Three models were employed to fit the experimental data. The values of Gibbs free energy (ΔG), enthalpy (ΔH^0) and entropy (ΔS^0) changes were estimated.

MATERIALS and METHODS

HDC production and characterization

Chitosan was obtained from shrimp wastes (*Penaeus brasiliensis*). Firstly, chitin was extracted through the chemical treatments to eliminate carbonates, proteins and

pigments content. After, demineralization, deproteinization and deodorization/decolorization steps were carried out [9]. The deacetylation reaction was performed at 240 min, using concentrated sodium hydroxide solution (421 g L^{-1}) at $130 \pm 1^\circ\text{C}$ (solution:chitin ratio of 60:1 mL g^{-1}), under constant agitation of 50 rpm in order to obtain $95 \pm 1\%$ of deacetylation (DD) (5% of average degree of acetylation, AD) [10]. After, chitosan was purified through dissolution in diluted acetic acid solution (1%), centrifuged and precipitated by addition of sodium hydroxide until pH 12.5, followed by neutralization until pH 7.0. The resulting chitosan suspension was centrifuged for separation of the supernatant [9] and spouted bed dried [11]. Chitosan powder were sieved until the discrete particle size of $72 \pm 3 \mu\text{m}$ and characterized in relation to degree of deacetylation (potentiometric method) [12] and molecular weight (viscosimetric method, $K=1.8 \times 10^{-3} \text{ mL g}^{-1}$ and $\alpha=0.93$) [10]. The functional groups were identified by Fourier transform infrared spectroscopy (FT-IR) (Prestige, 21210045, Japan) [13].

Batch adsorption experiments

Stock Cr (VI) solutions (1 g L^{-1}) were prepared from $\text{K}_2\text{Cr}_2\text{O}_7$ at pH 3 (the pH was adjusted using buffer disodium phosphate/citric acid solution 0.1 mol L^{-1} , and measured by Mars, MB10, Brazil). The batch adsorption experiments were performed as follows: Firstly, 200 mg of HDC (dry basis) were added in 100 mL of Cr (VI) solutions with initial concentrations from 50 to 400 mg L^{-1} . After, these solutions were stirred (100 rpm) at different temperatures (298, 308, 318, 328 K) until the equilibrium. The Cr (VI) concentration was determined by spectrophotometry (Quimis, Q108, Brazil) at 540nm using 1,5-diphenyl carbazide as the complexing agent [7]. All experiments were carried out in replicate ($n=3$) and blanks were performed. The equilibrium adsorption capacity (q_e) was determined by Eq. (1):

$$q_e = \frac{V(C_0 - C_e)}{m} \quad (1)$$

where, C_0 is the initial Cr (VI) concentration in liquid phase (mg L^{-1}), C_e is the Cr (VI) concentration in liquid phase at equilibrium (mg L^{-1}), m is HDC dosage (g) and V is the volume of solution (L).

Isotherm analysis

The experimental equilibrium data were evaluated by the Langmuir, Freundlich and Sips models.

The Langmuir model assumes that the solid surface carries a limited number of sites that are characterized by equal energy of adsorption [14]. The Langmuir model is given by Eq. (2):

$$q_e = \frac{q_m k_L C_e}{1 + k_L C_e} \quad (2)$$

where, q_m is the maximum adsorption capacity (mg g^{-1}) and k_L is the Langmuir constant (L mg^{-1}).

The Freundlich model assumes that the adsorption surface is heterogeneous and can be represented by the Eq. (3) [15]:

$$q_e = k_F C_e^{1/n} \quad (3)$$

where, k_F is the Freundlich constant ($(\text{mg g}^{-1})(\text{mg L}^{-1})^{-1/n}$) and $1/n$ is the heterogeneity factor.

The Sips model is a Langmuir and Freundlich isotherm combination [16] and can be represented by Eq (4):

$$q_e = \frac{q_{ms} (K_s C_e)^m}{1 + (K_s C_e)^m} \quad (4)$$

where, q_{ms} (mg g^{-1}) is the maximum adsorption capacity of Sips, K_s (L mg^{-1}) the Sips constant and "m" the exponent of Sips model.

The isotherm models coefficients were estimated by nonlinear regression using Statistica 7.0 software (Statsoft, USA). The objective function was Quasi-Newton. The fit quality was evaluated by the coefficient of determination (R^2) and average relative error (ARE).

Thermodynamic parameters

The Gibbs free energy (ΔG) (kJ mol^{-1}), enthalpy (ΔH^0) (kJ mol^{-1}) and entropy (ΔS^0) changes ($\text{kJ mol}^{-1} \text{K}^{-1}$) were estimated by Eqs. (5) and (6) [17]:

$$\Delta G^0 = -RT \ln K \quad (5)$$

$$\ln K = -\frac{\Delta H^0}{RT} + \frac{\Delta S^0}{R} \quad (6)$$

where, K is the thermodynamic equilibrium constant, T is the temperature (K) and R is the universal gas constant ($8.314 \text{ J mol}^{-1} \text{ K}^{-1}$). The K values were estimated from the parameters of the best fit isotherm model [17].

RESULTS and DISCUSSION

HDC characterization:

The chitosan deacetylation degree obtained at 240 min was $95.0 \pm 0.9\%$. The molecular weight was 120 ± 4 kDa. Fig. 1 shows the FT-IR spectrum of HDC.

It was observed at 3350 and 3150 cm^{-1} (Fig. 1) the chitosan characteristic stretches of N-H and O-H. The C-N stretching of amides can be identified at 1550 cm^{-1} . The angular deformations of C-O-H and H-C-H appear in 1450 cm^{-1} . At 1075 cm^{-1} , the C-N stretching related to amino groups was identified. An overlap of C=O stretching bond of amide on the angular deformation of N-H is verified between 1600 and 1700 cm^{-1} .

Equilibrium and thermodynamics

The equilibrium adsorption isotherms were obtained from 298 to 328K. Fig. 2 shows the equilibrium experimental data of Cr (VI) adsorption onto HDC in all studied temperatures.

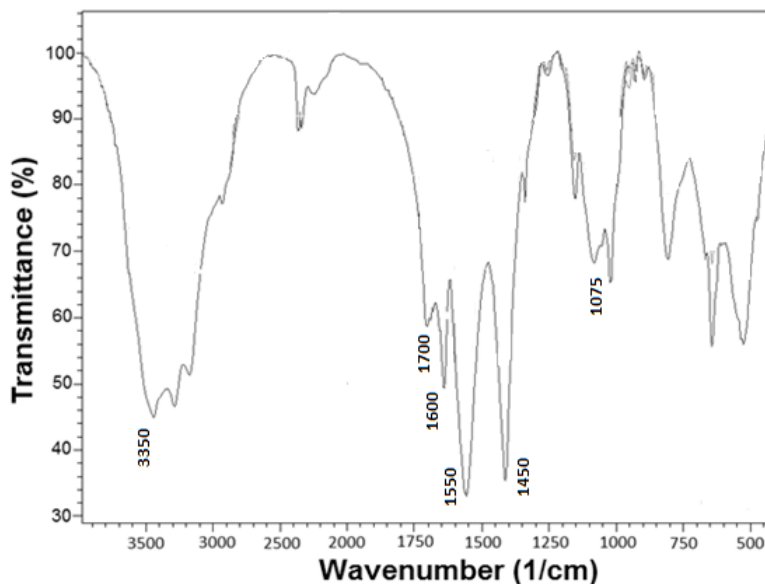


Figure 1: FTIR spectrum of HDC.

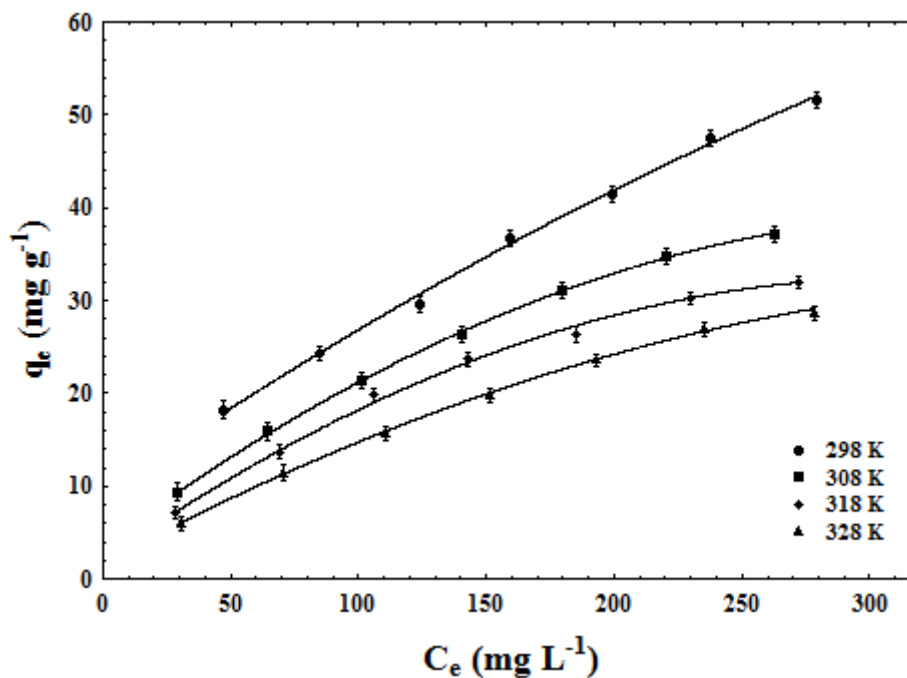


Figure 2: Equilibrium experimental data of Cr (VI) adsorption onto HDC.

It can be seen in Fig. 2, the isotherms were characterized by an initial increase in the adsorption capacity (indicating the great affinity between chitosan and Cr (VI) and a large number of accessible sites), tending a convex shape, which is associated with monomolecular layer adsorption [14]. It was observed that the temperature increase caused a decrease in adsorption capacity (Fig. 2). This can have occurred because the temperature increase causes an increase in Cr (VI) solubility [7], so, the interaction forces between Cr (VI) and the solvent become stronger than those between Cr (VI) and chitosan. Similar behavior was reported by Aydin and Aksoy (2009) [7].

In order to establish the most appropriate correlation to the equilibrium curves and estimate the isotherm parameters, three models (Langmuir, Freundlich and Sips) were fitted to the experimental data. Table 1 shows the isotherm parameters for Cr (VI) adsorption onto chitosan in all studied temperatures.

Table 1: Isotherm parameters for Cr (VI) adsorption onto HDC.

Temperature (K)	Langmuir				Freundlich				Sips				
	Q_m	KL	R^2	ARE	KF	n	R^2	ARE	Q_{mS}	KL	m	R^2	ARE
298	128.0	0.0022	0.99	3.86	0.705	1.36	0.99	1.33	97.4	0.002	0.82	0.99	1.41
308	236.4	0.0005	0.97	6.76	0.117	0.99	0.97	6.48	45.1	0.006	2.18	0.99	2.38
318	142.1	0.0008	0.95	11.85	0.103	1.01	0.96	9.72	36.0	0.006	2.45	0.99	2.24
328	220.8	0.0004	0.96	24.43	0.063	0.90	0.97	7.78	35.9	0.005	2.29	0.99	2.11

The coefficients of determination ($R^2 > 0.99$) and average relative errors (ARE < 2.5%) presented in Table 1 show that the Sips model was the more appropriate to fit the equilibrium experimental data in all studied conditions. Thus, this model can be used to represent the equilibrium data of Cr (VI) adsorption onto chitosan. The parameter q_{mS} (Table 1) increased with temperature decrease, reaching a maximum value of 97.4 mg g⁻¹ at 298 K. Literature shows maximum adsorption capacities for Cr (VI) using several adsorbents in the range from 2.8 to 110 mg g⁻¹ [1-7]. This shows that chitosan used in this study presented a good adsorption capacity.

Table 2 shows the thermodynamic parameters of Cr (VI) adsorption by HDC.

Table 2: Thermodynamic parameters for the Cr (VI) adsorption onto HDC.

Temperature (K)	298	308	318	328
ΔG^0 (kJ mol ⁻¹)	-4.87±0.01	-4.80±0.01	-4.75±0.02	-4.68±0.01
ΔH^0 (kJ mol ⁻¹)			-6.57±0.10	
$\Delta S^0 \times 10^3$ (kJ mol ⁻¹ K ⁻¹)			-5.77±0.01	

In Table 2, the negative values of ΔG^0 indicated that the Cr (VI) adsorption by HDC was a spontaneous and favorable process. The negative value of ΔH^0 shows that the adsorption process was exothermic. Comparing ΔH^0 and ΔS^0 values it can be seen that the Cr (VI) adsorption by HDC was predominantly an enthalpy controlled process.

CONCLUSION

The Sips model was the most adequate to represent the equilibrium adsorption isotherms. The maximum adsorption capacity was 97.4 mg g⁻¹ obtained at 298 K. The negative values of ΔG^0 , ΔH^0 and ΔS^0 showed that the Cr (VI) adsorption by chitosan was a spontaneous favorable and exothermic process. HDC is a good adsorbent to remove Cr (VI) from aqueous solutions.

REFERENCES

- [1] Albadarin, A. B., Mangwandi, C., Al-Muhtaseb, A. H., et al (2012). Kinetic and thermodynamics of chromium ions adsorption onto low-cost dolomite adsorbent. *Chemical Engineering Journal*, 179, 193–202.

- [2] Wan Ngah, W. S., Kamari, A., Fatimathan S., et al. (2006). Adsorption of chromium from aqueous solution using chitosan beads. *Adsorption*, 12, 249–257.
- [3] Wan, M. W., Kan, C. C., Rogel, B., & Dalida, M. L. P. (2010). Adsorption of copper (II) and lead (II) ions from aqueous solution on chitosan-coated sand. *Carbohydrate Polymers*, 80, 891–899.
- [4] Garcia-Reyes, R. B., & Rangel-Mendez, J. R. (2010). Adsorption kinetics of chromium (III) ions on agro-waste materials. *Bioresource Technology*, 101, 8099–8108.
- [5] Guibal, E. (2004). Interactions of metal ions with chitosan-based sorbents: a review. *Separation and Purification Technology*, 38, 43–74.
- [6] Wan Ngah, W. S., Teong, L. C., & Hanafiah, M. A. K. M. (2011). Adsorption of dyes and heavy metal ions by chitosan composites: A review. *Carbohydrate Polymers*, 83, 1446–1456.
- [7] Aydin, Y. A., & Aksoy, N. D. (2009). Adsorption of chromium on chitosan: Optimization, kinetics and thermodynamics. *Chemical Engineering Journal*, 151, 188–194.
- [8] Crini, G., & Badot, P. M. (2008). Application of chitosan, a natural aminopolysaccharide, for dye removal from aqueous solutions by adsorption processes using batch studies: A review of recent literature. *Progress in Polymer Science*, 33, 399–447.
- [9] Weska, R. F., Moura, J. M., Batista, L. M., et al (2007). Optimization of deacetylation in the production of chitosan from shrimp wastes: Use of response surface methodology. *Journal of Food Engineering*, 80, 749–753.
- [10] Moura, C. M., Moura J. M., Soares, N. M., & Pinto L. A. A. (2011). Evaluation of molar weight and deacetylation degree of chitosan during chitin deacetylation reaction: Used to produce biofilm. *Chemical Engineering and Processing*, 50, 351–355.
- [11] Dotto, G. L., Souza, V. C., & Pinto, L. A. A. (2011). Drying of chitosan in a spouted bed: The influences of temperature and equipment geometry in powder quality. *LWT—Food Science and Technology*, 44, 1786–1792.
- [12] Jiang, X., Chen, L., & Zhong, W. I. (2003). A new linear potentiometric titration method for the determination of deacetylation degree of chitosan. *Carbohydrate Polymers*, 54, 457–463.
- [13] Silverstein, R. M., Webster, F. X., & Kiemle, D. J. (2007). *Spectrometric identification of organic compounds*. (7th ed.). New York: John Wiley & Sons.
- [14] Langmuir, I. (1918). The adsorption of gases on plane surfaces of glass, mica and platinum. *Journal of the American Chemical Society*, 40, 1361–1403.
- [15] Freundlich, H. (1906). Over the adsorption in solution. *Journal of Physical Chemistry*, A57, 358–471.
- [16] Sips, R. (1948). On the structure of a catalyst surface. *The Journal of Chemical Physics*, 16, 490–495.
- [17] Milonjić, S. K. (2007). A consideration of the correct calculation of thermodynamic parameters of adsorption. *Journal of the Serbian Chemical Society*, 72, 1363–1367.

PHYSICO-CHEMICAL STUDIES ON THE CARBOXYMETHYLATION OF CHITOSAN

D. S. SILVA^{1*}, S. P. CAMPANA-FILHO¹

IQSC, Universidade de São Paulo, Av. Trab. São Carlense, 400, CP 780, CEP13560-970. São Carlos, SP, Brazil. (e-mail: danyss8@hotmail.com)

Abstract

Beta-chitin extracted from squid pens (*Loligo sp*) was subjected to the ultrasound assisted deacetylation (USAD process) aiming the production of extensively deacetylated chitosan (Ch0). Then, the extensively deacetylated chitosan ($\overline{DA}=4.5\%$) was submitted to the carboxymethylation reaction to result in O-carboxymethylchitosan (O-CMCh) presenting average degree of carboxymethylation (\overline{DS}) in the range $0.20 < \overline{DS} < 0.45$ depending of the molar ratio chitosan / monochloroacetic acid employed in the reaction. The ¹H NMR spectroscopy revealed the occurrence of N-carboxymethylation, evidenced by the signals observed in the range of 3.0 ppm - 3.4 ppm, assigned to the mono and disubstituted amino groups. However, as these signals exhibited low intensity, it was concluded that the N-carboxymethylation occurred in low extension when compared to O-carboxymethylation. The O-CMCh samples were soluble in acid (pH < 3.0), neutral (pH \approx 7.5) and alkaline (pH > 8.0) media due to the occurrence of charges along its chains. The occurrence of depolymerization simultaneously to the carboxymethylation reaction was observed since the O-CMCh samples showed lower viscosity average molecular weight as compared to the parent chitosan.

Keywords: chitin, chitosan and O-carboxymethylchitosan

Introduction

Chitosan has some properties that distinguish it from other polymers, such as its atoxicity, antimicrobial activity, biocompatibility and biodegradability [1]. The potential applications of chitosan are enhanced by the fact that it may be submitted to structural changes, resulting in derivatives with different characteristics and properties, and because it can be prepared in different forms such as solutions of controlled viscosity, gels, films, microspheres, nanoparticles and nanofibers [2].

Aiming to improve the physicochemical properties of chitosan and consequently their applications, some derivatization reactions have been suggested, such as N-acetylation [3], N-ftaloylation [4], O-carboxymethylation [5], and also the preparation of Schiff bases [6] and N-alkyl chitosan [7;8]. Accordingly, the proposed structural changes aim to improve properties such as solubility, swelling capacity, complexation of metal ions, and the interaction with other polymers, enzymes, proteins and organic substances. The derivatization reactions of chitosan are usually carried out under mild conditions, thereby avoiding the rupture of glycosidic bonds and the hydrolysis of acetamido groups.

The conversion of chitosan in a product more soluble in aqueous medium can be achieved by carrying out the carboxymethylation reaction, which results in a polyelectrolyte, namely carboxymethylchitosan (CMCh), having interesting physical, chemical and biological properties, such as high viscosity, low toxicity, biocompatibility, ability to form gels and solubility in a wide range of acidity [9]. The

interest in the carboxymethylation of chitosan has grown considerably, especially for producing soluble derivatives in physiological media, a very important property aiming the applications in the medical and pharmaceutical fields [10-13].

The main objective of this study is the production of O-carboxymethylchitosan by reacting extensively deacetylated chitosan with monochloroacetic acid in presence of excess sodium hydroxide. The influence of the molar ratio chitosan / monochloroacetic acid on the efficiency of the carboxymethylation reaction and on the structural characteristics and physicochemical properties of the O-carboxymethylchitosan samples is evaluated.

Materials and Methods

The deacetylation of beta-chitin, extracted from squid pens (*Loligo sp.*), was carried out according to the procedure reported by Delezuk [14]. Thus, the ultrasound-assisted deacetylation process was carried out twice consecutively to result in extensively deacetylated chitosan (sample Ch0). The carboxymethylchitosan samples were prepared according to Chen [5] and the molar ratio chitosan / monochloroacetic acid was 1:2.5, 1:5 and 1:10, producing samples CMCh-2.5, CMCh-5 and CMCh-10, respectively.

The structural and morphological characteristics of beta-chitin, chitosan and carboxymethylchitosan were determined as reported in the literature by using nuclear magnetic resonance and infrared spectroscopy [15], and X-rays diffraction [16-18]. Viscosity measurements were employed to determine the viscosity average molecular weight of chitosan and O-CMCh [15]. The solubility of O-CMCh samples in aqueous solution of different pHs was investigated by UV / visible spectroscopy [5] while the thermal stability was studied by thermogravimetric analysis [15]

Results and Discussion

The main results are discussed with emphasis on structural changes and properties resulting from carboxymethylation of chitosan and on the influence of the molar ratio chitosan/monochloroacetic employed in the reaction on the characteristics of the CMCh samples.

The vibration modes characteristics of beta-chitin, chitosan and O-CMCh were identified by IR spectroscopy analysis. The main characteristic peaks of chitin were observed at 3600-3000 cm^{-1} (axial deformation of O-H e N-H), 1660-1550 cm^{-1} (axial deformation of C=O and angular deformation of N-H), 1450-1370 cm^{-1} (symmetrical angular deformation of C-H), 1300-1315 cm^{-1} (axial deformation of CN), 1150-1155 cm^{-1} (axial deformation of O-H at hydrogen bond) and 1020-1080 cm^{-1} (angular deformation of C-O). The IR spectrum of chitosan exhibited the band due to the axial deformation of CO (1625 cm^{-1} , amide I), but the band in 1550 cm^{-1} , observed in the spectrum of beta-chitin, was not observed in the spectrum of chitosan.

The spectrum of the sodium salt form of O-CMCh (Figure 1) presented bands at 1405 cm^{-1} ($-\text{COO}^- \text{Na}^+$) and 1620 cm^{-1} (NH_2) while the acid form exhibited bands at 1731 cm^{-1} ($-\text{COOH}$), 1070-1136 cm^{-1} ($-\text{C-O}-$), 1622 cm^{-1} and 1517 cm^{-1} ($-\text{NH}_3^+$) [5;19]. Additionally, the acid and sodium salt forms of CMCh are clearly distinguished by the occurrence of an intense and broad band in the range 3400-2500 cm^{-1} due to stretching of strongly H-bonded hydroxyl group of the former, typical of carboxylic acid. The values of average degree of substitution (\overline{DS}) were determined from the IR spectra of

the O-CMCh samples [15], showing that the higher the excess of monochloroacetic acid used in the carboxymethylation reaction, the higher the average degree of substitution of the chitosan derivative (Table 1).

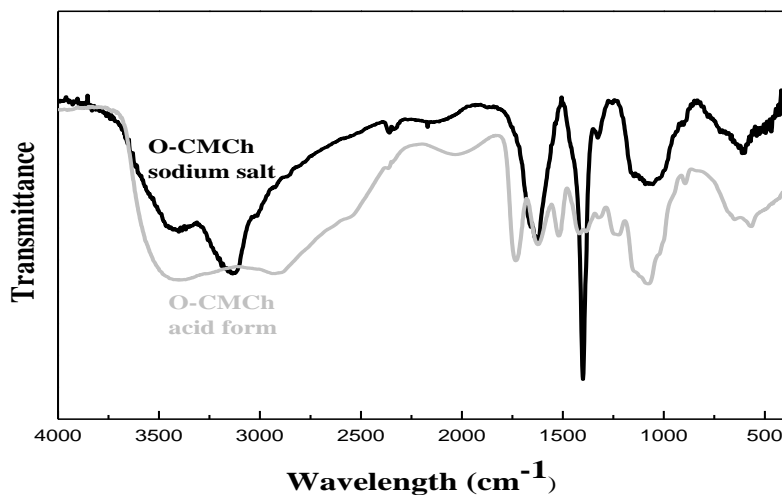


Figure 1- Infrared spectra of sample O-CMCh 10 as sodium salt and in acid form.

The structural modifications introduced by carboxymethylation were also evidenced by comparing the ^1H NMR spectra of chitosan (Figure 2) and O-CMCh (Figure 3). The ^1H NMR spectra of the O-CMCh samples revealed that the carboxymethylation of chitosan occurred in different extents depending on the reaction conditions. The occurrence of N-carboxymethylation was evidenced by the signals observed in the range of 3.0 ppm - 3.4 ppm, assigned to mono and disubstituted amino groups. However, as the signal intensity was much lower as compared to the signals occurring at 4.05 ppm - 4.55 ppm, attributed to the hydrogens of the carboxymethyl groups ($-\text{CH}_2-\text{COOD}$) introduced at the hydroxyl groups bonded to C3 and C6, it was concluded that the N-carboxymethylation occurred in low extension.

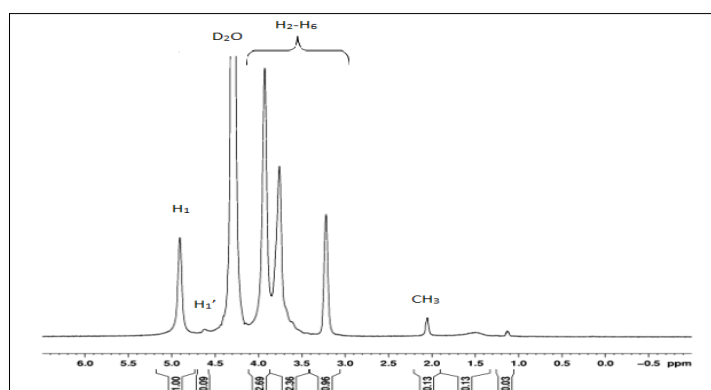


Figure 2- ^1H NMR (500 MHz) spectrum of chitosan (DCI/D₂O 1% (v/v)), 90°C.

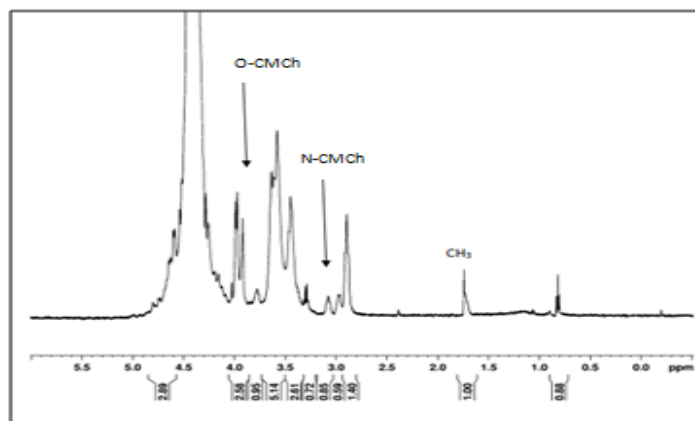


Figure 3- ^1H NMR (500 MHz) spectrum of CMCh-10 (DCI/D $_2$ O) 1% (v/v), 90 °C.

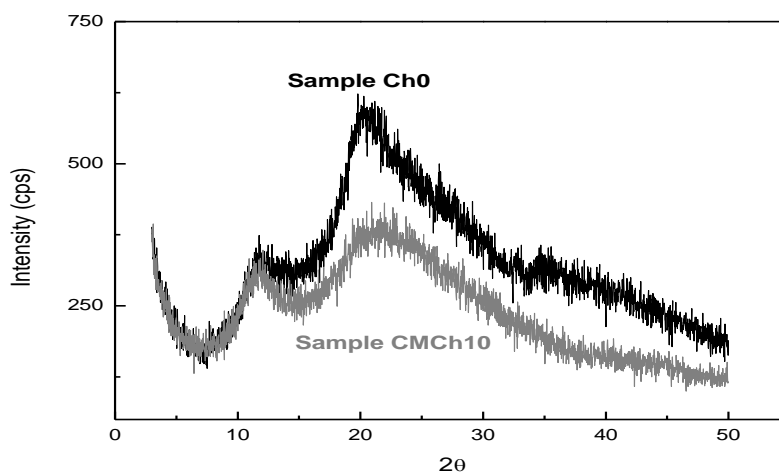


Figure 4: X-rays diffraction patterns of chitosan (sample Ch0) and carboxymethylchitosan (sample CMCh10, sodium salt form).

The X-ray diffraction analysis revealed that the carboxymethylation of chitosan provoked important changes in the arrangement of the polymer chains in the solid state, resulting in less organized arrangements (Table 1). Indeed, the spectra of carboxymethylchitosan exhibit broader and less intense peaks as compared to chitosan (Figure 4), which is attributed to the substitution of hydrogen atoms by carboxymethyl moieties, resulting in an important excluded volume effect and in repulsive interactions involving the sodium carboxylate groups.

Table 1- Values of intrinsic viscosity $[\eta]$, viscosity average molecular weight (M_v), average degree of substitution (DS) and the degree of order (DO) of chitosan and carboxymethylchitosan.

Samples	$[\eta]$ (mL/mg) ^(a)	$\overline{M}_v \times 10^5$ (g/mol) ^(b)	\overline{DS}	$\overline{DO}^{(a)}$
Ch0	0,9304	2,30	-	80
CMCh-2.5	0,8558	1,08	0,33	58
CMCh-5	0,8054	1,01	0,36	53
CMCh-10	0,5276	0,66	0,43	50

a) the values of DO were determined from the X-rays diffraction spectra according to the literature [18]

The solubility of chitosan and carboxymethylchitosan in aqueous media of different pHs was investigated, showing that chitosan is soluble in acid medium ($1.0 < \text{pH} < 6.5$) as described in literature [8], while carboxymethylchitosan is soluble in acid ($\text{pH} < 3.0$), neutral ($\text{pH} \approx 7.5$) and alkaline ($\text{pH} > 8.0$) media due to the occurrence of charges along its chains [15].

Conclusions

The average degree of substitution of the O-CMCh samples varied in the range $0,20 < \overline{DS} < 0,45$ depending on the molar ratio chitosan / monochloroacetic acid, the occurrence of N-carboxymethylation in a low extent being also observed. The carboxymethylation reaction has also resulted in depolymerization, as indicated by viscosity measurements, probably via alkaline hydrolysis of glycosidic linkages. The derivatization reaction resulted in improved solubility as the O-CMCh samples showed solubility in acid ($\text{pH} < 3.0$), neutral ($\text{pH} \approx 7.5$) and alkaline ($\text{pH} > 8.0$) media while chitosan is soluble only in acid medium ($1.0 < \text{pH} < 6.5$).

Acknowledgements

This research was supported by FAPESP, CNPq and CAPES.

References

1. AGULLO, E.; RODRÍGUEZ, M. S.; MATO, R.; TAPIA, C.; VALENZUELA, F.; PENICHE, C.; CABALLERO, A. H.; RAMÓN, J. S.; GOYCOOLEA, F.; ARGUELLES, W.; HIGUERA, I.; NAKAMATSU, J.; MAYORGA, A.; ABRAM, A. P. (2004). Quitina y Quitosano: Obtención, caracterización y aplicaciones. Fondo.
2. DOMARD, A. (2011). A perspective on 30 years research on chitin and chitosan. *Carbohydr. Polym.*, v. 84, n. 2, p. 696-703.
3. ANTHONSEN, M. W.; VÅRUM, K. M.; SMIDSRØD, O. (1993). Solution properties of chitosans: Conformation and chain stiffness of chitosans with different degrees of N-acetylation. *Carbohydr. Polym.*, v. 22, n. 3, p. 193-201.
4. SELMER-OLSEN, E.; RATNAWEERA, H. C.; PEHRSON, R. (1996). A novel treatment process for dairy wastewater with chitosan produced from shrimp-shell waste. *Water Sci. Technol.*, v. 34, n. 11, p. 33-40.
5. CHEN, X.-G.; PARK, H.-J. (2003). Chemical characteristics of O-carboxymethyl chitosans related to the preparation conditions. *Carbohydr. Polym.*, v. 53, n. 4, p. 355-359.
6. CAVALHEIRO E. T. G., CAVALHEIRO. C. C. S., CAMPANA-FILHO. S. P. (2009). Chitosan-Schiff bases: Preparation and applications. In: JAYAKUMAR, R.;

PRABAHARAN, M. (Ed.). Current Research and Developments on Chitin and Chitosan in Biomaterials Science. Cap.5. p. 89-106. Research Signpost.

7. CURTI, E.; DE BRITTO, D.; CAMPANA-FILHO, S. P. (2003). Methylation of Chitosan with Iodomethane: Effect of Reaction Conditions on Chemoselectivity and Degree of Substitution. *Macromol. Biosci.*, v. 3, n. 10, p. 571-576.

8. SASHIWA, H.; SHIGEMASA, Y. (1999). Chemical modification of chitin and chitosan 2: Preparation and water soluble property of N-acylated or N-alkylated partially deacetylated chitins. *Carbohydr. Polym.*, v. 39, n. 2, p. 127-138.

9. CHEN, L.; YUMIN, D.; X., Z. Relationship between the molecular structure and moisture-absorption and moisture-retention abilities of carboxymethyl chitosan. II. Effect of degree of deacetylation and carboxymethylation. *Carbohydr. Res.*, v. 3382003. p. 333-340.

10. ZHU, A. L., J.; YE, W. (2006). Effective loading controlled release of camptothecin by O-carboxymethylchitosan aggregate. *Carbohydr. Polym.*, v. 63, n. 1, p. 89-96.

11. AIPING, Z.; JIANHONG, L.; WENHUI, Y. (2006). Effective loading and controlled release of camptothecin by O-carboxymethylchitosan aggregates. *Carbohydr. Polym.*, v. 63, n. 1, p. 89-96.

12. RAMESH, H. P. V., S.; THA. (2004). Safety evaluation of formulations containing carboxymethyl derivatives of starch and chitosan in albino rats. *Carbohydr. Polym.*, v. 58, n. 4, p. 435-441.

13. ZHAO, A. Y., P.; KANG, C.; YUANG, X.; CHANG, J.; PU, P. (2005). Synthesis and characterization of tat-mediated O-CMC magnetic nanoparticles having anticancer function. *J. Magn. Mater.*, v. 295, p. 37-43.

14. DELEZUK, J. A. D. M.; CARDOSO, M. B.; DOMARD, A.; CAMPANA-FILHO, S. P. (2011). Ultrasound-assisted deacetylation of beta-chitin: Influence of processing parameters. *Polym. Int.*, v. 60, n. 6, p. 903-909.

15. ABREU, F. R.; CAMPANA-FILHO, S. P. (2009). Characteristics and properties of carboxymethylchitosan. *Carbohydr. Polym.*, v. 75, n. 2, p. 214-221.

16. CAMPANA-FILHO, S. P.; BRITTO, D. D.; CURTI, E.; ABREU, F. R.; DELEZUK, J. A. D. M.; CARDOSO, M. B.; BATTISTI, M. V.; SIM, P. C.; GOY, R. C.; SIGNINI, R.; LAVALL, R. L. (2009). Extraction, Structures and Properties of alpha- and beta-chitin. In: JAYAKUMAR, R.; PRABAHARAN, M. (Ed.). Current Research

and Developments on Chitin and Chitosan in Biomaterials Science. Cap.7. p. 123-136. Research Signpost.

17. SUN, L.-P.; DU, Y.-M.; SHI, X.-W.; CHEN, X.; YANG, J.-H.; XU, Y.-M. (2006). A new approach to chemically modified carboxymethylchitosan and study of its moisture-absorption and moisture-retention abilities. *J. Appl. Polym. Sci.*, v. 102, n. 2, p. 1303-1309.

18. FOCHER, B.; BELTRAME, P. L.; NAGGI, A.; TORRI, G. (1990). Alkaline N-deacetylation of chitin enhanced by flash treatments. Reaction kinetics and structure modifications. *Carbohydr. Polym.*, v. 12, n. 4, p. 405-418.

19. LIU, X. F.; GUAN, Y. L.; YANG, D. Z.; LI, Z.; YAO, K. D. (2001). Antibacterial action of chitosan and carboxymethylated chitosan. *J. Appl. Polym. Sci.*, v. 79, n. 7, p. 1324-1335.

Chemical Modifications and Advanced Materials

Preparation, Characterization and Releasing Studies of a Captopril Chitosan salt

Mariá Del Bianco Luppi, Rita de Cássia da Silva and Éder Tadeu Gomes Cavalheiro*

*Instituto de Química de São Carlos – USP. Av. Trab. São-carlense, 400, CP 780, CEP 13560-970
São Carlos, SP, Brazil.*

*cavalheiro@iqsc.usp.br

ABSTRACT

A salt from chitosan (Ch) and the antihypertensive captopril (Cap) was prepared and characterized by elemental analysis, thermogravimetry, differential scanning calorimetry and infrared spectroscopy. These techniques revealed the majority of the free amine sites of Ch reacted with the carboxylic groups in the drug, considering a deacetylation degree of 75,7%. HPLC was used to measure the drug released from the salt against time revealing a pH dependence in such release. A releasing mechanism was also proposed.

Keywords: chitosan, biopolymer, drug release, thermal analysis, HPLC

INTRODUCTION

The controlled release of drugs is a technology based on knowledge of a range of disciplines including chemistry, bioengineering, pharmacology, biology, polymer science and medicine. As the name suggests the main purpose of this procedure is to disseminate the drug where it is needed and how and in an appropriate *dosis* [1]. Chitosan (Ch) has numerous applications, including most importantly the use of body weight loss, tissue regeneration, prevention of metastasis, the removal of metals in waste water, reducing cholesterol and inhibition of cancer cells [2].

Several studies have been reported regarding the controlled release of drugs, from Ch. [3,4,5]. However the single weak adsorption forces results in a fast release of the drug, obliging to introduce crosslinking agents or other strategies to hold the drug into the matrix tighter. Such agents can difficult the liberation as well as to promote side effects.

The presence of the amino and hydroxyl groups in the Ch molecule allows to perform reactions for the preparation of many chitosan derivatives [6]. One of such modifications include the possibility of preparing salts from the free amine groups in Ch and carbonylated drugs, representing the simplest approach for such modification with no need of other agents. Our idea in this case, is that not only weak intermolecular or adsorptive forces are present, but a ionic bond linking the drug to the carrier, diminishing the need for crosslinkers or other agents.

Captopril (Cap) is a antihypertensive drug widely used all around the world and presents a carboxylic group in its chemical structure.

Thus this work presents the preparation and characterization of a chitosan-captopril salt with a large reaction extent, from the neutralization of Cap (acid) by Ch (base), in order to prepare a model controlled drug release system and evaluate the effect of pH in such releasing system.

MATERIALS and METHODS

Low molecular weight Ch (Aldrich) was purified by dissolving with 0.5 mol L⁻¹ acetic acid and retaken with 1:3 (v/v) ammonium hydroxide solution. After washing until neutral pH and drying, Ch was grinded and stored in a dessicator over silica gel. The deacetylation degree (DA) of the purified Ch was determined by potentiometric titration in the presence of a glass electrode [7,8,9].

Based in the *DA*, Ch samples was left to react with of Cap, by stirring a stoichiometric amount in 50 mL of water at room temperature during 24h. After this time the reaction mixture was totally dissolved, evidencing that a neutralization reaction has occurred. The resulting solution was lyophilized to dryness.

The thermogravimetric curves were obtained in a SDT Q-600 modulus (TA-Instruments) under a nitrogen atmosphere flowing at 100 mL min⁻¹ at a heating rate of 10 °C min⁻¹ up to 800 °C, and sample mass of about 5.5 mg. The DSC curves were obtained in a Q10 apparatus (TA-Instruments). The samples were cooled to -70 °C at a cooling rate of 10 °C min⁻¹ and kept in isotherm for one minute. Then, they were heted up to 150 °C at 10 °C min⁻¹, and kept in isotherm for one minute. Analysis were made under dynamic atmosphere of nitrogen flowing at 100 ml min⁻¹ with sample masses used of c.a. 2 mg.

UV-vis spectrophotometry was used to investigate the wavelength of maximum absorption of captopril in different pH, in order to choose the wavelength for detection in HPLC. Solutions of *c.a.* 3.8 mg of the Ch-Cap salt in 50.0 mL of 0.10 mol L⁻¹ HCl pH 1.0, 0.10 mol L⁻¹ HCl pH 2.0, 0.10 mol L⁻¹ acetate buffer pH 3.7, 0.10 mol L⁻¹ acetate buffer pH 4.7 and 0.10 mol L⁻¹ phosphate buffer pH 7.4 were prepared, placed in a thermostated cell and kept at 37.0 ± 0.1 °C (thermostatic bath, Marconi MA184), under constant stirring. Aliquots of 50 µL were taken, using a chromatographic syringe and filter at regular intervals for analysis of the release profile of the the drug from the matrix. These aliquots were analyzed by HPLC¹⁰, to determine the content of free drug. The chromatographic determinations were performed in a Shimadzu SCL-10Avp, using a mobile phase containing 0.11% phosphoric acid and methanol 45:55 (*v/v*), flowing at 0.7 mL min⁻¹, a C-18 column (Supelco, 25.0 cm), at 22 ± 1 °C, UV detection at 210 nm¹⁰. An analytical curve for Cap was previously obtained under exactly the same conditions.

RESULTS and DISCUSSION

The potentiometric titration revealed that the Ch used here presented a *DA* = 75.7%. Thus, it was used a stoichiometric amount of Cap based in this *DA*. The average molar mass of the Ch was calculated considering the Eq. 1

$$\overline{MM} = 0.757MM_{Dac} + 0.243MM_{Ac} + 18.02x \quad (1)$$

in which \overline{MM} , MM_{Dac} and MM_{Ac} are is the Ch average molar mass, the molar mass of the deacetylated unit and the molar mass of the acetylated unit respectively, while *x* is the % of water (*m/m*) determined by thermogravimetry.

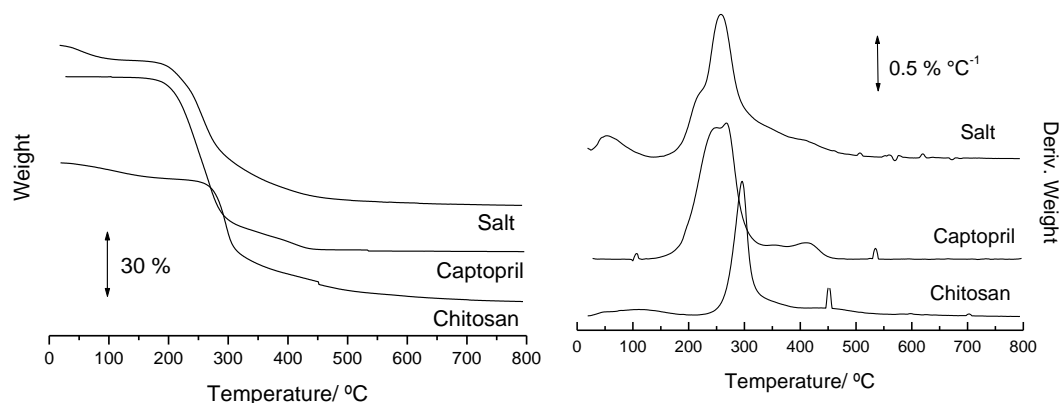
Table 1 resumes the thermal events observed for the Ch, Cap and the salt in their TG curves. The Ch TG/DTG curves (Figure 1.a) presented a dehydration process equivalent to 7.39%, followed by decomposition in a single step with 36.17% of residue. Cap decomposed in a single step, almost without residue at 800°C. The salt lost water between 100 and 200 °C and decomposed in a single step, resulting in 26.07% of residue.

The thermogravimetric curves (TG/DTG, Fig. 1) showed that the decomposition profile of the salt closely resembles that of Cap, after dehydration. In addition, the decomposition of Ch starts at a higher temperature than the decomposition of pure drug and salt. These facts suggests that the salt assumes a thermal behavior intermediate between the precursors. The DTG profiles (Fig. 1.b) corroborates such observations.

The carbon, hydrogen and nitrogen contents were determined by elemental analysis in order to evaluate the composition of the salt formed by the biopolymer and captopril. The results of elemental analysis (C, H, N and S) and those calculated for each sample are listed in Table 2, considering a water content of 7.39% as determined by the TG and described above.

Table 1. Temperature intervals and mass losses observed in each thermal event of Cap, Ch and salt decomposition

$\Delta T / ^\circ\text{C}$	Captopril / %	Chitosan / %	Salt / %	Attribution
25 - 100	-	-	6.233	dehydration
100 - 200	5.60	7.395	3.271	dehydration
200 - 600	92.17	56.434	63.27	decomposition
600 - 750	1.169	36.17	26.07	residue

**Figure 1.** (a) TG and (b) DTG curves of chitosan, captopril and salt.**Table 2.** Results of elemental analysis of chitosan, captopril and salt

Sample	Exp (calc)/ %		
	C	H	N
Chitosan	41,50 (41,45)	7,35(7,18)	7,33(7,45)
Captopril	49,01(49,77)	6,88(6,91)	6,43(6,45)
Salt*	44,06 (43,20)	6,91(7,27)	6,46(6,66)

*Considering 9.67 % water

From this table it is possible to see that the results are consistent with the degree of acetylation of 75.7% and the water content of 9.67%, using Eq. 1.

A comparison between the bands in the infrared spectra of Ch, Cap and the salt are presented in Table 3. These bands reveals the appearance of NH_4^+ in the salt spectra and changes in the position of the Ch carbonyl from 1674 to 1619 in the salt.

Table 3. Characteristic bands in the infrared region for chitosan, captopril and salt

Attribution	ν Chitosan (cm^{-1})	ν Captopril (cm^{-1})	ν salt (cm^{-1})
C=O	1674	-	1619
C-O	-	1752	-
C-O-H	-	1383	-
N-H	1400	-	1400
NH_4^+	-	-	2360

Figure 2 presents the DSC curves of Ch, Cap and salt. The DSC curve of captopril reveals an endothermic peak at 105.5 °C, related to the melting of the sample ($\Delta H_{fus} = 114.6 \text{ J g}^{-1}$). Meanwhile the Ch curve only presents a broad endotherm with peak higher than 100 °C. The curve of the salt also presents this dehydration endotherm, but with peak at 72.7°C. However the disappearance of the Cap melting signal associated to the changes in the TG profile, clearly shows that there is a strong interaction between Ch and Cap.

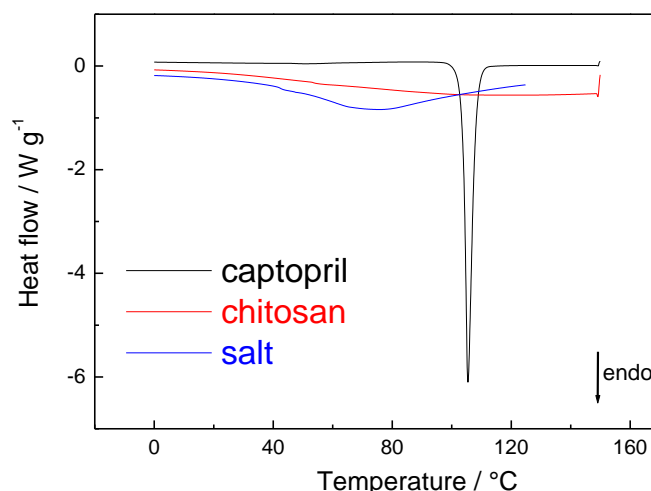
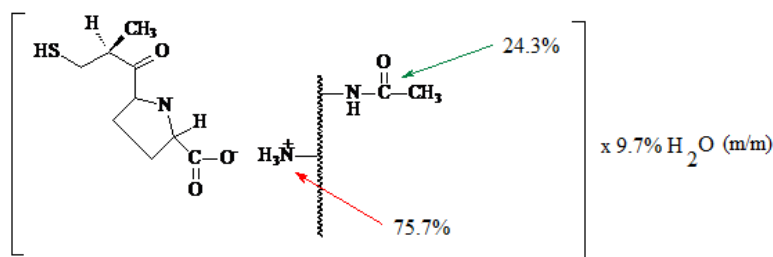


Figure 2. DSC curves of chitosan, captopril and salt.

In Scheme 1 is represented a structure of the salt according to the TG, elemental analysis and FTIR data.



$$\text{MMsalt} = [(\text{MMcap} \times 0.757) + (\text{MMdeacetyl.chit} \times 0.757) + (\text{MM acetyl chit} \times 0.243)]/0.903$$

Scheme 1: Representation of the structure of the salt of chitosan, and a relationship to calculate the average molecular mass.

Cap release profiles as a function of time has been evaluated in pH 1.0, 2.0, 3.7, 4.7 and 7.4, as presented in Table 4. Figure 3 shows chromatograms of the salt, at different times in 0.10 mol L⁻¹ HCl pH = 1.0, as an example.

The first peak with retention time (Rt) of about 2.4 min, refers to HCl, followed by a peak at 3.7 min, which was assigned to Cap as confirmed by adding a small amount of the drug to the system. The third peak was attributed to Ch soluble in HCl medium, as confirmed by the addition of non salified biopolymer to the sample. This third peak has not been described by Azevedo et al [10], when they worked only with Cap, which also confirms this hypothesis.

Release profiles were obtained measuring the areas of peaks at 3.7 min, at different times, resulting in release profiles shown in Figure 4, also as an example. From the profile presented by the curve of relative area versus time, there is a steady increase since the dissolution until about forty minutes, when a decreasing trend is observed in the released concentration up to about one hundred minutes and then a tendency to stabilize. A spread in the results were attributed to the relative complexity of the system once Ch tends to form a gel when in solution. By the other hand, the filtration process can lead to retention of random amounts of analyte.

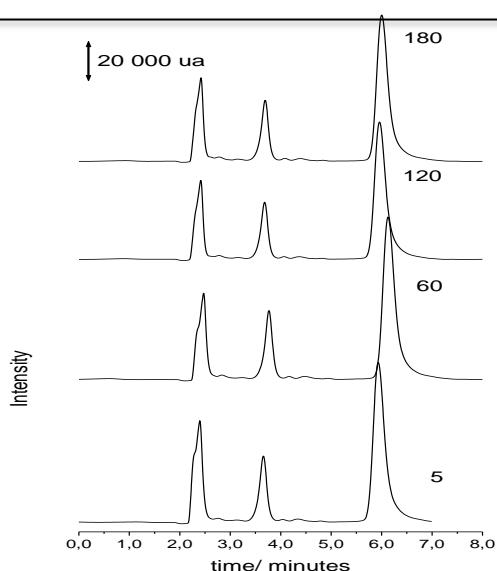


Figure 3. HPLC chromatograms of the salt solutions obtained under the experimental conditions described in the text after 5, 60, 120 and 180 minutes of preparation of the solution in 0.1 mol L⁻¹ HCl pH =1.

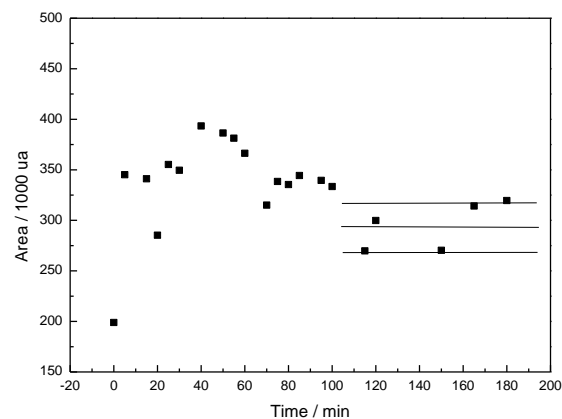


Figure 4. Releasing profile of Cap in 0.1 mol L⁻¹ HCl pH =1. The central line above 180 min. represents the average of the last five points while the side lines mark the standard deviation.

An estimative of the Cap concentration was performed by HPLC data, based on a calibration curve obtained from the chromatograms of standard solutions over the concentration range between 5 and 50 mg mL⁻¹, under the same experimental conditions, resulting in the following linear equation:

$$\text{Area} = -1967 + 14440 C_{\text{Cap}} (\mu\text{g}^{-1} \text{ mL}) \quad (R = 0,999, n=8) \quad (2)$$

which was obtained by measuring the relative areas of eight captopril solutions with increasing concentrations in the range above and three injections for each point.

The average of the five points over 100 minutes in Figure 10, resulted in an area of 295076 + 23822 r.u. leading to a concentration of 20.6 mg mL⁻¹, after equilibration, corresponding to approximately 514 mg of free Cap in the cell, whereas 25.0 mL of buffer.

The same procedure was performed in a solution of the 0.01 mol L⁻¹ HCl, pH 2.0; as well as in acetate buffer pH 3.7; acetate buffer 4.7 and in phosphate buffer pH 7.4, as presented in Table 4. It can be seen that there is a decrease in the amount released as the medium becomes less acidic.

Table 4: Results of the captopril released from the Chitosan salt in different media, among 120 -180 minutes

pH	medium	Startin salt mass* / mg	captopril released**	
			$\mu\text{g mL}^{-1}$	mass / μg
1.0	HCl	3.8	21 ± 2	514 ± 50
2.0	HCl	3.9	22 ± 1.5	538 ± 38
3.7	Acetate	3.8	18.0 ± 0.9	450 ± 22
4.7	Acetate	3.8	11.2 ± 0.9	281 ± 22
7.4	Phosphate	3.8	-	-

* initial mass of the salts

** captopril released in the 25,0 mL of solution at 37,0 ± 0,1 °C, - non detected

Considering the molar mass of the salt as confirmed from the elemental analysis and considering the water content from the TG curves, it was estimated *c.a.* 1.7 mg of captopril has been placed into 3.8 mg the Ch matrix.

According to the data in Table 4, it were released a maximum of *c.a.* 500 μg of captopril, from 3.8 mg of salt, which represents *c.a.* 30% of the total mass of the drug in the sample, meaning that 70% still in the carrier matrix to be released further. Any release was found in pH 7.4, until 120 min.

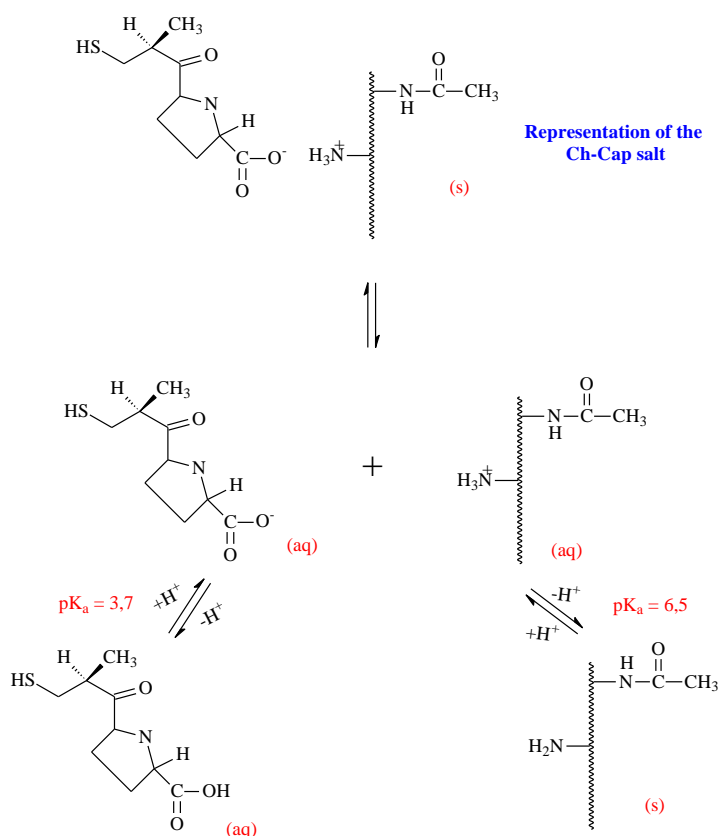
Regarding the change in the amount of Cap released in different pH and media, one can conclude that there is an influence of the pH in the releasing profile, which should follow the mechanism described in Scheme 2.

In this scheme it is proposed that initially the salt in the solid phase may dissociate releasing a molecule of captopril and a protonated ammonium site in the matrix of chitosan, which also has acetylated sites.

In acidic medium, Cap tends towards protonation ($\text{pK}_a = 3.7$), favoring the dissociation of salt. This would explain why at pH 1 and 2 the release is of the same order, while it decreases when the pH changes from 3.7 to 4.7. At pH = 7.4, it seems that there is no enough free H^+ in the medium and the release occurs in a very small extension.

In addition Ch is protonated in acidic medium, which also facilitates the salt dissociation and solubilization of the biopolymeric matrix.

So, the release of captopril would be facilitated in an acid medium, by both the protonation of the carboxylic Cap and amminic Ch groups suggesting that a pH-controlled release can be established.



Scheme 2. Proposed mechanism for Cap release from the salt, with the steps of dissociation of the salt in water and the protonation/deprotonation of the species involved.

CONCLUSION

Using the DA determined from potentiometric titration, TG and elemental analysis data for a Ch sample it was possible to propose a neutralization reaction to prepare a salt with captopril. The resulting salt (also called ionic complex in the literature) was characterized using TG, FTIR and elemental analysis, suggesting a large extension of the neutralization reaction. Finally the dissociation of the salt was evaluated by HPLC at 37.5°C, revealing that it is strongly dependant on the pH of the medium, being facilitated in acidic medium.

ACKNOWLEDGEMENTS

Authors are indebted to Brazilian agencies Fapesp and CNPq for fellowships (MDBL and RCS, respectively) and research grant (12/09933-3).

REFERENCES

- [1] Dunn, R. L. and Ottendrite, R. M. (2000). Polymeric Drugs and Drug Delivery Systems. ACS Symposium Series N. 469.
- [2] Damian C.; Beirão, L. H.; Espírito Santo, M. L. P.; Francisco, A. and Teixeira, E. (2005). Quitosana: um amino polissacarídeo com características funcionais. *Alimento e Nutrição*, Araraquara, 16, 195-205.
- [3] Paños, I.; Acosta, N. and Heras, A. (2008). New Drug Delivery Systems Based on Chitosan. *Current Drug Discovery Technologies*, 5, 333-341.
- [4] Gong, K.; Darr, J.A.; Rehman, I.U. (2006) Supercritical fluid assisted impregnation of indomethacin into chitosan thermosets for controlled release applications. *International Journal of Pharmaceutics*, 315, 93-98.
- [5] Maciel, J. S.; Paula, H. C. B.; Miranda, M. A. R.; Sasaki, J. M. and Paula, R. C. M. (2006). Reacetylated Chitosan/Cashew Gum Gel: Preliminary Study for Potential Utilization as Drug Release Matrix. *Journal of Applied Polymer Science*, 99, 326-334.
- [6] Tirkistani, F. A. A.; (1998). Thermal analysis of some chitosan Schiff bases. *Polymer Degradation and Stability* 60, 67-70.
- [7] Tolaimate A.; Desbrières J, M.; Rhazi, A.; Alagui, Vincendon, M.; Vottero, P. (2002) Influence of the nature of the metal ions on the complexation with chitosan. Application to the treatment of liquid waste. *European Polymer Journal* 38, 1523-1530.
- [8] Raymond, L.; Morin, F. G.; Marchessault, R. H.; (1993) Degree of deacetylation of chitosan using conductometric titration and solid-state NMR. *Carbohydrate Polymers*. 246, 331-336.
- [9] Terayama H. (1986). Method of colloid titration. A new titration between polymer ions. *Journal of Polymer Science*, 8, 243-253.
- [10] Azevedo, M. M. M. Nanoesferas e liberação controlada de fármacos. Monografia. Instituto de Química da Unicamp. 2002.

INFLUENCE OF STARCH OXIDATION IN DRUG DELIVERY BEHAVIOR OF CHITOSAN/ CORN STARCH FILMS

Mateus Batista Simões, Marília M. Horn, Virginia C. Amaro Martins, Ana Maria de Guzzi Plepis*

*Instituto de Química de São Carlos, Universidade de São Paulo, USP,
Av. Trab. São-carlense, 400, CP 780, CEP 13560-970, São Carlos-SP-Brasil.
E-mail address: amplepis@iqsc.usp.br*

ABSTRACT

The aim of this study was to investigate the *in vitro* drug release behavior of chitosan/starch films intended for controlled drug delivery application. Ciprofloxacin was the model drug incorporated in polysaccharides films prepared using a casting method. The films were prepared varying the polyol type (ethylene glycol, glycerol and sorbitol) and also the effect of starch oxidation in the drug release mechanism was investigated. Drug release amount is affected by polyols and also by the starch oxidation. Drug release mechanism was fitted to Korsmeyer-Peppas model suggesting that ciprofloxacin in the films of chitosan/gelatinized starch in presence or absence of plasticizer and chitosan/oxidized starch without plasticizer follow Fickian diffusion. However for chitosan/oxidized starch in the presence of polyols showed an anomalous behavior.

Keywords: Chitosan, oxidized starch, polyols, drug release.

INTRODUCTION

Drug delivery systems have an advantage compared to conventional dosage forms, which includes improved efficacy, improved patient compliance and convenience and reduced toxicity [1]. Films prepared with polysaccharides such as chitosan and starch are biocompatible and biodegradable, which are the basic characteristics for polymers used as drug delivery systems [2].

Chitosan is an attractive material for biomaterial and biomedical applications since it is a non toxic polymer that stimulates the cellular proliferation, reduces the cicatrization time and has antimicrobial activity [3,4].

Starch is a natural polysaccharide that presents good biocompatibility, biodegradability, non toxicity and excellent ability to form films. [5,6]. Starch is formed by two different components: amilose and amilopectin. Amilose is formed by glucose residues linked by glucosidic linkages α 1-4 creating a linear chain. Amilopectin is formed by a branched structure, linked by α 1-4 and α 1-6 glucosidic linkages. The proportion between these components differs depending on botanical source, maturation degree and varieties of determinate specie [7].

Chitosan/starch films show a great potential to act as drug release systems. However, this kind of material is weak and brittle and modifications are recommended to improve the mechanical properties [8]. Among these modifications, plasticizers addition, starch and/or chitosan modifications, such as oxidation and cross-linking are the most common and used techniques [9].

The objective of this study was to investigate the chitosan/starch films as support for drug delivery systems. Films were prepared varying the polyol type (sorbitol, ethylene glycol and glycerol), using oxidized starch to investigate the effect in drug delivery behavior and ciprofloxacin as a drug model.

MATERIALS and METHODS

Polyols: Sorbitol and ethylene glycol, purchased from Merck and glycerol, supplied by Aldrich with analytical grade were used as plasticizers.

Chitosan: Pens of *Loligo sp* were treated with 0.55 mol L⁻¹ HCl at room temperature for 2 h. Afterward, material was washed with water until neutral and dried at 37°C. The obtained solid was heated in 0.3 mol L⁻¹ NaOH at 80°C for 1 h, washed with water until neutral and dried. The obtained β -chitin was treated with 40% (w/w) NaOH at 80°C for 3 h in nitrogen atmosphere [10]. A 1% chitosan solution was prepared by dissolution in 1% acetic acid.

Corn Starch Gelatinization: Corn starch powder (Sigma-Aldrich – 73% amylopectin and 23% amylose) and 50 mL of deionized water were mixed with mechanical stirring and gelatinized at 90°C for 30 min, and then cooled at room temperature, forming a homogeneous solution [11]. An aqueous solution of 2% (w/w) of gelatinized starch was used in the films preparation.

Corn starch oxidation: Starch powder was oxidized with 5% periodic acid (H₅IO₆) during 24 h at 25°C under stirring. After, the material was dialyzed with deionized water during 72 h and then lyophilized [12]. An aqueous solution of 2% (w/w) of oxidized starch was used for films preparation.

Films preparation: Films were prepared by mixture in proportion 2:1:1 starch/chitosan/polyol and were labeled as: CS (chitosan/starch), CSGL (chitosan/starch/glycerol), CSSO (chitosan/starch/sorbitol) and CSEG (chitosan/starch/ethylene glycol). Ciprofloxacin was added (5%, w/w) to each solution. Films were obtained by casting at 25°C on rectangular Teflon® molds. The same method of preparation was used to obtain the films with oxidized starch, and they were labeled as: CSox (chitosan/oxidized starch), CSoxGL (chitosan/oxidized starch/glycerol), CSoxSO (chitosan/oxidized starch/sorbitol) and CSoxEG (chitosan/oxidized starch/ethylene glycol). All films were stored at controlled humidity of 65% at least 7 days before the tests.

In vitro drug delivery studies: *In vitro* delivery study was performed by immersion of films in an acrylic cell containing 100 mL of phosphate saline buffer solution (pH 7.4), with 50 rpm of stirring and constant temperature of 37°C. Aliquots of 1.0 mL were withdrawn at appropriate time intervals and immediately replaced by 1.0 mL of buffer solution to maintain the volume. Collected samples were analyzed for ciprofloxacin content by measuring the absorbance at 271 nm using an UV spectrophotometer (HITACHI model U-1100) and calculating the concentration by the interpolation of a calibration curve. *In vitro* release studies were performed in triplicate.

RESULTS AND DISCUSSION

Degree of acetylation of prepared chitosan was measured by potentiometric titration according to procedure carried by Raymond et al. (1993) [13], founding a value of 9.05 % \pm 0.35. The molecular weight value obtained for chitosan was 4.28x10⁵ measured by capillary viscosimetry method [14].

All films were homogeneous, transparent, thin, flexible and were easily removed from the cast plate, with good handling characteristics. Formation of homogeneous chitosan and gelatinized starch films can be attributed to strong interactions via hydrogen bonds between functional groups of two polysaccharides. The crystalline structure of starch molecule is disorganized by gelatinization process that exposure the hydroxyl groups that quickly form hydrogen bonds with amino groups of chitosan [15]. In the case of oxidized starch the aldehyde groups are essential to the formation of a network with

chitosan. Oxidation introduces carbonyl groups into starch chains that interact with amino groups of chitosan by ionic associations, without use of any crosslink agent.

Delivery of antibiotic in a specific wound is a challenge for the development of new support matrix. Ciprofloxacin as a drug model was added to chitosan solution during the preparation of chitosan/starch films, and its *in vitro* release behavior is shown in Figure 1.

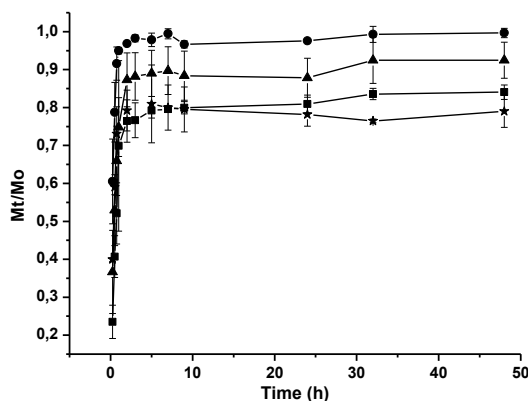


Figure 1. Average release of ciprofloxacin in films of chitosan/gelatinized starch for different plasticizers: no plasticizer (▲), ethylene glycol (■), glycerol (●) and sorbitol (★).

The initial release of ciprofloxacin from chitosan/gelatinized starch films was very rapid, and the release rate remains constant after 2 h. The initial release in all films was higher than 70% indicating that part of ciprofloxacin molecules entrapped diffused rapidly since ciprofloxacin is a soluble drug in aqueous solution.

After that, the constant behavior observed in the second stage can be attributed to the ciprofloxacin entrapped into the film that can be released due to the swelling and as well as film degradation. An initial release with high drug concentration is desirable in the case of delivering antibiotics, since is necessary a high dose to combat bacterial infections effectively.

Although for all the samples release behavior is similar, the quantity of ciprofloxacin released is different for each plasticizer (Table 1). It is observed that for the three used plasticizers, glycerol is the only one that increases the amount of drug released with respect to the film without plasticizer. This probably occurs because glycerol is the polyol with less steric hindrance, filling a larger amount of gaps of three-dimensional network formed by chitosan and starch, hindering the interaction of ciprofloxacin with such network, so that almost all the drug is released (96.8%).

Table 1. Ciprofloxacin released and release time for each plasticizer in films of chitosan with gelatinized or oxidized starch

Film	Drug release (%)
CS	87.3
CSEG	76.4
CSGL	96.8
CSSO	79.2
CSox	78.1
CSoxEG	40.2
CSoxGL	28.5
CSoxSO	66.5

On the other hand, sorbitol and ethylene glycol influence the formation of the network similarly to each other, and the amount of drug released is close, being 79.2 and

76.4% respectively. The presence of these polyols turn the chitosan/starch network more compacted, so that the drug becomes more trapped, making it difficult to be released.

An effective method used to change the release profile is the chemical modification in some component of the film. In this study, starch chemical modification was proposed to verify the changes in drug release behavior of ciprofloxacin. Figure 2 show the release profile of films prepared with oxidized starch. Starch oxidation process cleaves the C-2 – C-3 linkages of glucose units and forms dialdehyde groups that interact with amino groups of chitosan by electrostatic attraction [16].

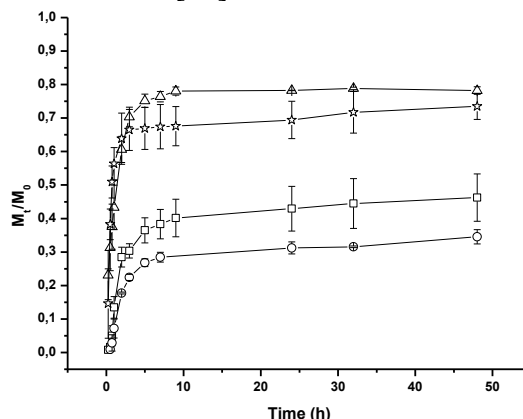


Figure 2. Average release of ciprofloxacin in films of chitosan/oxidized starch for different plasticizers: no plasticizer (Δ), ethylene glycol (\square), glycerol (\circ) and sorbitol (\star).

In the films with oxidized starch, the initial drug release was always smaller than the films with gelatinized starch (Table 1). This can be attributed to formation of a more effective interaction between the aldehyde groups of oxidized starch and the amino groups of chitosan, trapping ciprofloxacin [17] and therefore hindering the drug release. Furthermore, the presence of plasticizers in these films contributes to the formation of a more effective network, trapping the ciprofloxacin, decreasing the amount of drug released.

Release kinetics was also verified using Korsmeyer-Peppas relation (Figure 3) aiming to elucidate release mechanism.

$$Mt/M_0 = Kt^n$$

where Mt is the amount of drug release in time t , M_0 is the initial amount of drug, K is the constant for Korsmeyer-Peppas model and n indicates the release mechanism.

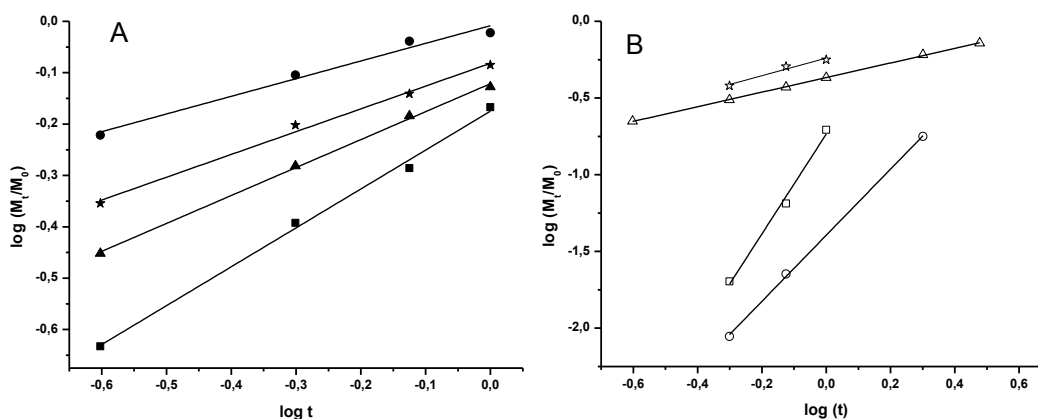


Figura 3. Korsmeyer -Peppas plots for the release studies with different plasticizers in films of chitosan/gelatinized starch (A) and chitosan/oxidized starch (B): no plasticizer ($\blacktriangle, \triangle$), ethylene glycol (\blacksquare, \square), glycerol (\bullet, \circ) and sorbitol (\star, \star).

Linearity is observed in all cases, since the correlation coefficients were very close to unity (Table 2). Thus, it follows that the release mechanism of ciprofloxacin in films of chitosan/gelatinized starch containing glycerol and sorbitol as plasticizers obeys Fick's Law of diffusion ($n < 0.45$). In the case of films containing ethylene glycol and no plasticizer, there is an anomalous behavior ($0.45 < n < 0.89$), which considers the diffusion of the drug through the matrix, besides the interference caused by the swelling of the matrix. However, the value of the film without plasticizer is very close to the limit value of n , and Fickian diffusion exerts a great influence on the release mechanism [18].

In the film of chitosan/oxidized starch without plasticizer, the slope is very close to the limit value of 0.45, and a mechanism controlled by Fickian diffusion. The film containing sorbitol has a value between 0.45 and 0.89, an anomalous behavior, and the Fickian diffusion and swelling of the matrix exerts influence on the release, but the rate at which the solvent diffuses through the matrix is less than speed of movement of polymer chains of chitosan/oxidized starch.

Table 2. Korsmeyer -Peppas parameters for studies of release of ciprofloxacin in films of chitosan/gelatinized and chitosan/oxidized starch.

Film	Angular Coefficient (n)	Correlation Coefficient
CS	0.54	0.9978
CSEG	0.76	0.9944
CSGL	0.35	0.9727
CSSO	0.44	0.9915
CSox	0.48	0.9996
CSoxEG	3.25	0.9866
CSoxGL	2.15	0.9990
CSoxSO	0.57	0.9422

For films of chitosan/oxidized starch containing ethylene glycol and glycerol, the coefficients are above 0.89, characteristic of the super transport mechanism type II, in which swelling of the matrix exerts influence on the release, along with Fickian diffusion, however, the diffusion rate of the solvent is much greater than the movement of the polymer chains [18].

CONCLUSION

The ciprofloxacin release in the films of chitosan/gelatinized starch has a rapid initial release. The addition of plasticizers do not influence the time of release but modified the amount released. Glycerol was the only plasticizer which increased the amount released while the ethylene glycol and sorbitol decreased, indicating that the addition of plasticizers more effectively forms a network which better entraps the drug, hindering its release. In films containing oxidized starch, it was observed that the presence of polyols reduces the released amount in any case, even compared with the films of gelatinized starch, and the release time was also different. Release mechanism studies through empirical equation of Korsmeyer-Peppas, provided that the Fickian diffusion plays a major role in the release for gelatinized starch. The evaluation of the release mechanism for chitosan/oxidized starch showed that addition of plasticizers also modifies the release mechanism, which was purely for the Fickian diffusion CSox, has the anomalous behavior for CSoxSO and presenting a super transport type II behavior for CSoxEG and CSoxGL.

AKNOWLEDGEMENTS

M.B.S. and M.M.H. gratefully acknowledges the financial support of Conselho Nacional de Pesquisa (CNPq) and PIBIC/CNPq.

REFERENCES

- [1] Desai, K.G.H.; Park, H.J. (2005). Preparation and characterization of drug-loaded chitosan-tripolyphosphate microsphere by spray drying. *Drug Delivery Res.*, 64, 114-128.
- [2] Liu, C.S.; Desai, K.G.H.; Meng, X.H.; Chen, X.G. (2007). Sweet potato starch microparticles as controlled drug release carriers: preparation and *in vitro* drug release. *Drying Technol.*, 25, 689-693.
- [3] Jayakumar, R.; Prabakaran, M.; Kumar, P.T.; et al (2011). Biomaterials based on chitin and chitosan in wound dressing applications. *Biotechnol. Adv.*, 29, 322-337.
- [4] Yusof, N.L.B.M.; Lim, L.Y., Khor, E. (2001). Preparation and characterization of chitin beads as a wound dressing precursor. *J. Biomed. Mater. Res.*, 54, 59-68.
- [5] Pauli, R.B.; Quast, L.B.; Demiate, I.M.; Sakanaka, L.S. (2011). Production and characterization of oxidized cassava starch biodegradable films. *Starch*, 63, 595-603.
- [6] Serrero, A.; Trombotto, S.; Cassagnau, P.; et al (2010). Polysaccharide gels based on chitosan and modified starch: structural characterization and linear viscoelastic behavior. *Biomacromol.*, 11, 1534-1543.
- [7] Denardin, C.C. (2008). Influência do teor de amilose e beneficiamento do arroz na resposta biológica de ratos. Dissertação (Mestrado em Tecnologia de Alimentos) Universidade Federal de Santa Maria, Santa Maria-RS.
- [8] Zhang, Y.R.; Zhang, S.D.; Wang, X.L.; et al (2009). Effect of carbonyl content on the properties of thermoplastic oxidized starch. *Carbohydr. Polym.*, 78, 157-161.
- [9] Junfeng, S.; Jianjun, C. (2011). Modified methods in starch-based biodegradable films. *Adv. Mater. Res.*, 183-185, 1635-1641.
- [10] Horn, M.M.; Martins, V.C.A.; Plepis, A.M.G. (2009). Interaction of anionic collagen with chitosan. Effect on thermal and morphological characteristics. *Carbohydr. Polym.*, 77, 239-243
- [11] Liu, F.; Qin, B.; He, L.; Song, R. (2009). Novel starch/chitosan blending membrane: antibacterial, permeable and mechanical properties. *Carbohydr. Polym.*, 78, 146-150.
- [12] Horn, M.M.; Martins, V.C.A.; Plepis, A.M.G. (2011). Effects of starch gelatinization and oxidation on the rheological behavior of chitosan/starch blends. *Polym. Int.*, 60, 920-923.
- [13] Raymond, L.; Morin, F.G.; Marchessault, H. (1993). Degree of deacetylation of chitosan using conductometric titration and solid-state NMR. *Carbohydr. Res.*, 246, 331-336.
- [14] Rinaudo, M. (2006). Chitin and chitosan: properties and applications. *Progress in Polym. Sci.*, 31, 603-632.
- [15] Pelissari, F.M.; Yamashita, F.; Garcia, M.A.; et al (2012). Constrained mixture design applied to the development of cassava starch-chitosan blown films. *J. Food Eng.*, 108, 262-267.
- [16] Tang, R.; Du, Y.; Fan, L. (2003). Dialdehyde starch-crosslinked chitosan films and their antimicrobial effects. *J. Polym. Sci.: Polym. Phys.*, 41, 993-997.
- [17] Zamudio-Flores, P.B.; Torres, A.V.; Salgado-Delgado, R.; Bello-Pérez, L.A. (2010). Influence of the oxidation and acetylation of banana starch on the mechanical and water barrier properties of modified starch and modified starch/chitosan blend films. *J. Appl. Polym. Sci.*, 115, 991-998.
- [18] Singhvi, G.; Singh, M. (2011). Review: In-vitro drug release characterization models. *Int. J. Pharm. Stud. Res.*, 2, 77-84.

SURFACE MODIFIED CHITOSAN FILM FOR TRANSDERMAL DRUG DELIVERY

Audrey Tourrette^{a*}, Shaan Chamary^a, De Geyter^b, Rino Morent^b, Plamen Kirilov^a, Sophie Cazalbou^a

^a *Université de Toulouse, CIRIMAT, UPS-INPT-CNRS, Faculté de Pharmacie, 118 Route de Narbonne, 31062 Toulouse cedex 4, France*

^b *Department of Applied Physics, Faculty of Engineering and Architecture, Ghent University (UGent), Sint-Pietersnieuwstraat 41, B-9000 Ghent, Belgium*

*E-mail: audrey.tourrette@univ-tlse3.fr

Keywords

Film, Surface modification, transdermal

INTRODUCTION

The worldwide transdermal market is the most successful non-oral systemic drug delivery system. Physico-mechanical and bioadhesive characteristics are important parameters in the product development of films for transdermal drug delivery devices. There are two main requirements of bioadhesive films for transdermal application; (1) that they should stick firmly to a difficult substrate (skin) and (2) that they should be easily and cleanly removed from that substrate when desired. This research concerns the elaboration of chitosan based film with specific surface modification/functionalization processes for achievement of the desired surface characteristics of the transdermal drug delivery system (adhesion and easy skin removal properties).

The main objective of this research is the elaboration of chitosan film with good mechanical properties and good skin adhesion. It is composed of two main axes:

- (1)- The study of the preparation of chitosan based film having good mechanical and adhesive properties;
- (2)- Chitosan film surface modification by grafting a temperature responsive polymer (poly-N-isopropylacrylamide, PNiPAAm).

MATERIALS and METHODS

1. Preparation of chitosan film

1.1 Physical gel

Chitosan (D.A. 18%, 260 000 g/mol) solution was prepared by dissolving 3% (w/v) into an aqueous solution of acetic acid (1% (v/v)). The mixture is then mechanically stirred for about 12h at 500rpm. Once the chitosan was completely dissolved, the plasticizers were added (20% of the total mass of polymer) to the mixture for plasticized samples. The solution was then mechanically stirred at 500rpm for 30min. The mixture is sonicated in order to remove all the trapped bubbles and then poured into Petri dishes (48g into 12cm diameter Petri dish and 40g into 10cm diameter Petri dish). Drying takes place at 50°C for 2 days. Once the mixture is dried the film is removed from the mould and the chitosan network neutralized with an aqueous solution of NaOH (1M). The film is rinsed with deionized water until neutrality of the supernatant. Lastly the film is dried between glass plates at 50°C for 48h.

1.2 chemical gel

The protocol used for cross-linked chitosan films (sample name: Genipin pH 5 and Genipin pH 13) is the following: chitosan film obtained by the above described method was immersed in 15 mL genipin solution (1% v/v acetic solution- pH5 or Tris buffer solution-pH 13.6) and let react for 6 hours. After washing with deionized water and drying, uncross-linked amine groups were neutralized with NaOH 1M and dried again (only for the sample Genipin pH 5).

2. PNiPAAm/ microgel preparation (PN/CS)

The microparticles of PNiPAAm/chitosan hydrogel (PN/CS) were prepared by a surfactant-free dispersion copolymerization method according to the procedure reported previously [1]. Their physico-chemical characterizations have been already published and their thermosensitivity confirmed.

3. Incorporation of PN/CS microgel onto activated chitosan film surface

3.1 Activated chitosan film surface by plasma treatment

The aim of chitosan film treatment with plasma (air) was to produce radicals, ions and active sites on the cotton fabric surface in order to facilitate the incorporation of PN/CS microgel. This treatment has been done according to the procedure we reported previously [2]. Then the activated films were immersed into 75 ml of microgel suspension and stirred for 2h30. The films were then thoroughly washed with deionized water in order to eliminate unreacted moieties. The films were dried between teflon plates for 24h at 50°C.

3.2 Activated chitosan film surface by UV treatment

Chitosan film was immersed into 75 ml of microgel suspension. Irradiation then took place at 365 nm for 40min. The medium was then stirred for 2h30. The films were then thoroughly washed with deionized water in order to eliminate unreacted moieties. The films were dried between teflon plates for 24h at 50°C.

RESULTS and DISCUSSION

1. Elaboration of chitosan film with appropriate mechanical properties

Mechanical properties are important, since films for transdermal drug delivery application need to exhibit desirable resistance to external forces, so that damage, such as tearing, will not occur during storage or use. The film should be removable without tearing. The film has to be resistant (high tensile strength, TS) with a good flexibility (high elongation at break value, EB). In this study, we used two different methods for the preparation of chitosan films: a) elaboration of chitosan physical gel including the incorporation of plasticizer agents, b) elaboration of chitosan chemical gel using a natural crosslinker (genipin). A physical gel is a reversible three-dimensional network. A variation of the pH or temperature can modify the system since the network is formed by weak interactions. The chemical gel is constituted by a stronger network with covalent interactions. Those gels are irreversible but can be deformed and regain their shape. An interesting property of these gels is that they can adhere to solid surfaces due to their elasticity.

Several samples were prepared and analyzed with a tensile tester in order to determine the formulation which leads to chitosan film with the best chemical properties (**Table 1**). Apart from polymer and solvent other excipients such as plasticizers or crosslinkers can be incorporated into the formulation. The plasticizer exerts a strong

influence on the properties of the formed film. In polymeric films plasticizer interacts with the polymer chains reducing the number of active centers available for rigid polymer - polymer contacts [3]. These interactions result on the one hand in a decrease in glass transition temperature and a higher flexibility of the films, on the other hand in a changed permeability for drug substances and water vapor [4]. Therefore determining the right amount of plasticizer is essential for a successful formulation of this dosage form. It is important to note that the adequate plasticizer concentration is individual for every plasticizer - polymer combination as the efficiency of a plasticizer is polymer dependent.

Table 1. Chitosan films formulation

Film Code	PEG 200	PEG 400	Glycerol	Genipin/pH réticulation
Physical Gels				
CS	-	-	-	-
CS-PEG200-20%	20%	-	-	-
CS-PEG400-20%	-	20%	-	-
CS-PEG200-Gly20%	20%	-	20%	-
CS-PEG400-Gly20%	-	20%	20%	-
Chemical Gels				
CS Genipin 5	-	-	-	0.1% / pH 5
CS Genipin 13.6	-	-	-	0.1% / pH 13.6

1.1. Mechanical properties characterization of plasticized chitosan films (physical gel)

Chitosan physical gel film was prepared by means of a casting/ solvent evaporation technique. An acidic chitosan solution was poured into a Petri dish and dried for water evaporation. Then the pH was increased above chitosan pKa (6.5) in order to form hydrogel network.

All mechanical properties, tensile strength (TS, in MPa) indicating the maximum tensile stress that the film can sustain, elongation at break (EB, in %) as the maximum change in the length of a test film before being broken, are summarized in **Table 2**.

Table 2. Mechanical properties of different chitosan films

Film Code	TS (MPa)	E (%)
CS	58.94 ± 2.94	16.29 ± 2.25
CS-PEG200-20%	35.67 ± 11.82	39.98 ± 4.72
CS-PEG400-20%	49.12 ± 1.40	36.90 ± 0.51
CS-PEG200-Gly 20%	44.09 ± 1.09	27.00 ± 4.22
CS-PEG400-GLY 20%	49.03 ± 4.08	59.61 ± 4.55
CS Genipin 5	53.69 ± 13.89	15.37 ± 5.62
CS Genipin 13.6	49.00 ± 5.20	38.60 ± 5.70

The plasticized films had significantly higher elongation at break (**Table 2**) than chitosan film (CS). However no significant differences in tensile strength (TS) were observed. PEG addition caused an increase of the percentage of elongation-at-break (**CS-PEG200 20%** and **CS-PEG400 20%**), which is enhanced with the presence of glycerol (**CS-GLY-PEG200 20%** and **CS-GLY-PEG400 20%**). We assume that the resultant plasticizing effect was due to hydrogen bonding between O-H groups that were present in both plasticizers and O-H and NH₂ groups of chitosan. We can also observe that PEG molecular weight influences the plasticizing effect: the higher the molecular weight, the greater the plasticizing effect obtained (**CS-PEG200 20%** and **CS-PEG400 20%**).

Two conclusions could be derived from these results: plasticizers addition does not significantly modify the TS and caused a significant increase of the elongation to the break value. Those properties were also influenced by PEG molecular weight.

1.2. Mechanical properties characterization of cross-linked chitosan films (chemical gel)

Genipin cross-linked chitosan films were prepared based on chemical gel network. Genipin is an aglycone derived from an iridoid glycoside called Geniposide present in fruit of *Gardenia jasminoides*. It has a low toxicity and is an excellent natural cross-linker for chitosan or collagen and gelatin cross-linking [5],

CS Genipin 5 film presents similar mechanical properties than chitosan film (CS). Indeed, small size cross-linking agents such as genipin produce films with decreased free volume and less variable physical properties [6]. The small cross-linking molecules freely diffuse through the membranes and interact with the free amino groups of chitosan, leading to the formation of uniform three-dimensional network structures [7]. In contrast, the bulky cross-linking agents (e.g., polymers with reactive multifunctional groups (PEG)) produce films with more free volume, resulting in higher variation of physical properties. In addition to the above cross-linking networks, the mechanical properties of chitosan based films depend on the degree of deacetylation, distribution of acetyl groups along the chain (random or block wise), degree of crystallinity, and molecular weight and its distribution [8].

CS-Genipin 5 sample presents higher TS but lower EB values than **CS Genipin 13.6**. This result is due to the environmental cross-link pH condition, which plays an important role in influencing the cross-linking reactions of the preparation of genipin cross-linked chitosan gels [9]. In acidic conditions, the hydrogel network consists of short chains of cross-linking bridges (dimer, trimer, tetramer). In contrast, the chitosan gel crosslinked with genipin under strong base consists of long chains cross-linking bridges (7-88 monomers). In addition, the extent of cross-linking was significantly dependant on the pH conditions. Hydrogel cross-linked at pH 13.6 presents a lower cross-linking density than hydrogel cross-linked at pH 5. There is a direct relationship between the condition of cross-link reaction, and polymer network: basic conditions leads to less cross-linked network with long bridges while in acidic condition the extent of cross-linking is higher but the bridges smaller. **CS Genipin 5** polymer network is constituted by a lot of short genipin bridges. Therefore this film is resistant (high TS) but less flexible (low EB). We can observe the opposite behavior for sample **Genipin 13.6**, which is composed by few long Genipin bridges. This film is more flexible, which is a better mechanical property for TDD application.

1.3. Determination of the film presenting the best mechanical properties

The final use of polymeric films for TDD Systems application strongly depended on their mechanical properties at room temperature. They must be flexible enough to follow the movements of the skin without breaking but at the same time they show an increased strength to prevent abrasion of the film caused for example by contact with clothing. Clearly, the blend film containing 20% PEG 400 and 20% glycerol (**CS-PEG400-GLY 20%**) shows the highest EB value and good TS value for obtaining films with suitable toughness and flexibility. This film will be used for subsequent surface modification.

2. Incorporation of PN/CS microgel onto chitosan film surface

PN/CS microgel was incorporated by a batch method onto untreated, plasma and UV treated chitosan films. On untreated chitosan film (**Un(CS-PEG400-GLY 20%)-PN/CS**), this process is based on adsorption (Van der Waals interaction, acid-base interaction, electrostatic interaction and hydrogen bonding) of the microgel onto chitosan film surface without covalent bonding. However, as the consequence of the presence of radicals at the

substrate surface, covalent bonding can be additionally expected between the plasma and UV treated substrate and the microgel particles (**Plasma(CS-PEG400-GLY 20%)-PN/CS** and **UV(CS-PEG400-GLY20%)-PN/CS**).

Surface features of untreated, plasma and UV treated chitosan films with incorporated PN/CS microgel were studied by SEM (Figure 6). The incorporation of PN/CS microgel significantly changed the visual aspect of the film surface. This is clearly exhibited in case of plasma and UV pretreated films (Figure 1, c, c' and d,d'), where it was easy to locate surface deposition of PN/CS micro particles and to distinguish their form, size and amount present at the film surface. However the repartition is more homogeneous for plasma activated film than UV treated film (Figure 1, c' and d'). We can observe the presence of polymer on the surface of **UV(CS-PEG400-GLY20%)-PN/CS** sample, which could be formed under UV treatment Figure 1, d'). Previously untreated chitosan film (**Un(CS-PEG400-GLY 20%)-PN/CS**) presents a heterogeneous surface, where microparticles are aggregate.

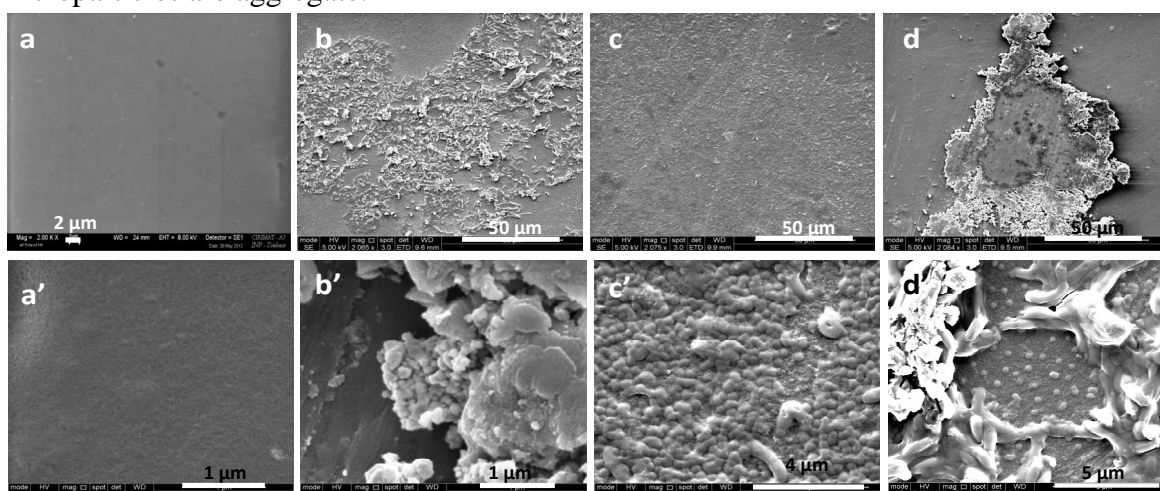


Figure 1. SEM pictures of CS film (a and a'), Un(CS-PEG400-GLY 20%)-PN/CS (b and b'), Plasma(CS-PEG400-GLY 20%)-PN/CS (c and c') and UV(CS-PEG400-GLY 20%)-PN/CS (d and d')

The enhancement of the adhesion between microgel and plasma treated chitosan film can be attributed both to physical and chemical modification. The physical modification is the surface roughening of the film surface by the sputtering effect, producing an enlargement of contact area that increases the friction between the film surface and the microgel. The chemical modification is the increase of the functional groups presence on the film surface, hence enabling a number of chemical bonds to be formed between the film and the microgel. After plasma and UV treatments, there are still a lot of free radicals that remain on the treated film surface, which can play a role in forming new functional groups and bonds between the film and the microgel.

CONCLUSION

Chitosan films surface was modified by thermosensitive microgel incorporation by non-thermal plasma or UV treatment. The results implied better microgel incorporation after plasma or UV treatment. All these results demonstrate the interest of this system as TDDS for drug delivery. In our future investigations, the wetting, spreading and peeling properties of the chitosan film will be realized with regard to confirm its ability to be used as effective delivery system. After physico-chemical characterization, the stability of a model drug incorporated in the film and drug release kinetic study will be envisaged.

ACKNOWLEDGEMENTS

Financial support for this work (BIOTRANSOS project) was provided by Marie Curie European Reintegration Grant (FP7-PEOPLE-2010-RG).

REFERENCES

- [1] Jovic, D. (2009). The Application of Temperature- and pH-responsive Microhydrogels for Functional Finishing of Cotton Fabric. *Technology: Advanced Performance Materials*, 24, 1-10.
- [2] Tournette, A., (2009). Incorporation of poly(N-isopropylacrylamide)/chitosan microgel onto plasma functionalized cotton fibre surface, *Colloids and Surfaces A: Physicochemical and Engineering Aspects*, 352, Issues 1-3, 126-135.
- [3] Aulton, M.E. (1981). The mechanical properties of hydroxypropylmethylcellulose films derived from aqueous Systems, part I: the influence of plasticizers, *Drug Dev. Ind. Pharm.* 7, 649-668.
- [4] Lin, S.Y. (1995). Drug-polymer interactions affecting the mechanical properties, adhesion strength and release kinetics of piroxicam-loaded Eudragit E films plasticized with different plasticizers, *J. Control. Release*, 33, 375-381.
- [5] Muzzarelli, A.A. (2009) Genipin-crosslinked chitosan hydrogels as biomedical and pharmaceutical aids. *Carbohydrate Polymers*, 77, Issue 1, 1-9.
- [6] Jegal, J. (1999). *J. Appl. Polym. Sci.*, 71, 671-675.
- [7] Chen, H. (2006). *Biomacromolecules*, 7, 2091-2098.
- [8] Rinaudo, M. (2006). *Prog. Polym. Sci.*, 31, 603-632.
- [9] Yuan Y. (2007). The effect of cross-linking of chitosan microspheres with genipin on protein release. *Carbohydrate Polymers*, 561-567.

Nanotechnology

PREPARATION OF OPTICALLY TRANSPARENT CHITIN NANOFIBER/POLYSILSESQUIOXANE COMPOSITES

Shinsuke Ifuku^{1*}, Akiko Ikuta¹, Minoru Morimoto¹, Hiroyuki Saimoto¹

¹Graduate School of Engineering, Tottori University 4-101 Koyama-cho Minami, Tottori 680-8552, Japan

*E-mail address: sifuku@chem.tottori-u.ac.jp

ABSTRACT

Chitin nanofibers (CNFs) reinforced silsesquioxane-urethaneacrylate (SSQ-UA) copolymer films were prepared. The nanocomposite films were highly transparent due to the nanometer sized CNFs inside the hybrid organic-inorganic SSQ-UA copolymer. CNFs due to their crystalline structure considerably increased Young's moduli and the tensile strengths of the composite and decreased the thermal expansion. Poly-SSQ improved heat resistance of CNFs.

Keywords

Chitin Nanofiber, Silsesquioxane, Nanocomposite, Low thermal expansion, Reinforcement

INTRODUCTION

Silsesquioxane (SSQ) is the compound with the chemical formula $(\text{RSiO}_{3/2})_n$, where R is either hydrogen or organic group, and has various structural orders including cage, ladder, and irregular structures. Its characteristic structure with intermediate between organic compounds and ceramics offers great potential to prepare multifunctional materials. Multifunctional properties resulting from organic/inorganic hybrid groups of SSQ increases its flexibility, optical transparency, and thermal stability. Therefore SSQ is recognized as a strong candidate for high performance substrate for future electrooptical devices. High temperature dimensional stability is strongly required for these applications, because thermal expansion causes damage for several substances deposited on an electronic substrate during the thermal assembly process. However, silsesquioxane polymer film has generally high thermal expansion, due to the organic part of the hybrid polymer.

Recently, we have prepared chitin nanofibers from crab and prawn shells and mushroom cell-wall [1-5]. The chitin nanofibers have a highly uniform structure with a 10-20 nm width and a high aspect ratio (Fig. 1). Since the nanofiber has excellent mechanical properties, it is useful for a reinforcement filler to create high-performance nanocomposites [6]. We expect that the nanofiber filler reduce the thermal expansion and improve thermo-mechanical properties of polysilsesquioxane due to the reinforcement effect. In this study, we prepared chitin nanofiber reinforced polysilsesquioxane to make a high and multi performance materials and characterized their optical, thermal, and mechanical properties for the development of substrates for future electrooptical devices [7].

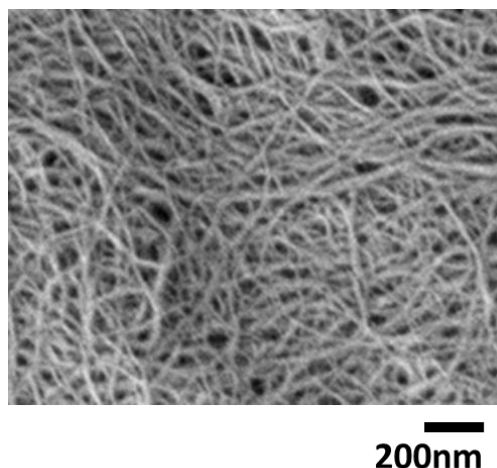


Figure 1. Chitin nanofibers isolated from crab shell

MATERIALS and METHODS

2.1. Materials

Chitin powder from crab shells was purchased from Nacalai Tesque, Inc. The average degree of acetylation of chitin was 3.9%, which was calculated from the C and N content in the elemental analysis data. Silsesquioxane was obtained from Nagase ChemteX Co., Ltd. Bifunctional urethaneacrylate oligomer (EBECRYL 9270, M_w 1,000) was obtained from Daicel-Cytec Co., Ltd. 2-Hydroxy-2-methylpropiophenone photo initiator was obtained from Tokyo Kasei Kogyo Co., Ltd.

2.2. Preparation of polysilsesquioxane (PSSQ) nanocomposite reinforced with CNFs

CNFs were prepared from commercially available chitin powder isolated from crab shell according to the previously reported procedure [2]. The CNFs were diluted to 0.1 wt.% in distilled water. The suspension was filtered under reduced pressure to make a CNF sheet. The wet sheet was then dried by pressing at 100 °C. The CNFs sheet was cut into 5 cm x 5 cm and had approximately 50 μm thickness and 90 mg weight. The sheet was impregnated into the matrices of mixtures SSQ and UA under reduced pressure. Five different types of matrices mixtures were prepared by mixing silsesquioxane (SSQ) and bifunctional urethane acrylate (UA) in the ratio of SSQ/UA = 5/0, 4/1, 3/2, 2/3, and 1/4 (w/w) with a photoinitiator. The SSQ-UA impregnated CNFs sheets of all the above SSQ/UA mixture were cured by UV irradiation with wavelength of 365 nm. The cured nanocomposites reinforced with CNFs thus obtained had approximately 70 μm thick, and the NF content was approximately 50 wt.%. SSQ-UA films without CNFs were also obtained by same protocol and used as control.

2.3. Measurements

The regular light transmittances of optically transparent nanocomposite films were measured by a UV-vis spectrophotometer (JASCO-V550). Tensile strengths and Young's moduli were measured by a universal testing instrument (AG-X, Shimadzu), for samples 50 mm long and 10 mm wide at a cross head speed of 1 mm min^{-1} with a gage length of 30 mm. The coefficients of thermal expansion (CTE) were evaluated with a thermomechanical analyzer (Q400, TA instruments). Specimens for CTE measurement were 30 mm long and 3 mm wide with a 20 mm span. The measurements were carried out from 30 to 165 °C by raising temperature at a rate of 5 °C min^{-1} . Thermogravimetric

analyses were carried out with TG8120 (Rigaku) apparatus. Measurements were conducted in the range 100-500 °C at a heating rate of 10 °C min⁻¹.

RESULTS and DISCUSSION

3.1. Transparency of CNFs composite films

CNFs were prepared from commercially available dry chitin powder as described in the literature [2]. We prepared SSQ based nanocomposite films reinforced with CNFs by impregnation of SSQ oligomer into CNF sheet followed by photopolymerization. The SSQ oligomer used in this study has mixed structure of irregular and ladder shape (Fig. 2).

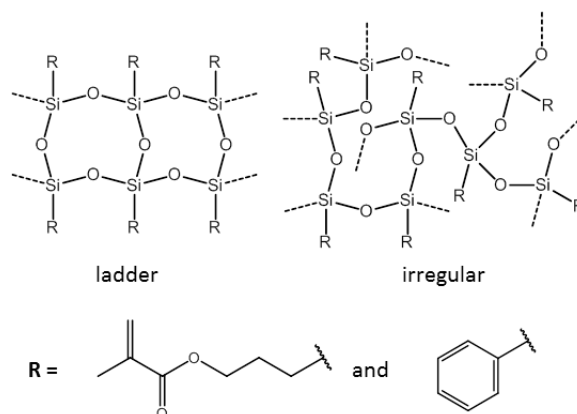


Figure 2. Chemical structures of silsesquioxane oligomer

The organic moieties of the hybrid oligomer consist of 75% 3-methacryloyloxypropyl group and 25% phenyl group. Due to the high crosslink density, polymerized SSQ was too brittle. Therefore, bifunctional UA oligomer was mixed as reactive diluent in the ratio of SSQ/UA = 5/0, 4/1, 3/2, 2/3, and 1/4, and copolymerized. Neat CNF sheet was not transparent at all (Fig. 3).

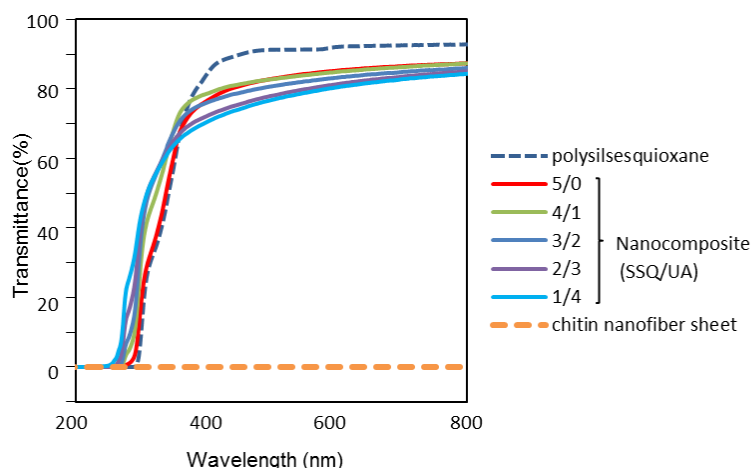


Figure 3. Regular light transmittance spectra of chitin nanofiber composite films

On the other hand, neat poly-SSQ film had approximately 90% transmittance. After SSQ-UA matrix impregnation and subsequent polymerization, the obtained CNFs nanocomposites in different ratios of SSQ/UA became highly transparent for visible light. CNFs sheets blended with SSQ-UA had good transparency (85% at 600 nm) in case of

SSQ/UA ratio 5/0. Blending with 1/4 ratio of SSQ/UA, CNFs sheet transparency decreased slightly to 80%. The composite films became transparent due to nano-sized composition of CNF sheet. Since the width (10-20 nm) of CNFs was much smaller than the wavelength of visible light (400-800 nm), the nanocomposites cause less light scattering than a microfiber reinforced composite at the interface between nanofiber and SSQ/UA matrix [8]. At 600 nm since transmittance of nanocomposites were 80-85%, the optical loss caused by nanofiber reinforcement were only in the range 5-10% despite the high fiber content of 50 wt.%. The chitin nanofiber sheet obtained in this study was available like a paper, though the novel paper is composed of nano-meter thick fibers. Several patterns can be printed on the nanofiber paper that we have prepared using a domestic inkjet printer (Fig. 4). The printed NF paper became transparent after matrix impregnation. This newly established technique of transparent printing on such a thin composite sheet can have application in printing of wiring used in electronic devices or electronic papers.

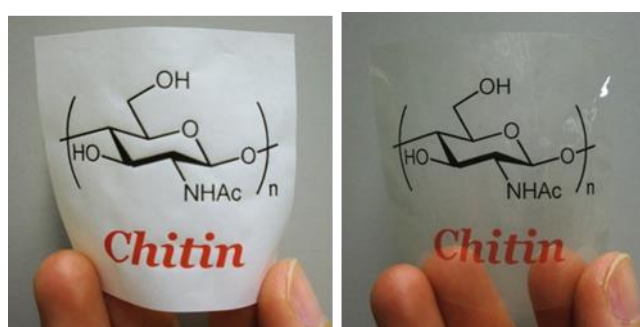


Figure 4. Appearance of chitin nanofiber sheet (left) and nanocomposite (right)

3.2. Thermal characterization of CNF composite films

Since CNFs show an efficient Young's modulus due to the extended crystal structure, the coefficient of thermal expansion (CTE) of crystalline chitin compound is $1.4 \times 10^{-6} \text{ K}^{-1}$ [9]. Therefore CNFs are better material as reinforcing element to reduce the high thermal expansion of poly-SSQ. Figure 5 shows the CTE of neat CNFs and its composites. Although neat poly-SSQ (SSQ/UA = 5/0) was too fragile to measure the thermal expansion, the CNF reinforced nanocomposite was tough for CTE measurement. CTE of CNF sheet without SSQ matrix was only $8.0 \times 10^{-6} \text{ K}^{-1}$.

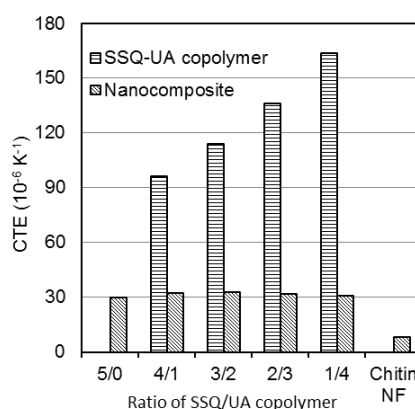


Figure 5. Thermal expansion of SSQ-UA copolymer and their chitin nanofiber composite films

While CTE of SSQ-UA copolymer films without CNFs was high in the range $96.2-164.0 \times 10^{-6} \text{ K}^{-1}$ depending on the ratio of SSQ/UA as shown by bars in Fig. 5. CTEs of all nanocomposites decreased significantly to a constant value of approximately $30 \times 10^{-6} \text{ K}^{-1}$.

These values corresponded to 66-81% decreased compared to the corresponding to the SSQ-UA matrices used. Thus, CNFs with low CTE worked effectively to decrease the thermal expansion of SSQ-UA copolymer film.

Due to the inorganic component, SSQ has high thermal stability and have been used to improve heat resistance property of polymers. Therefore, we investigated heat resistant property of nanocomposites to study effect of complexation of CNFs with SSQ-UA copolymers. Though, decomposition temperature of CNFs was at 318 °C, the decomposition bands shifted to higher temperatures when CNF blended with SSQ-UA copolymer. Decomposition of composites occurred at higher temperature was due to the blending of CNF with SSQ of high thermal stability of 420 °C. Thus, the thermal stability of the chitin nanofiber was improved by compounding with thermally stable SSQ. In general, since carbohydrate polymer has low decomposition temperature, this finding is advantageous for expanding the application of the chitin nanofibers as filler for nanocomposite materials.

3.3. Mechanical characterization of CNF composite films

CNFs have excellent mechanical properties and they are good materials to use as reinforcing element to improve mechanical properties of composite materials. Young's moduli and tensile strengths of SSQ-UA copolymer films and their CNFs composites were shown in Figure 6. Young's moduli of SSQ-UA with the ratio of 3/2, 2/3, and 1/4 without CNFs decreased from 1571 to 128 MPa with increasing the ratio of reactive diluent UA oligomer. The SSQ-UA films with the ratio of 5/0 and 4/1 were too fragile to measure the mechanical properties. On the other hand, nanocomposites were tough enough for the testing due to CNF support. Young's moduli of these nanocomposites considerably increased and reached in the range 3.36-4.29 GPa. The tensile strengths also considerably increased in the range 31-59 MPa. The enhancements of mechanical properties of composite strongly support that a CNF sheet with a high Young's modulus (1.80 GPa) and a high tensile strength (30 MPa) worked effectively as a reinforcement filler for SSQ-UA copolymer.

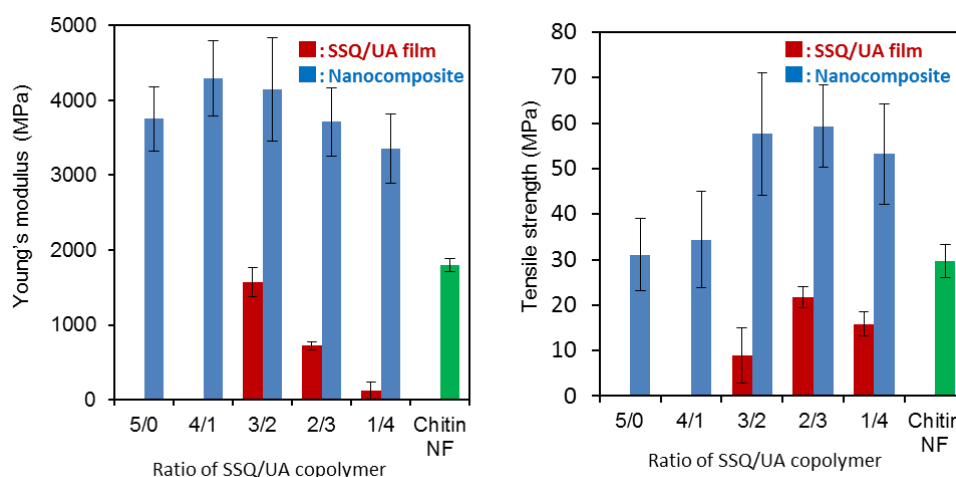


Figure 6. Young's modulus and tensile strength of silsesquioxane films and their nanocomposites

CONCLUSION

SSQ-UA films reinforced with CNFs were prepared and characterized in detail for transparency, thermal and mechanical properties. Neat CNFs sheet was not transparent, but when the cavities of NFs were filled by transparent SSQ hybrid material, the composites of

CNFs-SSQ-UA became transparent in a number of ratios of SSQ to UA. For different SSQ to UA ratios, the coefficient of thermal expansion of composites decreased in the range 66-81%. The decrease of thermal expansion is due to the contribution of low thermal expansion of CNFs. Moreover, the thermal stability of the chitin nanofiber was significantly improved owing to the inorganic component of SSQ with high thermal stability. Young's modulus and tensile strength of composites increased compared to neat CNFs or SSQ-UA copolymer due to nano-sized width of CNFs. Thus, SSQ-UA copolymer film reinforced with CNFs with high transparency, high mechanical properties, low thermal expansion, and high thermal stability will be advantageous to use as high performance nanocomposite as substrates for electrooptical devices like electronic paper.

REFERENCES

- [1] Ifuku, S., Nogi, M., Abe, K., Yoshioka, M., Morimoto, M., Saimoto, H., et al. (2009). Preparation of chitin nanofibers with a uniform width as α -chitin from crab shells. *Biomacromolecules*, 10, 1584-1588.
- [2] Ifuku, S., Nogi, M., Yoshioka, M., Morimoto, M., Yano, H., and Saimoto, H. (2010). Fibrillation of dried chitin into 10-20 nm nanofibers by a simple method under acidic conditions. *Carbohydrate Polymers*, 81, 134-139.
- [3] Ifuku, S., Nogi, M., Yoshioka, M., Morimoto, M., Yano, H., and Saimoto, H. (2011). Simple preparation method of chitin nanofibers with a uniform width of 10 to 20 nm from prawn shell under the neutral condition. *Carbohydrate Polymers*, 84, 762-764.
- [4] Ifuku, S., Nomura, R., Morimoto, M., and Saimoto, H. (2011). Preparation of chitin nanofibers from mushrooms. *Materials*, 4, 1417-1425.
- [5] Ifuku, S., and Saimoto, H. (2012). Chitin nanofibers: Preparations, modifications and applications. *Nanoscale*, 4, 3308-3318.
- [6] Ifuku, S., Morooka, S., Nakagaito, A. N., Morimoto, M., and Saimoto, H. (2011). Preparation and characterization of optically transparent chitin nanofiber/(meth)acrylic resin composites. *Green Chemistry*, 13, 1708-1711.
- [7] Ifuku, S., Ikuta, A., Hosomi, T., Kanaya, S., Shervani, Z., Morimoto, M., and Saimoto, H. (2012). Preparation of polysilsesquioxane-urethaneacrylate copolymer film reinforced with chitin nanofibers. *Carbohydrate Polymers*, 89, 865-869.
- [8] Yano, H., Sugiyama, J., Nakagaito, A. N., Nogi, M., Matsuura, T., Hikita, M., et al. (2005). Optically transparent composites reinforced with networks of bacterial nanofibers. *Advanced Materials*, 17, 153-155.
- [9] Wada, M., and Saito, Y. (2001). Lateral thermal expansion of chitin crystals. *Journal of Polymer Science B: Polymer Physics*, 39, 168-174.

“SMART” CO-CROSSLINKED CHITOSAN-BASED NANOPARTICLES FOR NANOBIO TECHNOLOGY

Celina Vila-Sanjurjo^{1,2}, Carmen Remuñán-López¹, Laurent David³, Cyrille Rochas⁴,
Francisco M. Goycoolea^{1,2}

¹ *Departament of Pharmacy and Pharmaceutical Technology. Universidad de Santiago de Compostela, 15782 Spain;* ² *Institut für Biologie und Biotechnologie der Pflanzen, Westfälische Wilhelms-Universität Münster. Schlossplatz 3; 48149 Münster, Germany;* ³ *Université de Lyon, Université Lyon 1, UMR CNRS 5223, Ingénierie des Matériaux Polymères (IMP), Laboratoire des Matériaux Polymères et des Biomateriaux, 15 Boulevard A. Latarjet, Bâtiment ISTIL, F-69622 Villeurbanne Cedex, France;* ⁴ *CERMAV-CNRS, Grenoble, France.*

*E-mail address: goycoole@uni-muenster.de

ABSTRACT

Ionically and covalently co-crosslinking of chitosan (CS) to harness nanoparticles (NPs) is described here as new route towards the development of nanobiotechnological approaches intended to biopharmaceutical and biomedical application. The aim of this study was to evaluate the effect of chemical co-crosslinking of CS-tripolyphosphate (TPP) NPs with genipin (GNP) on their biophysical characteristics and on their capacity to adsorb specific molecules known to act as autoinducers in bacterial *quorum sensing* (QS). The co-crosslinked CS NPs were found with enhanced capacity to adsorb 3-oxo-C6-hexanoyl homoserine lactone (3OC₆HSL) as a first evidence of their potential application in the development of antibiotic-free approaches against Gram (-) pathogenic bacteria.

Keywords

Chitosan nanoparticles, genipin, crosslinking, synchrotron SAXS, quorum quenching, N-acyl-homoserine lactone.

INTRODUCTION

Co-crosslinking chitosan-based nanoparticles (CS NPs) both ionically and covalently is a strategy to design new nanobiotechnological platforms and approaches intended to biopharmaceutical applications. Ionic crosslinking has been widely described for the development of non-toxic CS-based hydrogels, as well as for the preparation of CS-based micro- and nanosystems. The use of covalent crosslinkers makes CS to be more stable against pH, temperature, biological and mechanical degradation [1]. Genipin (GNP) is a recently discovered natural crosslinking agent of chitosan that is sourced from the glycosilated geniposide that occur in the fruits of *Gardenia jasminoides* Ellis and *Genipa americana*. GNP has been reported to be much less cytotoxic and more compatible than other well-known chemical crosslinkers of CS, such as glutaraldehyde. Thus, the use of GNP as a crosslinker has become a promising alternative to develop fully biocompatible materials [2,3]. The chemical crosslinking reaction between GNP and CS takes place in two steps. The first and faster involves the nucleophilic attack on the GNP C3 carbon atom by a CS primary amine group and the formation of a GNP heterocyclic compound linked to a glucosamine residue. The second step is slower and consists in the nucleophilic substitution of the GNP ester group (C11), with the formation of a secondary amide linkage with CS and further formation of crosslinked bridges [2].

The use of covalent crosslinkers allows to overcome the pH barrier of CS in solution, to preserve its thermosensitive character, and to enhance the extent of crosslinking in the matrix in order to modulate the network structure [1]. By controlling the extent of chemical crosslinking, other properties can be exploited, such as the ability of the resulting systems to adsorb and release biomolecules of particular interest for bionanotechnological or biopharmaceutical applications. This includes the capacity to target specific signals and receptors in bacteria, fungi and mammalian cells and to respond to physical and chemical stimuli. A very active field of research is to develop alternative approaches to the indiscriminate use of antibiotics against pathogenic bacteria. In this respect, the development of new nanomaterials aimed to interfere with pathogenicity is of particular interest. *Quorum sensing* (QS) is a cell-cell communication mechanism involved in virulence and other behaviors, by which bacteria count their own numbers by producing and detecting the accumulation of signaling molecules [4].

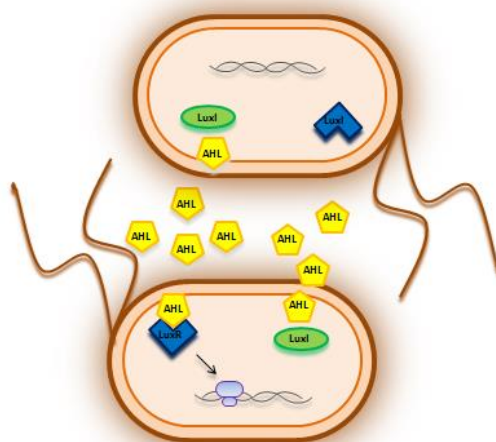


Figure 1. Schematic representation of QS signaling in Gram(-) bacteria. QS is a mechanism whereby bacteria produce and detect the accumulation of a signaling molecule (autoinducer, here represented by acyl-homoserine lactone signal molecules, AHLs, produced by the LuxI synthase) that they export into their environment. The binding of the AHLs to specific receptors (in the figure, LuxR protein) governs the expression of certain genes involved in community QS behaviours [4]. Strategies aimed to interfering with QS signaling, or quorum quenching, are currently proposed as potential alternatives to the massive use of antibiotics [5].

Recently, an approach has been described whereby a synthetic molecularly imprinted polymeric material showed enhanced capacity to adsorb N-acyl-homoserine lactones (AHLs) and inhibit the bioluminescence and biofilm formation responses in *Vibrio fischeri* and *Pseudomonas aeruginosa*, respectively [6,7]. Nanomaterials are bound to offer several advantages in this respect that can be exploited to interfere with QS, such as having a huge surface to volume ratio thus resulting in an enhanced capacity to adsorb QS signals.

This study aimed to investigate a “bottom-up” approach to exploit CS capacity to self-assemble by ionotropic gelation in the presence of pentasodium tripolyphosphate (TPP) and further co-crosslink with GNP so as to harness a new type of NPs with improved characteristics and performance. To this end, the effect of chemical co-crosslinking of CS-TPP NPs with GNP on their biophysical characteristics was addressed. Furthermore, a first account is presented here on the capacity of the co-crosslinked CS-based NPs to adsorb AHL molecules and hence, to potentially interfere with QS signaling in Gram (-) bacteria.

MATERIALS and METHODS

Materials

CS was a commercial sample of high purity grade in the hydrochloride salt form (ProtasanUP CL113, Mw ~125 kDa, DA ~14%, according to the manufacturer) purchased from Novamatrix (FMC-Biopolymer, Norway). GNP was purchased from Challenge Bioproducts (Taiwan). TPP and N-(3-oxo-hexanoyl)-L-homoserine lactone (3OC₆HSL) were purchased from Sigma-Aldrich (Germany). Milli-Q water was used throughout. All reagents were of analytical grade.

Optimization of the composition of CS-TPP NPs

CS-TPP NPs were prepared according with the general ionotropic gelation protocol described by Calvo *et al.* [8] with minor modifications. In order to assess optimal composition to obtain NPs of average size ≤ 200 nm and a low polydispersity (PDI ~0.1-0.2), different CS:TPP mass ratios were screened in two solvent environments, namely water or 85 mM NaCl. To this end, stock solutions of CS (2-3 mg/mL) and TPP (1-1.25 mg/mL) were prepared in both solvents and aliquots of the two components were mixed in a 96-well microplate in order to obtain CS-TPP NPs with various CS:TPP mass ratios (3.8:1 to 9.0:1). Larger batches of NPs with optimal size and PDI, at a given CS:TPP mass ratio, were prepared by scaling up of the preparation technique. Briefly, 11.25 mL of the TPP solution were poured onto 18.75 mL of the CS solution under magnetic stirring (500 rpm). When necessary, NPs were isolated by centrifugation (40 min, 10000 $\times g$, 25 °C) in 1.5 mL vials containing a glycerol bed and the pellets were resuspended in 100 μ L of water.

Co-crosslinking of CS-TPP NPs

The CS-TPP NPs were covalently co-crosslinked with GNP at different GNP:CS mass ratios (0.06:1 – 1.7:1). Aliquots of a GNP solution (5 mg/mL) were added to the NPs at a final concentration of 1 mg/mL in water. The NPs were incubated at 37°C under shaking (≈ 1400 rpm) for times ranging from 24-244 h.

Characterization of NPs

The size distribution of the nanoparticles was determined by dynamic light scattering using non-invasive back scattering (DLS-NIBS, measuring angle 173°) using a Malvern Zetasizer NanoZS ZEN 3600 (Malvern Instruments UK) equipped with a 4mW He/Ne laser beam operating at $\lambda=633$ nm. All measurements were performed at $25^\circ \pm 0.2$ °C. The kinetics of the crosslinking reaction was monitored by UV/VIS spectroscopy (Beckman-Coulter DU® DU 730 - Life Science UV/Vis Spectrophotometer) and by synchrotron small-angle X-ray scattering (SAXS, ESRF Grenoble, France; BM02-D2AM, E = 14 keV; sample-to-detector distance: 1.51 m).

Evaluation of the adsorption capacity of QS signals by CS-TPP NPs using a fluorescence *E.coli* biosensor

The BioBrick standard biological part BBa_T9002, ligated into the pSB1A3 (http://partsregistry.org/Part:BBa_T9002) was a gift sample from Prof. Anderson Lab (UC

Berkeley, USA). The part BBa_T9002 was transformed by chemical transformation into *E. coli* Top 10 (Invitrogen, Life Technologies Co., UK) and stored in a 30% glycerol stock at -80°C . The part BBa_T9002 comprises the transcription factor (LuxR), which is constitutively expressed but it is active only in the presence of a cell-cell signaling molecule (3OC₆HSL), which acts as an exogenous input. At an adequate concentration, two molecules of 3OC₆HSL bind to two molecules of LuxR and activate the expression of GFP (output), under the lux pR promoter from *Vibrio fischeri*. The fluorescence biosensor was calibrated for different 3OC₆HSL concentrations as described in Canton et al [9]. Ten mL of Luria Bertani broth, supplemented with 200 $\mu\text{g}/\text{mL}$ ampicillin, were inoculated with a single colony from a freshly streaked plate of Top10 containing BBa_T9002 and incubated for 18 h at 37°C with shaking at 100 rpm. The culture was diluted 1:1000 into 20 mL of M9 minimal medium supplemented with 0.2% casamino acids and 1 mM thiamine hydrochloride [9] and ampicillin (200 $\mu\text{g}/\text{mL}$) and grown to an OD₆₀₀ of 0.15 (~ 5 h) under the same conditions as before. The 3OC₆HSL was dissolved in acetonitrile to a stock concentration of 1×10^{-1} M and stored at -20°C until further usage. Prior to each experiment, serial dilutions from the stock solution were made in water to afford solutions of concentration ranging from 1×10^{-2} to 1×10^{-11} M. Twenty μL aliquots of the different 3OC₆HSL solutions were transferred into the wells of a flat-bottomed 96-well plate (Greiner Bio-One, cat. # M3061) and 180 μL aliquots of the bacterial culture were added to each well to yield AHL final concentrations ranging from 1×10^{-12} to 1×10^{-2} . Blank wells were filled with 200 μL of medium to measure the absorbance background. Control wells were filled with 180 μL of bacterial culture and 20 μL of water to measure the fluorescence background. The plate was incubated in a Safire Tecan-F129013 Microplate Reader (Tecan, Crailsheim, Germany) at 37°C and assayed with an automatically repeating protocol of fluorescence measurements ($\lambda_{\text{ex}}=485$ nm and $\lambda_{\text{em}}=520$ nm, 40 μs , 10 flashes, gain 100, top fluorescence), absorbance measurements (OD₆₀₀) ($\lambda=600$ nm absorbance filter, 10 flashes) and shaking (5 s, orbital shaking, high speed). Time between repeated measurements was 6 min. For each experiment, the fluorescence intensity (FI) and OD₆₀₀ data were corrected by subtracting the values of absorbance and fluorescence backgrounds and expressed as the average for each treatment. Data was represented in terms of FI/OD₆₀₀ versus incubation time. For the calibration of the biosensor, the rate of the evolution of FI/OD₆₀₀ was estimated from the value of the slope of a linear fit of FI/OD₆₀₀ during the first 100 min of incubation. The dependence of rate of FI/OD₆₀₀ as a function of AHL concentration was fitted to a non-linear growth sigmoidal Hill function by a minimization iteration process (OriginPro 8G, OriginLab Co., MA, USA) that allowed to determine the best-fit parameters. All measurements were conducted in triplicate.

To test the adsorption efficiency of the co-crosslinked CS NPs towards 3OC₆HSL, 2.5×10^{-9} M AHL was incubated in 1.5 mL vials with 1 mg/mL of non-isolated CS-TPP NPs (CS:TPP mass ratio 3.33:1), both in the presence and absence of GNP (final GNP:NP mass ratio 0.24:1), at 37°C with shaking (100 rpm), for 24 h. As controls the same concentration of AHL was incubated both alone or in the presence of GNP, without NPs. The final volume was 1 mL in all cases and all the reaction vials were prepared in triplicate. The vials were centrifuged at 13,000 rpm at room temperature for 30 min and 20 μL of the supernatants were applied to the fluorescence *E. coli* biosensor, to record the OD₆₀₀ and FI, as previously described.

RESULTS and DISCUSSION

Optimization of the formation of CS/TPP NPs

In order to assess the optimal NP composition that would afford particles with lowest average diameter and PDI, the CS:TPP mass ratio was varied in a range of 3.8:1 to 9.0:1 during the formation of NPs in both water or in 85 mM NaCl. Figure 2 illustrates the contour plots (upper and middle panels) for the dependence of the size and polydispersity of CS-TPP NPs with composition in water and in 85 mM NaCl. The lower frames summarize the dependence of the average diameter size in both solvent environments.

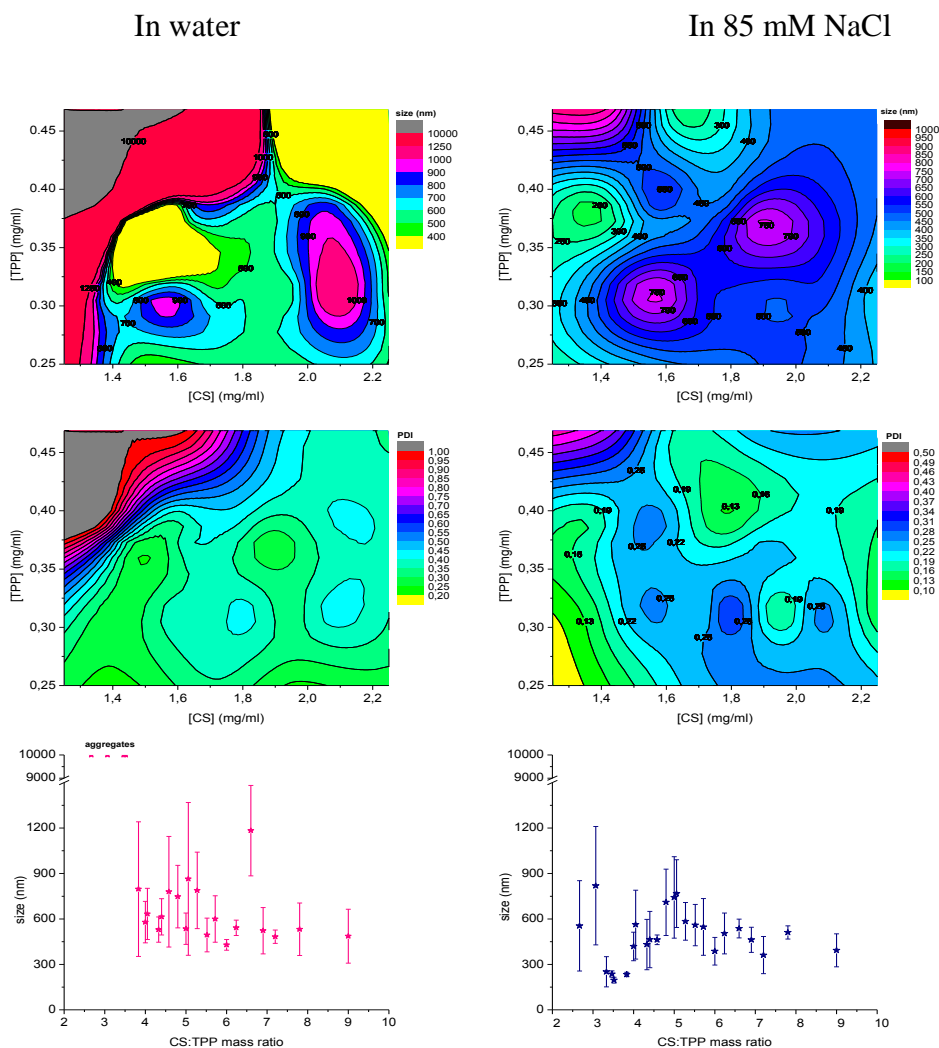


Figure 2. Contour plots (upper and middle panels) for the dependence of the size and PDI of CS/TPP NPs with composition in water (left panels) and in 85 mM NaCl (right panels). The lower frames summarize the evolution of size in both solvent environments.

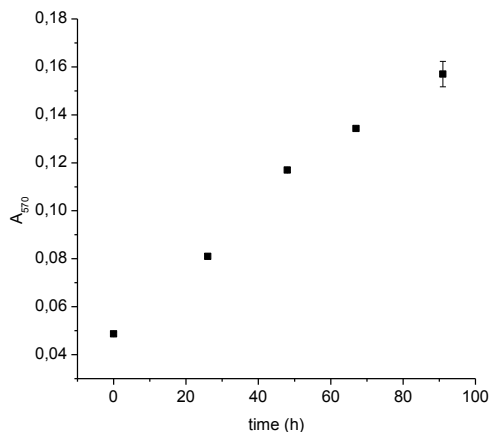
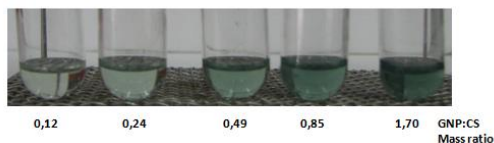
In the contour frames, the purple-to-gray color scale can be considered as hills for high PDI or size values, whereas the green-to-blue color scale would correspond to valleys for sub-micron and low-medium PDI values. Inspection of the plots reveals that the solvent environment plays an important role on the final NP size and polydispersity, showing that it is possible to obtain NPs with a size of ~200 nm and a fairly low PDI~0.2-0.3 under a narrow range of CS:TPP mass ratios ~3:1- 4:1 in 85 mM NaCl. In water and under

identical range of composition, the NP size and PDI values are much larger. Other studies have reported that the ionic strength affects the NP size, since the addition of monovalent ions to the solutions may overcome the electrostatic repulsion of the charged amino groups, leading to an increased flexibility and compaction of the CS backbone [10]. According with the evidence gathered here, the addition of NaCl improves the feasibility to formulate NPs at a relatively high concentration of both CS and TPP, which increases the final NP production yield (results not shown) without leading to aggregation.

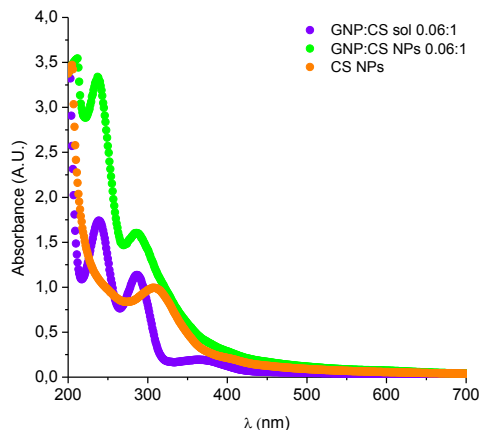
Co-crosslinking reaction kinetics

CS-TPP NPs of optimal composition prepared in 85 mM NaCl were covalently co-crosslinked with GNP at different GNP:CS mass ratios (0.06:1 – 1.7:1) at 37°C. The kinetics of the co-crosslinking reaction with GNP was studied by UV/VIS spectroscopy and synchrotron SAXS. The formation of blue pigments in CS-GNP co-crosslinked systems is attributed to the oxygen-radical-induced polymerization of GNP and dehydrogenation of an intermediate compound that occur once the first series of crosslinking reactions had taken place [2]. The upper frame of Figure 3A is a photograph that illustrates the evolution of the intensity of blue color at increasing GNP:CS mass ratios for CS-TPP NPs. In turn, the lower frame in Figure 3A represents the time-course evolution of the absorbance at $\lambda=570$ nm, which is proportional to the concentration of yellow-bluish pigments that have been proposed to form as an oxidation secondary product of the genipin cross-linking reaction of CS and GNP [3]. This is a first evidence that the crosslinking reaction proceeded in CS-TPP NPs at a GNP:CS mass ratio of 0.24:1. Notice in the plot that the A_{570} intensity increases linearly during the first 50 h of incubation while no stationary state is observed up to 100 h of incubation, although the slope of the curve is slightly reduced after 50 h. Figure 3B illustrates full UV-VIS scans 48 h after the crosslinking reactions of CS in solution and CS/TPP NPs with GNP at a GNP:CS mass ratio of 0.06:1, using non-covalently crosslinked CS-TPP NPs as a control. The crosslinking reaction of CS with GNP has been reported to exhibit a characteristic increase in the intensity of two peaks centered at $\lambda=240$ and 280 nm [3]. It can be noticed from the UV-VIS that the intensity of both peaks is significantly higher in the case of the CS-TPP NPs when compared with the CS solution at identical GNP:CS mass ratio and CS concentration. It appears that contribution of uncrosslinked NPs to the absorbance could account for this overall increase. However, it is also evident that in uncrosslinked NPs the bands at 240 and 280 are absent and there is only one a band at $\lambda=325$ nm. Figure 3C shows the time-course evolution of the crosslinking reaction of CS in solution (dashed lines) and CS/TPP NPs (solid lines) with GNP at three different GNP:CS mass ratios as monitored by the evolution of the intensity of the absorbance at $\lambda=300$ nm. Again, the traces show that the overall absorbance intensity is invariably higher for the CS-TPP NPs than for the CS in solution at the different tested GNP:CS mass ratios. Clearly, as the GNP:CS mass ratio increases in both CS solution and CS-TPP NPs, so does the rate of the reaction, as noticed by the slope of the A_{300} vs. time during the first 50 h. The crosslinking reaction for systems with lowest GNP:CS mass ratio, seemed to reach equilibrium after ~175 h, whereas at higher GNP:CS mass ratios it appeared not to have been then completed.

(A)



(B)



(C)

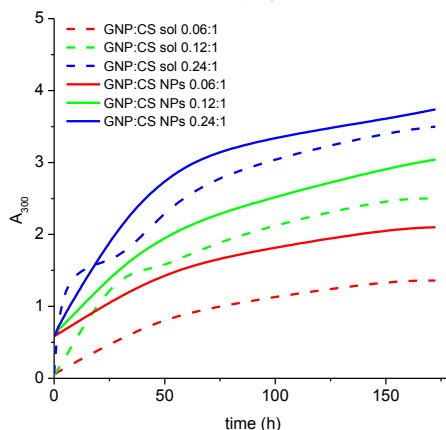


Figure 3. (A) Formation of blue color from secondary reaction product at different GNP:CS mass ratios and time-course evolution of genipin cross-linking reaction for CS-TTP NPs as monitored by the formation of yellow-blue color ($\lambda=570$ nm) at 37°C. (B) Comparison between UV-VIS scans for the covalent crosslinking reactions of CS in solution and CS/TTP NPs with GNP at a GNP:CS mass ratio of 0.06:1, and for non-crosslinked CS-TTP NPs, after 48 h incubation at 37°C. (C) Time-course evolution of the crosslinking reaction of CS in solution (dashed lines) and CS-TTP NPs (solid lines) with GNP at various GNP:CS mass ratios as monitored the absorbance at $\lambda=300$ nm.

The spectroscopic evidence presented here is consistent with the notion that the reaction of GNP crosslinking does occur when CS is present in the form of NPs and its kinetics does not seem to be modified.

To gain further insight into the structural modifications that take place at the CS-TPP nanoparticles during the crosslinking reaction with GNP, synchrotron SAXS studies were conducted. These studies sought to probe the structure of the nanoparticle systems at scales in the range 1 to 50 nm. Figure 4 shows representative scattering curves for CS-TPP nanoparticles at various GNP:CS mass ratios in co-crosslinked NPs after 24 h incubation at 37°C, in which the slope analysis (A) and the modified Porod core-shell model (B) were fitted.

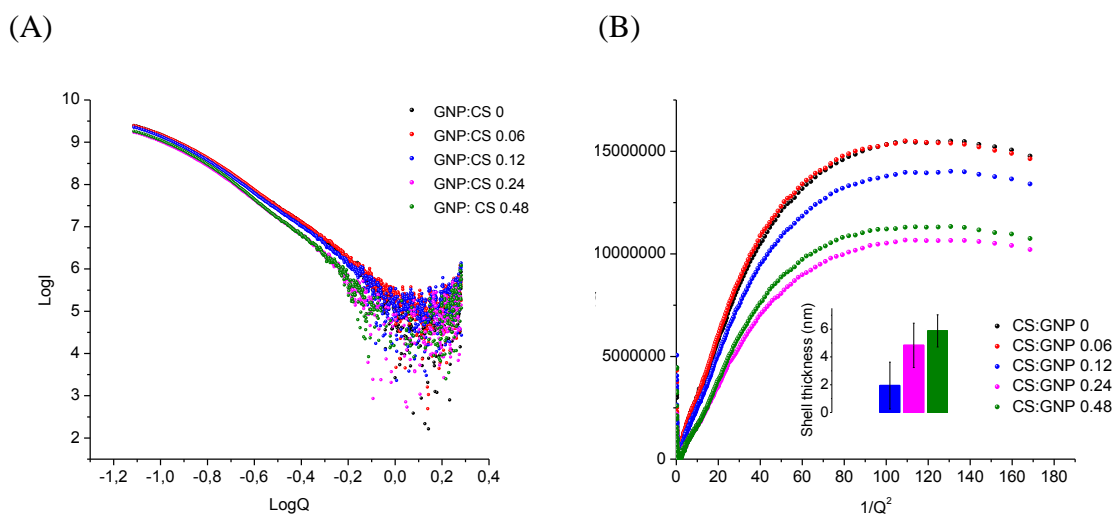


Figure 4. (A) Synchrotron SAXS scattering intensity curves and (B) Modified Porod representation for CS-TPP co-crosslinked NPs at varying GNP:CS mass ratios after 24 h incubation at 37°C. The inset in (B) represents the calculated thickness of the shell of the various systems.

As the slope of the plot $\log I$ vs. $\log q$ invariable assumed values larger than 4.0, the classical Porod's treatment is not applicable and hence a modified treatment consistent with the existence of a core-shell structure is applied to estimate the thickness of the shell of the NPs, using the following equation [11, 12]

$$I(q) * q^2 = -B + 1/q^2 * C \quad (1)$$

By virtue of this analysis it was possible to calculate the thickness of the interface of the transition layer (i.e. the shell thickness, L_i) during the course of the covalent reaction as a function at varying degrees of genipin crosslinking, from the expression:

$$L_i = \sqrt{B * 12\pi / C} \quad (2)$$

where C and B are the intercept and slope linear fit parameters of the modified Porod treatment (Eq. 1), respectively. The inset in Figure 4B represents the thickness of the shell of the various systems after 24 h incubation. As shown in the bar diagram, only for the NPs at GNP:CS mass ratios of 0.12-0.24, it was possible to fit the core-shell model and

estimate average values of shell thickness. It was found that the shell thickness increases with the GNP:CS mass ratio, ranging from ~2-6 nm. This evidence is consistent with the suggestion that the crosslinking reaction of GNP with CS-TPP NPs occurs preferentially at the nanoparticle surface.

Evaluation of the adsorption capacity of QS signals using a fluorescence *E. coli* biosensor

The fluorescence *E. coli* biosensor bearing the BbaT9009 genetic device, can be considered as an AHL receiver whose output (GFP expression) can be measured by fluorescence, as described by Canton et al. [9]. In order to estimate the sensitivity of the fluorescence biosensor, we have performed a series of experiments to calibrate the output response (FI/OD₆₀₀) to ranging 3OC₆HSL input concentrations. The data was successfully fitted to a three parameter Hill model, agreeing with already reported results for the same genetic device [9]. Nevertheless, the *E. coli* biosensor showed that, in our experimental conditions, a 10-fold increase in sensitivity can be achieved when compared with already reported data. As shown in Figure 5 the switch point, that is, the 3OC₆HSL concentration required for half-maximal FI/OD₆₀₀, is $3.22 \times 10^{-10} \pm 1.22 \times 10^{-10}$ M and at AHL concentrations higher than 1×10^{-9} M, the fluorescence response is saturated.

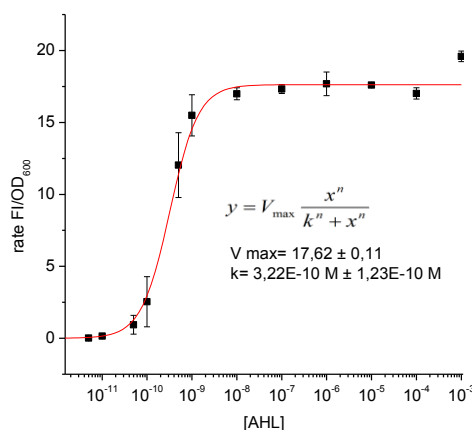


Figure 5. Rate of fluorescence expression normalized by the OD₆₀₀ at various AHL concentrations. The continuous line represents the best fit of the Hill function to the experimental data (shown in inset).

Figure 6 shows the effect of the co-incubation of NPs with AHL on FI (A), bacterial OD₆₀₀ (B) and normalized FI/OD₆₀₀ (C), after 3 h treatment of the *E. coli* biosensor with the supernatants. Figure 6D reveals the effect of the different treatments on the rate of FI/OD₆₀₀ during the first 55 min of bacterial growth. As shown in the plots, the fluorescence response is reduced and retarded in the case of the NP treatments, being more for the co-crosslinked NPs, when compared with the control AHL, which was not pre-incubated with NPs. The reduced fluorescence cannot be related to any toxic effect of the treatments as evidenced by the response of the optical density (OD₆₀₀). Hydrophobic interactions seem to be at play in governing the enhanced AHL adsorption to co-crosslinked NPs, as previously reported for other CS-GNP hybrid materials aimed to the adsorption of poor soluble molecules [2].

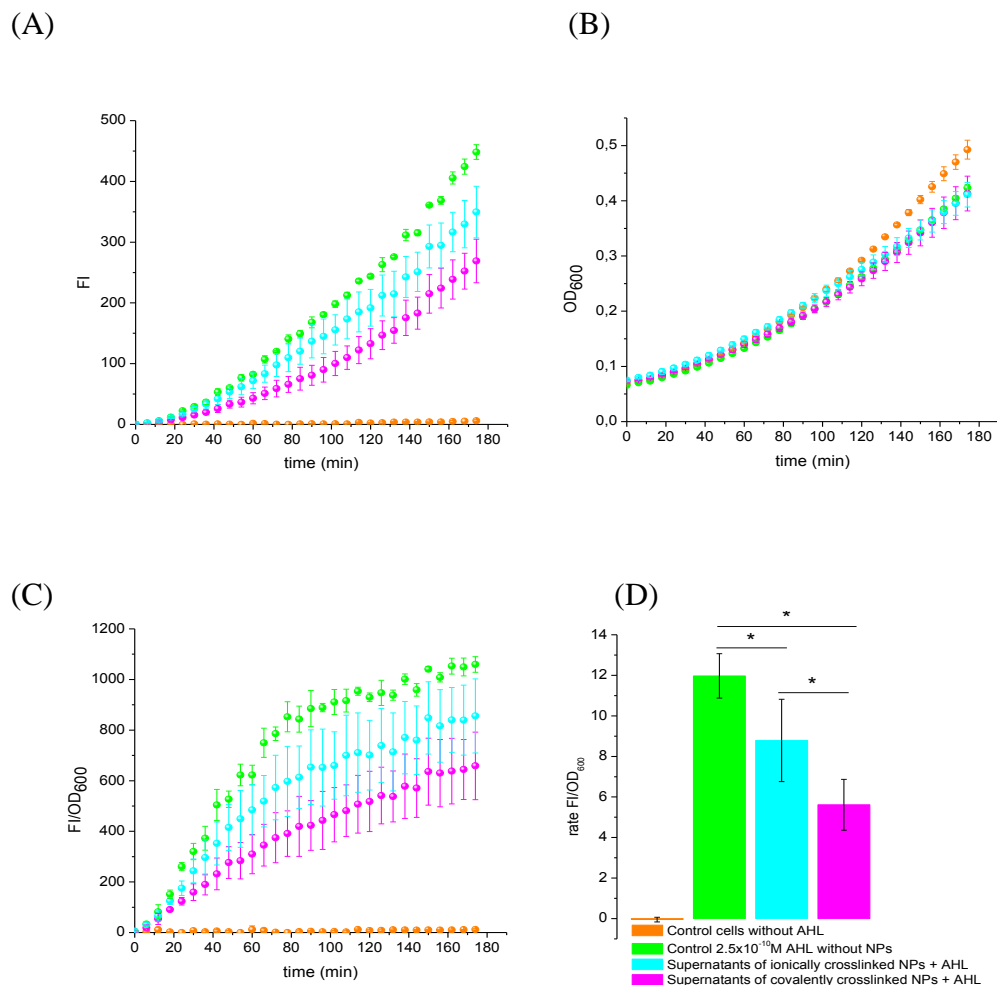


Figure 6. Effect of the co-incubation of NPs with AHL on FI (A), bacterial OD₆₀₀ (B) and normalized FI/OD₆₀₀ (C), after 3h treatment of the *E.coli* biosensor with the supernatants. (D) Effect of the different treatments on the rate of FI/OD₆₀₀ during the first 55 minutes of bacterial growth represented as mean ± standard deviation (n=3 for all groups, $p \leq 0.05$).

CONCLUSIONS

We have gathered evidence that by controlling the chemical modifications and the gelation process of the GNP-crosslinked CS NPs we can develop new nanomaterials modified at their surface. Our data suggest that our NP prototypes can be used as a platform to design new nanosystems than can exert an efficient microbial control via its ability to inhibit the expression on the genes involved in AHL-based QS signaling pathways.

ACKNOWLEDGMENTS

The European Commission (Marie Curie IIF – BioNanoSmart_DDS–No. 221111); “Consolidation and Structuration of Competitive Research Units (“Competitive Reference

Groups)⁴, REF. 2010/18; FEDER Financiation (Spain); Grants No. SC2774 and CH 3386 of European Synchrotron Research Facility (Grenoble, France) and Project FIS PS09/00816 from the Spanish Government-ISCIII. C.V. acknowledges fellowships granted by Xunta de Galicia and Ministerio de Educación y Ciencia (FPU), DAAD (Germany) and Fundación Pedro Barrié de la Maza. Help and advice of Mr. J.P. Fuenzalida with the synchrotron SAXS results is thanked.

REFERENCES

- [1] Moura, M.J., Faneca, H., Lima, M.P., Gil M.H., Figueiredo, M.M. (2011) In situ forming chitosan hydrogels prepared via ionic/covalent co-cross-linking. *Biomacromolecules*, 12, 3275-3284.
- [2] Espinosa-García, B.M., Argüelles-Monal, W.M., Hernández, J., Félix-Valenzuela, L., Acosta, N., Goycoolea, F.M. (2007). Molecularly imprinted chitosan-genipin hydrogels with recognition capacity towards *o*-xylene. *Biomacromolecules*, 8, 3355-3364.
- [3] Butler, M.F., NG, Y-F., Pudney, P.D.A. (2003). Mechanism and kinetics of the crosslinking reaction between biopolymers containing primary amine groups and genipin. *J. Polym. Sci. A Polym. Chem.*, 41, 3941-3953.
- [4] Bassler, B.L., Losick, R. (2006). Bacterially speaking. *Cell*, 125, 237-246.
- [5] Clatworthy, A.E., Pierson, E., Hung, D.T. (2007). Targeting virulence: a new paradigm for antimicrobial therapy. *Nat. Chem. Biol.*, 3 (9), 541-548.
- [6] Piletska, E.V., Stavroulakis, G., Karim, K., Whitcombe, M.J., Chianella, I., Sharma, A., Eboigbodin, K.E., Robinson, G.K., Piletsky, S.A. (2010). Attenuation of *Vibrio fischeri* quorum sensing using rationally designed polymers. *Biomacromolecules*, 11, 975-980.
- [7] Piletska, E.V., Stavroulakis, G., Larcombe, L.D., Whitcombe, M.J., Sharma, A., Primrose, S., Robinson, G.K., Piletsky, S.A. (2011). Passive control of quorum sensing: prevention of *Pseudomonas aeruginosa* biofilm formation by imprinted polymers. *Biomacromolecules*, 12, 1067-1071.
- [8] Calvo, P., Remuñán-López, C., Vila-Jato, J.L., Alonso, M.J. (1997). Novel hydrophilic chitosan-polyethylene oxide nanoparticles as protein carriers. *J. Appl. Polym. Sci.*, 63, 125-132.
- [9] Canton, B., Labno, A., Endy, D. (2008). Refinement and standarization of synthetic biological parts and devices. *Nat. Biotechnol.*, 26 (7), 787-793.
- [10] Jonassen, H., Kjoniksen, A., Hiorth, M. (2012). Effects of ionic strength on the size and compactness of chitosan nanoparticles. *Colloid. Polym. Sci.*, 290, 919-929.
- [11] Kim, M.H. (2004). Modified Porod's law estimate of the transition-layer thickness between two phases: test of triangular smoothing function. *J. Appl. Crystallogr.*, 37, 643-651.

Applications in Life Science

ANTIFUNGAL POTENTIAL OF MICRO AND NANOPARTICLES OF CHITOSAN CROSSLINKED WITH SODIUM TRIPOLYPHOSPHATE

O. COTA-ARRIOLA¹, M.O. CORTEZ-ROCHA¹, J. LIZARDI-MENDOZA², J.M. EZQUERRA-BRAUER¹, M. ROBLES-SÁNCHEZ¹, M. PLASCENCIA-JATOMEA*¹

¹ Department of Food Research and Graduate, University of Sonora, Mexico, ² CIAD A.C., Hermosillo, Sonora, México.

ABSTRACT

There are few studies on the antifungal activity and the effect of sodium tripolyphosphate (TPP) on the antimicrobial potential of particles of chitosan (CS) cross-linked with TPP. In this study, micro and nanoparticles of CS produced by ionotropic gelation with TPP were structurally characterized by transmission and scanning electron microscopy, Fourier transformed infrared spectroscopy and with respect to antifungal activity. Spherical particles were obtained from 80 nm to 20 μ m, depending on the concentration of CS and TPP. Comparing with CS in solution, the particles of CS were more effective to delay the radial growth and spore germination of *Aspergillus parasiticus*, causing morphologic alterations in hyphae and spores. The inhibitory effect can be attributed to the particle size and the available functional groups of CS/TPP (amino and phosphate groups), suggesting a possible synergistic effect between CS and TPP.

Keywords: Chitosan, *Aspergillus parasiticus*, antimicrobial activity, ionotropic gelation

INTRODUCTION

The study of chitosan has increased due to its ability to form micro and nanoparticles, mainly for biomedical and pharmaceutical applications for drug delivery [1, 2, 3]. It has been recently reported that the antibacterial activity of micro and nanoparticles of chitosan is higher as compared to chitosan solutions [4] due to a major interaction with the cellular membranes of fungi and bacteria, causing permeability alterations and possibly the penetration towards the interior of the cell [4]. Also it has been demonstrated that the size, shape and zeta potential are related to the antimicrobial potential of micro and nanoparticles of chitosan [5]. However, information about the antifungal effect of micro and nanoparticles based on chitosan matrixes and its possible mechanism of action is scarce. Several methods can be used for the preparation of chitosan matrices and ionotropic gelation is the most used at present, which consist in the electrostatic interaction between chitosan protonated amino groups and TPP anions [3]. The aim of this study was to obtain micro and nanoparticles of low viscosity chitosan by ionotropic gelation with TPP; also, to characterize the structure of particles and evaluate their antifungal activity against *Aspergillus parasiticus* (ATCC 16992).

MATERIALS and METHODS

Preparation of micro and nanoparticles of CS-TPP.

The micro and nanoparticles were prepared by the ionotropic gelation method [5]. Low viscosity chitosan (Sigma-Aldrich) solutions were prepared at 0.2, 0.35 and 0.5% (w/v) in

0.1 M of acetic acid solution. Each chitosan solution was added, independently, to different solutions of TPP (2.0, 6.0 and 10% w/v) to a CS:TPP ratio of 80:100 (v/v). The pH of the solution was adjusted to pH 5.6 with acetic acid solution. Nine particles sizes were obtained according to the used concentrations of chitosan and TPP. The nomenclature of materials was: TPP₂CS_{0.2}, TPP₂CS_{0.35}, TPP₂CS_{0.5}, TPP₆CS_{0.2}, TPP₆CS_{0.35}, TPP₆CS_{0.5}, TPP₁₀CS_{0.2}, TPP₁₀CS_{0.35}, TPP₁₀CS_{0.5}, indicating the subscript the used concentration of CS and TPP.

Fourier Transformed Infrared Spectroscopy. The spectra of the micro and nanoparticles of CS-TPP were obtained in a FT-IR spectrum Perkin Elmer GX equipment (Waltham, MA, USA), with an average of sixteen scans in a spectral range of 4000–400 cm⁻¹ [6].

Morphological properties. The morphology and size of the chitosan microparticles were determined using a scanning electron microscope (SEM) (JEOL DSM-54101V) equipped with EDS. The size and morphology of chitosan nanoparticles were determined using a transmission electron microscope (TEM) (JEOL JEM-2010F) operated at 200 kV [6].

Antifungal activity of micro and nanoparticles of CS-TPP on *Aspergillus parasiticus*

Radial growth kinetics. Petri dishes containing Czapek agar medium with added 5x10⁻³ g of micro and nanoparticles of chitosan were inoculated with 1x10⁵ spores/ml of *A. parasiticus* by a point-wise deposition of the inoculum in the center of the plate, and incubated at 28°C. The radial extension growth of the colony was measured each 12 h [7].

Spore germination. Petri dishes containing Czapek liquid medium with added 5x10⁻³ g of micro and nanoparticles of chitosan were inoculated with 1x10⁴ spores/ml of *A. Parasiticus*. The plates were incubated at 28°C and the number of germinated spores were counted each 5 h [7].

Morphometric parameters. The images of spores and hyphae of *A. parasiticus* grown in the presence of the micro and nanoparticles of chitosan were obtained by image analysis (Image Pro-Plus Version 6.3. Media Cybernetics, USA) [7].

Statistical analysis. A completely randomized design using a two-way factorial analysis with three levels and analysis of variance (ANOVA), was carried out. JMP software version 5.0 (SAS Institute Inc., USA) at a significance level of $P=0.05$, was used. Homogenous groups were separated using the multiple comparisons Tukey test (Tukey's post hoc test) at a confidence interval of 95%.

RESULTS and DISCUSSION

Morphology

Poncellet (2006) considers a nanoparticle when its size is less than 1 μm and a microparticle when the size is less than 1 mm [8]. In this study, nanoparticles and microparticles obtained (Fig. 1) were spherical and ranged in size from 80 nm to 20 μm. The particles size depends on the concentration of CS-TPP. The nanoparticles prepared with 0.2% of chitosan (TPP₂CS_{0.2}, TPP₆CS_{0.2} and TPP₁₀CS_{0.2}) showed a less than 1 μm size

and the microparticles prepared with 0.35 and 0.5% of chitosan showed a size between 1 and 20 μm .

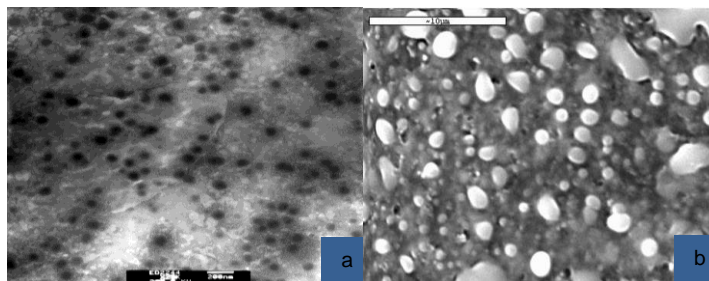


Fig. 1 Micrographs of chitosan-based micro and nanoparticles. **a)** CS-TPP nanoparticles observed by analysis TEM; **b)** CS-TPP microparticle observed by SEM analysis.

Infrared spectroscopy (FT-IR)

Infrared spectra of micro and nanoparticles showed the characteristics bands of chitosan and TPP (Fig. 2). The spectra of chitosan-TPP micro and nanoparticles (Fig. 2) shows the peak of the primary amide of chitosan at $1560\text{--}1650\text{ cm}^{-1}$. Also, stretching vibrations of the P=O group of the phosphate ion around $1228\text{--}1115$ and $889\text{--}750\text{ cm}^{-1}$, and the band at 527 cm^{-1} corresponding to the deformation vibrations of P=O, were observed. When the TPP concentration increased, the intensity of the band corresponding to the phosphate groups in the spectra was higher. This can be attributed to an increased number of available phosphate groups due to the excess of TPP. This verifies the presence of chitosan-TPP in the development of micro and nanoparticles [9,10].

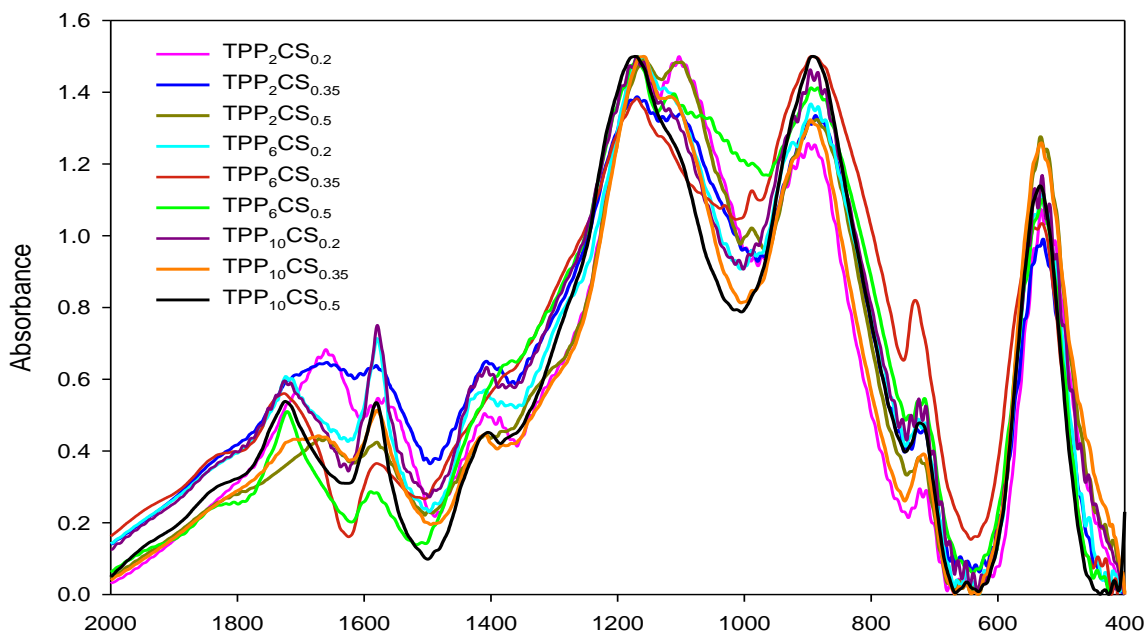


Fig. 2 Fourier Transform Infrared spectra of micro and nanoparticles of CS-TPP prepared at different concentrations.

Radial growth of *Aspergillus parasiticus*

Chitosan-micro and nanoparticles of CS-TPP decreased the radial extension of the colony of *A. parasiticus* with respect to the control (Table 1). A higher effect was observed when the TPP concentration was increased and the fungal growth was delayed until 12 h. A lower ($p \leq 0.05$) fungal growth in the presence of TPP₁₀CS_{0.2}, TPP₁₀CS_{0.35} and TPP₁₀CS_{0.5}, was observed. Table 1 shows the percentage of inhibition of *A. parasiticus*, at 168 h. The inhibitory effect can be attributed to the interaction of the phosphate ions with divalent metals such as Ca⁺² and Mg⁺² that are important for the fungi growth, or with components of positive charge of the plasma membrane such as proteins [11,12].

Since the particles with stronger fungistatic activity on *A. parasiticus* showed higher absorbance intensity of the bands corresponding to the primary amide (N-H) group of CS and bands related to the TPP phosphate ion (Fig. 2), the above results suggest that the fungistatic effect of micro and nanoparticles of CS-TPP are mainly related to the amino groups of CS and TPP phosphate ions available after the electrostatic interaction between CS and TPP.

The TPP₁₀CS_{0.2} nanoparticles showed the highest inhibitory effect after 108 h, which can be related to their smaller size. It has been reported that the particle size affects the antibacterial potential. Smaller particles increases the surface contact between the particle and the membrane of bacteria [4], being able to cause toxicity or cellular death in bacteria due to a possible cellular penetration of the smaller nanoparticles [4].

Table 1 Inhibition percentages of the radial extension colony (at 168 h) and spores germination (at 30 h) of *A. parasiticus* inoculated in Czapek media amended with micro and nanoparticles of chitosan-tripolyphosphate, incubated at 28°C.

Treatment	Inhibition (%) at 168 h	Inhibition (%) at 30 h
Control (Ac)	00.00	00.00
CS _{0.5}	16.67±0.36 ^b	42.43±1.47 ^{bc}
TPP ₁₀	0.00±0.36 ^a	48.11±1.47 ^{cde}
TPP ₂ CS _{0.2}	24.47±0.36 ^c	36.76±1.47 ^{ab}
TPP ₂ CS _{0.35}	26.60±0.36 ^d	40.27±1.47 ^b
TPP ₂ CS _{0.5}	28.65±0.36 ^f	43.78±1.47 ^{bcd}
TPP ₆ CS _{0.2}	27.66±0.36 ^{de}	38.65±1.47 ^b
TPP ₆ CS _{0.35}	27.66±0.36 ^{de}	48.10±1.47 ^{cde}
TPP ₆ CS _{0.5}	23.55±0.36 ^c	55.68±1.47 ^f
TPP ₁₀ CS _{0.2}	51.42±0.36 ^h	53.78±1.47 ^{ef}
TPP ₁₀ CS _{0.35}	40.07±0.36 ^g	52.97±1.47 ^{ef}
TPP ₁₀ CS _{0.5}	38.30±0.36 ^g	77.02±1.47 ^g

Data followed by their standard errors, are means of three experiments. Treatment means followed by different subscripts are significantly different ($P \leq 0.05$).

Morphological alterations were found in hyphae and spores of *A. parasiticus* grown in the presence of micro and nanoparticles of CS-TPP (TPP₁₀CS_{0.2}, TPP₁₀CS_{0.35}, TPP₁₀CS_{0.5}) (Fig. 3). Compared with the controls, thicker and irregular hyphae with low amount of spores were observed. Also, the color of the fungal mycelium was white in the presence of TPP₁₀CS_{0.2}, TPP₁₀CS_{0.35}, TPP₁₀CS_{0.5}, while in the control media was green (normal mycelia of *A. parasiticus*) (Fig. 3). The low amount of produced spores can be attributed to the presence of TPP as phosphate ions interact with metals such as Ca⁺, Fe⁺, and Mg⁺ [13], being these partly responsible for the spore germination of the fungus [7].

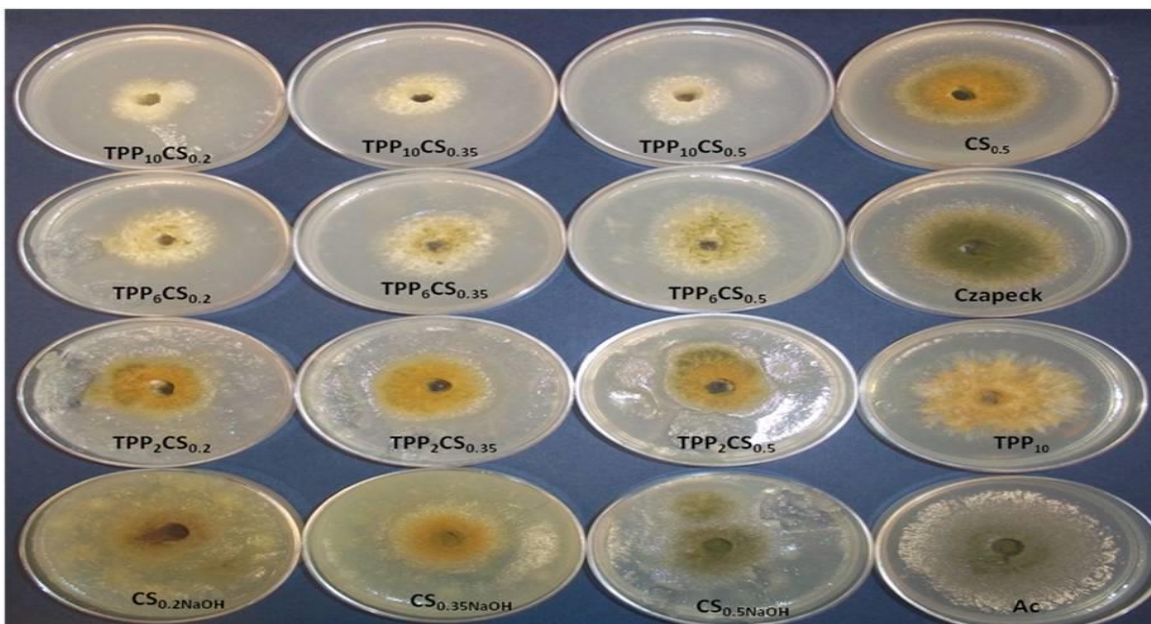


Fig. 3 Colonies of *Aspergillus parasiticus* grown on Czapek medium with amended chitosan-tripolyphosphate particles, incubated at 28°C, at 96 h.

Spore germination

The presence of micro and nanoparticles delayed the germination process compared with the control and the effect on the germination was dependent on the TPP concentration. The inhibitory activity of the micro and nanoparticles of CS-TPP increased as their concentration was increased (Table 1).

The size of the chitosan particles affected the germination of spores of *A. parasiticus*. Lower inhibitory effect on the germination was observed at smaller particle size, which can be attributable to the particles agglomeration, providing a surface where the spores can adhere to germinate. The morphological changes found in mycelium and spores were more marked and evident in the media added with smaller particles (image not showed), which can be explained on the basis of the ratio area/volume. The contact surface increases when the particle size is smaller; therefore there is greater electrostatic interaction [5] between chitosan and the fungi plasma membrane.

CONCLUSION

The micro and nanoparticles of CS-TPP showed a higher fungistatic effect on *A. parasiticus* compared with the CS and TPP in solution. This effect was depending on the particle size. Besides morphological changes in hyphae, a white mycelium and low amount of spores in media amended with CS particles prepared with TPP, were observed. The results suggest that the antifungal activity of CS/TPP micro and nanoparticles on *A. parasiticus* can be associated to a synergistic effect between CS and TPP in the matrix.

ACKNOWLEDGEMENTS

To CONACyT for funding provided through key projects and No. 58249 y No. 53493 J1, and scholarship for postgraduate studies.

REFERENCES

- [1] Il'ina, A.V., Varlamov, V.P., Yu, A.E., Orlov, V.N., Skryabin, K.G. (2008) Chitosan is a natural polymers for constructing nanoparticles. *Chemistry.*, 42, 199-201.
- [2] No, H.K., Meyers, S.P., Prinyawiwatkul, W., Xu, Z. (2007) Applications of chitosan for improvement of quality and shelf life of food: A review. *J Food Sci.*, 72(5), 87-100.
- [3] López-León, T., Carvalho, E.L.S., Seijo, B., Ortega-Vinuesa, J.L., Bastos-González, D. (2005) Physicochemical characterization of chitosan nanoparticles: electrokinetic and stability behavior. *J Colloid Interf Sci.*, 283, 344-351.
- [4] Du, W.L., Xu, Y.L., Xu, Z.R., Fan, C.L. (2008) Preparation, characterization and antibacterial properties against *E. Coli* K₈₈ of chitosan nanoparticle loaded copper ions. *Nanotechnology.*, 19, 1-5.
- [5] Ali, S.W., Joshi, M., Rajendran, S. (2010) Modulation of size, shape and surface charge of chitosan nanoparticles with reference to antimicrobial activity. *Adv Sci Lett.*, 3, 452-460.
- [6] Ruobao, L., Chunling, Z., Weifen, Z., et al. (2009) Comparison study of chitosan/ β -cyclodextrin microspheres. *J Nat Sci.*, 14,362-368.
- [7] Cota-Arriola, O., Cortez-Rocha, M.O., Rosas-Burgos, E.C., et al. (2011) Antifungal effect of chitosan on the growth of *Aspergillus parasiticus* and production of aflatoxin B1. *Polym Int.*, 60(6), 937-944.
- [8] Poncelet, D. (2006) Microencapsulation: fundamentals, methods and applications, in surface chemistry in biomedical and environmental science. Ed J.P. Blitz and V.M. Gun'ko, Springer, Heidelberg Publishers pp. 23-34.
- [9] Mathew, S., Abraham, T.E. (2008) Characterization of ferulic acid incorporated sterch-chitosan blend films. *Food Hydrocolloids.*, 22,826-835.
- [10] Xu, Y., Du, Y. (2003) Effect of molecular structure of chitosan on protein delivery properties of chitosan nanoparticles. *Int J Pharm.*, 250,215-226.
- [11] Brumkar, D.B., Pokhakar, V.B. (2006) Studies on effect of pH on cross-linking of chitosan with sodium tripolyphosphate: A technical note. *AAPS Pharm Sci Tech.*, 7,20-25.
- [12] Plascencia-Jatomea M, Viniera G, Olayo R, Castillo-Ortega MM, Shirai K (2003) *Macromol Biosci* 3:582-586
- [13] Vareltozidis, K., Soultos, N., Koidis, P., et al. (1997) Antimicrobial effects of sodium tripolyphosphate against bacteria attached to the surface of chicken carcasses. *Lebensmittel Wissenschaft and Technologie.*, 30,665-669.

Barrier Properties of Chitosan Film Incorporated with Essential Oil

H. S. DEBONE¹, C. M. P. YOSHIDA¹, C. F. DA SILVA^{1*}

¹UNIFESP, Universidade Federal de São Paulo, Rua São Nicolau, 210, Diadema – SP, CEP 09913-030, Brazil
E-mail: cfsilva@unifesp.br

ABSTRACT - The application of chitosan as a dressing for healing burns presents advantages like low toxicity, biocompatibility, as well as bacteriostatic and fungistatic activities. Chitosan is a natural polymer abundant in nature and derived from chitin. In this paper, emulsified oil chitosan films were produced by the casting technique in order to use them as wound dressings. Two concentrations of essential oil were evaluated. The barrier properties of the films were evaluated according to American standards (Water Vapor Permeability, WVP) and British standards (Fluid Handling Capacity, FHC). The results showed that the FHC of the films was lower than the values desired for dressings, although the values were equal or very close to the values observed for commercial dressings. Moreover, the increase in oil concentration promotes a decrease in the WVP of the films.

Keywords: chitosan, emulsified film, essential oil, wound dressing

INTRODUCTION

Various formulations such as ointments and wound dressings have been developed for the treatment of severe burn wounds or ulcers. Wound dressings have greatly enhanced burns healing treatment. Wound healing is a complex biological process and damaged tissue requires biocompatible materials like chitosan, which has high film-forming capacity. The most cited advantages of chitosan are the physico-chemical and biological properties, including antimicrobial, anti-inflammatory, antitumoral, bacteriostatic, fungistatic, and homeostatic activities, as well as adsorption properties (PAUL and SHARMA, 2004; WANI *et al.*, 2010).

Chitosan film is homogeneous, flexible, transparent, resistant, and slightly yellow in color. It has been described as a compact and uniform filmogenic matrix without pores or cracks (YOSHIDA *et al.* 2009). The application of the wound dressing promotes drainage and prevents the build-up of exudates. In addition to antimicrobial activity, which is interesting for the healing process, chitosan promotes activation and proliferation of inflammatory cells in granular tissues (ALEMDAROĞLU *et al.*, 2006), stimulates cell proliferation, reorganizes the histoarchitecture of the tissue (MUZZARELLI, 1989), and affects the function of macrophages, thus accelerating the healing process (BALASSA and PRUDDEN, 1984). Chitosan showed a substantial decrease in healing time and minimal scarring in several animals (PAUL and SHARMA, 2004).

These and other properties can be potentiated with the incorporation of some essential oils. The aim of this work is to evaluate the effect of essential oil concentration on the barrier properties of chitosan films in treating burns.

MATERIALS AND METHODS

Commercial chitosan (deacetylation $\approx 82\%$ and $M_w \approx 1.47 \times 10^5$ g/mol) was supplied by Polymar (Fortaleza, Brazil) without any prior purification, and acetic acid (Synth, Brazil) was used as the acid medium. Essential oil obtained from a Brazilian plant was used as the active compound.

Chitosan Suspension

Chitosan (1.0 % w/w) was dissolved in acetic acid aqueous solution. The stoichiometric amount of acetic acid was calculated from the sample weight, by taking into account the degree of acetylation required to achieve the protonation of all the NH₂ sites plus 50% of the amount. The suspension was homogenized for 2 h prior to the preparation of the chitosan film in order to complete the chitosan solubilization.

Preparation of the Chitosan Films

Films were prepared by the casting technique. The chitosan solution (1% w/w) and the essential oil was emulsified beforehand (24,000 rpm/10 min). We tested two concentrations of essential oils: 0.5% and 1.0% w/w. The chitosan emulsion was poured into polyethylene Petri dishes. The films were dried in a forced air oven at 40°C for 24 h. As the mass of the suspension applied onto the Petri dishes was kept constant, the total solid content per gram of dried films was 0.21 g/cm². The films were further characterized.

Fluid Handling Capacity (FHC)

The FHC of the film is defined as the sum of the Absorbency (ABS) and Moisture Vapor Transmission Rate (MVTR). The FHC was examined according to the European Standard BS EN 13726-1 for hydrocolloids and dressings. In this test, five samples of each film (or dressing) were applied to the modified Paddington cups (Figure 1), to which were added 20 ml of simulated exudate fluid (SEF).

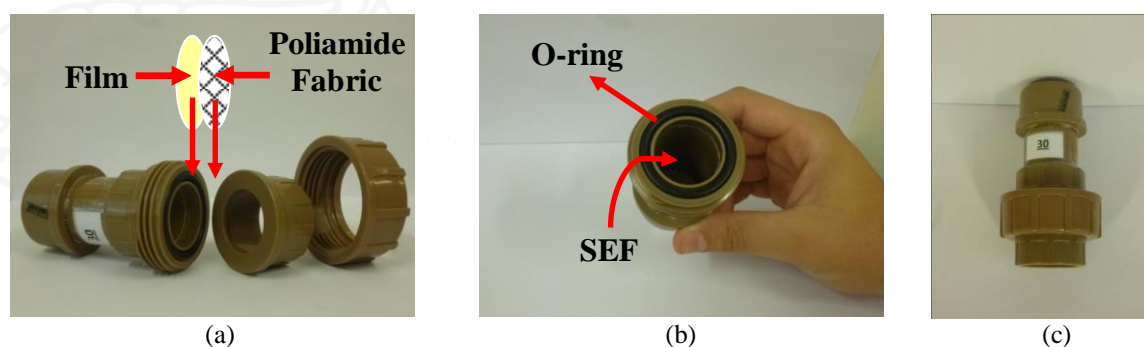


Figure 1. Modified Paddington cups used for the determination of Fluid Handling Capacity (FHC).

The cups were weighed using a calibrated analytical balance, inverted so that the dressing came into contact with the SEF (Figure 1c) solution, and then placed in a temperature and humidity controlled incubator to maintain an environment of 37°C ± 2°C and a relative humidity below 20%, for a period of 24 h. At the end of the test, the cups were removed from the incubator and were allowed to equilibrate at room temperature for a period of 30 min prior to reweighing on the analytical balance. The FHC, ABS, and MVTR values were calculated by the following equations:

$$MVTR = \frac{x - y}{\text{time} \times \text{surface}} \quad (1)$$

$$ABS = \frac{b - a}{\text{time} \times \text{surface}} \quad (2)$$

$$FHC = MVTR + ABS \quad (3)$$

where x is the total weight of the system (film + SEF solution + cup) at the beginning of the test; y is the total weight of the system (film + SEF solution + cup) after 24 h; b is the weight of the film at the beginning of the test; and a is the weight of the film after 24 h.

Water Vapor Permeability (WVP)

The WVP and water vapor transmission rate (WVTR) of the films were determined using the ASTM E96-02 gravimetric standard method (ASTM, 1995). The films were fixed on the top of test cells containing a desiccant (silica gel). The test cells were placed in a chamber with controlled temperature and relative humidity (25°C and 75% RH). Permeation cells were weighed before and at least four times after the incubation, and then the acquired weight was used to calculate the WVP. Linear regression was used to fit the data and weight versus time, and also to calculate the G value in g/s for the slope of the resulting straight line. The WVP and WVTR of the films were calculated from the following equations:

$$WVP = \frac{G \cdot x}{A \cdot \Delta P} \quad (4)$$

$$WVTR = \frac{G}{\text{time} \times \text{surface}} \quad (5)$$

where x is the film thickness; A is the area of exposed film; and ΔP is the partial water vapor pressure differential across the film, which was calculated based on the chamber temperature and the relative humidity inside and outside the cup. Five specimens were tested for each film type.

Scanning Electron Microscopy (SEM)

SEM analysis was performed on fractured cross-sections and the surfaces of gold sputtered films using an LEO 440i scanning electron microscope (LEO Electron Microscopy Ltd.) with 10 kV and 100 pA.

Statistical Analysis

All of the characterizations were done in replicate. The Tukey test was performed for comparison of means, using the BioEstat 5.0 software.

RESULTS AND DISCUSSION

Figure 2 shows SEM micrographs of the films containing essential oil. The films prepared with essential oil showed structural discontinuities associated with the formation of two phases (lipid and polymer) in the matrix. The oil-free films had a smooth and homogeneous microstructure with no irregularities like air bubbles or oil droplets detected (micrograph not shown). The greater the number of oil droplets, the higher the concentration of oil. YOSHIDA *et al.* (2010) also observed a more amorphous matrix with the incorporation of palmitic acid in emulsified chitosan films. Lipid droplets were also observed in emulsified films with caseinate/tung oil (PEREDA *et al.*, 2010) and hydroxypropylmethylcellulose/tea tree essential oil (SANCHEZ-GONZALEZ *et al.*, 2009). Pores and cavities were also present on the surface of the films containing essential

oil and this can affect the results of vapor permeation through the film, as will be seen in the results for FHC, ABS, and MVTR for 0.5% essential oil.

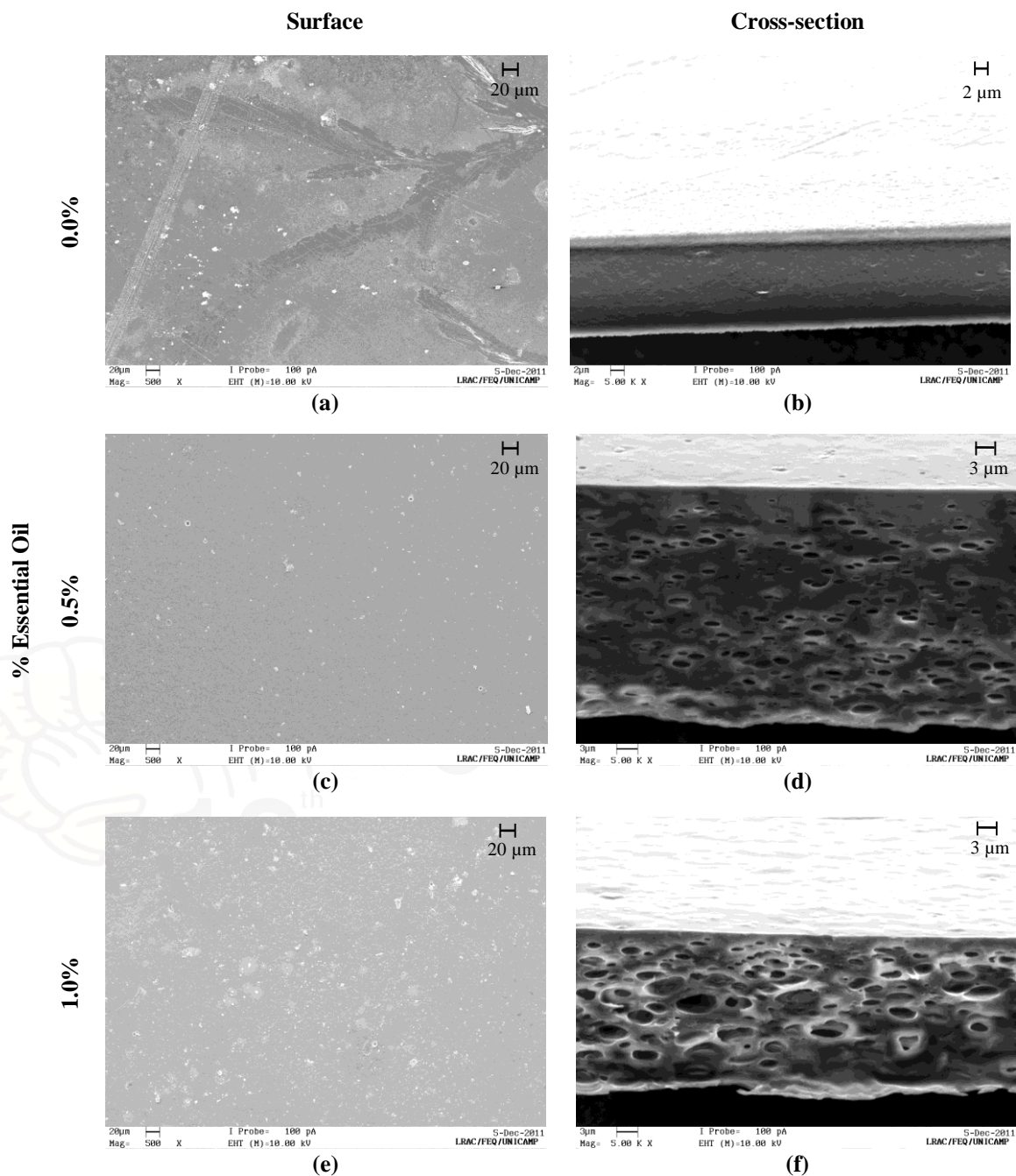


Figure 2. SEM micrographs of chitosan-essential oil films: (a), (c), and (e) show the surfaces at a magnification of 500 x; while (b), (d), and (f) show cross-sections at a magnification of 5,000 x.

Table 1 shows the results for FHC, ABS, and MVTR for the films. The addition of 0.1% of oil did not change the properties of the film, indicating that the amount of oil is insufficient for any structural modification of the film (data not shown). However, when adding 0.5% of oil, all the properties increased, and subsequently reduced with the addition of 1.0% of oil. The reduction of the values of these properties is due to the hydrophobic character of the oil. The increase in values occurring with 0.5% of oil may be due to the formation of pores that are preferred paths for facilitating the passage of fluid when the film is hydrated.

It was observed that the MVTR and ABS values are similar to those observed by THOMAS and YOUNG (2008) for some commercial dressings in which the same measurement technique was used. They found that the ABS value was equal to 3.44 ± 0.04 g/10cm²/24h and 4.32 ± 0.04 g/10cm²/24h for the ActivHeal and Allevyn Adhesive Dressing, respectively. The MVTR was equal to 1.67 ± 0.11 g/10cm²/24h and 12.35 ± 0.42 g/10cm²/24h for the ActivHeal and Allevyn Adhesive Dressing, respectively. Our results are also in accordance with AICKIN *et al.* (2010) for the following dressings: Tielle Plus, Allevyn Adhesive Border, Allevyn Gentle, and Biatain Adhesive.

According to Lamke *et al.* (1977), and also cited by THOMAS and YOUNG (2008), third-degree burns, donor sites and unspecified granulating wounds generate between 3.4 and 5.1 g of exudate/10cm²/24h. Thus, in order to apply a dressing for burns it is necessary that the dressing provides absorption of exudate to keep the burned surface moist, and, in particular, allow the passage of the exudate so that the MVTR is greater than that presented by the production of exudate at the site where the dressing is applied. Regarding the application of dressing films for third-degree burns, and considering the production of exudate, only the films containing 0.5% of oil showed an MVTR very close to the rate of exudate production. However, the MVTR value is higher than that presented by THOMAS and YOUNG (2008) for the ActivHeal dressing.

The oil hydrophobicity reduces the FHC values, due to the reductions in MVTR and ABS values. However, it was observed that the oil in some concentrations did not change the values of these properties. For example, for the film containing 0.5% of oil, there was an increase in the value of these properties compared to the film without oil. This increase is probably due to the formation of pores and cavities on the film surface when it is hydrated by SEF, which removes part of the oil from the film and promotes the capillary effect in these spaces. When the concentration of oil is 1.0%, the hydration is not so high and the film does not alter the FHC value enough.

Table 1 shows that the increase in the essential oil concentration promotes a reduction in WVPR and WVP values. No direct contact between the films or any fluid is provided in determining the WVP and WVPR, so the results show different behaviors from those observed for FHC. Increasing the concentration of essential oil promotes a reduction in WVP and also in WVPR, both due to the hydrophobicity of the oil.

Table 1. Barrier properties of chitosan film with essential oil.

	Essential Oil Concentration (%)***		
	0.0	0.5	1.0
Moisture Vapor Transmission Rate (MVTR)	1.73 ± 0.07^a	2.80 ± 0.25^b	1.41 ± 0.11^c
Absorbency (ABS)*	1.67 ± 0.12^a	2.41 ± 0.15^b	0.76 ± 0.02^c
Fluid Handling Capacity (FHC)	3.40 ± 0.14^a	5.21 ± 0.29^b	2.17 ± 0.11^c
Water Vapor Transmission Rate (WVTR)	0.58 ± 0.02^a	0.38 ± 0.03^c	$0.42 \pm 0.05^{b,c}$
Water Vapor Permeability (WVP)**	5.47 ± 0.37^a	4.41 ± 0.36^b	3.45 ± 0.21^c

*in g/10 cm²/24h; ** in (g/m.s.Pa) x 10¹¹; ***Means on the same line with different letters differ significantly at $p \leq 0.05$.

CONCLUSION

The chitosan films with essential oil showed regular morphology and the presence of oil droplets homogeneously dispersed in the polymeric matrix. The ABS and MVTR values of the films only achieved adequate levels for use as dressings for the film containing 0.5% of essential oil. Moreover, the increase in the concentration of essential oil promotes a reduction in water vapor permeability.

ACKNOWLEDGEMENTS



The authors are grateful to FAPESP (Process number 2010/17.721-4) for the financial support.

REFERENCES

- American Society for Testing and Materials (2000) ASTM E 96-00. Standard test methods for water vapor transmission of materials.
- British Standards (2002) BS EN 13726-1. Test methods for primary wound dressings. Part 1: Aspects of Absorbency, section 3.3 Fluid Handling Capacity.
- Alemdaroğlu, C., Değim, Z., Çelebi, N., Zor, F., Öztürk, S., Erdoğan, D. (2006) An investigation on burn wound healing in rats with chitosan gel formulation containing epidermal growth factor. *Burns*, 32, 319-327.
- Balassa, L. L., Prudden, J. F. (1984) Applications of chitin and chitosan in wound healing acceleration. In *Chitin, Chitosan and Related Enzymes* (JP Zikakis, ed.) pp. 296-305, Academic Press.
- Muzzarelli, A. A. (1989) Amphoteric derivatives of chitosan and their biological significance. In *Chitin and Chitosan* (G. Skjak-Braek, T. Anthonsen, P. Sandford, eds.), Elsevier Applied Science.
- Paul, W. and Sharma, C. (2004) Chitosan and Alginate Wound Dressings: A Short Review. *Trends in Biomaterials and Artificial Organs*, 18, 18-23.
- Yoshida, C. M. P., Oliveira-Júnior, E. N., Franco, T. T. (2009) Chitosan Tailor-Made Films: The Effects of Additives on Barrier and Mechanical Properties. *Packaging Technology and Science*, 22(3), 161-170.
- Aickin, S., Delbono, M., Lindsay, L., Mistry, P., Clark, R., Cullen, B. (2010) Evaluating Current in-vitro Assays for Assessing Fluid Handling Properties of Dressing and their Clinical Relevance. *Wounds UK*.
- Lamke, L.O., Nilsson, G.E., Reithner, H.L. (1977) The evaporative water loss from burns and water vapor permeability of grafts and artificial membranes used in the treatment of burns. *Burns*, 3, 159-165.
- Pereda, M., Aranguren, M. I., Marcovich, N. E. (2010) Caseinate films modified with tung oil. *Food Hydrocolloids*, 24, 800-808.
- Sánchez-González, L., Vargas, M., González-Martínez, C., Chiralt, A., Cháfer, M. (2009) Characterization of edible films based on hydroxypropylmethylcellulose and tea tree essential oil. *Food Hydrocolloids*, 23, 2102-2109.
- Thomas, S. and Young S. (2008) Exudate-handling mechanisms of two foam-film dressings. *Journal of Wound Care*, 17(7), 309-315.
- Yoshida, C. M. P., Bastos, C. E. N., Franco, T. T. (2010) Modeling of potassium sorbate diffusion through chitosan films. *LWT - Food Science and Technology*, 43, 584-589.
- Wani, M. Y., Hasan, N., Malik, M. A. (2010) Chitosan and Aloe Vera: Two Gifts of Nature. *Journal of Dispersion Science and Technology*, 31, 799-811.

EQUILIBRIUM AND KINETIC STUDIES ON THE ADSORPTION OF RED 2 BY CHITOSAN-CELLULOSE BEADS

E. Alva-Navarrete¹, B. García-Gaitán^{1*}, J. L. García-Rivas¹, R. E. Zavala-Arce¹, J. G. Luna-Bárceñas², M. C. Díaz-Nava¹, C. R. Muro-Urista¹

¹Instituto Tecnológico de Toluca, Av. Tecnológico S/N Col. La Virgen, Metepec, México, Méx.

²CINVESTAV-Unidad Querétaro, Libramiento Norponiente #2000, Fracc. Real de Juriquilla, Querétaro, Querétaro México. 76230

*E-mail address: beatrizggmx@yahoo.com

ABSTRACT

Chitosan-cellulose hydrogel beads (CCHB) were synthesized and tested for its anionic dye removal capacity from aqueous solutions. CCHB were used for adsorption of trisodium 2-hydroxy-1-(4-sulphonato-1-naphthylazo) naphthalene-3,6-disulphonate, a water-soluble hazardous azo dye (red 2 also called amaranth). Equilibrium and kinetics batch adsorption studies were performed to assess hydrogel's dye removal capacity. At initial pH 5.7, red 2 was removed efficiently. Specific rate constants for the processes were calculated by kinetics and adsorption time dependency measurements. Adsorption data were well described with a pseudo-second-order kinetic model. Isothermal adsorption data fit well the Langmuir model. Results in this study indicated that chitosan-cellulose hydrogel beads are an attractive candidate for removing red 2 from dye wastewater.

Keywords

Chitosan, cellulose, adsorption, dye, amaranth.

INTRODUCTION

Water pollution is caused by numerous pollutants including dyes. Dyes have become one of the main sources of severe water pollution as a result of the rapid development of the industries. The release of the colorant effluents has triggered a major concern on the human health as well as marine lives [1]. It is known that wastewaters containing dyes are very difficult to treat since the dyes are recalcitrant molecules (particularly azo dyes), resistant to aerobic digestion, and are stable to oxidizing agents. Another difficulty in the treatment of wastewaters arises when low concentrations of dye molecules are present [2]. The high cost to remove trace amounts of impurities causes the conventional methods of removing dyes become unfavorable to be applied at a large scale [1,3]. Recently, adsorption techniques using chitosan composites have been developed to adsorb dyes as an alternative to conventional wastewater treatment processes [4,5]. The objective of this work was to assess chitosan-cellulose hydrogel beads (CCHB) as adsorbent for removal of red 2 (R2) dye from aqueous solutions. R2 is a dark red to purple azo dye (Amaranth, CI Number 16185, EEC Number E123, FD&C Red 2, Acid Red 27, C.I. Food Red 9, Azorubin S) with molecular formula $C_{20}H_{11}N_2Na_3O_{10}S_3$ and a molar mass of 604.55 Da. R2 has been used as a food dye, in cosmetics and it can be applied to natural and synthetic fibers, leather, paper, and phenol-formaldehyde resins. R2 usage is still legal in some countries including Mexico. Its carcinogenic nature is still debatable; however, it has been recently proven that high concentration of this dye can adversely affect human/animal health; it may cause tumors, allergic and respiratory problems. There are

also some evidences which suggest that it may also cause birth defects [6]. R2 is highly soluble in water, it increases the risk of being found as a contaminant in industrial effluents.

MATERIALS and METHODS

Medium molecular weight chitosan flakes (75% deacetylated), microgranular cellulose powder and ethylene glycol diglycidyl ether (EGDE) 50 wt% in water, were used as received (reagent grade from Sigma–Aldrich Co.). NaOH and acetic acid were purchased from J. T. Baker (analytical grade). Red 2 (R2) was purchased from Sensient Co. and it was used as target molecule. Distilled water was used to prepare all solutions in sorption experiments. Figure 1 presents the chemical structure of the R2 dye.

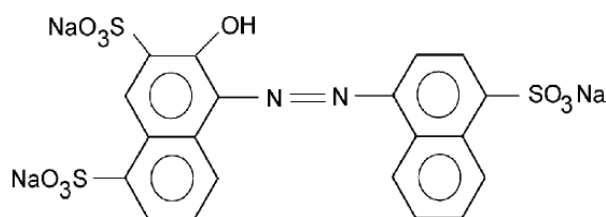


Figure 1. Chemical structure of the R2 used in this study.

Preparation of chitosan-cellulose hydrogel beads was performed according to the methodology described by Li and Bai [7] with minor modifications. 1 g of chitosan flakes was added to 50 mL of 0.4 M acetic acid in a beaker; this mixture was stirred in a hot plate at 70 °C and 250 rpm for 4 h. Additionally, 1 g of cellulose powder and 10 mL of 0.4 M acetic acid were added to the chitosan solution and the mixing was continued for another 5 h at room temperature. The final mixture was injected as droplets, using a 1 mL syringe (20 G needle) into a 1 M NaOH solution under agitation to form chitosan–cellulose hydrogel beads. Chitosan–cellulose beads were kept in the NaOH solution with slow stirring at room temperature for another 12 h for hardening and coarsening. The hardened beads were finally decanted from the NaOH solution and were washed with distilled water in a large beaker until the solution pH became the same as that of the fresh distilled water. The beads were then stored in distilled water for further use.

Chitosan–cellulose hydrogel beads were crosslinked with EGDE. Prior to crosslinking, the hydrogel beads were removed from distilled water and dried by placing them on filter paper. An equivalent volume of 7 mL of beads was suspended into 25 mL of distilled water in a beaker; the pH was adjusted to 12 by the addition of 0.1M NaOH solution. This mixture was placed in a two-neck flask, which was placed in a water bath with continuous agitation; this mixture was heated to 70 °C. Here, a 0.1 mL of EGDE solution was added to the flask and the crosslinking reaction was allowed to proceed at 70 °C for 6 h in a water bath with continuous agitation and nitrogen atmosphere. Finally, the mixture was cooled to room temperature and the crosslinked chitosan–cellulose hydrogel beads (CCHB) were washed with sufficient distilled water until the pH of the solution became the same as the fresh distilled water. The CCHBs were stored in high density polyethylene (HDPE) container with distilled water for further use.

Adsorption of R2 onto CCHB was studied in a batch mode. To determine the effect of contact time on the removal of R2 dye with CCHB, kinetic experiments were carried out by varying the contact time from 0 to 4320 min by triplicate under identical conditions into

a set of HDPE containers. Samples containing 30-50 mg of CCHBs and 10 mL of R2 solution (100 mg L^{-1}) were added without adjusting pH during the batch experiments (initial pH 5.7). HDPE containers were agitated on an orbit shaker (Unimax 1010 Heidolph) at 100 rpm and $20 \text{ }^\circ\text{C}$. Dye concentration, after adsorption experiments, was measured using a UV-Vis spectrophotometer (Lamda 35 Perkin Elmer) at the maximum absorbance wavelength of 520 nm. The amount of dye adsorbed q_t (mg g^{-1}) at time t , was calculated. In this study, the kinetic models of pseudo-first order (Lagergren) and pseudo-second order (Ho-McKay) were used to fit adsorption data.

Equilibrium studies were conducted at $20 \text{ }^\circ\text{C}$ for 24 h using 8 dye concentrations (5, 10, 20, 30, 40, 50, 60 y 70 mg L^{-1}) and q_e (mg g^{-1}) values were also calculated. Equilibrium experiments were identical to those of the kinetics tests. All q_e values represent the average of three independent experiments. Adsorption data were fitted to the Langmuir and Freundlich models.

RESULTS and DISCUSSION

Kinetic experiments. The dye adsorption capacity (adsorption uptake rate), q_t was calculated from the mass balance equation given by equation (1):

$$q_t = \frac{V(C_0 - C_e)}{m} \quad (1)$$

; where C_0 and C_e are the initial and final dye concentrations (mg L^{-1}) respectively, V is the volume of solutions (L), and m is the mass of adsorbent (mg) [9].

Data were modeled using both pseudo-first (Lagergren) and pseudo-second order (Ho-McKay) kinetic models. The pseudo-first order assumes that the rate of change is proportional to the amount of remaining unoccupied surfaces sites; in this study it was used the non-linearized equation (2):

$$q_t = q_e (1 - e^{-K_1 t}) \quad (2)$$

; where q_t and q_e are the adsorbed amounts (mg g^{-1}) at time t (min) and at equilibrium, respectively, and K_1 the Lagergren adsorption rate constant (min^{-1}) [10].

The pseudo-second-order model assumes the rate is proportional to the square of the number of remaining free surface sites [10]. The equation (3) is the non-linearized model:

$$q_t = \frac{K_2 q_e^2 t}{1 + K_2 q_e t} \quad (3)$$

; where K_2 is the pseudo-second-order adsorption rate constant ($\text{g mg}^{-1} \text{ min}^{-1}$). Parameters of kinetics models are presented in Table 1.

Table 1. Kinetics parameters for the adsorption of R2 onto CCHB.

Lagergren constants			Ho-McKay constants		
K_1 (min^{-1})	q_e (mg g^{-1})	R^2	K_2 ($\text{g mg}^{-1} \text{ min}^{-1}$)	q_e (mg g^{-1})	R^2
2.12E-3	43.1	0.964	5.81E-5	48.8	0.982

It can be seen from Figure 2 that adsorption equilibrium was reached at *ca.* 24 h and the maximum value of q_t reached was 47.2 mg g^{-1} . The kinetic model Ho-McKay fits well the experimental data; this supports the assumption that the rate-limiting step may be chemical adsorption or chemisorptions involving valency forces through sharing or exchange of electrons between sorbent and sorbate.

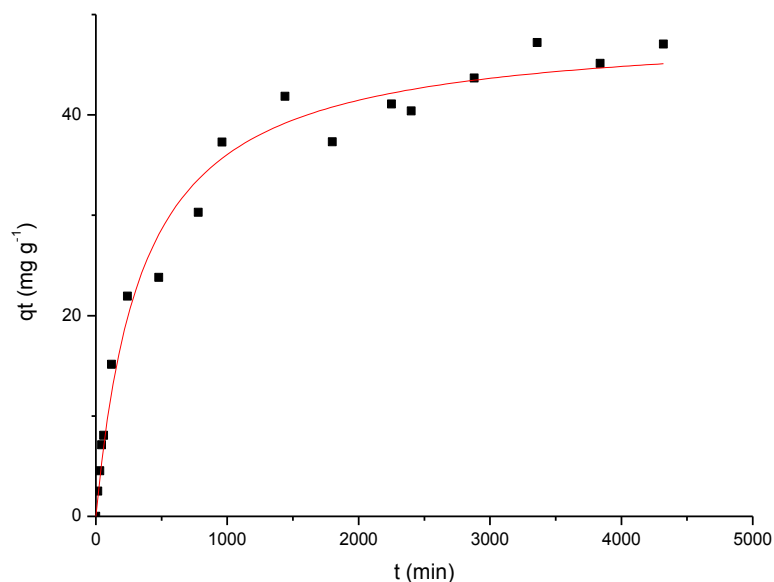


Figure 2. Kinetic data fitted to the Ho-McKay model.

Adsorption Isotherm. The distribution of dye between the liquid phase and the adsorbent is a measure of the equilibrium in the adsorption process and it can be generally expressed by two of the most popular isotherm theories; namely, the Freundlich and the Langmuir adsorption models.

The Langmuir model is adequate for monolayer sorption such that it considers the sorbent surface contains only one type of binding site and sorption of one ion per binding site [2]. Equation (4) is the non-linearized Langmuir model:

$$q_e = \frac{q_{emax}bC_e}{1+bC_e} \quad (4)$$

; where q_e is the amount adsorbed at equilibrium (mg g^{-1}), q_{emax} is the monolayer adsorption capacity (mg g^{-1}), b is the Langmuir constant related to adsorption energy (L mg^{-1}) and C_e the equilibrium concentration (mg L^{-1}).

The Freundlich model describes the heterogeneous surface energies by multilayer adsorption and it is expressed by equation (5):

$$q_e = K_F C_e^{1/n} \quad (5)$$

; where K_F indicates adsorption capacity ($\text{mg g}^{-1} \text{L}^{1/n} \text{mg}^{-1/n}$) and n empirical parameter related to the intensity of adsorption which varies with the heterogeneity of the adsorbent. The value n is always greater than 1; the exponent $1/n$ represents the intensity of adsorption and heterogeneity in a range between 0 and 1. The high n values for isotherms indicate relative uniformity at the surface, whereas low values suggest high adsorption at

low concentrations in solution. Furthermore, low values of n indicate the existence of a higher proportion of active sites with high energy [2].

Fitting parameters of the experimental data to the non-linearized isotherm models and calculated constant values are given in Table 2. Langmuir model fits better the experimental data than the Freundlich model. It is likely that the limiting step on the adsorption process is chemisorption on a set of well-defined localized sorption sites that have the same sorption energies independent of surface coverage and no interaction between adsorbed molecules.

Table 2. Model constants for the adsorption of R2 onto CCHB.

	Isotherm equation		
	Langmuir	Freundlich	
q_{emax} (mg g ⁻¹)	98.31	K_F (mg g ⁻¹ L ^{1/n} mg ^{-1/n})	40.74
b (L mg ⁻¹)	0.360	n	4.481
R^2	0.964	R^2	0.912

A plot of q_e versus C_e was obtained from non-linearized Langmuir model is shown in Figure 3.

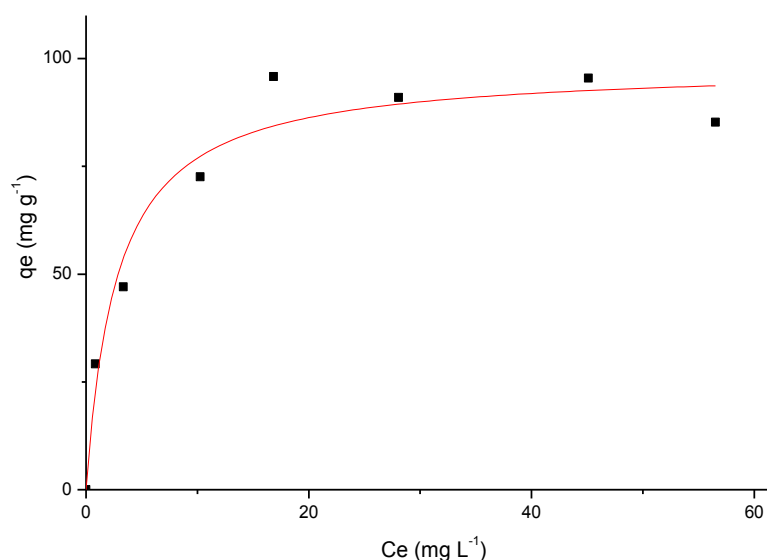


Figure 3. Non-linear Langmuir model for the adsorption of R2 onto CCHB.

CONCLUSION

Chitosan-cellulose hydrogel beads (CCHB) prepared in this work are suitable for R2 adsorption in a batch process from aqueous solutions at initial pH 5.7 and 20 °C. Kinetic experiments show that the adsorption equilibrium time was reached at 24 h and the data were well fitted to the Ho-McKay model (pseudo-second order) indicating that the adsorption process is governed by the surface reaction. Also, Langmuir model fitting confirms this behavior. On the other hand, the maximum adsorption capacity of R2 calculated using Langmuir model on CCHB is 98.31 mg g⁻¹.

ACKNOWLEDGEMENTS

The authors thank financial support of this work by PROMEP ITTOL-CA-1 2011-2012.

REFERENCES

- [1] Wan Ngah W.S., Teong L.C., M.A.K.M. Hanafiah M.A.K.M. (2011). Adsorption of dyes and heavy metal ions by chitosan composites: A review. *Carbohydr. Polym.*, 83, 1446–1456.
- [2] Crini G., Badot P.M. (2008). Application of chitosan, a natural aminopolysaccharide, for dye removal from aqueous solutions by adsorption processes using batch studies: A review of recent literature. *Prog. Polym. Sci.*, 33, 399–447.
- [3] Gong R., Ding Y., Li M., Yang C., Liu H., Sun Y. (2005). Utilization of powdered peanut hull as biosorbent for removal of anionic dyes from aqueous solution. *Dyes Pigments*, 64, 187-192.
- [4] Mouzdahir Y., Elmchaouri A., Mahboub R., Gil A., Korili S.A. (2010). Equilibrium modeling for the adsorption of methylene blue from aqueous solution on activated clay minerals. *Desalination*, 250, 335–338.
- [5] Huang X.Y., Bu H.T., Jiang G.B., Zeng M.H. (2011). Cross-linked succinyl chitosan as an adsorbent for the removal of methylene blue from aqueous solution. *Int. J. Biol. Macromol.*, 49, 643-651.
- [6] Koutsogeorgopoulou L., Maravelias C., Methenitou G., Koutselinis A. (1998). Immunological aspects of the common food colorants, amaranth and tartrazine. *Vet. Hum. Toxicol.*, 40, 1-4.
- [7] Li N., Bai R. (2005). Copper adsorption on chitosan–cellulose hydrogel beads: behaviors and mechanisms. *Sep. Purif. Technol.*, 42, 237-247.
- [8] Gong R., Sun Y., Chen J., Liu H., Yang C. (2005). Effect of chemical modification on dye adsorption capacity of peanut hull. *Dyes Pigments*, 67, 175-181.
- [9] Laus R., Costa T.G., Szpoganicz B., Fávere V.T. (2010). Adsorption and desorption of Cu(II), Cd(II) and Pb(II) ions using chitosan crosslinked with epichlorohydrin-triphosphate as the adsorbent. *J. Hazard. Mater.*, 183, 233-241.

RUBUS FRUTICOSUS SUSPENSION-CULTURED CELLS ELICITED WITH CHITOOLOGOSACCHARIDES PRODUCED FROM POLYMERIC CHITOSAN USING CHITOSANOLYTIC ENZYMES FROM SOLID STATE FERMENTATION

T. L. Honorato^{1*}, S. Rodrigues², N. E. El Gueddari³, B. M. Moerschbacher³, T. T. Franco¹

¹ FEQ, University of Campinas, Av. Albert Einstein, 500, 13083-852 Campinas-SP, Brazil.

² DETAL, Federal University of Ceará, Pici Campus, Bloco 858, P.O. Box 1268, 60021-970, Fortaleza-CE, Brazil.

³ IBBP, University of Muenster, Hindenburgplatz 55, Postal Code 48143, Muenster, Germany.

*E-mail address: talitalh83@gmail.com

ABSTRACT

The aim of this work was to develop a simple fermentation process yielding a chitosanolytic enzyme extract which can convert partially acetylated chitosan polymers into bioactive chitooligosaccharides (COS). Solid-state fermentation (SSF) of *Trichoderma polysporum* was performed with induction by shrimp shells. SSF crude enzyme extract was selected for further analysis due to the low complexity of its chitosanolytic activities. The resulting crude enzyme extract was analysed using SDS-PAGE followed by protein staining as well as semi-native PAGE and IEF followed by zymography using chitosans with different fractions of N-acetylglucosamine (F_A) as substrates. SSF extract catalysed the hydrolysis of three different chitosans with F_A of 0.15, 0.27, and 0.56, and the resulting COS were analysed by thin layer chromatography (TLC) and ESI-quadrupole-TOF-tandem-MS. Results showed that the SSF extract was dominated by chitobiase and/or N-acetylglucosaminidase with low but significant endo- and possibly exo-chitinase activity. *Rubus fruticosus* suspension-cultured cells elicited with COS reacted with a rapid and transient generation of H_2O_2 , with chitosan oligomers with F_A 0.56 being the most active ones.

Keywords

Chitooligosaccharides, Fungal enzymes, Solid-state fermentation, Chitosanases, Shrimp shells, Oxidative burst

INTRODUCTION

Chitin and its partially de-N-acetylated counterpart chitosan are among the most versatile and the most promising biomaterials. While the unique physico-chemical properties of chitosan polymers are typically exploited for applications in the material sciences, life science applications rely on specific biological functionalities of chitosan oligomers and food science and biotechnological applications often profit from both. Water-soluble chitooligosaccharides (COS) have been reported to have attractive biological activities, i.e., they induce apoptosis of tumour cells [1], have antioxidant activity, inhibit growth of fungi [2,3], elicit resistance against phytopathogens in crop plants, and promote plant growth in sustainable agricultural systems [4]. The biological activities of COS have been proposed to be governed by their degree of polymerisation

(DP), fractions of N-acetylglucosamine (F_A), and their patterns of acetylation (PA), and enzymatic methods of COS production, thus, appear to be promising [5]. Due to their selectivity, a given enzymatic process allows the generation of rather large amounts of a rather narrow spectrum of COS, thus reducing the costs of separation, provided a suitable enzyme substrate combination, can be found, which gives rise to the right mixture of COS exhibiting the desired biological functionalities. Therefore, enzymatic hydrolysis has become popular due to its low environmental impact, and high reproducibility of results [6].

In a screening of potentially suitable fungi, *Trichoderma polysporum* was identified as the most promising due to its good growth in SSF on shrimp shells (unpublished results of the authors). *Trichoderma* species are the most intensely studied biocontrol agents commercially available as biopesticides and biofertilizers for agriculture, and they are also employed to produce enzymes [7,8]. As entomopathogenic fungi, *Trichoderma* are known to synthesise a range of hydrolytic enzymes, including chitinases [7]. Some species are mycoparasites, invading and destroying fungal cells and then feeding on the dead cell contents, and chitinases have been found to be involved in cell wall hydrolysis during mycoparasitic attack. An unidentified chitinase is supposed to release oligomers from the host cell walls which then act as inducers of further chitinase formation [9].

The present study identified a microorganism suited for growth on Solid-State Fermentation (SSF) using abundantly available agro-industrial residues such as wheat bran and shrimp shells and to produce a mixture of chitosanolytic enzymes suitable for converting polymeric chitosans into potentially bioactive COS.

MATERIALS and METHODS

Microorganisms and inoculum preparation

T. polysporum was isolated by Embrapa Semi-Arido (Petrolina – PE, Brazil) as a biocontrol agent and kindly donated to our laboratory. The spore culture of *T. polysporum* was maintained in wheat bran at 4°C. Sterile 0.01% (v/v) Tween 80 solution (30 mL) was added to an Erlenmeyer flask containing the spore culture. The spores were counted in a haemocytometer (10^7 spores mL⁻¹).

Preparation of solid culture media

Shrimp shell waste from commercial shrimp farming operations in the state of Ceará, Brazil was used as a substrate. Prior to storage, the shells were washed with water and dried for 24 h at 60°C. Wheat bran was purchased from the local market (Mercado São Sebastião, Fortaleza – CE, Brazil).

T. polysporum was grown on a solid substrate containing 2 g wheat bran, 1 g shrimp shells, and 2.5 mL of a mineral medium (pH 5.5) containing 1 g L⁻¹ each of NaNO₃, (NH₄)₂HPO₄, MgSO₄·7H₂O and NaCl. Optimisation of the production of chitosanolytic enzymes by solid-state fermentation has already been studied [10]. The contents were then mixed thoroughly and incubated at 27°C for 72 h, statically for SSF.

Preparation of enzyme extracts

Enzymes were extracted from the fermented solid substrate by adding 20 mL of 200 mM acetate buffer (pH 5.5) to the flask and shaking at 27°C, 150 RPM, for 6 min. The enzyme extracts were then separated by filtration through analytical filter paper (70 mm) and then through 0.2 µm pore size Filtropur S (Sarstedt, Nümbrecht, Germany) syringe filters. The filtrates (enzyme extract) were concentrated in Vivaspin20 10,000 MWCO (Sartorius, Goettingen, Germany), desalted on prepacked Sephadex G-25 columns (PD-10,

Amersham Bioscience), equilibrated with 50 mM ammonium acetate buffer (pH 5.5) eluted with the same buffer, and stored in vials at 4°C.

Enzymatic hydrolysis

The enzyme extracts were incubated overnight at 37°C with 2 g L⁻¹ chitosans with three different F_A (commercial chitosan from Sigma F_A 0.15, chitosan F_A 0.27 with Mw 143.000 g mol⁻¹, and chitosan with F_A 0.56 with Mw 184.520 g mol⁻¹) in 50 mM ammonium acetate buffer (pH 5.5). Chitosans with F_A 0.27 and F_A 0.56 were prepared by acetylation of purified chitosan with F_A of 1.5 from Mahtani Chitosan Pvt. Ltd. (India). Each hydrolysate was mixed with a solution of ethanol/ammonia (7:3, v/v) at a 1:3 (v/v) ratio. The precipitated fraction was discarded and the supernatant was freeze-dried and then resuspended in distilled water.

Thin layer chromatography

Aliquots of hydrolysates were applied on silica gel 60 thin-layer chromatography (TLC) plates (Merck Co., Berlin, Germany) using *n*-butanol–methanol–25% ammonia solution–water (5:4:2:1, v/v/v/v) as a solvent system. The plates were sprayed with aniline-diphenylamine reagent (4 ml of aniline, 4 g of diphenylamine, 200 ml of acetone, and 30 ml of 85% phosphoric acid) to see the oligomers and spots developed by heating at 180°C for 3 min. The R_f of the samples was compared with R_f of authentic N-acetylglucosamine (degree of polymerisation, DP, 1, 3, 4, 5, 6) and D-glucosamine (DP 1 to 6) from Seikagaku Corporation patterns (Japan).

Mass Spectrometry

Nano electrospray quadrupole time-of-flight tandem mass spectrometry (nanoESI-Q-ToF-MS/MS) experiments were carried out with a quadrupole time-of-flight (Q-TOF) mass spectrometer (Micromass, Manchester, UK) in the positive ion mode. The QTOF mass spectrometer was interfaced to a personal computer running MassLynx software to control the instrument and to acquire and process the mass spectra. Gas-phase ions were generated from solutions containing approximately 7.5 pmol μL⁻¹ of the freeze-dried hydrolysate dissolved in water/methanol/formic acid (49/49/2, v/v/v) by nanoESI in the positive ion mode using a Z-spray source. Typical source parameters were as follows: a source temperature of 80 °C, a desolvation gas (N₂) flow rate of 75 L h⁻¹, a capillary voltage potential of 1.1 kV, and a cone voltage of 40 V.

Oxidative burst measurement in cell cultures

Aliquots of 300 mg of Blackberry (*Rubus fruticosus*) cells were suspended in 5 mL pre-incubation medium (3% sucrose (w/v) and 10 mM MES in 5% (v/v) MS medium supplemented with 2,4-D and sucrose (pH 5.8) as described by Ortmann et al. [11]) in a six-well plate and incubated under culture conditions for 5 h. Oxidative burst was determined by a method based on H₂O₂-dependent luminol chemiluminescence in accordance with Warm and Laties [12] using a luminometer (Lumat LB 9501 Berthold). The micromolar (μM) H₂O₂ concentration was determined using a standard calibration curve.

RESULTS and DISCUSSION

The crude SSF enzyme extract was incubated with polymeric chitosans with different F_A values, namely F_A 0.15, 0.27, and 0.56, and the resulting oligomeric products were analysed using TLC (Figure 1). As expected, and corroborating the presence of chitinases rather than chitosanases, the DP of the products decreased with increasing F_A of the

substrate. The major products of the most highly acetylated chitosan were from monomers to trimers, while the chitosan with a medium F_A was mostly from dimers to hexamers. In contrast, the chitosan with the lowest F_A gave rise to a broad range of oligomers with DPs ranging from one to more than six.

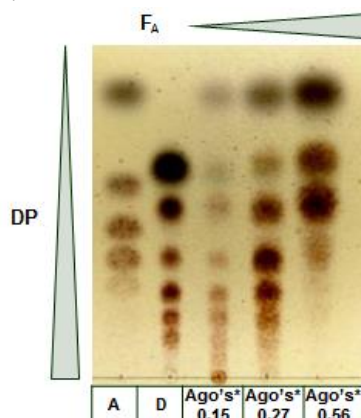


Figure 1. TLC analysis of chitosan oligomer profile produced by hydrolysis of chitosans with F_A of 0.15, 0.27, and 0.56 by SSF enzyme extract. Standards are listed from top to bottom: (A) N-acetylglucosamine standards DP 1, 3, 4, 5, and 6; (D) glucosamine standards DP 1, 2, 3, 4, 5, and 6; (Ago's) Chitosan oligomers.

Similar results were reported by de Assis et al. [13], who found a small concentration of acetylated dimeric to pentameric products when hydrolysing chitosan with F_A 0.15 using an SF enzyme extract of *Metarhizium anisopliae*, and by Sørbotten et al. [14], who found higher oligomer lengths for substrates with lower F_A values in the degradation of chitosans with varying degrees of acetylation by bacterial chitinase from *Serratia marcescens* overexpressed in *Escherichia coli*.

The compositions of the oligosaccharide mixtures were further analysed using ESI-QTOF-MS (Table 1), corroborating the trend of higher DP oligomers resulting from lower F_A polymers and thus the presence of chitinases rather than chitosanases.

Table 1. Chitosan oligomer profile* produced by hydrolysis of chitosans with different F_A using the SSF enzyme extract, identified by ESI-QTOF-MS.

F_A of substrate	DP of products						
	1	2	3	4	5	6	7
0.15	D ₁ (A ₁)	D₂	D₃ D ₁ A ₂ D ₂ A ₁	D₄ D ₁ A ₃ D ₂ A ₂ D ₃ A ₁	D₅ D ₄ A ₁ (D ₃ A ₂)	(D ₆) (D ₅ A ₁) (D ₄ A ₂)	(D ₅ A ₂)
0.27		(D ₂) (D ₁ A ₁)	D ₃ D ₁ A ₂ D₂A₁	D ₄ (D ₁ A ₃) D₂A₂ D₃A₁	(D ₅) D₄A₁ D₃A₂ (D ₂ A ₃)	(D ₅ A ₁) (D ₄ A ₂) (D ₃ A ₃)	
0.56	(A ₁)	(D ₂) D ₁ A ₁	D₁A₂ D₂A₁ (A ₃)	(D ₁ A ₃) D ₂ A ₂ (D ₃ A ₁) (A ₄)	(D ₁ A ₄) (D ₃ A ₂)		

*major products are given in bold, products present in trace amounts only are given in parentheses.

Trimers (D₂A₁, D₁A₂) were found to be the most abundant products in the hydrolysate derived from chitosan with a F_A of 0.56, but dimer (D₁A₁) and tetramer (D₂A₂) as well as traces of other small oligomers were also present. A trimer (D₂A₁), two tetramers (D₃A₁, D₂A₂), and two pentamers (D₄A₁, D₃A₂) were the most abundant oligomers in the chitosan hydrolysate with F_A 0.27, and traces of oligomers with DP from

2 to 6 were also seen. Only the chitosan with F_A 0.15 yielded products of DP 7 (D_5A_2), but the most abundant COS in this material were two trimers (D_3 , D_1A_2), a tetramer (D_4), and a pentamer (D_5).

The complete absence of the fully acetylated dimer, which would be expected to occur more abundantly than the larger fully acetylated chitin oligomers, corroborates the presence of chitobiase, and the near absence of other fully acetylated oligomers indicates the presence of low N-acetylglucosaminidase activities. This enzyme is most likely also responsible for the presence of fully deacetylated oligomers, which probably result from partial digestion of the products of a chitinase cleaving the glycosidic linkage between a deacetylated and an acetylated unit [15]. Such a cleavage would yield oligomers with a glucosamine unit at the reducing end and an N-acetylglucosamine unit at the non-reducing end, which can then be removed by the action of the N-acetylglucosaminidase. The alternative explanation for the occurrence of the fully deacetylated oligomer products, namely the action of a chitosanase cleaving the glycosidic linkage between two deacetylated glucosamine units, is highly unlikely given that such an enzyme would most likely also break down the larger glucosamine oligomers into dimers and trimers [2]. The presence of these fully deacetylated oligomers also proves the absence of a glucosaminidase. None of the major products contain more than two acetylated units and almost all of them contain more deacetylated than acetylated units. Most likely, none of the major products contain two adjacent acetylated units, which would be the preferred cleavage site of chitinases.

When cells of *R. fruticosus* were treated with COS ($10 \mu\text{g mL}^{-1}$), an oxidative burst response was induced, as shown in Figure 2. H_2O_2 production reached a peak value in the first 7-14 min of reaction and after this period the generation of H_2O_2 decreased progressively. The chitosan oligomer-induced burst was slightly increased by treatments with chitosan oligomers with F_A 0.56, but the oxidative burst kinetics were not significantly different from those induced by chitosan oligomers with F_A 0.15 and 0.27. The rapid and transient production of huge amounts of reactive oxygen species, the so-called oxidative burst, is one of the earliest reactions of plant cells against pathogen attack [4]. It has been shown previously that chitosan oligomers generated by partial chemical N-acetylation and, thus, random PA can induce an oxidative burst in plant cells [16].

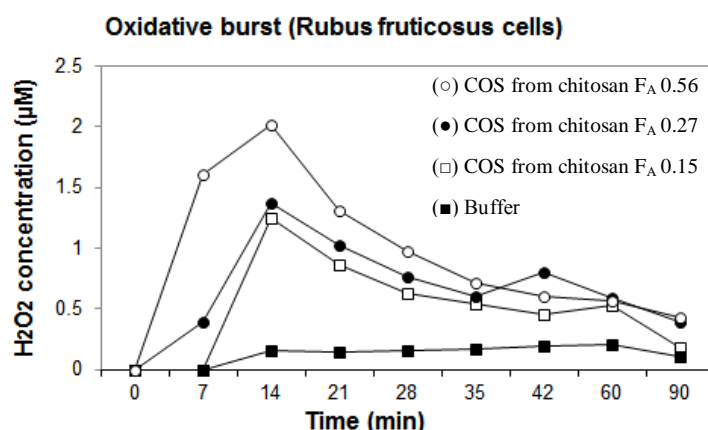


Figure 2. Time-response curves of H_2O_2 generation by suspension-cultured cells of *R. fruticosus* elicited with chitosan oligosaccharides F_A 0.15, 0.27, and 0.56 at a concentration of $10 \mu\text{g mL}^{-1}$.

Here, COS produced enzymatically and, thus, presumably with a non-random PA, are also elicitor active. It has been suggested that this action could be due to physico-chemical interaction between the positively charged COS and the negatively charged cell membrane [19] or to receptor-mediated recognition [20]. Therefore, more experimental

verifications must be performed in suspension-cultured cells of dicot and monocot angiosperm species with elicitors with different features and concentrations.

ACKNOWLEDGEMENTS

Financial support by FAPESP, CNPq, Capes, DAAD and EU through their PolyModE and NanoBioSaccharides projects is gratefully acknowledged.

REFERENCES

- [1] Liang, T.W., Chen, Y.J., Yen, Y.H., Wang, S.L. (2007). The antitumor activity of the hydrolysates of chitinous materials hydrolyzed by crude enzyme from *Bacillus amyloliquefaciens* V656. *Process Biochem* 42 (4):527-534.
- [2] Aam, B.B., Heggset, E.B., Norberg, A.L., Sørli, M., Vårum, K.M., Eijsink, V.G.H. (2010). Production of chitooligosaccharides and their potential applications in medicine. *Marine Drugs* 8 (5):1482-1517.
- [3] Oliveira, E.N., El Gueddari, N.E., Moerschbacher, B.M., Peter, M.G., Franco, T.T. (2008). Growth of phytopathogenic fungi in the presence of partially acetylated chitooligosaccharides. *Mycopathologia* 166 (3):163-174
- [4] Moerschbacher, B.M. (2005). In: *Emerging Trends in Plant-Microbe Interactions*. Madras, Chennai, 186-190.
- [5] El Gueddari, N., Schaaf, A., Kohlhoff, M., Gorzelanny, C., Schneider, S., Moerschbacher, B.M. (2007) In *Advances in Chitin Science 10*: 119-126, Antalya, Turkey.
- [6] Binod, P., Sandhya, C., Suma, P., Szakacs, G., Pandey, A. (2007). *Bioresour Technol* 98 (14):2742-2748.
- [7] Archer, D.B., Wood, D.A. (1994). Fungal Exoenzymes. *The Growing Fungus*. In: Gow NAR, Gadd GM (eds). Springer Netherlands, pp 137-162.
- [8] Harman, G.E., Howell, C.R., Viterbo, A., Chet, I., Lorito, M. (2004). *Trichoderma* species - Opportunistic, avirulent plant symbionts. *Nat Rev Microbiol* 2 (1):43-56.
- [9] Seidl, V. (2008). Chitinases of filamentous fungi: a large group of diverse proteins with multiple physiological functions. *Fungal Biology Reviews* 22 (1):36-42.
- [10] da Silva, L.C.A., Honorato, T.L., Franco, T.T., Rodrigues, S. (2012). Optimization of Chitosanase Production by *Trichoderma koningii* sp Under Solid-State Fermentation. *Food Bioprocess Tech* 5 (5):1564-1572.
- [11] Ortmann, I., Conrath, U., Moerschbacher, B.M. (2006). Exopolysaccharides of *Pantoea agglomerans* have different priming and eliciting activities in suspension-cultured cells of monocots and dicots. *FEBS Letters*, 580:4491-4.
- [12] Warm, E., Laties, G. (1982). Quantification of hydrogen peroxide in plant extracts by the chemiluminescence reaction with luminol. *Phytochemistry*, 21:827-31.
- [13] De Assis, C.F., Araújo, N.K., Pagnoncelli, M.G.B., Da Silva Pedrini, M.R., De Macedo, G.R., Dos Santos, E.S. (2010). Chitooligosaccharides enzymatic production by *Metarhizium anisopliae*. *Bioprocess and Biosystems Engineering* 33 (7):893-899.
- [14] Sørbotten, A., Horn, S.J., Eijsink, V.G.H., Vårum, K.M. (2005). Degradation of chitosans with chitinase B from *Serratia marcescens*: Production of chito-oligosaccharides and insight into enzyme processivity. *Febs J* 272 (2):538-549.
- [15] Yong, Z., Wan-Taek, J., Ro-Dong, P. (2010). Enzymatic Modifications of Chitin and Chitosan. In: *Chitin, Chitosan, Oligosaccharides and Their Derivatives*. CRC Press, pp 185-192.
- [16] Santos, A., El Gueddari, N., Moerschbacher, B.M. (2008). Partially Acetylated Chitosan Oligo- and Polymers Induce an Oxidative Burst in Suspension Cultured Cells of the Gymnosperm *Araucaria angustifolia*. *Biomacromolecules*, 9:3411-15.
- [17] Kauss, H., Jeblick, W., Domard, A. (1989). The degrees of polymerization and N-acetylation of chitosan determine its ability to elicit callose formation in suspension cells and protoplasts of *Catharanthus roseus*. *Planta*, 178:385-92.
- [18] Silipo, A., Erbs, G., Shinya, T., Dow, J.M., Parrilli, M., Lanzetta, R., Shibuya, N., Newman, M.A., Molinaro, A. (2010). Glyco-conjugates as elicitors or suppressors of plant innate immunity. *Glycobiology* 20 (4):406-419.

Characterization of a new H₂S chitosan intelligent sensor and study of the influence of moisture content

E.T. KATO JR.¹, E. Guibal³, C.M.P. Yoshida^{2*} and T.T. Franco¹

¹ School of Chemical Engineering –State of University of Campinas, UNICAMP, CEP13083-852, Campinas – SP, Brazil.

² Federal University of São Paulo-UNIFESP, Department of Exact and Earth Science, Av. Prof. Arthur Riedel, 275, CEP 09972-270, Diadema – SP, Brazil.

³ Laboratoire Génie de l'Environnement Industriel, Ecole des Mines d'Alès, 6 avenue de Clavières, 30319 Alès cedex, France.

*E-mail address: cristiana.yoshida@unifesp.br

ABSTRACT

A new, biodegradable, fast, simple manufacturing and colorimetric indicator of hydrogen sulfide gas (H₂S) was developed combining chitosan as tridimensional biopolymer matrix and a non toxic colorimetric indicator. Card paper sheets were coated adapted from Kato *et al.*^[1] with chitosan suspension (2.0%, w/w) containing the colorimetric indicator (0.25%, w/w). The water sensibility of the intelligent sensor was characterized by adsorption isotherms and water absorption capacity (Cobb Test). After different relative humidity conditions exposition, the samples were exposed to hydrogen sulfide gas (100 ppm) in a closed gas chamber to evaluated the colour variation. The mechanical properties (Young's modulus, fracture strain, stretching, traction resistance and resistance to bending results indicated that the intelligent sensor presented similar characteristics as compared to the cardpaper. In a range of 10% to 100% of RH, the sensor changes the colour with the same intensity at different times, indicating that the humidity influenced in the time response. Chitosan sensor is characterized by reversibility of color indication. A quantitative analysis study showed that the chitosan matrix keep an important amount of sulfur compounds (67,8% of the concentration after the first exposure). Despite of the presence of this sulfur compounds the chitosan matrix of the intelligent sensor it remain workable. This work is innovative and has derived in a patent request deposited at the INPI (2009) and the Patent Cooperation Treaty (PCT-2010).

Keywords

Chitosan, H₂S sensor, colourimetric, hydrogen sulfide gas.

INTRODUCTION

Chitosan is a polysaccharide derived from chitin by removing the acetyl groups with alkali. Chitin is very abundant in nature, as it found in fungal walls and the exoskeletons of crustaceans and insects^[2]. Chitosan is an excellent film-forming linear polymer with a backbone consisting of β -(1-4)- 2-acetamido-2-deoxy-D-glucose (N-acetyl glucosamine - GlcNAc) residues and glucosamine residues (GlcN). It is characterised by the degree of acetylation (DA) and the average molecular weight (MW), among other properties, e.g. degree of polymerization^[3]. Chitosan has a low toxicity and is biodegradable. Also,

depending on its molecular structure, size and concentration, may inhibit the growth of fungi, bacteria and yeasts^[4].

The association of chitosan to paper sheets provides interesting functionalities and maintains the environment-friendly characteristic of the material. Chitosan associated with cellulose have been studied as additive on paper production and paper surface treatment by decades. This combination increases the mechanical resistance and improves the color retention of the cardpaper^{[5][6][7]}. The printability increases with the chitosan addition^[8], possible due to the reduction of water absorptiveness.

Hydrogen sulfide (H₂S) is a flammable and colorless gas with a sweetish taste and characteristic odor of rotten eggs that can be poisonous at high concentrations.

An hydrogen sulfide (H₂S) indicator system was characterized in this study. This system detects and indicates the presence of hydrogen sulfide (H₂S). This indicator system has wide application, since applications in control of leaks in the petrochemical industry communicating the presence of H₂S in case of leaks in the line of recovery in critical points (joints, valves, connections, etc.), even in quality control of food products informing the consumer a potential microbiological changes in the product during transportation and storage, indicating the state of product freshness.

Objectives

The aim of this work was to investigate the influence of humidity on the efficiency response, tensile properties and water absorption of the H₂S indicator system.

MATERIALS and METHODS

Materials

Commercial chitosan used in this study was provided by Primex (Island), obtained from the exoskeleton of coldwater shrimps with a DA of 18 % and a molecular weight, MW, of $2.38 \times 10^5 \text{ g mol}^{-1}$ (dn/dc of 0.135 mL.g^{-1}) and polydispersivity of 2.89. Glacial acetic acid (Synth – Brazil), iron(II) sulphate heptahydrate (Sigma – Germany; 99 +%), ferrous sulphide (Synth – Brazil; 25 %), sodium carbonate (Synth – Brazil, 99 +%) and card paper (Triplex TP 250) (250 g m^{-2} , Suzano Papel e Celulose, Brazil) were also used.

Methods

Chitosan sensor production

The methodology of the film suspension producing was adapted from Yoshida *et al.*^[9]. Chitosan (3.0%, w/w) was dispersed in aqueous acetic acid. The dispersions were homogenized by magnetic stirring at room temperature for 60 minutes until complete dissolution. After the FeSO₄ aqueous solution (1.5%) was added and the chitosan suspension was supplemented to 100g. The sheets of cardboard were coated with aliquots of 2.0g of the chitosan film suspensions according to the methodology described by Kato *et al.*^[11].

Cardboard sheets (0.045m^2) were previously superficially impregnated with 3mL of sodium carbonate (Na_2CO_3) solution (4%, w/w).

Mechanical characterization

The stiffness and tensile properties (mean force, elongation, tensile energy absorption, tensile strength, breaking length and tensile index) of the indicator system was measured in accordance with the ASTM^[10] standard method. The samples were cut in both directions: machine direction (MD) and cross-machine direction (CMD).

Water absorption (COBB TEST)

Water absorption capacity was determined in accordance with standard T441om-90.^[11] The weight gain was measured using Mettler AE 163 analytical scales.

Sorption Isotherms

Adsorption isotherms were determined following procedure adapted from the COST 90 Project^[12]. The samples were cut (squares of 3 mm) and dried over silica in a desiccator during at least 7 days. Approximately 1g of each samples were weighted and placed in hermetic chambers containing saturated salt solutions with different water activity (a_w): 0.11 (LiCl), 0.33 (MgCl_2), 0.43 (K_2CO_3), 0.54 ($\text{Mg}(\text{NO}_3)_2$), 0.59 (NaBr), 0.76 (NaCl), 0.85 (KCl), 0.90 (BaCl_2), 0.94 (CuSO_4) at temperature of $25 \pm 2^\circ\text{C}$. The initial moisture content of each samples was measured in triplicate on dry basis by drying in an oven with renewal and air circulation (Mod TE-394/2, TECNAL, Brazil) at 105°C until constant weight^[13]. Equilibrium moisture content of the films was measured in triplicate. Isotherms models (GAB, BET, HALSEY, HENDERSON and OSWIN)^[14] were used for fitting the sorption data. Equations parameters were estimated by non linear regression (Statistic version 5.1) in terms of regression coefficient (R^2) values.

Scanning electron microscopy with X-ray energy dispersive spectrometer (SEM-EDS)

SEM-EDS determinations were performed at the *Centre de Recherche Louis Leprince-Ringuet – Laboratoire de Génie de l'Environnement Industriel* with cooperation of *Centre des Matériaux de Grande Diffusion – CMGD (École des Mines d'Alès – France)*. The instrument was a Quanta 200 FEG (FEI Company) operated at 15 kV and 0.60 torr equipped a backscattered electrons detector (BSE) integrated into an X-ray energy dispersive spectrometer (INCA Energy 350 – Oxford Instruments). Samples of the colorimetric sensor with about 10x10 mm in size were cut from the central part and mounted on SEM aluminium stubs using double-sided carbon tape. EDS spectra (working distance 10 mm) were collected for 50 s and the elemental composition obtained.

Evaluation of humidity influence on the efficiency of H₂S indicator system response

The samples were stored in desiccators with controlled relative humidity of 54% (Mg(NO₃)₂) 85% (KCl) and 100% humidity until the equilibrium were reached. The samples were exposed to H₂S gas (74.5 ppm) in a closed system, to determine the influence of moisture content in the time of detection of the gas in function of the concentration of indicator in the chitosan matrix. Initially, vacuum was made in the reactor system (230 mL) and after it was reached (-600 mmHg) the H₂S gas was introduced into the system and starts the counting of time until a color change from yellow to black was noted.

Statistical analyses

Statistical analyses were carried out with the Statistic version 5.0 program (Statistic Inc., USA). Differences between the means were detected using a multiple comparison Tukey test.

RESULTS and DISCUSSION

The H₂S indicator system presents a slightly continuous and homogeneous yellow color. Mechanical characterization is an important property of materials that measures the ability to resist the process of production. The values obtained for both directions of the cardpaper (MD and CMD) of stiffness are shown in Table 1.

Table 1. Stiffness (g.cm) of H₂S indicator system and uncoated card paper.

Sample	CMD				MD			
	R	L	Bending moment (g.cm)	Bending moment (mN.m)	R	L	Bending moment (g.cm)	Bending moment (mN.m)
Uncoated Card paper	60±3.12 ^a	84.5±2.85 ^b	72.25±2.19 ^d	7.09±0.21 ^f	135±4.32 ^a	172±3.39 ^c	153.33±3.30 ^e	15±0.34 ^g
Intelligent sensor	65±8.88 ^a	94±6.70 ^c	79.48±2.79 ^e	7.80±0.30 ^g	140±7.19 ^b	187±6.43 ^d	163.44±4.89 ^f	16.18±0.29 ^h

a-h: different letters in the same column are statistically different with 95% of confidence. Tukey's test $p < 0,05$.

The bending moment in the CMD of intelligent sensor showed an increase from 72.25 to 79.48 g.cm, on direction MD showed an increase from 153.33 to 163.44 g.cm, when compared with the uncoated card paper. According to Rhim and Kim^[15] the stiffness of card paper increased with a PLA coating. Samyn et al.^[16] reported that card paper coated with styrene maleic anhydride (SMA) had stiffness similar to uncoated card paper and Reis et al.^[17] reported that Kraft paper coated with chitosan emulsion film presented lower stiffness than uncoated Kraft paper. The mechanical properties remained almost unchanged, according to Bordenave et al.^[18] the system chitosan/cellulose was modified by the introduction of chitosan, but the cellulose fibers network still drive the mechanical behavior of the materials, i.e. the amount of chitosan was not enough to disturb the interactions between the potentially negatively charged cellulose fibers.

Table 2. Mechanical properties and Water absorptiveness of H₂S indicator and uncoated card paper.

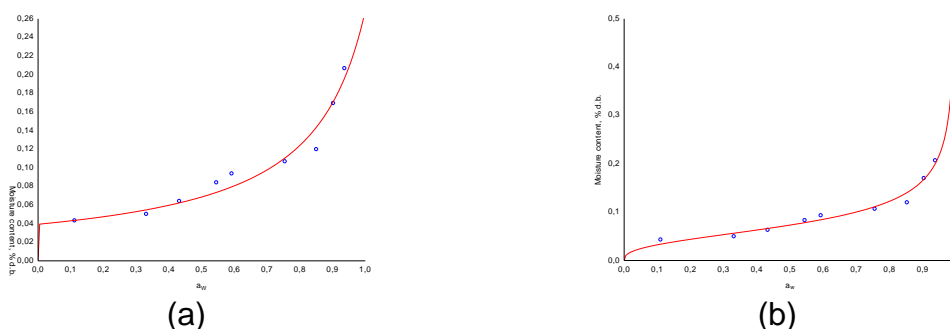
Sample		Mean force (N)	Elongation (%)	Tensile energy absorption (J.m ⁻²)	Tensile strength (kN.m ⁻¹)	Breaking length (km)	Tensile index (kN.m.kg ⁻¹)	Absorption (g/m ²)
Intelligent (MD)	sensor	244.53±4.37	3.69	368.21	16.30	6.65	2.65	100,75±3,10
Intelligent (CMD)	sensor	135.82±2.85	7.04	446.38	9.22	3.76	0.79	
Uncoated paper (MD)	card	236.31±7.47	3.55	342.75	15.75	6.43	2.66	54,09±20,37
Uncoated paper (CMD)	card	138.25±3.65	7.11	440.78	9.05	3.69	0.76	

In agreement with Samyn et al.^[16] and Kibirštis & Kabelkaitė^[19] the mean force in MD is higher compared to CMD due to anisotropy of the paper. Reis et al.^[17] reported that the mechanical properties of chitosan coated kraft paper remained almost unchanged with a 13.3 % reduction in the the elongation

The water absorption was determined for the H₂S indicator system and uncoated card paper (Table 2). In cellulosic materials, water absorption depends on the type of cellulose and the coating material^[17]. The water absorptiveness was increased with the biopolymer coating when compared with the uncoated card paper. The same result was observed by Rhim, Lee & Hong^[20], which was associated to hydrophilicity of the chitosan. Reis et al.^[17] reported a reduction in water absorption by up to 35% even using chitosan as coating.

Sorption Isotherms

Sorption isotherms were obtained at 25°C, GAB and Oswin models (Figure 1) were best fit to the experimental data of sorption.

**Figure 1** - Sorption isotherm of the H₂S indicator system at 25°C (a) GAB and (b) Oswin.

The GAB and Oswin models showed higher values of R² and explained variance in relation to other models. It also follows that the H₂S indicator system presents a behavior similar to the cardpaper, i.e. their sorption isotherms exhibit the same profile as the isotherms of the uncoated paperboard.

Evaluation of humidity influence on the efficiency response of the H₂S indicator

The distribution of the adsorbed specie Fe³⁺ in the chitosan matrix was performed for the H₂S indicator system, Figure 2 shows (a) a SEM image and (b) a BSE image of the H₂S indicator system.

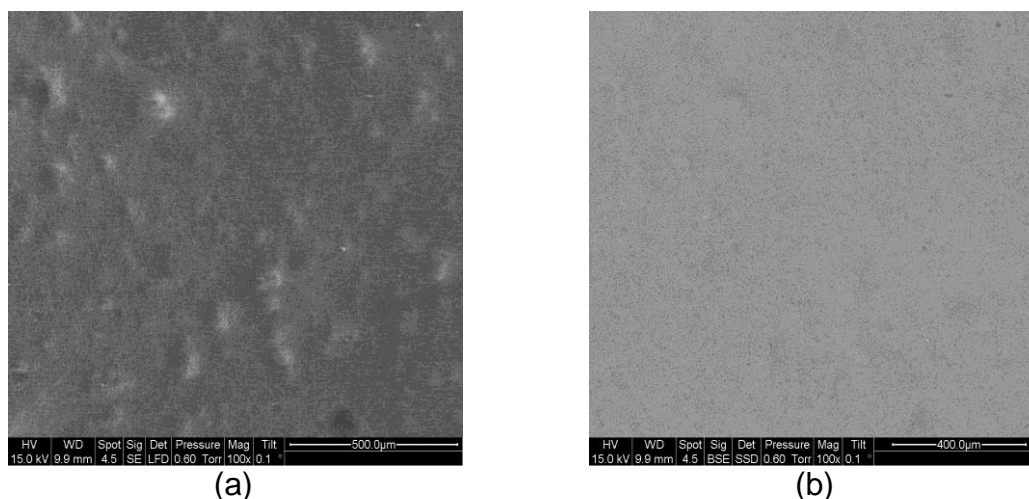


Figure 2 – SEM image of the H₂S indicator system, (a) SEM image and (b) BSE image

In the phase image (Figure 2b) is noticed the well distribution of the Fe³⁺ ions, i.e. areas of Fe³⁺ concentration, represented by white spots are not observed.

In Figure 3 the column represents a different concentration of the colorimetric indicator in the chitosan matrix. The moisture content acts as a facilitator in the indication of the presence of H₂S gas. Independent of the concentration of the H₂S indicator added to the chitosan matrix an increase in humidity decreases the time of detection of H₂S gas. It was possibly due to swelling of the chitosan polymer matrix thereby facilitating H₂S gas inlet and the subsequent interaction with the colorimetric indicator.

After a short period of absence of the H₂S gas the H₂S indicator system return to its original color (yellow), due to this reversibility a quantitative analysis were performed to evaluate the presence of sulfur compounds, the quantitative results of the EDS analysis showed that after 2 months of no contact with the H₂S gas, i.e. after the H₂S indicator system turn-back to its original colour (yellow), almost 87% of the concentration of sulfur content detected after the first exposure to the gas remains in the chitosan matrix. Even with this high concentration of sulfur contend in the H₂S indicator system, it remain functional, i.e. once exposed to a H₂S gas source it become black indicating the H₂S gas presence.

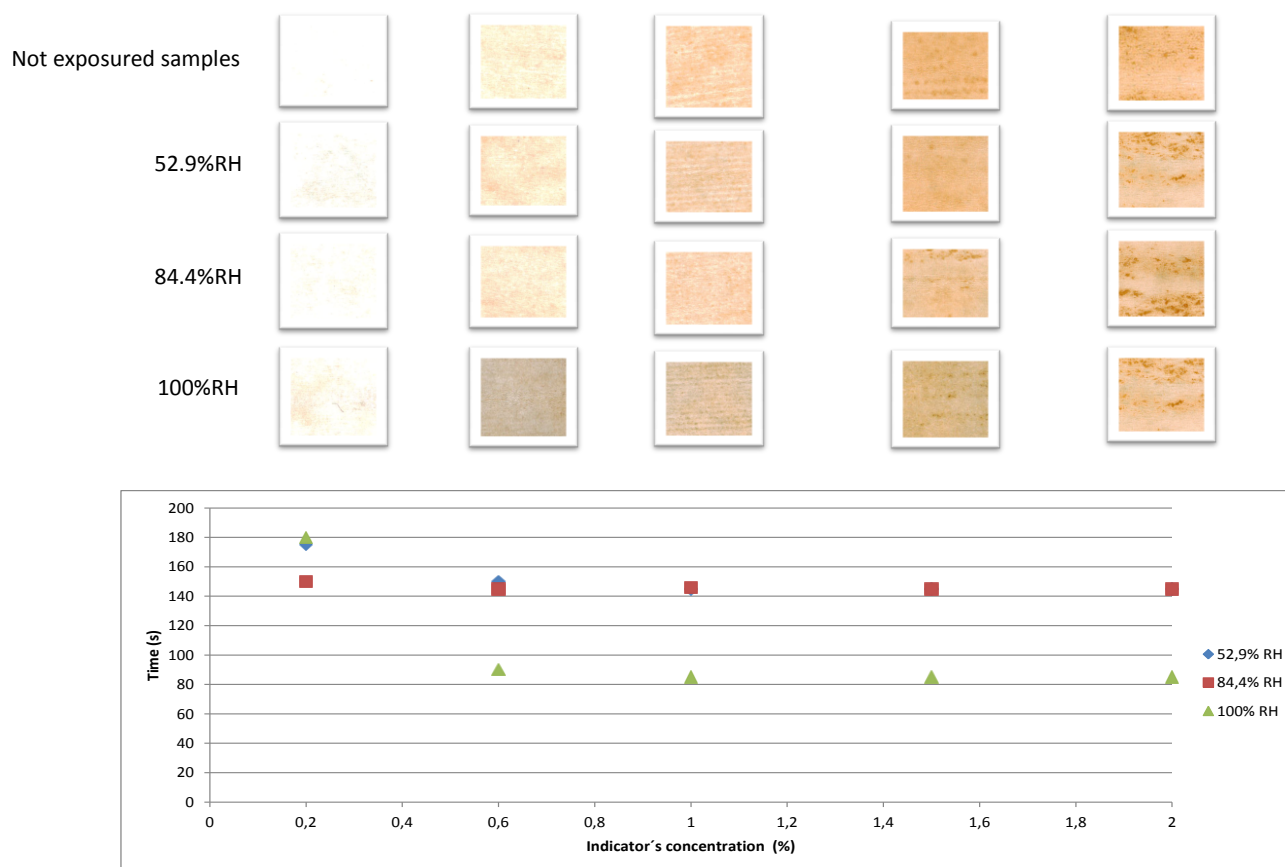


Figure 3 - Effect of moisture content in function of the concentration of the indicator in the H₂S indicator system response.

CONCLUSIONS

The H₂S indicator system changes the colour with the same intensity at the different times according to the RH, indicating that the humidity influenced in the time response. It was probably due to the swelling of the chitosan matrix facilitating the interaction between the H₂S gas and the iron entrapped in the chitosan matrix. Despite of the presence of this sulfur compounds the chitosan matrix of the intelligent sensor it remain workable, i.e. with a novel contact with H₂S gas the H₂S indicator system turn black indicating its presence. The application of chitosan suspension coating on the production of H₂S indicator system lead to an increase in stiffness compared with the uncoated card paper and the tensile properties did not change. The water absorptiveness increased almost 100% compared to uncoated card paper it was associated with the hydrophilicity of the polymer matrix. The distribution of metal ions (Fe³⁺) in the chitosan matrix was homogeneous.

ACKNOWLEDGEMENTS

This work was financially supported by FAPESP, CNPq and CAPES. The authors thank Primex for providing the chitosan samples.

REFERENCES

- [1]Kato Junior, E.T.; Yoshida, C.M.P.; Reis, A.B.; Melo I.S. and Franco, T.T., 2011. Fast detection of H₂S using a biodegradable colorimetric indicator system, *Polymer International*, v.60, Issue 6. (Article first published online : 2 MAY 2011, DOI: 10.1002/pi.3095).
- [2]Peter, M.G. *CHITIN AND CHITOSAN FROM FUNGI*, in: A. Steinbüchel (Ed.), *Biopolymers*, Vol. 6: Polysaccharides II , Weinheim: *Wiley-VCH*, 2002, pp. 123 - 157 (ISBN 3-527-30227-1).
- [3]Muzzarelli R.A.A. CHITOSAN-BASED DIETARY FOODS, *Carbohydr. Polym.*, 29: 306-316, 1996.
- [4]Tikhonov V.E, Stepnova EA, Babak VG, Yamskov IA, Palma-Guerrero J, Jansson H-B, Lopez-Llorca LV, Salinas J, Gerasimenko DV, Avdienko ID and Varlamov VP, BACTERICIDAL AND ANTIFUNGAL ACTIVITIES OF A LOW MOLECULAR WEIGHT CHITOSAN AND ITS N-2(3)-(DODEC-2-ENYL)SUCCINOYL-DERIVATIVES. *Carbohydrate Polymers*. Vol. 64. Pp. 66-72, 2006.
- [5]Allan,G.G.,Carroll, J. P.,Hirabayashi,Y.,Muvundamina,M.,&Winterown, J. G. CHITOSAN-COATED FIBERS ADVANCES IN CHITIN AND CHITOSAN, *Proceedings of international conference, fourth*, pp. 765–76, 1989.
- [6]Makino, Y., & Hirata, T. MODIFIED ATMOSPHERE PACKAGING OF FRESH PRODUCE WITH A BIODEGRADABLE LAMINATE OF CHITOSAN–CELLULOSE AND POLYCAPROLACTONE. *Postharvest Biology and Technology*, 10, 247–254, 1997.
- [7]Struszczyk, H. & Kivekäs, O. (1990). MICROCRYSTALLINE CHITOSAN - SOME AREAS OF APPLICATION. *British Polymer Journal*, 23, 261–265. *Technologies*, v.6, n.4, p.459-464, 2005.
- [8]Thomson, G. MAKING BETTER PAPER WITH SHRIMPS. *Pulp and Paper International*, 26, 33, 1985.
- [9]Yoshida, C.M.P.; Oliveira-Junior, E.N.; Franco, T.T., 2009. Chitosan Tailor-Made Films: the effects of additives on barrier and mechanical properties. *Packaging Science and Technology*, 22, 161-170.
- [10]ASTM. *Annual Book of ASTM Standards*. American Society for Testing and Materials, Atlanta, 1993.
- [11]TAPPI TEST METHODS. Technical Association of the Pulp and Paper Industry, Atlanta, GA, 1994.
- [12]Jowitt, R.; Escher, F.; Hallstom, B.; MEFFERT, H. F. T.; SPIESS, W. E. L. e VOS, G. *Physical properties of foods*. Applied Science Publishers, London and New York, 1983.
- [13]AOAC. 1990. *Official methods of analysis of the Association of Official Analytical Chemists*. 15th edition. Washington, DC, Association of Official Analytical Chemists.
- [14]Miranda, M.; Vega-Gálvez, A.; Sanders, M.; López, J.; Lemus-Mondaca, R.; Martínez, E. and Di Scala, K. Modelling the water sorption isotherms of quinoa seeds (*chenopodium quinoa willd.*) and determination of sorption heats. *Food Bioprocess Technol*, 2012. 5:1686–1693.
- [15]Rhim, J.-W. and Kim, J.-H. PROPERTIES OF POLY(LACTIDE)-COATED PAPERBOARD FOR THE USE OF 1-WAY PAPER CUP. *Journal of Food Science—Vol. 74, Nr. 2*, 2009.
- [16]Samyn, P.; Deconinck, M.; Schoukens, G.; Stanssens, D.; Vonck, L. and Abbeele, H. V. MODIFICATIONS OF PAPER AND PAPERBOARD SURFACES

WITH A NANOSTRUCTURED POLYMER COATING. Progress in Organic Coating. 69, p. 442-454, 2010.

[17] Reis, A.B.; Yoshida, C.M.P.; Reis, A.P.C. and Franco, T.T. APPLICATION OF CHITOSAN EMULSION AS A COATING ON KRAFT PAPER. (wileyonlinelibrary.com) DOI 10.1002/pi.3023. Society of Chemical Industry, 2011.

[18] Bordenave, N. Grelier, S. Pichavant, F. and Coma V. WATER AND MOISTURE SUSCEPTIBILITY OF CHITOSAN AND PAPER-BASED MATERIALS: STRUCTURE-PROPERTY RELATIONSHIPS. J. Agric. Food Chem. 55, p. 9479-9488, 2007.

[19] Kibirkštis, E.; Kabelkaitė, A. RESEARCH OF PAPER/PAPERBOARD MECHANICAL CHARACTERISTICS. Mechanika. Nr.3(59), p. 34-41, 2006.

[20] Rhim, J.W.; Lee J.H. and Hong, S.I. WATER RESISTANCE AND MECHANICAL PROPERTIES OF BIOPOLYMER (ALGINATE AND SOY PROTEIN) COATED PAPERBOARDS. LebensmWiss Technol. 39: p.806-13, 2006.

PREPARATION AND CHARACTERIZATION OF A CHITOSAN/PECTIN POLYELECTROLYTE COMPLEX

Vinicius Maciel¹, Cristiana Yoshida^{2*}, Telma Franco¹

¹FEQ, State University of Campinas, Av. Albert Einstein, 500 - 13083-852 Campinas, Brazil.

²UNIFESP, Federal University of São Paulo, Rua Artur Riedel, 275 - 09974-000 Diadema, Brazil.

*E-mail address: cristiana.yoshida@unifesp.br

ABSTRACT

Biodegradable polymers as chitosan and pectin are used to form a polyelectrolyte complex. Chitosan forms flexible and resistant films with an efficient oxygen barrier and film structure allows the water absorption. Pectin forms gels with high facility. Polysaccharides that have opposite charges as chitosan and pectin could interact resulting in a very strong intermolecular interaction and highly ordered orientation of the rigid-chain polymers. In this paper was studied polyelectrolyte complex (PEC) between chitosan and pectin at pH 4.0 and different weight ratios chitosan/pectin, by mixing solutions of pectin and chitosan with the same ionic strength. There was a higher PEC formation on ratio 3:1 (pectin/chitosan) with 58.1% of yield. The increase on amount of pectin promoted higher complex formation. However, very high amounts of pectin did not result in better yields, that could be associated to lack of amino groups ionized of chitosan for complexation. FTIR analysis confirmed PEC formation. Scanning electron microscopy (SEM) analysis indicated homogeneous matrices without pores or defects.

Keywords

Chitosan, pectin, polyelectrolyte complex.

INTRODUCTION

Among biodegradable polymers there are polysaccharides chitosan and pectin obtained from renewable sources. Chitosan is a linear cationic polysaccharide obtained from chitin, found in shells of shrimps, lobsters and crabs. It is characterized to form flexible and resistant films with an efficient oxygen barrier [1; 2]. It is composed by *N*-glucosamine and a small amount *N*-acetyl glucosamine and is classified according to the degree of deacetylation [3]. Because the amino groups on the *N*-glucosamine repeating units can be positively charged in an acidic environment. Chitosan can dissolve in acidic solutions, thus being a basic polysaccharide (polycation) [4]. Pectin is a natural, low toxicity and anionic polysaccharide extracted from cell walls of most plants such as apple, orange, pear, etc. It is characterized by the gelling property and branched structure. The pectin molecules consist primarily of D-galacturonic acid with a part of the carboxyl groups being methoxylated [5].

Ionic interactions occur between polyanions (pectin) and polycations (chitosan), leading to the formation of a polyelectrolyte complex (PEC). The PEC has unique properties which are significantly different from those of the initial components. They have been used successfully in medicine and other areas. PEC formed natural polymers are attracting much interest due to their valuable properties. In these polysaccharide structures the presence of polar functional groups results in very strong intermolecular interaction and

highly ordered orientation of the rigid-chain polymers [4; 6]. Different interactions (Van der Waals, electrostatic, hydrophobic, and hydrogen and coordination bonding) can occur between the different groups in polymer-polymer complexes. The stability of these complexes depends on the pH, temperature, charge density, ionic strength among other environmental conditions [1].

Many studies, mainly in medical area and drug delivery, have been developed involving matrices production and characterization obtained from PEC formed between chitosan and pectin [1; 6; 7; 8; 9; 10; 11].

The aim of the current study was develop and characterize the PEC formation from chitosan and pectin obtained in different proportions. The PEC yield formation was evaluated at pH 4.0 and different molar ratios pectin:chitosan by mixing solutions of pectin and chitosan with same ionic strength. FTIR and SEM were analyzed to study the degree of interactive strength between polyions.

MATERIALS and METHODS

Materials

Chitosan (Primex, molecular weight of $2,38 \times 10^5$ g/mol and degree acetylation of 15%, Iceland), acetic acid (Synth, Brazil) and pectin (from citrus fruits) of high degree of methoxylation (above 50% of esterified groups) (CPKelco, GENU® 105 rapid set, Brazil).

Methods

Determination of the degree of deacetylation of chitosan

The procedure was adapted of Raymond *et al.* [12] and Santos *et al.* [13]. Amount of 0.5 g of chitosan were solubilized in 50 ml hydrochloric acid 0.1 mol/L (v/v). The suspension was stirred by 30 minutes at room temperature ($25 \pm 2^\circ\text{C}$). Samples were titrated with NaOH solution (0.092 mol/L). Changes in conductance were measured in pHmeter using results in mV. Degree of deacetylation (DDA) was calculated by $\text{DDA} = (16.1 * [\text{base}] * (V_2 - V_1)) / m$. Degree acetylation (DA) was calculated by $\text{DA} = 100 - \text{DDA}$.

Determination of the degree of esterification of pectin

According to Bocek *et al.* [14], 0.2 g of the pectin was placed in a weighing bottle for titration and wetted with ethanol (95%). Distilled water was heated at 40°C (20 mL) and added. The polymer was dissolved with stirring for 2 h. The solution was titrated with 0.1 M NaOH in the presence of phenolphthalein to pale rose colour and the results annotated recorded as initial titrated (T_i). The pH of the solution was measured. 0.1 M NaOH solution (10 ml) was added to neutralize galacturonic acid of sample and stirred at room temperature for 2 h to saponify the esterified carboxy groups of the polymer. 0.1 M HCl (10 ml) was added. Excess HCl was titrated with 0.1 M NaOH. The number of the esterified carboxy groups was calculated from the volume of 0.1 M NaOH solution spent for titration (T_f). The degree of esterification (DE) of pectin was calculated by Equation 1:

$$\text{DE (\%)} = \frac{T_f}{T_i + T_f} * 100 \quad \text{Eq. 1}$$

Where, T_i : volume (mL) of NaOH used on initial titration and T_f volume (mL) used on final titration.

Polyelectrolyte complex (PEC) preparation

PECs were prepared according to adapted methodology of Bigucci *et al.* [7] and Ghaffari *et al.* [3]. Chitosan (0.50 g/100 g) and pectin (0.50 g/100 g) were dissolved separately in aqueous acetic acid (the stoichiometric amount of acetic acid was calculated from sample weight, taking into account the value of DA and the weight to achieve the protonation of all the NH₂ sites [15]) and distilled water, respectively. Chitosan and pectin suspensions were magnetic stirred at room temperature (45 minutes) and 60°C (30 minutes), respectively. The pH of chitosan and pectin suspensions was adjusted to 4.0 using 0.1 M HCl or 0.1 M NaOH solutions. Therefore, chitosan suspension was slowly added to the pectin aqueous suspension. The suspension obtained was maintained under stirring for 1 hour. Different weight ratios of pectin:chitosan were studied (1:1, 2:1, 3:1, 4:1, 5:1, 1:2, 1:3 and 1:4). Afterward, the PEC formed between pectin and chitosan was separated by ultracentrifugation at 20,000 rpm for 30 minutes at 5°C. The precipitate was dried at 40°C during 18 hours and weighted for the determination of solid PEC weight (yield).

Fourier transform infrared (FTIR) spectroscopy

FTIR analysis was performed on pectin, chitosan and PECs in the range of 4000-900 cm⁻¹, using a NICOLET 6700 spectrophotometer (USA), operating in the ATR mode. Data collection was performed with a 4 cm⁻¹ spectral resolution and 128 scans.

Scanning electron microscopy (SEM) of PEC

SEM analysis of PEC films was performed on fractured cross-sections and the surface of gold-sputtered CH-Sys using a LEO 440i scanning electron microscope (LEO Electron Microscopy Ltd., England) under the following conditions: accelerating voltage = 15 kV, distance = 25 mm, current = 200 pA, vacuum = 10⁻⁵ torr (1.3 x 10⁻³ Pa) [16].

RESULTS and DISCUSSION

The degree of deacetylation (DDA) is one of the most important properties of chitosan. DDA influences on the physicochemical properties of this polymer and its applications. In the current work, titration method was used for the DDA determination of chitosan. The value of 90.9% was estimated for DDA of chitosan.

According to titrimetric method suggested Bocek *et al.* [14], the degree of methoxylation or esterification of pectin was 72.0%. Therefore, it is classified as high methoxylated pectin.

Polyelectrolyte complex (PEC) preparation

PECs are formed by interacting the two oppositely charged polyelectrolytes in an aqueous solution. In this particular system, the electrostatic attractions between the ionized amino groups of chitosan (NH³⁺) and the ionized carboxyl acid groups (COO⁻) of pectin are the main interactions leading to the formation of the pectin/chitosan PECs. In order to form a PEC, both polymers have to be ionized and with opposite charges. This means that the formation of PECs between a weak polybase (like chitosan) and a weak polyacid (like pectin) occurs most extensively in the pH range between the pK_a's of the two polymers.

The pH range in which more than a half of the ionic groups of both polymers are ionized. For the chitosan and pectin system this corresponds to pH values between 3.5-4.5 (pKa range of pectin [17]) and 6.2-7.0 (pKa range of chitosan [18]). Besides pH, which is the most important factor affecting PECs formation and properties, other factors such as the proportion and loading of the two polymers, temperature and ionic strengths are also considered.

Table 1 shows the yield product of PEC samples at pH 4.0 at different pectin/chitosan ratios. The optimum weight ratio was taken at the point where a maximal yield of solid complex was obtained. The maximum yield (58.1%) was obtained at the ratio of pectin/chitosan of 75:25 (% , w/w).

Table 1. Composition of polyelectrolyte complexes of pectin and chitosan at pH 4.0.

PEC samples	Pectin:chitosan weight ratio (%) w/w	Product yield (%)
PEC 1	50.0:50.0	33.3
PEC 2	66.7:33.3	41.6
PEC 3	75.0:25.0	58.1
PEC 4	80.0:20.0	42.3
PEC 5	83.3:16.7	23.1
PEC 6	33.3:66.7	17.9
PEC 7	25.0:75.0	15.3
PEC 8	20.0:80.0	11.5

Ghaffari *et al.* [3] studying the PEC formation between pectin (high methoxylated) and chitosan at pH 5.4, founded yields in order to 70.0%, considering a ratio of 2:1 (pectin/chitosan). Naidu *et al.* [8] preparing a mixing polymeric solutions of gum kondagogu and chitosan as diclofenac carriers obtained yields on PEC formation in order to 90.0% for ratios of 5:1 and 3:1 (gum kondagogu/chitosan). Bigucci *et al.* [7] investigated the influence of polyelectrolyte complexes of chitosan and pectin on the release behaviour of vancomycin, verifying the best results in complexes prepared with 1:9 and 3:7 (chitosan/pectin) at pH 5.0.

Fourier transform infrared (FTIR) spectroscopy

The infrared spectra of the mixed polymers and their components are depicted in Figure 1. In the FTIR spectrum of pectin, bands related to C=O stretching of the ester and carboxyl group could be observed at 1748 and 1628 cm⁻¹, respectively. The C=O stretching vibration (amide I) at 1649 cm⁻¹ and the NH bending (amide II) band at 1577 cm⁻¹ region were observed in the IR spectrum of chitosan. The spectrum of pectin/chitosan complex indicated the main changes in the range of 1800-1600 cm⁻¹, evidenced of the interaction of the amino and carboxyl groups. A strong peak at 1621 cm⁻¹ (asymmetric stretching vibration of carboxylate) appeared and indicated the formation of interchain or intermolecular ionic salt bonds, i.e. PEC between amino groups of chitosan and carboxyl groups of pectin [4; 6; 11; 19].

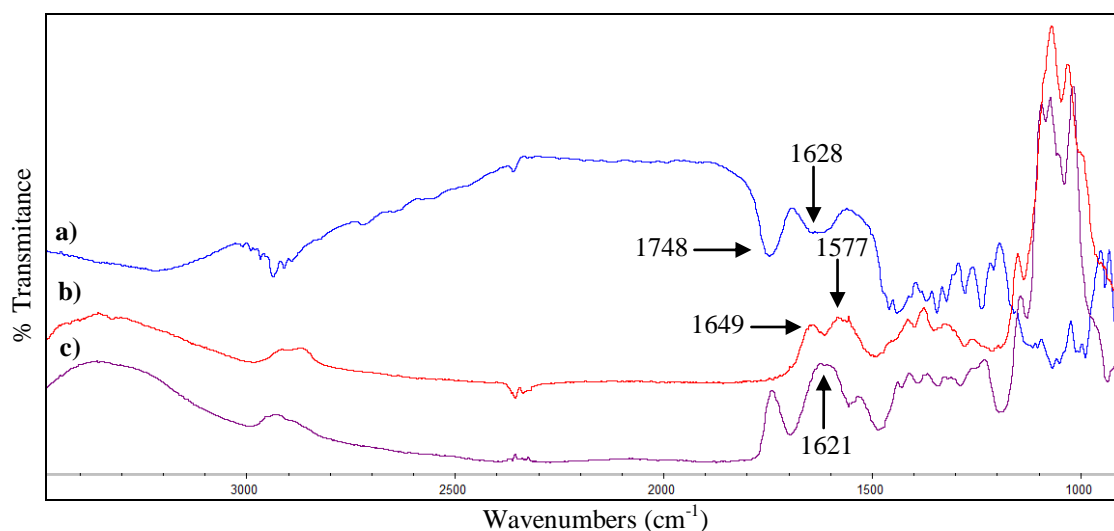


Figura 1. FTIR spectra of (a) pectin; (b) chitosan; (c) pectin/chitosan complex (3:1).

Scanning electron microscopy (SEM) of PEC

Figure 2 shows the SEM micrographs of the pectin/chitosan complex films. It can be seen (Figure 2a) has relatively homogeneous and smooth morphology. It was observed in cross-section (Figure 2b) a compact film that could indicate an interaction between polysaccharides.

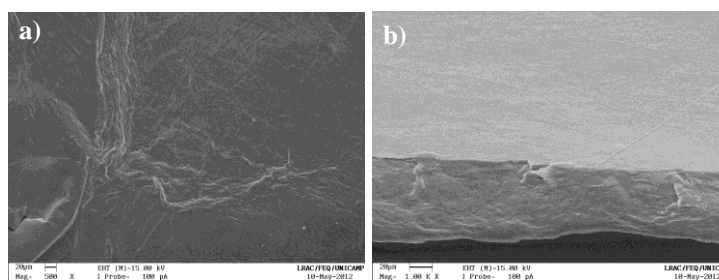


Figure 2. Micrographs of the pectin/chitosan complex (3:1): (a) superficial area and (b) cross-section.

Films of the polyelectrolyte complex between pectin and chitosan were prepared by casting/solvent evaporation method. The results of the present investigation verified the formation of polyelectrolyte complex (PEC) between pectin and chitosan at pH value in the vicinity of the pK_a interval of the two polymers. The optimal weight ratio of pectin to chitosan for PEC formation was 75:25 (% , w/w), which produced highest product yield.

ACKNOWLEDGEMENTS

The current study was developed with the support of CNPq, FAPESP and CAPES.

REFERENCES

- [1] Recillas, M., Silva, L. L., Peniche, P., Goycoolea, F. M., Rinaudo, M., Románe, J. S. and Argüelles-Monal, W. M. (2011). Thermo- and pH-responsive polyelectrolyte complex membranes from chitosan-g-N-isopropylacrylamide and pectin. *Carbohydr. Polym.*, 86, 1336-343.

- [2] Yoshida, C. M. P., Bastos, C. E. N. and Franco, T. T. (2010). Modeling of potassium sorbate diffusion through chitosan films. *Food Sci. Technol.*, 43, 584-89.
- [3] Ghaffari, A., Navaee, K., Oskoui, M., Bayati, K. and Rafiee-Tehrani, M. (2007). Preparation and characterization of free mixed-film of pectin/chitosan/Eudragit_ RS intended for sigmoidal drug delivery. *European J. Pharmac. and Biopharmac.*, 67, 175-86.
- [4] Chen, P-H., Kuo, T-Y., Kuo, J-Y., Tseng, Y-Po., Wang, D-M., Lai, J-Y. and Hsieh, H-J. (2010). Novel chitosan-pectin composite membranes with enhanced strength, hydrophilicity and controllable disintegration. *Carbohydr. Polym.*, 82, 1236-242.
- [5] Giancone, T., Torrieri, E., Masi, P. and Michon, C. (2009). Protein-polysaccharide interactions: Phase behaviour of pectin-soy flour mixture. *Food Hydrocol.*, 23, 1263-269.
- [6] Rashidova, S. S., Milusheva, R. Y., Semenova, L. N., Mukhamedjanova, M. Y., Voropaeva, N. L., Vasilyeva, S., Faizieva, R. and Ruban, I. N. (2004). Characteristics of interactions in the pectin-chitosan system. *Chromatographia*, 59, 779-82.
- [7] Bigucci, F., Luppi, B., Cerchiara, T., Sorrenti, M., Bettinetti, G., Rodriguez, L. and Zecchi, V. (2008). Chitosan/pectin polyelectrolyte complexes: Selection of suitable preparative conditions for colon-specific delivery of vancomycin. *Euro. J. Pharm. Sci.*, 35, 435-41.
- [8] Naidu, V. G. M., Madhusudhana, K., Sashidhar, R. B., Ramakrishna, S., Khar, R. K., Ahmed, F. J. and Diwan, P. V. (2009). Polyelectrolyte complexes of gum kondagogu and chitosan, as diclofenac carriers. *Carbohydr. Polym.*, 76, 464-71.
- [9] Cunha, A. G. and Gandini, A. (2010). Turning polysaccharides into hydrophobic materials: a critical review. Part 2. Hemicelluloses, chitin/chitosan, starch, pectin and alginates. *Cellulose*, 17, 1045-065.
- [10] Coimbra, P., Ferreira, P., Sousa, H. C., Batista, P., Rodrigues, M. A., Correia, I. J. and Gil, M. H. (2011). Preparation and chemical and biological characterization of a pectin/chitosan polyelectrolyte complex scaffold for possible bone tissue engineering applications. *Int. J. Biolog. Macromol.*, 48, 112-18.
- [11] Brinques, G. B. and Ayub, M. A. Z. (2011). Effect of microencapsulation on survival of *Lactobacillus plantarum* in simulated gastrointestinal conditions, refrigeration, and yogurt. *J. Food Eng.*, 103, 123-28.
- [12] Raymond, L., Morin, F. G. and Marchessault, R. H. (1993). Degree of deacetylation of chitosan using conductometric titration and solid-state NMR. *Carbohydr. Res.*, 246, 331-36.
- [13] Santos, J. E., Soares, J. P. and Dockal, E. R. (2003). Caracterização de Quitosanas Comerciais de Diferentes Origens. *Pol.: Ciênc. Tecnol.*, 13, 242-49.
- [14] Boček, A. M., Zabivalova, N. M. and Petropavlovskii, G. A. (2001). Determination of the esterification degree of polygalacturonic acid. *Russian J Appl. Chem.*, 74, 796-99.
- [15] Notin, L., Viton, C., David, L., Alcouffe, P., Rochas, C. and Domard, A. (2006). Morphology and mechanical properties of chitosan fibers obtained by gel-spinning: Influence of the dry-jet-stretching step and ageing. *Acta Biom.*, 2, 387-402.
- [16] Reis, A. B., Yoshida, C. M. P., Reis, A. P. C. and Franco, T. T. (2011). Emulsion chitosan application as coating on Kraft paper. *Polym. Int.*, 60, 963-69.
- [17] Rolin, C. (2002). Pectins and their Manipulation. In *Commercial Pectins Preparation* (C. Seymour, and P. Knox, eds.) pp. 222-41, Blackwell.
- [18] Vaarum, K. M. and Smidsrod, O. (2005). Structure-Property Relationship in Chitosans. In *Polysaccharides: Structural Diversity and Functional Versatility* (S. Dumitriu, ed.) pp. 625-60, Marcel Dekker Inc.
- [19] Stuart, B. H. (2004). *Infrared Spectroscopy: Fundamentals and Applications*, John Wiley & Sons.

EFFECT OF CHITIN NANOFIBRILS ON ULCERATIVE COLITIS MOUSE MODEL AND ITS MECHANISM

Saburo Minami^{1*}, Kazuo Azuma¹, Tomohiro Osaki¹, Shinsuke Ifuku², Hiroyuki Saimoto², Takeshi Tsuka¹, Tomohiro Imagawa¹, Yoshiharu Okamoto¹

¹School of Veterinary Medicine, Tottori University, Tottori 680-8553, Japan

²Graduate School of Engineering, Tottori University, Tottori 680-8552, Japan

*E-mail address: minami@muses.tottori-u.ac.jp

ABSTRACT

We prepared newly developed chitin nanofibrils (chitin-NFs) from crab shells by a grinding method, and also investigated bioactivities of the chitin-NFs. In this study, we examined the preventive effects of chitin-NFs in a mouse model of dextran sulfate sodium (DSS)-induced acute ulcerative colitis and also investigated mechanism of anti-inflammatory effect. The results indicated that chitin-NFs improved clinical symptoms and suppressed ulcerative colitis (UC). Conversely, chitin powder did not suppress the colitis. The chitin-NFs suppressed myeloperoxidase activation in the colon and decreased serum interleukin-6 concentrations. Chitin-NFs decreased positive areas of nuclear factor- κ B staining in the colon tissue. Chitin-NFs also decreased serum monocyte chemoattractant protein-1 concentration in DSS-induced acute UC. Moreover, chitin-NFs suppressed the increased positive areas of Masson's trichrome staining in colon tissue. On the other hand, chitin powder suspension did not show these effects in DSS-induced acute UC mice model. Our results indicated that chitin-NFs have the anti-inflammatory effect via suppressing NF- κ B activation and the anti-fibrosis effects in DSS-induced acute UC mice model.

Keywords

Chitin nanofibrils, DSS induced colitis model, mouse, nuclear factor- κ B, monocyte chemoattractant protein-1

INTRODUCTION

Recently, it is suggested that the size of the chitin is important to determine the effects in immune cells. Native chitins in crustacean shells are highly crystalline with strong hydrogen bonding. Especially in the crystalline structure of α -chitin, their microfibrils are arranged in an antiparallel fashion. These microfibrils consist of nanofibers about 2-5 nm diameter and about 300 nm in length embedded in a protein matrix. Chitin nanofibers are considered to have great potential such as tissue engineering scaffolds, drug delivery, wound dressing, separation membranes and antibacterial coat [1]. A cytocompatibility of chitin nanofibers had been studied such as promotion of cell attachment and spreading of normal human keratinocytes and fibroblasts compared to chitin microfibrils [2]. Our co-worker Ifuku demonstrated that α -chitin nanofibrils (chitin-NFs) were prepared from dried-crab shell, which have complex hierarchical structure with uniform width of approximately 10-20 nm by the grinding method with acetic acid [3]. However, no study was described effects of chitin nanofibers by oral administration *in vivo*.

Inflammatory Bowel Disease (IBD) is common and refers to a group of conditions characterized by inflammation in the intestinal tract. Crohn's disease (CD) and ulcerative colitis (UC) account for the majority of these conditions. Now some experimental animal models are used for IBD researches. A model of dextran sulfate sodium (DSS) induced colitis is one of common model of IBD, which developed acute and chronic colitis resembling UC.

Glucosamine hydrochloride (GlcN) is likely to suppress cytokine-induced activation of intestinal epithelial cells *in vivo*, thereby possibly exhibiting anti-inflammatory action in a DSS-induced rat UC model [4]. However, there is no study about effects of chitin or chitin derivatives in a DSS-induced UC model. The aim of this study is to evaluate the preventive effects of chitin-NFs compare to the effects of chitin powder on mice DSS-induced acute UC model. Furthermore, we investigate the mechanism of anti-inflammatory reaction by orally administered chitin-NFs on the model.

MATERIALS and METHODS

Reagents

Dextran sulfate sodium (molecular weight 36-50 kDa; reagent grade) was purchased from MP Biomedicals LLC (Solon, OH, USA). Chitin powder was purchased from Nacalai Tesque (Lot no.: M0A3811; Kyoto, Japan). The average diameter of Chitin powder was about 200 μm . Chitin-nanofiber gel (1%, pH3; chitin-NFs) was prepared previously described method (Ifuku et al, 2009). Chitin powder suspension (1%, pH3; Chitin-PS) were prepared, deacetylated ratio of chitin-PS was 3.9 %.

Animals

Sixty-eight C57BL/6 mice (female, 6 weeks old) for study 1 and thirty C57BL/6 mice (female, 5 weeks old) for study 2 were purchased from CLEA Japan (Osaka, Japan). The animals were maintained at a conventional condition. The use of these animals and the procedures they undergo were approved by the Animal Research Committee of Tottori University.

Study design

In the study 1, mice (n=68) were randomized into six groups: control (+) group was administered only DSS (n=17), control (-) group was administered tap water (n=5), chitin-NFs (+) group was administered chitin-NFs and DSS (n=17), chitin-NFs (-) group was administered only chitin-NFs (n=7), chitin-PS (+) group administered chitin-PS and DSS (n=16) and Chitin-PS (-) group administered only chitin-PS (n=6). To elicit colitis, mice were administered with 3% DSS *ad libitum* for 6 days; from day 0 to day 6. For 7 days before starting administration of DSS, chitin-NFs (+), chitin-NFs (-), chitin-PS (+) and chitin-PS (-) group were administered 0.1 % chitin-NFs or chitin-PS dissolved in tap water *ad libitum*. Blood collection and colon sampling were done at day 3 and day 5 in control (+), chitin-NFs (+) and chitin-PS groups (each n=5) and at day 6 in all groups (each group: n=5-7). **In the study 2**, mice (n=30) were randomized into 6 groups: the control (+) group was administered only DSS (n=5); the control (-) group was administered tap water (n=5); the chitin-NFs (+) group was administered chitin-NFs and DSS (n=5); the chitin-NFs (-) group was administered only chitin-NFs (n=5); the chitin-PS (+) group was administered chitin-PS and DSS (n=5); and the chitin-PS (-) group was administered only chitin-PS (n=5). To induce colitis, mice were administered 3% DSS *ad libitum* for 6 days

from day 0 to day 5. For 7 days before starting the administration of DSS, chitin-NFs (+), chitin-NFs (-), chitin-PS (+), and chitin-PS (-) groups were administered 0.1% chitin-NFs, or chitin-PS dissolved in tap water *ad libitum*. Blood collection and colon sampling were done on days 5 in all groups.

Clinical analysis for the both studies

Ulcerative colitis was evaluated using a disease activity index (DAI), as described by Melger et al.[5] with a slight modification, using parameters of body-weight loss, stool consistency and bleeding. The length and weight of the colon were measured, and tissue obtained from each colon was processed for further assays.

Histological evaluation of colitis for the both studies

Colon tissues were fixed in 10% buffered formalin. Each sample was made thin sections (3 μ m) for histological observation with hematoxylin-eosin staining. Each section was examined microscopically, and histological scoring was performed, as described by Ohkawara et al [6]. In brief, tissue damage was categorized into six grades: 0: normal mucosa; 1: infiltration of inflammatory cells; 2: shortening of the crypt by less than half height; 3: shortening of the crypt by more than half height; 4: crypt loss; 5: destruction of epithelial cells. Histological scoring was performed in ten fields observations at $\times 100$ magnification using three mice in each group. Means of scores in thirty fields were considered as the histological score in each group.

Myeloperoxidase (MPO) staining for the study 1

Myeloperoxidase (MPO) staining, which is one of a marker of leukocyte invasion to tissue, was performed in a routine manner. Counts of MPO positive cells in a submucosal layer were performed in twenty fields observations at $\times 400$ magnification using two mice in each group. Means of scores in forty fields were considered as the number of MPO positive cells in each group.

Measurements of serum IL-6 concentration for the study 1

Serum IL-6 was quantified by a sandwich enzyme-linked immunosorbent assay (ELISA) using a Mouse IL-6 ELISA kit (Thermo SCIENTIFIC, Rockford, USA), according to manufacturer's protocol.

Masson's trichrome (MT) staining for the study 2

In the DSS-induced UC, the fibrosis of mucosal and submucosal layers of the colon was observed at acute and chronic phase. To measure the fibrosis area of the mucosal and submucosal layers of the colon, we performed quantitative digital morphometri analysis of extracellular matrix (ECM) for colonic sections with MT staining according to a protocol adapted from that described in detail by Suzuki et al (2011)[7]. In brief, 10 randomly chosen high-power fields ($\times 200$ magnification) for each cross section were photographed with a digital camera attached to an Olympus microscope system (Olympus Corporation, Tokyo, Japan). The color wavelengths of the copied image were transformed into digital readings, by using Lumina Vision software (Mitani corporation, Tokyo, Japan) allowing for quantification of the various color wavelength with pixels as the unit of measure. By using the original image for comparison, the color spectra were analyzed and those corresponding to ECM were quantified. The percentage of the ECM tissues in mucosal and

submucosal layers was calculated by dividing the total pixel area of the ECM by the total pixel area corresponding to the total colonic tissue in the field of view. The colons of three mice were analyzed in each group. The mean scores for 30 fields were considered the percentages of fibrosis areas for each group.

Immunohistochemical detection of nuclear factor- κ B (NF- κ B) in the colon for the study 2

NF- κ B has been reported to be activated in inflamed colonic mucosa of IBD. Colon tissue sections (3 μ m) on glass slides were deparaffinized, washed by ethanol and water and soaked by PBS. The sections were treated by microwave with 0.01 M citrate buffer (pH 6.0) for 5 minutes. Then, the sections were washed with PBS and incubated with 1% hydrogen peroxide methanol for 30 minutes at room temperature. Washing with PBS, the sections were incubated with rabbit polyclonal anti-NF- κ B p65 antibody (1:500, sc-372; Santa cruz biotechnology, inc., California, USA) for 60 min at room temperature. The slides were washed with PBS, and envisioned for 30 minutes at room temperature (Code No. K3466, Dako, Glostrup, Denmark). Tissue sections were visualized by incubating with diaminobenzidine tetrahydrochloride, and counterstained with hematoxylin. We calculated the positive areas of NF- κ B in colon epithelium. The imaging analysis of NF- κ B were performed as well as those of colon fibrosis. The colons of three mice were analyzed in each group. The mean scores for 30 fields were considered the percentages of fibrosis areas for each group.

Measurements of serum monocyte chemotactic protein 1 concentrations for the study 2

Serum monocyte chemotactic protein 1 (MCP-1/CCL2) were quantified by a sandwich enzyme-linked immunosorbent assay (ELISA) using commercial mouse MCP-1 ELISA kit (Quantikine®, R&D Systems Inc., Minneapolis, USA) according to the manufacturer's protocol.

RESULTS and DISCUSSION

Results in the study 1

Effects of chitin-NFs on DAI in DSS induced acute UC mice

Weight loss, loose faces of stool and bleeding were observed at day 3 in the control (+), the chitin-PS (+) groups and at day 4 in the chitin-NFs (+) group (Table 1). The chitin-NFs (+) group significantly reduced DAI at day 4, day 5 and day 6 compared to the control (+) group ($p < 0.05$), and at day 5 ($p < 0.01$) and day 6 ($p < 0.05$) compared to the chitin-PS (+) group (Table 2). No change of DAI was observed among the control (-), the chitin-NFs (-) and the chitin-PS (-) groups.

Effects of chitin-NFs on colon length and colon weight/length in DSS induced acute UC mice

Administration of 3% DSS induced shorting colon length and increased colon weight/length ratio (mg/cm) in C57BL/6 mice [5]. In the chitin-NFs (+) group, colon lengths were significantly longer than those of the control (+) group at day 3, day 5 and day 6 ($p < 0.05$ at day 3 and day 5, $p < 0.01$ at day 6). Moreover, colon length in the chitin-NFs (+) group was significantly longer than the chitin-PS (+) group at day 3, day 5 and day 6 ($p < 0.05$ at day 3 and day 5, $p < 0.01$ at day 6). No change of colon length was observed

among the control (-), the chitin-NFs (-) and the chitin-PS (-) groups. Colon weight/length ratio (mg/cm) was decreased in the chitin-NFs (+) group at day 5 and day 6 compared to the control (+) group. At day 5, colon weight/length ratio (mg/cm) of chitin-PS (+) group was significantly decreased compared with the control (+) group ($p < 0.05$). At day 6, colon weight/length ratio (mg/cm) of the chitin-NFs (+) group was significantly decreased compared to the control (+) and chitin-PS (+) group ($p < 0.01$). No change of weight/length ratio (mg/cm) was observed among the control (-), the chitin-NFs (-) and the chitin (-) groups.

Table 1. Effect of chitin-NF administration on the DAI in DSS-induced acute UC mice

	Da y0	Da y 1	Day 2	Day 3	Day 4	Day 5	Day 6
Control	0.0 ± 0.0	0.0 ± 0.0	0.0 ± 0.0	0.3 ± 0.2	1.1 ± 0.4	3.6 ± 0.3	6.9 ± 0.5
Chitin- NF	0.0 ± 0.0	0.0 ± 0.0	0.0 ± 0.0	0.0 ± 0.0	0.2 ± 0.1*	2.3 ± 0.3*††	5.1 ± 0.4*†
Chitin- PS	0.0 ± 0.0	0.0 ± 0.0	0.0 ± 0.0	0.3 ± 0.2	1.0 ± 0.4	4.0 ± 0.5	7.0 ± 0.8

* $p < 0.05$ compared with chitin-NF (+) and control (+) groups, †† $p < 0.01$ compared with chitin-NF (+) and chitin-PS (+) groups, and † $p < 0.05$ compared with chitin-NF (+) and chitin-PS (+) groups.

Effects of chitin-NFs on histological changes in DSS induced acute UC mice

The damage of intestinal mucosa was microscopically evaluated by histological scoring. In the control (-), the chitin-NFs (-) and the chitin-PS (-) groups, No histological change was observed. At day 3, in both of the control (+) and the chitin-NFs (+) groups, infiltrations of inflammatory cells were observed. At day 5, erosions, shorting or destruction of crypt and edema were observed in the control (+) group. At day 5, in the chitin-NFs (+) group, some erosions were observed, however, shorting or destruction of crypt was markedly suppressed; moreover edema was slightly suppressed. At day 6, in the control (+) and chitin-PS (+) groups, severe erosions, crypt destructions and edema were observed; moreover some ulcers were observed. In the chitin-NFs (+) group, erosions, crypt destructions and edema were markedly suppressed compared to the control (+) and the chitin-PS (+) groups. The severity of tissue damage was evaluated by using histological scoring of hematoxylin-eosin stained sections. Histological scores of the chitin-NFs (+) were significantly decreased at day 5 compared to the control (+) group ($p < 0.01$), and at day 6 compared to the control (+) and the chitin-PS (+) groups ($p < 0.01$, Figure 1).

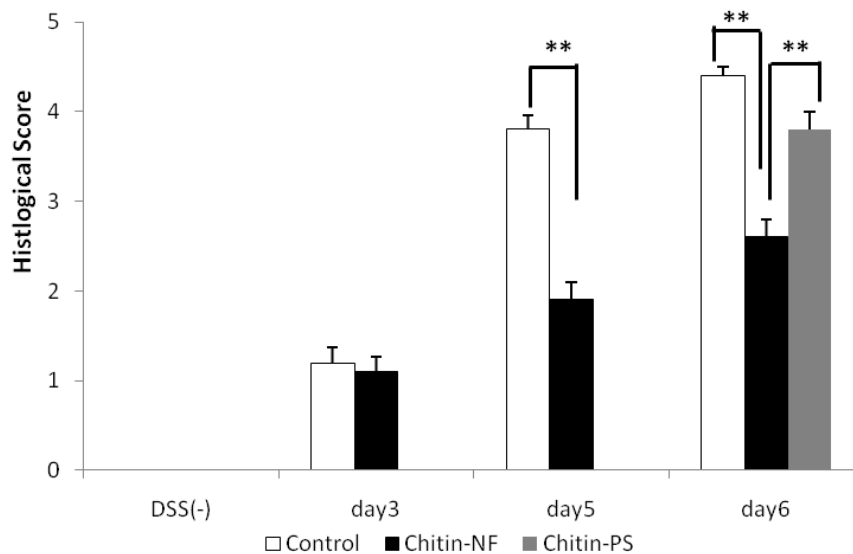


Figure 1. Effect of chitin-NFs administration on histological damage score of intestinal mucosa in DSS-induced acute UC mice.

Effects of chitin-NFs on colon MPO positive cells in DSS induced acute UC mice

The results of MPO were shown in Figure 2. In the control (-), the chitin-NFs (-) and the chitin-PS (-) groups, there is 0-1 MPO positive cell / $\times 400$ fields (Figure 2). In the control (+) and the chitin-NFs (+) groups, the counts of MPO positive cells were gradually increased from day 3 to day 6. In the chitin-NFs (+) group, however, counts of MPO positive cells were significantly fewer than the control (+) group at day 3, day 5 and day 6 ($p < 0.01$). In the chitin-PS (+) group, count of MPO positive cell was slightly fewer than the control (+) group, however, no significant difference was observed between them.

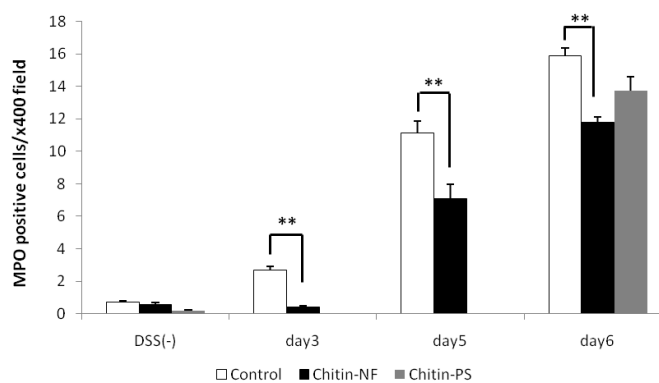


Figure 2. Effect of chitin-NFs administration on the MPO positive cells counts/ $\times 400$ fields of colon in DSS-induced acute UC mice.

MPO is a marker of oxidative stress, in DSS-induced UC model, high MPO activities were indicated. In the chitin-NFs (+) group, MPO positive cells were significantly fewer than the control (+) group.

Effects of chitin-NFs on serum IL-6 concentrations in DSS induced acute UC mice

At day 5, serum IL-6 concentration of the chitin-NFs (+) group (85.8 ± 1.2 pg/ml) was significantly lower than the control (+) group (237.1 ± 41.9 pg/ml) ($p < 0.01$).

Results in the study 2

The results of the clinical findings and the histological findings in the study 2 are almost same results as in the study 1 (Data were not shown).

Effects of chitin-NFs on fibrosis of the colon in DSS-induced acute UC mice

For evaluating the area of collagen deposition in mucosal and submucosal layers, we performed digital image analysis. The percentages of collagen deposition areas in mucosal and submucosal layers are shown in Figure 3. In the chitin-NFs (+) group, the score was significantly lower than that in the control (+) group ($p < 0.05$). In the control (-), chitin-NFs (-), and chitin-PS (-) groups, the scores were 1.5–1.9%.

Effects of chitin-NFs on NF- κ B of the colon epithelium in DSS-induced acute UC mice

To evaluate the effects of chitin-NFs on NF- κ B of the colon epithelium, immunohistochemical detections of NF- κ B were performed. The percentages of positive areas of NF- κ B in epithelium cells are shown in Figure 4. In chitin-NFs (+) group, the score was significantly lower than that in the control (+) group ($p < 0.05$). In the chitin-PS (+) groups, the scores were slightly suppressed. In the control (-), chitin-NFs (-), and chitin-PS (-) groups, the scores were 1.8–3.0 %.

Effects of chitin-NFs on serum MCP-1 concentrations in DSS-induced acute UC mice

The results were shown in Figure 5. In the chitin-NFs (+) group, serum MCP-1 concentration was significantly lower than the control (+) groups ($p < 0.05$).

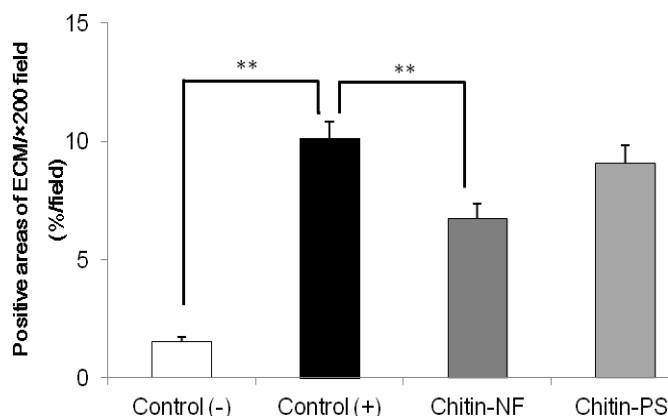


Figure 3. Effects of chitin-NFs on colon fibrosis in DSS-induced acute UC mouse model

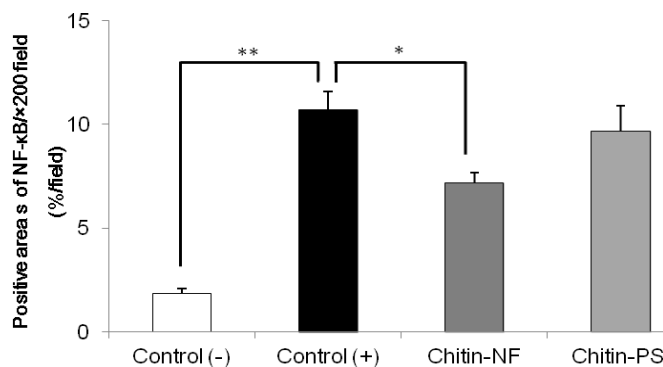


Figure 4. Effects of chitin-NFs on colon NF-κB activation in DSS-induced acute UC mouse model

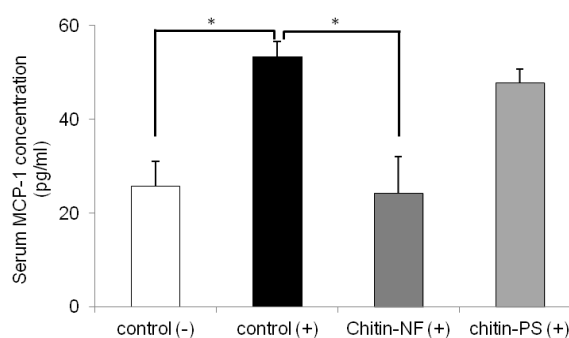


Figure 5. Effects of chitin-NFs on serum MCP-1 concentration in DSS-induced acute UC mouse model

In the DSS-induced UC model mice, fibrosis in the colon was observed not only chronic phase but also acute phase. It is described that MCP-1 induces fibrogenic response of the gut in IBD model [8]. Chitin-NFs suppressed the fibrosis and decreased serum MCP-1 concentration in DSS-induced acute UC mouse model. These results indicated that chitin-NFs have the suppressive effects of fibrosis in DSS-induced acute UC mouse model. It was indicated one mechanism of suppressive effects on fibrosis by chitin-NFs came from suppressing the action of MCP-1. NF-κB occupies a pivotal position in several innate immune signaling pathways. So far, it has been shown that NF-κB is the critical transcription factor needed to express genes associated with a proinflammatory response [9]. NF-κB activity is increased in the colon during active episodes of IBD. Chitin-NFs suppressed the activation of NF-κB in colon epithelium in DSS-induced acute colitis model. MCP-1 plays an important role in the pathogenesis of experimental colitis model to the recruitment of immune and enterochromaffin cells. The absence of MCP-1 is associated with a significant reduction in inflammation in experimental colitis model. Ju et al. demonstrated that pro-inflammatory cytokine induced the expression of MCP-1 via p38 mytogen-activated protein kinase (MAPK) and NF-κB signaling [10]. Chitin-NFs decreased serum MCP-1 concentration compared with control (+) group. These results indicated that chitin-NFs suppressed the increase of MCP-1 in serum via suppressing NF-κB activation. So far, it is not unclear how chitin-NFs absorb and metabolize *in vivo* and *in vitro*. To understand the anti-inflammatory mechanism of chitin-NFs, the study focusing on absorption and metabolism of chitin-NFs must be performed.

REFERENCES

- [1] Jayakumar, R., Prabakaran, M., Nair, S.V. and Tamura, H. (2010). Novel chitin and chitosan nanofiber in biomedical applications. *Biotech. Ad.*, 28, 142-50.
- [2] Noh, H.K., Lee, S.W., Kim, J.M., Oh, J.E., Kim, K.H., Chung, C.P., Choi, S.C., Park, W.H. and Min, B.M. (2006). Electrospinning of chitin nanofibers: degradation behavior and cellular response to normal human keratinocytes and fibroblasts. *Biomaterials*, 27, 3934-44.
- [3] Ifuku, S., Nogi, M., Abe, K., Yoshioka, M., Morimoto, M., Saimoto, H. and Yano, H. (2009). Preparation of chitin nanofibers with a uniform width as alpha-chitin from crab shells. *Biomacromol.*, 10, 1584-88.
- [4] Yomogida, S., Kojima, Y., Tsutsumi-Ishii, Y., Hua, J., Sakamoto, K., & Nagaoka, I. (2008). Glucosamine, a naturally occurring amino monosaccharide, suppresses dextran sulfate sodium-induced colitis in rats. *Int. J. Mol. Med.*, 22, 317-23.
- [5] Melgar, S., Karlsson, A. and Michaëlsson, E. (2005). Acute colitis induced by dextran sulfate sodium progresses to chronicity in C57BL/6 but not in BALB/c mice: correlation between symptoms and inflammation. *Am. J. Physiol. Gastro. Liver Phys.* 288, G1328-38.
- [6] Ohkawara, T., Nishihira, J., Takeda, H., Miyashita, K., Kato, K., Kato, M., Sugiyama, T. and Asaka, M. (2005). Geranylgeranylacetone protects mice from dextran sulfate sodium-induced colitis. *Scand. J. Gastroent.* 40, 1049-57.
- [7] Suzuki, Y., Okamoto, Y., Morimoto, M., Sashiwa, H., Saimoto, H., Shigemasa, Y. and Minami, S. (2000). Influence of physico-chemical properties of chitin and chitosan on complement activation. *Carbohydr. Polym.*, 42, 307-10.
- [8] Motomura, Y., Khan, W.I., El-Sharkawy, R.T., Verma-Gandhu, M., Verdu, E.F., Gauldie, J. and Collins, S.M. (2006). Induction of a fibrogenic response in mouse colon by overexpression of monocyte chemoattractant protein 1. *Gut*, 55, 662-70.
- [9] Elson, C.O., Cong, Y., McCracken, V.J., Dimmitt, R.A., Lorenz, R.G. and Weaver, C.T. (2005). Experimental models of inflammatory bowel disease reveal innate, adaptive, and regulatory mechanisms of host dialogue with the microbiota. *Immunol Rev.*, 206, 260-76.
- [10] Ju, Y., Hua, J., Sakamoto, K., Ogawa, H., Nagaoka, I. (2008). Modulation of TNF-alpha-induced endothelial cell activation by glucosamine, a naturally occurring amino monosaccharide. *Int. J. Mol. Med.*, 22, 809-15.

SYNTHESIS, CHARACTERIZATION AND STUDY OF AMPHIPHILIC QUARTENARY DERIVATIVES OF CHITOSAN: IN VITRO STUDY AGAINST *Aspergillus flavus*.

Mirelle Takaki, Rafael de Oliveira Pedro, Ricchard Hallan F. V. de Souza, Amanda Manchini Dias, Juliana dos Santos Gabriel, Marcio J. Tiera and Vera Ap. de Oliveira Tiera*.

Department of Chemistry and Environmental Sciences, Institute of Biosciences, Humanities and Exact Sciences – IBILCE, São Paulo State University – UNESP, São José do Rio Preto, Brazil.

*E-mail: verapoli@ibilce.unesp.br

ABSTRACT

In this work we present the synthesis, characterization, and antifungal activity of new amphiphilic derivatives of chitosan. The derivatives were synthesized using deacetylated chitosan in a two step process: first the reaction with pentyltrimethylammonium bromide followed by reductive amination with dodecylaldehyde (Dod). The derivatives were characterized by ¹H-NMR and the degrees of substitution by Dod were varied to improve the antifungal activity. The antifungal activity of deacetylated chitosan and its derivatives against *Aspergillus flavus* was tested by varying the polymer concentration from 0.01 to 1.0 mg/mL. The derivatives substituted only with pentyl groups showed modest inhibition against *A. Flavus*, similar to that obtained with deacetylated chitosan. Results show that the amphiphilic derivatives containing dodecyl groups exhibited increasing inhibition indexes with polymer concentration and hydrophobic (Dod) content. At 0.75 mg/mL, amphiphilic derivatives containing 5.0 and 30 % of Dod and 74% de pentyl groups completely inhibited the fungal growth.

Keywords: Chitosan derivatives, *Aspergillus flavus*, quaternary, antifungal activity, deacetylated chitosan.

INTRODUCTION

Chitosan and its derivatives have received increased attention due to their potential applications in the food industry and agriculture for protection of seeds and improvement of quality and shelf life of various foods. Among the natural properties of chitosan, its capability of inhibiting the fungal growth of microorganisms such as *Fusarium*, *Alternaria*, *Helminthosporium Botrytis cinerea*, *Rhizoctonia solani* has been well documented [1]. This property has been explained based on the interaction between the cationic groups of the polysaccharide chain and the anionic components of the microorganisms surface, which in turn may result either in the disruption of cell wall and leaking of its constituents or chitosan chains may form an impermeable layer around the cell, thus blocking the transport of essential solutes into the cell [2, 3]. However, the exact mechanism of the antimicrobial activity of chitosan is still unknown and has been recently reviewed by Kong et al. [4]. On the other hand, it has been shown that the activity may depend on various parameters such as molecular weight, pH and temperature. A number of reports show that its activity can be boosted via chemical modification of its structure and quaternized chitosan derivatives have been reported to exhibit improved antimicrobial activity [5]. Generally, the antifungal activity tends to increase with the degree of quaternization and

hydrophobic content, however, it also depends on the type of fungus and is more prominent with microorganisms having negatively charged cell surfaces [4]. Moreover, recent studies show that, for quaternized chitosans and its derivatives, the hydrophobic/hydrophilic balance plays an important role on their effectiveness [4,6]. The purpose of this paper is to report a simple and reliable method to prepare chitosans derivatives with improved capabilities of inhibiting the growth of *A. flavus*. Therefore, the synthesis characterization and antifungal activity of amphiphilic derivatives of chitosan against the fungus *A. flavus* is described. Chitosan derivatives were obtained through the reaction of chitosan amino groups with pentyltrimethylammonium bromide followed by reductive amination with dodecylaldehyde (Dod). Aiming to evaluate the effect of the hydrophobe content of the derivatives on the growth of the fungus *in vitro*, the content was increased. The results of the antifungal activity of these derivatives were presented and discussed taking into account the degree of hydrophobic substitution of the derivatives.

MATERIALS AND METHODS

Materials

Commercial chitosan (C-CH, degree of deacetylation (DDA) 85%) was purchased from Polymar Co., Brazil, (5-bromopentyl) trimethylammonium bromide, sodium hydroxide, dodecylaldehyde, sodium acetate, and acetic acid were purchased from Sigma Aldrich Chemical Co., Brazil. Spectra/pore membranes (Spectrum) were employed for dialysis. All solvents were of reagent grade and used as received. Water was deionized using a Gehaka water purification system.

Preparation and characterization of the pentyltrimethylammonium-modified chitosan (CH-Pentyl) and its amphiphilic derivatives

The pentyltrimethylammonium-modified derivatives were obtained from a highly deacetylated chitosan sample (DDA 99%) and their synthesis have been described [7]. Following, the quaternized derivative (CH-Pentyl) was modified with dodecylaldehyde via a reductive amination reaction and the procedure is illustrated below for the synthesis of Dod₅-CH-Pentyl. A solution of dodecylaldehyde (0.025 g, 0.14 mmol) in ethanol (76 mL) was added dropwise to a solution of CH-Pentyl (1.008 g, 2.72 mmol monosaccharide residue) in aqueous acetic acid (110 mL, 2 wt %) at room temperature. At the end of the addition, the solution was stirred for 30 min. The pH of the reaction mixture was adjusted to 5.0 by adding aqueous NaOH (1.0 M). The reaction mixture was stirred for 1 hr at room temperature. Sodium cyanoborohydride (0.510 g, 8.10 mmol) was added under stirring. Thereafter, the reaction mixture was stirred for 20 hrs. The reaction mixture was purified by dialysis followed by lyophilization and samples extracted with chloroform in a soxhlet system as described previously [11]. The degree of substitution (DS) was determined by H-NMR in a Bruker Instrument, 500 MHz. Polymer solutions (10 mg/mL) were prepared in D₂O/DCI (100/1, v/v). Their H NMR spectra were recorded at 70 °C. The characterization of the derivatives is shown in Table 1.

Viscosity measurements

Viscosity measurements were carried out in water thermostated bath with a capillary calibrated viscosimeter for dilution Cannon-Ubbelohde 9722M-50 (Cannon Instr. Co.) at pH 4.5 acetic acid (0.3M)/sodium acetate(0.2M) buffer. The mean viscosimetric molecular weight of chitosan and its derivatives were determined by using the Mark-Houwink equation, with constants $a = 0.796$, $K = 0.079 \text{ mL g}^{-1}$ [8].

Pathogen, cultures and Antifungal assays

The microorganism chosen to test the antifungal activity of chitosan and its derivatives was *A. flavus*. The strain was kindly provided by Brazilian Collection of Microorganisms from the Environment and Industry – CBMAI, Campinas – São Paulo, Brazil, and it was maintained on potato dextrose agar (PDA) (potato infusion from 200 g/L, 20 g/L dextrose, and 15 g/L agar) in the dark at 25 ± 2 °C. The antifungal activities of deacetylated chitosan and its quaternary derivative were compared to those of the amphiphilic derivatives modified with a dodecyl groups whose degree of substitution varied from 5 to 30%. The polymers solution were prepared at pH 5.5 in acetic acid and added at concentrations of 0.0 (control plate) and from 0.01 to 1.0 g/l. The culture was carried out as described previously [7]. Inhibition index of the fungus by the polymers was calculated as follows:

$$\text{Antifungal Index (\%)} = (1 - D_a/D_b) \times 100,$$

where D_a is a diameter of the growth zone in the test plates and D_b is growth zone in the control plate, according to Guo *et al.* [9]. Each experiment was performed in quadruplicate, and the data were averaged. The student T- test and the Kruskal-Wallis test with Dunn's multiple comparison were used to evaluate the differences in antifungal index in antifungal tests. Results with $P < 0.01$ were considered statistically significant.

Table 1. Properties and DS (degree of substitution) of the chitosan derivatives.

Polymer	Molar ratio* Dod/Gluco	DS Pentyl (%)	DS _{DA} Dodecyl (%)	M _v (kDa)
CH	-	-	-	18.3
CH-Pentyl	-	74.1	-	5.6
Dod ₅ -CH-Pentyl	0.05	74.1	4.81	-
Dod ₃₀ -CH-Pentyl	0.30	74.1	24.1	-

*Molar ratio of dodecylaldehyde (Dod) to glucosamine units (Gluco)

RESULTS AND DISCUSSION

Preparation of the Derivatives

The functionalization of chitosan with quaternary amino groups was performed as described before using a nucleophilic substitution of the C-2 amine groups in a slightly alkaline medium [7]. The strategy to synthesize was successively carried out by using the pentyltrimethylammonium bromide. Deacetylated chitosan (CH, 99%) was used as starting material and the substitution by Pentyl groups was reached by setting the initial molar ratio of *N*-pentyltrimethylammonium to glucosamine units to 3. The ¹H NMR spectra of the quaternized derivative (CH-Pentyl) and the derivative having 30% of dodecyl groups are shown in Figure 2. The ¹H NMR spectrum of deacetylated chitosan (CH) shows the characteristic peaks of chitosan spectrum with a doublet at δ 5.43 ppm, which are due to the resonance of the anomeric proton (H1), a singlet at 2.56 ppm attributed to the acetamido methyl protons and a singlet at δ 3.74 ppm corresponding to the proton linked to carbon 2 of the glucosamine ring (data not shown). The degree of deacetylation for CH was determined as described before using the two later described peaks [10]. The ¹H NMR of the quaternized derivative exhibited a singlet at 3.50 ppm, which was attributed to the resonance of the trimethylammonium protons of the *N*-pentyltrimethylammonium moiety and also exhibited a signal at δ 1.87 ppm corresponding to the resonance of the methylene

protons located in the middle of the hydrocarbon chain of the cationic substituent $\text{CH}_2\text{CH}_2\text{CH}_2\text{CH}_2\text{CH}_2\text{N}^+(\text{CH}_3)_3$ (Fig. 2b) [7].

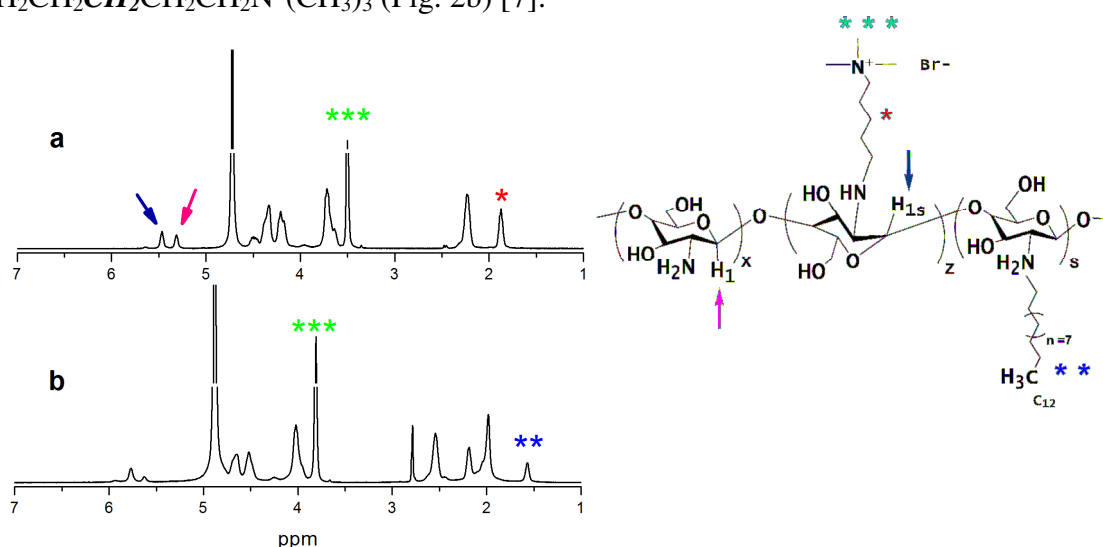


Figure 1. Structure and ^1H NMR spectra of the chitosan derivatives (a) CH-Pentyl and (b) Dod₃₀-CH-Pentyl recorded at 70 °C in D₂O/DCI (100/1, v/v).

The signal corresponding to the anomeric proton also undergoes a downfield shift from 5.31 ppm to 5.47 ppm, which confirms the success of the substitution reaction. The degree of substitution (DS) was determined from the areas of the signal at δ 1.87 ppm (Fig. 2b), which corresponds to the resonance of the methylene protons $\text{CH}_2\text{CH}_2\text{CH}_2\text{CH}_2\text{CH}_2\text{N}^+(\text{CH}_3)_3$ and the area of the signals due to the anomeric protons of pentyltrimethylammonium substituted and unsubstituted glucosamine residues, H_{1s} and H₁, respectively by the relationship previously described [7] (Fig. 2a). The amphiphilic derivatives were obtained by setting the initial proportions of dodecylaldehyde (Dod) to glucosamine units to 0.05 and 0.30. The degrees of substitution by dodecyl groups were determined using the area of the signal at δ 1.56 ppm due to terminal methyl protons (I_{CH₃}) (Figure 2b) from the dodecyl chain, and the area of the peaks corresponding to anomeric protons at δ 5.5-6.0 ppm (I_{H₁} + I_{H_{1s}}) of the glucosamine rings, by using the relationship previously described [11]. The obtained derivatives were substituted with 74% of pentyl groups and 4.80, and 27,6% of dodecyl groups, denoted as CH-Pentyl, Dod₅-CH-Pentyl, Dod₃₀-CH-Pentyl, respectively (Table 1). The molecular weight was determined by viscosity measurements and, as can be seen from Table 1, the molecular weight (M_v) decreased about 3 times, which occurred probably due to the long time of reaction [7]. These derivatives were tested for their antifungal activities in vitro against *Aspergillus Flavus* and their results are presented and discussed in the following section.

Antifungal activity of commercial chitosan and its deacetylated and quaternary derivatives.

Figure 2 shows the inhibition indexes of the growth in vitro of *A. Flavus* in the presence of commercial chitosan (C-CH) deacetylated Chitosan CH, and its derivatives containing Pentyl (CH-Pentyl) and dodecyl groups (Dod_x-CH-Pentyl). The modification of chitosan clearly leads to significant differences in the inhibition indexes and the results presented in Fig. 2 correspond to the inhibition on the 7th day. As can be seen from Fig. 2 commercial chitosan C-CH, CH and the quaternized derivative CH-Pentyl, exhibited similar inhibition indexes, which remained around 10-15% , however, for CH-Pentyl the

inhibition activity showed a tendency to decrease for concentrations higher than 0.5 mg/mL.

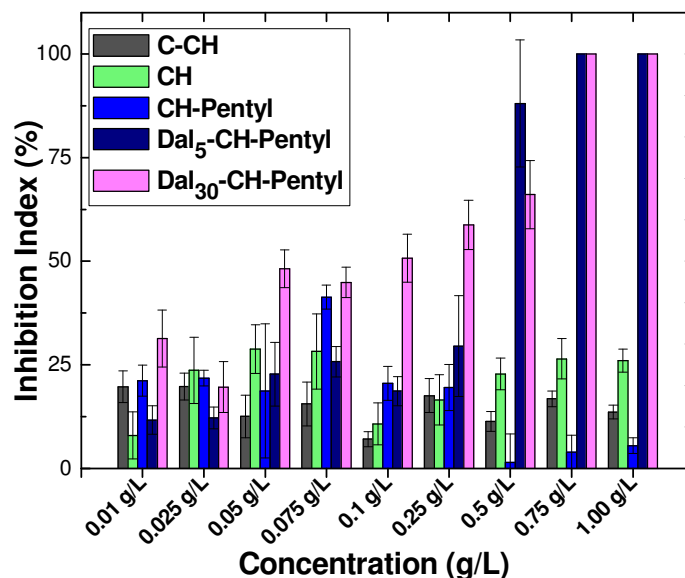


Figure 2. Inhibition percentages of commercial chitosan (C-CH), deacetylated chitosan CH and its derivatives CH-Pentyl, Dod₅-CH-Pentyl, Dod₃₀-CH-Pentyl on *Aspergillus flavus* growth “in vitro” at increasing polymer concentrations (0.01 to 1.0 mg/mL, mean \pm SD, n = 4). Amphiphilic derivatives containing dodecyl groups are statistically different from deacetylated chitosan with $p < 0.001$.

Although initially unexpected, the presence of cationic charges did not significantly affect antifungal activity when compared to deacetylated chitosan, which can be due to the higher hydrophilicity of this derivative, that in turn may decrease the interaction between the polymer chain and the cell wall. This explanation is reinforced by comparing the results to the amphiphilic derivatives Dod₅-CH-Pentyl and Dod₃₀-CH-Pentyl, which showed a clear increase in their inhibition indexes at higher polymer concentrations. At 0.05 mg/mL the most substituted derivative, Dod₃₀-CH-Pentyl, exhibited an inhibition percentage of around 50%. Moreover, derivatives Dod₅-CH-Pentyl and Dod₃₀-CH-Pentyl, completely inhibited the fungal growth for concentrations higher than 0.75 mg/mL. The Student t-test was applied to independent samples of Dod₅-CH-Pentyl and Dod₃₀-CH-Pentyl. At a level of significance of 0.001, the inhibition indexes were significantly different when compared to commercial and deacetylated chitosan CH, showing clearly that hydrophobic modification for these derivatives significantly increases the antifungal activity. These results can be attributed to the grafted dodecyl chains, which may favor a hydrophobic and stronger interaction with the cell membrane, blocking the transport of essential solutes into the cell or causing the formation of pores on the cell, that can lead to the leaking of the constituents of the cell [4].

CONCLUSIONS

Amphiphilic quaternary derivatives can be synthesized by nucleophilic attacks to amino groups of chitosan, which is an easy and reliable method to improve the antifungal activity of chitosan. However, in the first step the molecular weight decreases due to degradation during reaction time. The amount of hydrophobic groups attached to chitosan

chain can be controlled by setting the proportion of dodecylaldehyde in the reaction media. The antifungal activity of quaternary derivatives of chitosan against *A. Flavus* depends on the polymer concentration. The in vitro study showed that hydrophobic groups play an important role and can be adjusted to maximize antifungal activity.

ACKNOWLEDGEMENTS

Financial support by FAPESP (Grant No. 2012/03619-9), FUNDUNESP (Grant 430/09). M.T., R.O.P and J.S.G. thank FAPESP and CAPES for undergraduate fellowship. We thank David R.M.Mercer for English revision.

REFERENCES

- [1] Kumar, M. N. V. R. (2000). A review of chitin and chitosan applications. *Reactive and Functional Polymers*, 46, 1-27.
- [2] Zheng, L. Y., Zhu, J. F. (2003). Study on antimicrobial activity of chitosan with differentmolecular weights. *Carbohydrate Polymers*, 54, 527-30.
- [3] Lifeng, Q., Zirong, X., Jiang, X., Zou, X. (2004). Preparation and antibacterial activity of chitosan nanoparticles. *Carbohydr. Res.*, 339, 2693-700.
- [4] Kong, M., Chen, X. G., Xing, K., Park, H. J. (2010). Antimicrobial properties of chitosan and mode of action: A state of the art review. *Intern. J. Food Microbiology*, 144, 51-63.
- [5] Xie, Y.J., Liu, X.F., Chen, Q. (2007). Synthesis and characterization of water-soluble chitosan derivate and its antibacterial activity. *Carbohydr. Polym.*, 69, 142-7.
- [6] Sajomsang, W., Gonil, P., Saesoo, S., Ovatlarnporn, C. (2012).Antifungal property of quaternized chitosan and its derivatives. *Int. J. Biol. Macromol.*, 50(1), 263-9.
- [7] De Oliveira Pedro, R., Takaki, Gorayeb, T. C. C., Del Bianchi, V. L., Thomeo, J. C., Tiera, M. J., De Oliveira Tiera, V. A. (2012). Synthesis, characterization and antifungal activity of quaternary derivatives of chitosan on *Aspergillus flavus*. *Microbiological Res.*, Article in Press.
- [8] Roberts, G. A. F., Wang, W. (1996). Evaluation of Mark-Houwink viscosimetric constants for chitosan. In: *Advances in chitin science*. J. Domard, R. Muzzarelli, ed. pp. 279-84, Lyon: Jacques Andre.
- [9] Guo ZY, Chen R, Xing R, Liu S, Yu H, Wang P. (2006). Novel derivatives of chitosan and their antifungal activities in vitro. *Carbohydr. Res.*, 341(3), 351-4.
- [10] Tiera, M. J., Qiu, X. P., Bechaouch, S., Shi, Q., Fernandes, J. C., Winnik, F. M. (2006). Synthesis and charac-terization of phosphorylcholine-substituted chitosans soluble in physiological pH conditions. *Biomacromolecules*, 7(11), 3151-6.
- [11] De Oliveira Tiera, V. A., Tiera, M. J., Winnik, M. F. (2010). Interaction of amphiphilic derivatives of chitosan with DPPC (1,2-dipalmitoyl-sn-glycero-3-phosphocholine. *Journal of Thermal Analysis and Calorimetry*, 100, 309-13.

CHITOSAN BASED SUTURE – FOCUSING ON THE REAL ADVANTAGES OF AN OUTSTANDING BIOMATERIAL

Rivelino Montenegro^{1*}, José R. G. Godeiro²

¹ Medovent GmbH, Friedrich-Koenig-Str. 3, Mainz 55129 Germany.

² UFERSA, Univ. Fed. Rur. Semi-Arido, KM 47, BR 110, s/n, Mossoro-RN Brazil

*rivelino@medovent.com

ABSTRACT

The real advantages of a chitosan based suture can be summarized as a low inflammatory response, pain free removal and long term bacteriostatic property. An *in vivo* study in rats showed that in comparison to nylon, chitosan based suture (QiGel®) induced a lower tissue reaction with a lower number of macrophages, less fibroblast and lower deposition of collagen. QiGel® provides the option for a controlled dissolution in just few hours by applying a lower pH solution to dissolve the thread without any pain. Since chitosan is inherently bacteriostatic due to its positively charged chain, QiGel® has the advantage of a long term bacteriostatic effect. In an *in vitro* test, QiGel® provided the bacteriostatic effect for a period of time twice as long as a commercially available antibiotic loaded suture.

Keywords

Chitosan, Suture, Biocompatibility, Bacteriostatic, Dissolution

INTRODUCTION

A suture is a medical device meant to hold a wound close until the natural healing process has fully taken place. They can be made of different materials such as silk, cotton and collagen or synthetic polymers such as nylon, polyglycolic acid and many others.

Sutures exist in different sizes, from different materials and for different purposes. According to Mackenzie [1] sutures have been used since pre-historical time to reapproximate soft tissue. Chitosan has become an attractive material to be used as a suture since it shows interesting properties such as nontoxicity, biocompatibility, and biodegradability [2], moreover chitosan possesses antimicrobial activity, wound healing, hemostatic, and tissue regeneration properties [3-9].

Chitin/Chitosan sutures have been known among scientists for almost 30 years [10], but they have not been adopted by the medical community and they are basically inexistent in the market.

Since every suture must be at least biocompatible and strong enough to hold a wound close, what could be unique in a chitosan suture to differentiate it from other materials?

This paper reports the development of a chitosan based suture (QiGel®) and the evaluation of the most important advantages over the commercially available options.

MATERIALS and METHODS

Chitosan sutures

Medovent GmbH has developed a wet spinning method to produce chitosan fibers (QiGel®) that can be used as material for the production of monofilament sutures. The fibers are not chemically crosslinked and free from any toxic compound. QiGel® is produced under clean room conditions and sterilized after packaging.

***In vitro* dissolution**

On a petri dish 2 cm long chitosan fibers were placed in contact with slightly acidic solution soaked textile. Pictures were taken every hour for 5 hours.

Animal study

Thirty Wistar female rats (*Rattus norvegicus*) were used for the *in vivo* tests. The rats were 80 days old, weighting 220±12g. The animals were acclimatized at 25°C and submitted to the same conditions of handling and feeding.

The animals were distributed in two groups of 15 rats each. Group 1 corresponded to the chitosan group while group 2 corresponded to the group with a commercially available nylon suture (Ethicon). Each group was subdivided in three observation periods with 5 animals each to be sacrificed at the 3rd, 7th and 14th day.

Each animal was anesthetized with zolazepam (Zoletil®) and tiletamine chlorhydrate applying a 45mg/kg intramuscular dose. A 3 cm longitudinal cut was made through all the abdominal wall layers and sutured with a USP 4/0 suture. The animals were sacrificed using an intraperitoneal lethal dose (100mg/kg) of sodium thiopental.

The histological analysis was done on the fragments of the peritoneum fixed in 10% formaldehyde. Slides of 5µm in thickness were prepared and stained according to the hematoxiline-eosine method [11]. The density of the histological components was made by optical microscopy using an Olympus model BX51 with 400x magnification. The cell counting was done via the software Image Pro Plus, version 6.0.

***In vitro* bacteriostatic test**

In order to compare the bacteriostatic properties of a chitosan based suture (QiGel®) to a commercially available antibiotic loaded one (Vicryl® Plus – Eticon) the following test was performed: For an overnight culture 20 ml of TrypticSoyBroth-media were inoculated with a *S. carnosus* and incubated overnight at room temperature under mild shaking. The OD₅₀₀ of the overnight culture showed a value of 3.5. A 500 µl of the *S. carnosus* overnight culture were plated on a Mueller-Hinton-Agar plate pH 5.5 and put in contact with a 4 cm long suture piece overnight in the incubator at 37°C. After 24h of incubation the process was repeated with the same fibers on a new plate.

RESULTS and DISCUSSION

Lower inflammatory response

The first important advantage of a chitosan suture is its lower inflammatory response in comparison to other commercially available sutures. Biocompatibility of suture materials describes how sutures, which are foreign materials to the body, could affect surrounding tissue and how the surrounding tissues could affect the properties of sutures [12].

The normal tissue reaction to sutures has three stages, characterized by the appearance of a variety of inflammatory cells. They are [12]:

- initial infiltration of polymorphonuclear leukocytes, lymphocytes and monocytes in the first 3 to 4 days (i.e. acute response);
- occurrence of macrophages and fibroblasts from day 4 to 7 and
- beginning of maturation of fibrous connective tissue formation with chronic inflammation after the 7th day.

Bennett [13] has described that the highest tissue reactivity happen to silk and cotton sutures (non-absorbable) and to Catgut (absorbable).

It is also well known from the literature that multifilament sutures cause more inflammatory reaction than monofilament [12] and from the multifilament sutures; silk is the worst offender as already stated before.

From a biocompatibility perspective monofilaments are a better choice than multifilament sutures, especially in closing contaminated wounds. This is because not only do multifilament sutures elicit more tissue reactions, which may lessen tissue ability to deal with wound infections, but also multifilament sutures have a capillary effect that could transport microorganisms from one region of the wound to another [12].

The reason multifilament sutures generally elicit more tissue reactions than monofilament is that inflammatory cells are able to penetrate the interstitial space within a multifilament suture and invade each filament [12].

Chitosan suture is also a natural material (polysaccharide), but differently from silk, chitosan does not elicit such high inflammatory response, first because it is not a protein structure such as silk (the major constituent of silk is a fiber protein called fibroin) [12] additionally chitosan can be made in to a monofilament fiber with the required mechanical properties.

The Table 1 presents the results of the *in vivo* test where chitosan sutures induced a lower tissue reaction, with a lower number of macrophages, less fibroblast and a lower deposition of collagen when compared to a nylon monofilament.

Table 1. Density average of macrophages, fibroblasts and collagen during the wound healing of sutured peritoneum of rats. Comparison between QiGel[®] and nylon [14].

Group	Time of observation		
	3 days	7 days	14 days
	Macrophages		
Chitosan	110.45±9.89	116.12±7.69	-
Nylon	129.95±11.64	132.70±7.81	-
	Fibroblasts		
Chitosan	-	136.24±4.70	-
Nylon	-	148.42±9.00	-
	Collagen		
Chitosan	-	-	158.01±2.06
Nylon	-	-	187.97±5.55

As shown above chitosan based suture induced a lower tissue response when compared to nylon. These results also indicate a potentially smaller scar formation, which would be of great advantage in the plastic surgery sector.

Pain free removal

Biodegradable sutures do not have to be removed, but they have usually an undefined degradation time. On the other hand non-biodegradable sutures must be surgically removed. This removal is often painful.

The presence of a suture can lead to complications and in some cases even absorbable sutures must be removed. Holzheimer [15] reports 12 cases of complications with absorbable sutures, where unexpected tissue reactions were observed such as inflammation, granulation, extrusion, fistula and abscess. Some of the patients experienced healing only after the suture removal.

Chitosan sutures can be dissolved from the skin just by applying a slightly acidic solution for few hours. The Table 2 shows the time need for a full dissolution of a chitosan suture based on the pH of the solution.

Table 2. Time vs pH for complete dissolution (+) of a chitosan suture (QiGel®).

pH	Time				
	1 h	2 h	3 h	4h	5 h
5.5	-	-	-	-	+
5.0	-	-	+	+	+

This is especially advantageous in the case of sensitive patients such as children or in sensitive areas such as the face.

This dissolution property can be of great advantage since due to the normal tissue reaction, fibrous and/or epidermic tissue ingrowth into sutures may pose a problem during removal of sutures, particularly for those sutures placed through the cutaneous surface due to the ingrowth of epidermis in addition to fibrous connective tissue. This problem is particularly profound in multifilament sutures because of the available interstitial space within these sutures for tissue infiltration. The formation of a perisutural cuff due to a down growth of epidermis along the suture path has been found to be responsible for 70 to 80% of the force required to remove a suture [13, 16 - 17].

Bacteriostatic properties

Although bacteriostatic sutures (e.g. Vicryl® Plus) are known among physicians, this property is shown for a short time only, since the incorporated antibiotics diffuse away from the suture while in contact with body fluids. Chitosan, however, is inherently bacteriostatic due to its positively charged chain.

The *in vitro* bacteriostatic test show a clear inhibition zone in the case of the antibiotic loaded suture (Vicryl® Plus) as well for the chitosan based QiGel® suture (see Figure 1 A and B). The same fibers were placed again in a new plate to repeat the experiment. Now the inhibition zone from the Vicryl® Plus suture was clearly smaller than the one from the chitosan suture (see Figure 1 C and D).

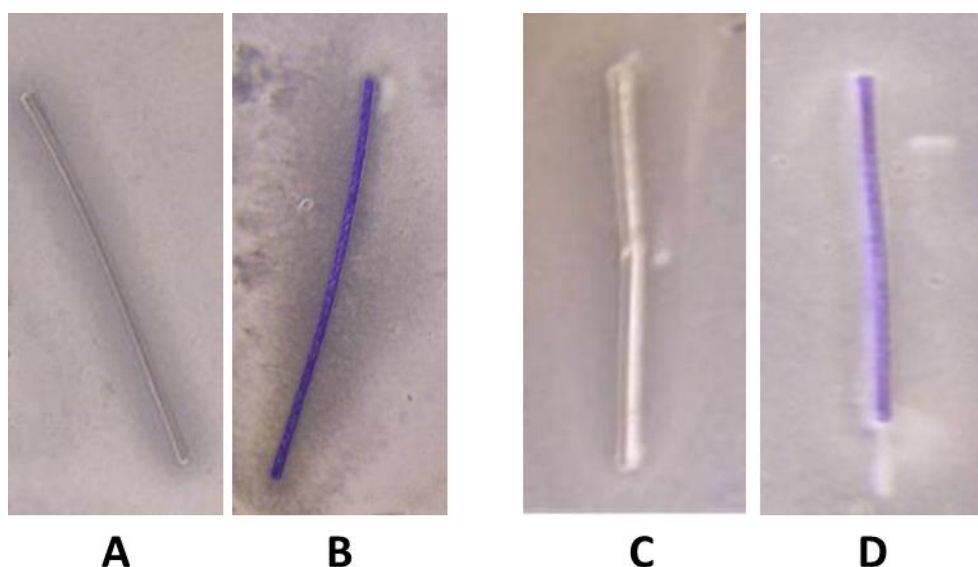


Figure 1. Bacteriostatic properties of QiGel[®] (A, C) compared to antibiotic loaded Vicryl[®] Plus (B, D). *In vitro* test against *S. carnosus*.

After a day in contact with media the antibiotics presented in the Vicryl[®] Plus suture was leached out, allowing the proliferation of bacteria on it, while chitosan keeps its inherent bacteriostatic property due to its positively charged chain, remaining bacteriostatic for a longer period of time.

Loading antibiotics in medical devices is a well know strategy, but is a short term solution [18 – 20]. The concentration of the released antibiotic will eventually drop below the minimal inhibitory concentration [21].

As demonstrated above chitosan presents real advantages in comparison to commonly used materials for the manufacture of sutures, since it shows a lower inflammatory response, a pain free removal option and a long term bacteriostatic property.

CONCLUSION

Chitosan based sutures have a great potential in medicine.

The high biocompatibility of chitosan is directly observed by the lower inflammatory response as in comparison to nylon sutures, which could potentially lead to a lower scar formation.

Due to the solubility property of chitosan in slightly acidic aqueous solutions, such sutures can be dissolved from the surface instead of removed as shown by the *in vitro* experiment. This ingenious removal process is a pain free method, different from the mechanical procedure as commonly used in the cases of non-biodegradable sutures.

Although other bacteriostatic fibers exist in the market, none of them can offer a long term protective effect, since the incorporated antibiotics will leach out quickly in contact with tissue fluids. Chitosan sutures show bacteriostatic properties for a period at least twice as long as in comparison to a commercially available suture.

As discussed in this paper, chitosan offers exceptional properties as a suture material for both veterinary and human medicine.

REFERENCES

- [1] Mackenzie, D. (1973). The history of sutures. *Med. Hist.* 17, 158-168

- [2] Felt, O., Buri P., Gurny, R. (1998). Chitosan: A unique polysaccharide for drug delivery. *Drug Dev. Ind. Pharm.* 24, 979–993.
- [3] Carlson, R. P., Taffs, R., Davison, W.M., Stewart, P. S. (2008). Anti-biofilm properties of chitosan-coated surfaces. *J. Biomater. Sci. Polymer Edn*, 19, No 8, 1035-1046.
- [4] İkinci, G., Senel, S., Akıncıbay, H., Kas, S., Ercis, S., Wilson, C.G., Hıncal, A.A. (2002). Effect of chitosan on a periodontal pathogen: *Porphyromonas gingivalis*. *Int J Pharm.* 255, 121–127.
- [5] Jumaa, M., Furkert, F.H., Müller, B.W. (2002). A new emulsion formulation with antimicrobial efficacy using chitosan. *Eur J Pharm Biopharm.* 53, 115–123.
- [6] Muzzarelli, R.A.A., Baldassare, V., Conti, F., Ferrara, P., Biagini, G., Gazzanelli, G., Vasi, V. (1988). Biological activity of chitosan: Ultrastructural study. *Biomaterials.* 9, 247–252.
- [7] Klokkevold, P.R., Lew, D.S., Ellis, D.G., Bertolami, C.N. (1991). Effect of chitosan on lingual hemostasis in rabbits. *J. Oral Maxillofac. Surg.* 49, 858–863.
- [8] Okomato, Y., Shibazaki, K., Minami, S., Matsushashi, A., Tanioka, S., Shigemasa, Y. (1995) Evaluation of chitin and chitosan on open wound healing in dogs. *J. Vet. Med. Sci.* 57, 851–854.
- [9] Lee, Y.M., Park, Y.J., Lee, S.J., Ku, Y., Han, S.B., Klokkevold, P.R., Chung, C.P. The bone regenerative effect of platelet derived growth factor-bb delivered with a chitosan/tricalcium phosphate sponge carrier. (2000). *J. Periodontol.* 71, 418–424.
- [10] Nakajima, M., Atsumi, K., Kifune, K., Miura, K., Kanamaru, H., *Jap. J. Surg.* (1986). Chitin is an effective material for sutures. 16, 418 – 424
- [11] LUNA, L.G. (1968). *Manual of histologic staining methods of the armed forces institute of pathology.* 3. ed. New York: Mc Grav Hill.
- [12] Chu, C. C., von Fraunhofer, J. A., Greisler, H. P. (1996). *Wound Closure Biomaterials and Beveices*, CRC Press.
- [13] Bennett, R. G. (1988). Selection of wound closure materials, *J. Am. Acad. Dermatol.* 18, Part 1, 619-637.
- [14] Godeiro, J. R. G. (2010). Estudo comparativo da reação tecidual induzida entre fios de nylon e quitosana em suturas no peritônio de ratos, UFERSA.
- [15] Holzheimer, R. G. (2008). Adverse events of suture. Possible interactions of biomaterials? *Eur. J. Med. Res.* 10, 521-526.
- [16] Homsey, C. A., McDonald, K. E., Akers, W. W. (1968). Surgical suture – Canine tissue interaction for six common suture types, *J. Biomed. Mater. Res.* 2, 215-230.
- [17] Freeman, B. S., Homsey, C. A., Fissette, J., Hardy, S. B. (1970). An analysis of suture withdrawal stress, *Surg. Gynecol. Obstet.* 131, 441-448.
- [18] Harris, L.G., Mead, L., Müller-Oberländer, E., Richards, R.G. (2006). Bacteria and cell cytocompatibility studies on coated medical grade titanium surfaces. *J. Biomed. Mater. Res.* 78A, 50-58.
- [19] Stigter, M., de Groot, K., Layrolle, P. (2002) Incorporation of tobramycin into biomimetic hydroxyapatite coating on titanium. *Biomaterials*, 23, 4143-4153.
- [20] Darouiche, R.O., Mansouri, M.D., Zakarevycz, D., Alsharif, A., Landon, G.C. (2007) In vivo efficacy of antimicrobial-coated devices. *J. Bone Joint Surg. Am.* 89, 792-797.
- [21] Walder, B., Pittet, D., Tramer, M.R. (2002) Prevention of bloodstream infections with central venous catheters treated with anti-infective agents depends on catheter type and insertion time: Evidence from a meta-analysis. *Infect. Control Hosp. Epidemiol.* 23, 748-756.

CHITOSAN IN BIOMEDICINE. FROM GELS TO NANOPARTICLES

Liliam Becherán¹, Michel Bocourt², Javier Pérez³, Carlos Peniche^{2*}

¹*Institute of Science and Technology of Materials, IMRE, University of Havana, Havana, Cuba.*

²*Center of Biomaterials, University of Havana, Havana, Cuba.*

³*Center of Natural Products, Faculty of Chemistry, University of Havana, Havana, Cuba.*

Email: peniche@reduniv.edu.cu

ABSTRACT

This article presents the preparation of chitosan gels and nanoparticles and illustrates their potential for drug release applications. Interpenetrated polymer networks of chitosan (CHI), polyacrylic acid (PAA) and polyacrylamide were prepared by free radical polymerization. Swelling studies showed that the water uptake of these hydrogels was highly dependent on composition and pH. The hydrogels were loaded with bovine serum albumin. Sustained protein release was observed at pH 6.8 and 7.4. The integrity of the protein released was unaffected. The hydrogels were not cytotoxic.

Chitosan nanoparticles were prepared by two routes. In the first one nanoparticles were obtained by the interpolyelectrolyte reaction between chitosan acetate and the sodium salt of PAA and alginic acid. It was found that the appropriate conditions for nanoparticle formation depend on the nature of the reacting polyelectrolytes. The CHI-PAA nanoparticles loaded with 5-fluorouracil released the drug with a pH dependent kinetics. In the second route, the preparation of self-assembled nanoparticles of α -tocopherol modified glycol chitosan and succinyl-chitosan is illustrated. The size of nanoparticles in aqueous solution ranged from 254 to 496 nm. At pH 6 the nanoparticles give sustained release of α -tocopherol with almost constant rate during the first 4-7 hours.

Keywords chitosan, hydrogel, polyelectrolyte complex, nanoparticles, drug delivery

INTRODUCTION

Chitosan, (1,4)-[2-amino-2-deoxy- β -D-glucan] is a deacetylated derivative of chitin, a natural occurring polymer. It is widely studied in pharmaceutical and biomedical fields because of its unique variety of biological properties, such as: biocompatibility, biodegradability, bioactivity, antimicrobial activity, chemiotactic action, immunoestimulating activity, mucoadhesivity and epithelial permeability[1-2]. The functional amino and hydroxyl groups in chitosan allow the preparation of chitosan derivatives with improved properties under relatively mild conditions.

One important application of chitosan is in drug delivery where its main role is to perform as a matrix for the delivery of drugs. The solubility of chitosan in diluted acid solutions allows it to produce micro/nanoparticles, films and membranes. In combination with hydrophilic polymers, chitosan hydrogels can be prepared. Because of its polycationic character, chitosan is able to form polyelectrolyte complexes with polyanions.

The aim of this article is to present some of our results on the preparation of different chitosan based systems with potential application in drug delivery: pH sensitive hydrogels obtained from the polymerization of acrylic monomers in the presence of chitosan, and nanoparticles prepared by two different routes: complex coacervation and self assembling of soluble chitosan derivatives grafted with lipophilic drugs.

CHITOSAN HYDROGELS

Hydrogels can be used to target the release of a drug or protein to a specific area of the body and simultaneously control the release kinetics due to their three-dimensional

structure. They have become popular carriers for drug delivery applications due to their biocompatibility and resemblance to biological tissues. Macromolecular hydrogels based on the intimate mixture of natural or synthetic macromolecules and polymer chains can be formed by polymerization reaction in the presence of the macromolecular template.

The most interesting systems are the result of the grafting of synthetic polymers onto polysaccharides and the formation of template interpenetrating polymeric networks (IPNs) prepared by the free radical polymerization of vinyl and acrylic monomers embedded in natural macromolecular systems including polysaccharides and proteins. In this sense, chitosan as a polymeric ionic template has been extensively used for the preparation of macromolecular templates with ionizable acrylic monomers like acrylic acid, methacrylic acid, acrylamide and several derivatives of acrylamide [3].

In this work interpenetrated polymer networks were prepared by the free radical copolymerization of acrylamide (AM) and acrylic acid (AA) in the presence of chitosan (CHI) and *N,N,N',N'*-tetramethylenebisacrylamide (MBA) as cross-linker [4]. The use of the bifunctional monomer MBA in the reacting mixture promotes the formation of a tridimensional interpenetrated polymer network reinforcing the mechanical properties of the hydrogel as well as restraining its swelling capacity.

Some hydrogels were washed in double distilled water for approximately 2 weeks to remove unreacted monomer and are named (CHI/PAA/PAM)A and others were hydrolysed with 1 mol/L sodium hydroxide solution during 3 hours and washed with double distilled water until pH 7 was reached. These are identified as (CHI/PAA/PAM)S. The compositions of the reacting mixtures for the different hydrogels prepared are shown in Table 1.

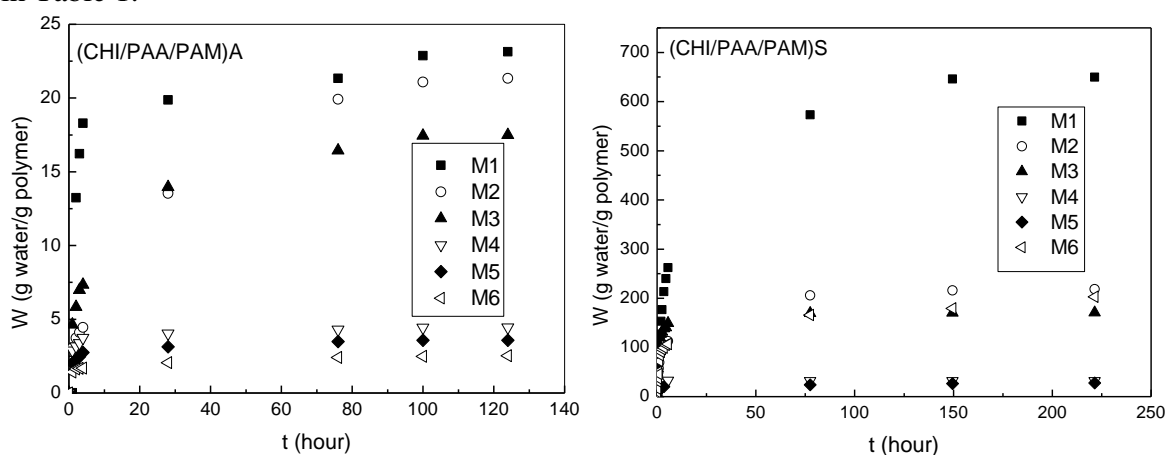


Figure 1. Swelling of CHI/PAA/PAM hydrogels in water at 37°C. The composition of hydrogels are reported in Table 1.

Swelling of (CHI/PAA/PAM)A and (CHI/PAA/PAM)S hydrogels in water was followed at 37°C for long time to ensure equilibrium. The resulting swelling curves are shown in Figure 1 and the equilibrium water uptakes for all compositions are shown in Table 1. A strong dependence of the swelling degree on composition is observed. For instance, swelling of (CHI/PAA/PAM)A hydrogels decrease as the AM/AA ratio decreases, due to the formation of hydrogen bonding between carboxylic groups in PAA and amide groups in AM. These hydrogen bonds introduce additional cross-links to the hydrogel network decreasing its swelling capacity.

During the alkaline treatment, amide groups are hydrolyzed into carboxylate ions. These negatively charged carboxylate ions are highly solvated and the repulsion between them provokes the expansion of the hydrogel network, absorbing more water than the neutral amide groups. This explains the greater swelling in water observed for (CHI/PAA/PAM)S

hydrogels in Figure 1 and Table 1. It was found that the swelling process of both hydrogels was dependent on the relaxation of chains [5]. The pH dependence of the swelling capacity of (CHI/PAA/PAM)S hydrogels was evaluated at pH 5 and pH 1.2 and the results are also reported in Table 1. Swelling of (CHI/PAA/PAM)S hydrogels is considerably higher at pH 5 than at pH 1.2 due to the dissociation of the carboxylic units of AA above pH 4.7 (pKa = 4.7).

Table 1. Swelling of hydrogels at different pH. The composition of the reaction mixtures for the preparation of (CHI/PAA/PAM) systems is indicated.

SAMPLES	AM/AA/CHI (wt-%)	(CHI/PAA/PAM)A	(CHI/PAA/PAM)S		
		Water	Water	pH=5	pH=2
M1	90/0/10	23.1±0.8	819.9	228.4	22.12
M2	80/10/10	21.3±0.6	218.6	149.0	20.69
M3	70/20/10	17.5±0.6	170.9	107.6	18.13
M4	45/45/10	4.4±0.2	32.0	27.5	12.82
M5	20/70/10	3.5±0.1	28.0	27.0	10.32
M6	0/90/10	2.52±0.1	202.8	138.5	6.25

The gels were loaded with bovine serum albumin (BSA) and the release of the protein was followed at various pH for all compositions. They are shown in Figure 2 for (CHI/PAA/PAM)S hydrogels. As expected, protein release was highly dependent on both parameters. It was verified that the loading-release process did not affect the integrity of BSA. In addition to that it was found that (CHI/PAA/PAM)S hydrogels are non-cytotoxic to human skin dermal fibroblasts [4].

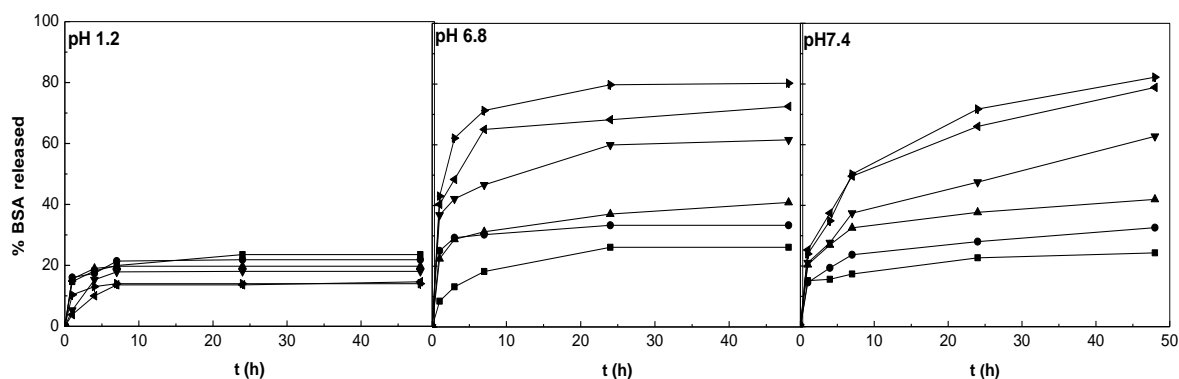
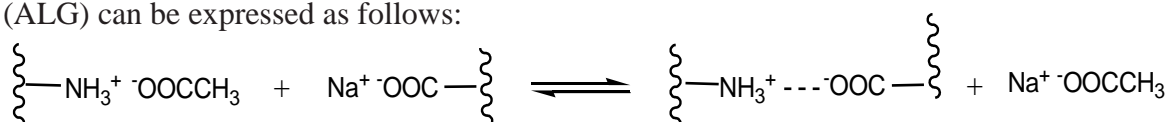


Figure 2. *In vitro* cumulative release profiles of BSA from (CHI/PAA/PAM)S hydrogels at various pH. (■) M1; (●) M2; (▲) M3; (▼) M4; (◄) M5; (►) M6.

The fact that (CHI/PAA/PAM)S hydrogels exhibited limited BSA release in simulated gastric fluid and sustained release in simulated intestinal fluids suggests that they are good candidates as matrices for colon-specific sustained protein release formulations.

CHITOSAN BASED POLYELECTROLYTE COMPLEX NANOPARTICLES

Polyelectrolyte complex formation between chitosan acetate and the sodium salt of negatively charged polyelectrolytes, such as poly(acrylic acid) (PAA) or alginic acid (ALG) can be expressed as follows:



The complex is obtained spontaneously in the form of a suspension when the reactants are mixed. There are several factors affecting the size and morphology of the particles in the suspension, such as the order of addition of the polymer solutions, the initial concentration and molar ratio of the polyelectrolytes, the stirring speed, and the pH of the starting solutions, among others. For instance, it has been reported that nanoparticles of the CHI-PAA complex are obtained when the concentrations of both polyelectrolytes are fixed at 0.02 wt-% [6]. However, considerable volumes of the solutions have to be handled in order to obtain a reasonable amount of nanoparticles. Additionally, Chen et al. reported that the best results are obtained when the molar ratio of the polymers in the reaction mixture is $n(\text{CHI}/\text{PAA})=1.25$ because excess CHI provides the particles with a net positive charge, increasing the stability of the CHI-PAA complex suspensions [7]. In our studies we have found that CHI-PAA complex nanoparticles can be obtained when mixing 0.1 wt-% solutions of both polyelectrolytes in a molar ratio $n(\text{CHI}/\text{PAA})=1.25$ and stirring at 1 300 rpm [8]. In contrast, nanometric particles of the CHI-ALG PEC were formed with 0.04 wt-% polymer solutions, molar ratio $n(\text{CHI}/\text{ALG})=1.35$ and stirring at 4 000 rpm.

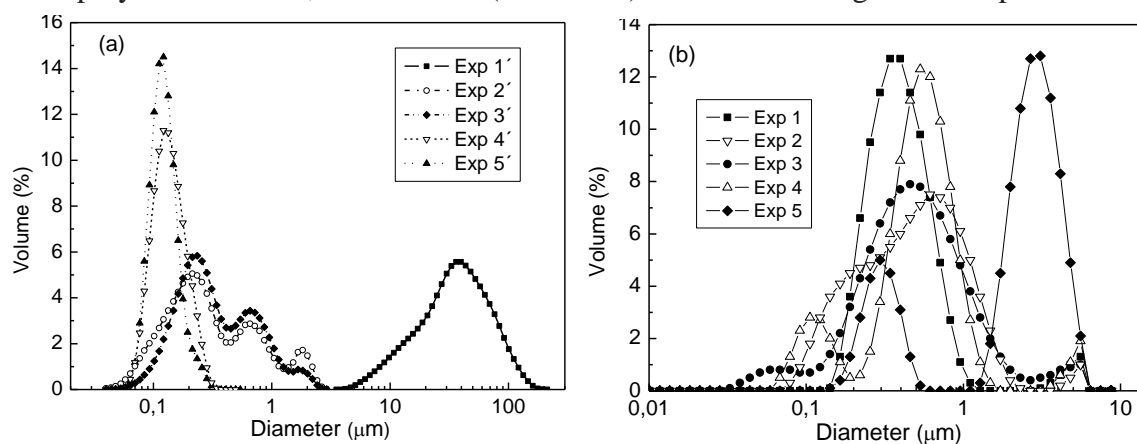


Figure 3. Dependence of complex formation on the pH. (a) CHI-PAA; (b) CHI-ALG.

The fact that CHI is a weak polybase and PAA and ALG are both weak polyacids suggests that their interaction must be strongly influenced by the degree of dissociation of both polyelectrolytes in aqueous solution, which in turn is dependent on the pH. This fact led us to study the influence of this parameter on the particle size distribution and yield of the complexes formed at different pH values of the corresponding polyelectrolyte solutions. The size distributions of the suspensions of the PECs obtained in these experiments are shown in Figure 3 and the experimental conditions as well as the mean diameters of the particles and their yield are collected in Tables 2 and 3.

Table 2. Dependence of CHI-PAA complex formation on pH.

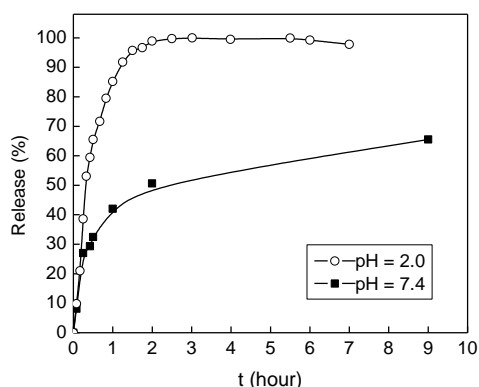
Exp.	pH			Mean diameter (μm)	Particle content < 1 μm (%)	Yield (%)
	CHI	PAA	Suspension			
1'	5.53	5.40	5.51	$44.33 \pm 0,03$	5.1	115.7
2'	5.53	3.20	5.45	$0.49 \pm 0,01$	87.4	107.4
3'	4.50	3.20	4.48	$0.477 \pm 0,008$	90.1	97.5
4'	2.87	5.40	2.98	$0.138 \pm 0,003$	100	43.6
5'	2.87	3.20	2.90	$0.149 \pm 0,005$	100	41.2

Table 3. Dependence of CHI–ALG complex formation on pH.

Exp.	pH			Mean diameter (μm)	Particle content < 1 μm (%)	ξ (mV)	Yield (%)
	CHI	ALG	Suspension				
1	3.0	3.8	3.47	0.338 ± 0.003	93 ± 4	60 ± 5	61 ± 3
2	3.0	6.5	3.24	0.327 ± 0.003	98 ± 1	47 ± 4	63 ± 2
3	4.5	3.8	4.31	0.347 ± 0.005	96 ± 3	63 ± 1	75 ± 1
4	5.8	3.8	5.68	0.460 ± 0.004	96 ± 3	43.9 ± 0.9	84 ± 4
5	5.8	6.5	6.44	0.980 ± 0.012	23 ± 2	32.2 ± 0.6	96 ± 3

As it can be seen in Tables 2 and 3, the pH of the reactant solutions had a great influence on both the particle size and the yield of the complexes formed. In fact, for both systems it is clear that the higher the pH of the resulting suspension the greater the yield of particles. The most convenient pH values of the starting solutions for obtaining CHI-PAA nanoparticles with a yield near 90 % were 4.5-5.5 for CHI and 3.2 for PAA. On the other hand, for the CHI-ALG PEC nanoparticles are obtained with CHI solutions at pH between 4.5 and 5.8 and ALG solutions at pH = 3.8. It is worth mentioning that the particle size distributions of the suspensions formed in these conditions did not vary appreciably after the suspensions were kept still for one month under atmospheric conditions at temperatures between 20 and 23°C).

Some preliminary studies were performed in order to evaluate the potential of these particles as drug delivery systems. With this purpose, CHI-PAA nanoparticles were loaded with 5-fluorouracil (5-FU), a chemotherapy agent. The release profiles in phosphate buffer at pH=2.0 and 7.4 are shown in Figure 4. At pH = 2 almost 100% of the drug had been released after 2 hours. Otherwise, at pH 7.4 only 65% of the encapsulated drug had been released after 9 hours. The results were analyzed using different mathematical models and the best results were found for a zero order kinetic behavior at acid pH ($k = 1.47 \pm 0.05$; correlation coefficient = 0.991). These results are in good agreement with the fact that, under these conditions, the CHI-PAA complex breaks down, with the subsequent dissolution of the nanoparticles. On the other hand, under basic conditions the best results were observed for the model proposed by Ritger and Peppas [9] ($k = 0.40 \pm 0.12$; $n = 0.43 \pm 0.06$; correlation coefficient = 0.979). The value of the diffusion coefficient (n) suggests that Fickian diffusion is the predominant mechanism for the release of the drug.

**Figure 4. Release profiles of 5-fluorouracil from CHI-PAA complex nanoparticles.**

SELF-ASSEMBLED CHITOSAN NANOPARTICLES

Self-assembled polymeric nanoparticles, engineered with controlled composition and defined properties, have received increasing interest recently for their potential applications in medicine, biotechnology and food chemistry, particularly as drug delivery systems and carriers [10]. These amphiphilic nanoparticles consist of a hydrophobic core, usually a long hydrocarbon chain and/or aromatic groups, shielded by a hydrophilic shell

in aqueous solution [11-12]. Chitosan is particularly promising for the preparation of these nanoassemblies, due to its aforementioned biological properties. However, the limited water solubility and precipitation of these chitosan self-aggregates restricts its practical application. Nevertheless, the use of some water soluble chitosan derivatives, such as glycol chitosan, O6-succinyl chitosan and fructose chitosan overcome this limitation.

In our studies we have used the abovementioned water soluble derivatives to prepare self-assembled chitosan nanoparticles for the sustained release of lipophilic drugs such as vitamin D2 [13], vitamin E [14] and testosterone [15]. In order to link the lipophilic drugs to the chitosan derivatives, Vitamin D2 hemisuccinate, vitamin E monoesters and testosterone hemisuccinate were synthesized by basic-catalyzed traditional esterification with dicarboxylic acids in pyridine [16].

For instance, we prepared self-assembled nanoparticles of modified glycol chitosan and succinyl-chitosan for the controlled release of α -tocopherol (vitamin E)[17]. To this end the monoesters of α -tocopherol with succinic acid (MST), maleic acid (MMT) and itaconic acid (MIT) were first obtained. The structures of DL- α -tocopheryl monoesters (MST, MIT, MMT), O6-partially succinylated chitosan (SCS) and glycol chitosan (GC) are shown in Figure 5.

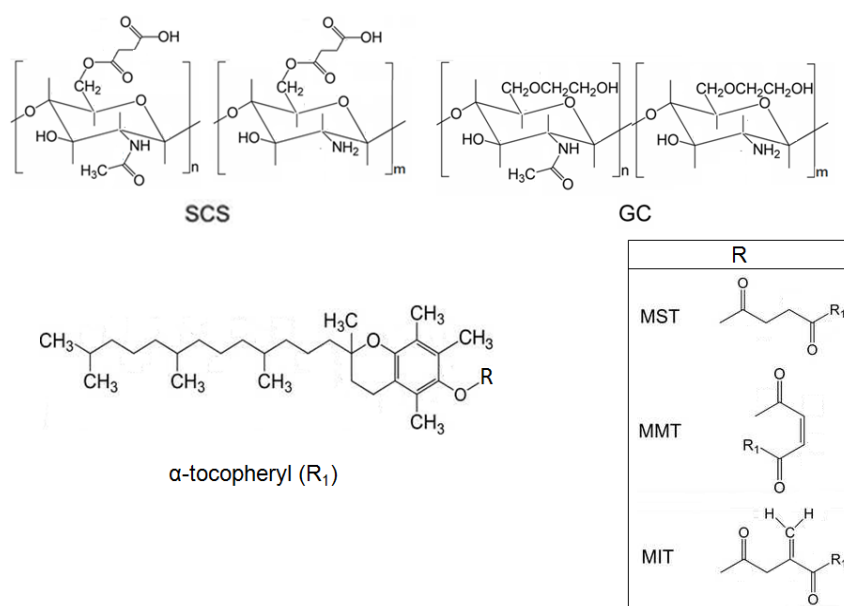


Figure 5. Structures of O6-partially succinylated chitosan (SCS), glycol chitosan (GC) and DL- α -tocopheryl monoesters (MST, MIT, MMT).

The monoesters were conjugated to the chitosan derivatives by reaction with 1-ethyl-3-(3'-dimethylaminopropyl) carbodiimide hydrochloride (EDC) and N-hydroxysuccinimide. The employed method afforded chitosan-vitamin conjugates with substitution degrees by elemental analysis of up to 22.8 mol% (GC-MST), 36.3 mol% (GC-MIT), 20.9 mol% (GC-MMT), 16.2 mol% (SCS-MST) equivalent to DL- α -tocopherol contents of 29.7 wt-% (GC-MST), 38.6 wt-% (GC-MIT), 28.1 wt-% (GC-MMT) and 27.6 wt-% (SCS-MST), respectively.

These conjugates formed nanoparticles in aqueous solution with average particles diameters by dynamic light scattering studies of 392 ± 8 nm with a PDI of 0.211 ± 0.006 (GC-MST), 284 ± 3 nm with a PDI of 0.02 ± 0.01 (GC-MIT), 496 ± 5 nm with a PDI of 0.30 ± 0.08 (GC-MMT) and 254 ± 4 nm with a PDI of 0.25 ± 0.03 (SCS-MST). These

nanoparticles were accompanied by c.a. 1-8 mol% aggregates of about 4.4-5.6 μm sizes. The SEM and TEM images of dried particles showed almost spherical shaped nanoparticles with 25-90 nm mean diameters. Zeta potential values of 18.5 ± 0.6 mV (GC-MST), 36.5 ± 0.6 mV (GC-MIT), 11.7 ± 0.4 mV (GC-MMT) and 36.3 ± 0.9 mV (SCS-MST), can be attributed to some positively charged amino groups of chitosan moieties on the surface of nanoparticles.

The *in vitro* vitamin E release profiles at $37 \pm 2^\circ\text{C}$ in PBS solution (pH = 6.0), expressed as per cent cumulative release of DL- α -tocopherol against time from tocopheryl-*N*-modified glycolchitosans and O6-partially succinylated chitosan nanoparticles are presented in Figure 6. In all cases sustained release with almost constant release rate (zero order kinetics) during the first 4-7 hours is observed. Release rate decreases in the sequence (GC-MMT) > (GC-MST) > (GC-MIT) indicating that as the substitution degree increases the particles become more compact and more resistant to hydrolysis. The greater release rate of (SCS-MST) particles compared to (GC-MIT) particles suggests that the nature of the chitosan derivative also influences release.

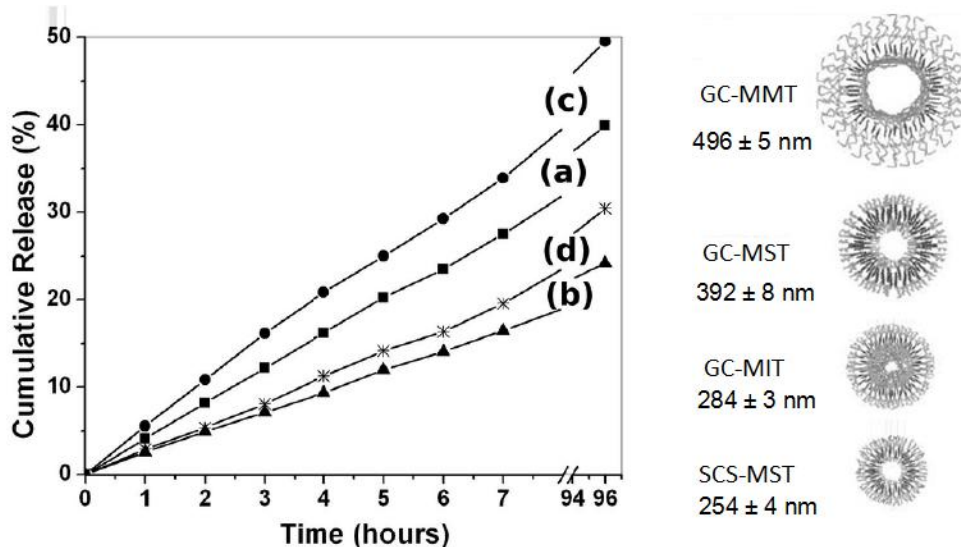


Figure 6. *In vitro* release profiles at $37 \pm 2^\circ\text{C}$ from: (a) GC-MST, (b) GC-MIT, (c) GC-MMT y (d) SCS-MST in phosphate buffer (pH = 6.0)[17]

CONCLUSION

The extraordinary biological properties of chitosan and the reactivity of the primary amino and hydroxyl groups of its chemical structure are unmatched by other polysaccharides. Therefore, the chitosan based gels and nanoparticles described in the present article exemplify only some of the enormous possibilities of this versatile polysaccharide for biomedical applications, and more specifically for developing advanced drug delivery systems.

REFERENCES

- [1] Francesko, A., Tzanov, T. (2011). Chitin, Chitosan and Derivatives for wound healing and tissue engineering. *Adv Biochem Engin/Biotechnol*, 125, 1-27.
- [2] Muzzarelli, R. A. A. (2009). Chitins and chitosans for the repair of wounded skin, nerve, cartilage and bone. *Carbohydr. Polym.*, 76, 167-82.
- [3] Bhattarai, N., Gunn, J., Zhang, M. (2010). Chitosan-based hydrogels for controlled, localized drug delivery. *Adv. Drug. Deliver. Rev.*, 62, 83-99.
- [4] Bocourt, M., Argüelles, W., Cauich, J. V., Bada, N., Peniche, C. (2011). Interpenetrated chitosan-poly(acrylic acid-co acrylamide) hydrogels. Synthesis, characterization and sustained protein release studies. *Mater. Sci. Appl.*, 2, 509-20.

- [5] Bocourt, M., Bada, N., Argüelles-Monal, W., Peniche, C. (2009). Síntesis y caracterización de redes poliméricas interpenetradas de quitosana-poli(ácido acrílico-co-acrilamida). *Rev. CENIC Ciencias Químicas*, 40, 81-8.
- [6] Hu, Y., Jiang, X., Ding, Y., Ge, H., Yuan, Y., Yang, C. (2002). Synthesis and characterization of chitosan-poly(acrylic acid) nanoparticles. *Biomaterials*, 23, 3193-201.
- [7] Chen, Q., Hu, Y., Chen, Y., Jiang, X., Yang, Y. (2005). Microstructure formation and property of chitosan-poly(acrylic acid) nanoparticles prepared by macromolecular complex. *Macromol. Biosci.*, 5, 993-1000.
- [8] Davidenko, N., Blanco, M. D., Peniche, C., Becherán, L., Guerrero, S., Teijón, J. M. (2009). Effects of different parameters on the characteristics of chitosan-poly(acrylic acid) nanoparticles obtained by the method of coacervation. *J. Appl. Polym. Sci.*, 111, 2362-71.
- [9] Ritger, P. L., Peppas, N. A. (1987). A simple equation for description of solute release. II. Fickian and anomalous release from swellable devices. *J. Control. Release*, 5, 37-42.
- [10] Chen, X., Choi, K., Choi, Y., Jeong, S. Y., Leary, J. F., Lee, D.-E. (2011). Tumor-homing photosensitizer-conjugated glycol chitosan nanoparticles for synchronous photodynamic imaging and therapy based on cellular on/off system. *Biomaterials*, 32, 4021-29.
- [11] Beheshti, N., Kjøniksen, A.-L., Knudsen, K. D., Nyström, B., Zhu, K. (2009). Rheological and structural aspects on association of hydrophobically modified polysaccharides. *Soft Matter*, 5, 1328-39.
- [12] Jing-Mou, Y., Li-Yan, Q., Yi, J., Yong-Jie, L. (2008). Self-aggregated nanoparticles of cholesterol-modified glycol chitosan conjugate: Preparation, characterization, and preliminary assessment as a new drug delivery carrier. *Eur. Polym. J.*, 44, 555-65.
- [13] Pérez-Quiñones, J., Gothelf, K. V., Kjems, J., Heras-Caballero, A. M., Schmidt, C., Peniche-Covas, C. (2012). Self-assembled nanoparticles of glycol chitosan-ergocalciferol succinate conjugate, for controlled release. *Carbohydr. Polym.*, 88, 1373-77.
- [14] Pérez-Quiñones, J., Gothelf, K. V., Kjems, J., Heras-Caballero, A. M., Schmidt, C., Peniche-Covas, C. (2013). N,O6-partially acetylated chitosan nanoparticles hydrophobically-modified for controlled release of steroids and vitamin E. *Carbohydr. Polym.*, 91, 143-51.
- [15] Pérez-Quiñones, J. P., Gothelf, K. V., Kjems, J., Heras-Caballero, A. M., Schmidt, C., Peniche-Covas, C. (2012). Novel self-assembled nanoparticles of testosterone-modified glycol chitosan and fructose chitosan for controlled release. *J. Biomater. Tissue Eng.*, (in press).
- [16] Abe, T., Hasunuma, K., Kurokawa, M. (1976). Vitamin E orotate and a method of producing the same. US: 3,944,550.
- [17] Pérez-Quiñones, J., Gothelf, K. V., Kjems, J., C. Yang, Heras-Caballero, A. M., Schmidt, C., Peniche-Covas, C. Self-assembled nanoparticles of modified-chitosan conjugates for the sustained release of DL- α -tocopherol. *Carbohydr Polym*, (*in press*),

THE BIODEGRADABILITY OF CHITOSAN FILM-COATED KRAFT PAPER SHEETS

A.B.Reis^{1*}, C.M.P. Yoshida², I. S.Melo³, T.T.Franco⁴

^{1*}UFVJM - Universidade Federal dos Vales do Jequitinhonha e Mucuri, Diamantina-MG, Brazil.

² UNIFESP - Universidade Federal de São Paulo, Diadema-SP, Brazil.

³ EMBRAPA - Laboratório de Meio Ambiente, Jaguariúna-SP, Brasil.

⁴ UNICAMP - Universidade Estadual de Campinas, Campinas-SP, Brazil.

*e-mail: arlete.reis@ufvjm.edu.br

ABSTRACT

Different recyclable materials for packaging have been studied, including cellulosic packaging such as cardboard, paperboard, kraft paper, among others. The kraft paper, the main component of making sheets of cardboard has good mechanical properties but low resistance to moisture. The use of natural polymers is an alternative to petroleum-derived polymers that can reduce industrial waste and contribute to environmental protection. The application of natural polymers in the packaging has been studied, due to the biodegradable nature of same. Among the possible biodegradable polymers can cite chitosan, which has the property of forming films and these in turn can be used as cover. This study has assessed the biodegradability of chitosan film-coated Kraft paper sheets, as well as uncoated Kraft paper sheets. In order to assess mechanical properties was tensile tests and the biodegradability, analyses on Scanning Electron Microscopy (SEM), percentage of degradation with gravimetry analysis were performed.

Keywords: Biodegradability, biopolymer, chitosan films, Kraft paper.

1 - INTRODUCTION

Paper is a biodegradable material widely applied on packaging sector and essentially comprises spontaneous crosslinks between cellulose fibers by hydrogen bondings. Kraft paper is widely used in packaging applications but its porous structure makes it highly permeable to gases and it is formed of a structural matrix that connects cellulose and non cellulose chains (hemicellulose and lignin) by H-bondings. Its low cost favors its application in the packaging sector (electronics, food, pharmaceuticals, etc.). A good example of such efforts is the packaging industry that, steadily growing in the market, prioritizes the development of new technologies intended to mitigate recycling, environmental pollution and biodegradation problems, among others. Within this context, the replacement of synthetic polymers for biopolymers is an alternative reduce the use of non-renewable materials. Biopolymers are polymers derived from natural renewable sources and are usually biodegradable and less toxic. They can be produced by biological systems or synthesized whether by chemical or enzyme catalysis [1]. In addition to presenting an alternative to polymers derived from petroleum, most of them are degraded in weeks. The biodegradability of polymers depends on the chemical and physical structure, on the chain length and on the crystalline structure [2]. The biodegradation of these polymers is usually initiated at the less crystalline parts due to the greater mobility of

polymer chains, facilitating the access of microorganisms to the substrate [3]. Factors such as light, temperature, humidity, morphologic structure of the surface, pH, among others, also influence the degradation [4];[5]. There are several biodegradable polymers; one of them is chitosan, which consists of a linear sequence of β -(1- β -4)2-acetamide-2-deoxy-D-glucose (N-acetylglucosamine) monomeric sugars and glucosamine from chitin deacetylation [6]. Chitosan is obtained from the processing of fishing industry waste by the following operations: discoloration, deproteinization and deacetylation. It is able to form resistance films, difficult to break, becoming a potential substitute for synthetic polymers in different industrial sectors, such as the packaging industry [7]. The application of chitosan as a coating on Kraft paper sheets could be an alternative to bilayer commercial systems that often use synthetic polymers as coating. Advantages are its biodegradability and recyclability, which could reduce the amount of waste, and is readily compatible with paper matrix. The combination of chitosan with paper is not new. It has been used as an additive of papermaking and for surface treatments improving the paper properties. This study has assessed the biodegradability of chitosan film-coated Kraft paper sheets as uncoated Kraft paper sheets. In order to assess mechanical properties was percentage of elongation tests and the biodegradability with gravimetry and analyses on Scanning Electron Microscopy (SEM) were performed.

2-MATERIALS AND METHODS

2.1 – Materials

Chitosan (Primex, ChitoClear®, lot TM 2227, Iceland), acetic acid (Synth, Brazil) and Kraft paper sheet having a grammage of 200g/m² (Rigesa, Brazil) were used.

2.2 – Methods

Chitosan solubilization

The chitosan filmogenic suspensions were prepared by dispersing 4.0% chitosan (w/w) in aqueous acetic acid under continuous agitation. The stoichiometric amount of acetic acid was calculated from the weight of the sample, taking account of the degree of acetylation of the chitosan (DA=18%), to achieve protonation of all the NH₂ sites. The dispersion was stirred until the chitosan was fully dissolved.

Preconditioning

Uncoated and coated Kraft paper sheets were preconditioned at 23 ± 1 °C and 50 ± 2% relative humidity before analysis, in accordance with the standard method [8].

Kraft Paper/Film Packaging Systems

Sheets of Kraft paper (0.45m²) were coated with filmogenic suspensions of chitosan equivalent to 35g/m² (each coated sheet) using a 80µm wire bar coater (TKB Ericksen, Brazil). The coated paper sheets were dried at over T=200°C for 1 minute.

2.3 - Mechanical Properties

Tensile Properties – Force and Elongation

The tensile properties were determined as specified with the standard method [9]. Uncoated and coated Kraft paper were cut into sheets with a width of 15.0 ± 0.1 mm and a length of 180.0 ± 0.1 mm, machine direction (MD) and cross direction (CD), using a guillotine (Regmed, Brazil). Tensile properties were measured by a dynamometer (Mod. D-21, Regmed, Brazil) using a 500N load cell and a speed of 20mm/min. Tensile initial grip separation was set at 180 mm. The tensile strength was expressed in kgf/15mm and elongation was calculated from the difference in distance between grips holding the samples before and after break. There were at least ten replicates per experiment.

Statistical analysis

Statistical analysis was carried out with the Statistic version 5.0 program (Statis Inc., USA) and differences between the means were detected by multiple comparison Tukey's test.

Scanning Electron Microscopy

The KCF and KC received gold deposition for three minutes under a 25,000 Ampere current and then had their structure and biofilm formation analyzed by a Gemini Leo 982 Leica Zeiss high resolution scanning microscope from the laboratory of Environmental Microbiology of *Embrapa Meio Ambiente*, under the following conditions: voltage = 10Kv; working distance = 16mm.

Gravimetric Analysis – Percentage Degradation

The gravimetric analysis consists in storing the KCF and KC samples in nylon bags. The bags were prepared containing about 0.80g of samples dried in an oven at 105°C. Then they were buried in 10cm deep common soil furrows (without treatment). The collections were performed in: 1, 3, 7, 15, 30 and 60 days. In each collection, samples were taken off the bags, dried in an oven at 105° C and weighted in a Scientech SA 210 analytical balance. The mass of samples that may have been degraded by microorganisms in soil was determined by their weight difference. The analyses were performed in triplicate and the results were expressed in grams:

4 - RESULTS and DISCUSSION

4.1 - Mechanical Properties

Tensile Properties – Elongation

The mechanical properties of bilayer Kraft paper were analyzed by elongation and maximum force at break. The tensile tests were performed on the KCF, KC, as show in Table 1. The decrease could be associated to the lower strength between fiber-fiber interactions on paper matrix, which may be partially due to the coated material impregnated into cellulose structure. The mechanical properties of chitosan-Kraft paper systems were still controlled by the cellulose fiber matrix which is dependent on the strength of fibers, their surface area and length and the bonding strength between them.

In relation to mechanical properties, the coating did not significantly change the properties of elongation of the Kraft paper sheets (Table 1).

Table 1: Mechanical properties content, maximum force and elongation at break of uncoated Kraft CF and Kraft C.

Samples	Force (Kgf/15mm)		Elongation (mm)	
	MD	CD	MD	CD
Kraft CF	19,33 ±0,94 ^a	9,05 ±1,10 ^a	3,30 ±0,21 ^a	4,09 ±1,06 ^a
Kraft C	21,11 ±1,85 ^b	10,54 ±1,41 ^b	3,74 ±0,39 ^b	4,82 ±1,25 ^{ab}

a-b Means in the same column with different superscripts differ significantly (p 0.05) according to Tukey's test.
CD - Cross direction; MD - Machine direction

4.2 - Scanning Electron Microscopy

The scanning electron microscopy analyses showed the surface of each sample (KCF and KC), whether with or without coating, in pictures taken in crescent time intervals in order to follow-up the formation of films throughout the soil microorganisms and to view bacteria colonies (Figure 1).

The greater evidence of biofilm formation was seen in the KC samples (8h), what may be related to the beginning of the paper degradation process in soil. It was possible to visualize a greater formation of bacterial cells in the KC samples after 72h, indicating that the chitosan film coating acted a substrate for the cellular reproduction, also noticed by the increase of bacterial cell formation during the collection periods when compared to the KCF samples (times: 8, 12 and 72 hours). The KC samples as the number of cells increased, the times of collection were increased. Was observed the formation of colonies of *Pseudomonas paucimobilis* bacterium in cellulose acetate films under composting process [10].

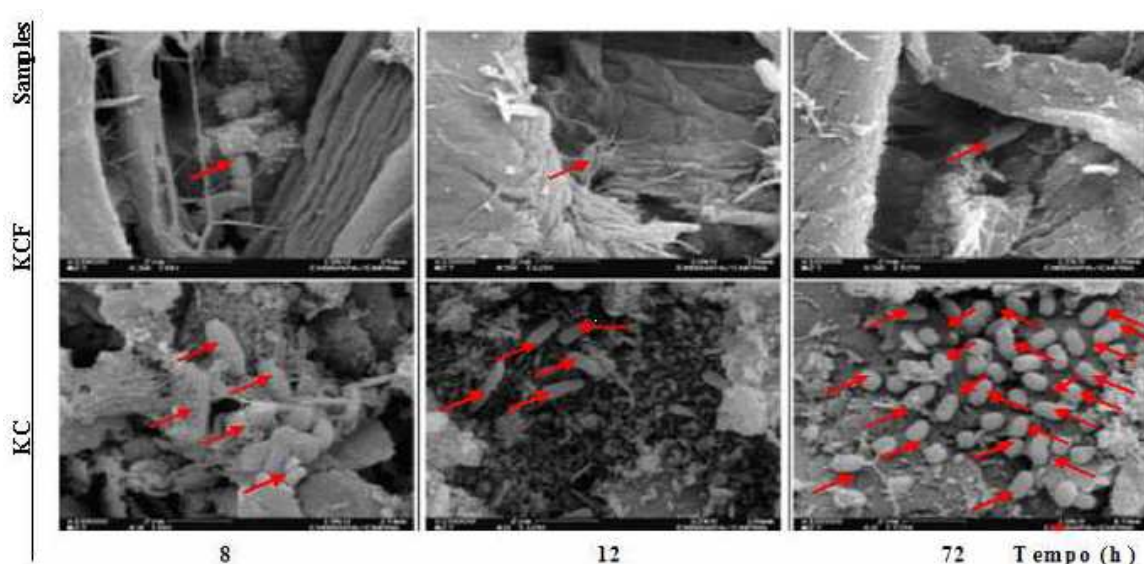


Figure 1 – SEM pictures of Kraft paper sheets: KC and KCF.

The formation of biofilms consists in a process in which a diversified and complex microorganism community is established on a surface [11].

4.3 - Gravimetric Analysis

The gravimetric analysis of soil degradation was performed based standard method [12], and consisted in the difference of mass of the samples buried in soil (initial weight) and the samples weight after a certain period (final weight). The collections were performed at: 1, 3, 7, 15, 30 and 60 days for the KC and KCF (Table 2).

It was observed in all samples the gradual reduction of masses in relation to the times of collection and even more in the degradation behavior regarding the KC and KCF samples.

Table 2 – Percentage of degradation of the KCF and KCF systems under gravimetric soil analysis.

Time (days)	% Degradation	
	Samples	
	KCF	KC
1	5.56 ± 0.07	4.72 ± 0.03
3	4.84 ± 0.02	4.96 ± 0.02
7	12.10 ± 0.04	13.94 ± 0.04
15	21.57 ± 0.01	21.52 ± 0.01
30	38.54 ± 0.06	42.80 ± 0.06
60	62.70 ± 0.02	67.63 ± 0.08

The KCF and KC samples presented increasing degradation percentage of 38, 42 and 45% in 30 days and 62, 67 and 49% in 60 days, indicating that they were degraded, however, Table 1).

The biodegradation studies in 50% chitosan and 50% nylon 11, in comparison to pure nylon 11 films. They observed that the weight loss percentage was 4 times greater for the films containing chitosan than for those of pure nylon 11. Thus, they found out that the films containing a higher chitosan percentage degraded faster within a 10-40 day period. The researchers also found out that the greater biodegradation can be caused by higher water absorption, which is a chitosan film feature [13].

5 - Conclusions

- It was possible to see in MEV analysis the formation of microbial biofilms in 8h in KC samples and during the collecting periods (3, 8, 12 and 72h) it was possible to see the gradual growth of KC, the bacterial cells when compared to the KCF samples, indicating that the chitosan film chitosan-based coatings act as a substrate to the microorganisms, inducing their growth.
- It was observed in all samples the gradual reduction of masses in relation to the times of collection and even more in the degradation behavior regarding the FQ and FAP samples. The KCF, KC samples presented increasing degradation percentage of 38, 42% in 30 days and 62, 67% in 60 days, indicating that they were degraded.
- In relation to mechanical properties, the coating did not significantly change the properties of elongation and tensile strength of the Kraft paper sheets.

6 - ACKNOWLEDGEMENTS

We thank Fapesp, CNPq, CAPES, for the financial support and EMBRAPA – *Meio Ambiente*.

7 – REFERENCES

- [1] FLIEGER, M.; KANTOROVÁ, M.; PRELL, A.; REZANKA, T.; VOTRUBA, J. Biodegradable Plastics from Renewable Sources. **Folia Microbiol.** 48 (1), 27-44, 2003.
- [1] ABNT Associação Brasileira de Normas Técnicas – Sistema Nacional de Metrologia, Normalização e Qualidade Industrial, NBR 10.004-Classificação de Resíduos Sólidos.
- [2] MASSADIER-NAGEOTTE, V., PESTRE, C., CRUARD-PRADET, T., BAYARD, R. Aerobic and anaerobic biodegradability of polymer films and physico-chemical characterization. **Polymer degradation and stability**, v.91, p.620-627, 2006.
- [3] ZUIDEVELD, M., GOTTSCHALK, C., KROPFINGER, H., THOMANN, R., RUSU, M., FREY, H. Miscibility and properties of linear poly(L-lactide)/branched poly(L-lactide) copolyester blends. **Polymer**, *on line-in press*, 2006.
- [4] SHANGGUAN, Y-Y, WANG, Y-W, WU, Q., CHEN, G-Q The mechanical properties and in vitro biodegradation and biocompatibility of UV-treated poly(3-hydroxybutyrate-co-3-hydroxyhexanoate). **Biomaterials**, v.27, p. 2349-2357, 2006.
- [5] OHTAKE, Y.; KABAYASHI, T., ASABE, H., MURAKAMI, M. Studies of biodegradation of LDPE – observation of LDPE films scattered in agricultural fields or in garden soil. **Polymer degradation and stability**, v.60, p.79-84, 1998.
- [6] MUZZARELLI, R.A.A. Chitosan-based dietary foods. **Carbohydrate Polymers**, v.29,p. 309-316, 1996.
- [7] JOHN, M.J.; THOMAS, S.; **Biofibres and biocomposites**. **Carbohydrate Polymers**, v.71.p. 343-364, 2008.
- [8] ASTM (1997) D 685-93- Conditioning paper and paper products for testing, ASTM Book of Standards, Philadelphia, PA.
- [9] ASTM (1997) D823-93- Standard test method for tensile properties of paper and paperboard using constant-rate-of-elongation apparatus, ASTM Book of Standards, Philadelphia, PA.

- [10] GU, J.-D.; McCARTY, S.P.; SMITH, G.P.; EBERIEL, D.E.; GROSS, R.A. *Polym. Mat. Sci. Eng.* V. 67, 230-231, 1992. (anotar o título deste referência)
- [11] GROSS, R.A.; GU, J.-D.; EBERIEL, D.; NELSON, M.; McCARTY, S.P. Cellulose acetate biodegradability in simulated aerobic composting and anaerobic bioreactors as well as by a bacterial isolate derived from compost. In: Kaplan, D.; Thomas, E.; Ching, C. (Eds), *Fundamentals of Biodegradable Materials and Packaging*. **Technomic Publishing Co, Lancaster, Pennsylvania**, p.257-279, 1993.
- [12] ABNT(1987)- Associação Brasileira de Normas Técnicas-NBR 10.004 – Classificação de Resíduos Sólidos.
- [13] KUO, P.C.; SAHU, D.; YU, H.H. Properties and biodegradability of chitosan/nylon 11 blending films. **Polymer Degradation and Stability**, v.91. p.3097-3102, 2006.

SYNTHESIS AND CHARACTERIZATION OF ANTIMICROBIAL CHITOSAN CO-CITRIC FILMS.

I. Corona¹, M. Gimeno², A. Tecante², J. Sepúlveda¹, K. Shirai^{1*}

¹Universidad Autónoma Metropolitana, Departamento de Biotecnología, Laboratorio de biopolímeros. Av. San Rafael Atlixco No. 186, Col. Vicentina, C.P.09340, México.

² Universidad Nacional Autónoma de México. Facultad de Química.

*E-mail address: smk@xanum.uam.mx

ABSTRACT

Non-toxic procedure to prepare chitosan co-citric acid (CCA) films by covalent attachment of chitosan has been successfully achieved using sorbitol as plasticizer. ATR-FTIR analyses on films suggested C6 carbon of the chitosan linked to C1 carbon of citric acid (CA). The characteristic peaks of CA were observed in the purified material by ¹HNMR spectroscopy, with up to 41.94% of CA incorporation onto chitosan. The mechanical properties of native chitosan films (0.07 ± 0.01 kPa) were improved with greater resistance under stress (0.46 ± 0.07kPa). Molecular functional groups migration during casting in film formation was monitored by ATR. It was also observed that CCA presented characteristic bands of amino groups, with fungistatic properties attributed to acidic pH. Finally we determined the biomasses of *P.chrysogenum* obtained with media that contained films and control (culture media), therein, biomasses obtained were significantly lower than in the control. Percentage of inhibition of 73.03 ± 4.22% and 61.13 ± 0.78% were observed for CCA and Chitosan, respectively. This inhibitory activity was confirmed with SEM analysis during the interaction of fungi to CCA and in the film.

Keywords: Chitosan films, chitosan co-citric, *Penicillium chrysogenum*.

INTRODUCTION

Chitosan-based materials present interesting bio-functional properties, such as antimicrobial ability, biodegradability and biocompatibility [1,2]. The use of polycarboxylic acids, such as citric acid (CA) for chemical chitosan modification have the advantage of a mild and nontoxic method toward extended practical uses [3,4]. In addition, CA might also promote inhibition of the microorganisms [5]. In this regard, antimicrobial activity of polycationic form chitosan is suggested to undergo by the positively charged amino group interacting with negatively charged microbial cell membranes [6], leading to the leakage of proteinaceous and other intracellular constituents of the microorganisms. According to that, the release of biocide agents, often contained in commercial bioactive food packaging, might not be required using Chitosan-based films (CBF)s and moreover, it would overcome legal issues and standards concerning migration rates of natural or synthetic agents in packaging into food products [7]. Recently, we reported a nontoxic method for covalent crosslinking of chitosan to cotton fibers using citric acid (CA) with up to 27 mg of incorporated chitosan per gram of cellulose [3]. That material was highly inhibitory, decreasing biomass and germination of spores of *Penicillium chrysogenum* and significant inhibition of *Escherichia coli*. In the present work, we have successfully established a nontoxic methodology to prepare CBFs using CA for application in food preservation. Film characterization as well as its mechanical and antimicrobial properties have been evaluated.

MATERIALS and METHODS

Chitosan was supplied from Primex ingredients ASA (grade 3 cosmetic) with medium molecular weight and 93.58% of deacetylation. CA, sorbitol and NaH₂PO₄ were supplied by

J.T. Baker (México). Acetic acid was purchased to Mallinckrodt Chemicals. In a typical procedure for our CBF formation, chitosan was dissolved in water containing CA and heated at 70 °C prior to addition of NaH₂PO₄. Then, solution was kept under stirring for 30 min. [3]. After cooling the reaction, sorbitol was added and left stirred for 12 h. Solution was placed in petri dishes of 9 cm diameter and dried at room temperature for 24 h to form films, which were heated at 60 °C until constant weight. The purification was carried out by dissolution in a phosphate buffer 0.1 M (pH 5) and precipitated in excess of cold ethanol. Then, precipitate was recovered by filtration and freeze-dried prior to chemical analysis. Infra-red spectra were directly recorded on the films using an ATR FTIR-spectrometer (Perkin Elmer 100). Each sample was registered by triplicate with 16 scans. ATR-FTIR analyses of functional groups migration was carried out following the methodology reported by Lagaron [8]. Proton nuclear magnetic resonance (¹HNMR) spectra of the samples of chitosan and chitosan-co-CA were obtained in a Bruker Advance III 500 spectrometer (Germany) at 200 MHz at 298°K using deuterated 3-(Trimethylsilyl) propionic acid as internal reference. Samples were dissolved in HCl/D₂O. DA was calculated according to earlier reports [9]. Percentage of covalent incorporation of CA onto chitosan was obtained by integration of the assigned signals on ¹H NMR spectroscopy on samples after purification from unreacted reagents. To determine mechanical properties of stress-strain, films were placed in a desiccator for conditioning following ASTM [10] at ambient temperature (23 ± 2 ° C) and relative humidity of 50 ± 5% by oversaturated solutions of Mg(NO₃)₂ for 48 h. Film thickness was measured after conditioning with a micrometer (Fowler digital micrometer 0-1") at 5 random positions for each film, four on the perimeter and one in the center. The mechanical properties were calculated considering an average thickness value. Mechanical properties were evaluated in terms of fracture strength in the puncture and fracture strength in extension in mechanical testing equipment SINTECH 1/S (MTS, USA) using clamps with a 100N load cell, varying between the two tests (puncture and extension). Force fracture puncture was determined by the method described by Gontard [11]. Samples were evaluated by triplicate. Force fracture extension was evaluated based on standard method ASTM [12]. *Penicillium chrysogenum* from Spanish culture collection (CECT 2267) was maintained in potato dextrose agar (PDA, BD Bioxon, México) at 10 °C. Spore suspension of *P. chrysogenum* was obtained in sterilized solution of Tween 80 (0.1%wt) up to a concentration of 1x10⁶ spores/mL. Biomass was determined by gravimetric method from Czapeck media agar. Subsequently, pre-weighed chitosan or chitosan-co-CA films were placed in the center of each plate. Then, plates were incubated at 30°C for 120 h. The percentage of inhibition was calculated considering the mass of control (culture media) and those with the chitosan film. SEM observations were made in a (JEOL JSM-5900LV) after 24, 72 and 120 h of treatment with inoculated *P. chrysogenum* spores on the films of chitosan-co-CA, control (culture media) and films without inoculation. For observations 0.5x0.5cm were cut in the peripheral part of the film to observe the interaction of fungi with the film.

RESULTS and DISCUSSION

The synthesis scheme of CCA is depicted in Figure 1 [3].

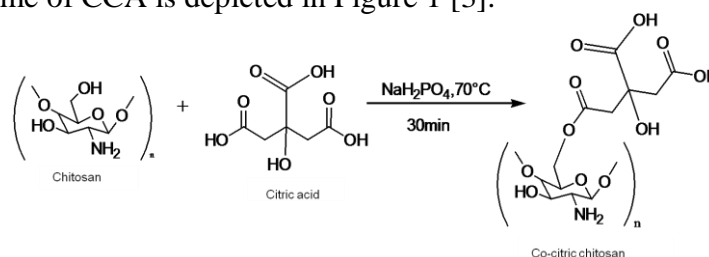


Figure 1. Proposed scheme reaction for the cross-linking of CA to chitosan using NaH₂PO₄

ATR-FTIR analysis of the CBF showed a characteristic band at $1,707.75\text{ cm}^{-1}$ (Figure 2) assigned to carbonyl stretching of the ester linkage between CA and chitosan [3]. Evidence of ester formation was also ascertained with bands at $1,186.94\text{ cm}^{-1}$ and $1,064.22\text{ cm}^{-1}$ assigned to CO-O stretching absorptions.

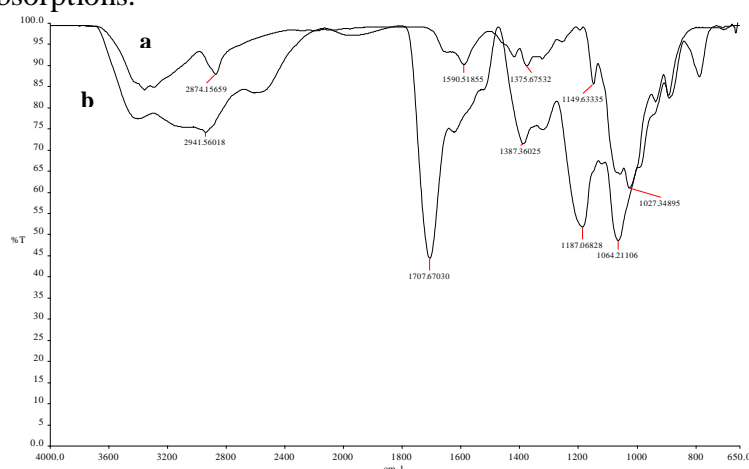


Figure 2. Infrared spectrum of film of: a) chitosan, b) chitosan co-citric.

The progress of the reaction during the formation of the chitosan-co-CA film was monitored by the ATR. CCA showed the same band assigned to water ($1,630\text{ cm}^{-1}$), which decreases as that strong band assigned to ester bond of chitosan-co-CA ($1,706\text{ cm}^{-1}$) increase. The band at $1,391\text{ cm}^{-1}$ pointed out the presence of CA (carboxyl group) (Figure 4a).

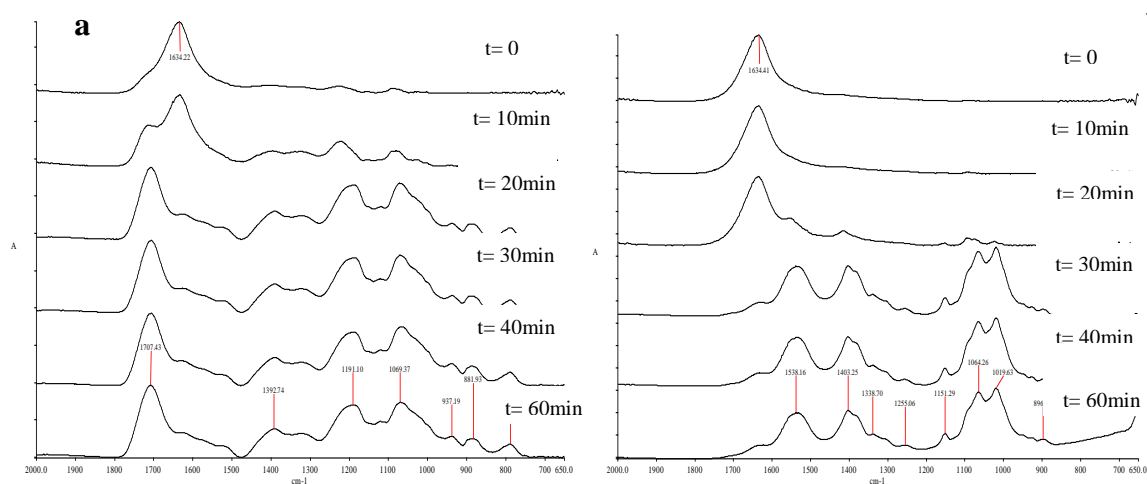


Figure 4. Infrared spectra of the formation of CCA (a) and chitosan (b) films of native chitosan.

Likewise in the case of the chitosan acetate salt the two bands at $1,186$ and $1,071\text{ cm}^{-1}$ were used as reference bands. In contrast to the spectra obtained from the chitosan acetate, the amino group is protonated to a lesser extent and even its absorption band is overlapped with water. The protonated amino group positively charged, which band appears at $1,531.9\text{ cm}^{-1}$ and that of the negatively charged carboxyl group at $1,402.9\text{ cm}^{-1}$ from the acid are responsible for the functionality of chitosan as an antimicrobial agent at pH between 8 and 5 (Figure 4b). The analyzed chitosan-co-CA seems to owe its functionality mainly to the pH decrease due to the CA, thus changing the environment for the microorganism and with a lesser extent to the protonated amino group. Purification of the cross-linked material was carried out to remove low molecular weight products and to assess the covalent linkage of CA onto chitosan. ^1H NMR spectrum of the functionalized sample after precipitation in ethanol (Figure 3) gave a molar ratio of 2.38:1 of chitosan to CA (41.94% of CA incorporation). CA

resolved into two characteristic doublets with displacements at 3.01 ppm and 2.84 ppm [13]. Integration of corresponding signals of CA with the protons of massive A of chitosan could be perfectly carried out to assess the molar incorporation of the acid on native chitosan.

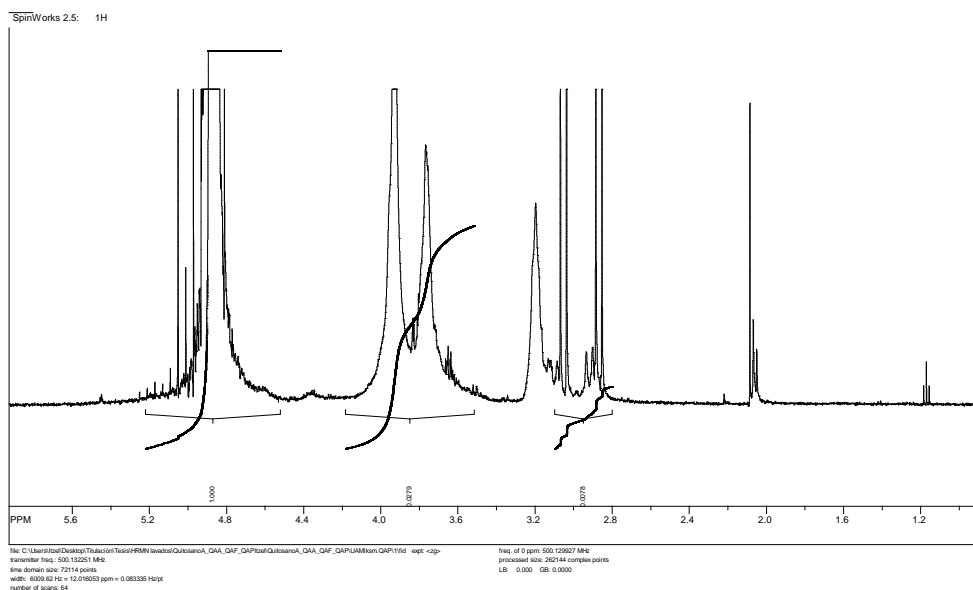


Figure 3. Chitosan-co-citric ¹H NMR spectrum.

The mechanical properties were improved and a greater force was needed to break during stress (0.46 ± 0.07 kPa) as compared to chitosan films (0.07 ± 0.01 kPa).

The antifungal activity of chitosan-co-CA films was determined on *P. chrysogenum* with films of chitosan, CCA and commercial polyethylene used as control (Figure 5a). As observed, the CCA film showed significant inhibition as compared to other treatments. Figure 5b shows the percentage of inhibition of apical growth of the fungus every 24 and for each of treatment where CCA displays a constant inhibition throughout the experiment, while the others increased the inhibition with time. Percentages of inhibition of $73.03 \pm 4.22\%$ and $61.13 \pm 0.78\%$ were observed for CCA and Chitosan, respectively.

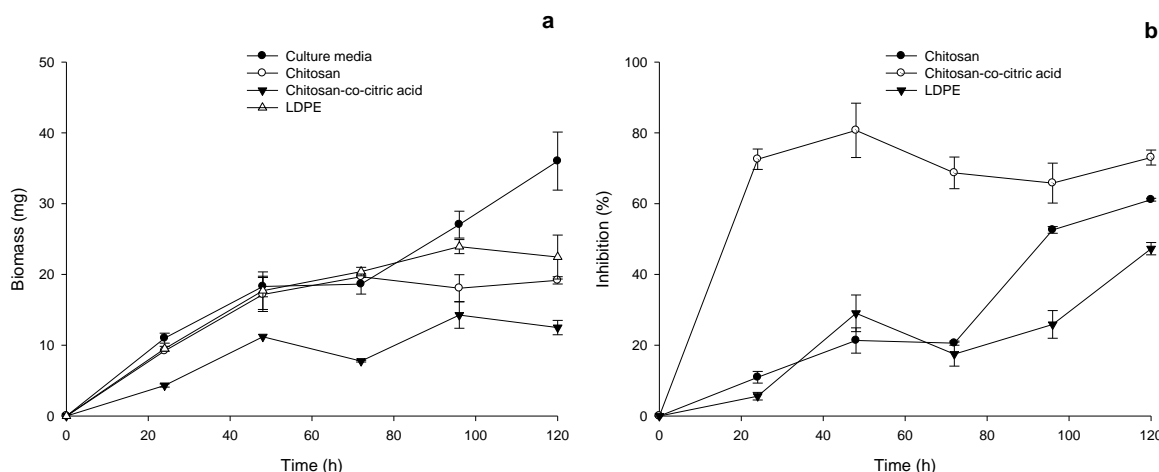


Figure 5. Kinetic of *P. chrysogenum* growth within CCA, chitosan, LDPE and culture media (a). Percent inhibition of *P. chrysogenum* within CCA, chitosan and LDPE (b).

This inhibitory activity was confirmed by SEM analysis of inoculated agar with CCA films (Figure 6a and 6b), in which the proliferation of fungi was observed in the agar (Figure 6c and 6e). Despite of spores from the surrounding (agar) invaded the film; these did not display germination or polarization (Figure 6d and 6f), thus confirming the CCA fungistatic property.

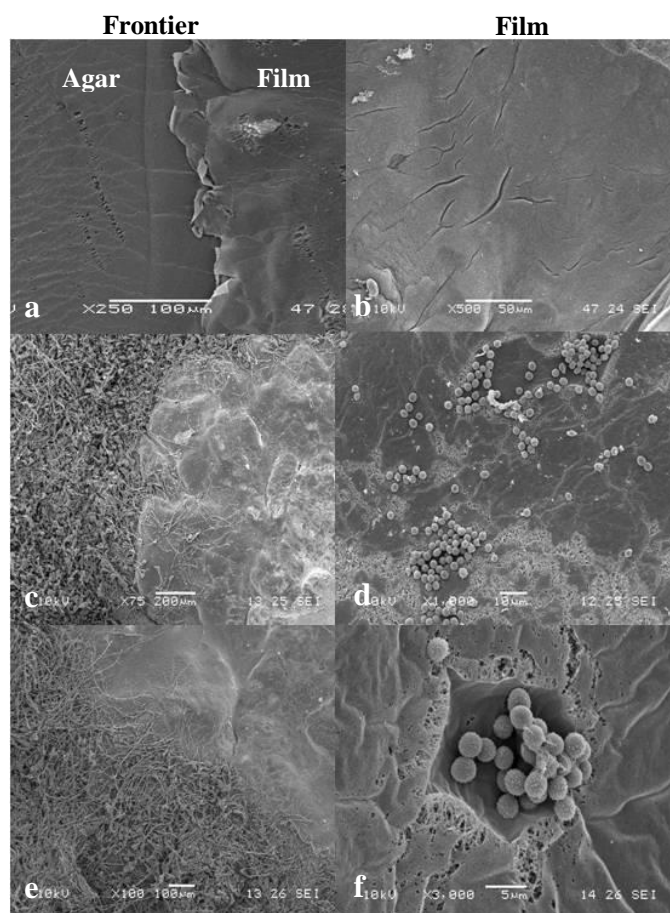


Figure 6. SEM of culture media and films of CCA inoculated with spore of *P. chrysogenum* at time of growth of: a & b) 24 h, c & d) 72 h and e & f) 120 h.

CONCLUSION

Films prepared with chitosan modified with CA showed improved physico-chemical, mechanical and fungistatic properties over its native chitosan.

ACKNOWLEDGEMENTS

The authors acknowledge the financial support from Institute of Science and Technology of Mexico City (ICyTDF) (Project no.PICSA 11-69) and to CONACYT for scholarship grant to ICJ.

REFERENCES

- [1] Park, S., Lee, B., Jung, S., Park, H. (2001). *Mater Res Bull* 36, 511-519.
- [2] Synowiecki, J., and Al-Khateeb, N. A. (2003). *Crit Rev Food Sci* 43, 145-171.
- [3] Alonso, D., Gimeno, M., Olayo, R., Vázquez-Torres, H., Sepúlveda-Sánchez, J., Shirai, K. (2009). *Carbohydr Polym* 77, 536-543.
- [4] Alonso, D., Gimeno, M., Sepúlveda, J., Shirai, K. (2010). *Carbohydr Res* 345(6), 854-859.
- [5] Nielsen, M., Arneborg, N. (2006). *Food Microbiol* 24, 101-105.
- [6] Pacheco, N., Larralde-Corona, P., Sepúlveda, J., Trombotto, S., Domard, A., Shirai, K. (2008). *Int J Biol Macromol* 43, 20-26.
- [7] Möller, H., Grelier, S., Pardon, P., Coma, V. (2004). *J Agr Food Chem.* 52, 6585-6591.
- [8] Lagaron, J., Fernandez-Saiz, P., Ocio, M. (2007). *J Agr Food Chem.* 55, 2554-2562.
- [9] Hirai, A., Odain, H., Nakajima, A. (1991). *Polym Bull* 26, 87.
- [10] ASTM D618-00 (2003). Standard practice for conditioning plastics for testing.
- [11] Gontard, N., Guilbert, S., Cuq, J. (1993). *J Food Sci* 58(1), 206-211.

[12] ASTM D882-97 (2003). Standard test method for tensile properties of thin plastic sheeting.

[13] Rodriguez, J., Erny, G., Barros, A., Esteves, V., Brandao, T., Ferreira, A., Cabrita, E., Gil, A. (2010). *Analytica Chimica Acta* 674, 166-175.

STRESS-RESPONSE OF *Aspergillus niger* EXPOSED TO CHITOSAN: COMPARISON OF THE GROWTH KINETICS MODELS IN SOLID AND LIQUID MEDIA

J.M. Velez-Haro¹, E.C. Rosas-Burgos¹, M.O. Cortez-Rocha¹, F.J. Almendariz-Tapia², M. Plascencia-Jatomea^{1*}

¹Departamento de Investigación y Posgrado en Alimentos, ²Departamento de Ingeniería Química y Metalurgia, Universidad de Sonora, Hermosillo, Sonora, México, CP 83000.

*E-mail: mplascencia@guayacan.uson.mx

ABSTRACT

Aspergillus niger is a toxigenic filamentous fungi which infest most of the agricultural products and stored food, contaminating them with mycotoxins. Chitosan have antifungal activity, which varies depending mainly on its molecular weight, degree of deacetylation, concentration, microorganism and mode of application. The aim of this work was to evaluate and compare the stress-response of *Aspergillus niger* in liquid and solid Czapek media amended with different concentrations of chitosans with different molecular weight. The effect on the spore's germination of *A. niger* was determined and the growth kinetic parameters were estimated and correlated applying logistic model. The diameter of the fungi spores and hyphae and number of branches of the terminal hyphae were also determined by image analysis. Microscopical observations and measurements shown differences ($p < 0.05$) of the antifungal activity of chitosan with respect to control. At all chitosan concentrations tested, a stronger ($p < 0.05$) inhibition was founded in Czapek liquid media with respect to Czapek agar media.

Keywords

Chitosan, *Aspergillus niger*, logistic model, morphometric.

INTRODUCTION

Fungi spoil around the 10% of the world's annual harvests and the *Aspergillus* genus, including several opportunistic pathogens, toxin producers, and industrial species, are responsible for the majority of agricultural contamination [1, 2]. *A. niger* is one of the most common species and is considered as the main cause of deterioration of several seeds, besides their potential to produce ochratoxins and human aspergillosis [3,4,5]. In addition, the emergence of fungal resistance to chemicals compounds is a serious challenge and has led to an overwhelming demand for new antimicrobial agents [6]. Chitosan exhibit inhibitory effects on the growth of microorganisms, especially plant pathogens [7]. The fungicidal activity of chitosan has been well documented both in *in vitro* and *in situ* studies [8]. In general, the action of chitosan is fungistatic, however, fungicide activity has been reported at higher polymer concentrations [9]. In this study, the antifungal effect of commercial chitosan of different molecular weights and concentrations on the stress-response of *A. niger* in liquid and solid Czapek media, were determined and compared.

MATERIALS and METHODS

Materials. Commercial chitosan (Sigma-Aldrich, USA) with molecular weights of 121.6 (Q_{LMW}), 152.6 (Q_{MMW}), and 211.3 kDa (Q_{HMW}), deacetylation degree between 75-

85%, were used. Solutions from each polymer (1.4, 2.8, 4.2 and 5.7 g/L) were prepared in 0.1 M of acetic acid and mixed with sterile Czapek liquid and solid media. Czapek media pH adjusted to 5.4 ± 0.1 was used as control (C_{ac}). A strain of *Aspergillus niger* (NRRL-3) was activated in PDA media (Difco, USA), and incubated at 25 ± 2 °C for 5 days. Spores were harvested by pouring a sterile solution of 0.1% (v/v) Tween 80 into the flask and stirring with a sterile magnetic bar for 5 min. The spore concentration of the suspension was determined using a Neubauer chamber (Brand, Germany) and adjusted at a final concentration of 1×10^5 spores/mL [10].

Antifungal assay. The spore's germination of *A. niger* in Czapek agar and broth media with added with chitosan solutions, was analyzed. In broth media, Petri dishes containing sterile cover glass were used. All plates with agar and broth media were inoculated with the spore's suspension of *A. niger* [11] incubated at 30 ± 2 °C. Fungistatic inhibition (%) was determined using Equation (1), where S_i was the percentage of spores germinating in the chitosan treatments, and S_c was the percentage of spores germinating in the control media. Each germination experiment was carried out by quadruplicate. Experimental data were adjusted to the logic model (Equation 2) to estimate the growth kinetic parameters of spore germination, where S was the percentage of germinated spores after time (t), S_0 was the initial percentage of germinated spores, S_{max} was the maximal percentage of germinated spores ($t \rightarrow \infty$), and k was the spore germination rate [12].

$$\text{Fungistatic inhibition (\%)} = 1 - [S_i/S_c] \times 100 \quad (1)$$

$$S = S_{max} / [1 + ((S_{max} - S_0) / S_0) \exp^{-kt}] \quad (2)$$

The diameters of the fungi spores (SD) and hyphae (HD), the long terminal hyphae (TH) and the number of branches (NB) was used only the chitosan solution of 5.7 g/L, determined by image analysis using Image-Pro Plus version 6.3 software (2008 Media Cybernetics Inc., USA), using an optical microscope (Olympus CX31, Japan) connected to an Infinity 1 camera (Media Cybernetics, USA), and using a 40× objective. Statistical analysis were carried out using the SPSS 17.0 (SPSS, Inc., USA) program ($p < 0.05$) and the Statistica 8.0 (2007) program was used for the estimation of the germination parameters.

RESULTS and DISCUSSION

Many cellular aspects of the apical extension of hyphae and branching in filamentous fungi are well understood, which may be linked to the growth kinetics of individual hyphae and branching mycelia on solid or liquid media [13]. The micotoxigenic effect of chitosan has mostly dealt with colony growth inhibition of plant-pathogenic fungi and the associated with ultrastructural changes in the hyphae and spores. However, as is expected, there are great variations in tolerance to chitosan between the different fungi tested [14]. *Aspergillus sp.* is the best example for chitosan resistant fungus [15], being *A. niger* one of the most studied species [9,10,12,16].

In this study, differences were observed on the spore's germinations of *A. niger* (Figure 1). In liquid media, lowest values were obtained for the three chitosans tested. Comparing with control, the spore's germination of *A. niger* decreased when the chitosan concentration increased. The biopolymer delayed the germination process (Figure 2) in both, liquid and solid media (Table 1).

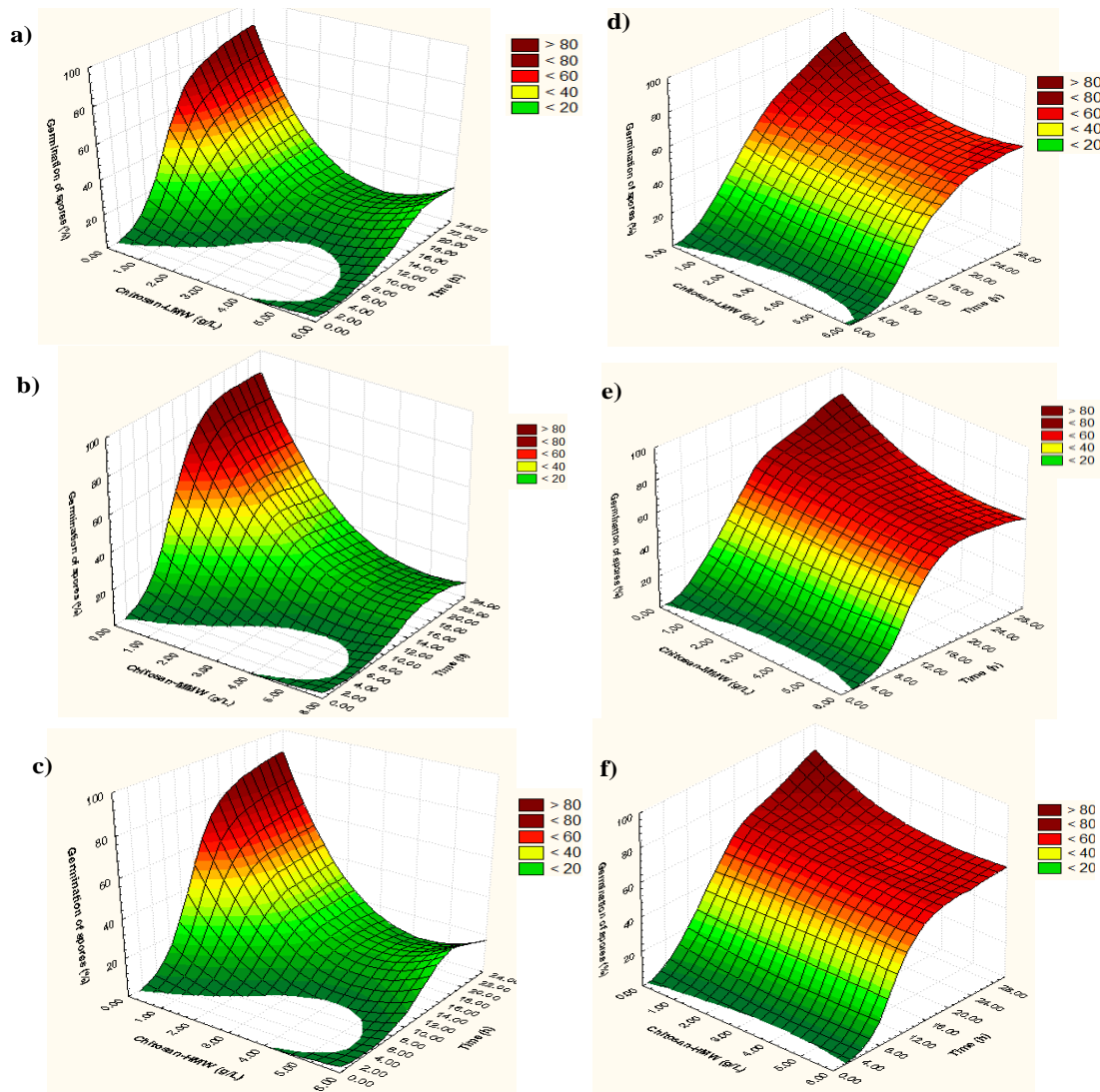


Figure 1. Effect of the chitosan concentration of Q_{LMW} (a, d), Q_{MMW} (b, e) and Q_{HMW} (c, f), on the spore germination (%) of *Aspergillus niger* in Czapek liquid (a-c) and solid (d-f) media, at 30 ± 2 °C.

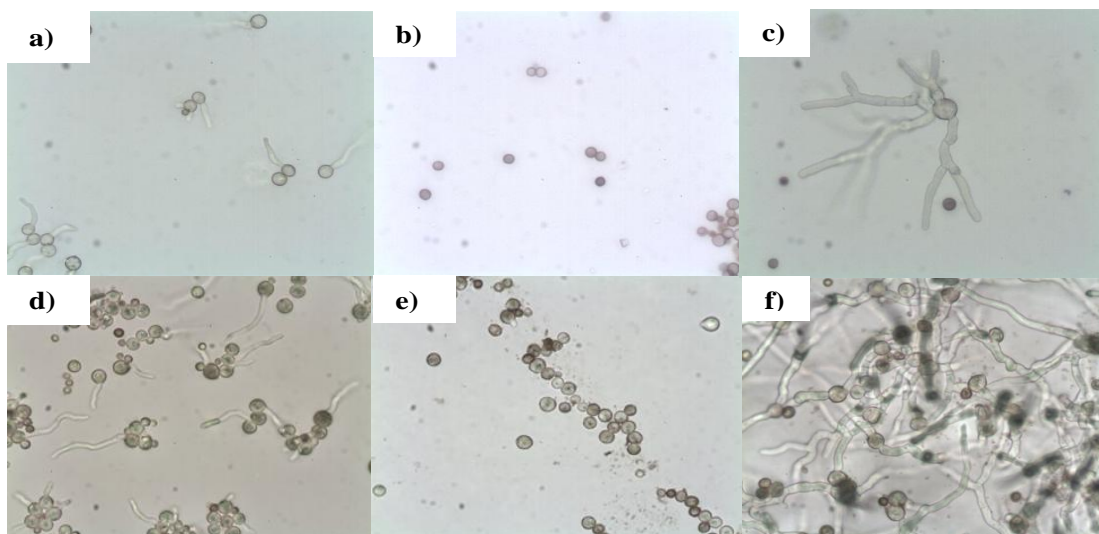


Figure 2. Observation on first hours *Aspergillus niger* grown at liquid (a-c) and solid (d-f) Czapek media with Q_{MMW} 5.7 g/L (b-c and e-f) and control (a and d), at 40x. Observation Time at: 8h (a-b, and d-e) and 20 h (c and f).

The use of mathematical models when evaluating the antifungal activity of chitosan is little reported [12,16], being evaluated mostly the effect on germination and fungal biomass. In this study, differences ($p < 0.05$) were observed in the adjusted parameters using the logistic model. In solid media, higher values ($p < 0.05$) of both S_{max} and k , were obtained.

Table 1. Spores germination parameters of *Aspergillus niger* inoculated in Czapek solid (sol) and liquid (liq) media with amended chitosan (5.7 g/L), estimated by logistic model.

Treatment (g/L)	Fungistatic inhibition (%)*	S_{max} (%)	S_0 (%)	k (h^{-1})	R^2	
C_{ac}	sol	-	80.12	2.22	0.29	0.98
	liq	-	88.63	0.00	1.26	0.99
Q_{LMW}	sol	33.17 ^a	53.05	0.00	1.10	0.98
	liq	80.28 ^a	18.14	0.00	0.75	0.85
Q_{MMW}	sol	31.64 ^a	59.48	0.00	1.19	0.99
	liq	91.60 ^b	8.76	0.00	0.93	0.96
Q_{HMW}	sol	27.83 ^a	60.48	0.00	1.22	0.99
	liq	82.97 ^a	19.01	0.00	0.94	0.92

Lowercase letters are significantly different ($P < 0.05$) between treatments of only one type of chitosan.

*: measures at: at 22h in liquid media, and 28h in solid media.

It has been reported that chitosan kill cells through the plasma membrane permeabilization, and it has been recently shown that different sensitivities to chitosan are due to different plasma membrane fluidities in different fungi [14]. Conditions that induce a faster mycelial growth also reduce sporulation; therefore spore formation occurs when the growth rate is reduced [17]. In this study we observed that the morphometry of *A. niger* is affected by the chitosan addition (Table 2). The diameter of the fungi spores and hyphae, the length of terminal hyphae, and the number of hyphae branches showed differences ($p < 0.05$) between almost all chitosan with respect to the control.

Table 2. Activity of chitosan (5.7 g/L) on morphometric parameters of *A. niger* in solid (sol) and liquid (liq) Czapek media.

Treatment (g/L)	SD (μm)*	HD (μm)*	TH (μm) ^{&}	NB ^{&}	
C_{ac}	sol	6.61 ^{aA}	3.97 ^{aAB}	32.03 ^{bA}	1.41 ^{bcB}
	liq	6.12 ^{aA}	3.33 ^{aA}	9.80 ^{aA}	1.30 ^{aA}
Q_{LMW}	sol	7.67 ^{bB}	3.97 ^{aB}	33.88 ^{bA}	1.22 ^{aAB}
	liq	7.47 ^{bB}	4.57 ^{cB}	27.88 ^{bcD}	1.89 ^{bB}
Q_{MMW}	sol	6.74 ^{aB}	3.74 ^{aA}	36.27 ^{cdA}	1.32 ^{aA}
	liq	8.36 ^{bB}	4.58 ^{bB}	21.10 ^{bcC}	1.80 ^{bC}
Q_{HMW}	sol	7.39 ^{bB}	4.03 ^{abcB}	36.73 ^{bA}	1.20 ^{aA}
	liq	8.18 ^{bB}	4.65 ^{cB}	18.57 ^{bB}	3.71 ^{cd}

Data are means of four experiments. Treatment means are significantly different ($P < 0.05$ according to Tukey test). Lowercase letters are significantly different ($P < 0.05$) between treatments of only one type of chitosan. Uppercase letters are significantly different ($P < 0.05$) between treatments of type chitosan. *: measures at: at 22h in liquid media, and 24h in solid media. &: measures at 20h both media.

Chitosan had a major effect in the first stages of the spores germination of *A. niger*. The resistance of fungi to chitosan can be attributed to the cellular composition. *A. niger* contains 10% of chitin in its cell wall [18], and 26.1% of chitosan [19].

CONCLUSIONS

This study showed the strong effect of chitosan on the first growth stages of *A. niger*. The importance of the mode of application is a determinant factor in order to evaluate the fungistatic effect of chitosan, the dosage and how to apply. Beverages, juices, and liquid or semiliquid foods can be formulated with chitosan as a preservative agent.

ACKNOWLEDGEMENTS

Projects FOMIX-Sonora No. 80891 and CONACyT No. 53494 are gratefully acknowledged.

REFERENCES

- [1] Shapiro, R. S., Robbins, N. and Cowen, L. E. (2011). Regulatory circuitry governing fungal development, drug resistance, and disease. *Microbiol. Mol. Biol. Rev.*, 75, 213-267.
- [2] Normile, D. (2010). Spoiling for a fight with mold. *Science*, 327, 807.
- [3] Meijer, M., Houbraeken, J. A., Dalhuijsen, S., et al. (2011). Growth and hydrolase profiles can be used as characteristics to distinguish *Aspergillus niger* and other black aspergilli. *Stud. Mycol.*, 69, 19-30.
- [4] Palumbo, J. D., O'Keeffe, T. L., Abbas, H. K. (2008). Microbial interactions with mycotoxigenic fungi and mycotoxins. *Toxins Reviews*, 27, 261-285.
- [5] Palencia, E. R., Hinton, D. M., and Bacon, C. W. (2010). The black *Aspergillus* species of maize and peanuts and their potential for mycotoxin production. *Toxins*, 2, 399-416.
- [6] Li, P., Zhou, C., Rayatpisheh, S., et al. (2012). Cationic peptidopolysaccharides show excellent broad-spectrum antimicrobial activities and high selectivity. *Adv. Mater.*, 24, 4130-4137.
- [7] Xia, W., Liu, P., Zhang, J., et al. (2011). Biological activities of chitosan and chitooligosaccharides. *Food Hydrocolloids*, 25, 170-179.
- [8] Bautista-Baños, S., Hernández-Lauzardo, A. N., Velázquez-del Valle, M.G., et al. (2006). Chitosan as a potential natural compound to control pre and postharvest diseases of horticultural commodities. *Crop Protection*, 25, 108-118.
- [9] Alfredsen, G., Eikenes, M., Militz, H., et al. (2004). Screening of chitosan against wood-deteriorating fungi. *Scand. J. For. Res.*, 19, 4-13.
- [10] Martínez-Camacho, A. P., Cortez-Rocha, M. O., Ezquerro-Brauer, J. M., et al. (2010). Chitosan composite films: Thermal, structural, mechanical and antifungal Properties. *Carbohydr. Polym.*, 82, 305-315.
- [11] Cota-Arriola, O., Cortez-Rocha, M. O., Rosas-Burgos, E. C., et al. (2011). Antifungal effect of chitosan on the growth of *Aspergillus parasiticus* and production of aflatoxin B1. *Polym. Int.*, 60, 937-944.
- [12] Plascencia-Jatomea, M., Viniestra, G., Olayo, R., et al. (2003). Effect of chitosan and temperature on spore germination of *Aspergillus niger*. *Macromol. Biosci.*, 3, 582-586.
- [13] Prosser, J. I. (1993). Growth kinetics of mycelial colonies and aggregates of ascomycetes. *Mycol. Res.*, 97, 513-528.
- [14] Palma-Guerrero, J., Jansson, H. B., Salinas, J., et al. (2008). Effect of chitosan on hyphal growth and spore germination of plant pathogenic and biocontrol fungi. *J. Appl. Microbiol.*, 104, 541-53.

- [15] Natarajan, V., Gnana, G. K. Sang, S. H., et al. (2009). Synthesis and characterization of potential fungicidal silver nano-sized particles and chitosan membrane containing silver particles. *Iran. Polym. J.*, 18, 383-392.
- [16] Ávila-Sosa, R., Paulo, E., Jiménez-Munguía, M.T., et al. (2011). Antifungal activity by vapor contact of essential oils added to amaranth, chitosan, or starch edible films. *Int. J. Food Microbiol.*, 153, 66-72.
- [17] Lahlali, R., Serrhini, M. N., Friel, D., et al. (2007). Predictive modelling of temperature and water activity (solutes) on the in vitro radial growth of *Botrytis cinerea* Pers. *Int J Food Microbiol.*, 114, 1-9.
- [18] Palma-Guerrero, J., Larriba, E., Güerri-Agulló, B., et al. (2010). Chitosan increases conidiation in fungal pathogens of invertebrates. *Appl. Microbiol. Biotechnol.*, 87, 2237-2245.
- [19] Kumaresapillai, N., Basha, R. A., Sathish, R. (2011). Production and evaluation of chitosan from *Aspergillus niger* MTCC strains. *Iran. J. Pharm. Res.*, 10, 553-558.

KINETIC AND ISOTHERMS STUDIES OF Cu^{+2} SORPTION USING CHITOSAN-CELLULOSE CRYOGEL

R. Garcia-Gonzalez^{1,2}, R.E. Zavala-Arce^{1*}, P. Avila-Perez³, R.M. Gomez-Espinosa², B. Garcia-Gaitan¹, F. Cortes²

¹ DEPI, Instituto Tecnológico de Toluca, Av. Tecnológico s/n Fracc. La Virgen, Metepec, Mex.

² Centro Conjunto de Investigación de Química Sustentable, UAEM-UNAM.

³ ININ, G. Ciencias Amb., Carr. Mexico-Toluca, s/n, La Marquesa Ocoyoacac, C.P.52750, Salazar, Mexico.

E-mail address: rzavala@ittoluca.edu.mx, zavalaarce@yahoo.com

ABSTRACT

The increase in the concentration of heavy metals in water bodies, attributed to industrial and agricultural activities, requires the use and development of most efficient technologies for their removal [1, 2]. The sorption is considered the most appropriate method to remove heavy metals under field conditions due to its easy operation, high removal efficiency and little or no sludge production [3]. Currently, the most used sorbents are those based on polysaccharides such as chitosan (Q) and cellulose (C), whose use has proven to be efficient [4, 5]. The cryogels can be used as sorbents, they are comprised of an interconnected macroporous network that can provide a surface area for adsorption [6-7].

The aim of this paper is to show the results of the evaluation of the sorption of Cu^{+2} in aqueous solution using cryogel chitosan-cellulose (Q-C), the kinetics and sorption isotherms were studied. The kinetics showed that maximum value reached of q_t was 20.63 mg/g. The data were adjusted to the Ho model. The adjusted data to the Langmuir and Freundlich model showed that the better fit is the Freundlich model.

Keywords

Chitosan, cellulose, cryogels, sorption, copper

INTRODUCTION

Biological methods for the removal of heavy metals have become important due to their high efficiency and low operating costs. One of these methods is biosorption, in this method natural materials are used to remove heavy metals and it is useful in industrial effluents. Natural materials that have been investigated for their low cost are: bacteria, fungi, yeasts, algae, and chitosan, and they have shown an adequate sorption capacity of heavy metals [8] [9]. In particular, chitosan (Q) is a known sorbent effective in the uptake of transition metals because the amino groups on Q chains serve as coordination sites. Chemical modifications of Q such as carboxyalkyl-substitution, aldehyde-crosslinking, ligand-crosslinking, and poly-amination are required to prevent its dissolution in acidic media ($\text{pH} < 2$) or to enhance adsorption ability, or both. This Q sorption capacity was evaluated by using powder, hydrogel, flakes, among others. A structure which is only beginning to be evaluated for this purpose is as cryogel, it has a macroporous structure that consists of "walls" of material, which was initially dissolved in the aqueous phase, and after that, a drying process surrounds empty areas that previously resided in the ice crystals. Therefore the aim of this study was to evaluate the sorption capacity of a cryogel Cu^{+2} synthesized from cellulose (C) and Q at 30 ° C.

MATERIALS AND METHODS

The cryogel was synthesized procedure described by Garcia [6]. The chitosan (deacetylation 75%), cellulose and ethylene glycol diglycidyl ether were purchased from Sigma Aldrich. Cu^{+2} standard solution (1000 mg/L), and acetic acid were obtained by Merck. The reagents were used without further purification. The orbital shaker Unimax Heidolph mark 1010 was used.

Adsorption experiments

Sorption experiments of copper ions were performed in a batch system with two replicates at a temperature of 30 °C and initial pH of 6, without controlling the pH.

Sorption kinetics experiments

0.170 g of Q-C cryogel was added to the solution of Cu^{+2} of 20 mg/L as initial concentration. The solution was stirred at 150 rpm at 30°C for 5 minutes to 48 hours. Then, the supernatant was filtered and was adding 10 μL of HNO_3 . The adjustment of atomic absorption results followed Lagergren (Equation 1) and Ho (Equation 2) models.

$$\log(q_e - q_t) = \log(q_e) - \frac{k_1}{2.303} t \quad 1$$

$$\frac{t}{q_t} = \frac{1}{k_2 q_e^2} + \frac{1}{q_e} t \quad 2$$

Equilibrium sorption experiments

The experiments were performed with solutions of concentrations 1, 4, 8, 12, 16, 20 mg/L of Cu^{+2} and 0.170 g of Q-C cryogel was added to each solution of Cu^{+2} . The solutions were stirred at 150 rpm at 30°C for 5 minutes to 48 hours. Then, the supernatant was filtered and was adding 10 μL of HNO_3 on each experiment. The atomic absorption data were fit to Lagmuir and Freundlich models (Equation 3 and 4).

$$q_e = \frac{q_{e,\text{máx}} b C_e}{1 + b C_e} \quad 3$$

$$q_e = k_f C_e^{\frac{1}{n}} \quad 4$$

RESULTS and DISCUSSION

The sorption kinetics experiments

The kinetics experiments show the equilibrium of maximum adsorption capacity of Cu^{+2} on the cryogels. Besides, the adsorption behavior of Cu^{+2} was analyzed using a theoretical model. Figure 1 shows the kinetics of copper at 30 °C, the remotion values increase during the first 300 minutes, having the value of q_t of 17.78 mg/g, this value tends to stabilize during the next 120 min; however, the sorption of copper increases until a maximum value of q_t of 20.63 mg/g at 720 min.

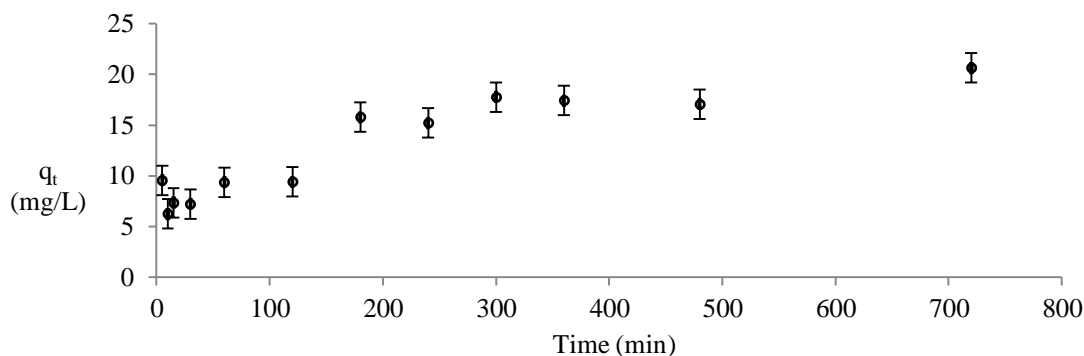


Figure 1. Sorption kinetics of copper at 30 ° C.

Figure 2 shows the values adjusted to the Lagergren model, applied to the kinetics at 30 ° C, which shows that only values between 10 and 60 minutes correspond to a straight line as shown in Figure 3a, so that these values were used to obtain the rate constant k1 pseudo first order (min⁻¹), as shown in Table 1.

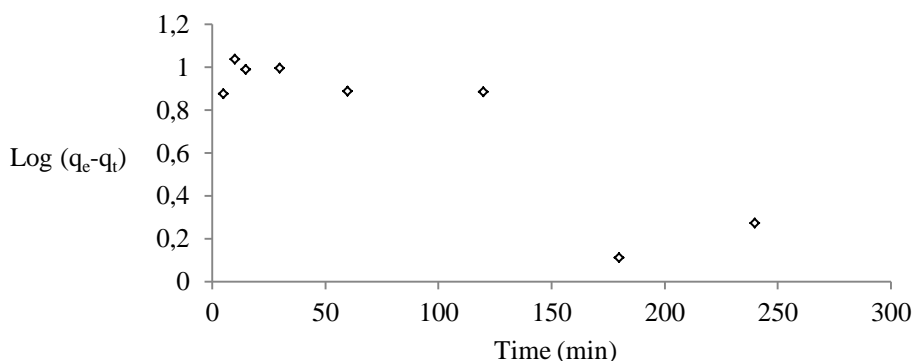


Figure 2. Pseudo-first order model applied to copper at 30 ° C.

Figure 3b shows the set values of the model Ho for the pseudo second order kinetics at 30 ° C for the values between 5 and 720 min, could be obtained the pseudo-rate constant second order k2 (min⁻¹), according to the Table 1.

It is also noted that the pattern of the kinetic of pseudo second order reproduces well the experimental results with a correlation coefficient of 0.97 and a maximum sorption capacity of 20.8 mg/g.

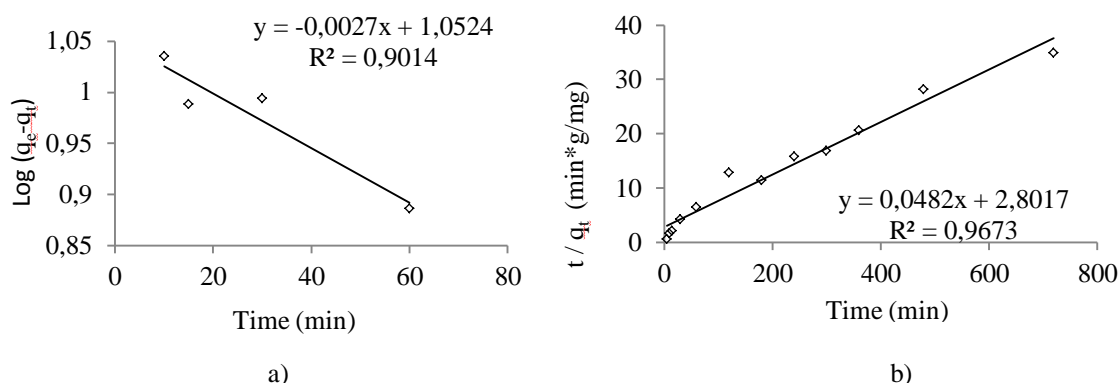


Figure 3. Experimental data fitting of adsorption kinetics at 30 ° C to kinetic models a) pseudo first order and b) pseudo second order.

Table 1. Summary of the kinetic models applied to the kinetics at 30 ° C

Model	Parameters	Values at 30 ° C
Pseudo first order (Lagergren)	r^2	0.90
	k_1	0.0062 min ⁻¹
	q_e	11.3 mg g ⁻¹
Pseudo second order (Ho)	r^2	0.97
	k_2	0.0014 g mg ⁻¹ min ⁻¹
	q_e	22.4 mg g ⁻¹

Sorption equilibrium experiments

Figure 4 shows the behavior of the copper adsorption capacity, q_e (mg copper/gcryogel) versus the equilibrium concentration of copper in the aqueous phase, C_e (mg/L of copper). This figure shows that the behavior of the isotherm corresponds to a type IV isotherm according to the classification established by ISO 15901-2:2006. According to this classification this isotherm is characteristic of mesoporous solids and is characterized by a hysteresis loop due to its porous network properties, so it is considered that stops growing near the saturation concentration. However, the Q-C cryogel can adsorb another monomolecular layer of copper on the surface.

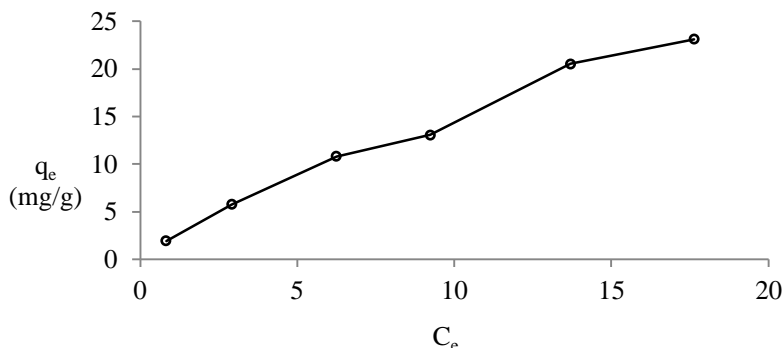


Figure 4. Sorption isotherm of Cu²⁺ on QC cryogel at 30 ° C.

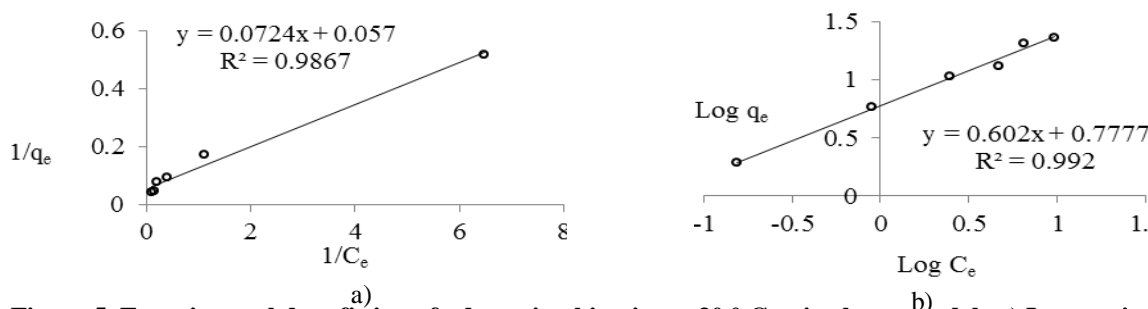


Figure 5. Experimental data fitting of adsorption kinetics at 30 ° C to isotherm models a) Langmuir and b) Freundlich.

Figure 5 shows the experimental data settings of the sorption isotherm of Cu^{+2} at 30°C to Langmuir and Freundlich models.

According to data observed in Figure 5 the two models give a good correlation value and the Table 2 shows the summary of the values obtained for the parameters of these models.

Table 2 Summary of the models applied to the isotherm at 30°C .

Model	Equation	Parameters
		$r^2 = 0.986$
Langmuir	$q_e = \frac{q_{e,max} b C_e}{1 + b C_e}$	$q_{e,max} = 17.5 \text{ mg g}^{-1}$ $b = 0.787 \text{ L mg}^{-1}$
		$r^2 = 0.992$
Freundlich	$q_e = K_F C_e^{\frac{1}{n}}$	$K_F = 5.9 (\text{mg g}^{-1})(\text{L mg}^{-1})^{1/n}$ $n = 1.7$

Comparing the value of the correlation coefficients reported in Table 2, shown that in both models reproduced the experimental results of the isotherm at 30°C in an acceptable way, but Freundlich is the model that best describes the balance between copper ions and the Q-C cryogel with a correlation coefficient of 0.992. The values K_F and n (Freundlich constants) involving the biosorbent affinity for the metal ions and the adsorption strength respectively, show affinity of the biomass for the copper, since n values were higher than 1.0, so that the sorption of the metal in the cryogel is strong [10], which represents a favorable sorption [11].

4. CONCLUSIONS

Based on the results obtained in experiments of kinetics and equilibrium sorption we can conclude: The equilibrium time of contact between Q-C cryogel and Cu^{+2} aqueous solution, have to be at least of 600 min. The kinetic model of the pseudo second order is the best model that reproduced the experimental kinetic results at 30°C . This model proposes that the mechanism for the sorption is chemical. In the sorption equilibrium experiments conducted at 30°C , it was observed that the Freundlich model is the best model that describes the data, an affinity coefficient was obtained of $K_F = 5.9$ and q_{max} of 23,100 mg/g. Then, Freundlich model is an empirical model that considers the material has a heterogeneous surface [12].

ACKNOWLEDGEMENTS

We thank to ITT, ININ and acknowledge financial support by 2342.09-P project DGEST and 241364 scholarship CONACYT.

REFERENCES

- [1] Prasad, M., Saxena, S., Amritphale, S. (2002). Adsorption models for sorption of zinc on francolite mineral. *Ind. Eng. Chem Res.* 41 (1), 105.
- [2] Reddad, Z., Gerente, C., Andres, and., Le Cloirec, P. (2002). Adsorption of several metal ions onto a low-cost biosorbent kinetics and equilibrium studies. *Env. Sci and Tech*, 36, 2067.
- [3] Kannan, N. y Rengasamy, G.(2005). Comparison of cadmium ion adsorption on various activated carbons. *Wat, Air, and Soil Poll.* 163, 185.
- [4] Ho, Y. S., McKay, G. (1999). The sorption of lead (II) ions on peat. *Wat Res.* 33 (2), 578.
- [5] Li N. y Bai R. (2004). Copper adsorption on chitosan–cellulose hydrogel beads: behavior and mechanisms. *Sep and Purif Tech.* 42, 237.
- [6] Garcia, G. R. (2011). Synthesis and characterization of a quitosan and cellulose cryogel. Master Degree Thesis. Instituto Tecnológico de Toluca, Mexico.
- [7] Wang X., Chung S. C., Lyoo W. S. y Byug G. M. (2006). Preparation and properties of chitosan/polyvinyl alcohol blend foams for copper adsorption. *Pol International.* 5,1230.
- [8] Ho, Y. S., McKay, G. The sorption of lead (II) ions on peat. *Water Research.* 32 (2). 1999.
- [9] Vijayaraghavan, K., Palanivelu, K., Velan, M. (2006). Biosorption of copper (II) and cobalt (II) from aqueous solutions by crab and shell particles. *Biores Tech.* 97.
- [10] Sanchez T. E. L, Garza G. M. T., Almaguer C. V., Saenz T. I. C., Liñan M. A. (2008). Kinetic study and sorption isotherms of Ni(II) and Zn(II) sorption using *Chlorella* sp. biomass. *CIENCIA UANL.* 118.
- [11] El-Sayed G O, Dessouki H A, Ibrahim S S.(2010). Biosorption of Ni (II) and Cd (II) ions from aqueous solutions onto rice straw. *Chem Sci J, CSJ-9.*
- [12] Smith. J. M. (1991). *Chemistry kinetics engineering.* COMPAÑIA EDITORIAL CONTINENTAL, S. A. DE C. V.

MELON PRODUCTION (*Cucumis melo* L.) AS AFFECTED BY SOIL APPLICATIONS OF CHITOSAN OLIGOMERS UNDER VARYING LEVELS OF IRRIGATION

C. A. Pérez-Cabrera¹, H. Ortega-Ortiz^{1*}, E. Treviño-López¹, M. Cabrera-De la Fuente², A. Benavides-Mendoza², E. De la Cruz-Lázaro³

¹Centro de Investigación en Química Aplicada Enrique Reyna #140, CP 25294, Saltillo, Coahuila, México. Tel. +52 844 438 98 30.

²Universidad Autónoma Agraria Antonio Narro. Calzada Antonio Narro 1923. CP 25315, Buenavista, Saltillo, Coahuila, México.

³División Académica de Ciencias Agropecuarias. Universidad Juárez Autónoma de Tabasco. Carretera Villahermosa-Teapa. Km 25. R/A La Huasteca. Centro, Tabasco, México.

*E-mail address: hortensia.ortega@ciqa.edu.mx

ABSTRACT

The effect of chitosan oligomers (CsO) on yield of melon plants (*Cucumis melo* L.) grown in the open field was studied. Plants were irrigated with varying levels of irrigation: 100%, 75%, 50% and 25%, totaling 4.25, 3.56, 2.82 and 2.07 m³, respectively, during a growing season of 91 days. Treatments consisted of a control with not CsO and three CsO treatments with different viscometric molecular weights (CsO1, CsO2, and CsO3). Chitosan oligomers were applied six times to the soil during the growing season. The CsO influenced positively melon production with different irrigation treatments. Plants with CsO3 recorded the highest total fruit production when soil irrigation was 25%, while at 50% the highest yield was obtained with CsO2; however to increase the irrigation to 75% the control treatment (t0) exceeded the effect of CsO. Even when plants were provided with 100% irrigation, the CsO1 and CsO2 were associated with the highest yield compared with t0. For °Brix and fruit hardness no significant effect were detected.

Keywords

Cucumis melo, chitosan oligomers, levels of irrigation, production, open field.

INTRODUCTION

Mexican muskmelon is a widely acknowledged produce that has maintained a consistent acceptance in the international market for its excellent quality. The main muskmelon grower in the world is China with 63% of global production with over 14 million tons per year; the United States produces over one million tons; and Mexico is ranked in the eleventh place. In Mexico, the main type of cultivated muskmelon is Cantaloupe, as in 2005 491,164.32 tons were produced, the second place with 39,781 t is the Valencian type and the third place is the Honey dew type with 137 tons [1]. Nutrition of muskmelon plants is of foremost importance in order to obtain a high quality and yield of fruits. Nutrient deficiencies are responsible for a reduction of 50% of yield and 70% of fruit quality [2]. Fertilization also affects plant susceptibility to pests and diseases, a factor that also affects the yield and quality. Besides the appearance of stress during the phenological stages of flowering, maturity fruit and fruit development, causing a sharp reduction in the number of fruits due to a sharp fall them. Water stress can inhibit photosynthesis, reducing contribution of carbohydrates to fruit and thereby stopping its

growth [3]. Different chitosan derivatives have been implicated in the induction of resistance to insect attack and pathogens, mainly through the jasmonate pathway, which is also involved in the response to water stress. [4] So far the information that are available on signaling with polyacrylic acid-chitosan complexes is only doing by our working group, with the most significant results which are detailed below. The hypothesis of the physiological effect of the complexes was verified by demonstrating that in the tomato the presence of chitosan complexes activate two of antioxidant enzymes (catalases and peroxidases) associated with abiotic stress tolerance [5]. Application of chitosan-polyacrylic acid complex with PAA of lower molecular weight (106,000) increases a 40% the growth of plants of lettuce (*Lactuca sativa L.* var. Great Lakes) and onion (*snow ball*) under conditions of high salinity [6, 7]. The objective of this study is to determine the effect of different molecular weights of the chitosan oligomers applied on the soil under melon production in open field and four levels of moisture.

MATERIALS and METHODS

The experiment was conducted in the spring-summer of 2011 in the experimental field of the Research Center for Applied Chemistry (CIQA) in Saltillo Coahuila, between the geographical coordinates of 25° 27' N latitude, 101° 02' longitude West of the Greenwich meridian and at a height of 1610 m above sea level.

Soil preparation and seeding

In March 2011 there were four beds that were used for the culture with application of chitosan oligomers (CsO) via soil, on March 18 of that year was the black plastic mulch to beds and the same day was planting the crop melon cv. Muskmelon F1 Hybrid trading house SAKATA. The seeding was being planted directly in the open one seed per hole. The distance between beds was 1.8 m and the distance between plants was 0.30 m.

Fertigation, pest and disease control

The irrigation system used was drip cintilla NETA FIM caliber 6000 with a dropper expense of 0.91 L/h, the first irrigation was applied the next day after planting (DAP) during four hours to all treatments. Fertilization was 178-85-221-120-25 of N, P, K, Ca and Mg kg per hectare respectively; micronutrients were added with Multi Poliquel (GBM). The control of pests and diseases was done with products such as dimethoate, imidacloprid, 1-2 mL/ L of water to whitefly (*Bemisia tabaci* sp), aphids (*Aphis gossypii*). With copper-based products 1mL/ L of water to control blights; early blight and late blight (*Alternaria solani* and *Phytophthora infest*) as it was the presence of these entomopathogenic cultivation, in addition to the presence of nematodes in soil not be able to control and damage to the ripe melon by rats or rabbits.

Chitosan Oligomers

The oligomers of chitosan used in this experiment were obtained enzymatically from the chitosan commercial of high molecular weight, brand Marine Chemicals India in CIQA, to which were determined by viscosimetric molecular weight (M_v) and the degree of deacetylation by infrared spectroscopy: Oligomer 1 (CsO1) with $M_v = 12,000$; Oligomer 2 (CsO2) with $M_v = 8,000$ and the Oligomer 3 (CsO3) with $M_v = 5,000$ and all of them with degree of deacetylation close to 100%. Chitosan oligomers solutions were prepared by dissolving it in 1% acetic acid at a temperature of 50°C for one hour and then was do the dilution 1:10 with distilled water to obtain the end use solution.

Treatments

The first application of CsO via soil was at 19 days after planting (DAP) and later applications were every 14 days (33, 47, 61, 75 and 89 DAP) carried out a total of six

applications of chitosan oligomers during the cultivation cycle (Table 1). Water stress began to apply when the melon plants were 27 days after emergence. The amount of water applied in all the cultivation cycle for the treatment of 100% irrigation was 4,258.80 L, whereas treatment with 75%, 50% and 25% the irrigation applied to cultivation melon to soil was 3564.00 L, 2066.4 L and 2815.20 L respectively, with a growing season of 91 days.

Table 1. Distribution of treatments with the application of chitosan oligomers (CsO) via soil with varying levels of irrigation.

100	75	50	25
CsO1	CsO3	CsO2	CsO1
T0	CsO2	T0	CsO3
CsO2	T0	CsO3	CsO2
CsO3	CsO1	CsO1	T0

Harvest

The first cut of the fruit was carried out on June 9, 2011 at 83 DDS, treatments were harvested separately to make the fruit quality analysis ($^{\circ}$ Brix and firmness). Harvest was completed on 17 of the same month at 91 DAP. Throughout the cycle were made 5 cuts.

Experimental design

This work was set with a split plot design with randomized complete block design, with 16 treatments and 7 repetitions, taking a plant as experimental unit, with a total of 112 plants in the field. The data obtained were subjected to statistical analysis using analysis of variance ANOVA and comparison of means according to the multiple range test of Tukey ($p \leq 0.05$) using the Statistical Analysis Systems (SAS) version 9.0.

Production variables

At the end of the experiment at 91 DAP sampling was applied destructive end to make determinations that are recorded immediately.

Foliar area: This variable was determined with the foliar area meter brand LICOR 3100 that passing the leaves of the plants by the meter displays data directly in cm^2 .

Biomass sampling was conducted only at the end of the experiment, plant leaves were dried in an oven at 60°C for 48 hours. Then weighed and the results expressed in g.planta^{-1} .

Polar diameter of fruit. We measured the circumference of the fruit when it was in a state of maturity with a tape measure in cm.

Equatorial diameter of fruit. We measured the circumference of the fruit when it was in a state of maturity with a tape measure in cm.

Yield. Was determined by weighing the total fruit per plant, eliminating those that had poor quality, thereby was obtaining the total yield per plant, expressed in g per m^2 .

Quality variables

$^{\circ}$ Brix. A drop of mature of muskmelon flesh was put on the brand manual refractometer ATAGO and note the reading.

Hardness of the fruit: It was determined with a penetrometer (QA SUPPLIES brand, model FT 327) in Kg, was to peel the fruit and later take his record, two repetitions were performed to get an average.

RESULTS and DISCUSSION

Production variables

The foliar area variables and dry weight were measured at the end of the experiment, observing no significant differences ($p \leq 0.05$) between the different irrigation systems and the chitosan oligomers applications. These results are consistent with those published by Benavides-Mendoza *et al.* [8] who found no statistical differences in fresh and dry biomass, both above and roots.

Table 2 shows that there were significant differences between the number and weight of fruits per square meter at the end of the cultivation cycle at 91 DAP, by the effect of varying levels of irrigation to which the plants were subjected and not for the chitosan oligomers that were applied to the soil. As adverse moisture conditions are reflected in the plant tissue with a rapid reduction in the cell division and elongation [9] resulting in a reduction in stem [10], leaves [11, 12] and fruits [3] growth. For polar and equatorial diameter of fruits, not significant differences were detected for the effect of water stress and also for chitosan oligomers of these variables.

Table 2. Influence of varying levels of irrigation and applications of chitosan oligomers on the soil melon under production variables.

		Fruit Number per m ²	Weight of fruits per m ² (g)	Polar diameter of fruit (cm)	Equatorial diameter of fruit (cm)
Irrigation	100	3.5a ^z	4393.9a	46.14a	45.00a
	75	2.83ab	3227.2b	45.33a	44.38a
	50	2.75ab	3043.8bc	44.12a	43.11a
	25	2.25b	2350.9c	42.99a	42.08a
Chitosan oligomers	T0	3.17a	3607.5a	44.74a	43.65a
	OQ1	2.42a	3038.2a	45.83a	44.75a
	OQ2	3.00a	3264.8a	44.85a	43.74a
	OQ3	2.75a	3105.4a	43.18a	42.43a
^y ANOVA					
	Irrigation	*	***	NS	NS
	Chitosan oligomers	NS	NS	NS	NS
	Irrigation*Oligomers	NS	**	NS	NS
	CV (%)	35.17	23.60	7.06	6.56

^zMedia with the same letter in each column parameter are equal according to the multiple comparison test of Tukey with $p \leq 0.05$.

^yAnalysis of variance, NS, *, **, ***, significant and not significant at $p \leq 0.05$, 0.01, 0.001, respectively. CV. - coefficient of variation. T0.- control), CsO.- chitosan oligomer.

The following figure shows that when applying CsO3 to soil and with an irrigation of 25% the higher total fruit production per square meter was recorded, being higher at 63.57% and 76.55% at T0 and the CsO2 respectively. The intermediate value of production was obtained with CsO1 exceeding to T0 by 7.05%, this may be due to chitin derivatives that may cause favorable changes in the metabolism of plants and fruits. The CsO2 was the best behaved with an irrigation of 50% obtaining a production of 3721.95 g per square meter, exceeding T0 by 14.73% of the production, but the CsO1 and CsO3 were lower than T0 in 16.62 and 22.82% of the muskmelon. Increasing by 75% soil irrigation T0 (4956.64 g) the highest production of muskmelon compared with chitosan oligomers CsO1 CsO2, CsO3 was obtained. On the other hand when the cultivation is irrigated at 100%, the

chitosan oligomers CsO2 and CsO1 had the highest value of production of 23.96 and 8.54% compared with T0. The lowest value of production was obtained with CsO3 with 3613.13 g. The data are consistent with those reported by Benavides-Mendoza *et al.* [8], who mentioned that with applications of PAA-Cs and benzoic acid in the nutrient solution these have a positive effect on the number of leaves and the yield, in which the PAA-Cs was higher than the control in a 60%. In contrast Perez *et al.* [2] mentioned that nutrient handling is essential for obtaining quality and a high fruit yield and the nutritional deficiencies are able to reduce the yield in 50% and fruit quality in 70%.

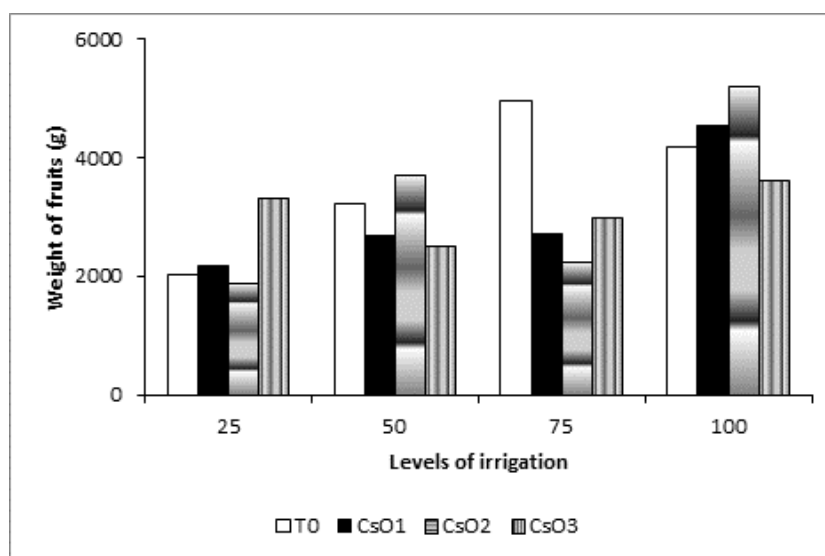


Figure 1. Effect of the interaction of moisture and chitosan oligomers with different molecular weights applied on soil under fruit weight per square meter of melon cv. muskmelon at 93 days after planting.

Quality variables

Based on the statistical analysis we observed not significant differences ($p \leq 0.05$) with respect to the levels of irrigation and chitosan oligomers applied to soil for the parameters of fruit quality of muskmelon (hardness and °Brix) done at 87 DAP. This may be attributed to water stress that stimulates the production of ethylene in the plant [13], and consequently influences the acceleration of a number of physiological processes in different harvests. There was also no interaction between irrigation and chitosan oligomers used in the experiment, these data are not consistent with those published by Benavides-Mendoza *et al.* [8], who mentioned that the PAA-Cs positively influenced the firmness and storage life.

ACKNOWLEDGEMENTS

The authors acknowledge the support provided by CONACyT through the project: CB-80425.

REFERENCES

- [1] www.siap.sagarpa.gob.mx Servicio de Información y Estadística Agroalimentaria y Pesquera SIAP, SIACON, SAGARPA. Consulta de Indicadores de Producción Nacional de Melón.
- [2] Pérez, Z. O.; Cigales, R. M. R.; Orozco, S. M.; Pérez, C. E. G. (2004). Tensión de humedad del suelo y fertilización nitrogenada en melón Cantaloupe Parte II. *Agrociencia* 38:261-272.
- [3] Blanke, M.M., Bower, J. P. (1991). Small fruit problem in Citrus trees. *Trees-Structure and Function* 5(4), 239-243.
- [4] Munemasa, S., Oda, K.; Watanabe-Sugimoto, M., Nakamura, Y., Shimoishi, Y., and Murata, Y. (2007). The coronatine-insensitive 1 mutation reveals the hormonal signaling interaction between abscisic acid and methyl jasmonate in Arabidopsis guard cells. Specific impairment of ion channel activation and second messenger production. *Plant Physiol* 143, 1398-1407.
- [5] Ortega-Ortiz, H.; Benavides-Mendoza, A.; Mendoza-Villarreal, R.; Ramírez-Rodríguez, H.; De Alba Romenus, K. (2007). Enzymatic Activity in Tomato Fruits as a Response to Chemical Elicitors, *J. Mex. Chem. Soc.*, 51(3), 141-144.
- [6] Benavides-Mendoza, A., H. Ortega-Ortiz, H. Ramírez, R. K. Maiti. (2004). Use of interpolyelectrolyte complexes of poly(acrylic acid)-chitosan as inducers of tolerance against stress in horticultural crops. *Crop Research* 28(1), 42-49.
- [7] Ortega-Ortiz, H., A. Benavides-Mendoza, S. Alonso-Corona. (2002). "Uso de los complejos interpolielectrolíticos de poliácido acrílico-quitosán como inductores de tolerancia al estrés en hortalizas", II Simposio Iberoamericano de Quitina y Quitosán (II SIAQ), Acapulco, México, 10-15 de Noviembre de 2002.
- [8] Benavides-Mendoza, A., Burgos-Limón, D., Ortega-Ortiz, H., Ramírez, H., (2007). El ácido benzoico y poliácido acrílico-quitosán en la calidad y el rendimiento del tomate cultivado en suelo calcáreo. *Terra Latinoamericana*, 25(3), 1-8.
- [9] Graebe, J. E. (1987). Gibberellins biosynthesis and control. *Ann. Rev. Plant Physiol.* 38:419-465.
- [10] Kobayashi, M., P. Gaskin., C. R. Spray., Y. Susuki., B. O. Phlnney and J. MacMillam. (1993). Metabolism and biological activity of gibberelin A4 in vegetative shoots of *Zea mays*, *Oriza sativa* and *Arabidopsis thaliana*. *Plant Physiol.* 102,379-386.
- [11] García-Martínez, J. L. and P. Hedden. (1997). Gibberellins and fruit development. In: Tomás-Barberan, F. A. and R.J. Robins., eds. *Phytochemistry of fruit vegetables*. Pp 263-285. Clarendon Press. Oxford.
- [12] Glimour, S. J., J. A. D. Zeevaart., L Schwenen and J. E. Grabe. (1986). Gibberelin metabolism in cell free extracts from spinach leaves in relation to photoperiod. *Plant Physiol.* 82: 190-195.
- [13] Riov, J. and S. F. Yang. (1982). Effect of exogenous ethylene on ethylene production in citrus leaf tissue. *Plant Physiol.* 70:136-141.

PREPARATION AND CHARACTERIZATION OF POROUS CHITOSAN AND CARBOXYMETHYLCHITOSAN MEMBRANES FOR PREVENTING POSTSURGICAL PERICARDIAL ADHESIONS

A. Fiamingo¹, J. B. Lopes², S.P. Campana-Filho¹

¹*IQSC, Universidade de São Paulo (USP). Av. Trab. são-carlense, 400 CEP 13560-970, São Carlos-SP, Brazil.*

²*FMB, Universidade Federal da Bahia (UFBA). Av. Reitor Miguel Calmon, s/n°, CEP 40110-100, Salvador-BA, Brazil.*

**E-mail address: anderson_fiamingo@iqsc.usp.br*

ABSTRACT

This study aimed the production of porous chitosan (Ch) and carboxymethylchitosan (CMCh) membranes and the evaluation of the influence of the average degree of crosslinking on the X-ray diffraction and thermal stability of the membranes. According to the results, increasing the concentration of glutaraldehyde increased the average degree of crosslinking of the membranes. The X-ray diffraction analyses showed a significant decrease in the peaks intensities and the occurrence of peak broadening in the spectra of the cross-linked membranes as compared to those acquired from the same samples in powder form, indicating that the degree of order was much lower in the former cases. The thermal analysis also revealed that the form of the sample (powder or cross-linked membrane) affected both the onset temperature as well as the loss of mass associated with the thermal event occurring in the range 200 – 350^oC. These results, along with those concerning the evaluation of the mechanical properties and susceptibility to lysozyme (data not shown), indicate that the CMCh membranes exhibit the physicochemical properties and morphological characteristics proper as to act in the prevention of pericardial adhesions.

KEYWORDS

Carboxymethylchitosan; chitosan; pericardial adhesions; X-ray diffraction; thermal stability.

INTRODUCTION

The pericardial adhesions are the result of surgical interventions on the heart and great vessels. Many medical problems are reported as a consequence of the existence and the severity of postoperative pericardial adhesions as they cause serious difficulties to future approaches, increasing the rate of morbidity and mortality in the reoperations [1].

Krause et al. [2] described by the first time, the use of carboxymethylchitosan in the prevention of pericardial adhesions, and this study showed an important decrease of postoperative adhesions in large animal models without undesirable side effects.

Carboxymethylchitosan seems to be promising because it has many characteristics that are important for the use in the biomedical area such as, its biocompatibility, biodegradability, atotoxicity, low immunogenicity, antimicrobial activity, capacity to form gels and solubility in a wide range of acidity [3].

A recent work proposed a new approach, using the keratinocyte growth factor (KGF) associated to a carboxymethylchitosan gel to result in effective reduction in pericardial adhesions [3]. However, the use of solutions and gels of CMCh is limited to surgical procedures in which the post-surgery drainage is not necessary. Consequently, the development of films or membranes is necessary for enlarging the range of applications, for example, in cardiovascular surgery.

In this study the influence of the morphology of membranes on the X-ray diffraction and thermal stability of chitosan and carboxymethylchitosan membranes is investigated.

MATERIALS and METHODS

Porous Membranes

The porous membranes were prepared by freeze-drying solutions of chitosan (Yue Planting/China; purified as described in the literature [4], sample Ch) and carboxymethylchitosan (Dayang Chemicals/China; purified in the sodium form as described in the literature [4], sample CMCh). The solutions of chitosan (Ch) were prepared by dissolving the polymer (1.0 g) in 100 ml of acetic acid 0.1 mol L^{-1} , while the solutions of carboxymethylchitosan (CMCh) were prepared by dissolving it (2.0 g) in 100 ml of deionized water. Then, 25% aqueous glutaraldehyde (Acros Organics/USA) was added to the solution of CMCh to result in different cross linker concentration ($0.25 \times 10^{-3} \text{ mol L}^{-1}$; $0.5 \times 10^{-3} \text{ mol L}^{-1}$; $1.0 \times 10^{-3} \text{ mol L}^{-1}$; $2.5 \times 10^{-3} \text{ mol L}^{-1}$ and $5.0 \times 10^{-3} \text{ mol L}^{-1}$). The resulting solutions were submitted to ultrasound treatment in an ultrasonic bath to remove air bubbles, and then they were poured into Petri dishes (dish area / solution volume = $2.0 \text{ cm}^2 \text{ mL}^{-1}$) and maintained at room temperature for 6 hours to allow the crosslinking to occur. Following, the membranes were frozen, freeze-dried, neutralized with acetic acid 0.3 mol L^{-1} / sodium acetate 0.2 mol L^{-1} buffer (pH = 4.5) in the cases of CMCh membranes, and with NaOH 0.1 mol L^{-1} in the case of Ch membrane, and washed with distilled water to remove the glutaraldehyde excess and salts. After washing, the membranes were freeze-dried again.

The identification of the membranes as well as the concentration of glutaraldehyde used for crosslinking are shown in Table 1.

Table 1 – Composition of Ch and CMCh membranes.

Samples	Description
M-Ch	Chitosan membrane
M-CMCh	Carboxymethylchitosan membrane
M-CMCh-2,5	Carboxymethylchitosan membrane cross-linked with $0.25 \times 10^{-3} \text{ mol L}^{-1}$ of glutaraldehyde.
M-CMCh-5	Carboxymethylchitosan membrane cross-linked with $0.5 \times 10^{-3} \text{ mol L}^{-1}$ of glutaraldehyde.
M-CMCh-10	Carboxymethylchitosan membrane cross-linked with $1.0 \times 10^{-3} \text{ mol L}^{-1}$ of glutaraldehyde.
M-CMCh-25	Carboxymethylchitosan membrane cross-linked with $2.5 \times 10^{-3} \text{ mol L}^{-1}$ of glutaraldehyde.
M-CMCh-50	Carboxymethylchitosan membrane cross-linked with $5.0 \times 10^{-3} \text{ mol L}^{-1}$ of glutaraldehyde.

Average Degree of Crosslinking

The average degree of crosslinking of the membranes was determined by using the ninhydrin assay [5]. Thus, the sample was freeze-dried for 24 h and then weighed. Following, the freeze-dried sample was heated with a ninhydrin solution for 20 min, and the optical absorbance of the solution was recorded in a spectrophotometer (UV-VIS: JASCO model V-630). A calibration curve was elaborated by treating glucosamine hydrochloride at various known concentrations with ninhydrin, as described above.

X-Ray Diffraction

The X-ray diffraction analyses were carried out to evaluate the crystallinity of the samples, allowing the evaluation of the influence of the sample form (powder or membrane) on the degree of order. These analyses were carried out in a RIGAKU diffractometer with copper tube ($\lambda = 1.54 \text{ \AA}$) in the range $3\text{--}50^\circ$, using continuous scan speed of 1° min^{-1} . The voltage and current used were 40kV and 30mA, respectively.

Thermal Stability

The thermal stability of the samples was analyzed by thermogravimetric analysis, which was carried out in equipment SHIMADZU (TGA-50), in dynamic atmosphere of synthetic air (20% O_2 and 80% N_2) at flow rate 20 mL min^{-1} . Initially, the samples were heated with a rate of $10^\circ\text{C min}^{-1}$ from 25°C to 110°C and remained at 110°C for 10 min to eliminate water, and then they were heated at the same rate from 110°C to 800°C . The samples ($\approx 8.0 \text{ mg}$) were previously stored in a desiccator containing silica gel for 15 days.

RESULTS and DISCUSSION

Membrane Crosslinking

After carrying out the crosslinking reaction, it was observed that the colour of the resulting membranes turned yellowish. Indeed, the reactions between the glutaraldehyde and the amino groups forming Schiff bases have been reported as the main cause for the occurrence of browning [6]. As shown in **Fig. 1** the average degrees of crosslinking of the CMCh membranes increased with increasing concentration of glutaraldehyde ($p < 0.05$).

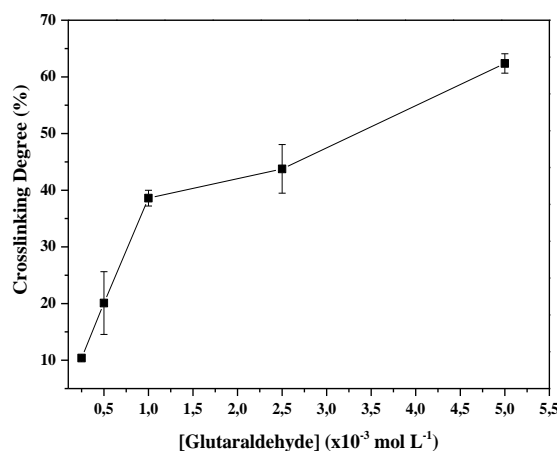


Fig. 1. Average degree of crosslinking of the carboxymethylchitosan membranes as a function of the glutaraldehyde concentration ($n=3$).

X-Ray Diffraction

The X-ray diffraction analyses were carried out aiming to evaluate the occurrence of different arrangements of the samples in powder and in membrane form (Fig. 2).

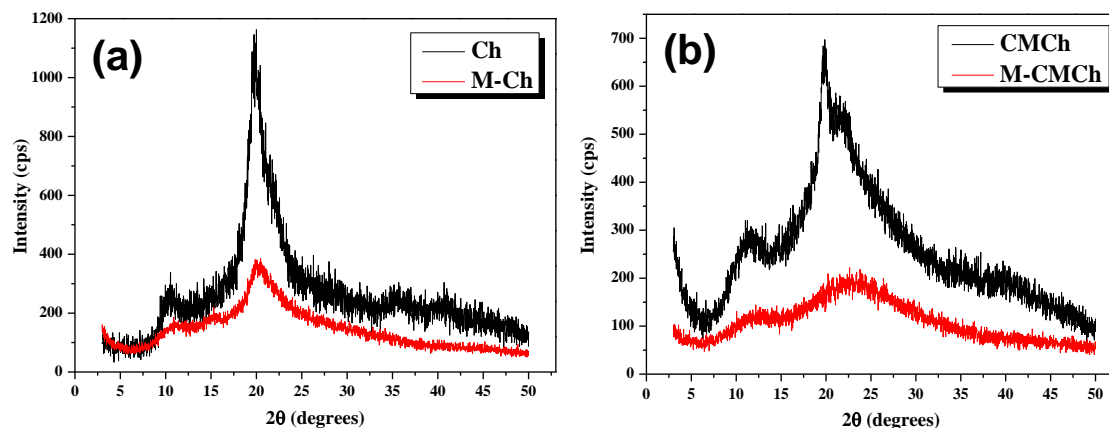


Fig. 2. X-ray spectra of chitosan (a) and carboxymethylchitosan (b).

A significant decrease in the peak intensity and the occurrence of peak broadening were observed in the spectra of the membranes as compared to those of the samples in the powder form (Fig. 2), indicating that the degree of order was reduced. Indeed, for preparing the membrane the polymer solution was quickly frozen and then it was submitted to freeze-drying, a procedure which preserved the disordered structure existing in solution while in the powder form of both polymers, chitosan and carboxymethylchitosan, there are amorphous as well as ordered regions. The same is true in the cases of the cross-linked membranes, the concentration of glutaraldehyde used in the crosslinking step having no effect in the peak intensity (data not shown).

Thermal Stability

The thermogravimetric curves of chitosan (Ch) and carboxymethylchitosan (CMCh) are shown in Fig. 3.

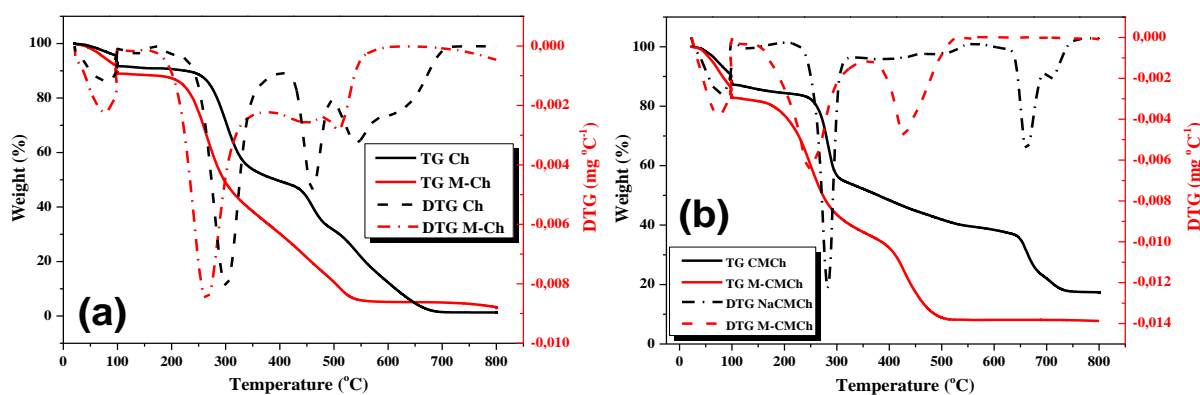


Fig. 3. Thermogravimetric curves of Ch (a) and CMCh (b).

According to the thermal analyses (**Fig. 3**), the form of the sample (powder or membrane) affected both the onset temperature as well as the loss of mass associated with the thermal event occurring in the range 200°C – 350°C (**Tab. 2**). Also, it was observed that the onset, maximum and endset temperatures were lower in the case of the membranes, which could be attributed to their lower crystallinity.

The thermogravimetric curves and values of the onset, maximum and endset temperatures of the crosslinked membranes are shown in **Fig. 4** and **Tab. 2**.

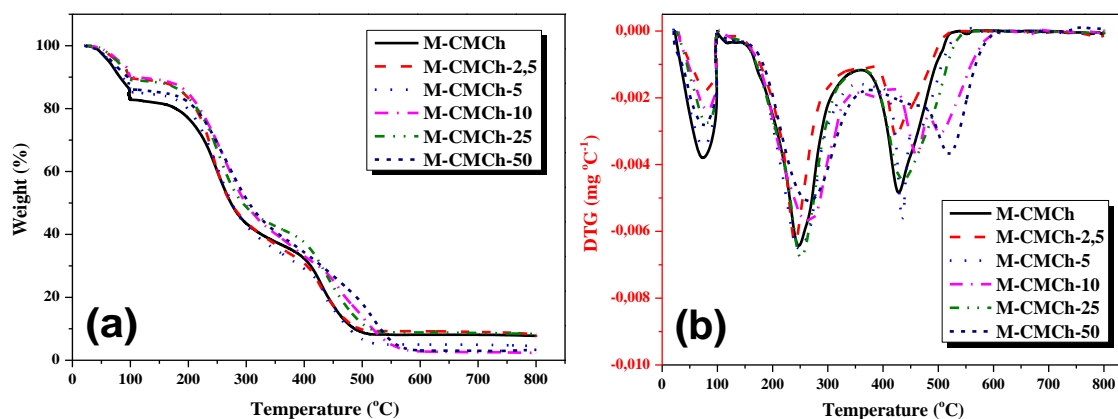


Fig. 4. TG (a) and DTG (b) curves of M-CMChs depending on the concentration of glutaraldehyde used in the crosslinking stage in synthetic air with flow rate of 20 mL min⁻¹ and heating rate of 10°C min⁻¹.

According to the thermal analyses of the cross-linked membranes (**Fig. 4**), it was observed that increasing the crosslinking degree increased the temperature of thermal degradation (onset, maximum and endset temperature), indicating that crosslinking led to the formation of the membranes thermally more stable.

Tab. 2. Temperatures (°C) corresponding to the onset, maximum and onset of the thermal event occurring in the range 200°C – 350°C of chitosan and carboxymethylchitosan as powders and membranes.

Samples	T _{onset}	T _{max}	T _{endset}	Weight loss (%)
Ch	276	307	331	36
M-Ch	227	264	283	41
CMCh	263	283	300	31
M-CMCh	202	240	280	40
M-CMCh-2,5	204	246	281	41
M-CMCh-5	204	248	282	41
M-CMCh-10	205	252	285	42
M-CMCh-25	205	265	291	40
M-CMCh-50	208	270	314	41

CONCLUSIONS

Porous membranes of chitosan and carboxymethylchitosan were successfully prepared by using glutaraldehyde as cross linker. The crosslinking reaction produced carboxymethylchitosan membranes exhibiting higher degree of crosslinking the higher the concentration of glutaraldehyde. The X-ray diffraction analyses of the membranes (M-Ch and M-CMCh) revealed a significant decrease in the intensity and broadening of the peak, indicating that the degree of order was much lower in these cases as compared to the samples in powder form (Ch and CMCh). The thermal analyses showed that the form of the sample (powder or membrane) affected both the onset temperature as well as the loss of mass associated with the thermal event occurring at 200°C – 350°C. These results, along with those concerning the evaluation of the mechanical properties and susceptibility to lysozyme (data not shown), indicate that the CMCh membranes exhibit the physicochemical properties and morphological characteristics to act in the prevention of pericardial adhesions.

ACKNOWLEDGEMENTS

The authors are grateful to CAPES, CNPq and FAPESP for financial support.

REFERENCES

- [1] Lopes, J.B.; Dallan, L.A.O.; Moreira, L.F.P.; Campana-Filho, S.P.; Gutierrez, P.S.; Lisboa, L.A.F.; Oliveira, A.S. and Stolf, N.A. (2010). Synergism between keratinocyte growth factor and carboxymethyl chitosan reduces pericardial adhesions. *Ann Thorac Surg.* 90, 566-572.
- [2] Krause, T.J.; Zazanis, G.; Malatesta, P.; Solina, A. (2001). Prevention of pericardial adhesions with N,O-carboxymethylchitosan in the rabbit model. *Journal of Investigative Surgery*, 14, 93-97.
- [3] Daroz, L.R.D.; Lopes, J.B.; Dallan, L.A.O.; Campana-Filho, S.P.; Moreira, L.F.P. and Stolf, N.A.G. (2008). Prevenção de aderências pericárdicas pós-operatórias com uso de carboximetilquitosana termoeestéril. *Revista Brasileira de Cirurgia Cardiovascular*, 23, 480-487.
- [4] Abreu, F. R. and Campana-Filho, S. P. (2009) Characteristics and properties of carboxymethylchitosan. *Carbohydrate Polymers*, 75, 214-221.
- [5] Mi, F.-L.; Shyu, S.-S. and Peng, C.-K. (2005). Characterization of ring-opening polymerization of genipin and pH-dependent cross-linking reactions between chitosan and genipin. *Journal of Polymer Science: Polymer Chemistry*, 43, 1985–2000.
- [6] Guangyan, L.; Baiyang, S.; Gan, W.; Yujun, W.; Yandao, G. and Xiufang, Z. (2009) Controlling the degradation of covalently cross-linked carboxymethyl chitosan utilizing bimodal molecular weight distribution. *Journal of Biomaterials Applications*, 23, 435-451.

INFLUENCE OF COPPER SPECIES ON CHITOSAN MEMBRANES FOR CHROMIUM ADSORPTION – AN XPS STUDY

Marisa Masumi Beppu^{1*}, Fernanda Condi de Godoi¹, Rodrigo Balloni Rabelo¹, Enrique Rodriguez-Castellon² and Eric Guibal³

¹FEQ, University of Campinas

² Facultad de Ciencias, Universidad de Málaga

³ Ecole des Mines d'Alès

*E-mail address: beppu@feq.unicamp.br

ABSTRACT

In this study, copper nanoparticles were synthesized by redox reaction between Cu(II) adsorbed on chitosan (CHI) membrane using sodium borohydride (NaBH₄) as reducing agent. CHI membrane containing copper nanoparticles (CHI-RED) was used as adsorbent in Cr(VI) dilute solution. X-ray photoelectron spectroscopy (XPS) revealed that the copper species on CHI-RED membrane surface was predominantly composed by Cu(I). After the Cr(VI) adsorption, Cu(I) was oxidized to Cu(II) which was found available to interact with CHI amino groups.

Keywords

Copper nanoparticles, Chitosan, hexavalent chromium, XPS

INTRODUCTION

The disposal of industrial wastes containing heavy metals is one of the leading causes of water pollution. In order to achieve low concentrations of heavy metals in wastewater, studies that use biopolymers as adsorbents are in constant evolution. Over the last years, many research groups are using metal nanoparticles supported on chitosan to improve the adsorption of metals such as Cr(VI). Geng et al. (2009a and 2009b) synthesized iron nanoparticles stabilized by chitosan in order to improve the removal of Cr(VI) in water. Chitosan nanoparticles with Fe(0) were prepared by in situ reduction of the Fe(II) with KBH₄ [1,2]. Wu et al.[3] used chitosan-tripolyphosphate chelating resin beads to fabricate zero-valent copper-chitosan nanocomposites. According to Wu et al., the adsorption behavior of hexavalent chromium from aqueous solution onto fabricated nanocomposites has better adsorption capacity than that of the chitosan-tripolyphosphate beads.

In this study, a CHI membrane with copper nanoparticles (CHI-RED membrane) was produced by submitting CHI membrane with adsorbed Cu(II) through a chemical reduction process using sodium borohydride (NaBH₄) as reducing agent. CHI-RED membrane was used as adsorbent for Cr(VI) solution. The choice of this metallic solution was based on the difference among the reduction potentials of the pairs Cu(II)/Cu(0) ($E^0=0.34$ eV) against Cr(VI)/Cr(III) ($E^0=1.33$ eV). X-ray Photoelectron Spectroscopy (XPS) analysis was conducted in order to investigate the Cr(VI) adsorption on CHI-RED-membrane. The XPS technique allowed to: (1) determine the oxidation state of the metallic species involved (Cu or Cr) on the sample surface and (2) evaluate possible modifications in the CHI-RED membrane surface composition after adsorption of Cr(VI).

MATERIALS and METHODS

CHI-RED membrane synthesis

Firstly, CHI-membrane was prepared by casting CHI solution (1.5 wt % in glacial acetic acid solution) on a Petri dish, followed by total solvent evaporation in an oven at 40°C. The CHI membrane was neutralized in alkaline solution ([NaOH] = 1 M) for 24 hours. The CHI-membranes were extensively washed to remove residual NaOH and stored in ultrapure water at 4°C. Then, Cu(II) was incorporated onto the CHI-membrane by immersing 0.1 g of CHI-membrane in a copper(II) sulphate solution with [Cu(II)] = 1.57 mM, for 48 hours (pH=4.5, T = 20°C).

The production of copper nanoparticles on CHI-membranes was performed by chemical reduction of the Cu(II) adsorbed on CHI-membrane as follows: 0.1 g of CHI-membrane with adsorbed Cu(II) was immersed in 80 mL of ultra-pure water with constant stirring at ambient temperature, under N₂ atmosphere (pH = 8, during 2 min). Then, 20 mL of a freshly prepared aqueous solution containing 0.1 g of NaBH₄ was added into the mixture until the membrane appears dark-brown (approximately 1.5 mins, under N₂ atmosphere). After the reduction process, the so called CHI-RED-membranes were quickly rinsed with Milli-Q® water and immediately submitted to the Cr(VI) adsorption batch experiment.

Batch adsorption experiment

For chromate adsorption on CHI-RED membrane, potassium dichromate (K₂Cr₂O₇) salt was dissolved in Milli-Q water with [Cr(VI)]₀=9,6 mM. The experiments were conducted at 20 °C. CHI-RED membrane (0.1 g) was added to 50 mL of metal salt solution set initially at pH = 4. The resulted sample of the adsorption batch experiment was called Cr-CHI-RED membrane.

XPS experiments

XPS measurements were carried out with a spectrometer Physical Electronics 5700, using an Mg-K α source (1253.6 eV) (model 04-548 Dual Anode X-rays Source). The X-ray source was run at a power of 300 W (10 keV and 30 mA). The pressure inside the vacuum chamber was 5×10^{-8} Torr. The samples were fixed on a stainless steel support and then stored for approximately 12 hours under high vacuum in the preparation chamber, being then transferred to the analysis chamber of the spectrometer. Two types of measurements were performed: (1) a low-resolution measure that afforded the survey spectra in order to identify the elements present in the sample surface, and (2) a high-resolution measure with irradiation time of 35 min that allowed the determination of the chemical state of the elements. A first acquisition was performed with 8 min of irradiation time in order to avoid the photo-reduction of Cu(II) species. All spectra were obtained using a 720 μ m diameter analysis area. Binding energies (BE) were referred to the C 1s line of adventitious carbon at 284.8 eV and determined with the resolution of ± 0.1 eV. The spectra were fitted assuming a Gaussian-Lorentzian distribution for each peak, in order to determine the binding energy of the various element core levels.

RESULTS and DISCUSSION

XPS analysis was conducted for CHI-RED and CHI-RED-Cr membranes in order to investigate the oxidation state of copper and chromium species adsorbed on surface. Table 1 summarizes the assignments of each peak (resulting from the deconvolution procedure) based on their binding energies (BE) and atomic concentrations (AC).

Table 1: Assignments of the decomposed peaks for CHI-RED and Cr-CHI-RED membranes.

<i>Elements</i>	<i>Binding Energy (eV)</i>		
	<i>CHI-RED</i>	<i>Cr-CHI-RED</i>	<i>Assignments</i>
C 1s	284.8 [76]	284.8 [73]	C-C or contaminated C
	286.3 [13]	286.2 [16]	C-N or C-O or C-O-C
	287.7 [11]	288.0 [11]	C=O or O-C-O
N 1s	-	398.5 [44]	-NH ₂ or -NH-
	399.8 [100]	399.8 [56]	
O 1s	-	531.4 [100]	C=O or C-O-C or chemisorbed H ₂ O
	532.4 [87]	-	>C-O or O-H or bound H ₂ O
	530.5 [12]	-	Cu ₂ O
Cu 2p _{3/2}	933.0 [38]	933.1 [12]	Cu(0) or Cu(I)
	935.2 [15]	935.1 [30]	Cu(II)
Cu 2p _{2/3} (Shake-up)	944.5 [15]	941.6 [11]	-
Cu 2p _{1/2}	952.6 [19]	944.1 [8]	Cu(0) or Cu(I)
	955.2 [7]	953.0 [6]	Cu(II)
Cu 2p _{1/2} (Shake-up)	962.0 [7]	955.0 [15]	-
Cu LMM*	337.2	337.1	-
Cr 2p _{3/2}	-	577.3 [67]	Cr(III)
Cr 2p _{1/2}	-	587.1 [33]	

* Value taken from XPS spectrum for Cu LMM region.

Figure 1 (a) shows the core level Cu 2p spectrum for the CHI-RED membrane. The spectrum noise signal is due to the short acquisition time that had to be applied in order to avoid, as much as possible, the photo-reduction of Cu ions by the X-rays action. A large asymmetric signal could be seen in Cu 2p_{3/2} core region that could be decomposed in two contributions at 932.9 and 934.4 eV. The shake-up lines for the bands 2p_{3/2} (944.5 eV) and 2p_{1/2} (962.0 eV) are evidence of an open 3d⁹ shell of Cu(II) [4].

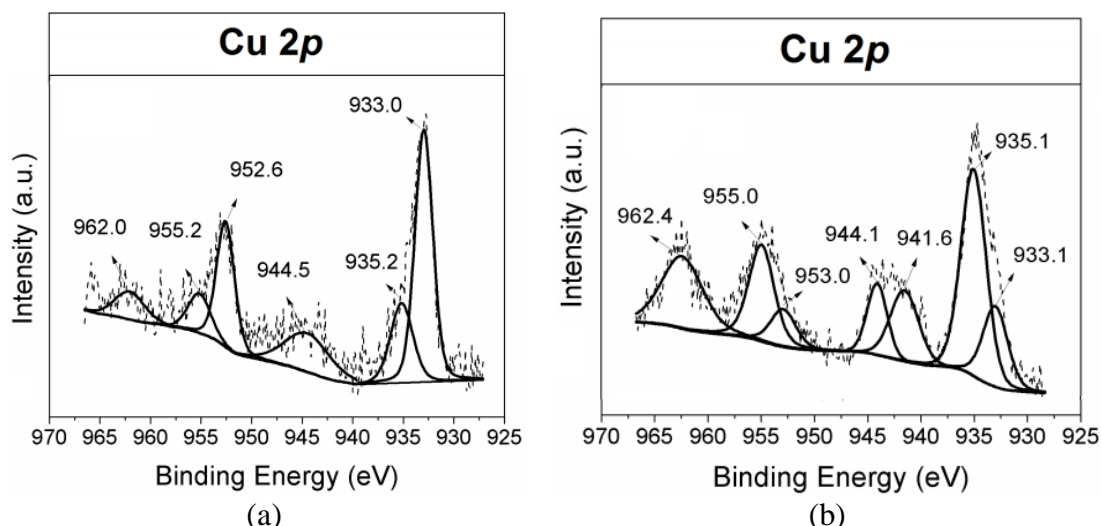


Figure 1: Decomposition of the Cu 2p XPS spectrum for (a) CHI-RED and (b) Cr-CHI-RED membrane.

Since XPS spectra for Cu(I) and Cu(0) are indistinguishable, the Wagner's plot was used for Cu 2p_{3/2} (also called State Diagram) in order to study the presence of Cu(0), Cu(I) and Cu(II) species. In this diagram (shown in Figure 2) the modified Auger parameter (α'_0) is represented by diagonal lines. The binding energy values, $BE_{Cu2p_{3/2}}$, and KE_{CuLMM} kinetic energy of the Cu LMM Auger electron are on the abscissa and ordinate, respectively [5]. The α'_0 value was calculated from the Eq. (1):

$$\alpha'_0 = KE_{CuLMM} - KE_{Cu2p_{3/2}} + 1253.6 \tag{1}$$

where $KE_{Cu2p_{3/2}}$ is the kinetic energy of the Cu 2p_{3/2} photo-electron and 1253.6 is the energy of the Mg Ka X-ray excitation source in eV. The detailed calculation for KE_{CuLMM} and $KE_{Cu2p_{3/2}}$ is as follows below.

$$KE_{CuLMM} = 1253.6 - BE_{CuLMM} = 916.4 \text{ eV}$$

$$KE_{Cu2p_{3/2}} = 1253.6 - BE_{Cu2p_{3/2}} = 320.6 \text{ eV}$$

From the Wagner's plot in Figure 2, it may be concluded that Cu(I) is the Cu species that predominates in CHI-RED membrane surface (72%). So, the doublet Cu 2p_{3/2} at 933.0 eV and Cu 2p_{1/2} at 952.6 eV were assigned to the presence of Cu(I). And the doublet Cu 2p_{3/2} at 935.2 eV and Cu 2p_{1/2} at 955.2 eV close to the shake-up satellite were associated to the presence of Cu(II) [5-7].

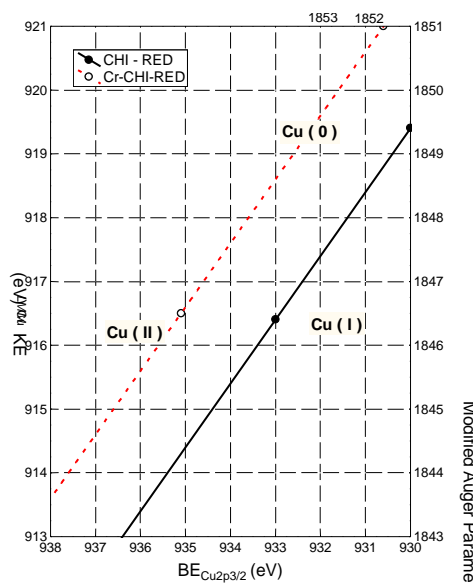


Figure 2: Wagner's plot for Cu 2p - CHI-RED and Cr-CHI-RED membranes.

C 1s spectrum for CHI-RED membrane could be decomposed into three contributions. The characteristic peaks described in Table 1 are consistent with the observation in previous studies for CHI [8-11]. The CHI-RED membrane had a symmetric peak at 399.8 eV for the N 1s XPS spectrum. This peak was assigned to the nitrogen atoms in the $-\text{NH}_2$ and/or the $-\text{NH}-$ groups of CHI [9]. CHI was not protonated, since the reduction process occurred at pH~8. The O 1s XPS spectrum revealed the presence of Cu_2O (correlated to the peak at 530.5 eV) [6]. The peak located at 532.4 eV can be assigned to C-O (alcohol and/or ether). Hydroxyl and ether groups can form metal complexes with copper, in which oxygen atoms donate electrons to Cu [11]. As seen in Cu 2p core level spectra for Cr-CHI-RED membrane (Figure 1 (b)), the increase of the relative intensity of the area occupied by the shake-up satellites after Cr(VI) adsorption indicative of copper species oxidation [6]. The same procedure that was used for CHI-RED membrane to calculate α'_0 , was also applied to Cr-CHI-RED membrane. Consequently, the percentage of Cu(I) decreased from 72% (CHI-RED membrane) for 29% after chromate adsorption.

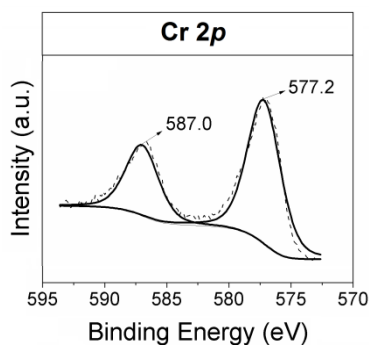


Figure 3: Decomposition of the Cr 2p XPS spectra for Cr-CHI-RED membrane.

Figure 3 shows the XPS spectra of Cr 2p for Cr-CHI-RED membrane. The main peaks of Cr $2p_{3/2}$ varied from 577.1 to 577.3 eV which were attributed to Cr(III), as Cr_2O_3 or CuCr_2O_4 (for membranes containing copper species) [12]. Contributions around 580.0 eV, typically detected for Cr(VI) species, were not observed.

Dambies *et al.* (2001) reported similar results for chromate adsorption on chitosan beads crosslinked with glutaraldehyde. In corroboration with the XPS data obtained by Vieira *et al.* (2011), for chromate adsorption on chitosan membranes (pristine and crosslinked with glutaraldehyde and epichlorohydrin). In both cases, Cr(VI) was reduced to Cr(III) form, confirming the ability of chitosan to reduce some metals [8,10]. Wu *et al.* (2009) showed that the Cr(VI) has been partially reduced to Cr(III) after adsorption on chitosan beads crosslinked with tripolyphosphate and containing metallic copper nanoparticles. In addition, these authors reported that after Cr(VI) adsorption, the metallic copper nanoparticles were oxidized to Cu(II) [3]. Geng *et al.* (2009) adsorbed Cr(VI) in solution on chitosan containing Fe(0) nanoparticles and they shown, by the XPS technique, that two simultaneous reactions occurred: (1) oxidation of Fe(0) nanoparticles and (2) reduction of Cr(VI) to Cr (III).

According to Table 1, C 1s spectra did not show significant difference for CHI-RED and Cr-CHI-RED membrane. In N 1s spectrum, membrane Cr-CHI-RED presented a second peak (398.5 eV) shifted to the right. The same binding energy of the second peak was observed by Vieira *et al.* (2011) for N 1s spectrum after adsorption of Cu(II) in CHI membranes. Thus, it is possible to infer that after the redox reaction between Cu(I) and Cr(VI), the Cu(II) is found available to interact with the CHI amino groups. The peak located in 399.8 eV for Cr-CHI-RED membrane was associated with presence of $-\text{NH}_2$ or $-\text{NH}-$. After chromate adsorption, the O 1s spectrum could be fitted in only one symmetric peak located at 531.4 for Cr-CHI-RED (Table 1). This confirms that the Cu (previously in oxide state -

Cu₂O) in CHI-RED membrane, was oxidized after the Cr(VI) adsorption and now interacts preferentially with the amino groups of chitosan.

Based on the redox potentials of the involved species, it might be concluded that the copper nanoparticles donate electrons to chromate anions in solution promoting the reductions Cr(VI)→Cr(III) and their own oxidation.

CONCLUSION

XPS demonstrated to be a powerful technique to qualitatively analyze the mechanism of Cr(VI) adsorption in CHI-RED membrane.

ACKNOWLEDGEMENTS

The authors are grateful to CAPES (process 4575-11-3), CNPQ, Universidad de Málaga and Ecole des Mines d'Alès.

REFERENCES

- [1] Geng, B., Jin, Z. H., Li, T. L., & Qi, X. H. (2009a). Kinetics of hexavalent chromium removal from water by chitosan-Fe-0 nanoparticles. *Chemosphere*, 75(6), 825-830.
- [2] Geng, B., Jin, Z. H., Li, T. L., & Qi, X. H. (2009b). Preparation of chitosan-stabilized Fe-0 nanoparticles for removal of hexavalent chromium in water. *Science of the Total Environment*, 407(18), 4994-5000.
- [3] Wu, S. J., Liou, T. H., & Mi, F. L. (2009). Synthesis of zero-valent copper-chitosan nanocomposites and their application for treatment of hexavalent chromium. *Bioresource Technology*, 100(19), 4348-4353.
- [4] Novakov, T. (1971). X-Ray Photoelectron Spectroscopy of Solids; Evidence of Band Structure. *Physical Review B*, 3(8), 2693-2698
- [5] Wagner, C. D., Gale, L. H., & Raymond, R. H. (1979). Two-dimensional chemical state plots: a standardized data set for use in identifying chemical states by x-ray photoelectron spectroscopy. *Analytical Chemistry*, 51(4), 466-482.
- [6] Ghijsen, J., Tjeng, L. H., van Elp, J., Eskes, H., Westerink, J., Sawatzky, G. A., & Czyzyk, M. T. (1988). Electronic structure of Cu₂O and CuO. *Physical Review B*, 38(16), 11322-11330.
- [7] Fleisch, T. H., & Mains, G. J. (1982). Reduction of copper oxides by UV radiation and atomic hydrogen studied by XPS. *Applications of Surface Science*, 10(1), 51-62.
- [8] Dambies, L., Guimon, C., Yiacoumi, S., Guibal, E. (2001). Characterization of metal ion interactions with chitosan by X-ray photoelectron spectroscopy. *Colloids and Surfaces A-Physicochemical and Engineering Aspects*, 177(2-3), 203-214.
- [9] Liu, C., & Bai, R. (2006). Adsorptive removal of copper ions with highly porous chitosan/cellulose acetate blend hollow fiber membranes. *Journal of Membrane Science*, 284(1-2), 313-322.
- [10] Vieira, R. S., Oliveira, M. L. M., Guibal, E., Rodríguez-Castellón, E., & Beppu, M. M. (2011). Copper, mercury and chromium adsorption on natural and crosslinked chitosan films: An XPS investigation of mechanism. *Colloids and Surfaces A: Physicochemical and Engineering Aspects*, 374(1-3), 108-114.
- [11] Kang, J., Liu, H., Zheng, Y.-M., Qu, J., & Chen, J. P. (2010). Systematic study of synergistic and antagonistic effects on adsorption of tetracycline and copper onto a chitosan. *Journal of Colloid and Interface Science*, 344(1), 117-125
- [12] Capece, F. M., Castro, V. D., Furlani, C., Mattoño, G., Fragale, C., Gargano, M., & Rossi, M. (1982). "Copper chromite" Catalysts: XPS structure elucidation and correlation with catalytic activity. *Journal of Electron Spectroscopy and Related Phenomena*, 27(2), 119-128.

ANTIBACTERIAL ACTIVITY OF FUNGAL CHITOSAN

PAIVA, W.S.*, SOUZA NETO, F. E., REBOUCAS, G.G., PRAXEDES JÚNIOR, F. H. A.,
BATISTA, A.C.L.

UFERSA, Univ. Fed. Rural do Semiárido, Av. Francisco Mota, 572 - 59625-900 Mossoró, Brazil

*E-mail address: wdsipaiva@gmail.com

ABSTRACT

The indiscriminate use of antibiotics are selecting microorganisms resistant to current antibacterial drugs, requiring the research and development of new drugs. Therefore we used the fungal chitosan as a new molecule antibacterial and verification of contact time required for action is effective. We used strains of *Escherichia coli* ATCC 11775 and *Staphylococcus aureus* ATCC 6538 and fungal chitosan (DD 94%) obtained by *Cunninghamella elegans* grew in YPD medium. Chitosan is a polymer soluble at pH lower than 6.5, for this reason, all tests were made in culture medium NA at pH 5.5. For bactericidal activity aliquots of 1 mL of fungal chitosan gel (1.5% in acetic acid 0.25% (w/v)) were distributed in conical tubes, after was added 100µL of bacterial culture (10^7 cells/mL) and incubate at 37°C in contact times 5, 10, 15, 20 and 30 minutes. Subsequently the samples grown on NA plates were incubated at 37 ° C for 24 and 48h. The cultures untreated were used as the control. Growth inhibition was observed in all samples treated with fungal chitosan in all contact times and the samples untreated grew normally at all intervals, demonstrating the efficacy of fungal chitosan against bacteria generally related clinical diseases.

Keywords : Antibacterial, fungal, chitosan.

INTRODUCTION

Chitin is the second most abundant polysaccharide in nature, being found in most shell exoskeleton of crustaceans and insects. Under the action of the enzyme chitin deacetylase (E.C. 3.5.1.41), chitosan is obtained naturally in the cell wall of some fungi, especially those belonging to the class Zygomycetes [1]. Chitosan is a copolymer, as well as chitin, presents in its units residue N-acetyl-2-amino-2-deoxy-D-glucose (glucosamine) and residues amino-2-deoxy-D-glucose (N-acetyl-glucosamine) [2].

The production of chitosan by enzymatic deacetylation of chitin is not the only way of obtaining such biocompound, the same current is generated on a commercial scale by deacetylation of most of the chemical residues of N-acetyl-D-glucosamine present in the chitin extracted from the shell crustaceans [3,4].

Chitosan was described in 1954 by Kreger, with an analysis of x-ray structure of the cell wall *Phycomyces blakesleeanus* [5], a procedure which is performed to this day as to characterize the crystallinity of chitosan [6]. Currently chitosan has been the subject of many studies, since according to its properties it has been used in several areas giving rise to the development of new research. It is known that the cosmetic industry, food, pharmaceutical and biotechnology, has made heavy use of this knowledge to generate economic growth to these companies [7,8,9].

The various options for the use of chitosan are the reasons for the growing interest in manipulating the same, it is also a product that contributes to the cost-benefit because it eliminates waste of crustaceans, which are used for food consumption, transforming them into chitosan with high value, by using cheap process [3].

Another way of using chitosan, is the exploitation of its antimicrobial potential. The action takes place through the disruption of the cell wall of bacteria, because the difference in charges between the structures in contact, where chitosan is positively charged and negatively cell wall [10].

In addition to this biocompound other molecules are exploited as antimicrobial agents, as in the case of caseicin, which is an enzyme that breaks a milk protein, casein, and act permeabilizing the cytoplasm, resulting in the leakage of intracellular components of microorganisms due to cationic caseicin characteristic of [11], as well as lectin, where studies report that the lectin originating from muramic acid and N-acetylmuramic acid, binds to the carbohydrate present in the cell wall of bacteria causing disturbance in the cell wall and thus destroying the pathogens [12,13].

The use of chitosan as an antimicrobial product, is growing according to the effectiveness of the results obtained from research carried out [14,15]. The importance of these new findings is due to resistance of microorganisms to antibiotics being utilized in recent years.

MATERIALS and METHODS

To demonstrate significant importance of fungal chitosan, which was obtained from *Cunninghamella elegans* grown in YPD medium (yeast extract 10 g, bacteriological peptone 20g, glucose 20g, distilled water 1000 ml) with 94% DD a new molecule with antibacterial activity was evaluated studies to verify the contact time required for antibacterial activity against *Escherichia coli* ATCC 11775 and *Staphylococcus aureus* ATCC 6538. The fungal chitosan used is soluble at pH 5.5; the tests were performed on Nutrient Agar -NA medium (5g beef extract, 10g peptone, and 1000 ml distilled water) at pH 5.5.

Test of Microdrop

The initial concentration of micro-organisms was performed by the microdrop technique [16]. The count of viable microorganisms was carried out in Petri dishes containing NA culture medium at pH 5.5. From the initial inoculum, serial dilutions were performed by transferring conical tubes to 0.900 ml saline with 0.3% Tween 80 and 0.100 ml of inoculum to obtain an initial dilution of 10^{-1} , successively performing this procedure until dilution of 10^{-8} . After, using micropipettes, four drops were transferred to a Petri dish,

each droplet being of 10 μ l, the plates were incubated in aerobic incubation at 37 °C for 24 hours. The final consideration is taken into account the average counts of drops quadrupled and were evaluated according to the method of biometric Cavalli-Sforza [17].

Test Antimicrobial

To test the bactericidal activity were used in 900 μ l of fungal chitosan gel (1.5% acetic acid 0.25% (w / v)) [18] distributed in conical tubes, and then was added 100 μ L bacterial culture (10⁻⁶ cells / ml for *E. Coli*) and (10⁻⁵ cells / ml for *S. aureus*) dilutions were established by reading the test results of the microdrop, then the plates were incubated at 37 °C contact five times pre-established: 5, 10, 15, 20 and 30 minutes. After contact with chitosan, the samples of each time were plated on NA and incubated at 37 °C were observed after 24 and 48 hours. Untreated cultures were used as control group.

RESULTS and DISCUSSION

According to the obtained results, we demonstrated the antibacterial activity of chitosan with high degree of deacetylation, corroborating with the results of Batista et al. [14], chitosan from crustacean that used with a high degree of deacetylation against *S. aureus* isolates from cattle with mastitis and *E.coli* ATCC.

The growth inhibition was observed in all samples treated with chitosan (Fig.1. A, C) in all time intervals tested, whereas the untreated samples grew normally (Fig.1. B, D) in all time intervals. This study demonstrates the potential antibacterial activity of fungal chitosan with a high deacetylation degree after 96 hours of growth in culture media, after 5 minutes of contact of bacteria with chitosan gel. In the literature, the time of 5 hours is described as a enough time of contact between crustacean chitosan and strains of *S. aureus* and *E. coli* as necessary for a satisfactory activity of growth inhibition in the culture medium, however, the fungal chitosan used in this study was efficient at only 5 minutes of contact [14]. In contrast, studies by Bento et al. [20] showed that chitosan obtained from *Mucor rouxii* with concentration of 2.5 mg.mL⁻¹ has antibacterial activity with 4 hours of contact with microorganisms.

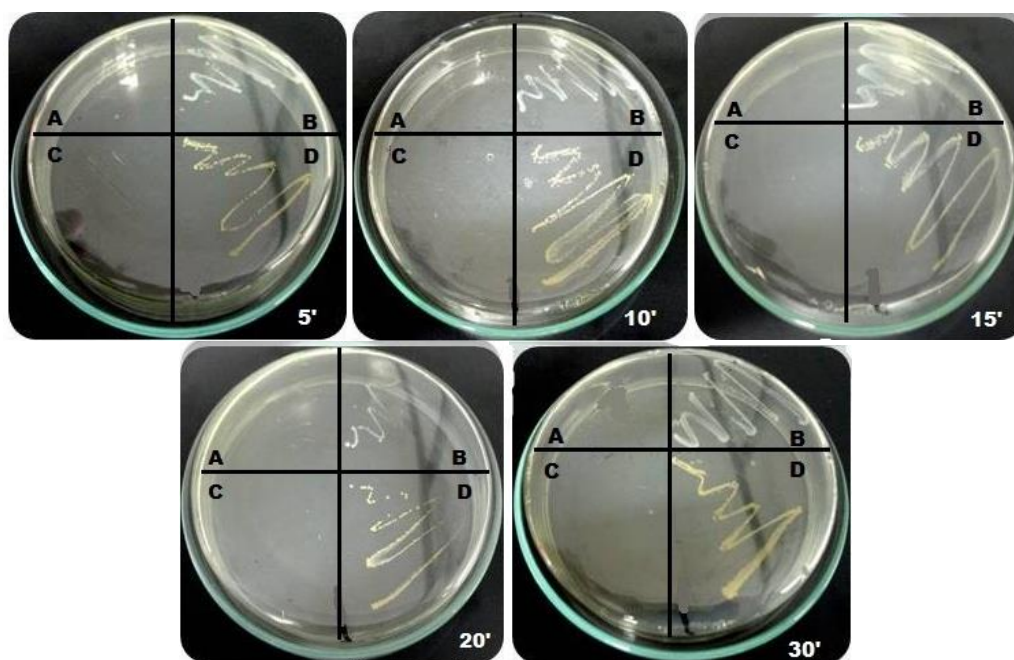


Figure.1. Antibacterial activity of fungal chitosan against micro-organisms *Escherichia coli* and *Staphylococcus aureus* ATCC in different contact times after 48 h of incubation. A – *E.coli* treated; B – untreated *E.coli*; C – *S.aureus* treated; D – untreated *S.aureus*.

From the data presented by Xiao et al. and Liu et al. [6.19], describing the results of chitosan contact with microorganisms, we can assume that the intensity of concentration, bactericidal caused damage in the cell wall of *E. Coli* and cell membrane rupture *S. aureus* [18].

In this study, the minimum time for the antimicrobial action of chitosan was 5 minutes, demonstrating the great potential of this polysaccharide in combating pathogenic microorganisms, and thus indicating the effectiveness of chitosan as a new fungal natural medicine against bacterial infections.

CONCLUSION

With this work we prove the antibacterial activity of chitosan obtained from the fungi *Cunninghamella elegans*. This chitosan was effective in controlling the growth of bacteria such as *E. coli* and *S. aureus* contact times between 5 to 30 minutes, giving fungal chitosan as a new alternative for the control of bacteria.

ACKNOWLEDGEMENTS

The authors acknowledge Prof. Dra Galba Maria de Campos Takaki (Nucleus of Research Studies in Environmental Sciences, Catholic, University of Pernambuco) and Prof Dr. Jean Berg Alves da Silva (Federal University Rural of Semi Árido) for kindly providing the fungal chitosan and bacteria, respectively, used in the experiment.

REFERENCES

- [1] Kafetzopoulos, D.; Martinou, A.; Bouriotis, V. (1993). Bioconversion of chitin to chitosan: Purification and characterization of chitin deacetylase from *Mucor rouxii*. Proc. Natl. Acad. Sci. USA., 90, 2564-2568.
- [2] Aranaz, I.; Harris, R.; Heras A. (2010). Chitosan Amphiphilic Derivatives. Chemistry and Applications. Current Organic Chemistry., 14, 308-330.
- [3] Radwan, M. A.; Farrag, S. A. A.; Abu-Elamayem, M. M.; Ahmed, N. S. (2012). Extraction, characterization, and nematocidal activity of chitin and chitosan derived from shrimp shell wastes. Biol Fertil Soils., 48, 463–468.
- [4] Kumar, M.N.V.R. (2000). A review of chitin and chitosan applications. React. & Func. Poly., 46, 1-27.
- [5] Kreger, D. R. (1954). Observations on cell walls of yeasts and some other fungi by x-ray diffraction and solubility tests. Biochim, Biophys. Acta, 13, 1-9.
- [6] Xiao, B.; Wan, Y.; Zhao, M.; Liu, Y.; Zhang, S. (2011). Preparation and characterization of antimicrobial chitosan-N-arginine with different degrees of substitution. Carbo. Poly.. 83, 144-150

- [7] Azevedo, V. V. C.; Chaves, S. A.; Bezerra, D. C.; Lia Fook, M. V.; Costa, A. C. F. M. (2007). Quitina e Quitosana: aplicações como biomateriais. *Revis. Eletr. de Mate. e Proce.*, 2.3, 27-34.
- [8] Costa Silva, H. S. R.; Santos, K. S. C. R. dos.; Ferreira, E. I. (2006). Quitosana: Derivados Hidrossolúveis, Aplicações Farmacêuticas e Avanços. *Quim. Nova.*, 29, 776-785.
- [9] Mendes, A. A.; Oliveira, P.C.; Castro, H. F.; Giordano, R. L. C. (2011). Aplicação de quitosana como suporte para a imobilização de enzimas de interesse industrial. *Quim. Nova*, 34, 831-840.
- [10] Holappa, J.; Hjálmarsdóttir, M.; Másson, M.; Rúnarsson, Ö.; Asplund, T.; Soininen, P.; Nevalainen, T.; Jarvinen, T. (2006). Antimicrobial activity of chitosan N-betainates. *Carbohydr. Poly.*, 65, 114–118
- [11] Norberg, S.; O'Connor, P.M.; Stanton, C.; Ross, P.; Hill, C.; Fitzgerald, G.F.; Cotter, P.D. (2011). Altering the Composition of Caseicins A and B as a Means of Determining the Contribution of Specific Residues to Antimicrobial Activity. *Appli. and Environ. Microbio.* 77, 2496-2501.
- [12] Santi-Gadelha T.; Gadelha C.A.A.; Aragaño K.S.; Oliveira C.C.; Mota M.R.L.; Gomes R.C., et al. (2006). Purification and biological effects of *Araucaria angustifolia* (Araucariaceae) seed lectin. *Biochemistry and Biophysics Research Community.*, 350, 1050-1055.
- [13] Ayouba A.; Chatelain, C.; Rouge, P. (1991). Legume lectins interact with muramic acid and N-acetylmuramic acid, *FEBS Lett.*, 289, 102–104.
- [14] Batista, A.C.L.; Dantas, G.C.; Santos, J.; Amorim, R.V.S. (2011). Antimicrobial Effects of Native Chitosan against Opportunistic Gram-negative Bacteria. *Microbio. Journ.* 1., 3, 105-112.
- [15] Kim, K.W.; Min, B.J.; Kim, Y-T.; Kimmel, R.M.; Cooksey, K.; Park, S.I. (2011). Antimicrobial activity against foodborne pathogens of chitosan biopolymer films of different molecular weights. *LWT - Food Science and Technology.*, 44, 565-569.
- [16] Romeiro, R. S. Métodos em bacteriologia de plantas. Viçosa: UFV, 2001. 279.
- [17] Cavalli-Sforza, L. (1974) *Biometric*. Stuttgart: Gustav Fisher.
- [18] Tao Y, Qian L.-H., Xie J. (2011). Effect of chitosan on membrane permeability and cell morphology of *Pseudomonas aeruginosa* and *Staphylococcus aureus*. *Carbohydrate Polymers.*, 86, 969–974.
- [19] Liu, H., Du, Y. M., Yang, J. H., & Zhu, H. Y. (2004). Structural characterization and antimicrobial activity of chitosan/betain derivative complex. *Carbohydrate Polymers.*, 55, 291–297.

-
- [20] Bento, R. A.; Stamford, T. L. M.; Campos-Takaki, G. M.; Stamford, T. C. M.; Souza, E.L. (2009). Potential of Chitosan from *Mucor rouxii* UCP064 as Alternative Natural Compound to Inhibit *Listeria monocytogenes*. *Brazi. Jour. of Microbio.*, 40, 583-589.

EVALUATION OF CHITOSAN BASED FILMS IN PRESERVATION OF MEXICAN FRESH CHEESE “QUESO RANCHERO”

M. Lopez-Chavez,¹A.Tecante,² A. Lopez-Luna,¹ K. Shirai^{1*}

¹ Universidad Autónoma Metropolitana, Dept. Biotecnología Lab. Biopolímeros. Av. San Rafael Atlixco 186. Col. Vicentina, México City. C.P.09340.

² UNAM, Facultad de Química, Ciudad Universitaria, C.P. 04510, México

*E-mail: smk@xanum.uam.mx

ABSTRACT

Chitosan was prepared by heterogeneous deacetylation from chitin extracted by biological method and characterized on their moisture content, ash, residual protein, acetic acid solubles, degree of acetylation and molecular weight. The synthesis of chitosan-lactic acid, chitosan-co-citric and chitosan-co-citric acid-co-hydroxypropylmethylcellulose were carried out and the materials were also characterized. Bags were prepared by cutting chitosan films heat-sealed and used for packaging commercial cheese ranchero. Cheeses were stored at 4°C with 20% relative humidity. It was observed that chitosan-co-LA showed the highest inhibition for aerobic mesophilic bacteria, molds and yeasts. The mechanisms of microbial inhibition by chitosan are explained by its direct interaction within the microbial cell wall but also for other extrinsic factors such as the reduction of moisture content observed during storage at low relative humidity. Since, none of the films prevented loss of moisture in the cheeses during storage time, pH was not significantly different in the control (unpacked) and cheese in the bags. Microbial growth inhibition was observed in fresh cheeses packaged in chitosan based films, however, further modification in the material is needed for maintaining the moisture content of cheeses during storage.

Keywords chitosan, cheese, lactic acid, citric acid

INTRODUCTION

The “queso ranchero” is a fresh cheese of soft paste not pressed produced in several states of Mexico. The short shelf life (up to 10 days) and its perishability are due to its high moisture content (45 and 55%), low salt content and near neutral pH (6.0–6.5) [1]. *Listeria monocytogenes* outbreak has been associated to consumption of fresh cheese [2]. Therefore, the extension of shelf life and food safety are challenges for the dairy food industry. For this purpose the use of films based on chitosan represents a potential commercial alternative for this product. Chitosan-based materials have gained growing interest owing to their bio-functional properties, such as antimicrobial ability, biodegradability and biocompatibility. Chitosan-based films (CBF) are mostly formed from acidic solutions of these biopolymers where plasticizers, cross-linkers and other additives are usually added to improve the resulting film properties, which vary on the type of chitosan, type of acidic dissolution and added compounds [3]. Then, many organic acids, vitamins, antibacterial agents such as nisin, essential vegetable oils or cross-linking with other compounds are reported for CBF formation [3-6]. CBF are applied for improvement of quality and shelf life of various foods from agriculture, poultry, and seafood by antimicrobial activity against a wide range of foodborne filamentous fungi, yeast, and bacteria [6]. In this work, we evaluated the effect of four different CBFs in preserving cheese ranchero; chitosan (Q), chitosan-co-LA(QLA), chitosan-co-citric (QC) and chitosan-co-citric acid-co-hydroxypropylmethylcellulose (QH).

MATERIALS and METHODS

Chitosan was obtained by heterogeneous deacetylation of biologically extracted chitin [3], glacial acetic acid (Merck, Germany), 85% Lactic acid (LA) (JT Baker, Mexico), citric acid (CA) (JT Baker, Mexico), hydroxypropyl methylcellulose (HPMC) (Derivados Macroquímicos, Mexico), ethanol (Hycel, Mexico), polyethylene glycol (Fluka, USA), potassium phosphate dibasic (JT Baker, Mexico), sorbitol (JT Baker, USA); sodium phosphate monobasic (JT Baker, Mexico). Commercial cheese "Ranchero" (Celaya Guanajuato, Mexico) was made 24h before use and stored at 4 °C. Standard count agar (Bioxon, Mexico) and potato dextrose agar (Bioxon, Mexico) were used for microbiological analysis.

Characterization of chitosan and chitin. Infrared spectra were recorded in an ATR-FTIR spectrophotometer (Perkin Elmer Spectrum100).⁶ The viscosity molecular weight (M_v) of chitosan was determined by the Mark-Houwink-Sakurada equation from acetic acid (0.2 M)/ammonium acetate (0.15 M) solutions.⁷ Degree of acetylation (DA) of chitosan was determined by ¹H-NMR spectrometry in a Bruker AC 200.⁸

Preparation of films. Chitosan-LA(QAL) Chitosan was dissolved in LA0.5N. QAL synthesis was conducted at 80°C for 2h. After cooling the reaction, sorbitol was added and the solution was distributed in Petri dishes, which were placed under vacuum at 80°C for 3h and dried at 60°C for 6h. Films were purified by Soxhlet with acetone for 18 h.

Chitosan-co-Citric (QC). Chitosan was dissolved in water containing CA (0.2M) and heated at 70 °C prior to addition of NaH₂PO₄. Then, solution was kept under stirring for 30 min.[7]. After cooling the reaction, sorbitol was added and left stirred for 12 h. The solution was placed in petri dishes and dried at 60 °C for 6 h.

Chitosan-citric acid-hydroxy propylmethyl cellulose (QH). Chitosan was dissolved in acetic acid (0.1 M), thereupon citric acid, sodium phosphate monobasic and sorbitol were added. A solution of hydroxy propylmethylcellulose (HPMC) and polyethylene glycol-600 diacid was prepared. Films were prepared by pouring 1:1 (v/v) chitosan/HPMC solutions onto Petri dishes, heat-treated (100 °C, 3 min) and oven dried (40 °C, 48 h).

Purification of crosslinked chitosan. Materials were dissolved in a phosphate buffer 0.1 M (pH 5) and precipitated in excess of cold ethanol, filtered by filtration and freeze-dried prior to chemical analysis.

Characterization of the chitosan based materials. Infrared spectra were directly recorded on the films using an ATR FTIR-spectrometer (Perkin Elmer 100). Each sample spectrum was registered by triplicate with 16 scans. Proton nuclear magnetic resonance (¹HNMR) spectra of the samples of Q and QC were obtained in a Bruker Advance III 500, (Germany) spectrometer at 200 MHz at 298°K and deuterated 3-(Trimethylsilyl) propionic acid as internal reference. Samples were dissolved in HCl/D₂O. The degree of acetylation (DA) was calculated according to earlier reports [8]. Percentages of covalent incorporation of CA, Lactic acid (LA) and HPMC onto chitosan were obtained by integration of the corresponding assigned signals on ¹HNMR spectra of samples obtained after anti-solvent purification. To determine mechanical properties of stress-strain, films were placed in a desiccator for conditioning following ASTM (ASTM D618, 2003) at ambient temperature (23 ± 2 ° C) and relative humidity of 50 ± 5% achieved with oversaturated solutions of Mg(NO₃)₂ for 48 h prior to determination. Film thickness was measured after conditioning with a micrometer (Mitutoyo, Japan) at 5 random positions for each film, four on the perimeter and one in the center. Mechanical properties were calculated considering an average thickness value. Mechanical properties were evaluated in terms of fracture strength in the puncture and fracture strength in extension in mechanical testing equipment SINTECH 1/S (MTS, USA) using clamps with a 100N load cell, varying between the two tests (puncture and extension). Force fracture puncture was determined by the method

described by Gontard et al.[9]. Samples were evaluated in triplicate. Force fracture extension was evaluated based on standard method ASTM [10]. Water vapor permeability (WVP) was determined at $4^{\circ}\text{C}\pm 2$ with relative humidity gradients (HR) 22 to 75% and 75 to 22%. Determinations were made by triplicate.

Evaluation of CBFs on wrapping Queso Ranchero. Bags of the CBF that contained cheeses were heat-sealed using grenetine. Wrapped cheeses were stored at $4^{\circ}\text{C}\pm 1$ and HR of $20\%\pm 1$ for 15 days. Unwrapped cheeses were used as control.

Analysis of cheese: Cheese samples were unpacked every 7 days and weight loss percentage (%W) was measured considering the initial weight and the final weight. Moisture content, pH and total titratable acidity (ATT) expressed as LA were determined according to procedure of A.O.A.C. [11] Cheese samples were liquefied with 100 mL of 0.9 % (w/w) saline solution for 2 min using an electrical homogenizer (Sper Scientific 460003, USA), further decimal dilutions were prepared. Each dilution was deposited in Standard count agar and potato dextrose agar plates and incubated at 30°C . Colonies were counted and expressed as CFU/g of aerobic mesophilic bacteria, molds and yeast.

Statistical analysis. A randomized design was carried out in triplicate for experiments with several CBF and control. NCSS (NCSS, PASS and GESS, 2001) software computed the analysis of variance with film thickness, WVP, quality attributes of cheeses (weight loss, pH, acidity and microbial enumeration) as response variables. Means were compared with Tukey Kramer multiple means comparison test ($P < 0.05$).

RESULTS and DISCUSSION

Demineralization (DM) of 61% was achieved during LA fermentation (LAF) according with a low acidification but high percentage of deproteinization (DP) (91%). The latter attributed to increased proteolytic activity at $\text{pH} > 5$ [12]. The moisture, ash and protein contents determined in shrimp waste, raw chitin obtained after LAF [13] and chitin are presented in Table 1. Chitosans DA lower than 15% (Table 2).

Table 1. Chemical compositions of shrimp waste, raw chitin and chitin.

Sample	Shrimp waste	Raw chitin	Chitin
Moisture (%)	76.38 \pm 0.24	62.17 \pm 0.86	3.32 \pm 0.40
Ash (%)	17.07 \pm 0.73	10.68 \pm 0.53	1.90 \pm 0.13
Protein (%)	40.29 \pm 0.08	6.29 \pm 0.03	1.68 \pm 0.05

Table 2. Characteristics of chitosans prepared from biologically extracted chitins.

Batch#	Moisture (%)	Ash (%)	Solubles ¹ (%)	DA ² (%)	M_v (kDa)
1	7.7 \pm 0.13	1.7 \pm 0.05	69 \pm 4.0	4.71 \pm 0.16	189.8
2	5.6 \pm 0.85	2.1 \pm 0.07	72 \pm 2.2	13.57 \pm 0.76	177.9

¹ in acetic acid 0.1M; ² DA determined by ¹HNMR

The lactyl units showed characteristic signal in the infrared spectra at $1,716.8\text{ cm}^{-1}$ assigned to C = O stretching, other signals are at $1,211.2$ and $1,120.2\text{ cm}^{-1}$ assigned to stretching of carbonyl group of an acid ester [14]. Figure 1a shows the chitosan ATR-FTIR spectrum, the characteristic signals are presented at $3,356.9\text{ cm}^{-1}$ corresponding to the OH groups of the polymer, at $3,281\text{ cm}^{-1}$ of the -NH group, at $2,916.4$ and $2,850.6\text{ cm}^{-1}$ -CH stretching, at $1,648.5\text{ cm}^{-1}$ carbonyl of acetamide, at $1,570.2\text{ cm}^{-1}$ amino group -NH₂, $1,418.5\text{ cm}^{-1}$ assigned to -CH₂, $1,375.5\text{ cm}^{-1}$ to the -CH stretching and deformation of C-CH₃, the band at $1,148\text{ cm}^{-1}$ is characteristic of the asymmetric stretching of group C-O-C, characteristic vibration of the skeletal structure of chitosan appears at $1,024.1\text{ cm}^{-1}$ and $1,064.6$ and 890.1 cm^{-1} showing the anomeric tension of CH group [15]. The QAL infrared spectrum showed the confirmative bands of chitosan at $1,562.6\text{ cm}^{-1}$ of the free NH₂ groups at $1,062$ and $1,020.6\text{ cm}^{-1}$ of characteristic vibration of the skeletal structure. Carbonyl

stretching at $1,719.3\text{ cm}^{-1}$ is observed indicating LA incorporation (Figure 1b). In spectra of QC and QH appear characteristic band at $1,707.75\text{ cm}^{-1}$ due to carbonyl stretching and assigned to ester linkage between CA and chitosan (Figure 1c and 1d). Evidence of ester formation is also ascertained with bands at $1,186.94\text{ cm}^{-1}$ and $1,064.22\text{ cm}^{-1}$ due to CO-O stretching absorptions (Figure 1c).

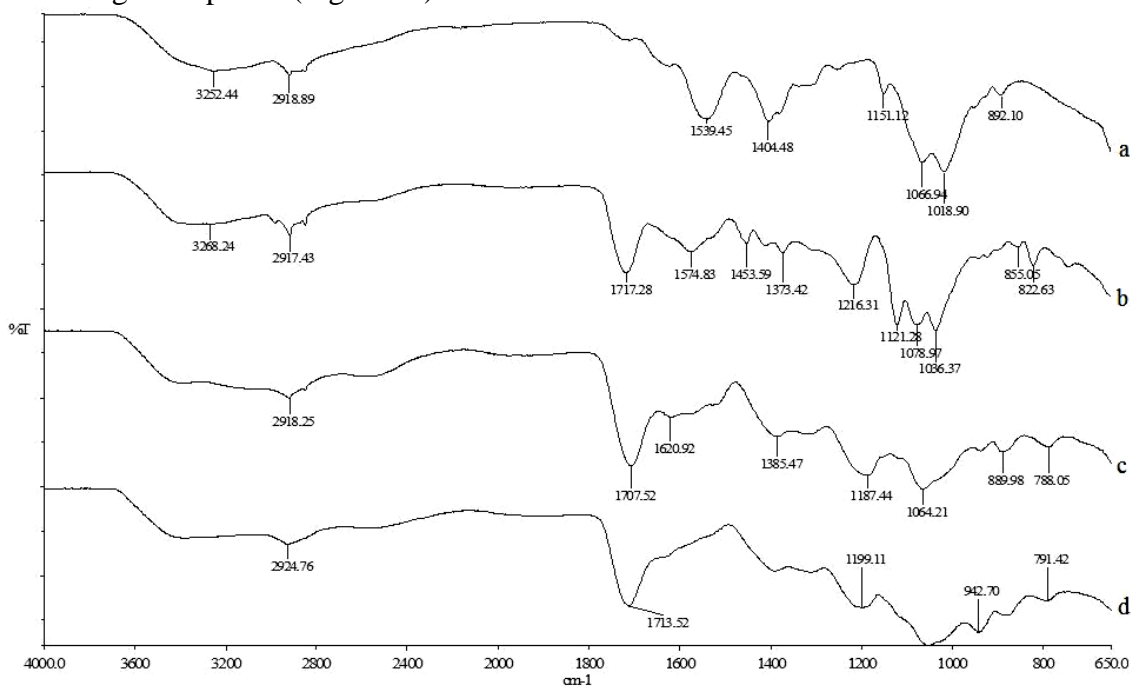


Figure 1. Infrared spectra of chitosan based films: a) Q, b) QAL, c) QC, d)QH

The weight of the films varied in relation to its composition and the addition of other compounds. Direct relationship was observed between the weight and thickness of the films, QH films were the thickest, while QAL and QC had similar thickness; the thinnest were the Q films (Figure 2). The thickness affects the WVP, as the film thickness increases the resistance to mass transfer increases, thus the partial pressure of water vapor in equilibrium also increase [16].

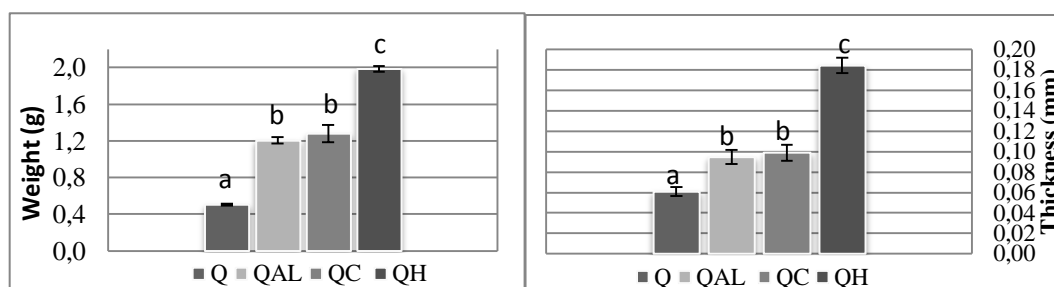


Figure 2. Weight and thickness of chitosan based films. Mean of ten measurements and their standard deviations . Histograms with the same letter did not display significant differences ($P < 0.05$)

The WVP was measured at $4\text{ }^{\circ}\text{C}$, simulating storage conditions within the bags made from CBF with cheeses, where HR test cell was 75%, corresponding to the moisture content of the cheese; while RH of the environmental chamber corresponded to the external moisture in the fridge (20%). WVP were also conducted by reversing the gradient of HR, in order to observe the behavior of moisture of CBFs. QAL and QH films showed higher values in the gradient WVP with 22/75, 1.53×10^{-3} and 1.46×10^{-3} $\text{gmm/m}^2\text{hkPa}$, respectively. Besides, the films of Q and QC presented smaller values of WVP with the same gradient, with

values of 6.96×10^{-4} and 5.94×10^{-4} gmm/m²hKPa, respectively (Figure 3). Another factor that influences the WVP was the addition of plasticizers, in this paper we used sorbitol. Trejo et.al. [17] observed an increase in the WVP of chitosan films when the amount of sorbitol was increased, this was attributed to the ability of sorbitol to reduce internal hydrogen bonds, reducing the intermolecular forces between the polymer chains, allowing larger spaces for the migration of water molecules.

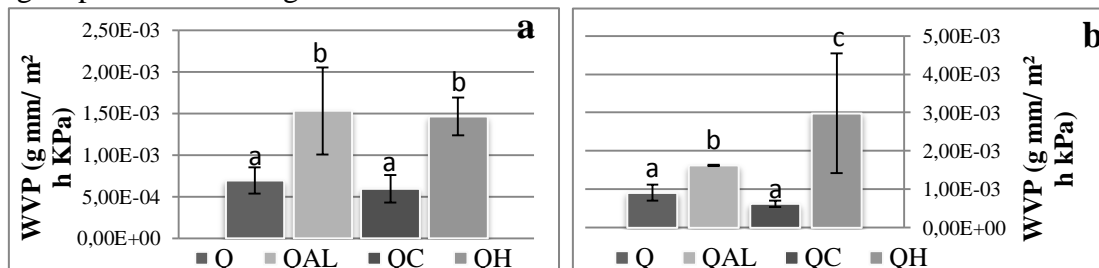


Figure 3. WVP of chitosan based films at HR gradients: a) 22/75 and b)75/22 at 4°C±2. Mean of three measurements and their standard deviations. Histograms with the same letter did not display significant differences (P<0.05)

On the mechanical properties, the cross-linking reaction among LA, CA or HPMC with chitosan produced less rigid and fragile films than the solely chitosan. QAL polymer shows high plasticity, but poor elasticity. While QC films were more elastic and less rigid than the ones prepared with Q (Table 3).

Table 3. Mechanical properties of chitosan based films.

Sample	Fracture strength to the extension			Fracture strength to the puncture		
	Young's Modulus (MPa)	Elongation at break (%)	Maximum tensile stress (MPa)	Young's Modulus (MPa)	Elongation at break (%)	Maximum tensile stress (MPa)
Q	2226±561.8	57.2±27.0	610.6±204.1	990.61±116.11	6.74±1.98	46.50±9.63
QAL	4331±8372	275.4±5.9	323.3±22.3	63.88±4.87	43.20±0.55	20.51±1.02
QC	327.2±97.2	238.4±14.4	474.0±80.5	316.79±134.06	35.88±0.78	53.06±6.28
QH	222.3±25.1	122.7±4.1	283.4±38.9	202.35±32.32	27.59±1.47	32.67±4.26

Evaluation of chitosan based films in rancho cheese.

The initial moisture of the cheese was $71.7 \pm 4.8\%$, after fifteen days of storage at the conditions given in the fridge and WVP of the films, cheeses presented a W of ca. 40% and only significant differences were determined between control and QC (Figure 4a). A higher loss of moisture content in the coated cheese than with the control, suggests an effect of drying. The final moisture content in cheeses displayed significant differences between treatments, showing a lower content of $26.6 \pm 0.39\%$, in cheese coated with QAL than other treatments (Figure 4b), this is consistent with results of WVP (Figure 4).

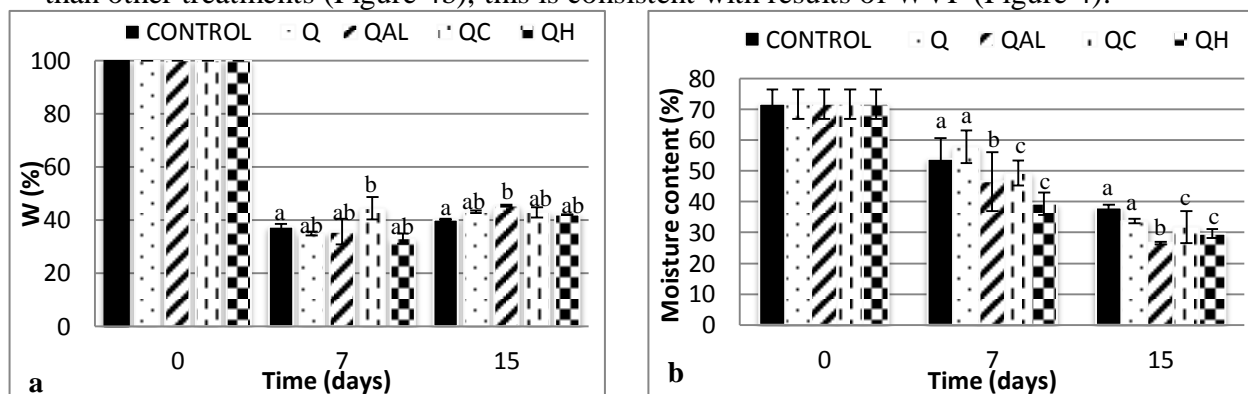


Figure 4. W (%) (a) and moisture content (%) (b) of cheeses packed in bags made with chitosan based films at HR 20% at 4°C±2. Mean of three measurements and their standard deviations. Histograms with the same letter did not display significant differences (P<0.05).

The pH with the control and Q was increased during the storage time until a final pH of 6.46 ± 0.0212 and 6.53 ± 0.0094 , respectively. The cheeses packaged with QAL, QC and QH showed a decrease in pH after seven days storage caused by acidification of the cheese probably due to the migration of the acidic components of the film with final pH of 5.73 ± 0.08 , 5.22 ± 0.19 and 5.05 ± 0.07 for cheese with QAL, QC and QH, respectively (Figure 5a). The TTA tend to increase with time of storage in the different treatments. The highest TTA was $3.04 \pm 0.87\%$ and $3.12 \pm 0.13\%$ in cheeses packaged with QC and QH, respectively (Figure 5b).

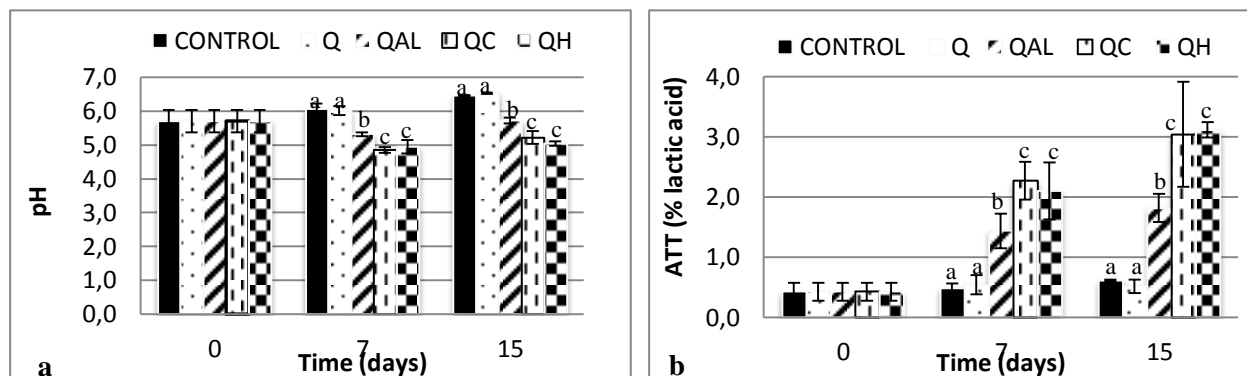


Figure 5. pH (a) and ATT (b) of cheeses packed in bags made with chitosan based films at HR 20% at $4^{\circ}\text{C}\pm 2$. Mean of three measurements and their standard deviations. Histograms with the same letter did not display significant differences ($P < 0.05$)

According to microbiological analysis, it was found that only the packed cheeses with QH and QAL presented significant differences in aerobic mesophilic microorganism inhibition compared to control (Figure 6a). QAL showed the greatest inhibition for bacteria, fungi and yeasts (Fig. 6). The counts obtained for QAL are even lower than the initial amount of microorganisms, indicating bactericide and fungicide effects besides of inhibition. The mechanism of inhibition of chitosan and LA is well known and explained the inhibitory effect of QAL.

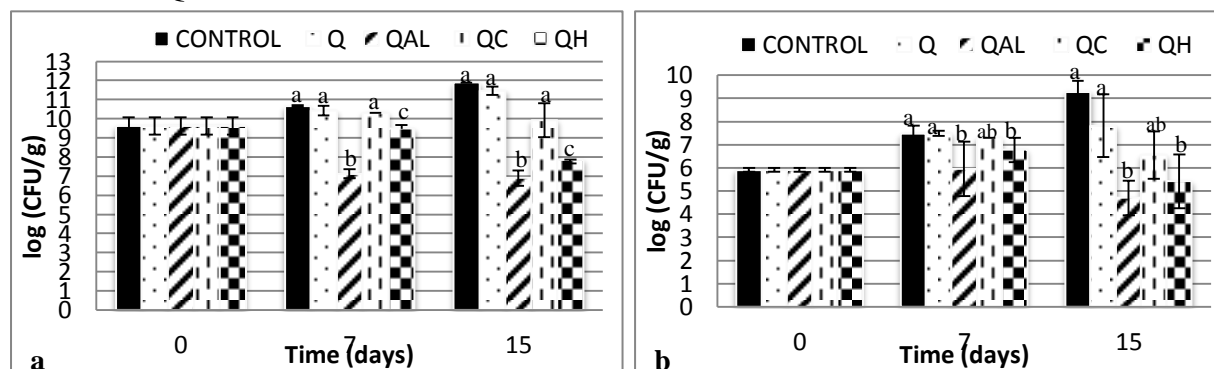


Figure 6. Colonies enumeration of mesophilic microorganism (a) and fungi (b) of cheeses packed in bags made with chitosan based films at HR 20% at $4^{\circ}\text{C}\pm 2$. Mean of three measurements and their standard deviations. Histograms with the same letter did not display significant differences ($P < 0.05$)

ACKNOWLEDGEMENTS

The authors thank Institute of Science and Technology of Mexico City (ICyTDF) (Project No. PICSA 11-69) for funding and scholarship grant (MLC).

REFERENCES

1. Villegas de G.A. 1993. Los Quesos Mexicanos. Manuales para educación agropecuaria SEP/trillas. México D.F.
2. Soni KA, Desai M, Oladunjoye A, Skrobot F, Nannapaneni R. 2012. International Journal of Food Microbiology 155 (1-2):82-88

3. Möller, H., Grelier, S., Pardon, P., Coma, V. (2004). *J. Agr Food Chem.* 52, 6585-6591.
4. Mi, F., Huang, C., Liang, H., Chen, M., Chiu, Y., Chen, C., Sung, H. (2006). *J Agr Food Chem.* 54 (9), 3290-3296.
5. Pranoto, Y., Rakshit, S., Salokhe, V. (2005). *LWT - Food Sci Technol.* 38(8), 859-865.
6. No, HK; Meyers, SP; Prinyawiwatkul, W; Xu, Z. (2007) *J Food Sci* 72, 5, 87-100
7. Pacheco, N., Garnica-González, M., Gimeno, M., Bárzana, E., Trombotto., David, L., Shirai. 2011. *Biomacromolecules.* 12:3285-3290.
8. Alonso, D., Gimeno, M., Olayo, R., Vázquez-Torres, H., Sepúlveda-Sánchez, J., Shirai, K. (2009). *Carbohyd Polym* 77: 536-543.
9. Hirai, A., Odani, H. and Nakajima, A. (1991). *Polym Bull* 26: 87-94.
10. Gontard, N., Guilbert, S. & Cuq, J.L. (1993). *J. Food Sci.* 58 (1), 206-211.
11. ASTM D882-97 (2003). "Standard Test Method for Tensile Properties of Thin Plastic Sheeting", Vol. 8.01, pp. 163-171.
12. AOAC. 1990. Official methods of analysis, 13th edition. Association of Official Analytical Chemists, Washington, D.C.
13. Pacheco N., Garnica-González M., Ramírez-Hernández Y., Flores-Albino B., Gimeno M, Bárzana E., Shirai K. 2009, *Bioresour. Technol.* 100: 2849-2854.
14. Cira L., Huerta S., Hall G., Shirai K., 2002, *Process Biochem.*, 37, 1359-1366pp.
15. Mazo P., Ríos L., Restrepo G., 2011, "Síntesis de poli ácido láctico y poli ricinoleato empleando calentamiento por microondas y su utilización en la producción de termoplásticos de poliuretano", *Polímeros: Ciencia e Tecnología*, vol. 21, núm. 2, 83-89 pp.
16. Jacinto C., Maza I., 2007, "Caracterización fisicoquímica de Quitosano para su Aplicación como Biosorbente de metales", *REVCUNI*, 11 (1), 1-5pp.
17. Bertuzzi, M. A.; Armada, M.; Gottifredi, J. C.; Aparicio, A. R.; Jimenez, P, 2002, "Estudio de la permeabilidad al vapor de agua de films comestibles para recubrir alimentos", Congreso regional de ciencia y tecnología NOA 2002, Producciones Científicas. Sección: Ciencias de la Ingeniería, Agronomía y Tecnología, Universidad Nacional de Catamarca, Buenos Aires.
18. Trejo V., Aragón N., Miranda P., 2001, *J. Mex. Chem. Soc.* año/vol. 45, número 001, México, México, pp. 1-5

BIODIESEL PRODUCTION FROM SUNFLOWER OIL REFINED USING CHITOSAN SPHERES WITH CALCIUM AS HETEROGENEOUS CATALYST

L.M.CORREIA, N.S.CAMPELO, R.S.VIEIRA*

Grupo de Pesquisas em Separações por Adsorção (GPSA), Departamento de Engenharia Química, Universidade Federal do Ceará (UFC), Campus do Pici, Blc. 709, CEP: 60455-760, Fortaleza-Ceará-Brasil.

**E-mail address: rodrigo@gpsa.ufc.br*

ABSTRACT

The production of biodiesel is routinely carried out by the transesterification reaction which the activity catalytic is maximized for heterogeneous catalysts with a more porous structure and higher surface area, providing more active sites for the reaction. Chitosan, can be used as directional structure agent by the insertion of the calcium oxide in its structure. The objective of this study was synthesize porous spheres of calcium oxide by coagulation of a chitosan solution and a metal precursor (calcium). These spheres were calcinated to obtain a porous catalyst without organic material. The structural properties of the material were investigated by X-ray diffraction, Fourier transform infrared spectroscopy and X-ray fluorescence. The calcined beads were tested in the transesterification reaction of sunflower oil and methanol. The results were optimized using a 3² factorial design with one central point. The best conversion of triglyceride to methyl esters was 56.12 ± 0.32 % w.t in the following reaction conditions: molar ratio (1:9), catalyst amount (3 % w.t), reaction time (4 h), temperature (60 °C). It can be concluded that the porous spheres based on calcium oxide exhibited considerable conversions for production of biodiesel and is therefore chitosan is a good directing agent to obtain a porous matrix.

Keywords: biodiesel, transesterification reaction, spheres, calcium oxide.

INTRODUCTION

Biodiesel, an alternative diesel fuel, is made from renewable biological sources such as vegetable oils and animal fats. It is biodegradable and nontoxic, has low emission profiles and so is environmentally beneficial [1]. Heterogeneous catalysis is an economically and ecologically important field in catalyst research. These catalysts have many advantages: they are environmentally benign, non-corrosive, and present fewer control problems. They are also much easier to separate from products and they can be designed to give best activity, selectivity and longer catalyst lifetimes [2]. Chitosan is a biopolymer obtained by deacetylation of chitin, a polysaccharide abundant found in marine invertebrates and insects [3]. Calcium oxide has prominent among other oxides of alkaline earth metals, for have relatively high base strength and less environmental impact due to its low solubility in methanol and being synthesized from inexpensive sources such as limestone and calcium hydroxide [4]. Among the different catalytic systems based on solids, CaO is one of the most active solid catalysts for the production of biodiesel [5-8]. This study proposes the immobilization of CaO on chitosan, in order to increase the surface area and reduce the calcium leaching and solubilization on the reaction system. The chitosan-metal complex was calcined and characterized by XRD, FTIR and XRF. The

porous spheres of calcium oxide were used to catalyze the transesterification of sunflower oil and methanol. The effect of oil/alcohol molar ration and catalyst weight was investigated on the methyl ester conversion.

MATERIALS and METHODS

Materials

The reagents used were: chitosan with deacetylation degree > 85% (POLYMAR); sunflower oil commercial obtained from a local supermarket (LIZA); methanol with a purity > 99.8% (VETEC); calcium nitrate tetrahydrate P.A (VETEC); methyl heptadecanoato with a purity of > 99.99% (SIGMA-USA) and analytic grade He, N₂ and Ar gases (WHITE MARTINS).

Preparation and catalyst activation

A chitosan solution 5% (w/w) prepared in acetic acid 5% (v/v) was mixed with tetrahydrated calcium nitrate in the monomer: calcium molar ratio of (1mol:1mol), under intense stirring. The chitosan-calcium solution was dripped into a ammonium hydroxide solution 50% (v/v) obtaining a hybrid spheres porous. The beads remained in the coagulante solution for 24 hours for groups amino neutralization, and then they were washed with distilled water repeatedly and dried at room temperature. Before the chitosan spheres could be used as a catalyst, it was necessary to be activated. The thermic process consisted of heating the material in a mufle and warming it to 900 °C for 1 h at a heating rate of 5 °C/min. The objective of activation was to promote the formation of calcium oxide basic and eliminate the organic matrix of the chitosan spheres.

Catalyst characterization

The methods used for the characterization of chitosan, spheres of chitosan with calcium (natural and calcined) were XRD, FTIR and XRF. All of these characterization tests were performed to observe the differences after the thermal process materials. The associated methods provided valuable information regarding: the identification of minerals and crystallography (XRD), the identification of organic groups (FTIR) and the elementary chemical composition (XRF).

Transesterification reactions of sunflower oil

The transesterification reactions were conducted in a three necked glass reactor with a condenser and magnetic stirrer with 60 mL of vegetable oil with different volumes of methanol and varied amounts of catalyst (over the weight of heavy oil). The oil/methanol ratios used were 1:6; 1:9 and 1:12 and the amounts of catalyst were 1, 2 and 3 % w.t. The temperature of the reaction was fixed at 60°C and the reaction time of 4 hours was obtained accomplishing the equilibrium reaction. The catalyst was separated by centrifugation at 2250 rpm for 30 minutes, and the reaction mixture (methyl ester and glycerine) was placed in a funnel for phase separation. The residual methanol in the methyl ester layer was evaporated out using a rotary evaporator at 100 °C to obtain the fatty acid methyl esters. The content of methyl esters in the biodiesel was determined according to the procedure described in the standard EN 14103 [9]. This analysis was done using a gas

chromatograph Varian CP-3800 equipped with a flame ionization detector (FID). The column was a "CP WAX 52CB" (30 x 0.25 x 0.05 m).

RESULTS and DISCUSSION

Catalyst characterization

Figure 1 shows the X-ray diffractograms of the parent chitosan (a) chitosan spheres with calcium (b) and the thermally modified chitosan spheres (c) 900 °C/1h. It was observed in the Figure 1 (a) the occurrence of two peaks at angles 2θ (11.17 and 23.11). The second peak is related to the deformation of the amorphous material [6]. For the spheres of chitosan with calcium in the XRD diffractogram were identified peaks at angles of 2θ (11.98, 23.02, 29.20 and 34.42) shown in Figure 1 (b). However, in the XRD shown in Figure 1 (c) for the spheres thermally modified, the peaks are related to the formation of crystalline material of calcium oxide found in the angles 2θ (21.14, 24.51, 26.98; 33.29, 34.91, 40.01, 42.08, 43.95, 46.16, 48.25, 50.48, 55.52, 59.83 and 64.31).

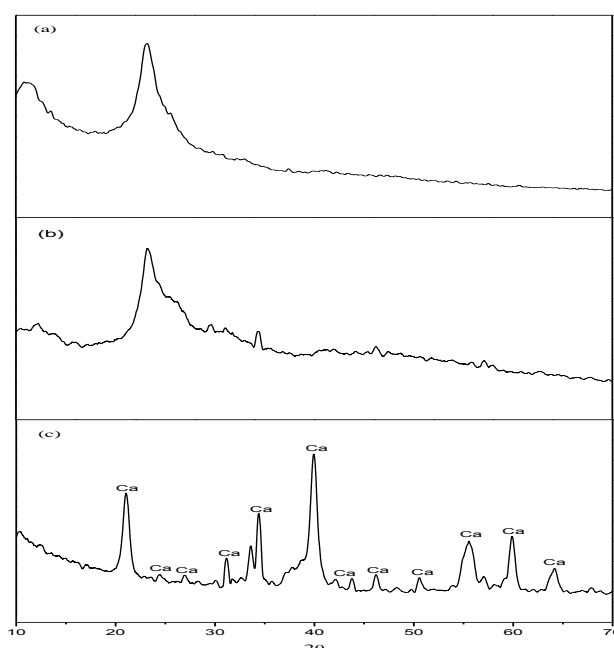


Figure 1. X-ray diffractograms of the parent chitosan (a) chitosan spheres with calcium (b) and the thermally modified 900 °C/1h chitosan spheres (c).

The Figure 2 presents the absorption spectrum in the infrared region between 4000 and 400 cm^{-1} for pristine chitosan (a) chitosan with calcium (b) chitosan with calcium after heat treatment (c). It was observed bands near 3400 cm^{-1} of from group hydroxyl stretch (OH). The appearance of a small band at 2887 cm^{-1} is due to the of groups stretch ($-\text{CH}_2$). There are at 1664 cm^{-1} axial strain of ($\text{C}=\text{O}$) group amide concerning of acetyl groups not deacetylated. There is the angular deformation of amino group at 1592 cm^{-1} and axial deformation amide group ($\text{C}-\text{N}$) at 1415 cm^{-1} . There is also symmetrical angular deformation ($-\text{CH}_3$) at 1378 cm^{-1} , the axial deformation of ($-\text{CN}$) groups amino around 1070 cm^{-1} and polysaccharide structures bands in the region between 1157 to 897 cm^{-1} . The similarity between (a) and (b) spectra indicate that not all the amino and hydroxyl groups are complexed with calcium ions. The spectrum of spheres in thermally calcined (c) was observed the appearance of the bands 3643 cm^{-1} was attributed to the of $\text{Ca}(\text{OH})_2$. The band at 1417 cm^{-1} was associated with the stretching of (CO_3^{-2}) due to chemisorption of

(CO₂) on the surface containing Ca(OH)₂. The band at 500-875 cm⁻¹ corresponding (Ca-O) bands.

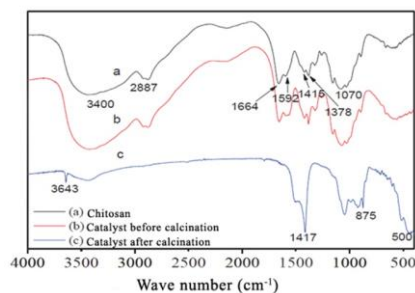


Figure 2. Infrared spectrum of the chitosan (a) spheres chitosan with calcium (b) spheres with calcium heat modified at 900 ° C / 1h (c).

The XRF analyses of chitosan spheres with calcium have not been performed in other studies. This analyze shows the metal content in the spheres. The chemical composition of chitosan spheres with calcium obtained by XRF showed that the predominant element is calcium (84.42 % w.t) (Table 1). The appearance of the element ruthenium (Ru) may be due to the contamination during the XRF analysis, and other elements are characteristic of chitosan is in its powder form. The chemical composition of chitosan has been demonstrated in different studies, using several techniques, such as, elemental analysis and XPS [10,11].

Table 1. Chemical composition of elemental calcium with chitosan spheres by XRF.

Elements (% w.t)								
Ca	Si	Fe	P	Sr	K	Cl	Ru	Σ
84.42	1.80	3.34	0.20	0.61	0.62	0.11	8.90	100.00

Transesterification reaction

Kinetic evaluation

The optimum reaction time for the transesterification reaction using the synthesized catalyst was determined by performing the reaction during 9h (Figure 3). The result showed that the methyl esters content significantly increased from 0-9h, giving the highest methyl ester content of 52.20 ± 0.08 % w.t in the 4 hours.

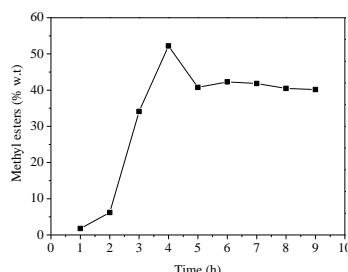


Figure 3. Influence of the reaction equilibrium time.

Experimental design

Table 2 shows the results obtained from the experimental design performed at different reaction conditions. Figure 4 shows the response surface plot of the methyl esters conversion in function of two variables (molar ratio and amount of catalyst). Negative values on the scale corresponding to lower values of the variable and positive values represent the higher values. According to the results obtained using an experimental design (3^2 + point central), it is noticed that the values of methyl esters are higher when using a larger amount of catalyst with a lower molar ratio.

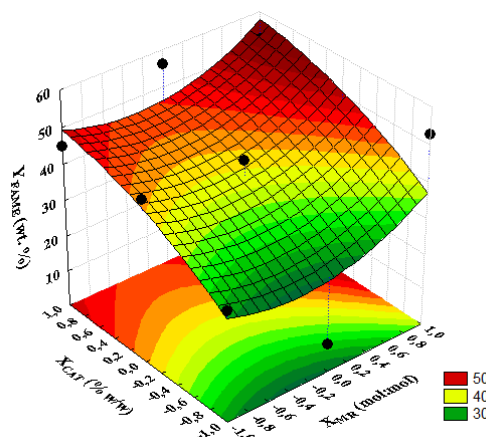


Figure 4. Response surface for the model of chitosan spheres with calcium.

The molar ratio between the reagents is an important variable in the transesterification reaction, since the reaction is a reversible type. The minimum ratio for producing biodiesel is 1:3, requiring an excess of this ratio to cause the equilibrium of the reaction towards the formation of methyl esters.

The results depicted in Table 2 showed an increase in the conversion of methyl esters as the methyl alcohol concentration increases in the reaction medium. The maximum conversion was 56.12 ± 0.32 with a X_{RM} of (1:9) and X_{CAT} of (3%). The kinetic point of view it is expected that increasing the molar ratio favors the conversion reaction, since a higher concentration of alcohol in the reaction shifts the chemical equilibrium to the product side. However, the use of a high volume of methyl alcohol may shift the equilibrium in the opposite direction, towards the formation of mono, di and triglycerides, decreasing the production of methyl esters, what happened in the X_{RM} (1:12). Also an increase in molar ratio complicates the process of separation by gravity between the ester and glycerin phases formed.

Table 2. Experimental design of transesterification reaction.

Run	Coded variables		Real variables		Conversion
	Molar ratio (X_{RM})	Catalyst Amount (X_{CAT})	Molar ratio (X_{RM})	Catalyst Amount (X_{CAT})	Methyl Esters (Y_o %)
1	-1	-1	1:6	1	30.64 ± 0.21
2	-1	0	1:6	2	44.97 ± 0.02
3	-1	1	1:6	3	44.72 ± 0.33
4	0	-1	1:9	1	7.81 ± 0.01
5	0	0	1:9	2	43.32 ± 0.05
6	0	1	1:9	3	56.12 ± 0.32
7	1	-1	1:12	1	52.67 ± 0.04
8	1	0	1:12	2	40.54 ± 0.32
9	1	1	1:12	3	52.20 ± 0.20
10	0	0	1:9	2	43.46 ± 0.06
11	0	0	1:9	2	43.38 ± 0.03
12	0	0	1:9	2	43.25 ± 0.12

CONCLUSIONS

The biopolymer chitosan served as structural driver in the production of porous calcium oxide. The results of XRD, XRF and FTIR confirmed the production of calcium oxide using the thermal process. The parameters for the transesterification reaction were optimized using an experimental design 3^2 and the best result was obtained at reaction conditions of 3 % w.t concentration of catalyst in molar ratio 1:9 (refined sunflower oil / methanol alcohol) in a time of 4 hours. The conversion to methyl ester was found 56.12 ± 0.32 % w.t. The applications of the catalyst in the transesterification of refined sunflower oil with methyl alcohol achieved high conversions of methyl esters.

ACKNOWLEDGEMENTS

The authors acknowledge to CNPq and FUNCAP for financial support.

REFERENCES

- [1]Shahid E.M., Jamal, Y. (2008). A review of biodiesel as vehicular fuel, *Renew. Sust. Energ.*, 12, 2484-94.
- [2]Watkins, S.R., Lee, K.F.A. (2004). Li-CaO catalysed tri-glyceride transesterification for biodiesel applications, *Green Chem.*, 7, 335-40.
- [3]Guibal, E. (2004). Interactions of metal ions with chitosan-based sorbents: a review, *Sep.Purif. Technol.*, 38, 43-74.

- [4] Zabeti, M.; Daud, W.M.A.W.; Aroua, M.K. (2009). Activity of solid catalysts for biodiesel production: A review, *Fuel Process. Technol.*, 90, 770-77.
- [5] Yang, R.; Su, M.; Li, M.; Zhang, J.; Hao, X.; Zhang, H. (2010). One-pot process combining transesterification and selective hydrogenation for biodiesel production from starting material of high degree of unsaturation, *Bioresour. Technol.*, 101, 5903-09.
- [6] Atadashi, I.M.; Aroua, M.K.; Aziz, A.A. (2010). Biodiesel separation and purification: a review Biodiesel separation and purification: a review, *Renew. Energ.*, 36, 437-43.
- [7] Granados, M.L.; Poves, M.D.Z.; Alonso, D.M.; Mariscal, R.; Galisteo, F.C, Moreno, T.R. (2007). Biodiesel from sunflower oil by using activated calcium oxide, *Appl. Catal. B-Environ.*, 73, 317-26.
- [8] Alba, R.A.C.; Santamaría, G.J.; Mérida, R.J.M.; Moreno, T.R.; Martín, A.D.; Jiménez, L.A. (2010). Heterogeneous transesterification processes by using CaO supported on zinc oxide as basic catalysts, *Catal. Today.*, 149, 281-87.
- [9] EN 14103 (2001). Fats and Oil Derivatives- Fatty Acid Methyl Esters (FAME). Determination of Ester and Linoleic Acid Methyl Ester Contents.
- [10] Rabelo, R.B.; Vieira, R.S.; Luna, F.M.T.; Guibal, E.; Beppu, M.M. (2012). Adsorption of copper (II) and mercury (II) ions onto chemically-modified chitosan membranes: Equilibrium and kinetic properties, *Adsorpt. Sci. Technol.*, 30, 1-21.
- [11] Vieira, R.S.; Oliveira, M.M.; Guibal, E.; Rodríguez-Castellón, E.; Beppu, M.M. (2011). Copper, mercury and chromium adsorption on natural and crosslinked chitosan films: An XPS investigation of mechanism, *Colloid. Surface A.*, 374, 108-114.

INFLUENCE OF THE ADDITION OF POTATO STARCH TO CHITOSAN MATRICES USED FOR CONTROLLED RELEASE

M. V. Debandi, M. E. Daraio, N. J. Francois*

*Grupo de Aplicaciones de Materiales Biocompatibles, INTECIN (UBA-CONICET).
Departamento de Química. Facultad de Ingeniería, Universidad de Buenos Aires
Av. Paseo Colón 850, C1063ACV, Ciudad Autónoma de Buenos Aires, Argentina.*

*E-mail address: nfranco@fi.uba.ar

ABSTRACT

The aim of this study was the preparation of polymeric matrices of chitosan-potato starch blends for the controlled release of triethanolamine hydroiodide which is a cosmetic active with an effective anti-cellulitic activity.

The dynamic rheological parameters (G' : elastic modulus and G'' : viscous modulus) and the kinetic behavior of blends prepared with different ratios of potato starch and chitosan keeping a 4.5 % w/w final polymer concentration were obtained. Rheological results indicated that the blends are not gels because a crossover between G' and G'' is observed, being $G' < G''$ at low frequencies. This viscoelastic behavior corresponds to entanglements networks that are present in concentrated polymer solutions.

The release experiments were performed using a vertical diffusion Franz cell with a cellulose membrane separating the upper and lower compartments of the cell. The release profile of the blend prepared with a chitosan/potato starch ratio of 70/30 showed the biggest difference compared to the release profile of the matrix prepared only with chitosan.

The analysis of the mechanical spectra and the kinetic profiles has demonstrated that the addition of 30 % of starch produces the optimum blend to achieve the longest release period while keeping the rigidity of the matrix.

Keywords

Chitosan, Potato starch, Blends, Polymeric dispersions, Controlled release

INTRODUCTION

Chitosan is a cationic polysaccharide obtained by the alkaline deacetylation of chitin which is the second most abundant polysaccharide in nature. There is great interest on it for medical, pharmaceutical and cosmetic applications, particularly for drug delivery. This interest is motivated by its physicochemical characteristics such as biodegradability, biocompatibility, mucoadhesion, non-toxicity, film-forming capacity, bioactivity as well as its bacteriostatic and fungistatic properties [1, 2].

In order to modify the characteristics of pure chitosan matrices, there have been a considerable number of researches evaluating hydrogels made of blends prepared with chitosan and several synthetic and natural polymers like xanthane, polyvinyl alcohol, alginate, carboxy methylcellulose, pectin, carragenan or starch [3, 4, 5, 6, 7].

Among all the polymers mentioned above, we have selected starch to prepare the blends because it is a natural, biodegradable and inexpensive polymer.

Starch is a mixture of two polymers, amylopectin and amylose, formed by a single type of carbohydrate, glucose. Amylose is a linear polymer and amylopectin is a highly

branched one. The average ratio of both polymers in potato starch is 21 % for amylose and 79 % for amylopectin [8]. When heated in water, potato starch granules disintegrate easily and form an homogeneous gel. Figure 1 shows the chitosan and starch chemical structures.

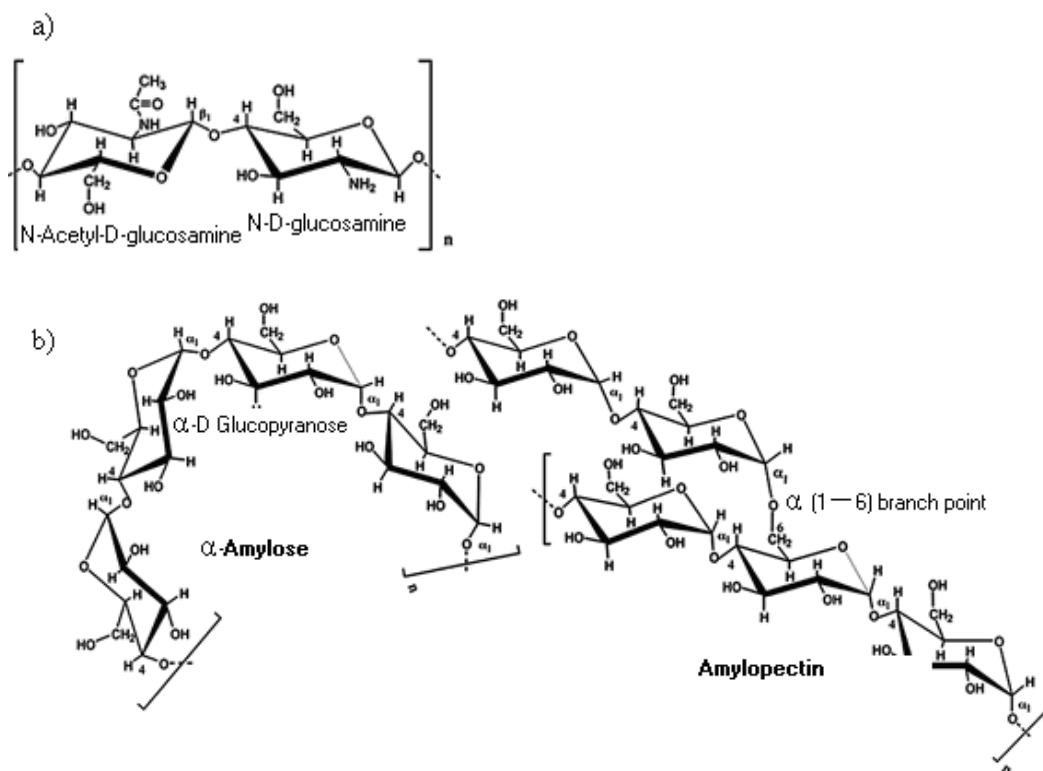


Figure 1. Chemical structure of: a) Chitosan; b) Starch [9]

Our goal was to evaluate the addition of gelatinized potato starch to a chitosan matrix and its effect on the release kinetics of a cosmetic active. The changes to the viscoelastic properties of the polymeric matrix after the addition of starch were analyzed with dynamic rheology.

MATERIALS and METHODS

Chitosan (CH) of medium molecular weight (Aldrich, deacetylation degree 83%) and hydrolyzed potato starch (Sigma Aldrich) were used as received from the providers.

The drug triethanolamine hydroiodide (TEAH) (Fabriquímica S.A., Argentina) with a final concentration of 0.75 % w/w was used for the kinetic experiments.

Samples preparation

CHI dispersions were obtained with a weighed amount of polymer dispersed in deionized water by magnetic agitation and the final pH was adjusted to 4.5 using lactic acid of analytical grade (Cicarelli, Argentina).

Aqueous potato starch (PS) solutions of the desired concentration were prepared by heating until reaching its gelatinization temperature (64 °C) under stirring.

To produce the blends, the gelatinized potato starch was mixed with the chitosan dispersion in order to obtain three different polymeric matrices. They were prepared with CH/PS ratios of 30/70 (CH:1.35 % w/w , PS: 3.15 % w/w), 50/50 (CH = PS: 2.25% w/w)

and 70/30 (CH:3.15 % w/w , PS: 1.35 % w/w). In each case the final total polymer concentration was 4.5 % w/w.

Dynamic rheological measurements

Each polymeric matrix was weighed and poured in order to cover completely the area of the 50-mm rough-flat plate device of a Paar Physica controlled stress rotational shear rheometer (MCR 300, Stuttgart, Germany). The temperature of each sample was kept constant at 25 °C using a Peltier system (Viscotherm VT2, Paar Physica, Germany).

To avoid the dehydration of the sample during the rheological measurement, a container with water was placed around the rheometer plate in order to keep a relative high humidity. Each sample was allowed to rest 10 minutes before the measurement in order to reach mechanical and thermal equilibrium.

For each sample, the linear viscoelastic range (LVR) was determined performing oscillatory stress sweeps and then a frequency sweep was obtained at a constant strain of 0.5 %. The rheological parameters obtained from the frequency sweeps were the storage modulus (G') and the loss modulus (G'').

Release measurements

The in vitro drug delivery experiments were accomplished at 32 °C using a 20 mL Flat Ground Joint type Franz Cell (PermeGear, PA). The lower compartment of the Franz Cell was filled with a buffer solution with a pH of 7.4 kept under constant stirring during the experiment. The upper compartment was filled with 10 gr of the polymeric matrix.

Between the upper and lower compartments there was a cellulose membrane with an average pore diameter of 48 Å and a Mw cut-off of 12,000 (Arthur Thomas).

The cumulative concentration of TEAH released was obtained measuring the absorbance of an aliquot taken from the receptor solution, at 240 nm with a Shimadzu UV-2401 spectrophotometer.

After each aliquot was taken, the volume (20 mL) in the receptor compartment was made up with the buffer solution, assuring a constant volume in the lower compartment and a full contact between the polymeric matrix supported by the membrane and the receptor liquid. Data reproducibility was assessed by running the experiments in duplicate.

Kinetic data treatment

Taking into account that the drug can only be released through the surface of the membrane in contact with the liquid of the receptor compartment, it is assumed that the release process is one dimensional. The cumulative concentration of TEAH was fitted to a power law type semiempirical equation [10]:

$$M_t = M_\infty k t^n \quad (1)$$

M_t and M_∞ are the cumulative amount of drug released after a time t and an infinite time respectively, k is a constant depending on kinetic characteristics and experimental conditions, and n is the exponent describing the release process.

M_∞ and k were included in k' , and equation (2) was used to fit the data:

$$M_t = k' t^n \quad (2)$$

RESULTS and DISCUSSION

For every sample tested, the frequency sweep (Figure 2) showed a crossover between G' and G'' , being $G' < G''$ at low frequencies. This viscoelastic behavior corresponds to entanglement networks occurring in concentrated polymer solutions [11].

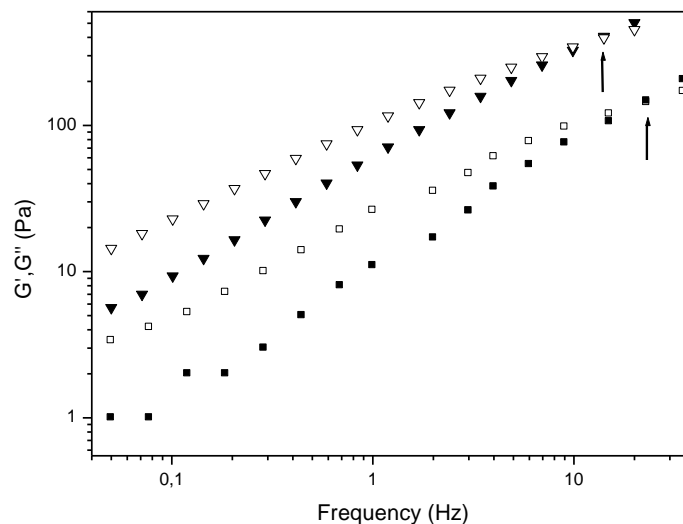


Figure 2. Frequency sweep for CHI 4.5 % w/w (\blacktriangledown) and CHI-St blend 50/50 (\blacksquare). Arrows show the crossover point. G' (solid symbols) and G'' (non-solid symbols).

An increase of the chitosan concentration in the blend produced a shifting of the crossover frequency towards lower values and a growing in G' and G'' values (see Table 1) which is indicative of an increase in the matrix rigidity due to the existence of more entanglements [12]. In particular the G' parameter can be used as an indicator of macroscopic hardness and as an indicator of structure [13].

Table 1. Crossover frequency (ω) and rheological parameters (G' , G'') for pure CHI and CHI/PS matrices from the frequency sweep

CH % w/w	PS % w/w	ω (Hz)	$G' = G''$ (Pa)
4.5	0	13	400
3.15	1.35	13	230
2.25	2.25	23	150
1.35	3.15	24.8	72

In the final matrix there are different types of interactions. The stronger ones belong to the entanglements between the chitosan chains. The pure chitosan matrix has the biggest G' which is indicative of more rigidity. In the case of the blends there are interactions between both biopolymers and interactions between starch chains. The hydroxyl groups of amylose can establish intermolecular hydrogen bonds with the amino groups of chitosan [14]. These interactions could affect the structure of the final matrix modifying the porosity and tortuosity of the polymeric matrix [4] with a consequent change on the G' value.

Tortuosity is a difficult parameter to quantify; it includes the average pore size, the pore size distribution and the pore interconnections [15]. Taking into account that effective diffusion path length for drug release is affected by the tortuosity, the final composition and the crosslinking of the matrices could determine the release profiles.

The kinetic profiles were obtained plotting the cumulative concentration of TEAH released from the polymeric matrix in function of time, as shown in Figure 3. The total drug quantities released during the first 2 h ranged from 16.8 % (blend CH/PS: 3.15 % w/w / 1.35 % w/w) to 22.1 % (CH: 4.5 % w/w).

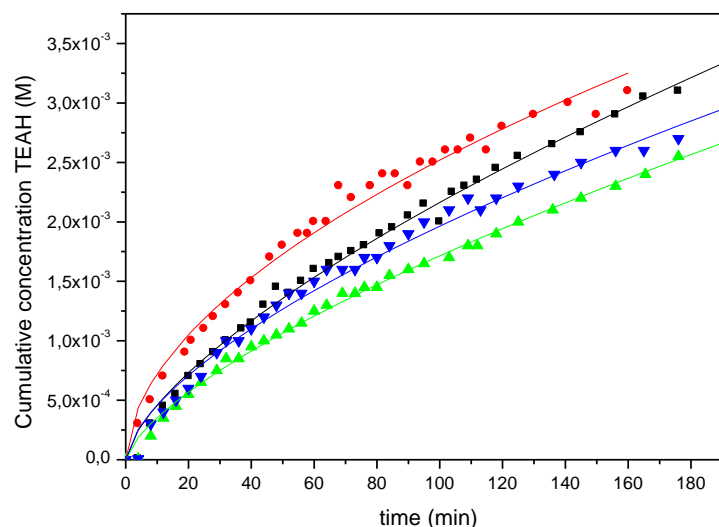


Figure 3. Cumulative concentration of TEAH released from CH/PS: 100/0 (●), CH/PS: 30/70 (■), CH/PS: 50/50 (▼), CH/PS: 70/30 (▲). Lines represent calculated concentration values obtained using equation (2). Best fit parameters were taken from Table 2.

These results indicate that the release of TEAH was dependent upon the ratio of CH/PS used.

The kinetic parameters obtained using equation (2) are shown in Table 2.

Table 2. TEAH release kinetic parameters

Polymeric matrix composition (% w/w)	k^2 ($M \text{ min}^{-n}$)	n	R^2
CH/ PS: 4.5 / 0	$(2.1 \pm 0.18) \times 10^{-4}$	0.54 ± 0.03	0.995
CH/ PS: 3.15 / 1.35	$(7.3 \pm 0.74) \times 10^{-5}$	0.67 ± 0.03	0.992
CH/ PS: 2.25 / 2.25	$(9.7 \pm 1.11) \times 10^{-5}$	0.67 ± 0.02	0.994
CH/ PS: 1.35 / 3.15	$(1.1 \pm 0.13) \times 10^{-4}$	0.63 ± 0.02	0.996

For slab geometry of the sample, the n kinetic parameter in equation (2) has two proposed physical meanings: $n = 0.5$ corresponds to a diffusion-controlled drug release mechanism and $n = 1.0$ indicates a relaxation-controlled drug release [8]. Values of n between 0.5 and 1 can be regarded as a superposition of the two mechanisms mentioned before and it is called an anomalous behavior.

Table 2 presents the results of the fitting using equation (2) for each matrix tested.

The data appears to be correctly described and fitted by this equation, as can be seen in Figure 3, and as it is reflected by the correlation coefficients (R^2) with values of 0.994 ± 0.002 . The n values indicate an anomalous kinetic mechanism for all the matrices assayed.

From the frequency sweeps of the rheological experiments, it can be concluded that the matrices studied herein are not gels but they are concentrated dispersions. They present a crossover between G' and G'' at a determined frequency depending on the matrix studied. The crossover frequency for the blends shifted to lower values when the

concentration of chitosan increased as a consequence of a bigger number of polymeric interactions.

Taking into account that the structure of the matrix is a factor that influences the diffusion of the solutes through the polymeric network, a higher porosity and a lower G' could be associated with a higher release of the drug.

ACKNOWLEDGEMENTS

Financial support from Universidad de Buenos Aires, Argentina (Grant 20020100100260, UBACyT 2011-2014) is gratefully acknowledged.

REFERENCES

- [1] Rinaudo, M. (2006). Chitin and chitosan: properties and applications. *Progress in Polym. Sci.*, 31, 603-632.
- [2] Varshosaz, J.; Jaffari, F.; Karimzadeh, S. (2006). Development of bioadhesive chitosan gels for topical delivery of lidocaine. *Sci. Pharm.*, 74, 209-223.
- [3] Martinez-Ruvaleaba, A.; Chornet E.; et al. (2007). Viscoelastic properties of dispersed chitosan/xanthan hydrogels. *Carb. Polym.*, 67, 586-595.
- [4] Viyoch, J.; Sudemark, T.; Srema, W.; et al (2005) Development of hydrogel patch for controlled release of alpha-hydroxyacid contained in tamarind fruit pulp extract. *Int. J. of Cosmetic Sci.*, 27, 89-99.
- [5] Berger, J.; Reist, M.; Mayer, J.; et al (2004) Structure and interactions in covalently and ionically crosslinked chitosan hydrogels for biomedical applications. *Europ. J. Of Pharm. and Biopharm.*, 57, 19-34.
- [6] Moller, H.; Grelier, S.; Pardon, P.; et al (2004) Antimicrobial and Physicochemical Properties of Chitosan-HPMC-Based Films. *J. Agric. Food Chem.*, 52, 6585-6591
- [7] Marudova, M.; Mac Dougall, A.; Ring, S. (2004). Pectin-chitosan interactions and gel formation. *Carbohydr. Research.*, 339, 1933-1939.
- [8] Swinkels, J. (1985). Composition and Properties of Commercial Native Starches. *Starch*, 37, 1-5.
- [9] Sá-Lima, H.; Caridade, S.; Mano, J.; et al (2010). Stimuli-responsive chitosan-starch injectable hydrogels combined with encapsulated adipose-derived stromal cells for articular cartilage regeneration. *Soft Matter*, 6, 5184-5195.
- [10] Ritger, P.; Peppas, N. (1987) Fickian and non-Fickian release from non-swelling devices in the forms of slabs, spheres, cylinders or discs. *J. of Controlled Rel.*, 5, 23-36.
- [11] Martinez-Ruvalcaba, A.; Chornet, E.; Rodrigue D. (2004). Dynamic rheological properties of concentrated Chitosan solutions. *Appl. Rheol.*, 14, 140-147
- [12] Serrero, A.; Trombotto, S.; Cassagnau P.; et al (2010) Polysaccharide-based adhesive for biomedical applications: correlation between rheological behavior and adhesion. *Biomacromol.*, 12, 1556-1566.
- [13] Narine, S.; Marangoni, A. (2000). Elastic modulus as an indicator of macroscopic hardness of fat crystal networks. *Lebensmittel-Wissenschaft und-Technologie*, 34, 33-40.
- [14] Xu, Y.; Kim, K.; Hanna, M.; et al (2005). Chitosan-starch composite film: preparation and characterization. *Ind. Crops and Products*, 21, 185-192.
- [15] Hoffman, A. (2002). Hydrogels for biomedical applications. *Advanced Drug Del. Rev.*, 43, 3-12.

CONTROLLED RELEASE OF FERTILIZERS: INFLUENCE OF XANTHAN AND HIDROXYPROPYLMETHYLCELLULOSE ADDITION TO CHITOSAN MATRICES

Mariana A. Melaj, Eugenia Andisco, Nora J. Francois*, Marta E. Daraio

*Grupo de Aplicaciones de Materiales Biocompatibles, INTECIN (UBA-CONICET).
Departamento de Química. Facultad de Ingeniería, Universidad de Buenos Aires
Av. Paseo Colón 850, C1063ACV, Ciudad Autónoma de Buenos Aires, Argentina.*

**E-mail address: nfranco@fi.uba.ar*

ABSTRACT

Tablets made of different polymeric blends were prepared to analyze the influence of the addition of xanthan (X) and hidroxypropylmethylcellulose (HPMC) to chitosan (CH) matrices on the release mechanism of KNO_3 , used as a model fertilizer, in order to obtain a controlled release fertilizer (CRF). Drug release was continuously monitored by conductimetry and the cumulative concentrations were determined as a function of time using a calibration curve. To fit the experimental data, a power law model was used in order to characterize the delivery kinetics of KNO_3 . Polymeric interactions caused a reduction of the release ratio of the drug. The CH:X blend forms a complex due to the opposite charges of these polymers, resulting in a release mechanism dominated by the relaxation of the macromolecules. When HPMC is added to Chitosan, a gel layer is formed and the release rate is independent of time. The addition of these polymers, X or HPMC, to a CH matrix affects the kinetic mechanism lowering the fertilizer release rate. Chitosan:HPMC blends would be an effective option to prepare a CRF, enabling the availability of the fertilizer for a longer period of time.

Keywords

Controlled-release fertilizer; release kinetics; fertilizer; chitosan; xanthan; hidroxypropylmethylcellulose.

INTRODUCTION

Nutrient use efficiency is conceived as the amount of nutrients taken up from the soil by plants compared with the amount of nutrients available in the soil during the same period of time. When a conventional fertilizer is applied, a fraction of it may be lost to the environment by different means, mostly by leaching, volatilization, breakdown by microorganisms and chemical processes such as hydrolysis or precipitation.

Slow and controlled release fertilizers contain a plant nutrient in a format which delays its availability for plant uptake and use after its application, or which extends its availability to the plant significantly longer than a reference rapidly available nutrient fertilizer such as ammonium nitrate or urea, ammonium phosphate or potassium chloride. With slow release fertilizers (SRFs), the rate, pattern and duration of release are not well controlled; they may be strongly affected by storage, transportation and distribution in the field, or by soil conditions such as microbiological activity, pH and moisture content. Controlled release fertilizers (CRFs) are the ones where the factors dominating the rate,

pattern and duration of the release are well-known and controllable during their preparation [1] CRFs based on polymers, minimize nutrient losses and offer additional benefits such as the controlled nutrient availability required by different crops. This capability reduces toxic concentrations and increases the efficiency of nutrient uptake by plants [2].

The use of biocompatible polymers as CRF's matrices reduces the risks of environmental contamination because they don't leave toxic waste in the soil.

Chitosan (CH), xanthan (X) and hidroxypropylmethylcellulose (HPMC) are polymers frequently used for drug controlled release [3]. Chitosan, poly- β -(1 \rightarrow 4)-D-glucosamine, is the only natural polysaccharide with a cationic nature and is produced by alkaline deacetylation of chitin [4]. This polymer is not only naturally abundant, but also biocompatible, biodegradable and nontoxic, and that's why it has many applications. It also has other properties that contribute to crop development. It acts as carbon source for soil microbes and may be used as a plant promoter [5]. When it is included in polymeric blends, the release kinetics of the drug is altered.

Xanthan gum is a microbial exopolysaccharide consisting of a cellulosic backbone with two mannose and one glucuronic acid side chains on every second glucose residue [4]. It is used in agriculture as a plant growth stimulator [6].

Hidroxypropil methylcellulose is a propylene glycol ether of methyl-cellulose. The hydroxypropyl substituent group, $-\text{OCH}_2\text{CH}(\text{OH})\text{CH}_3$ contains a secondary hydroxyl on the number two carbon. HPMC with higher molecular weight forms a more viscous gel and the drug release from an HPMC matrix tablet is slow. It is used as a dispersing agent in pesticides and fertilizers [7]. Figure 1 shows chitosan, xanthan and HPMC structures.

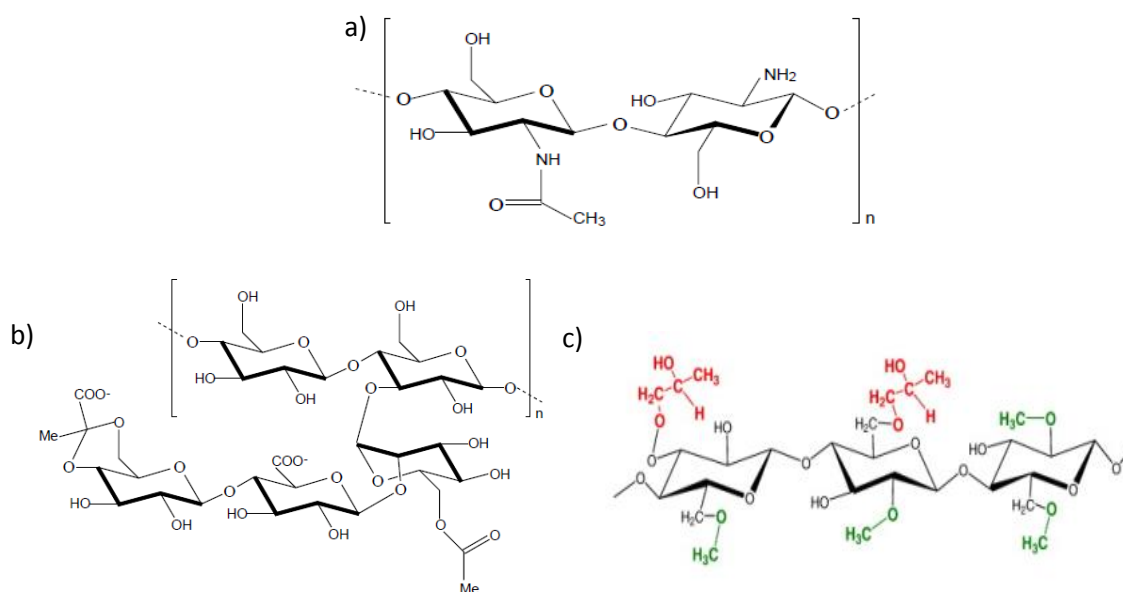


Figure 1: Chemical structure of: a) chitosan [8]; b) xanthan gum [8] and c) HPMC [9].

The objective of this work was to analyze the influence of the matrix composition on the release mechanism of one model fertilizer. We prepared tablets using two different polymeric blends: chitosan: xanthan (Q: X) and chitosan: HPMC (Q: HPMC).

MATERIALS and METHODS

Materials

Chitosan of medium molecular weight was supplied by Sigma-Aldrich with a deacetylation degree of 83%. Xanthan was provided by Fluka and HPMC from Colorcon (Methocel K100M Premium). As a model fertilizer it was used KNO₃ (Aldrich) and magnesium stearate as a lubricant (LU) (Mallinckrodt), both of analytical grade.

Methods

Preparation of matrix tablets

Multilayers tablets were prepared. They had two external layers containing a polymer blend and lubricant without fertilizer and a middle layer made of the same components plus the fertilizer KNO₃. The polymers were passed through a sieve with a mesh of 420 microns before processing them. The blend of components was mixed. Layered matrix tablets were prepared by adding a weighed amount of the powder mixture without the model fertilizer to a die and slightly compressing it for uniform spreading. The weighed amount of the powder mixture blended with the KNO₃ was placed over the first layer and again was slightly compressed. The other weighed mixture was subsequently placed and compressed at 6 Tons for 1 minute using a manual hydraulic press. The diameter of the tablets was 1.6 cm and the thickness was 0.3 cm. The final mass was 0.8000 g.

The composition of the samples is shown in Table 1.

Table 1. Compositions of the tablets

Sample	Composition (% w/w)				
	CH	X	HPMC	KNO ₃	LU
CH:X	33.7	33.7	----	31.2	1.4
CH:HPMC	33.7	----	33.7	31.2	1.4

Release of potassium nitrate

To measure the kinetic data, the tablets were placed in a stainless steel basket and immersed into a beaker containing 1,00L of distilled water at (25 ± 0.2) °C under a constant magnetic stirring at (250 ± 10) rpm. The delivery of KNO₃ to the water phase was continuously monitored by conductimetry and the cumulative concentrations were determined as a function of time using a calibration curve.

Drug release mechanism

The temporal behavior of the fertilizer concentration during the release process (the first 60% of the fractional release curve) was adjusted by a power-law type relationship [10, 11]:

$$C_t = k \times t^n \quad (1)$$

C_t is the molar cumulative concentration of KNO₃ at time t , k is a constant associated to the kinetic characteristics and the experimental setup, and n is a kinetic parameter related to the release mechanism. The percentage of drug released can be derived from (1):

$$KNO_3 \text{ released } (\%) = (C_t \times V \times M_r / m_o) \times 100 = k' \times t^n \quad (2)$$

V is the volume of distilled water, M_r is the fertilizer molecular weight and m_0 is the initial fertilizer mass in the tablet.

RESULTS and DISCUSSION

Previous studies show, under the same working conditions, that a pure CH matrix is not useful because the fertilizer is released too fast [12]. The addition of X or HPMC to the CH matrix causes a reduction in the release ratio of KNO_3 due to polymeric interactions.

Figure 2 shows the kinetic profiles for CH:X and CH:HPMC matrices, representing the percentage of KNO_3 during the release time.

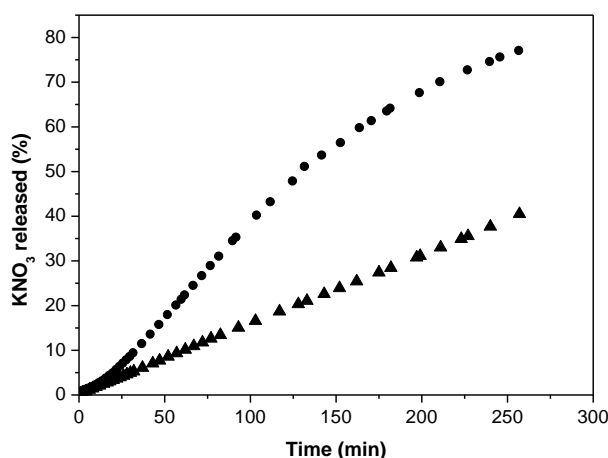


Fig. 2. Release kinetics of KNO_3 for CH:X (●) and CH:HPMC (▲).

For CH:X tablets we observed that the initial points (up to about 15 minutes) deviate from the behavior predicted by the power law. These points were not taken into account for fitting to eq (2). When a mixture of xanthan and chitosan is placed in an aqueous solution, these two oppositely charged polymers form a polyelectrolyte hydrogel due to a complexation reaction, involving the hydrophilic functions (R-COOH in the case of polyanions and $\text{R}'\text{-NH}_2$ for the polycations) [4]. This could be the reason for the observed initial delay. The CH:HPMC tablets showed a slower release than those made of CH:X polymeric matrices, in Fig 2 it can be observed that after 250 min the CH:HPMC matrix delivered only half of fertilizer compared to the CH:X tablet. The high swellability of HPMC has a significant effect on the release kinetics of the incorporated drug. When HPMC is added, the release rate decreases as consequence of the absorption of water by the polymer and the formation of a gelatinous barrier layer on the surface of the tablet matrix [13].

For a cylindrical geometry, the power law of eq (1) has two proposed physical meanings in the case of $n = 0.45$ (diffusion-controlled drug release) and $n = 0.89$ (swelling-controlled drug release or Case II transport). Values of n between 0.45 and 0.89 are described as anomalous or non-Fickian diffusion and can be regarded as a superposition of the two mechanisms. In the Case II transport, the relaxation process of the macromolecules occurring after the absorption of water by the system is the rate-determining mechanism. The n values are shown in Table 2 for this geometry.

Table 2: Diffusion exponent of the power law (eq (1)) and solute release mechanism for cylindrical shape.

Diffusion exponent (n)	Drug release mechanism
0.45	Fickian diffusion
$0.45 < n < 0.89$	Anomalous (non-Fickian) diffusion
0.89	Case-II transport
$n > 0.89$	Super case-II release kinetics

The kinetic parameters obtained fitting the release data with equation (2) are shown in Table 3.

Table 3. Kinetic parameters

Sample	n	k (min^{-n})	R^2
CH:X	0.86 ± 0.05	0.83 ± 0.20	0.9961
CH:HPMC	1.02 ± 0.03	0.14 ± 0.03	0.9876

In the case of CH:X, when the polyelectrolyte complex is formed, the diffusion of the model fertilizer and the relaxation of the macromolecules controls the release mechanism. The n value indicates an anomalous (non-Fickian) diffusion transport.

For CH:HPMC, the formation of a gel layer controls the kinetics of the incorporation of water into the tablet and consequently the model fertilizer release rate from the middle layer ($n < 0.89$). When the exponent n takes a value of 1.0, the model fertilizer release rate is independent of time. This case corresponds to zero-order release kinetics. The rate-controlling mechanism is the relaxation process of the macromolecules occurring upon water imbibition into the system [14].

The properties of chitosan used as a polymeric matrix for controlled release are enhanced when xanthan or HPMC are added. The structure formed when the matrix makes contact with the solvent causes the delay of the fertilizer release (forming a complex and a gel layer respectively). The addition of X or HPMC polymers to a CH matrix affects the kinetic mechanism decreasing the fertilizer release rate. Chitosan:HPMC blends would be an effective option to prepare CRF with the capability to extend the fertilizer availability.

ACKNOWLEDGEMENTS

We thank to Colorcon S.A. Argentina, for the supply of the HPMC polymer.

Financial support from Universidad de Buenos Aires, Argentina (Grant 20020100100260, UBACyT 2011-2014) is gratefully acknowledged

REFERENCES

- [1] Shaviv, A. (2000) Advances in Controlled Release of Fertilizers. Adv. Agron. 71, 1-49.

- [2] Davidson, D.; Gu, F. X. (2012) Materials for Sustained and Controlled Release of Nutrients and Molecules To Support Plant Growth. *J. Agric. Food Chem.*, 60, 870-876.
- [3] Sinha, V.; Singla, A.; Wadhawan, S.; et al. (2004) Chitosan microspheres as a potential carrier for drugs. *Int. J. Pharm* 274 (2004) 1–33.
- [4] Argyn-Soysal, S; Kofinas, P.; Lo, Y. M. (2009) Effect of complexation conditions on xanthan–chitosan polyelectrolyte complex gels. *Food Hydrocolloids*, 23, 202-209.
- [5] Ohta, K.; Atarashi, H.; Shimatani, Y.; et al. (2000) Effect of Chitosan with or without Nitrogen Treatments on Seeding Growth in *Eustoma Grandiflorum*. *J. Jpn. Soc. Hortic. Sci.*, 69, 63-65.
- [6] U.S.Congress, Office of Technology Assessment, Biopolymers, Making Materials Nature's Way – Background Paper, (1993) OTA – BP – E – 102 (Washington DC; U.S. Government Printing Office), Chapter 2, pp. 31.
- [7] Dow Chemical Company. (2000) Using METHOCEL Cellulose Ethers for Controlled Release of Drugs in Hydrophilic Matrix Systems. USA.
- [8] Hamman, J. H. (2010) Chitosan Based Polyelectrolyte Complexes as Potential Carrier Materials in Drug Delivery Systems. *Mar. Drugs*. 8, 1305-1322.
- [9] Patural, L.; Marshal, P.; Govin, A.; et al. (2011) Cellulose ethers influence on water retention and consistency in cement-based mortars. *Cement Concret Res* 41, 46-55.
- [10] Ritger, P. L.; Peppas, N. A. (1987). A simple equation for description of solute release. I. Fickian and non-fickian release from nonswellable devices in the form of slabs, spheres, cylinders or discs. *J. Controlled Release*, 5, 23- 36.
- [11] Ritger, P. L.; Peppas, N. A. (1987). A simple equation for description of solute release. II. Fickian and anomalous release from swellable devices. *J. Controlled Release*, 5, 37- 42.
- [12] Melaj, M.; Daraio, M. (2012) Matrices poliméricas sólidas basadas en Quitosano y Xantano para liberación controlada de fertilizantes. *Avances en Ciencia e Ing.*, 3 (1), 1-9.
- [13] Akbari J, Saedi M, Enayatifard R, Sagheb Doost M, (2010) Development and evaluation of mucoadhesive chlorhexidine tablet formulations. *Tropical Journ. of Pharm.l Research*, 9 (4) 321.
- [14] Siepmann, J.; Peppas, N. A. (2001) Modeling of drug release from delivery systems based on hydroxypropyl methylcellulose (HPMC). *Adv. Drug Delivery Rev.* 48, 139–157.

EFFECT OF USING FREEZE-THAWING CYCLES ON THE PROPERTIES OF CHITOSAN FILMS

S. Allo, M. Daraio, N. Francois*

*Grupo de Aplicaciones de Materiales Biocompatibles, INTECIN (UBA-CONICET).
Departamento de Química. Facultad de Ingeniería, Universidad de Buenos Aires
Av. Paseo Colón 850, C1063ACV, Ciudad Autónoma de Buenos Aires, Argentina.*

**E-mail address: nfranco@fi.uba.ar*

ABSTRACT

Biocompatible and biodegradable films with potential applications in agriculture, food and pharmacy industries were made using a polymeric solution of chitosan..

Films were made by casting the chitosan solution prepared without plasticizer by applying two different drying procedures: a room-temperature drying method and, a freeze–thawing cyclic process prior to the room-temperature drying process. The obtained films were characterized by physical studies including mechanical tests, swelling assays and water vapor transmission.

Based on the results obtained, when eight freezing–thawing cycles were applied during the film fabrication, a physical reinforcement of the structure was achieved, avoiding the use of a crosslinking chemical agent. Results point to an increase in the number of crosslinking points by Hydrogen-bonding..

Keywords

Chitosan, films, freeze- thawing, swelling, water vapor transmission

INTRODUCTION

Lately there has been a great interest to study and to develop films based on renewable natural polymers which can degrade naturally and faster, than the films obtained from synthetic polymers

In order to reduce and to control the negative effects of pollution associated with the use of conventional plastics, it is necessary to apply the scientific knowledge to generate low cost plastics derived from renewable sources [1].

In particular, there is great interest in studying films prepared from biopolymers because they are biodegradable and biocompatible. These characteristics makes them optimal to be used in food packaging and for coatings [2-5]. Among other features, these films are fragile and brittle [6].and for the mentionned applications they need to possess specific mechanical, morphological and thermal properties.

In the case of the food industry, these polysaccharide films can act as a support of additives or nutrients and they can also act as a barrier to gases and to water vapor. Among the most common additives we can mention the antioxidants and antimicrobials that are added to packaged food in order to minimize degradation reactions that alter the packaged product limiting its shelf life [2,3, 7]..

Chitosan is a polysaccharide with good film forming properties that can be used in edible films or coatings [8]. This cationic polymer is biocompatible and biodegradable, it has antimicrobial activity [9] and it is a good gas barrier [10].

However, polysaccharide based films have poor mechanical properties and consequently they do not provide an adequate physical protection for the product.

This paper studies the differences in mechanical response, barrier properties and the swelling behavior of chitosan films prepared with two different methods, the traditional drying process and one using 8 freeze-thaw cycles. The use of freeze-thaw cycles has the intention to increase the physical crosslinking of the polymeric chains producing an improvement in the characteristics needed for the food industry without introducing any chemical crosslinking agent with undesired side effects.

MATERIALS and METHODS

We used chitosan (CH) of medium molecular weight (Aldrich, deacetylation degree 83%) and a 1 % v/v aqueous solution of lactic acid to prepare the polymeric solution.

The water used on the preparation was obtained from a Millipore Simplicity device.

Films preparation

The polymeric solution was prepared dispersing the polymer powder in the acidic solution until dissolution. The dispersions were kept at constant temperature under magnetic agitation for 2 hours. The final polymeric concentration was 1 % w/w. Afterward the polymeric dispersion was poured onto polypropylene plates of 5 cm diameter with a relation mass/surface of 306 mg cm⁻².

Films were obtained by two different procedures:

I) Direct drying (DD): it consisted in placing the plates loaded with polymeric solution into a stove at 50°C for 1 hour. Finally, the films were dried out at atmospheric conditions until a constant weight was obtained.

II) Cycles of freezing-thawing (FT): it introduced 8 cycles of freezing-thawing of the polymeric solution previous to the drying process described in the direct drying item. Each FT cycle consisted of 24 hours at -20°C and 1 hour thawing at 25°C.

MECHANICAL TESTS

They were performed using a JJ Tensile Testing Machine T5002 according to ASTM D 638:03. The cross-head speed was fixed at 100 mm min⁻¹. Before the test, samples were equilibrated at atmospheric conditions and measured by triplicate.

The percentage of elongation and the tensile strength at the rupture point were obtained.

WATER VAPOR TRANSMISSION (WVT) AND PERMEANCE (P)

The WVT rate (g m²s⁻¹) is the steady water vapor flow measured in unit time through unit area of a body, normal to specific parallel surfaces, under specific conditions of temperature and humidity at each surface.

The WVT was obtained accordingly to the desiccant method described in ASTM E 96:00.

Acrylic water vapor permeation cells with an internal diameter of 5.0 cm, a depth of 3.5 cm and an external diameter of 8.5 cm were used.

The film was fixed with an acrylic ring shaped cover fastened with four screws. A film sample was placed between the water vapor permeation cell and the acrylic ring shaped cover.

A 10 mm air gap was left between the film and the CaCl₂ layer (0% relative humidity (RH), 0 Pa water vapor partial pressure) contained in the interior of the acrylic cell.

The cells were stored in a chamber maintained at a constant temperature of 27 °C and a relative humidity of 74 %, both of them checked regularly with a digital thermohygrometer.

Water vapor transport was determined from the slope of a plot of the weight gain of the cell in function of time

Another parameter useful to evaluate the film behavior as a water vapor barrier is the permeance that is the time rate of WVT through unit area induced by unit vapor pressure difference between two specific surfaces, under specified temperature and humidity conditions

P was calculated using equation (1)

$$P = WVT / S (Rh-R) \quad (1)$$

S is the saturation vapor pressure of water at test temperature (3565 Pa in our experiments), Re is the relative humidity at the test chamber (74%) expressed as a fraction and Rp is the RH inside the permeation cell (0%) expressed as a fraction.

.All tests were conducted at least twice.To ensure a stable WVT rate, the measurements were taken once a day.

SWELLING EXPERIMENTS

Dynamic swelling measurements were performed dipping the films, held inside of a steel basket, in distilled water at a constant temperature of 25 °C.

Swollen films were weighed with an electronic analytical balance (ACCULAB, capacity 210 g) to the nearest 0.1mg. at preset times in order to obtain the amount of water retained by the polymeric material.

The masic degree of swelling (Qm) of the films was calculated with equation (2):

$$Qm = (m_t - m_0) / m_0 \quad (2)$$

m_t is the weight of the film at time t and m₀ is the initial weight of the dry film.

RESULTS and DISCUSSION

Chitosan is a biocompatible polymer capable of producing films without the addition of plasticizers. Films prepared using both drying methods were uniform, homogeneous and easily removed from the polypropylene plate with an average thickness of 0.050± 0.002 mm.

Chitosan is a biocompatible polymer capable of producing films without the addition of plasticizers. Films prepared using both drying methods were uniform and homogeneous. They were easily removed from the polypropylene plate.

The structural strength of these films depends on several factors, among which we can mention the molecular weight of the polymer, the concentration of the chitosan dispersion, the type of acid and the type and concentration of the plasticizer used for their preparation.

If the water content is too low, the films are very brittle and fragile. As the water content increases, the film offers greater resistance to fracture, with an increase of the percentage of elongation and a decrease of the tensile strenght [4, 5].

For the films included in this study, the plasticizer is the residual water left after the drying process. In our case, this remaining water represents approximately a 40% of the final film mass.

Table 1. Results of mechanical tests

Sample	Tensile strength (MPa)	% Elongation
DD	3.61 ± 0.08	170 ± 10
FT	4.05 ± 0.06	117 ± 2

The mechanical tests results indicate (Table 1) that the matrix prepared using 8 cycles FT it proved to be more resilient and it had a lower percentage of elongation than the matrix prepared by direct drying..

We concluded that the cyclic FT process could favour an increasing in the structural integrity of the film without compromising the elasticity of the material because it only experienced a 31 % reduction in the percentage of elongation at the moment of rupture.

The weight gain of the permeation cells as a function of time showed a linear behavior. The slope of each curve was calculated by linear regression with the coefficient $R^2 > 0.997$ in every case.

Table 2. Water vapor transmission and permeability

Sample	WVT ($\text{g s}^{-1} \text{m}^{-2}$)	P ($(\text{g s}^{-1} \text{m}^{-2} \text{Pa}^{-1})$)
DD	$(5.22 \pm 0.27) 10^{-3}$	$(1.98 \pm 0.10) 10^{-6}$
FT	$(3.31 \pm 0.79) 10^{-3}$	$(1.25 \pm 0.29) 10^{-6}$

In Table 2 it is observed that the films obtained using the FT method are less permeable to water vapor than films obtained with the DD method (at 95 % of confidence level). A similar trend was obtained for another polysaccharide named Scleroglucan when the FT method was applied [11]. This reduction could be related to an increase in intermolecular interaction that produced a bigger compactness of the structure [12]. The FT cycles could affect the inner structure of the material increasing the tortuosity of the channels affecting the final behavior toward the WVT. [11].

Swelling measurements are employed as a rather simple method to characterize polymer networks. A lowering in the swelling degree can be helpful to deduce the existence of a higher number of crosslinking points in physical gels [13].

The phenomenon of solvent sorption by a polymeric film depends on the diffusion of water molecules within the gel matrix and the subsequent relaxation of macromolecular chains [14]. The effect of both preparation methods (DD and FT) on the swelling behavior of chitosan films is shown in Fig. 1.

On films prepared using the FT cycles, there is a significant reduction of the water uptake. This result suggested that FT cycles promoted an increased number of crosslinking sites, thus hindering the solvent diffusion into the films and thereby decreasing the degree of swelling.

This fact suggests the existence of a denser structure, very likely due to an increase in the physical crosslinking points.

The degree of swelling (Q_m) of the films decreases, after 1 hour, from 200 for the material obtained by the conventional method to 110 using the FT method.

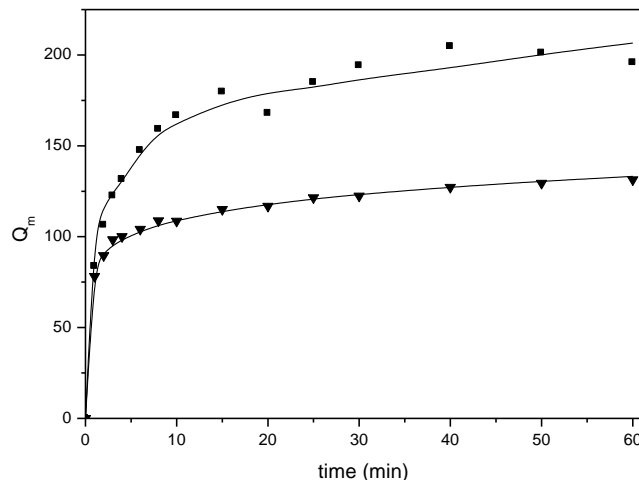


Fig. 1. Swelling degree for DD films (■) or FT films (▼)

During the freezing phase of the FT method, the material could achieved a more organized structure due to a disorder to order conformational transition. These transitions favored more associations between the ordered regions of polymeric chains generating an increment of the physical crosslinking process [11, 15].

The use of eight freezing-thawing cycles in the protocol of film preparation, produced a material easily to handle with a significant reduction of: the percentage of elongation, the WVT rate and the swelling degree, when compared to the films obtained by the DD method.

The FT cycling method is suitable for obtaining films with a reinforced network structure due to the increase of intermolecular interactions, avoiding the use of a crosslinking chemical agent.

ACKNOWLEDGEMENTS

Financial support from Universidad de Buenos Aires, Argentina (Grant 20020100100260, UBACyT 2011-2014) is gratefully acknowledged.

REFERENCES

- [1] Aider M: (2010). Chitosan application for active bio-based films production and potential in the food industry: Review. *LWT- Food Sc. And Tech.*, 43, 837-842.
- [2] No, H.; Meyers, S.; Prinyawiwatkul, W.; Xu, Z. (2007) Applications of Chitosan for Improvement of Quality and Shelf Life of Foods: A Review. *J. of Food Sci.*, 72, 87-100.
- [3] Sagoo, S.; Board, R.; Roller, S. (2002). Chitosan inhibits growth of spoilagemicro-organisms in chilled pork products. *Food Microbiol.*, 19, 175–82.
- [4] Lazaridou, A.; Biliaderis, G. (2002). Thermophysical properties of chitosan, chitosan-starch and chitosan-pullulan films near the glass transition. *Carb. Polym.*, 48, 179-190.

- [5] Caner C.; Vergano, P.; Wiles, J. (1998). Chitosan film mechanical and permeation properties as affected by acid, plasticizer, and storage. *J Food Sci.*, 63, 1049-1053.
- [6] Avanitoyannis I.; Nakayama, A.; Aiba, S. (1998). Chitosan and gelatine based edible films : state diagrams, mechanical and permeation properties. *Carbohydrate Polymers*, 37, 371-382.
- [7] Ji, J.; Yang, J.; Kim, N.; Hur, J. (2003). Effect of chitosan treatment on growth and shelf life of soybean sprouts. *J. Chitin. Chitosan*, 8, 214-9.
- [8] Jeon, Y.; Kamil, J.; Shahidi, F. (2002). Chitosan as an edible invisible film for quality preservation of herring and Atlantic cod. *J. Agric. Food Chem.*, 50, 5167-78.
- [9] No, H.; Park, N.; Lee, S.; Meyers, S. (2002). Antibacterial activity of chitosans and chitosan oligomers with different molecular weights. *Int. J. Food Microbiol.*, 74, 65-72.
- [10] Butler, B.; Vergano, P.; Testin, et al (1996). Mechanical and barrier properties of edible chitosan films as affected by composition and storage. *J. Food Sci.*, 61, 953-961.
- [11] Francois, N.; Daraio, M. (2009). Preparation and characterization of Scleroglucan drug delivery films: the effect of freeze-thaw cycling. *J. of Applied Pol. Sci.*, 112, 1994-2000.
- [12] Pranoto, Y. ; Rakshit, S.; Salokhe; V. (2005). Enhancing antimicrobial activity of chitosan films by incorporating garlic oil, potassium sorbate and nisin. *LWT* 38, 859-865
- [13] Chen, X.; Chen, Z.; Lu, G.; et al (2003). Measuring the swelling behavior of polymer microspheres with different crosslinking densities and the medium dependent color changes of the resulting latex crystal films. *J. of Colloid Int. Sci.*, 264, 266-270
- [14] Bajpai, A.; Sharma, M. (2005). Preparation and characterization of binary grafted polymeric blends of polyvinyl alcohol and gelatin and evaluation of their water uptake potential. *J. of Macromolecular Sc.- Pure Applied Chem.*, 42, 663-682.
- [15] Nugent M.; Hanley A.; Tomkins C.; et al. (2005). Investigation of a novel freeze-thaw process for the production of drug delivery hydrogels. *J. of Mat. Sci.: Materials in Med.*, 16, 1149-1158.

Applications in Material Science

PERFORMANCE EVALUATION OF MECHANICAL CHITOSAN/HYDROXYAPATITE BIOCOMPOSITES

Rita de Cássia Alves Leal^{1*}, Imarally V.S.R. Nascimento¹, Isabel Portela Rabello¹, Valéria Pereira Ferreira¹, Marcus Vinicius L. Fook¹, Hugo M. Lisboa¹

¹ Department of Materials Engineering, Federal University of Campina Grande, Campina Grande.

*E-mail address: ritaalvesleal@hotmail.com

ABSTRACT

The incorporation of calcium phosphate in polymer matrices for producing composites combines the flexibility of the polymers with the resistance, hardness and bioactivity of the inorganic phase. This study aimed to obtain rigid biocomposites using hydroxyapatite as mineral phase and chitosan as a polymer binder for the application as a biomaterial. To obtain the biocomposites, hydroxyapatite was added under constant stirring to a solution of chitosan in order to satisfy a 70:30 (HA/CS, wt%) ratio. XRD results showed no significant change in the profile of hydroxyapatite with the incorporation of chitosan. The analysis of scanning electron microscopy (SEM) of the biocomposite HA/CS, indicated that there was an excellent dispersion of HA particles in the polymeric matrix. Infrared Spectroscopy with Fourier Transform (FTIR) analysis proved an existing interaction between chitosan and hydroxyapatite. Flexural tests revealed that the biocomposites have lower flexural strength than those reported in literature for cortical bone. However, the values are adequate for trabecular bone substitution. It is considered that the present biocomposites are promising biomaterials for trabecular bone grafting

Keywords: Biocomposites, Hydroxyapatite, Chitosan.

INTRODUCTION

The techniques used in tissue engineering for regeneration/bone replacement include the use of material grafts from animal or human sources, and synthetic materials as well (metals, polymers and mainly ceramics) in the form plates, cement, granules or three-dimensional structures [1]. Today's commercial materials used for repair or replacement of tissues do not meet all the chemical and structural requirements, thereby stimulating the development of new biomaterials [2].

Hydroxyapatite $[\text{Ca}_{10}(\text{PO}_4)_6(\text{OH})_2]$ has been widely studied as an alternative to grafts in damaged bone tissue repair, because this is a calcium phosphate that naturally occurs as a mineral constituent of bone, with proven osseointegration and biocompatibility properties [3, 4], and also allow bone growth (osteoconductive), establishing links between hydroxyapatite and bone (bioactive), which indicates the great similarity of the surface chemistry [5].

There are some disadvantages that still limit the use of hydroxyapatite for hard tissue replacement, such as, it's fragile nature, due to the conflict between porosity and mechanical strength, and the problem of particle migration [6]. A possible solution to this problem comes in the form of composites comprising calcium phosphates and natural biopolymers, widely used as biomaterials for bone tissue repair and engineering [7-9]. The advantages of such composites include increased osteogenic potential by the inclusion of

hydroxyapatite and bioactive polymer matrix acting as a binder to prevent migration of hydroxyapatite [10].

Biomaterials based on chitosan are an emerging class with application in various biomedical fields such as tissue regeneration, particularly for cartilage; devices for controlled drug release systems and cell immobilization in gel [11]. Chitin and chitosan are promising materials for medical applications due to their bacteriostatic/bactericide properties, biocompatibility with human tissues, and ability to facilitate regenerative processes in wound healing [12].

The constant challenge of science and technology is to create mechanisms to improve the quality of life in all its aspects. Within this context, it is of major importance the development of biocomposites that enable reconstruction of bone tissue, meeting the growing demand for these materials in biological applications of diverse health areas. Therefore, the present study aimed to produce and characterize biocomposites - hydroxyapatite/chitosan - to be applied as a biomaterial.

MATERIALS and METHODS

Preparation of Calcium Phosphate Powder

Hydroxyapatite ceramic slurry was prepared using the neutralization reaction of calcium hydroxide (PA, VETEC) with phosphoric acid (Pa, VETEC), both at a concentration of 2.0 M, with a 1.67 (HA) mol ratio of Ca/P.

Preparation of Chitosan Solution 2g/100mL

An aqueous chitosan (POLYMAR, DD=86%, low molecular weight) solution of 0.02 g/mL was prepared by dissolving the polymer in a solution of 1%wt acetic acid (Pa, VETEC) under magnetic stirring for 24 hours to ensure full dissolution of chitosan. After this period, the final solution was vacuum filtered to remove residues.

Preparation of Chitosan/HA biocomposite

The biocomposites were prepared in a ratio of 70%wt hydroxyapatite and 30%wt chitosan. The slurry formed was stirred for 30 minutes at room temperature, then filtered. The weight retained was placed in a mold under a pressure of 2.5 tons for 30 minutes, then demolded and placed in an oven at 60 ° C for 20 hours.

Sample characterization

Composites morphology was observed with scanning electron microscopy Shimadzu Superscan SSX-550. The crystal structure of composite powder was examined using Shimadzu (model XRD 6000) with scanning angle between 10 and 70, the assembly of Bragg-Brentano θ - 2θ system, using Cu radiation ($\lambda 1$) with the scan step 0.02 (2θ). The characterization by Fourier Transformed InfraRed spectroscopy was performed on a spectrometer model Spectrum 400FT Mid-IR PerkinElmer to scan from 4000 to 400 cm^{-1} . Samples were prepared in the form of KBr discs. A three points bending test, using an equipment AS-50kN, with a crosshead speed of 0.5 mm/min were made according to ASTM C1161-08.

RESULTS and DISCUSSION

XRD analysis

The XRD analysis, Figure 1 shows that the presence of chitosan in the composites did not cause significant changes in the phase of hydroxyapatite, because all peaks correspond to this phase. Only a small deviation from the profile of hydroxyapatite was observed, referring to the peak of chitosan.

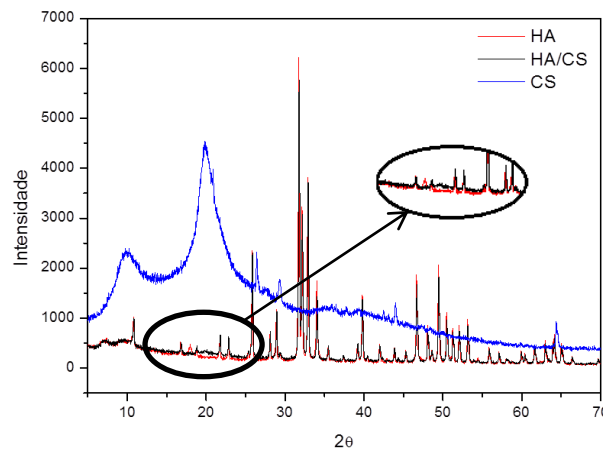


Figure 1 – X-Ray Diffractogram of HA(red), CS(Blue), HA/CS(Black).

SEM

Figure 2, shows a SEM image of the biocomposite HA/CS, revealing a small porous structure with an excellent dispersion between polymer and calcium phosphate. Figure 3, is a SEM image of the biocomposites after calcination, revealing that after chitosan degradation, an interconnected porous structure is imprinted in the calcium phosphate.

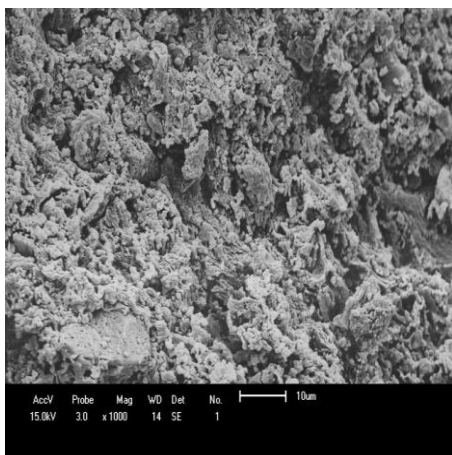


Figure 2: SEM of biocomposite HA / CS.

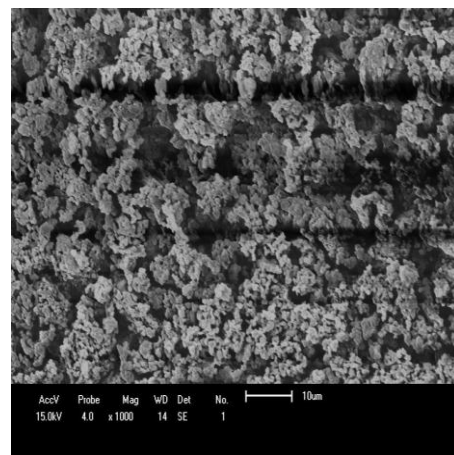


Figure 3: SEM of the sample calcined at 900 ° C.

FTIR

Figure 4 shows the FTIR spectrum of the CS/HA biocomposites developed. The bands in the region of 478, 562 and 1100 cm^{-1} correspond to stretching and bending vibrations of the PO_4^{3-} groups [13]. The bands around 3450 and 3590 cm^{-1} are assigned to the stretching of hydroxyl groups, OH, characteristic of HA. The bands between 1550-1700 cm^{-1} are assigned to a possible overlap between hydroxyapatite and NH-groups of the amide I and amide II of chitosan [14].

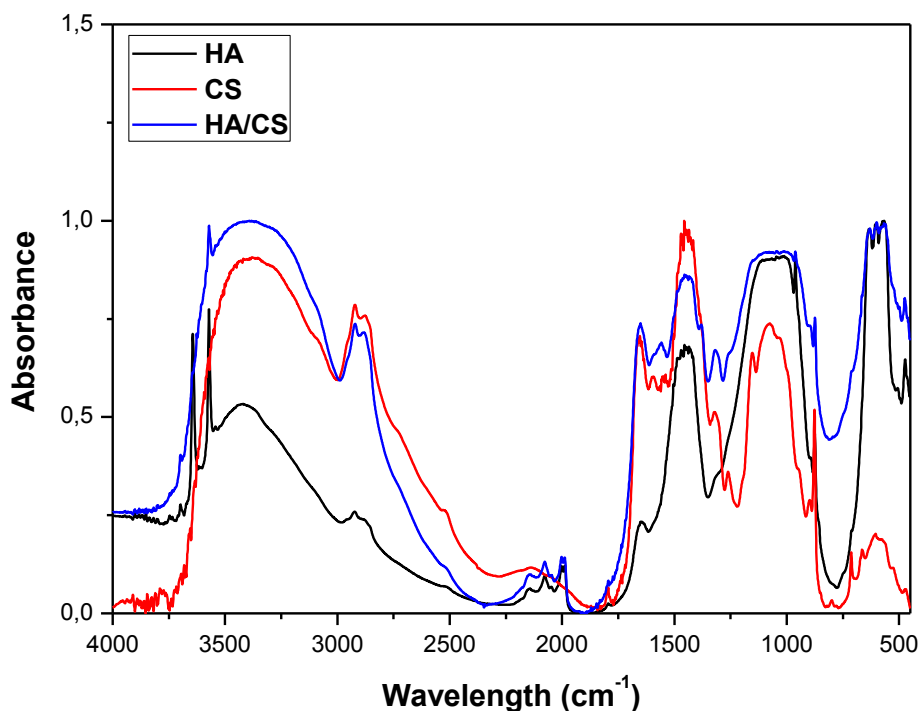


Figure 4: FTIR spectrum of HA(blue), CS(red) e HA/CS(black).

According to the spectrum shown in Figure 4, we can confirm that chitosan is not 100% deacetylated, confirmed by the band found in the region of 1646 cm^{-1} characteristic of an amide I ($\text{O} = \text{C-NHR}$). The expansion of the band at 1050 cm^{-1} reflects the presence of polymer and its interaction with phosphate groups [15].

Flexural Tests

Figure 5 illustrates the results of the bending test of biocomposites HA / CS. The biocomposites showed an average value for flexural strength of 44.65 MPa.

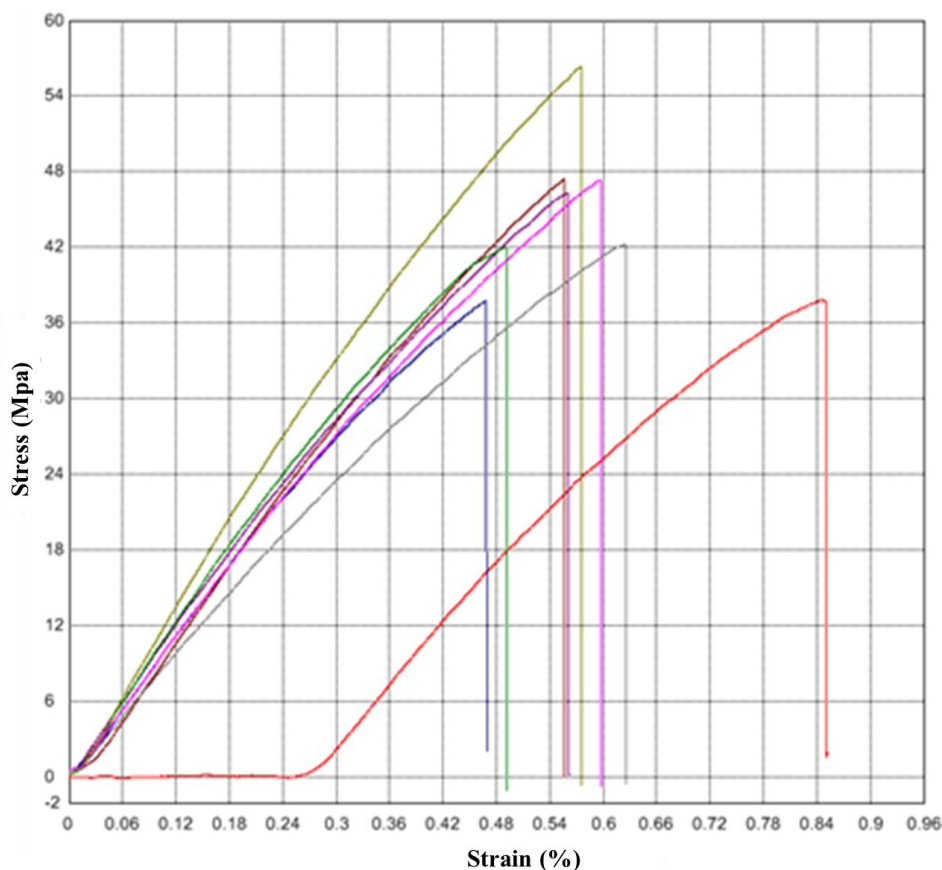


Figure 5: Stress-Strain curves for flexural tests of HA/CS biocomposites with 70:30 wt% HA/CS

The values obtained for the biocomposites HA / CS, approach the minimum value obtained for cortical bone, which have values in the range of 50 to 150 MPa [16]. However, if we compare this values with the trabecular bone, which has values in the range of 10 - 20 MPa, we can affirm that the biocomposites obtained showed values above the desirable for use as a trabecular bone replacement.

CONCLUSION

In the present work, HA/CS biocomposites were successfully produced revealing through SEM images an excellent dispersion and interconnected microporosity. The XRD analysis of the biocomposites revealed no major changes in hydroxyapatite while FTIR analysis revealed an interesting interaction between chitosan and hydroxyapatite. Flexural tests revealed that the HA/CS biocomposites present promising results for cortical and trabecular bone grafts. It is considered that further investigation is necessary to study the biological response of the human body to the presented biocomposite.

ACKNOWLEDGEMENTS

The authors acknowledge the Coordenação de Aperfeiçoamento Pessoal do Ensino Superior (CAPES) for post-graduation grants.

REFERENCES

- [1] Toro, C., Robiony, M., Zerman, N., Politi, M. *Minerva Stomatol.*, v.54, n.4,. p.199-206, 2005.
- [2] Shen, H., Hu, X., Yang, F., Bei,J.,Wang, S. *Acta Biomaterialia*, v.6, p.455–465, 2010.
- [3] Uchida, A.; Araki, N.; Shinto, Y.; Yoshikawa, H.; Kurosaki, E.; Ono, K. The use of calcium hydroxyapatite ceramic in bone tumor surgery.**J. Bone Joint Surg.** 72B (1990), 298-302.
- [4] Bohner, M. Calcium orthophosphates in medicine: from ceramics to calcium phosphate cements. **Injury**, vol. 31, pp. 37-47, 2000.
- [5]. Galea, L. G. *et al.* "Bone substitute: Transforming β -tricalcium phosphate porous scaffolds into monetice". *Biomaterials*, v.29, p. 3400-3407, 2008.
- [6] Sıvakumar, M.; Rao, K. P. Preparation, Characterization and In Vitro Release of Gentamicin from Coralline Hydroxyapatite-Gelatin Composite Microspheres. *Biomaterials*, v. 23, p. 3175-3181, 2002.
- [7] Wahl DA, Czernuszka JT. Collagen-hydroxyapatite composites for hard tissue repair. *Eur Cells Mater* 2006;11:43–56.
- [8]. Rusu VM, Chuen-How Ng, Wilke M, Tiersch B, Fratzl P, Peter MG. Size-controlled hydroxyapatite nanoparticles as self-organized organic-inorganic composite materials. *Biomaterials* 2005;26: 5414–5426.
- [9] Hu Q, Li B, Wang M, Shen J. Preparation and characterization of biodegradable chitosan/hydroxyapatite nanocomposite rods via in situ hybridization: A potential material as internal fixation of bone fracture. *Biomaterials* 2004;25:779–785.
- [10] Muzzarelli, C.; Muzzarelli, R.A.A.*Journal of Inorganic Biochemistry* 2002; 92: 89-94.
- [11] Laranjeira, M.C.M.; Fávere, V. Quitosana: Biopolímero Funcional com Potencial Industrial Biomédico.*Química Nova*, 32, 672-678, 2009.
- [12] Muzzarelli RAA. Chitins and chitosans for the repair of wounded skin, nerve, cartilage and bone. *Carbohydr Polym* 2009;76:167–182.
- [13] Finisie, Mellatie R; Josué, Atche; Fávere, Valfredo T; Laranjeira, Mauro C. M. **Synthesis of Calcium-Phosphate and Chitosan Bioceramics for Bone Regeneration**, 2000.
- [14] Jiang, L.; LI, Y.; Wang, X.; Zhang, L.; Wen, J. and GONG. M. Preparation and properties of nano-hydroxyapatite/chitosan/carboxymethyl cellulose composite scaffold. **Carbohydrate Polymers**. 74(2008) 680-684.

[15] Manjubala, I.; Scheler, S.; Bossert, J. and Jandt, K. D. Mineralisation of chitosan scaffolds with nano-apatite formation by double diffusion technique. **Acta Biomaterialia** 2(2006) 75-84.

[16] Hench, L. L.; Wilson, J. Introduction to bioceramics. Singapore: Word Scientific Publishing Co. Pte. Ltd., 1993, p. 1-15.

CHITOSAN-POLY (LACTIC ACID) COMPOSITE FILMS: MECHANICAL, THERMAL, AND ANTIFUNGAL PROPERTIES

A.P. Martinez-Camacho¹, M.M. Castillo- Ortega², J.M. Ezquerra-Brauer¹, P. Herrera-Franco³, M.O. Cortez-Rocha¹, M. Plascencia-Jatomea*¹

¹DIPA, ²DIPM, Universidad de Sonora, Hermosillo, Sonora, México. C.P. 83000, P.O. Box 1658.

³Unidad de materiales, Centro de Investigación Científica de Yucatán, A.C., Mérida, Yucatán, México.

* E-mail address: mplascencia@guayacan.uson.mx

ABSTRACT

Composite casting films were obtained from solutions of chitosan in acetic acid as and poly (lactic acid) in chloroform. Only the solutions of proportions 70:30 and 80:20 chitosan:PLA were homogeneous, and adequate to obtain films by casting. However, only the films with the proportion of 80:20 were strong enough to analyze. These films were used to assess the effect of the material structure on its functional properties, such as mechanical, thermal and structural. An infrared spectroscopy analysis of composite films showed a wider OH peak area, indicating a possible interaction of the polymers in the blend by hydrogen bonds. The mechanical dynamic analysis showed the presence of a sole possible Tg in the blend film, which is indicative of polymer miscibility in blends. The composite films had antifungal activity shown in the morphometric determination, especially in the spores. These changes in the form and size of fungi spores could be due to the chitosan effect on the permeability of membranes and cell walls; however more studies are needed to understand the effect of molecular arrangement in the films on their antimicrobial properties.

Keywords

Chitosan, poly (lactic acid), casting, films, composites, antifungal.

INTRODUCTION

Chitosan films have potential as a packaging polymer due to their good oxygen and carbon dioxide permeability, good mechanical properties, which are comparable with those of many medium strength commercial polymer, and also due to their antimicrobial activity [1]. However chitosan films are highly sensible to moisture, which limits its application as food packaging. The blending with other polymer with more resistance to moisture is a versatile, inexpensive and simple way to improve the chitosan films properties [1].

However this additional polymer has to conserve the chitosan properties, especially its biodegradability and antimicrobial activity.

The characteristics of the blend depend on the state of the mix and the miscibility of the components, as well as the phase morphology. For solvent cast film also the solvent selected is a determinant factor [2].

Blending with poly (lactic acid), a biodegradable and biocompatible polymer with high strength, thermoplastic behavior with molding and shaping feasibility, grease and oil resistance, and good aroma barrier, has been proved to obtain different chitosan composite materials [1, 3-5]. The limitations of PLA are their inherent brittleness and low toughness

[6]. Other properties including thermal stability and gas barrier properties of PLA still need to be improved before being used as food packaging.

However, one of the major problems with the blend of chitosan and poly (lactic acid) is the poor miscibility of the polymers in the blend [3]. Different factors such as the solvent and the process used to obtain the blend films have influence in the final characteristics of the blend material [3, 7]. Together with the mechanical and thermal resistance of the resulting chitosan-poly (lactic acid) blend films, the antimicrobial activity is important to establish and package feature advantage.

Even when in some cases blend films have been obtained, due to an interaction of the polymers, how this interaction could affect the antimicrobial activity, has been little studied. In this study we obtained chitosan-poly (lactic acid) casting films blend using acetic acid and chloroform as solvents. Also, we determinate the mechanical, thermal and structural properties of the film and contrasted with their antifungal activity.

MATERIALS and METHODS

Materials

Chitosan of low molecular weight from Sigma-Aldrich (viscosity 20.000 cps) with 80.81% deacetylation degree was used. Pellet form poly (lactic acid) (PLA) from Promoplast, trademark IngeoTM 2002D NatureWorks LLC for extrusion was used.

Chitosan solution concentration 3% in acetic acid at 90% and PLA solution at 6% in chloroform were mixed in different proportions (20:80, 40:60, 50:50, 60:40, 70:30 y 80:20, QB:PLA) for at least 24 h at room temperature. Chitosan and PLA blend films were made by casting [8].

Characterization of chitosan-poly (lactic acid) blends casting films.

The morphology of the surface of the obtained materials was analyzed by SEM, covering them with gold before being morphologically characterized using a scanning electron microscope (Jeol JSM-6360LV, Japan).

The infrared spectra of the materials were obtained using an infrared spectrophotometer FT-IR (Perkin Elmer FT-IR Spectrum GX), in a spectral range from 4000 to 400 cm^{-1} .

Mechanical resistance to rupture of the films was performance by a tension test in a microtensor, using an 18kg charge cell. Samples (12.5mm x 50 mm) were uniaxially stretched at a constant rate of 0.02mm/s. Width and thickness of the samples were previously measure to obtain the strain-stress curves.

A dynamic mechanical analysis (DMA) was done using a DMA7 Perkin Elmer equipment, with 1 Hz frequency, 0.8mm amplitude, from 30°C to 230°C, with a 90mN static force and a 75 mN dynamic force.

The thermal properties of the composite films were analyzed by differential scanning calorimetry (DSC) in DSC 8000 Perkin Elmer equipment, and using 8-10mg of the films and a temperature cycle (first 30° C to 190° C, hold 1min, cooled to -30° C rapidly, hold for 3min; and second from -30° C to 300°C at 10° C/min). An empty cup was used as reference [1, 3].

The antifungal activity of the films was determined by the analysis of the radial extension and the spore germination of *Aspergillus niger* inoculated on the surface of the films, by measures of the fungal colony radius and the quantity of germinated spores at different times [8]. Morphometric analysis were done by estimation of the germinated spore and hyphae diameters using digital images obtained in an optical microscope (Olympus Cx31), using the image analysis software Image-Pro Plus version 6.3 (2008 Media Cybernetics Inc., USA).

Statistics on a completely randomized design were determined using the one-way analysis of variance (ANOVA) procedure with JMP software (JMP version 5.0, SAS Institute Inc., USA), at a level of significance set at $P = 0.050$. Means for groups in homogeneous subsets were determined using the Tukey multiple comparisons test (Tukey's *posthoc* test), at 95% confidence interval. All data were presented as mean value with their standard error indicated (mean \pm SE). Differences were accepted as significant when $P \leq 0.05$.

RESULTS and DISCUSSION

Only proportions 80:20 (M1) and 70:30 (M2) chitosan:PLA casting films were obtained. However M2 could not be further analyzed due to the impossibility of separated the complete material from the petri dishes. This may be due to the low miscibility of both polymers [1, 2]. Films with different proportions (90:10, 80:20 y 70:30) have been obtained using a 1% chitosan and 10% PLA concentration [1]. However, increasing chitosan proportion raises viscosity, troubling solution homogenization and films obtaining. The chloroform used to dissolve PLA has low water solubility, while chitosan dissolves in an aqueous solution of acetic acid, a polar solvent; this also can influence homogenization of the solutions. Since chloroform evaporate so much faster than water or acetic acid from the casting membranes during the film formation, the membranes obtained could present separation of phases [7]. The direct addition of PLLA or PDLA to chitosan solutions causes a fast precipitation of PLA when mixing or a slow separation during the drying in casting. In this work, all the proportions tested, except the 80:20, showed a visible phase separation. Using a better homogenization technique could reduce this problem.

The micrographics of the films obtained by SEM (Figure 1) showed that the PLA films had 10mm of diameter pores. In the chitosan films spherical aggregates of less than 5mm of diameter were observed. In the blend of both polymers pores and irregular aggregates can be seen along the material surface.

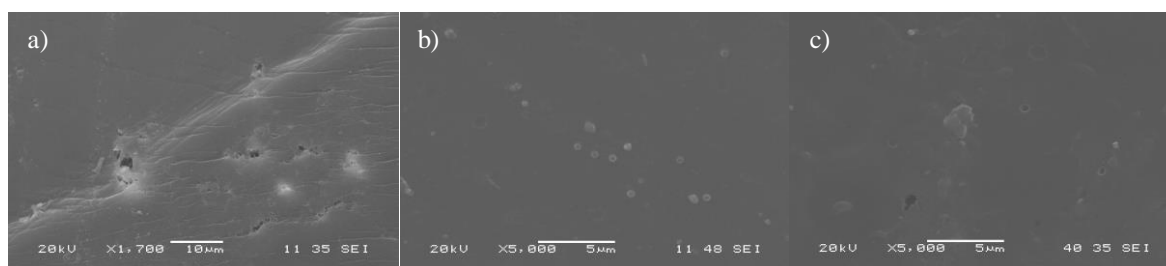


Figure 1. SEM images of a) poly (lactic acid) 6% in cloroform, b) chitosan 3% in acetic acid at 90% and c) 80:20 chitosan:PLA casting films.

Since the higher proportion of the blend used corresponds to chitosan, this polymer represents the continuous phase, while the disperse phase is the PLA, which can form spherical aggregates in the continuous matrix [7]. It is possible that the high viscosity of the chitosan solution (even at 1% concentration) and the low viscosity of PLA solution (even at concentrations above 5%), caused the formation of little drops that dispersed in the continuous phase during mixing, and remained even after the solution blend was poured in the plates to obtain films [7].

Miscibility and interactions between components of blends in the films were determined by an FT-IR analysis. In the chitosan film spectra (Figure 2) the characteristic peak for the polymer due to the amide I band appear around 1650 cm^{-1} , while in the PLA

film is located around the 1768 cm^{-1} , which corresponds to the stretching of the ester group [3].

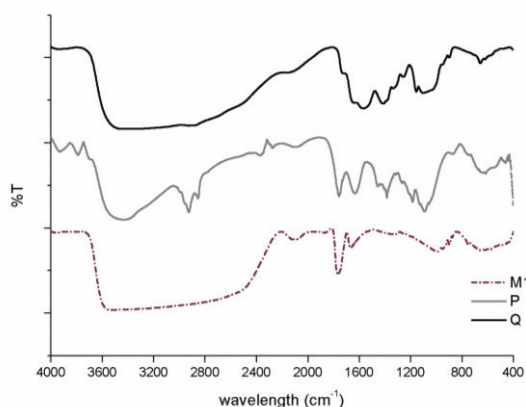


Figure 2. FTIR spectra from casting films of chitosan (Q), poly (lactic acid) film (P), and the blend in proportion 80:20 chitosan:poly (lactic acid) film (M1).

In the M1 blend both peaks can be seen, which leads to the assumption of a very low miscibility or nonexistent interaction by this representative groups between the two polymers [1, 3, 9]. However, the area around the 3000 cm^{-1} , corresponding to the O-H tension band and hydrogen bond formation, is almost as wide as in the chitosan film. Since the formation of hydrogen bonds usually induces the miscibility of the polymers blends, it is also likely that the possible interaction by hydrogen bonds between both polymers is located in this zone [8, 10]. The obtained 80:20 chitosan-poly (lactic acid) film blend, seems to be low or partially miscible blend.

DMA curve of PLA film shows a strong transition around 50°C , attributed to a glass transition temperature (T_g) of the polymer reported in pure films [3]. The chitosan film presented a less strong transition around 142°C possibly due to T_g related to molecular movement in the amorphous region [8, 11-13]. A minor transition around 195°C was also observed; although not corresponding to a thermal degradation of chitosan (estimated around 240°C), it could point out its beginning [1, 8]. The blend film presented transition at 137°C , however no evidence of other transition in the curve was found, thus this possibly corresponds to a T_g . Due to a the low PLA proportion in the blend, this transition is closer to chitosan T_g . The presence of a solely T_g in the blend could indicate miscibility of the components.

The mechanical properties of films are summarized in Table 1. The chitosan film exhibits the typical behavior of crystalline material; meanwhile the pure PLA film the curve presents the behavior typical to amorphous materials.

Table 1. Mechanical properties of chitosan and poly (lactic acid) blend casting films.

Film	Strength max (MPa)	Elongation (%)
Q	$13.690 \pm 2.331b$	$8.118 \pm 3.289a$
P	$9.994 \pm 3.557b$	$2.869 \pm 1.503a$
M1	$25.778 \pm 3.892a$	$5.725 \pm 1.979a$

(Q) chitosan film, (P) poly (lactic acid) film, (M1) 80:20 chitosan:poly (lactic acid) blend film. In each column, different letters indicate statistic difference ($P \leq 0.05$).

In the blend the crystalline behavior predominates, most likely because of the higher chitosan proportion. However the maximum strength was higher than for pure chitosan. It is possible the polymer chains arranged in such a way a more rigid and less elastic structure was formed, giving lower deformation values.

An increment of PLA in the blend tends to reduce the strength to tension, however this not happened in the blend obtained in this work.

The decrease in the strength would indicate an immiscibility of the blend components, but the registered increase could be related to the film obtaining method. An increase in the polymers chains arrangement during the film formation can result in a crystalline behavior. It is possible that the materials characteristics were affected by the solvent used. More studies must be done to clarify this behavior.

The differential scanning calorimetry was done to determinate the glass transition temperature of the blend films. For the poly (lactic acid) films only one temperature transition was detected around the 45.9°C (very similar to the Tg obtained in DMA) which is close to the reported glass transition temperature to this polymer [14]. For chitosan films the Tg was estimated around the 111.1°C. It is possible that this transition could be more related to the evaporation of residual water contained in the chitosan films which have shown strong affinity to water. For the chitosan and poly (lactic acid) blend films it was also founded a single Tg around the 113.5° C, which is similar to the estimated Tg obtained in the chitosan films, probably due to the greater chitosan proportion in the blend.

The antifungal effect of chitosan films on the extensional growth of *Aspergillus niger* was bigger than in the rest of the films. The composite films had a similar effect that the control (cellophane) films. Since chitosan and its composite films are hygroscopic, the contact with de culture media surface caused deformation of the film and probably damage in the structure, making easier the pass through the material to the agar, resulting in the growth of the fungi. Also it is possible that the chitosan's amino groups, responsible of their antimicrobial action, would be not available to interact with the negative charges of the fungi membrane. This due to the miscibility of both polymers in the blend, which is a result of the hydrogen bonds established between the hydroxyl and the amino groups. However no significant differences was found in the films analyzed ($P \leq 0.05$).

The greater chitosan antifungal effect seems to occur in the first stage of fungi growth, the spore germination, before the formation and proliferation of hyphae [8]. The determination of the spores and hyphae diameters is useful to estimate the growth of the fungi analyzed. It was observed that only the spore diameter in chitosan films were significant different from the other films (Table 2).

Table 2. Morphometric parameters of *Aspergillus niger* inoculated over the chitosan and poly (lactic acid) blend films.

Film	Hyphae diameter (mm)	Spore diameter (mm)
C	2.298 ± 0.003d	3.955±0.037b
M1	4.026 ± 0.018b	3.831±0.039b
P	2.505 ± 0.004c	3.962±0.048b
Q	5.119 ± 0.006a	4.177±0.037a

(C) Cellophane film as control, (Q) chitosan film, (P) poly (lactic acid) film, (M1) 80:20 chitosan:poly (lactic acid) blend film. In each column, different letters indicate statistic difference ($P \leq 0.05$).

Similar results were found in a previous work in two inoculation systems: under and over the films, assuming that chitosan is capable to disturb the membrane permeability of the spores and induce the increase in diameter [8]. All the films showed a significant

different hyphae diameter value. The biggest diameter was found on fungi inoculated over chitosan films, and the smallest in the control and poly lactic acid films. The increase in the hyphae diameter could be related to an imbalance of the membrane permeability resulting in the entrance of exterior water to the cytoplasm of the fungi cell. More detailed studies are needed to understand how the chitosan composite films exert their antimicrobial action.

ACKNOWLEDGEMENTS

REFERENCES

- [1] Suyatma, N. E., Copinet, A., Tighzert, L., & Coma, V. (2004). Mechanical and barrier properties of biodegradable films made from chitosan and poly (lactic acid) blends. *Journal of Polymers and the Environment*, 12, 1-6.
- [2] Peesan, M., Supaphol, P., & Rujiravanit, R. (2007). Effect of casting solvent on characteristics of hexanoyl chitosan/poly(lactide) blend films. *Journal of Applied Polymer Science*, 105, 1844–1852.
- [3] Peesan, M., Supaphol, P., & Rujiravanit, R. (2005). Preparation and characterization of hexanoyl chitosan/poly(lactide) blend films. *Carbohydrate Polymers* 60, 343–350.
- [4] Wu, H., Wan, Y., Cao, X., & Wu, Q. (2008). Interlocked chitosan/poly(DL-lactide) blends. *Material Letters*, 62, 330-334.
- [5] Ljungberg, N., & Wesslen, B. (2005). Preparation and properties of plasticized poly(lactic acid) films. *Biomacromolecules*, 6, 1789–1796.
- [6] Ahmed, J., Varshney, S. K., & Auras, R. (2010). Rheological and thermal properties of polylactide/silicate nanocomposites films. *Journal of Food Science*, 75, N17-N24.
- [7] Wan, Y., Wu, H., Yu, A., & Wen, D. (2006). biodegradable polylactide/chitosan blend membranes. *Biomacromolecules*, 7 (4), 1362-1372.
- [8] Martínez-Camacho, A. P., Cortez-Rocha, M. O., Ezquerro-Brauer, J. M., Graciano-Verdugo, A. Z., Rodríguez-Félix, F., Castillo-Ortega, M. M., Yépiz-Gómez, M. S., & Plascencia-Jatomea, M. (2010). Chitosan composite films: Thermal, structural, mechanical and antifungal properties. *Carbohydrate Polymers*, 82, 305-315.
- [9] Xu, J., Zhang, J., Gao, W., Liang, H., Wang, H., & Li, J. (2009). Preparation of chitosan/PLA blend micro/nanofibers by electrospinning. *Materials Letters* 63, 658–660.
- [10] He, Y., Zhu, B., & Inoue, Y. (2004). Hydrogen bonds in polymer blends. *Progress in Polymer Science*, 29, 1021–1051.
- [11] Mucha, M., & Pawlak, A. (2005). Thermal analysis of chitosan and its blends. *Thermochimica Acta* 427, 69–76.
- [12] Dong, Y., Ruan, Y., Wang, H., Zhao, Y., & Bi, D. (2004). Studies on glass transition temperature of chitosan with four techniques. *Journal of Applied Polymer Science*, 93, 1553–1558.
- [13] Suyatma, N. E., Tighzert, L., & Copinet, A. (2005). Effects of hydrophilic plasticizers on mechanical, thermal, and surface properties of chitosan films. *Journal of Agricultural and Food Chemistry*, 53, 3950-3957.
- [14] Suyatma, N. E., Copinet, A., Legin-Copinet, E., Fricoteaux, F., & Coma, V. (2011). Different pla grafting techniques on chitosan. *Journal of Polymers and the Environment*, 19, 166-171.

EFFECT OF INTRINSIC FACTORS OF CHITOSAN ON PROPERTIES OF CHITOSAN/2-GLYCEROPHOSPHATE THERMOSENSITIVE HYDROGEL CONTAINING SILVER NANOPARTICLES

Min-Lang Tsai*, Hsiang-Wei Chang, Ya-Shen Lin, Ying-Die Tsai

Department of Food Science, National Taiwan Ocean University, 2 Pei-Ning Road, Keelung 20224, Taiwan, ROC.

*E-mail address: tml@mail.ntou.edu.tw

ABSTRACT

This study focuses on investigating the effect of degree of deacetylation (DD) and molecular weight (MW) of chitosan on the properties of chitosan/2-glycerophosphate/nanosilver (CS/GP/NAg) thermosensitive hydrogel. Gelation temperatures for the hydrogel are 32-43°C via a manipulated chitosan's MW and DD. The porous structure, water vapor transmission rate and skin permeation of nanosilver for 88% DD chitosan hydrogel were better than those for 80% DD chitosan hydrogel. The nanosilver hydrogel was mildly cytotoxic for HS68 cells; cell viabilities were between 22.7-33.3% for 12 h and recovered to 49.2-59.0% after 48 h. The diameters of the hydrogel's inhibition zones for *Pseudomonas aeruginosa* and *Staphylococcus aureus* increased as the concentration of nanosilver increased and as the MW of the chitosan decreased.

Keywords

Chitosan; 2-Glycerophosphate; Nanosilver; Thermosensitive hydrogel; Degree of deacetylation; Molecular weight

INTRODUCTION

Chitosan solution has 2-glycerophosphate added, changing the mechanism of gelation from pH dependent to thermal-pH dependent. The state of chitosan/glycerophosphate (CS/GP) is a solution in the physiological pH range; it is converted into a gel state due to body heat [1]. A number of works have reported CS/GP hydrogel being applied in biomedicine, such as the drug delivery system, tissue engineering, and cancer treatment [1-2]. Nanosilver has been acknowledged as an antimicrobial agent for a long time. The typical minimum inhibitory concentration (MIC) and minimum bactericidal concentration (MBC) of nanosilver against standard reference cultures are 1.56-6.25 ppm and 12.5 ppm, respectively [3]. Sudheesh Kumar et al. [4] reported that prepared β -chitin/nanosilver composite scaffolds were bactericidal against *Escherichia coli* and *Staphylococcus aureus*. The scaffolds also showed good blood-clotting ability and vero cells were well attached to the scaffolds.

In this study, the intrinsic factors (DD and MW) of chitosan affecting the properties of CS/GP/NAg hydrogel were investigated, including gelation temperature, water vapor transmission rate, skin permeation of nanosilver, microstructure, antibacterial activity and cytotoxicity.

MATERIALS and METHODS

Materials

Chitosans with 80% DD (DD80) (MW 145, 161 and 335 kDa) and 88% DD (DD88) (MW 113, 146, 160 and 204 kDa), were used in this study. The preparation method is described in Tsai et al. [5].

Preparation of thermosensitive hydrogel

The preparation of CS/GP/NAg hydrogel solution is described by Tsai et al. [5]. In brief, 30 ml of 0.002 M sodium borohydride solution were chilled in an ice bath for 20 min, and 6 ml of 0.001 M silver nitrate solution were slowly dropped into the sodium borohydride solution. Then the pale yellow nanosilver formed. Chitosan was dissolved in 1% (v/v) aqueous acetic acid (9 ml) to prepare the 2% chitosan solution. Glycerophosphate was dissolved in distilled water to prepare the 5% glycerophosphate solution. Both the chitosan and glycerophosphate solutions were chilled at 4°C for 1 h, respectively; then these solutions were mixed and stirred for 2 min in an ice bath. Next, the hydrogel solution was shaken for 40 s by a vortex shaker. Finally, the hydrogel solution was obtained and the pH value of the solution was adjusted within the range of 6.5. The nanosilver solution (6 or 12 ppm) was added to the hydrogel solution by a vortex shaker. The concentration and size of nanosilver were determined by an atomic absorption spectrophotometer (Perkin-Elmer 510 OPC, Norwalk, CT, USA) and a scanning electron microscope (Hitachi, S-4800, Tokyo, Japan), respectively.

Observation of microstructure

The porous structure of CS/GP/NAg hydrogel was observed with a scanning electron microscope (SEM, Hitachi S-4800, Tokyo, Japan).

Determination of water vapor transmission rate

A modified ASTM standard method (inverted-cup, E96-90) was used to determine the water vapor transmission rate (WVTR) of CS/GP/NAg hydrogel [6].

Measurement of skin permeation

The permeability of the silver ion through a BALB/c mouse's skin was investigated using Franz diffusion cells with an effective diffusional area of 0.785 cm². The method is expatiated by Lin et al. [7].

Evaluation of cytotoxicity

HS68 human fibroblast cells were cultured in a DMEM media supplemented with 2.2 g/l sodium bicarbonate and 10% fetal bovine serum (FBS). Cells were subcultured according to ATCC recommendations without using any antibiotic. For cytotoxicity, cells were seeded on CS/GP hydrogel with or without 12 ppm nanosilver hydrogel on 48-well plates at 5×10^4 cells/well. Cell viability was determined at 0, 12 and 48 h, respectively. For each time point, 50 μ l of mammalian cells solution from a LIVE/DEAD[®] Viability/Cytotoxicity Kit was added to the culture medium, and monolayer cultured cells were used as the control. The samples were incubated at 37°C for 30 min. After washing them three times with PBS, the stained cells were observed using fluorescence microscopy (Olympus, BX-51, Japan).

Antibacterial activity

The *S. aureus* and *P. aeruginosa* were used to assay the antibacterial activity of CS/GP/NAg hydrogel by the modified Kirby–Bauer disc diffusion method. These bacteria were grown overnight in nutrient broth. The 50 μ l hydrogel solution was added into filter paper (8 mm). Then the papers were placed on a nutrient agar culture of *S. aureus* ($6 \times \log$ CFU/ml) and *P. aeruginosa* ($6 \times \log$ CFU/ml), respectively. All of the samples were cultured at 37°C for 24 h. Finally the sizes of the antibacterial circles were measured [4].

RESULTS and DISCUSSION

Appearance of the hydrogel

Figure 1 shows a discrepancy in appearance of the CS/GP hydrogel before and after gelation. Based on this illustration, the appearance of the hydrogel with a white stain color after gelation is apparently dissimilar to that prior to gelation. Figure 1 also shows a photograph of the CS/GP/NAg hydrogel solution after gelation. The hydrogel appears pale yellow due to the addition of nanosilver. The color is clearly different between the CS/GP hydrogel and CS/GP/NAg hydrogel.



Figure 1. Photograph of chitosan/2-glycerophosphate (CS/GP) and chitosan/2-glycerophosphate/nanosilver (CS/GP/NAg) hydrogels before and after gelation.

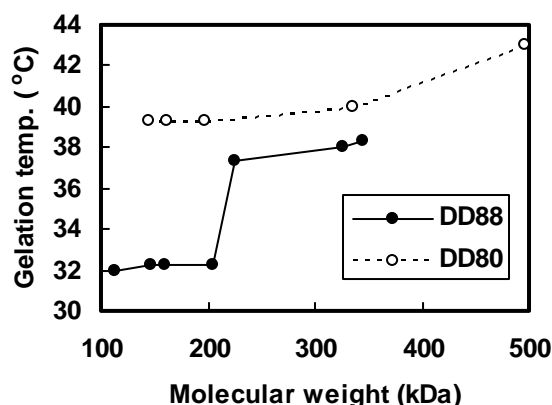


Figure 2. Effect of degree of deacetylation and molecular weight of chitosans on the gelation temperature of CS/GP/NAg hydrogel.

Gelation temperature

The gelation temperatures for the hydrogels were measured in the range of 32-43°C by manipulating the MW and DD of chitosan (Figure 2). Results show that the gelation temperatures of hydrogels which were prepared with chitosan that had different DDs but similar MWs, decreased with the increase in DD. We considered that a higher DD chitosan chain may be more flexible, making a change of the original conformation in the sol-gel process easier and resulting in a lower gelation temperature.

Figure 2 also shows that the gelation temperatures of CS/GP/NAg hydrogels, prepared with the same DD but different MW chitosans, increased with the increasing MW of chitosan. We reasoned that a higher MW chitosan has a larger hydrodynamic volume, and that it is more difficult to change the original conformation in the sol-gel process, resulting in a higher gelation temperature.

Microstructure of hydrogel

Figure 3 shows the microstructure of a cross-section of lyophilized CS/GP/NAg hydrogels prepared with DD80 and DD88 chitosan being formed for the two types of hydrogels. The structure of DD88 chitosan hydrogel is more porous, uniform and connective than the DD80 chitosan hydrogel. The DD88 chitosan hydrogel's superior porosity may be due to its having been prepared with a higher amount of DD chitosan which makes it more flexible and compact to form larger and more porous structures.

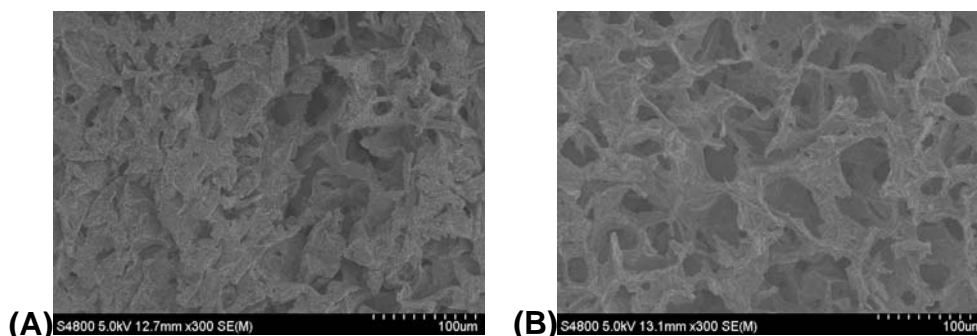


Figure 3. SEM graphs of CS/GP/NAg hydrogels, (A) DD80/MW161 300x, (B) DD88/MW160 300x.

Water vapor transmission rate of hydrogel

The water vapor transmission rate (WVTR) of CS/GP/NAg hydrogels prepared with DD80 and DD88 chitosan were 7150 ± 52 and 9044 ± 221 $\text{g} \cdot \text{m}^{-2} \cdot \text{d}^{-1}$, respectively, owing to the hydrogel's ability to form three-dimensional porous structures (Figure 2). It can be seen that both the DD80 and DD88 hydrogels with superior WVTRs may be suitable for wounds with more exudates, and for ulcers.

In vitro skin permeation studies

The permeability of the silver ion through a BALB/c mouse's skin was investigated using the Franz diffusion cell method. The size and initial concentration of nanosilver were 21.8 nm and 20.22 ppm, respectively. The results show that the permeation amounts of nanosilver from DD80 and DD88 CS/GP/NAg hydrogel were 3.82 and 4.99 $\mu\text{g}/\text{cm}^2$ for 24 h, respectively. The results correspond to the results for SEM and WVTR. The three-dimensional network of DD88 chitosan hydrogel has a more porous structure and favors nanosilver permeation.

Table 1. Effects of molecular weight (MW) of chitosan, with or without nanosilver (NAg, 12 ppm), and culture time on the viability (%) of HS68 epidermis fibroblasts incorporated in DD88 CS/GP/NAg hydrogels. Cell density: 5×10^4 cells/well.

MW (kDa)	0 ppm NAg 12 h	12 ppm NAg 12 h	12 ppm NAg 48 h
204	85.6 \pm 3.9 ^{xy}	27.1 \pm 7.3 ^x	59.0 \pm 7.9 ^x
160	83.6 \pm 4.8 ^{xy}	26.9 \pm 7.8 ^x	53.2 \pm 7.7 ^x
146	78.8 \pm 2.0 ^y	27.7 \pm 5.9 ^x	54.3 \pm 8.5 ^x
113	78.4 \pm 4.7 ^y	29.5 \pm 5.6 ^x	54.0 \pm 5.2 ^x

Each value represents mean \pm S.D. (n = 3). ^{x-y} Different letters in the same column and concentration of 2-glycerophosphate are significantly different ($p < 0.05$).

Cytotoxicity of hydrogel

Table 1 indicates that the cell viability of HS68 human fibroblast cells incorporated in CS/GP hydrogels with differing MW chitosan without nanosilver after 12 h was 77.9-87.9%. Chitosan is a non-toxic, biocompatible and biodegradable polysaccharide. Glycerophosphate has been approved by the FDA for veinal administration [2]. The material shows no cytotoxicity if the relative generative rate is $\geq 75\%$ [8]. Consequently, the chitosan/glycerophosphate hydrogels show no cytotoxicity for HS68 cells. However,

the cell viability of HS68 cells seeded in CS/GP hydrogels with 12 ppm nanosilver after 12 h was 22.7-33.3% and showed cytotoxicity for normal human cells. These HS68 cells continue proliferating for 48 h and cell viability recovered to 49.2-59.0%, indicating that the HS68 cells would resist nanosilver cytotoxicity via a prolonged culturing time. The result is similar to the cytotoxicity of silver-load chitosan/polyphosphate dressing for Neonatal Human Dermal Fibroblasts [9].

Table 2. Effects of concentration of nanosilver and molecular weight (MW) of chitosan on the inhibition zones (mm) for DD88 CS/GP/NAg hydrogels.

Species	Nanosilver (ppm)	MW (kDa)			
		204	160	146	113
<i>Pseudomonas aeruginosa</i>	0	13 ^a	13	13	14
	6	17	17	18	19
	12	19	20	20	22
<i>Staphylococcus aureus</i>	0	11	12	12	12
	6	17	17	18	20
	12	19	22	22	25

^a Data in table are the mean of every diameter of inhibition zone.

Antimicrobial activity of hydrogel

Table 2 shows the inhibition zones against *P. aeruginosa* and *S. aureus* for DD88 CS/GP hydrogels with different MW of chitosan (113, 164, 160 and 204 kDa) and different nanosilver concentrations (0, 6, 12 ppm). The results indicate that all of the diameters of the hydrogel inhibition zones for *P. aeruginosa* and *S. aureus* increased as the concentration of nanosilver increased. These results are similar to those of Sudheesh Kumar et al. [4] which showed that the diameters of the inhibition zones of β -chitin/nanosilver scaffolds against *S. aureus* and *E. coli* increased with the increased concentration of nanosilver. Jain et al. [3] indicated that the MIC₅₀, MIC₉₀ and MBC_{99.9} for nanosilver for *P. aeruginosa* were 3.12, 6.25 and 12.5 ppm, and the MIC₅₀ and MIC₉₀ for *S. aureus* were 6.25 and 12.5 ppm, respectively. It may be necessary for this hydrogel system to contain 6-12 ppm of nanosilver to have good antibacterial activity regardless of other factors.

Table 2 also shows that the diameters of the hydrogel inhibition zones for *P. aeruginosa* and *S. aureus* increased as the chitosan's MW decreased; this may be due to the lower MW chitosan's ability to more easily penetrate toward the nuclei of the bacteria and interfere with the synthesis of mRNA and proteins [10].

Table 2 shows that the antibacterial activity of hydrogel without nanosilver for *P. aeruginosa* (Gram-negative) was better than it was for *S. aureus* (Gram-positive). This may be due to the different structures and compositions of Gram-negative and Gram-positive cell walls. The major constituent of the Gram-positive bacteria cell wall is peptidoglycan and a small amount of protein. The cell wall of Gram-negative bacteria, on the other hand, is thinner but contains more complex and varied polysaccharides, proteins and phospholipids besides the peptidoglycan [10]. The peptidoglycan has a positive charge, while the phospholipid has a negative charge. The positively charged chitosan amino group can easily interact with the negatively charged phospholipid of Gram-negative bacteria, thus altering the cell membrane structure and resulting in changes to the cell membrane permeability as well as allowing more intracellular substances to leak out. Therefore, the antibacterial activity of chitosan is more effective against Gram-negative bacteria than Gram-positive.

CONCLUSIONS

Manipulating the chitosan's MW and DD and the concentration of glycerophosphate could lead to the gelation temperature of CS/GP/NAg being close to body temperature and becoming an in situ-form hydrogel. The porous structure, water vapor transmission rate and skin permeation of nanosilver for DD88 chitosan hydrogel were better than those of DD80 chitosan hydrogel. Nanosilver exhibited mild cytotoxicity on HS68 cells. The antibacterial activity of hydrogel was increased with the increased concentration of nanosilver. The hydrogel exhibited antibacterial activity for *P. aeruginosa* and *S. aureus* even without nanosilver; preparing the hydrogel with a lower MW chitosan resulted in higher antibacterial activity. Therefore, in order to reduce the cytotoxicity of nanosilver, a newly formulated hydrogel could be proposed that has similar antibacterial activity, made with lower MW chitosan and a lower concentration of nanosilver.

ACKNOWLEDGEMENTS

The authors wish to express their appreciation for the financial support from National Science Council, ROC (NSC 100-2313-B-019-004-MY3).

REFERENCES

- [1] Chenite, A., Chaput, C., Wang, D., Combes, C., Buschmann, M. D., Hoemann, C. D., Leroux, J. C., Atkinson, B. L., Binette, F., Selmani, A. (2000). Novel injectable neutral solutions of chitosan form biodegradable gels in situ. *Biomaterials*, 21, 2155-2161.
- [2] Wu, J., Wei, W., Wang, L. Y., Su, Z. G., Ma, G. H. (2007). A thermosensitive hydrogel based on quaternized chitosan and poly(ethylene glycol) for nasal drug delivery system. *Biomaterials*, 28, 2220-2232.
- [3] Jain, J., Arora, S., Rajwade, J. M., Omay, P., Khandelwal, S., Paknikar, K. M. (2009). Silver nanoparticles in therapeutics: Development of an antimicrobial gel formulation for topical use. *Mol. Pharm.*, 6, 1388-1401.
- [4] Sudheesh Kumar, P. T., Abhilash, S., Manzoor, K., Nair, S. V., Tamura, H., Jayakumar, R. (2010). Preparation and characterization of novel β -chitin/nanosilver composite scaffolds for wound dressing applications. *Carbohydr. Polym.*, 80, 761-767.
- [5] Tsai, M. L., Chang, H. W., Yu, H. C., Lin, Y. S., Tsai, Y. D. (2011). Effect of chitosan characteristics and solution conditions on gelation temperatures of chitosan/2-glycerophosphate/nanosilver hydrogels. *Carbohydr. Polym.*, 84, 1337-1343.
- [6] Wu, P., Fisher, A. C., Foo, P. P., Queen, D., & Gaylor, J. D. S. (1995). In vitro assessment of water vapour transmission of synthetic wound dressing. *Biomaterials*, 16, 171-175.
- [7] Lin, C. C., Lin, H. Y., Chen, H. C., Yu, M. W., Lee, M. H. (2009). Stability and characterisation of phospholipid-based curcumin-encapsulated microemulsions. *Food Chem.*, 116, 923-928.
- [8] Xie, F., Li, Q. F., Gu, B., Liu, K., Shen, G. X. (2008). In vitro and in vivo evaluation of a biodegradable chitosan-PLA composite peripheral nerve guide conduit material. *Microsurgery*, 28, 471-479.
- [9] Ong S. Y., Wu J., Mochhala S. M., Tan M. H., Lu, J. (2008). Development of a chitosan-based wound dressing with improved hemostatic and antimicrobial properties. *Biomaterials*, 29, 4323-4332.
- [10] Dutta, P. K., Tripathi, S., Mehrotra, G. K., Dutta, J. (2009). Perspectives for chitosan based antimicrobial films in food applications. *Food Chem.*, 11, 1173-1182.

ANTIFUNGAL PROPERTIES OF NEUTRALIZED AND NON-NEUTRALIZED CHITOSAN/POLYLACTIC ACID COMPOSITE FILMS

M.A. Méndez-Encinas^{1*}, A.P. Martínez-Camacho¹, E.C. Rosas-Burgos¹, A.Z. Graciano-Verdugo², M.S. Yépiz-Gómez¹, M. Plascencia-Jatomea¹

¹Departamento de Investigación y Posgrado en Alimentos. ²Departamento de Ciencias Químico-Biológicas. Universidad de Sonora. Blvd. Luis Encinas y Rosales S/N, Col. Centro, Hermosillo, Sonora, México.

*E-mail address: mayraa.mendez@correoa.uson.mx; mplascencia@guayacan.uson.mx.

ABSTRACT

The objective of this study was to evaluate the effect of the neutralization of chitosan/poly(lactic acid) (PLA) composite films on *Aspergillus niger* growth. Blends of different concentrations of chitosan:poly(lactic acid) were used (0:100, 85:15, 90:10, 95:5, and 100:0). The films were elaborated using the solvent evaporation technique (*Casting*), and neutralized by immersion in NaOH, KOH, NaOH-Na₂CO₃ and NaOH-NaHCO₃; afterwards, the films were placed in a Petri plate containing Czapek agar and inoculated with 1x10⁶ spores/mL. The average diameter of the developed spores was determined at 18 and 24 h, observing that the hyphae developed on Q:PLA films of 85:15 concentration, neutralized with NaOH, presented a higher ($P \leq 0.05$) diameter with respect to the cellophane control, at 18 h. Also, it was observed that at 24 h, the films elaborated with a 85:15 proportion, and neutralized with KOH, resulted in a high ($P \leq 0.05$) increase on the hyphae diameter. FT-IR analysis, showed that neutralized films presented a decrease in the hydrogen bonds interactions with respect to the non-neutralized films; moreover, it was observed the presence of characteristic bands of the amino groups, which indicates that it is possible to obtain antifungal Q:PLA films with a potential application for the use in antimicrobial food packaging.

Keywords

Chitosan; poly(lactic acid); *Aspergillus niger*; neutralization; antifungal properties.

INTRODUCTION

The increase in shelf life of food products is one of the main topics of interest in the food industry and the use of packaging is a method for preserving the life of these. Nowadays, traditional food packagings are made from nonrenewable synthetic materials, hardly degradable most of them, which represents a serious environmental pollution. This situation has led to look for packaging materials derived from natural biopolymers, which are partially or completely biodegradable [1].

Chitosan is a biocompatible polysaccharide edible, non toxic, biodegradable, with antimicrobial activity against different microorganisms [2]. In addition, it has excellent film forming properties, it is semipermeable, thin and resistant, which may be used in food packaging to extend shelf life [2, 3]. Unfortunately, there are some limitations to the application of chitosan film for packaging, because of its high sensitivity to moisture. One strategy to overcome this drawback is to associate chitosan with a moisture resistant polymer such as poly(lactic acid), while maintaining the overall biodegradability of the product [4].

Non-neutralized chitosan films contain available amino groups to inhibit microbial [6]. Recently, previous studies using chitosan films, showed that even after being neutralized in NaOH 0.1 M solution, films prepared by the casting method are effective to delay the growth of *Aspergillus niger* [5]. Neutralized chitosan-based films have better physicochemical properties compared to those of non-neutralized chitosan films, however its antimicrobial activity is not clear. The aim of this work was to study the effect of different agents to neutralize chitosan/PLA films, and subsequently evaluate the antifungal activity of the materials against the growth of *Aspergillus niger*.

MATERIALS AND METHODS

Materials

Commercial grade chitosan (Q) of medium molecular weight (Sigma Aldrich) and polylactic acid (PLA) pellets (Polymer 2002-D, Ingeo™ PLA, Lerma, Estado de México) were used.

Microorganism and growth conditions

A strain of *Aspergillus niger* (NRRL 3) was activated in potato dextrose agar media, PDA, and incubated at 25°C for 3-5 d. Developed spores were removed pouring a sterile solution of 0.1% (v/v) Tween 80 into the flask and stirring with a magnetic bar during 15 min. The spore concentration of the suspension was determined using a Neubauer chamber (Brand, Germany).

Preparation of chitosan/polylactic acid solutions and films

Chitosan solutions 1% (w/v) in acetic acid 90% (v/v) were prepared; PLA solutions were prepared through the dissolution of PLA pellets in chloroform (1% w/v). Both solutions were stirred with a sterile magnetic bar during 24 h at 25°C; subsequently, they were degassed and maintained at 25°C for 12 h.

The chitosan/polylactic acid films were elaborated using the solvent evaporation technique or *casting*. Mixtures of Q:PLA of different proportions: 95:5, 90:10 and 85:15 were prepared. Pure chitosan films (100:0), pure PLA films (0:100) and commercial cellophane films were used as controls. Film forming solutions were poured on polystyrene plates and left to dry at 25°C on a previously leveled surface, until total solvent evaporation. The dried films were carefully peeled from the plate and maintained at 25°C.

Neutralization of films

The films were separately neutralized by immersion in NaOH 1% (w/v), KOH 1% (w/v), NaOH 1% (w/v)/Na²CO³ 0.05% (w/v) and NaOH 1% (w/v)/NaHCO³ 0.5% (w/v). Afterwards, the films were washed with distilled water and left to dry at 25°C in a laminar flow chamber. Once neutralized, the films were cut in square pieces of 1 cm² and stored into a desiccator container.

Activity of chitosan/PLA films on the hyphae diameter

The films were sterilized by exposure to UV light during 5 min on each side before analysis. Petri plates with Czapek agar (Bioxon, USA) were used to evaluate antifungal activity. Before inoculation, the plates were opened and exposed to UV light during 10 min in order to dry the surfaces. The sterile film pieces were placed on the agar and maintained under UV light for 15 min. Then, a fungi inoculum with a concentration of 1.4x10⁶ spores/mL was deposited on the surface of each film and incubated at 25°C. Pictures of the mycelium were taken at 18 and 24 h, using an optical microscope (Olympus, Japan)

connected to a camera (Infinity 1, Media Cybernetics, USA), with a 40X objective. Hyphal diameter was determined by image analysis using Image Pro-Plus version 6.3 software (Windows Media Cybernetics, USA) [5].

Fourier transform infrared analysis (FT-IR)

Film samples were analyzed using a FT-IR spectrophotometry equipment (Perkin-Elmer Spectrum GX FTIR), in a spectral range from 4000 a 400 cm⁻¹.

RESULTS AND DISCUSSION

Hyphae diameter

The Q:PLA films of 85:15 proportion, neutralized with NaOH, caused a large increase in the *A. niger* hyphae diameter, at 18 h (Figure 1; Table 1), whereas at 24 h, this films, but neutralized with KOH, resulted in a further increase in hyphae diameter ($5.19 \pm 0.97 \mu\text{m}$).

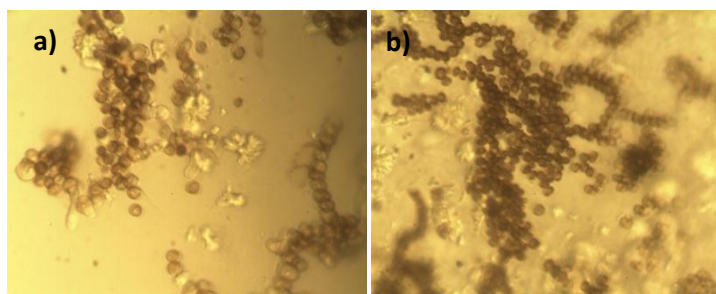


Figure 1. Hyphae and spores of *A. niger* inoculated on Q:PLA film of 85:15 proportion, neutralized with NaOH.

Related to 95:5 chitosan/PLA non neutralized films, a higher increase in the hyphae diameter was observed, which can be mainly attributed to the high content of chitosan and the presence of protonated amino groups, as well as acetic acid remaining after evaporation.

Antifungal activity has been reported in non neutralized chitosan/PLA films against *Fusarium proliferatum*, *F. moniliforme* and *Aspergillus ochraceus*, which was attributed to the antimicrobial activity of chitosan and not to the PLA [4]. However, it is possible that the PLA content in films may limit the absorption of nutrients, and therefore preventing or slowing the fungus development.

Table 1. Effect of neutralizing agents on mean hyphae diameter of *A. niger*, inoculated on Q:PLA films, at 18 h.

Agent	Diameter (μm)				
	0:100	85:15	90:10	95:5	100:0
NaOH	2.80 ± 1.34^a	5.30 ± 0.71^c	-	4.27 ± 1.81^{bc}	4.61 ± 0.83^{bc}
KOH	2.52 ± 0.55^a	4.89 ± 0.79^{bc}	4.84 ± 0.86^c	4.36 ± 0.71^{bc}	4.87 ± 0.88^c
NaOH/Na ₂ CO ₃	3.08 ± 0.58^a	3.07 ± 0.52^a	3.06 ± 0.82^a	4.17 ± 0.91^{bc}	3.06 ± 0.64^a
NaOH/NaHCO ₃	4.49 ± 0.63^c	-	3.41 ± 0.78^{ab}	3.34 ± 0.72^a	-
No neutralized	4.07 ± 1.43^{bc}	4.76 ± 0.67^{bc}	4.73 ± 0.74^c	4.52 ± 0.51^c	5.03 ± 1.06^c
Control	3.80 ± 2.85^b	3.80 ± 2.85^{ab}	3.80 ± 2.85^b	3.80 ± 2.85^{ab}	3.80 ± 2.85^{ab}

Superscript with same word in column, are not significantly different ($P \leq 0.05$). (-): No hyphae were observed. Control: commercial cellophane film.

The chelating ability of chitosan may indirectly limit the growth of filamentous fungi making cations such as calcium and some essential minerals inaccessible [7]. This may explain the presence of only few germ tubules in the non neutralized films. With respect to films neutralized with KOH, it is possible that the presence of K^+ ions remaining in the films has caused disturbances in the system of Ca^{+2} inside and outside the cell, whether acting as a transporting inhibitor or as an competent ion, thereby affecting the growth of the hyphae.

In Q:PLA films of 90:10 proportion, neutralized with NaOH and, 85:15 and 100:0 neutralized with NaOH-NaHCO₃, no hyphae were observed at 18. However, a large amount of spores as well as the formation of aggregations thereof was observed. Recent studies have reported that chitosan can induce aggregation of spores of *A. niger*, which increases the time of appearance or termination of dormancy of the spore [5]. It is possible that agglomerates may prolong the dormancy time of spores and therefore the germination. In addition to swelling, chitosan may produce excessive branching and malformations in the hyphae [8]. In this study we observed that as the concentration of chitosan increased, especially in non neutralized films, germ tubules and hyphae with several branches, swollen and with malformations were observed (Figure 2a); some spores showed hyphae development at both poles.

Previous studies have reported that the addition of chitosan to PDA agar media, cause deformation and surface damage on *A. niger* hyphae, and swelling in the diameter hyphae, which increases proportionally to the polymer concentration [9]. Contrary to this, the hyphae developed on commercial cellophane films and PLA (0:100) control showed a smooth appearance without any branching.

PLA is a polymer with non antimicrobial activity, for this reason, it can be assumed that the fungus can grow normally on PLA films; however, at 18 h, films neutralized with NaOH, KOH and NaOH/Na₂CO₃ showed a decrease in hyphae diameter compared with the commercial cellophane, while neutralization with NaOH/NaHCO₃ increased diameter, causing the opposite effect (Table 1, Figure 2b, c). It is likely that the low permeability of PLA films, due to its crystalline and compacted structure has not allowed adequate oxygenation and nutrient absorption [5], affecting fungal growth and reducing the hyphae diameter.

Regarding the increase in hyphae diameter, probably NaOH/NaHCO₃ interacted with PLA molecules, causing a molecular realignment and forming channels into the films, which were used by the fungus as channels for feeding [10]. Another reason can be attributed to the interaction that might have occurred between the neutralizing agent and the cell wall of the fungus, which altered the membrane permeability and led to swelling of the hyphae.



Figure 2. a) *A. niger* spores and hyphae inoculated on Q:PLA films of 100:0, neutralized with NaOH/Na₂CO₃; b) *A. niger* hyphae inoculated on PLA films, neutralized with NaOH/Na₂CO₃, at 18 h; b) PLA film neutralized with NaOH/NaHCO₃ at 18 h.

Fourier transform infrared analysis

The Q:PLA film of 85:15 proportion and neutralized with de NaOH/Na₂CO₃, showed a wider band corresponding to the –OH group stretching (2400-3600 cm⁻¹), which can be attributed to electrostatic interactions between PLA-chitosan, chitosan-NaOH/Na₂CO₃ and PLA-NaOH/Na₂CO₃ (Figure 3). A good definition of the characteristic amino group peaks of chitosan was not observed, which can be attributed to the possible interaction between –NH groups of chitosan with other molecules of the polymeric matrix, forming hydrogen bonds, contributing to the widening of the band [11].

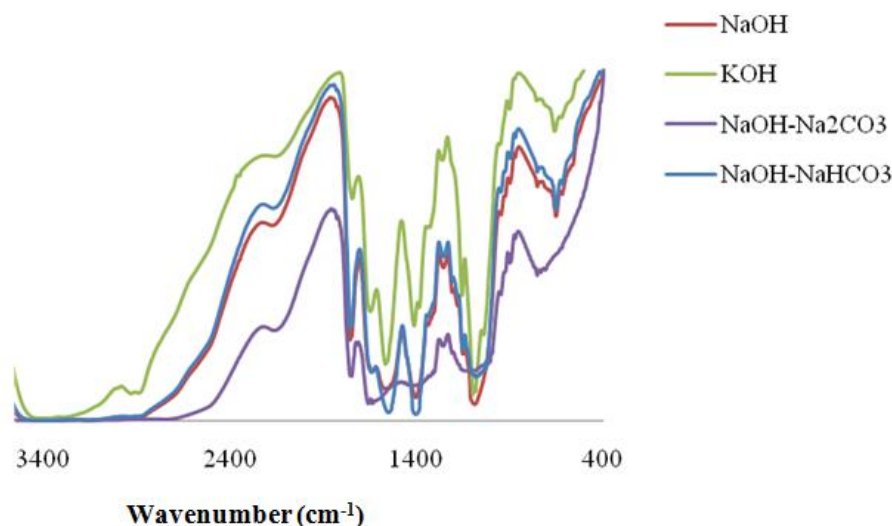


Figure 4. FT-IR spectra of chitosan:PLA films of 85:15 proportion, neutralized.

The film neutralized with KOH showed a good definition of the characteristic peaks of chitosan, –NH and NH₂ (1650 and 1590 cm⁻¹), and high intensity of the peak related with NH₃⁺ OOCCH ions (~1405 cm⁻¹). Fernández-Sainz et al. (2006) reported a band at 1405 cm⁻¹, which could be related to antimicrobial character of chitosan. Also, a low intensity peak for the C=O group (~1761 cm⁻¹) of PLA, which may indicate PLA interaction with other compounds was observed.

CONCLUSIONS

The Q:PLA film of 85:15 proportion presented a high effect on *A. niger* hyphae diameter at 18 h, (P<0.05). This proportion showed a high antifungal activity against the fungus, because it was observed mostly germ tubules and limited hyphae development. By neutralizing with KOH a slower hyphae development was observed, whereas NaOH/NaHCO₃ inhibited spore germination. This shows that it is possible to obtain antifungal materials made from chitosan and polylactic acid blends, which will assist in the design and development of methods and strategies for the development of more resistant functional packaging intended for food preservation.

ACKNOWLEDGEMENTS

This work was carried out with the financial support of CONACyT (Government of Mexico). Dra. Hisila Santacruz is greatly acknowledged for his assistance in FT-IR analysis.

REFERENCES

- [1] Srinivasa, P., & Tharanathan, R. (2007). Chitin/Chitosan — Safe, ecofriendly packaging materials with multiple potential uses. *Food Reviews International* , 23, 53–72.
- [2] Meng, Q., Hu, J., Ho, K., et al. (2009). The shape memory properties of biodegradable chitosan/poly(L-lactide) composites. *J Polym Environ* , 17, 212–224.
- [3] Agulló, E., Albertengo, L., Pastor de Abram, A., et al. (2004). *Quitina y Quitosano: Obtención, Caracterización y Aplicaciones*. Lima, Perú: Pontificia Universidad Católica del Perú.
- [4] Sébastien, F., Stéphane, G., Copinet, A., & Coma, V. (2006). Novel biodegradable films made from chitosan and poly(lactic acid) with antifungal properties against mycotoxinogen strains. *Carbohydrate Polymers* , 65, 185–193.
- [5] Martínez-Camacho, A., Cortez-Rocha, M., Ezquerro-Brauera, J., Castillo-Ortega, M.M., Yépiz-Gómez, S., Plascencia-Jatomea, M. (2010). Chitosan composite films: thermal, structural, mechanical and antifungal properties. *Carbohydrate Polymers* , 82 (5), 305–315.
- [6] Raafat, D., & Sahl, H.-G. (2009). Chitosan and its antimicrobial potential – a critical literature survey. *Microbial Biotechnology* , 2 (2), 186-201.
- [7] Li, X., Feng, X., Yang, S., Wang, et al. (2008). Effects of molecular weight and concentration of chitosan on antifungal activity against *Aspergillus Niger*. *Iranian Polymer Journal*, 17 (11), 843-852.
- [8] Bautista-Baños, S., Hernández-Lauzardo, A., Velázquez-del Valle, M., Hernández-López, M., et al. (2006). Chitosan as a potential natural compound to control pre and postharvest diseases of horticultural commodities. *Crop Protection* 25, 108–118.
- [9] Plascencia-Jatomea, M., Viniestra, G., Olayo, R., et al. (2003). Effect of chitosan and temperature on spore germination of *Aspergillus niger*. *Macromol Biosci* , 3, 582-586.
- [10] Nogueira, C., Ferreira, G., Cárdenas, G., & Inocentinni, M. (2005). Effects of neutralization process on preparation and characterization of chitosan membranes for wound dressing. *Macromol. Symp.* , 239, 253-257.
- [11] Cesteros, I. (2004). Aplicaciones de la FTIR al estudio de las interacciones polímero-polímero. *Revista Iberoamericana de Polímeros* , 5 (3), 111-132.
- [12] Fernández-Sainz, P., Ocio, M. J., & Lagaron, J. M. (2006). Film-forming process and biocide assessment of high-molecular-weight chitosan as determined by combined ATR-FTIR spectroscopy and antimicrobial assays. *Biopolymers* , 83, 577-583.

3D STRUCTURED CHITOSAN SCAFFOLDS FOR TISSUE ENGINEERING

Greyce Yane Honorato Sampaio^{1*}, Ana Carolina Brasil M. Fook¹, Thiago Bizerra Fidéles¹, Hugo Miguel Lisboa Oliveira¹, Anna Sylvia R. de R. M. Cavalcanti¹, Marcus Vinicius Lia Fook¹

¹ *Department of Materials Engineering, Federal University of Campina Grande, Av. Aprígio Veloso, 882 – 58429-140 Campina Grande, Brazil.*

**E-mail: greycesampaio@gmail.com*

ABSTRACT

Chitosan has been explored as a natural polysaccharide with suitable characteristics to be applied as porous matrices for reconstruction of body tissues using techniques in expansion in Tissue Engineering. The aim of this study is the development and characterization of porous chitosan scaffolds using the freeze drying technique. Chitosan solutions were prepared with concentrations of 1.5 % (w/t) and 2 % (w/t) and the solutions were poured into petri dishes and frozen in three different freezing rates. The scaffolds were characterized by Spectroscopy Fourier Transform Infrared (FTIR) and Scanning Electron Microscopy (SEM), and Compressive tests were performed. Through FTIR analysis all the characteristic bands of chitosan, regardless the concentrations studied, could be observed. The SEM micrographs obtained demonstrate the efficacy of the freeze drying technique and the influence of freezing rates in the final morphology of the scaffolds. The compression properties demonstrated increases in resistance proportionally to the freeze rate applied and to the concentration of the chitosan solution.

Keywords

Chitosan, scaffold, freeze drying, tissue engineering

INTRODUCTION

Tissue Engineering can be defined as the creation of new tissues for therapeutic reconstruction of the human body through the deliberate and controlled stimulation of selected target cells, in a systematic combination between mechanical and molecular signals [1]. Among the most important aspects of this area, the manufacture of three-dimensional porous scaffolds similar to the tissue extracellular matrix (ECM) stands out [2].

The basic requirements for biomaterials used in the scaffolds manufacture are biocompatibility, biodegradability, and surface properties appropriate to promote adhesion, proliferation, and cellular differentiation [3].

In this context, the biopolymer chitosan, a polysaccharide derived from chitin, has been investigated due to its biocompatibility, which minimizes additional local inflammation, intrinsic antibacterial activity, ability to recognize growth factors that favor the production of extracellular matrix, and biodegradability. The latter allows the biodegradation of the scaffolds according to the growth of the new tissue [4, 5].

Chitosan is the most important derivative chitins in terms of application. Chitin can be converted to chitosan by enzymatic route or by alkaline deacetylation, which is the method most used. During the course of alkaline deacetylation, part of the N-acetyl bonds are broken with the formation of D-glucosamine units containing a free amine group.

According to Antonino (2007), chitosan can be defined as a copolymer of 2-amino-2-deoxy- β -D-glucose and 2-deoxy-2-acetamino- β -D-glucopyranose of variable composition. That is according to the residual degree of acetylation whose the units are linked by glycosidic linkages β -(1.4) [6, 7, 8].

Besides, chitosan has the capacity to be processed in a variety of macro and nano shapes [9]. Among the techniques currently used to manufacture, chitosan matrices can be obtained by freeze drying process, in which it is possible to obtain scaffolds with different densities, shapes, and porosity, depending on the specific processing variables [10].

The knowledge of the physicochemical properties is critical for the understanding of biological properties of biomaterials designed with chitosan. It is particularly important to establish a relationship between the structures and the biological responses [11]. Thus, this work focuses on the development and characterization of porous chitosan matrices using the technique of freeze drying for application in tissue regeneration.

MATERIALS and METHODS

PREPARATION of CHITOSAN SCAFFOLDS

Chitosan (Sigma-Aldrich, Molecular weight (Mw) = 190×10^3 g/mol – 310×10^3 g/mol, Degree of Deacetylation (DD) = 75 % - 85 %), acetic acid (Vetec), absolute ethyl alcohol 99,5° GL (Vetec) and ethyl alcohol 70° INPM (TUPI), were used to prepare the scaffolds.

Chitosan solutions with concentrations of 1.5 % (w/t) and 2 % (w/t) were prepared by dissolving the polymer in a solution of acetic acid 1 % (v/v). The solutions remained under magnetic stirring at room temperature for 24 hours and were subsequently vacuum filtered to remove insoluble material. The scaffolds were obtained by the process of freeze and lyophilization of the solutions prepared, which allows the separation of solid-liquid phase and subsequent sublimation of the solvent to form porous structures [10].

In previous studies were established scales for the freezing rates in terms of °C/s: “very slow” (less than 0.01 °C/s), “slow” (0.01 °C/s to 0.06 °C/s), “fast” (0.06 °C/s at 50 °C/s) and “super-fast” (above 50 °C / s) [12]. In this research the solutions were poured into petri dishes and frozen at -20 °C, at “very slow” and “slow” freeze rate, and in liquid nitrogen (≈ -196 °C), at “rapid” freeze rate. After frozen, the solutions were lyophilized for 48 hours. The obtained scaffolds were neutralized by immersion in absolute ethyl alcohol for 1 hour and subsequent washing with ethyl alcohol 70°, frozen and lyophilized again.

CHARACTERIZATION of SCAFFOLDS

The chemical characterization of scaffolds was performed by Spectroscopy Fourier Transform Infrared (FTIR) analysis. The spectra were recorded on a spectrophotometer (Spectrum 400 FT-IR/FT-NIR Spectrometer Perkin Elmer) in the region of 400-4000 cm^{-1} with a resolution of 4 cm^{-1} and 20 scans.

Scanning Electron Microscopy (SEM, HITACHI, TM 1000) was used for analysis of the final microstructure of the scaffolds. Furthermore, the average pore diameter was determined by following the method described in literature [13]: was measured the width and length of the pores from SEM micrographs of scaffolds, and the average pore diameter determined by the expression $d = \sqrt{l \cdot h}$, where l and h are the average length and width of the pores, respectively. Measurements were taken in 20 pores per sample.

The compression properties of the scaffolds were tested with dry samples using an electromechanical universal testing machine (INSTRON, Model 5582) with a capacity of

100 kN, constant strain rate of 5 mm/min. and at room temperature. The scaffolds were cut in cylindrical shape with a ratio about 2 between the diameter and height of the samples. The compressive strength was calculated by dividing the maximum strain and the original area.

RESULTS and DISCUSSION

SPECTROSCOPY FOURIER TRANSFORM INFRARED

Through FTIR analysis could be observed the absorption of bands present in the scaffolds produced before and after neutralization. This was performed in different concentrations of chitosan and freezing rates. The spectra obtained are shown in Figure 1.

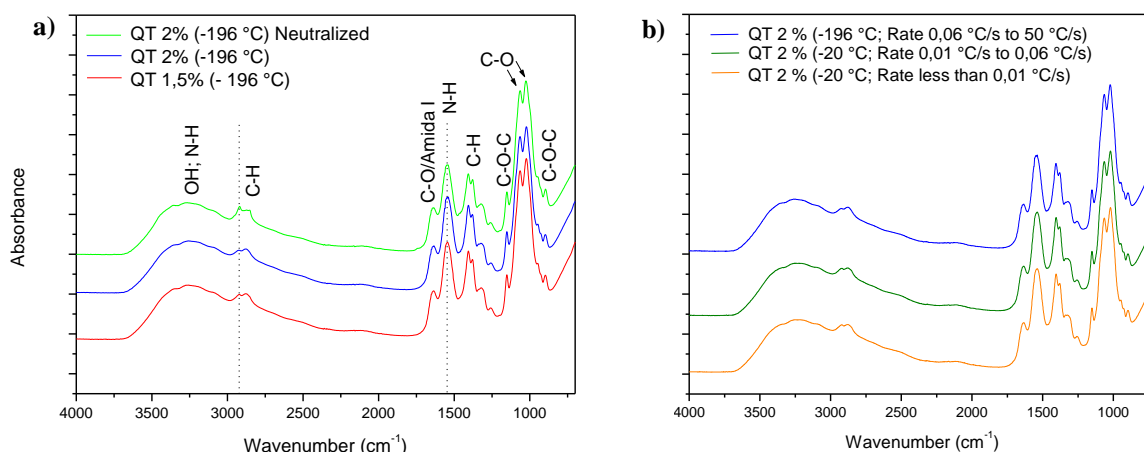


Figure 1. FTIR spectra of freeze-dried chitosan scaffolds: (a) chitosan 1,5 % (w/t) and 2 % (w/t), frozen in liquid nitrogen, before and after neutralization, and (b) chitosan 2 % (w/t), frozen at three different rates.

The spectra obtained show all characteristic bands of chitosan [6, 7, 14], regardless of the concentrations studied (Fig. 1a). Further, was observed no significant changes in the spectra of scaffolds independently of the freeze rate applied (Fig. 1b).

The samples characterized before the neutralization stage (Fig. 1a) presented a small increase in the absorption of amide group II (N-H, 1543 cm^{-1}), which becomes amide III, due to protonation of group ($\text{NH}_2 \rightarrow \text{NH}^{3+}$). Thus, the spectrum QT 2 % neutralized showed a small decrease in the peaks related to N-H stretch of the amine group NH_2 (1546 cm^{-1}) and an increase of the peak related to the stretching vibration of C-H asymmetric group (2920 cm^{-1}). According to previous studies [15], these differences were caused by neutralization stage.

SCANNING ELECTRON MICROSCOPY

The scaffold microstructure such as pore size, shape, and distribution have prominent influence on cell intrusion and proliferation, as previously reported [16]. To investigate if the scaffolds microstructure is related to the different freezing rates and concentrations of chitosan solutions, analysis were performed by SEM. These analysis were based on longitudinal sections of areas that represented the predominant morphology. The results were compared to scaffolds with concentration 1.5 % and 2 %, showed in Figure 2.

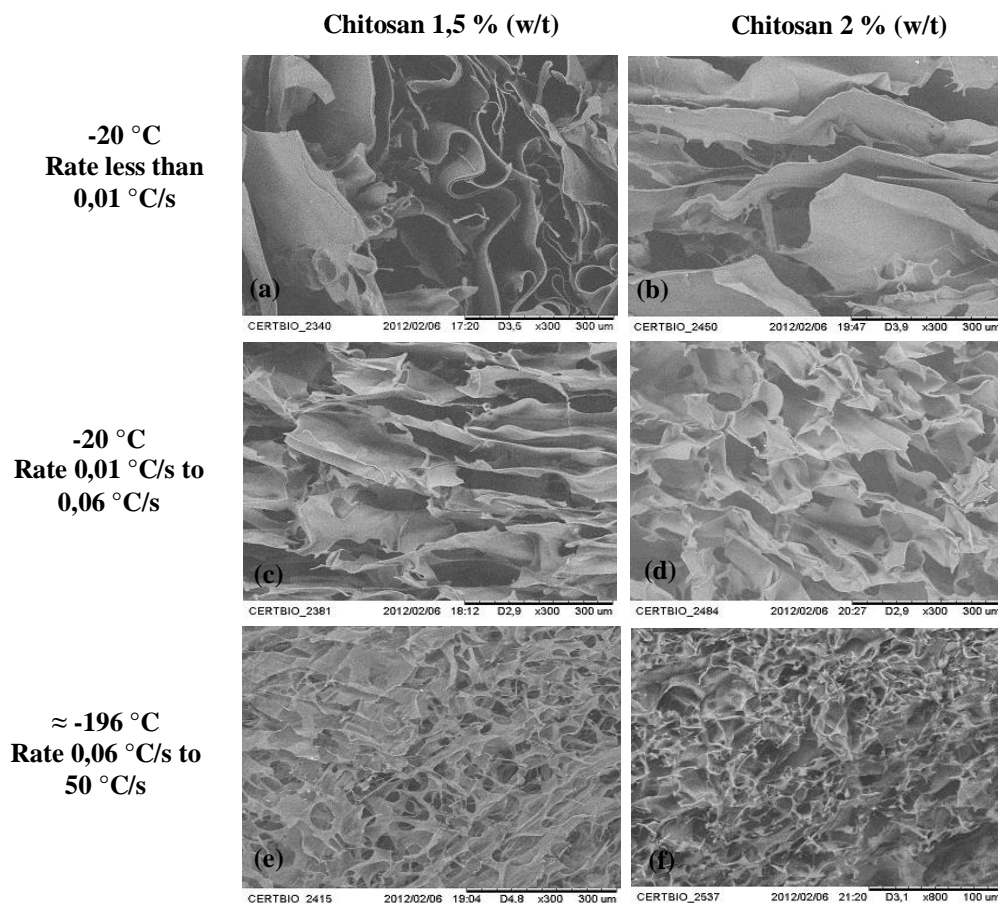


Figure 2. Micrographs (MEV) of longitudinal sections of freeze-dried chitosan scaffolds 1,5 % (w/t) (a-300x, b-300x, c-300x) and 2 % (w/t) (a-300x, b-300x, c-300x), frozen at $-20\text{ }^{\circ}\text{C}$, rate less than $0,01\text{ }^{\circ}\text{C/s}$ and rate $0,01\text{ }^{\circ}\text{C/s}$ to $0,06\text{ }^{\circ}\text{C/s}$, and at $\approx -196\text{ }^{\circ}\text{C}$, rate $0,06\text{ }^{\circ}\text{C/s}$ to $50\text{ }^{\circ}\text{C/s}$.

Through the figures 2(a, b), was observed the formation of plaque/blades arranged, with corrugated surface, that themselves organize predominantly in the form of channels. However, along these blades was not observed pores, which indicates a structure with poor interconnectivity. This alignment may be a consequence of the freezing stage. The “very slow” rate allows the formation of higher ice crystals. For this rate, the scaffolds 1.5 % and 2 % presented an average pore diameter of $63\text{ }\mu\text{m}$ and $85\text{ }\mu\text{m}$, respectively.

Figures 2(c, d) illustrate the internal formation of scaffolds frozen at “slow rate” (rate $0.01\text{ }^{\circ}\text{C/s}$ to $0.06\text{ }^{\circ}\text{C/s}$). The formation of blades with pores of different sizes on their surfaces, which allow an interconnection of the structure, was observed. Furthermore, the amount of pores is higher than that observed in figures 2(a,b), and the shape of pores is polygonal and more uniform, with average diameter of $60\text{ }\mu\text{m}$ for both scaffolds 1.5 % and 2 %. This architecture may be attributed to the increasing freeze rate, which provides a shorter time for the internal formation of ice crystals. Consequently, these crystals present smaller sizes throughout the frozen solution.

The micrographs obtained to the “fast” freeze rate ($0.06\text{ }^{\circ}\text{C/s}$ to $50\text{ }^{\circ}\text{C/s}$), figures 2(e, f), show more blades in the structure. These blades exhibit minimum space between themselves. The mean of pores was $40\text{ }\mu\text{m}$ and $50\text{ }\mu\text{m}$ to scaffolds 1.5 % and 2 %, respectively. Therefore, with the increase of the freeze rate, the ice crystals do not have much time to grow, resulting in smaller pores and with more uniform shape.

According to these results, independently of the chitosan concentrations was observed an increased number of pores with the increase of the freeze rate, as well as a

decrease in pore size. These results corroborate to those found by Madihally and Matthew (1999), Hshieh, Chang and Lin (2007) and Tigh, Karakeçili and Gümüşderelioglu (2007), in studies with similar methodology [17, 18, 16].

COMPRESSIVE MECHANICAL TEST

The knowledge of the mechanical properties of porous scaffolds utilized in tissue engineering has a particular importance, since these are closely linked to the strength, performance, and durability of the scaffolds during application [19].

Data related to compression elastic modulus (E) were collected and are listed in Table 1. According to these results may be inferred that the resistance of the scaffolds rises with the increase of freeze rate. Furthermore, was observed an increase in the compression modulus to the scaffolds with a concentration of 2 %.

Table 1. Compressive modulus of freeze-dried chitosan scaffolds

SCAFFOLDS	Compressive modulus - E (Mpa)	
	Chitosan 1,5 % (w/t)	Chitosan 2 % (w/t)
Freeze rate		
-20 °C (Rate less than 0,01 °C/s)	0,0014 ± 0,0002	0,0096 ± 0,0013
-20 °C (Rate 0,01 °C/s to 0,06 °C/s)	0,0026 ± 0,0006	0,0164 ± 0,0022
≈ -196 °C (Rate 0,06 °C/s to 50 °C/s)	0,0081 ± 0,0029	0,0318 ± 0,0019

These results are consistent with the morphology of the scaffolds observed by SEM. With the increase of freeze rate was noted a densification of the internal structures and the formation of walls perpendicular to the blades. These walls may allow a charge distribution in the scaffold and consequently higher resistance. The increase in concentration of chitosan may result in a higher polymer mass distributed throughout the architecture of the material, which may contribute to the rise of the compression modulus.

CONCLUSION

Through the Spectroscopy Fourier Transform Infrared (FTIR) was observed all the characteristic bands of chitosan, regardless of the concentrations studied, and no significant changes in the spectra of scaffolds varying the rate of freezing. The Scanning Electron Microscopy (SEM) demonstrated the efficacy of the freeze drying technique. The influence of the freezing rate in the final morphology of the scaffolds, which had channels and pores of various shapes, was also observed. The compression properties of the scaffolds revealed increases in resistance proportionally to the rate of freezing applied and to the concentration of the chitosan solutions.

ACKNOWLEDGEMENTS

The financial support of *Coordenação de Aperfeiçoamento de Pessoal de Nível Superior/CAPES* is gratefully acknowledged by the authors.

REFERENCES

- [1] Williams, D. F. (2008) On the mechanisms of biocompatibility. *Biomaterials*, 29, 2941-2953.
- [2] Tabata, Y. (2005) Significance of release technology in tissue engineering. *DDT*, 10, 23/24, 1639-1646.

- [3] Kim, I.-N.; Seo, S.-J.; Moon, H.-S.; Yoo, M.-K.; Park, I.-Y.; Kim, B.-C.; Cho, C.-S. (2008) Chitosan and its derivatives for tissue engineering applications. *Biotechnology Advances*, 26, 1-21.
- [4] Uragami, T and Tokura, S. (2006) *Material science of chitin and chitosan*. Kodansha Ltd.: Tokyo.
- [5] Dash, M.; Chiellini, F.; Ottenbrite, R.M.; Chiellini, E. (2011) Chitosan - A versatile semi-synthetic polymer in biomedical. *Progress in polymer science*, 36, 981-1014.
- [6] Antonino, N. A. (2007) Otimização do processo de obtenção de quitina e quitosana de exoesqueletos de camarões oriundos da indústria pesqueira paraibana. Federal University of Paraíba, João Pessoa.
- [7] Aimoli, C. G. (2007) Investigação da adequação de membranas de quitosana quimicamente modificadas para uso como biomaterial: estudo da calcificação *in vitro*. State University of Campinas, Campinas.
- [8] Dutta, J. and Dutta, P. K. (2011) Antimicrobial Activity of Chitin, Chitosan and Their Oligosaccharides. In: *Chitin, chitosan, oligosaccharides and their derivatives: biological activities and applications* (S.-K.Kim, ed.), Taylor & Francis Group: B R.
- [9] Correlo, V. M.; Gomes, M.E.; Tuzlakoglu, K.; Oliveira, J.M.; Malafaya, P.B.; Mano, J.F.; Neves, N.M.; Reis, L.R. (2007) *Tissue engineering using natural polymers*. In: *Biomedical polymers* (M. Jenkins, ed.) M. Woodhead Publishing Ltda.
- [10] Franks, F. (2007) *Freeze-drying of pharmaceutical and biopharmaceuticals: principles and practice*. RSC Publishing.
- [11] Domard, A. (2011) A perspective on 30 years research on chitin and chitosan. *Carbohydrate polymers*, 84, 696-703.
- [12] Pitombo, R. M. N. (1989) A liofilização como técnica de conservação de material de pesquisa. *SBPC Ciência e Cultura*, 427-431.
- [13] Yin, Y.; Ye, F.; Cui, J.; Zhang, F.; Li, X.; Yao, K. (2003) Preparation and characterization of Macroporous chitosan-gelatin/ β -tricalcium phosphate composite scaffolds for bone tissue engineering. *J Biomed Mater Res.*, 67, 844-855.
- [14] Fidèles, T. B. (2010) *Filmes reticulados de quitosana para aplicação como biomaterial*. Federal University of Campina Grande, Campina Grande.
- [15] Noriega, S.E. and Subramanian, A. (2011) Consequences of Neutralization on the Proliferation and Cytoskeletal Organization of Chondrocytes on Chitosan-Based Matrices. *International Journal of Carbohydrate Chemistry*, 2011, 1-13.
- [16] Tiğh, R. S.; Karakeçili, A.; Gümüşderelioğlu, M. (2007) In vitro characterization of chitosan scaffolds: influence of composition and deacetylation degree. *J Mater Sci: Mater Med.*, 18, 1665-1674.
- [17] Madhally, S. V. and Matthew, H. W. T. (1999) Porous chitosan scaffolds for tissue engineering. *Biomaterials*, 20, 1133-1142.
- [18] Hsieh, W.-C.; Chang, C.-P.; Lin, S.-M. (2007) Morphology and characterization of 3D micro-porous structured chitosan scaffolds for tissue engineering. *Colloids and surfaces B: biointerfaces*, 57, 250-255.
- [19] Wan, Y.; Wu, H.; Cao, X.; Dalai, S. (2008) Compressive mechanical properties and biodegradability of porous poly(caprolactone)/chitosan scaffolds. *Polymer Degradation and Stability*, 93, 1736-1741.

Intellectual Properties

EACH COIN HAS TWO SIDES: SCIENTIFIC AND COMMERCIAL ASPECTS OF CHITIN / CHITOSAN

Martin G. Peter

Universität Potsdam, Institut für Chemie, Karl-Liebknecht-Str. 25, D – 14476 Potsdam, Germany

E-mail address: Martin.Peter@uni-potsdam.de

ABSTRACT

Chitin is often compared with cellulose in abundance and importance. Counts of publications in scientific journals and of patents on chitin, chitosan, chitinases and chitosanases are analyzed and compared with cellulose, using searches in two databases, i.e. "SciFinder[®]" (Chemical Abstracts) and "Web of Science[®]" (Thomson Reuters). Criteria for refinement were the language of publication, the territorial distribution of the institutions from which publications originated, the field of investigation, and the titles of journals which publish articles on the topics. Some data on industrial demand and market volumes are cited. It appears that a major fraction of publications on chitin and derivatives deal with research on potential pharmaceutical and biomedical applications.

Keywords

Biopolymers, Cellulose, Databases, Literature, Market-Volume, Polysaccharides

INTRODUCTION

It is frequently stated that *chitin is the second most abundant "biopolymer" or "polysaccharide" on earth after cellulose*, but neither are figures given nor references cited. Other sources mention that *chitin is the second most important*, but they do not mention in which respect it is important. The statement is often even made when the subject of research is not at all dealing with the abundance or importance of chitin. Abundance would be interesting in the context of large technical applications, like paper and cardboard production or exploration of new renewable sources for energy generation, such as biofuel. Even thinking about using chitin for these purposes is totally unrealistic. Besides availability, the logistics, methods, and cost of securing and processing the raw material are very different for cellulose and chitin. Last not least: in terms of abundance and importance of polysaccharides, what about starch, alginates, hyaluronates, pectins, etc., etc. ?

In fact, chitin and derivatives are intensively investigated because of their unique, outstanding chemical and biological properties, and not because of their high abundance in nature. A remarkable number of scientific publications and patents on both, cellulose and chitin, appear daily, indicating a high interest in these polysaccharides. The aim of this study is to summarize some facts about the abundance and the areas of interest of chitin, and to correlate those with the industrial demand, applications, and the actual market situation, as far as information is available.

ABUNDANCE

Occurrence: Cellulose occurs mostly in plants but is also synthesized by some bacteria. It represents ca. 45 – 50 % of wood dry biomass, the rest being composed of polyphenolic lignin

(25–30 %) and polysaccharides named polyoses (hemicelluloses, 15 – 20 %), not considering minor components like other primary and secondary metabolites and salts. In terms of organic carbon (OC) present in the pedosphere, it is estimated that ca. 110–300 billion (= 110–300 × 10⁹) tons of OC are bound in cellulose (Table 1). Chitin is likewise widely distributed in the biosphere [1,2]. However, the amounts of OC bound in chitin, e.g. in arthropods and fungi, are unknown. Concerning the hydrosphere, i.e. freshwater, athalassohaline, and oceanic ecosystems, neither the OC bound in cellulose, mostly in algae, nor that in chitin occurring in fungi, some diatoms, annelids, arthropods, and tunicates, and other chitinous organisms have been estimated.

In consequence, statements according to which "chitin is the second most abundant polysaccharide or biopolymer" ignore the fact that polyoses are also polysaccharides, and that lignins, proteins, nucleic acids and others, such as poly-isoprenoids and natural polyesters, are also biopolymers. Last not least, comparison of unknowns is beyond scientific respectability. It necessarily ends up in fairy tales.

Table 1: Abundance of organic carbon on earth.

Compartment	tons of OC	Ref.
Pedosphere, total	2,600 × 10 ⁹	[3]
Dead Matter (mostly fossil deposits and humic substances)	1,750 × 10 ⁹	[4]
Plant Biomass	830 × 10 ⁹	[4]
Cellulose in Pedosphere	110 – 300 × 10 ⁹	[4,5]
Chitin in Pedosphere (fungi, arthropods, other)	unknown	
Hydrosphere, total	1,000 × 10 ⁹	[4]
Cellulose in Hydrosphere	unknown	
Chitin in Hydrosphere (zoo- and phytoplankton)	unknown	

Annual Regeneration: Cellulose originates from carbon dioxide through photosynthesis, while chitin biosynthesis proceeds from D-glucose and L-glutamine. Estimates for the annual global production of cellulose vary between 10¹⁰ and 10¹² metric tons per year (t×a⁻¹) [6]. Sandermann [7] estimated the synthesis of cellulose by trees alone to amount to 13×10⁹ metric tons which is equivalent to 5.7×10⁹ t×a⁻¹ OC. According to *Klemm* et al. [8], the total global cellulose synthesis is 1.5×10¹² t×a⁻¹ (667×10⁹ t OC). Estimates for chitin synthesized by arthropods vary between 1.36×10⁹ t×a⁻¹ (0.62×10⁹ t OC) in the hydrosphere [9] and 2.3×10⁹ t×a⁻¹ (1.1×10⁹ t OC) in marine ecosystems [10]. However, these estimates do not consider chitin production by fungi, arthropods, and other organisms in the pedosphere, while the amounts of cellulose produced in aquatic ecosystems have not been estimated, either.

SCIENTIFIC ASPECTS

Scientific interest in a topic is reflected by the numbers of publications and their variations over time. Thus it is of interest to extract information about research activities on chitin, chitosan, and relevant enzymes from two of the most comprehensive databases. Searches were carried out on June 10, 2012 and on October 14, 2012 in:

- SciFinder[®] (Chemical Abstracts) [11], including CAPLUS and MEDLINE. Query: "chitin or chitosan or chitinase or chitosanase".
- Web of Science[®] (WOS; Thomson Reuters) [12]. Social sciences, arts and humanities were excluded. Query: "chiti* or chito*".

The results are summarized in Table 2. Trends become clearly apparent by analysis of the citations, though restrictions are due to the fact that analysis in CAPLUS is limited to 15,000

records; information about the country of origin is not available without checking the individual citations in CAPLUS; some records may be counted multiple-fold in case of several countries of origin, research, and subject areas. WOS does not cite patents and some other types of publications, such as dissertations; definitions of subject areas and research topics are different in CAPLUS vs. WOS. The results were not evaluated with respect to details of content, quality and originality of research.

Table 2. Number of counts in the databases.

Date of search	Science Finder		WOS	
	2012-06-10	2012-10-14	2012-06-10	2012-10-14
Year of First Record	1875		1901	
Total Number of Records	96,146	100,221	39,506	40,911
1st Refinement: Database				
MEDLINE	17,064	17,782		
CAPLUS	79,082	82,439		
2nd Refinement, Type of Publication				
	CAPLUS		WOS	
Journal Articles	50,182	52,045	35,733	
Reviews	3,914	4,214	1,548	
Proceedings & Conference Papers	2,410	2,492	1,450	
Patents	26,026	27,423	0	
Dissertations	323	335	0	
Books	43	46	0	
Total	82,898	86,555	38,731	

According to an update, made on October 14, 2012, the number of journal articles recorded over all years was 52,045 in CAPLUS and 40,911 in WOS which means that, in the average, ca. 15 additional journal articles and 11 patents are registered daily in CAPLUS, and ca. 11 citations are added in WOS. Just for comparison: a search for "cellulose or cellulase" yielded 239,407 records of journal publications in CAPLUS.

Further refinement of "chitin, chitosan, chitinase, chitosanase" in CAPLUS is based on records from the last decade, as it appears that > 70 % of all the articles were published since 2001 (Fig. 1). CAPLUS includes a large number of journal articles published in Asian Journals which are not reported in Web of Science (Table 3). According to CAPLUS, ca. 72% of articles were written in English, 24 % in Chinese, 1.6% in Japanese, 1.0% in Russian, 0.6% in Korean, ca. 0.8% is written in a few other languages. According to WOS, 97.2% of articles are in English, but only 1.4% in Chinese, 0.3% each in Portuguese and Japanese, and 0.2 % in Spanish. Thus, researchers relying on WOS only may eventually not be aware of the scientific output in other major parts of the world.

Table 3. Language of publication in journal articles (CAPLUS: 2001 – 2012; WOS: all years).

Language	CAPLUS	WOS	Language	CAPLUS	WOS	Language	CAPLUS	WOS
English	25748	38025	French	33	151	Croatian	2	3
Chinese	8444	476	Persian	25	0	Lithuanian	2	0
Japanese	582	267	Ukrainian	23	0	Malay	2	0
Russian	358	163	Italian	20	5	Romanian	2	2
Korean	217	63	Czech	14	9	Azerbaijani	1	0
Portuguese	95	105	Slovak	12	0	Latvian	1	0
Polish	89	39	Bulgarian	3	0	Slovenian	1	0
Spanish	77	78	Hungarian	3	0	Thai	1	0
German	56	106	Indonesian	3	0	Turkish	1	4
Vietnamese	38	0	Serbian	3	0	SerboCroatian	0	4

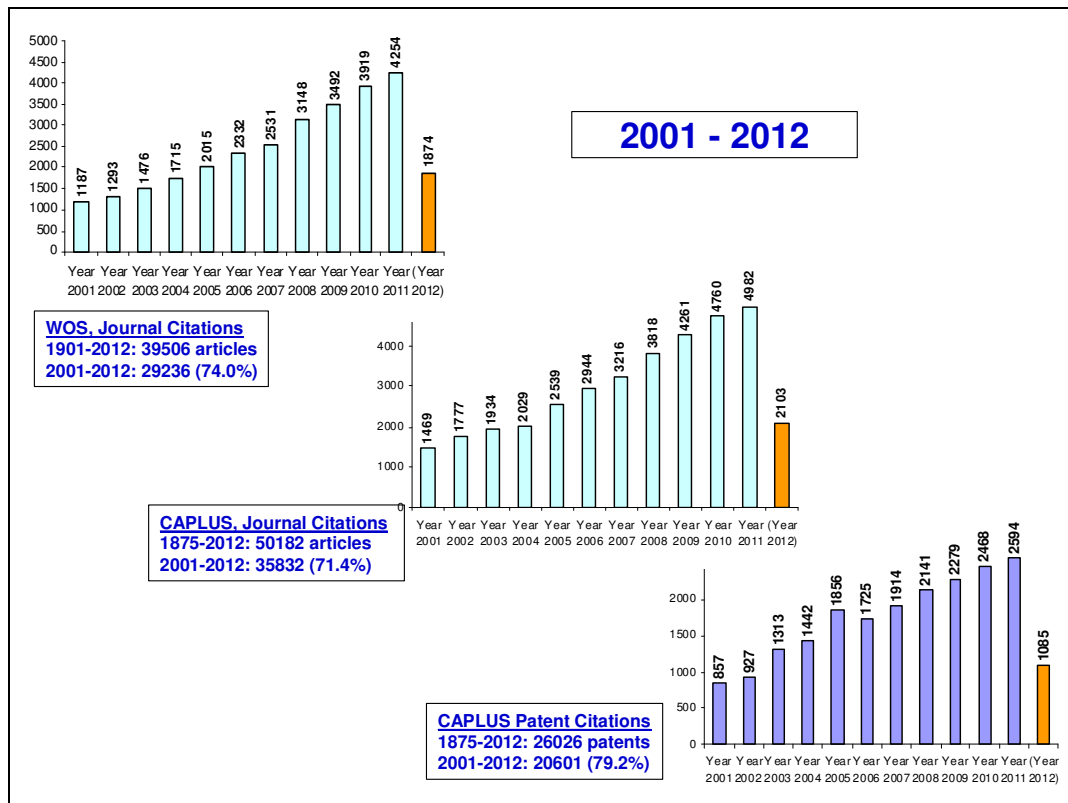


Figure 1. Journal articles and patents counts (year 2001 until 2012-06-10).

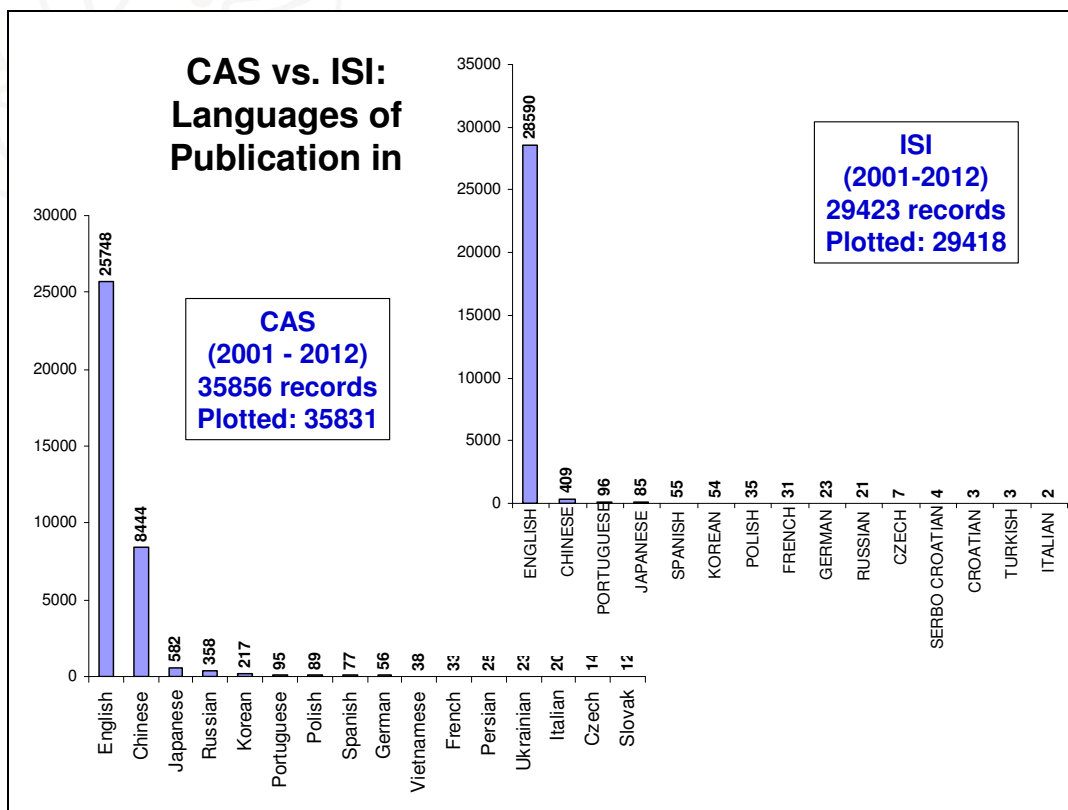


Figure 2. Languages of publications in journals.

The language profile is quite different from that of the territorial distribution of institutions of origin when evaluated WOS (Table 4). In this case, the number of records originating from Asian Institutions surpass those from the rest of the world. Apparently, WOS covers mostly articles and abstracts written with Latin characters, meaning that a large number of articles originating from Asian institutions are written in English.

Table 4. Territorial distribution of the institutions from which journal articles originated (WOS, all years, 50 of 128 entries are listed; sum of records: 39,506; total listed: 45,388, obviously containing multiple counts).

PR China	6905	Taiwan	1231	Iran	482	Austria	324	Greece	162
USA	6509	Italy	1201	Switzerland	471	Denmark	312	Slovakia	129
Japan	4445	Spain	1105	Mexico	447	Malaysia	300	Hungary	125
India	2352	Russia	912	Egypt	446	Argentina	296	Ireland	114
S. Korea	1967	Netherlands	655	Belgium	444	Czech Rep.	200	Cuba	113
France	1785	Thailand	640	Sweden	391	Finland	199	Bulgaria	109
Germany	1632	Australia	636	Israel	359	Romania	183	Fed Rep Ger	96
Canada	1592	Turkey	629	Singapore	354	S. Africa	183	USSR	95
England	1387	Poland	544	Norway	350	N. Zealand	165	Saudi Arabia	84
Brazil	1235	Portugal	520	Scotland	333	Chile	164	Pakistan	76

Nearly 30 % of the journal publications recorded in CAPLUS since year 2001 are dealing with pharmaceuticals (Fig. 3), followed by industrial carbohydrates (7.65 %), food and feed chemistry (5.92 %), microbial, algal, and fungal biochemistry (4.38 %), and enzymes (4.25%). For comparison: 7.12 % of the "cellulose" articles deal with pharmaceuticals.

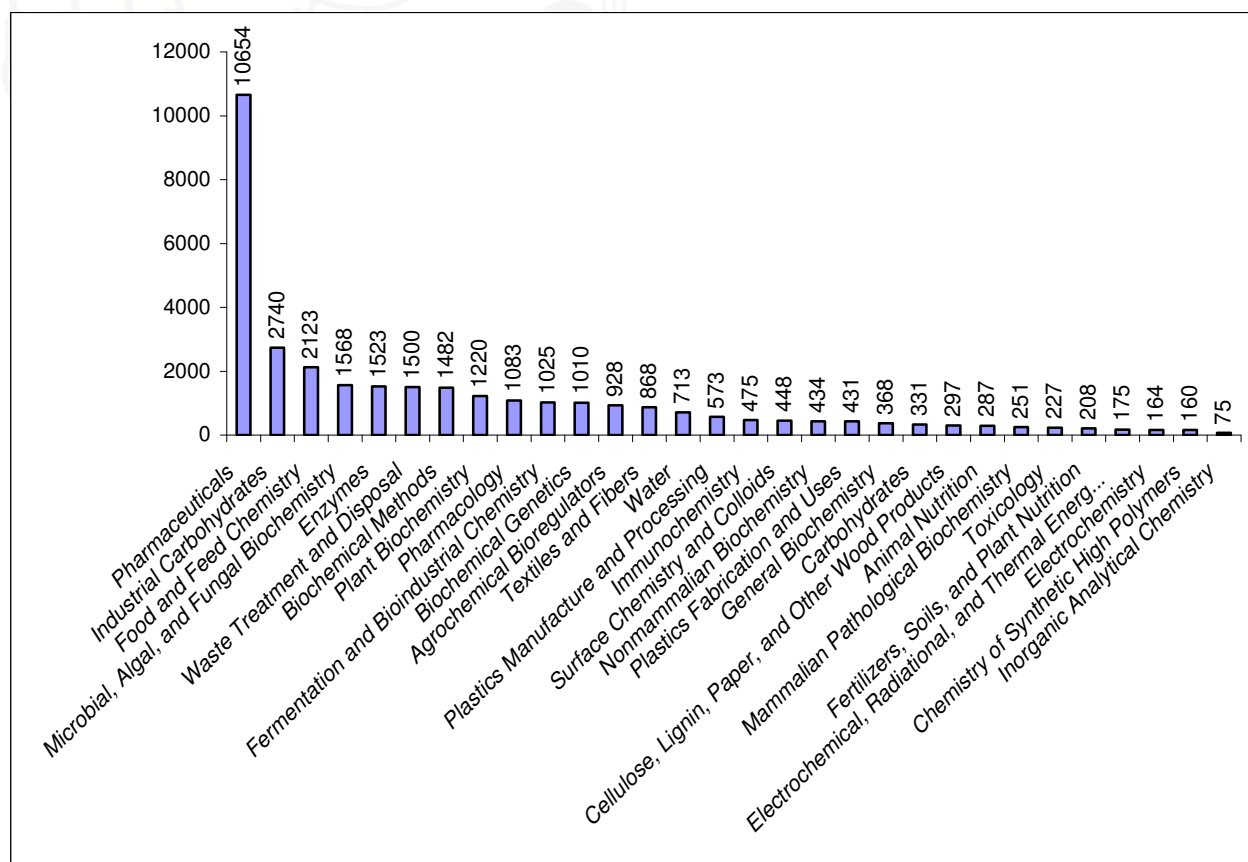


Figure 3. The 30 top subject areas (CAPLUS; 2001-2012; plotted: 33,341 out of 35,856 counts)

According to CAPLUS, articles on the topics "chitin, chitosan, chitinase, chitosanase" are published in more than 1,000 journals. On the top is *Carbohydrate Polymers* with 1021 articles (2.85 %) in the period 2001 until June 10, 2012, followed by *J. Appl. Polym. Sci.*, *Biomaterials*, *Biomacromolecules* and *Int. J. of Pharm. Sci.* (Fig. 4). It is interesting that *Advances in Chitin Science* stands in place 7. However, a closer inspection shows that no articles are cited after 2005, though several volumes have appeared since then. Obviously, Chemical Abstracts did not have access to the series after year 2005, meaning that some significant information is not available, neither in CAPLUS, nor in WOS where *Adv. Chitin Sci.* is not indexed at all.

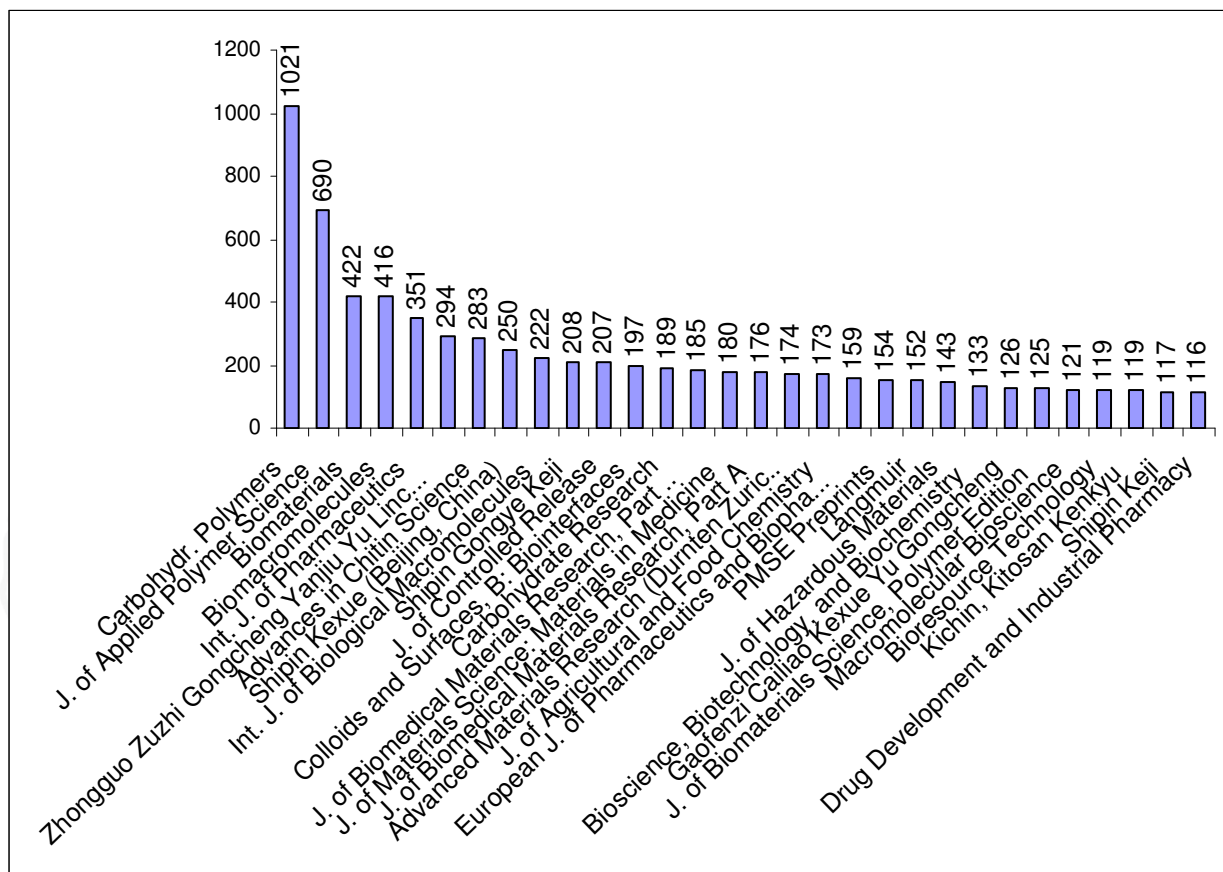


Figure 4. The 30 leading journals publishing articles on chitin, chitosan, chitinase and/or chitosanase (CAPLUS; 2001-2012; plotted: 7,222 out of 35,856 counts).

COMMERCIAL ASPECTS

The scientific as well as – in some sense – the commercial interest in a subject is also reflected by the number of patents filed on a particular topic. CAPLUS lists, over all years, 26,026 patents and patent applications on chitin, chitosan, chitinase, chitosanase. For comparison, the number of patents on "cellulose or cellulase" is 223,605. Nearly 80 % of all "chitin" patents were recorded in the period 2001 until 2012-06-10. Analysis of the period 2006 until 2012-06-10 shows that 14,206 patents and patent applications are written in 24 languages, more than 45 % of them are in Chinese (Table 4).

Table 5. Language of patents and patent applications (CAPLUS: 2006 – 2012-06-10; listed 14,206 of 14,206 counts)

Language	Count	%	Language	Count	%	Language	Count	%
Chinese	6473	45.57	Portuguese	73	0.51	Moldavian	2	0.01
English	4488	31.59	Polish	29	0.20	Slovak	2	0.01
Japanese	999	7.03	Italian	26	0.18	Turkish	2	0.01
Korean	938	6.60	Czech	7	0.05	Arabic	1	0.01
German	467	3.29	Romanian	7	0.05	Bulgarian	1	0.01
Russian	368	2.59	Norwegian	3	0.02	Latvian	1	0.01
French	234	1.65	Greek	2	0.01	Slovenian	1	0.01
Spanish	79	0.56	Hungarian	2	0.01	Swedish	1	0.01

The leading subject area in the last six years is, like in journal articles, pharmaceuticals, followed by food and feed chemistry, industrial carbohydrates, essential oils and cosmetics, and textiles and fibers

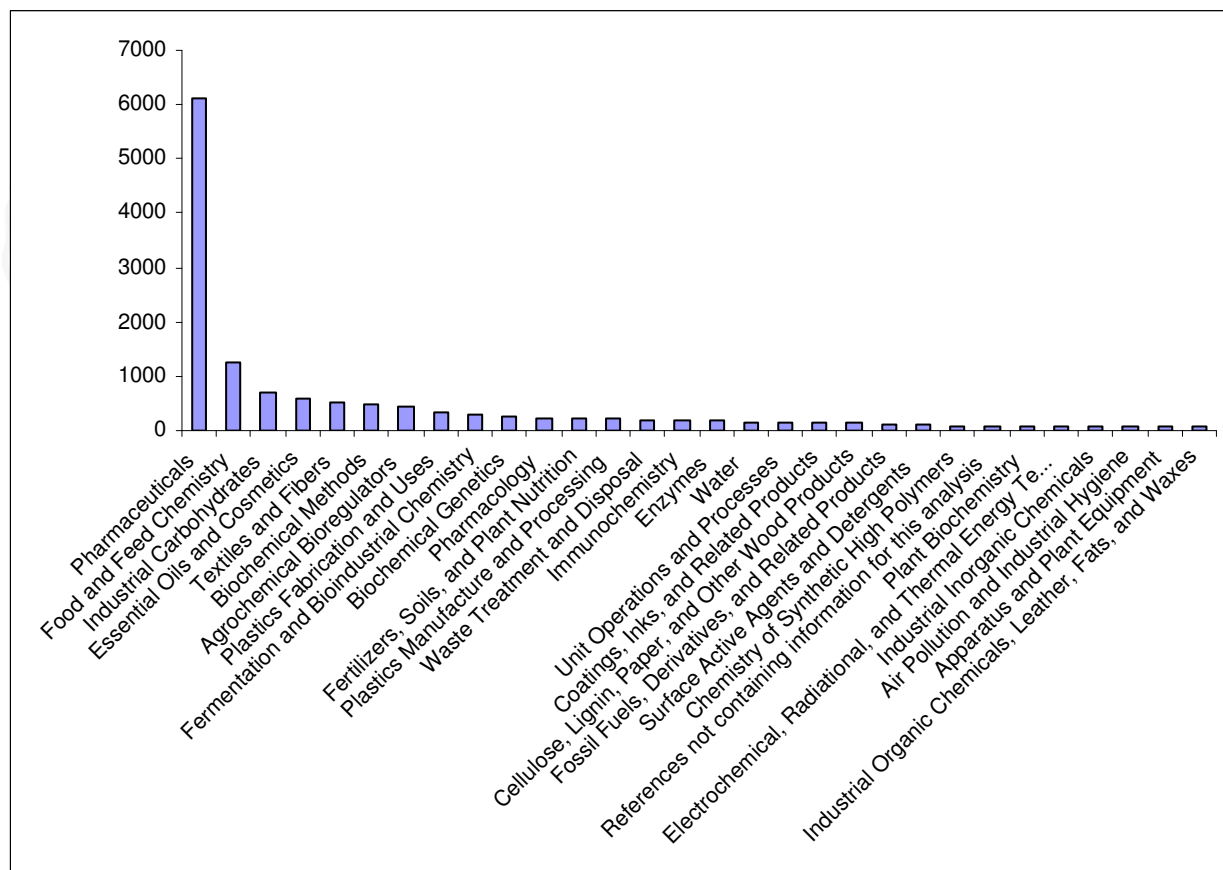


Figure 5. Patent Subject areas (CAPLUS; 2006-2012; plotted: 13,592 out of 14,206 counts).

The industrial demand for cellulose was $> 300 \times 10^6$ tons (year 2006 [6a,c;13]) with an estimated market volume of $> 2 \times 10^9$ US\$ (year 2007 [14]). The global annual demand for chitin was estimated at ca. 10,000 (year 2000 [15]) and 17,085 (year 1999 [16]) metric tons. Most of this (ca. 65%) was converted to glucosamine, 25% to chitosan, and 10% to

chitooligosaccharides. Figures for the chitin and derivatives market volume, including glucosamine, vary between 187×10^6 and 647×10^6 US\$ [15,16]. According to a recent commercial study [17], Japan alone produced 20,000 tons of chitin and derivatives in 2011. The compound annual growth (CAGR) chitin and derivatives is said to be at ca. 12% per year, reaching an estimated market volume of 63×10^9 US\$ in 2015 [17].

CONCLUSIONS

Coming back to the initial consideration of abundance it follows that chitin is not the second biopolymer or polysaccharide after cellulose. It is certainly one of the most abundant polysaccharides. In terms of industrial demand, there is a striking difference between the amounts as well as between the intensity of research on the two polysaccharides. Human welfare depends mostly on achievements in technical, health, nutrition, and social sciences, besides economic aspects. It is up to the reader to decide which of the many polysaccharides currently in use is more important in one or the other field. Research opportunities for chitin, chitosan, and derivatives are manifold.

REFERENCES

- [1] Muzzarelli, R.A.A. (1977). *Chitin*, pp. 5–16, Pergamon, Oxford.
- [2] Roberts, G.A.F. (1992). *Chitin Chemistry*, pp. 54–55, Macmillan, Houndmills.
- [3] Wang, Y.P., Law, R.M. Pak, B. (2010) *Biogeosciences*, **7**, 2261–2282.
- [4] Thieme Römpf-Online: "Kohlenstoff" and "Kohlenstoff-Kreislauf", <http://www.roempp.com/prod/>.
- [5] Ebert, G. (1993) *Biopolymere*, Teubner, Stuttgart.
- [6] a) Kirk-Othmer (Ed.) (1993), *Encyclopedia of Chemical Technology*, 4th Edn., Vol. 5, p. 476, John Wiley & Sons, New York. b) Klemm, D., Schmauder, H.-P., Heinze, T. (2002), in: Vandamme, E.J., De Baets, S., Steinbüchel, A. *Biopolymers*, Vol. 6, pp. 275-319, Wiley-VCH, Weinheim. c) *Ullmann's Encyclopedia of Industrial Chemistry* (1993), 5th Edn., Vol. A5, p. 375; Vol. B8, p. 172, Wiley-VCH, Weinheim.
- [7] Sandermann, W. (1973). *Holz Roh. Werkst.* **31**, 11; note that the figure given in this article, i.e. 13×10^9 , was wrongly cited as 1.3×10^9 in ref. [6c].
- [8] Klemm, D., Heublein, B., Fink, H.-P., Bohn, A. (2005). *Angew. Chem. Int. Ed.* **44**, 3358 – 3393.
- [9] Cauchie, H.-M. (2002). *Hydrobiologia* **470**, 63–96.
- [10] Jeuniaux C., Voss-Foucart M.F., Bussers J.C. (1993). *Aquat. Living Resour.* **6**, 331–341.
- [11] <https://scifinder.cas.org>
- [12] http://apps.webofknowledge.com/WOS_GeneralSearch_input.do?product=WOS&search_mode=GeneralSearch
- [13] Thieme Römpf-Online: "Papier", <http://www.roempp.com/prod/>
- [14] Wysokińska Z. (2010), *Fibr. Text. Eastern Europe*, 18, 7-13.
- [15] Sandford, P.A. (2002), *Adv. Chitin Sci.* **6**, 35–42.
- [16] http://evven.5u.com/text/future_opportunities.htm
- [17] Global Industry Analysts, Inc. (2010), *Chitin & Chitosan - A Global Strategic Business Report*; <http://www.strategyr.com/pressMCP-2039.asp>; note: figures cited here are taken from the abstract, the full record is not available to the author.



S I A Q

Sociedad Iberoamericana de Quitina

Sponsors

